Synthesis and Biological Evaluation of Novel MPTP Analogs as Potential Monoamine Oxidase B Inhibitors.

by

Amit S. Kalgutkar

Dissertation submitted to the Faculty of the Virginia Polytechnic Institute and State University in partial fulfillment of the requirements for the

degree of

Doctor of Philosophy

in

Chemistry

APPROVED BY:

Dr. Neal Castagnoli, Jr., Chairman

Dr. David G. I. Kingston

Dr. Harry W. Gibson

Dr. James Tanko

Dr. Joseph S. Merola

September, 1993

Blacksburg, Virginia

Synthesis and Biological Evaluation of Novel MPTP Analogs as Potential Monoamine Oxidase B Inihibitors.

by

Amit S. Kalgutkar

Professor Neal Castagnoli, Jr., Chairman

Abstract

The Parkinsonian-inducing neurotoxin 1-methyl-4-phenyl-1,2,3,6-tetrahydropyridine (MPTP) and close structural analogs are the only known cyclic tertiary amines with good monoamine oxidase substrate properties. In addition to its substrate properties, MPTP is a weak mechanism-based inactivator of monoamine oxidase-B (MAO-B). In an attempt to exploit the special interactions between this cyclic tertiary allylamine and MAO-B, studies were initiated to develop novel mechanism-based inactivators of this flavoenzyme. Analogs of MPTP bearing a variety of functional groups at either N or the C(4) position have been synthesized and their interactions with purified MAO-B have been characterized. The substituents selected included functionalities which were considered potential sources of enzyme generated electrophilic or radical intermediates that might alkylate and inactivate the enzyme. None of the C(4)-substituted compounds displayed significant enzyme inhibitor properties while the 4-phenyl-1-propargyl analog was a good mechanism-based inactivator of MAO-B but not MAO-A. The 4-phenyl-1-propyl derivative showed significant turnover with MAO-B suggesting that previous reports regarding the lack of

substrate properties of MPTP analogs bearing N-substituents larger than methyl must be viewed with caution.

The MAO-A and B generated dihydropyridinium metabolite derived from 1-methyl-4-phenoxy-1,2,3,6-tetrahydropyridine was observed to undergo rapid hydrolytic cleavage to yield phenol and 1-methyl-2,3-dihydropyridone, a chromophoric species that could be monitored spectrophotometrically. This reaction sequence was exploited to probe the active site of MAO-A and MAO-B with a variety of C(4)-aryloxytetrahydropyridine analogs bearing groups of different steric bulk on the aryloxy moiety. Almost all of the compounds displayed good to excellent substrate properties with MAO-A and MAO-B. In contrast to previous claims, these results argue that the active sites of both MAO-A and MAO-B will accomodate tetrahydropyridine derivatives bearing bulky groups at C-4. Consequently other factors are likely to contribute to substrate selectivity.

The results described in this thesis provide evidence that a variety of disubstituted tetrahydropyridine derivatives are good to excellent substrates for MAO-A and MAO-B. The new insights gained in terms of structure-activity relationships with the compounds studied here should set the stage for the design of other tetrahydropyridine analogs with therapeutic potential. The localization of MAO-A and MAO-B in specific cell types within the nervous system makes particularly attractive the possibility of designing tetrahydropyridine based prodrugs which will undergo bioactivation in selected cells in the nervous system resulting in the liberation of the pharmacologically active species.

This dissertation is dedicated to my parents.

Their love and encouragement have been a great

source of inspiration and comfort for me.

Acknowledgments

The Author wishes to express his gratitude and appreciation to his mentor, Peter's Professor Dr. Neal Castagnoli, Jr. for his constant enthusiasm and guidance. His patience and skills in solving scientific problems have made a lasting impression on the author's life.

Grateful acknowledgments are also made to Dr. David G. I. Kingston, Dr. Harry W. Gibson, Dr. James Tanko and Dr. Joseph S. Merola for their valuable advice and discussions.

The author is grateful to the members of the Castagnoli research group for valuable suggestions, assistance and friendship. The following are thanked:

Dr. Larry Hall (the general)

Dr. Babu Subramanium

Dr. Deepak Dalvie

Dr. Simon Kuttab

and above all Mrs. Kay Castagnoli and Ms. Lucy Liu for bearing with me for 4 years.

The author would like to also thank sincerely two undergraduate students, namely, Mr. Sam Murray and Ms. Andrea Hall for their effort particularly in the later stages of the project.

This work was supported by NIH and the Harvey W. Peters Research Center for Parkinson's Disease and Disorders of the Central Nervous System.

Table of Contents

List of Schemes

List of figures.

This dissertation is concerned with the enzyme catalyzed bioactivation of cyclic tertiary amines which may be neurotoxic and with the design, synthesis and biological evaluation of cyclic tertiary amine analogs with structural features that will impart inactivation properties to the resulting products upon enzyme processing. Results of our research also have led us to focus our attention on the design of cyclic tertiary amines bearing functionalities which convert the original substrate molecule to prodrug models which release the active drug moiety upon enzyme mediated bioactivation. The discussion which follows Chapter 1 will review the basic features of monoamine oxidase A and B (MAO-A and MAO-B), the particular enzymes of interest which have been utilized in our inhibition and prodrug design studies. Chapter 1 will include a discussion of the history of MAO inhibitors and a consideration of the mechanisms of inhibition of MAO. Chapter 2 will discuss the rationale and the proposed objectives of the thesis. In order to understand the approach taken in the design of the inhibitor and prodrug molecules, Chapter 2 will include a historical perspective on the neurotoxic tertiary amine MPTP which has been the key molecule upon which the thesis is based. Chapter 3, Section 3.1 will describe the synthetic work associated with this thesis. Chapter 3, Section 3.2 will report the substrate and inactivation studies on MAO-B and Chapter 4 will provide a discussion on the preliminary results of the interactions of selected MPTP analogs with human placental MAO-A. Chapter 5, Section 5.1 presents the experimental section on the synthetic work and Chapter 5, Section 5.2 will describe the experimental work on the isolation and

purification of MAO-B and MAO-A. This chapter also describes the substrate and inactivation assays utilized in this thesis.

Chapter 1. The Monoamine Oxidases A and B.

1.1.1. Catecholamines:

The term "catecholamine" refers generically to organic compounds that contain a catechol nucleus and an amino group. In practice the term includes the biogenic amines dopamine (DA, **1**), norephinephrine (NE, **2**) and epinephrine (E, **3**). The indolealkylamine 5-hydroxytryptamine (serotonin, 5-HT, **4**), while not a catecholamine, displays pharmacological properties related to the catecholamines. All of these compounds are water-soluble organic bases of low molecular weight which are derived from amino acid precursors by the action of specific enzyme systems.

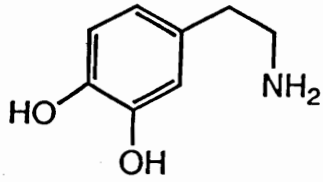

1

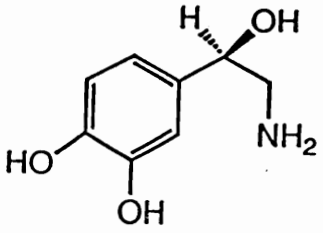

2

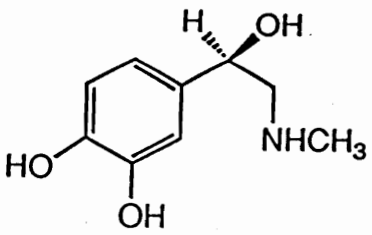

3

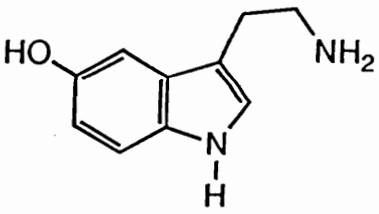

4

The characterization of the formation and fate of the catecholamines and indolealkylamine neurotransmittors and the development of drugs that alter the synthesis, storage, release, metabolism, transport and physiological activity of these compounds have greatly advanced our knowledge of the biochemistry, physiology

and pharmacology of the central nervous system. The biogenic amines that occur in the brain include dopamine (**1**), norepinephrine (**2**), and the indolealkylamine serotonin (**4**). In 1954 Vogt[1] was the first to report the uneven regional distribution of **2** and the striking effects that certain behaviour altering drugs had on its concentration in the mammalian brain. These early findings stimulated great interest in the biochemistry of the central biogenic monoamines.

In earlier studies[2] devoted to the field of naturally occuring biogenic or sympathomimetic amines, it was suggested that monoamines such as **2** may function as chemical transmitter substances at the terminals of peripheral sympathetic neurons. It is generally recognized today that, upon release from the presynaptic nerve endings, these chemical transmitters cause changes in the post-synaptic neuronal membrane potential that result in the generation of an impulse in the newly stimulated neuron. It was proposed[3a] subsequently that **1, 2, 3** and **4** also may function as transmitter substances (neurotransmitters) in the central nervous system as well.

Recent studies[3b-c] on the intracellular localization of the catecholamines and related metabolites in nerve tissue as well as on the functional correlation of catecholamines with the activity of nerve-end organs have contributed significantly towards our understanding of the pharmacological properties of these compounds. On the basis of previous studies,[3b-c] Bloom and coworkers[3d] described the life cycle of a biogenic amine in the brain as follows:

(1) The precursor α-amino acids [e.g. tyrosine (**5**) and tryptophan (**7**),

see Scheme 1 and Scheme 2] are transported across the blood-brain barrier and presumably also across the neuronal cell membrane. This step is enzymatically catalyzed by appropriate transporters.

(2) Synthesis of the amines take place in the neuron by a process involving appropriate enzyme catalyzed decarboxylation and hydroxylation steps.

(3) The amines thus formed are taken up by a membrane-bound granule and stored in association with a material that serves as the binding substance. The amines in this form are inactive but are in dynamic equilibrium with other, still poorly characterized pools in the neuron. These vesicles are then transported from the nerve cell bodies to the nerve terminals.

(4) Physiological release of the amines into the synaptic clefts in "active" forms then occurs in response to a stimulus.

(5) Dissociation of the amines from the receptor sites takes place with termination of the stimulus. The amines either succumb to enzymatic degradation or are taken up by the nerve terminals.

1.1.2. Distribution of the Biogenic Amines in the Nervous System.

In 1946 von Euler[4] in Sweden and shortly later Holtz[5] in Germany independently identified the presence of norepinephrine in adrenergic nerves. These findings laid the foundation for a new era of research in the field of catecholamines. Sympathetic ganglia and postganglionic fibers are known to contain equal concentrations of norepinephrine.[6] Of all the nerves studied, splenic nerves were found to have the highest content of norepinephrine.[7] The occurence of norepinephrine in a given

organ or nerve can, in general, be taken as evidence for the presence of noradrenergic fibers. Thus the absence of norepinephrine in bone marrow or placenta suggests the absence of adrenergic vasomotor nerves. Shortly after it was established that norepinephrine was the neurotransmitter substance of noradrenergic nerves in the peripheral nervous system, it was also identified as a normal constituent of the mammalian brain. The relative distribution of norepinephrine is quite similar in most mammalian species. The highest concentration is usually found in the hypothalamus and other central sympathetic areas.[8] More norepinephrine is generally found in gray matter than in white matter.

Dopamine is also found in the mammalian central nervous system and its distribution differs markedly from that of norepinephrine. In fact dopamine represents more than 50% of the total catecholamine content of the central nervous system in most mammals. The highest levels of dopamine are found in the neostriatum and the nucleus accumbens.[9] Dopamine is also present in the carotid body and superior cervical ganglion where it may play a role other than that of a precursor of norepinephrine.[10]

Epinephrine concentrations in the mammalian central nervous system are relatively low, approximately 5 to 17 percent of the norepinephrine content.[11] At present, the significance of the presence of epinephrine in certain brain areas is unknown.

1.1.3. Biosynthesis of the Biogenic Amines.

The biogenic amines are formed in the brain, sympathetic cells and

sympathetic ganglia from their amino acid precursor tyrosine (**5**) by a sequence of enzymatic steps. The amino acid precursor tyrosine is normally present in the bloodstream from which it is taken up and concentrated within the brain and presumably also in other sympathetic tissue by an active transport system. Once inside the peripheral neuron, tyrosine undergoes a series of structural transformations resulting in the ultimate formation of dopamine, norepinephrine, or epinephrine depending on the availability of the key enzyme systems. The biosynthetic pathway for the formation of catecholamines is shown in Scheme 1.[12] The first step involves the conversion of S-tyrosine (**5**) to DOPA (**6**) which is catalyzed by the enzyme tyrosine hydroxylase.[13] This enzyme is present in the adrenal medulla and in the brain and appears to be a unique constituent of catecholamine-containing neurons. The enzyme is stereospecific, requires molecular oxygen, Fe^{+2}, a tetrahydropteridine cofactor, and shows a fairly high degree of substrate selectivity. This is the rate determining step in the biosynthesis of catecholamines. The actual mechanism of this aromatic hydroxylation is poorly understood.

The second step in the biosynthetic pathway, the transformation of DOPA (**6**) to dopamine (**1**), is catalyzed by the enzyme DOPA decarboxylase.[14] This enzyme acts on all naturally occuring aromatic S-amino acids including histidine, tyrosine, tryptophan and phenylalanine. This enzyme is, therefore, more appropriately referred to as S-aromatic amino acid decarboxylase. The enzyme occurs in the cytoplasm of most tissue including the liver, stomach, brain, and the kidney, suggesting that

its function in metabolism is not limited solely to catecholamine biosynthesis.

The third step involves the conversion of dopamine (**1**) to norepinephrine (**2**). This step is catalyzed by the enzyme dopamine-β-hydroxylase. Dopamine-β-hydroxylase,[15] like tyrosine hydroxylase, is a mixed function oxidase. It requires dioxygen and utilizes ascorbic acid as a cofactor. The enzyme is a Cu^{+2} containing protein with about two moles of cupric ion/mole of enzyme. It is believed that this enzyme is localized primarily in the membrane of the amine storage granules. Dopamine-β-hydroxylase does not show a high degree of substrate selectivity and acts in vitro on a variety of substrates.

The last step in the biosynthetic pathway, the N-methylation of norepinephrine (**2**) to epinephrine (**3**), is catalyzed by phenylethanolamine-N-methyltransferase. This enzyme is localized[16] in the adrenal medulla although low levels of activity are known to occur in the heart and the mammalian brain. Demonstration of activity requires the cofactor S-adenosylmethionine. This enzyme, which shows poor substrate selectivity, catalyzes the methylation of a variety of β-hydroxylated amines.

Scheme 1. Biosynthesis of the Catecholamines.

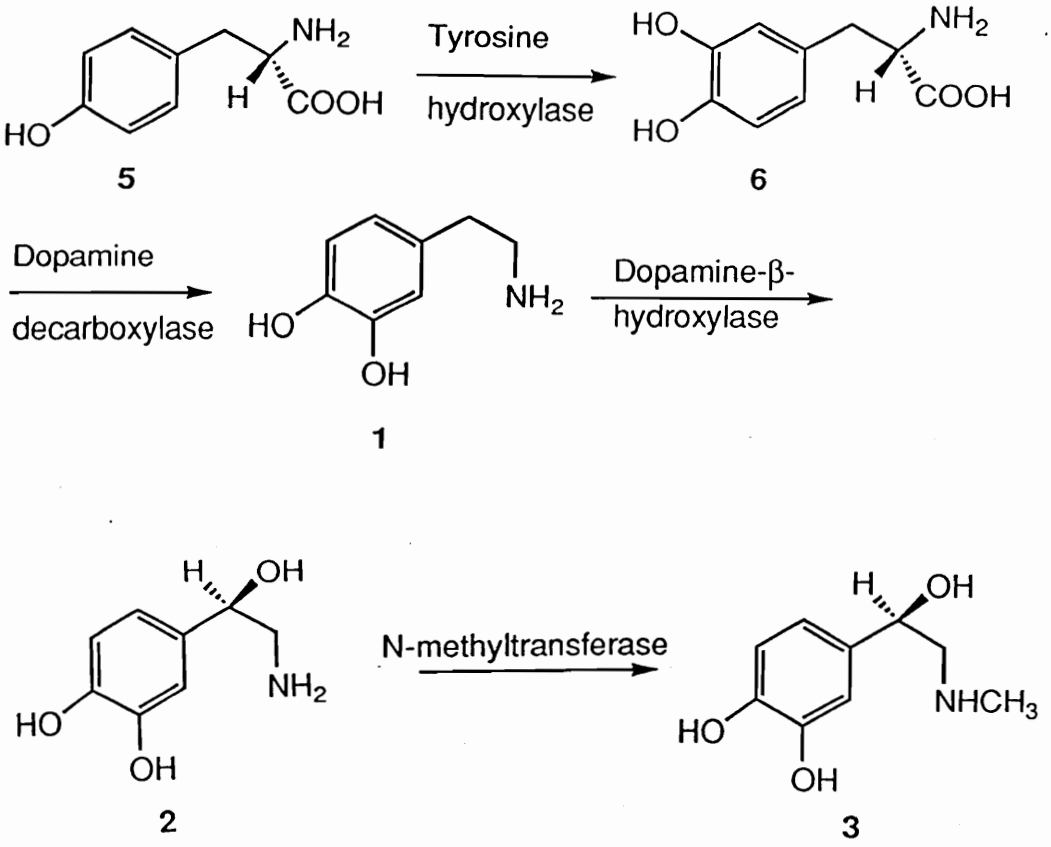

Serotonin (**4**) is found in many cells, such as platelets, which are non-neuronal.[17] In fact only a small percentage of serotonin in the whole body is found in the brain.[18] Nevertheless as serotonin cannot cross the blood brain barrier, it is clear that brain cells also are capable of synthesizing this amine. The biosynthesis of serotonin is summarized in Scheme 2.[19] The first step is the transporter mediated uptake of the amino acid tryptophan (**7**), the primary substrate for the biosynthesis of serotonin. The next biosynthetic step involves the hydroxylation of **7** at the 5-position to form 5-hydroxytryptophan (**8**). The enzyme required for this transformation is tryptophan hydroxylase which occurs in almost all

tissues in low concentrations. The enzyme appears to have an absolute requirement for dioxygen and reduced pteridine co-factor. The next step involves decarboxylation of 5-hydroxytryptophan (8) to yield serotonin (4). The enzyme responsible for this step is amino acid decarboxylase.

Scheme 2. Biosynthesis of Serotonin.

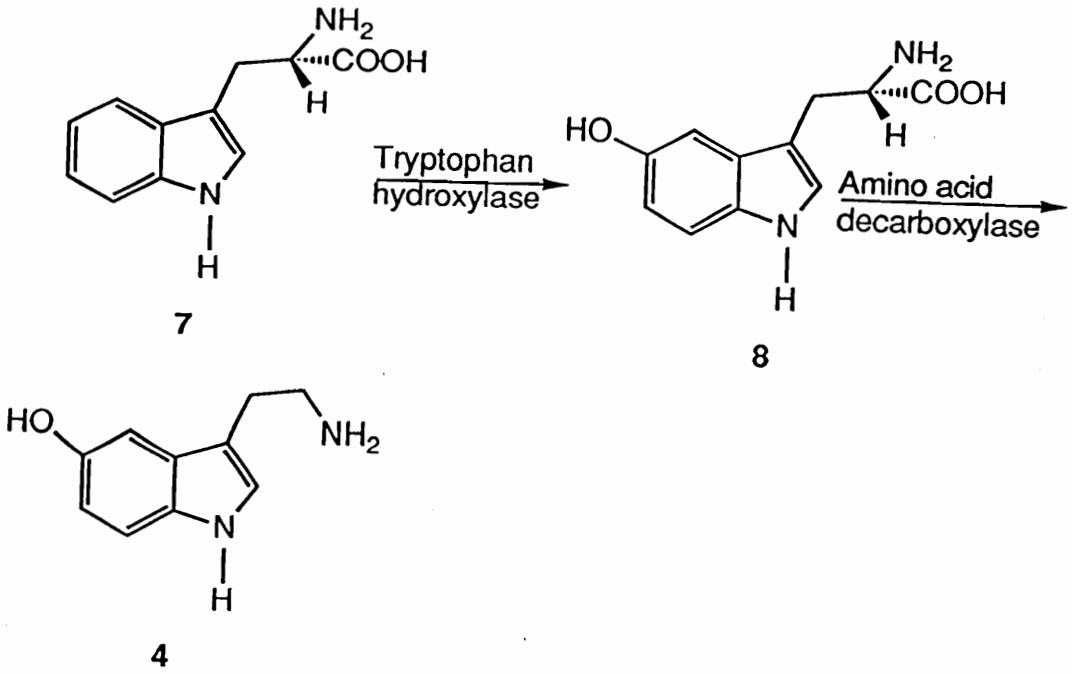

1.1.4. Metabolic Fate of the Biogenic Amines.

The major mammalian enzymes responsible for the metabolic degradation of catecholamines are monoamine oxidase (MAO)[20] and catechol-O-methyltransferase (COMT).[21] MAO, which will be reviewed in detail later, catalyzes the conversion of dopamine to 3,4-dihydroxyphenylacetaldehyde (**9a**) as shown in Scheme 3. Aldehyde intermediate **9a** is rapidly metabolized, usually oxidatively, by the enzyme aldehyde dehydrogenase, to the corresponding acid **10a**. In the

case of central norepinephrine (**2**), in addition to the corresponding oxidative pathway (**2** going to **9b** which goes to **10b**), reduction of the aldehyde metabolite **9b** by the enzyme aldehyde reductase to the glycol **10c** appears to be an important route.

Scheme 3. Metabolic Fate of the Catecholamines.

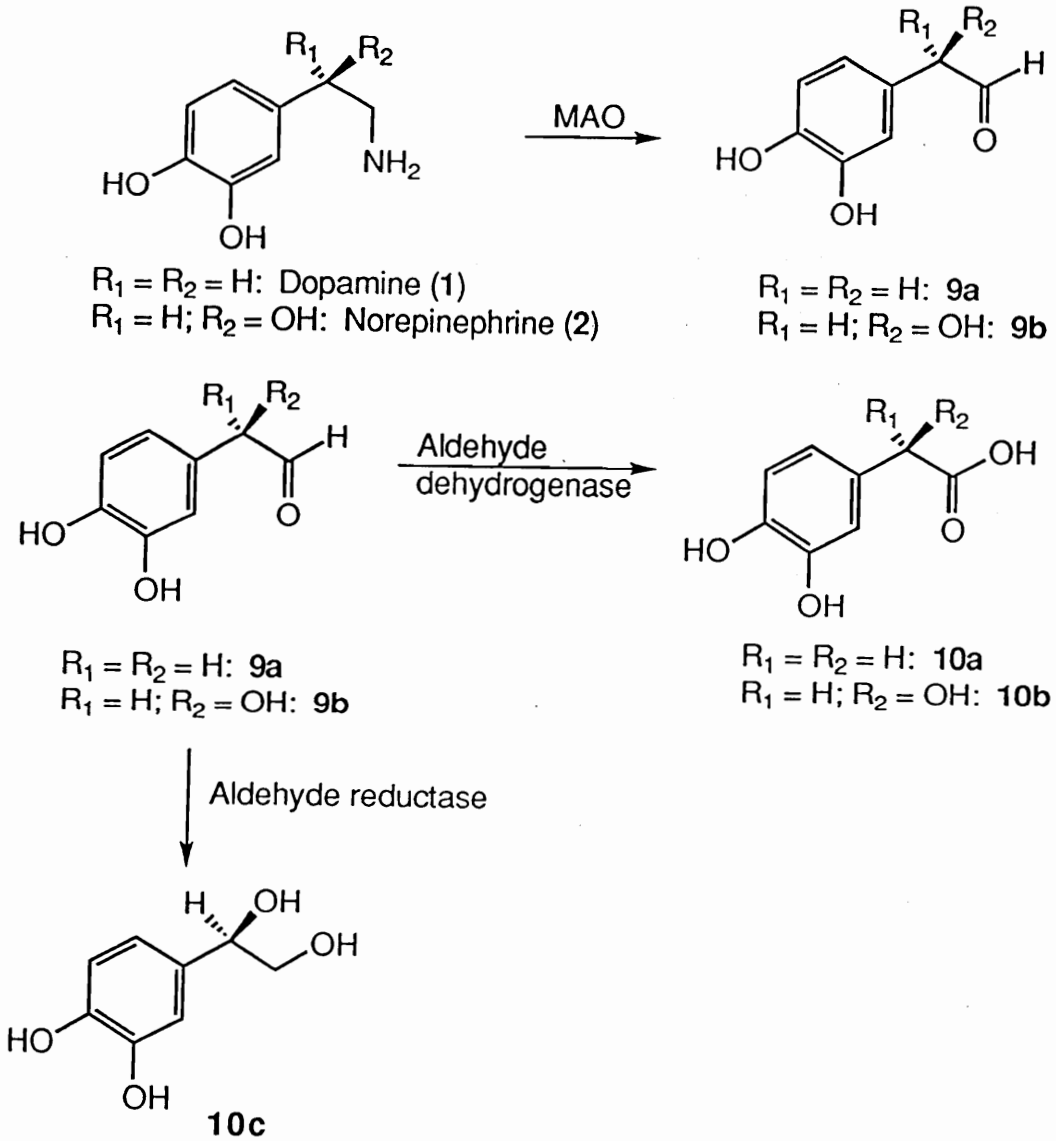

The second enzyme, COMT, is a relatively non-selective enzyme that catalyzes the transfer of methyl groups from *S*-adenosylmethionine to the *m*-hydroxy group of catecholamines and various other structurally related compounds.[21] The enzyme is found in the cytoplasm of most animal tissues and is particularly abundant in the liver and kidney. The enzyme requires Mg^{+2} and S-adenosylmethionine for activity.

The most effective route for the metabolism of serotonin (Scheme 4) is deamination by MAO.[22] The product of this reaction, 5-hydroxyindoleacetaldehyde (**11**), may be further oxidized to 5-hydroxyindoleacetic acid (**12**) or reduced to 5-hydroxytryptophol (**13**) depending on the NAD+/NADPH ratio in the tissue.

Scheme 4. Metabolism of Serotonin.

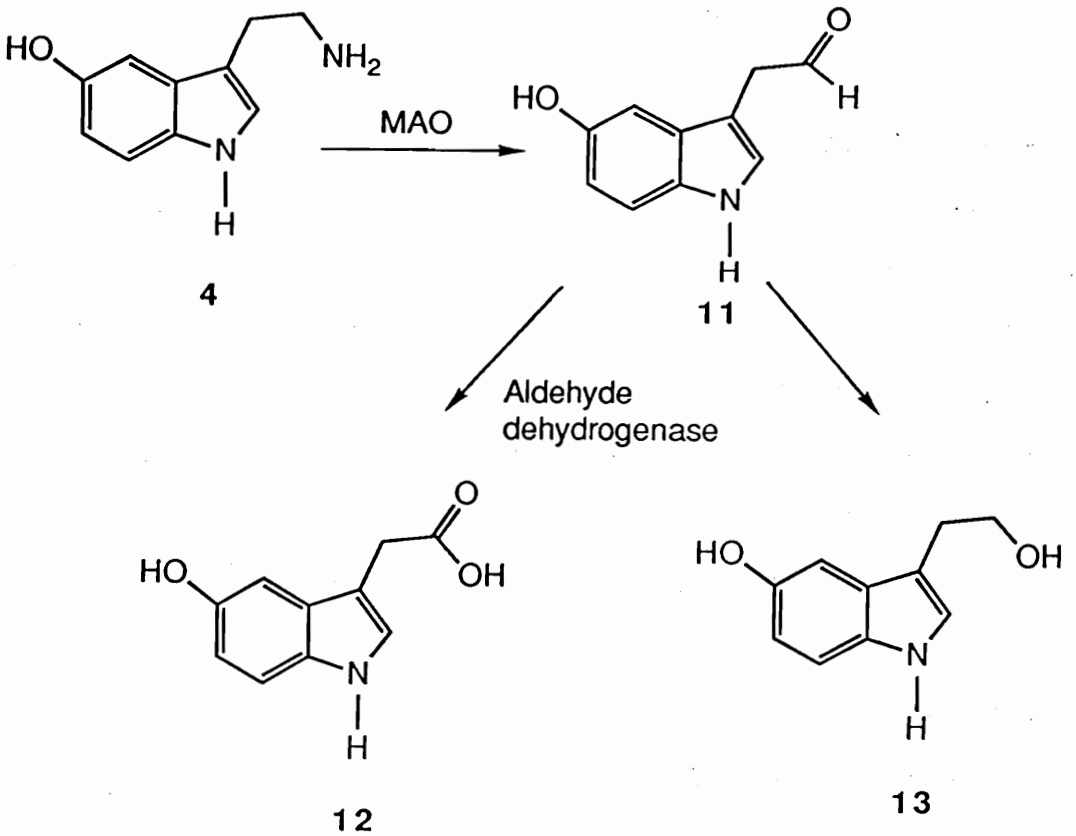

4 **11** **12** **13**

1.2. Amine Oxidases.

The oxidations of amines, diamines, and polyamines are catalyzed by amine oxidases,[23] the classification of which is based on the following criteria:

1. Substrate selectivity
2. Mode of oxidation
3. Sensitivity to inhibitors
4. Structure of enzyme and cofactor requirements

The first three criteria are based on individual properties of the enzyme. These properties are not absolute and may depend on environmental factors or on the procedures employed for their assay. The forth criterion, on the other hand, is much more characteristic and is based on the intrinsic properties of each of the respective enzymes.

1. Substrate selectivity

A common way to classify amine oxidases (AOs) is based on their substrate selectivity. AOs thus may be divided into monoamine oxidases (MAOs), diamine oxidases (DAOs), and polyamine oxidases (PAOs), according to their ability to catalyze the oxidation of monoamines, diamines or polyamines, respectively. The main disadvantage of this classification is that it tends to give a simplified picture of the many enzymes that lack strict substrate selectivities. Use of sensitive analytical techniques also may complicate the issue further by increasing the spectrum of possible substrates. For example Gorkin[24] showed that the substrate selectivity of mitochondrial monoamine oxidase could be altered by treatment of the enzyme with peroxides of oleic acid. Thus this

enzyme preparation which usually catalyzed the oxidation of monoamines only acquired an expanded substrate capability and also catalyzed the oxidation of polyamines.

2. Mode of oxidation

Amine oxidases also may be characterized by their catalytic mechanisms. Most of the enzymes catalyze the oxidative deamination of terminal primary amino groups. Such enzymes include the classical plasma amine oxidase and various bacterial enzymes. Another group of enzymes catalyze the oxidation of secondary amino groups including polyamines such as spermidine.

3. Sensitivity to inhibitors

The use of inhibitor selectivities as one of the criteria for AO classification was first proposed by Zeller[25] and was adopted by Malstrom[26] who first defined MAOs as enzymes which are inhibited by 2-phenylcyclopropylamine. DAOs on the other hand are inhibited by hydrazine and semicarbazide. In many cases, the selectivity to the drugs is not high. Thus aminoguanidine, which is regarded as a selective inhibitor of DAO, also inhibits the oxidation of polyamines.

4. Structure of enzyme and cofactors

The limitations summarized above argue for a better nomenclature of the AOs. One of the recent classifications is based on the structure of the enzyme and its cofactor requirement.[27] Most of the AOs have flavin or metal cofactors. The flavin cofactor in AOs is flavin adenine dinucleotide (FAD), which was shown to be present in mitochondrial MAO in a covalent linkage as 8-α-cysteinyl-FAD (see the

next section for a detailed discussion on the FAD-containing enzyme MAO). Many AOs do not contain an FAD cofactor but do contain stoichiometric amounts of copper which are needed for activity. These include the following: Bovine plasma AO: The crystalline enzyme has a molecular weight of 170,000 daltons and apparently contains two identical subunits. It contains 1 to 2 molecules of Cu^{++} and a pyridoxal phosphate like moiety. The enzyme catalyzes the oxidation of polyamines such as spermidine and spermine. Pig plasma AO: The crystalline enzyme has a molecular weight of about 195,000 and contains two molecules of copper per enzyme molecule. The enzyme selectively oxidises monoamines. Diamines and polyamines are not substrates. Pig kidney DAO: The purified enzyme has a molecular weight of approximately 170,000 and contains two molecules of copper and one molecule of pyridoxal phosphate like moiety per mole of enzyme. The enzyme is responsible for the oxidation of diamines, such as histidine. Pea seedling DAO: This enzyme contains 0.08 to 0.09% Cu^{++} which is firmly bound to the protein. It catalyzes the oxidation of polyamines. Aspergillus niger AO: The crystallized enzyme has a molecular weight of 273,000 and contains three molecules of Cu^{+2} per enzyme molecule. It also contains a pyridoxal-like material. The enzyme catalyzes the oxidation of monoamines.

The problem of developing a satisfactory nomenclature for the AOs has not been completely solved since the relative rates of activity by AOs on the monoamines, diamines and polyamines differ with differing preparations.[28] The classifications discussed above recognized as generally being useful.

A systematic scheme of classification was adopted by the International Union of Biochemistry in 1961. This classification is based upon three principles. The first principle of this system indicates that names of enzymes, especially those ending in *-ase*, should be used for single enzymes, i.e. single catalytic entities. They should not be applied to systems containing more than one enzyme. For example, the system catalyzing the oxidation of succinate by dioxygen which consists of succinate dehydrogenase, cytochrome oxidase, and several other intermediate carriers is named the succinate oxidase system and not succinate oxidase. The second principle refers to the nomenclature of enzymes according to the reaction catalyzed. Since this is a specific property it serves a way to distinguish one enzyme from another. The consequence of this concept is that a certain name designates not a single enzyme protein but a group of enzymes with the same catalytic properties. Enzymes from different sources are classified as one entry. The third principle requires that enzymes be divided into groups on the basis of the type of reaction catalyzed, and this, together with the names of the substrate provides a basis for naming individual enzymes. It is also the basis for classification and code numbers. The enzyme commission devised a system for classification of enzymes that also serves as a basis for assigning code numbers to them. These code numbers which are prefixed by EC are now widely used. They contain four elements separated by points with the following interpretation. The first number shows to which of the six main divisions (classes) the enzyme belongs. The six main classes based on this nomenclature are oxidoreductases,

transferases, hydrolases, lyases, isomerases and ligases. The second number indicates the sub-class. The third number gives the sub-sub-class and the fourth number is the serial number of the enzyme in its sub-sub-class. Thus, the flavoprotein monoamine oxidase is classified as EC 1.4.3.4. which expands to enzyme class (amine: oxygen oxidoreductase (deaminating) (flavin containing). Examples based on this system of classification are available in Enzyme Nomenclature (Recommendations of the Nomenclature Committee of the International Union of Biochemistry, Academic Press, Inc. 1978).

1.3. Monoamine Oxidase

1.3.1. Biochemical Background.

Although the history of amine oxidases can be traced back to Schmiedeberg, who showed that benzylamine was excreted in the dog as hippuric acid, it was Mary Hare in 1928[29] who first documented the enzyme-catalyzed oxidation of tyramine by tissue extracts and called the responsible enzyme tyramine oxidase. This was later renamed monoamine oxidase (EC 1.4.3.4) by Zeller[30] in an attempt to distinguish it as a member of the class of enzymes responsible for the oxidative deamination of monoamines. Monoamine oxidase is an FAD containing enzyme[31] which catalyzes the oxidation of amines to the corresponding aldehyde and ammonia. The stoichiometry of this oxidation reaction is as shown. The pathway will be discussed later.

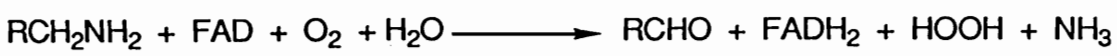

1.3.2. Multiplicity.

MAO is an integral protein of the mitochondrial outer membranes of neuronal, glial and other cells. Its roles include regulation of the levels of biogenic amines in the brain and the peripheral tissues by catalyzing their oxidative deamination.[32]

MAO exists in two forms termed MAO-A and MAO-B. These forms are distinguished by the availability of highly selective inhibitors. MAO-A is inhibited by nanomolar concentrations of clorgyline (**14**)[34] while MAO-B is inhibited by nanomolar concentrations of (S)-deprenyl (**15**).[33] Micromolar concentrations are required for opposite combinations.

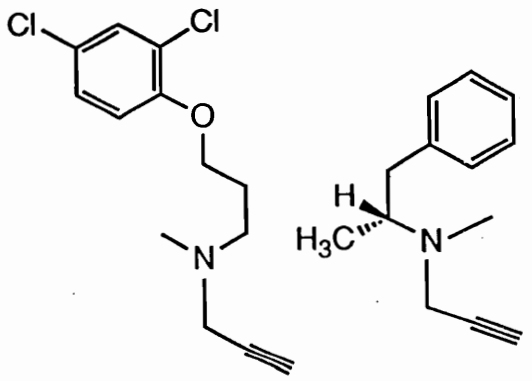

14 **15**

Although substrates of the A and B forms of MAO do not show absolute specificity, phenylethylamine is a preferred substrate of the B-form of the enzyme whereas 5-hydroxytryptamine is a preferred substrate of the A form. The existance of the A and B forms of MAO has been known since the work of Johnston[34] in 1968 who discovered the selectivity of clorgyline. The application of various chromatographic

techniques, however, had not provided unequivocal evidence for the two forms until the report of Pearce and Roth[35] who demonstrated that both the A and B forms of human brain MAO are separable with retention of enzymatic activity by simple chromatographic techniques. Further studies,[36] particularly those where monoclonal antibodies raised against each form of the enzyme were used, have provided additional evidence indicating that the two major enzyme sub-types are different proteins. Differences between these two had been proposed in terms of their lipid microenvironments.[37] Physical evidence that MAO-A and MAO-B are two distinct proteins was shown[38] in the deduced amino acid sequences. The subunit molecular weights of the A and the B forms have been calculated to be 59,700 and 58,800 daltons respectively. They have 70% amino acid sequence identity. Both sequences contain the pentapeptide Ser-Gly-Gly-Cys-Tyr in which the obligatory co-factor FAD is bound to cysteine.[39] Comparisons of immunological determinants,[40] subunit sizes, peptide maps[41] and cDNA clones fully document that MAO-A and MAO-B are unique proteins.[42]

1.3.3. Tissue Distribution.

MAO has been found in all the mammals examined. It is essentially a mitochondrial enzyme which is tightly bound to the outer membrane, whether in the nerve terminals or the liver. Some activity has been reported in microsomes. A few tissues express only one form of MAO. Thus, in the human most tissues express both MAO-A and MAO-B, although placenta contains predominantly MAO-A[43a] and platelets and lymphocytes express only MAO-B.[43b] Both forms of MAO seem to be

present in most areas of the brain. In spite of the fact that 5-HT is a selective substrate for the A form of the enzyme, MAO-B appears to be the main, if not the only, form present in serotonergic neurons[44] whereas MAO-A is localized in the catecholamine neurons.[45] Mammalian adrenal glands contain variable levels of MAO with both forms expressed in the cortex and medulla.[46] In the human fallopian tube, the intensity of MAO staining correlates with the phases of the menstrual cycle.[47] It was suggested that MAO may protect the fertilized ovum from circulating amines.

1.3.4. Subunit Structures and FAD Content.

Although these enzymes have never been crystallized, early titration experiments estimated that bovine liver MAO-B contained one FAD per 100 kDa protein.[48] These results were in good agreement with a ratio estimated by a spectrophotometric determination of flavin.[49] More accurate measurements show a ratio of one FAD per 63 kDa (MAO-A) and 57 kDa (MAO-B) human enzyme.[50] The above data in conjunction with the molecular weights obtained from cDNA studies[51] indicate that MAO consists of either one or more subunits, each of which binds one FAD molecule.

1.3.5. MAO Substrates.

The principal biogenic amines metabolized by MAO-A and MAO-B are dopamine (**1**), noradrenaline or norepinephrine (**2**), adrenaline or epinephrine (**3**), serotonin (**4**) and 2-phenylethylamine (**16**). Although substrates of the A and B forms of MAO do not show absolute specificity, 2-phenylethylamine is considered a prefered MAO-B substrate and

serotonin a preferential MAO-A substrate. In addition to the endogenous substrates of MAO, numerous substances of exogenous origin have been shown to be oxidatively metabolized by MAO.[52]

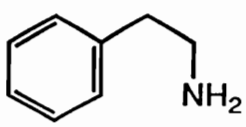

16

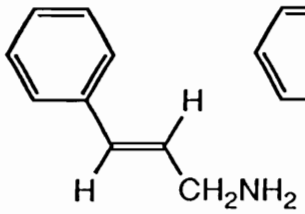

17a

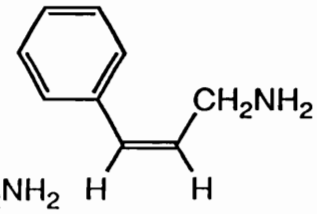

17b

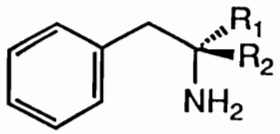

18a: $R_1 = H$; $R_2 = CH_3$
18b: $R_1 = CH_3$; $R_2 = H$

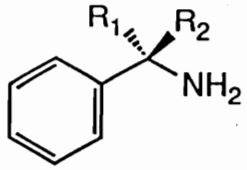

19a: $R_1 = H$; $R_2 = CH_3$
19b: $R_1 = CH_3$; $R_2 = H$

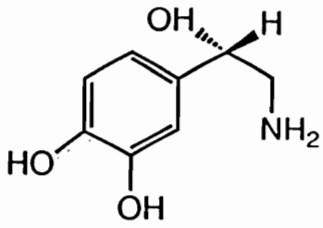

20

The MAOs which have wide substrate selectivities, catalyze the oxidation of primary, secondary and, to a lesser extent, tertiary amines. Primary and secondary amine derivatives are indiscriminately deaminated by both forms of MAO. By contrast compounds such as the N,N-dimethylaminoalkylindoles tend to be selective MAO-B substrates.[53a] Thus the ability to act upon tertiary amines is thought to be a selective feature of MAO-B. This observation suggests that the binding

site of MAO-A is more sensitive to steric interactions than that of MAO-B. However, other factors besides steric interactions should be involved in the selective recognition of substrates by MAO-A or MAO-B. Thus C-5 to C-10 linear aliphatic amines have been shown to be preferential MAO-B substrates,[53b] possibly in relation to their lipophilicity which appears to be a common property of the typical MAO-B substrates.

The ability of MAO-B to catalyze the selective oxidation of *E*- and *Z*-N-methylcinnamylamines (**17a**) and (**17b**) with almost equal efficiency[54] suggests that, in addition to an amine binding site, MAO has a hydrophobic site that binds the aromatic residue of substrates. If such a site exists, the high selectivity of cinnamylamine isomers, benzylamine, phenethylamine and aliphatic amines for MAO-B, and serotonin for MAO-A suggests a large difference in the nature of this binding site between MAO-A and MAO-B. Contrary to MAO-A, the hypothetical hydrophobic binding site of MAO-B must be an extensive one if both *E*- and *Z*-cinnamylamine isomers can be equally well accomodated.

MAO is thought to catalyze amine oxidation by a single electron transfer (discussed in detail in next section). Abstraction of an α-proton from the intermediate cation radical was suggested to be the rate limiting step in the oxidation process. The absolute stereochemistry of the abstraction of a hydrogen atom from the prochiral methylene group has been determined. Yu *et al.*[55a] using dopamine or benzyl amine as substrate, have established that both MAO-A and -B exhibit the same stereospecificity, that is, the pro-R-hydrogen is abstracted by both forms of MAO. Substitution of one α-hydrogen atom in MAO substrates by a

methyl group transforms these substrates into reversible and competitive inhibitors.[55b] Thus while 2-phenylethylamine (**16**) is an excellent substrate, α-methylphenethylamine or amphetamine (**18**) is resistant to MAO catalyzed oxidative deamination and acts as a reversible and competitive inhibitor.[55b] The S enantiomer (**18a**) of amphetamine, in which the methyl group occupies the position of the non-abstracted hydrogen atom, is a more potent inhibitor of MAO-A than its R counterpart.[55c] Both enantiomers display the same inhibitory potency towards MAO-B. Similarly, introduction of an α-methyl group into benzylamine, a highly selective MAO-B substrate, affords **19**, the R enantiomer of which was found to be a more potent MAO-A and MAO-B inhibitor than the S form.[55d] These results not only highlight the stereoselective nature of the active sites of MAO-A and MAO-B, but also clearly indicate that factors other than α-substitution of the side chain, such as distance between the aromatic ring and the nitrogen atom, can influence the specific recognition of arylalkylamine MAO inhibitors. Concerning the stereoselective nature at the β position for substrate recognition, it was shown that the R enantiomer of β-phenylethanolamine (**20**) only interacted with MAO-A wheras MAO-B did not exhibit any bias and deaminated both enantiomers.[55e] These data suggest that the active site of MAO-A would have steric constraints at the position corresponding to the β-carbon in arylalkylamines which do not exist for MAO-B. Additional details on substrate recognition, particularly, with regards to tertiary amines, by MAO are reviewed in Chapter 2.

Catalytic Mechanism.

The exact catalytic mechanism of MAO is still unclear. Many mechanistic studies[56a-b] dedicated to unraveling the MAO catalytic pathway have led to the working hypothesis summarized in Scheme 5a and Scheme 5b. Scheme 5a shows the proposed fate of the FAD. In its oxidized form FAD (**21a**) accepts an electron from the amine substrate to form the semi-reduced radical anion $FAD^{\cdot -}$(**21b**). A second electron transfer and protonation converts **21b** to the reduced flavin anion $FADH^-$ (**21c**). Finally protonation of **21c** yields $FADH_2$ (**21d**).

The key mechanistic feature of this catalytic pathway involves several steps which are initiated by the oxidation of amine substrates (**22**) via an initial one electron transfer from the amine to the oxidized flavin cofactor FAD to yield the intermediate radical cation **22a**. Intermediate **22a** loses a proton to generate the carbon centered radical **22b**. Loss of a second electron leads to the iminium species **22c**. The iminium species **22c** is then hydrolyzed to generate the corresponding aldehyde and ammonia.

Scheme 5a: Reduction of the Flavin

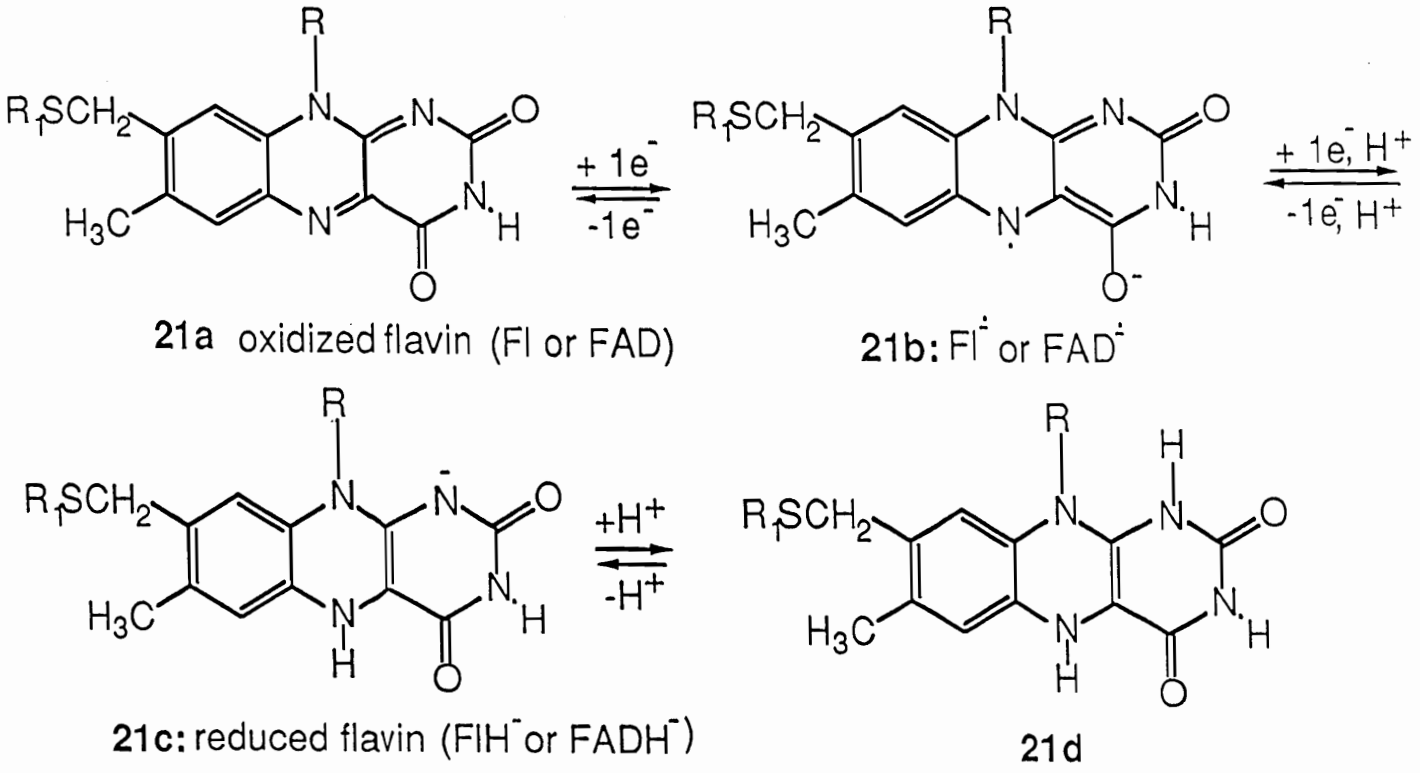

21a oxidized flavin (Fl or FAD)

21b: $Fl^{\cdot}$ or $FAD^{\cdot}$

21c: reduced flavin (FlH^- or $FADH^-$)

21d

Scheme 5b. Proposed Mechanism of Amine Oxidation by MAO.

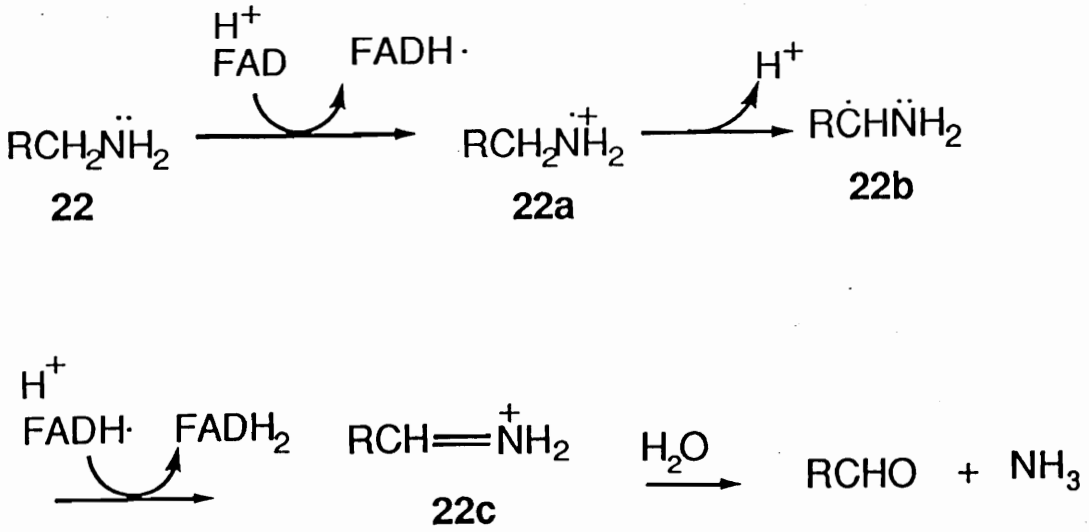

The proposed pathway is based primarily on the elegant studies by Silverman and coworkers who used cyclopropylamines and cyclobutylamines as probes for a one-electron transfer pathway for MAO (discussed in detail later). More direct evidence for a radical intermediate in the MAO-catalyzed amine oxidations was sought by carrying out the reaction of MAO with poor substrates such as cyclobutylamines in the presence of a radical spin trap in an ESR cell.[56a] Such studies have been attempted with benzylamine, the preferred MAO-B substrate, but no ESR spectral support[56b] could be obtained for a radical intermediate, even in the presence of spin traps, presumably due to the high reactivity of the generated radical intermediates. The oxidation of benzylamine may be so efficient that radical intermediates are processed rapidly prior to escape from the active site. Silverman and coworkers designed a new substrate, the aminoketone **23**, for MAO which upon oxidation may generate a

carbon centered radical species **23c** with an enhanced stability which could be trapped by suitable spin traps. Compound **23** proved to be a poor substrate (k_{cat} 2.0 min^{-1} and K_m = 330 μM) and a poor inactivator for (K_I = 16.7 mM and k_{inact} = 0.016 min^{-1}) MAO-B. When incubated with MAO-B for 17 hours in the presence of PBN (α-phenyl-N-tert-butylnitrone) a triplet of doublet signal consistent, with the trapped adduct **23d**, was observed. In the absence of enzyme or in the presence of enzyme previously inactivated with known inhibitors no ESR signals were observed. The mechanism of the inactivation is consistent with the single electron transfer from **23** to the flavin to generate the radical cation **23a** which then ring opens to the carbon-centered radical **23b**. Ring closure of **23b** gives the stable radical **23c**. The stable carbon-centered radical can be trapped by PBN to generate the nitroxyl radical **23d** (Scheme 5c). This evidence supports an initial one-electron transfer from the amine to the flavin.

Scheme 5c. Evidence for Electron Transfer Mechanism Using Spin Traps.

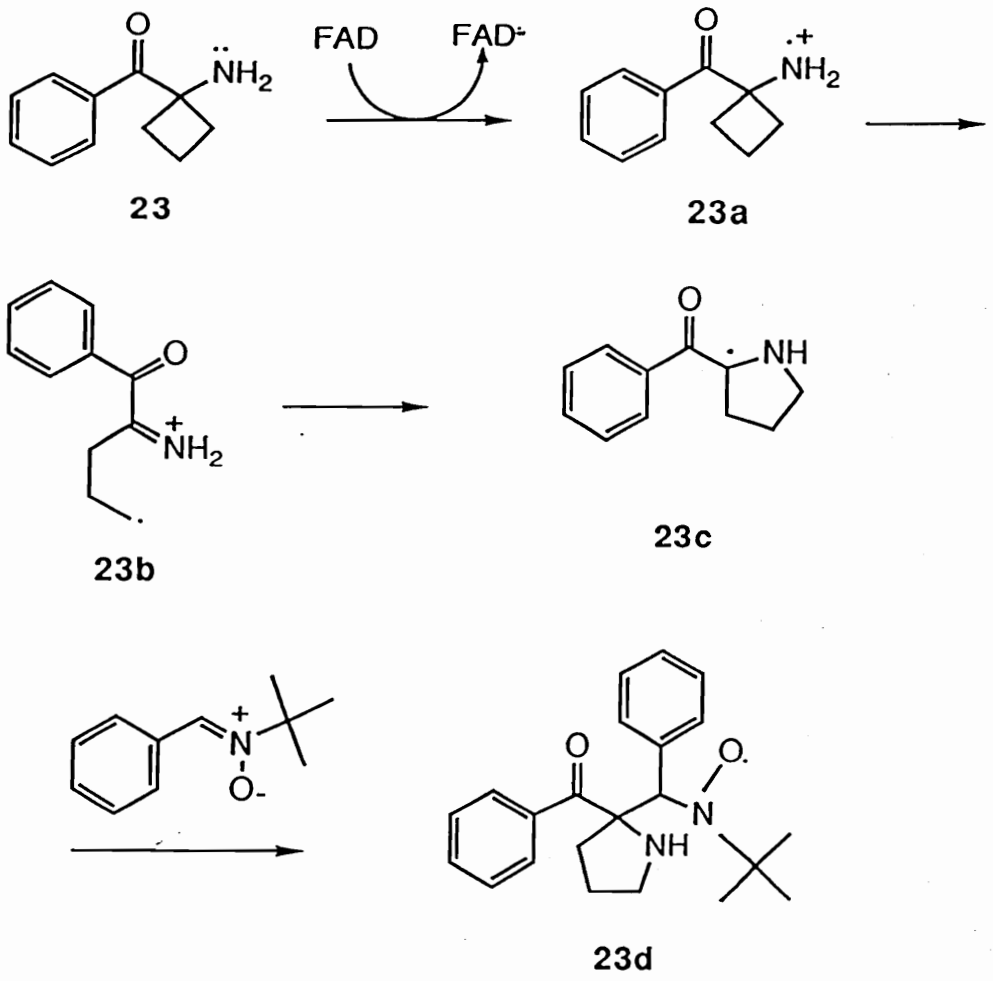

Recent studies with (aminomethyl)trimethylsilane and 5-(aminomethyl)-3-aryl-2-oxazolidinones (reviewed in detail later) also lend support to the pathway shown in Scheme 5b as the mechanism of MAO catalyzed oxidation.

The deprotonation step at the carbon centered radical **22b** as suggested in Scheme 5b is a commonly proposed reaction for many

organic cation radical intermediates. For example this is a generally accepted fate of alkylaromatic as well as tertiary amine cation radicals generated in chemical,[57a-b] photochemical[58] and enzymatic oxidation reactions.[59a-b] Nevertheless the step remains controversial and an alternative pathway also has been proposed in which loss of a hydrogen atom rather than a proton takes place.

Tertiary amine cation radical deprotonations have been the subject of considerable discussion in the recent literature. Nelson and Ippoliti[60] have argued that the high kinetic acidity previously proposed for tertiary amine radical cations might be incorrect and on the basis of thermodynamic acidity estimates they argued that cation radicals are not extremely acidic and therefore α-deprotonation of an amine radical cation is not as favorable a pathway as hydrogen atom abstraction. Dinnocenzo and coworkers[61] presented arguments based on model studies that the thermodynamic acidity is irrelevant and that the true pKa for amine radical cations determined by direct measurements, is no more than 10 which makes amine radical cations weaker acids than originally thought; consequently they suggested that α-deprotonation is a favourable and rate-limiting pathway. Studies with the tertiary amine cation radical salt **24**[61] and its subsequent reaction with quinuclidine (**25**) which led to the adduct **26** (Scheme 5d) indicated the reaction to be first order in both the reactants and to proceed with an isotope effect of 7.68 (for the disappearance of the aminium radical when comparing the reaction rate between **24** and **24-d$_3$**). This is clearly a primary isotope effect and requires that cleavage of the C-H(D) bond be rate determining and suggested a

deprotonation mechanism (Scheme 5d, pathway a) rather than a second electron transfer (Scheme 5d, pathway b) leading to the adduct **26**.

Scheme 5d (Pathway a). Proton Transfer Mechanism

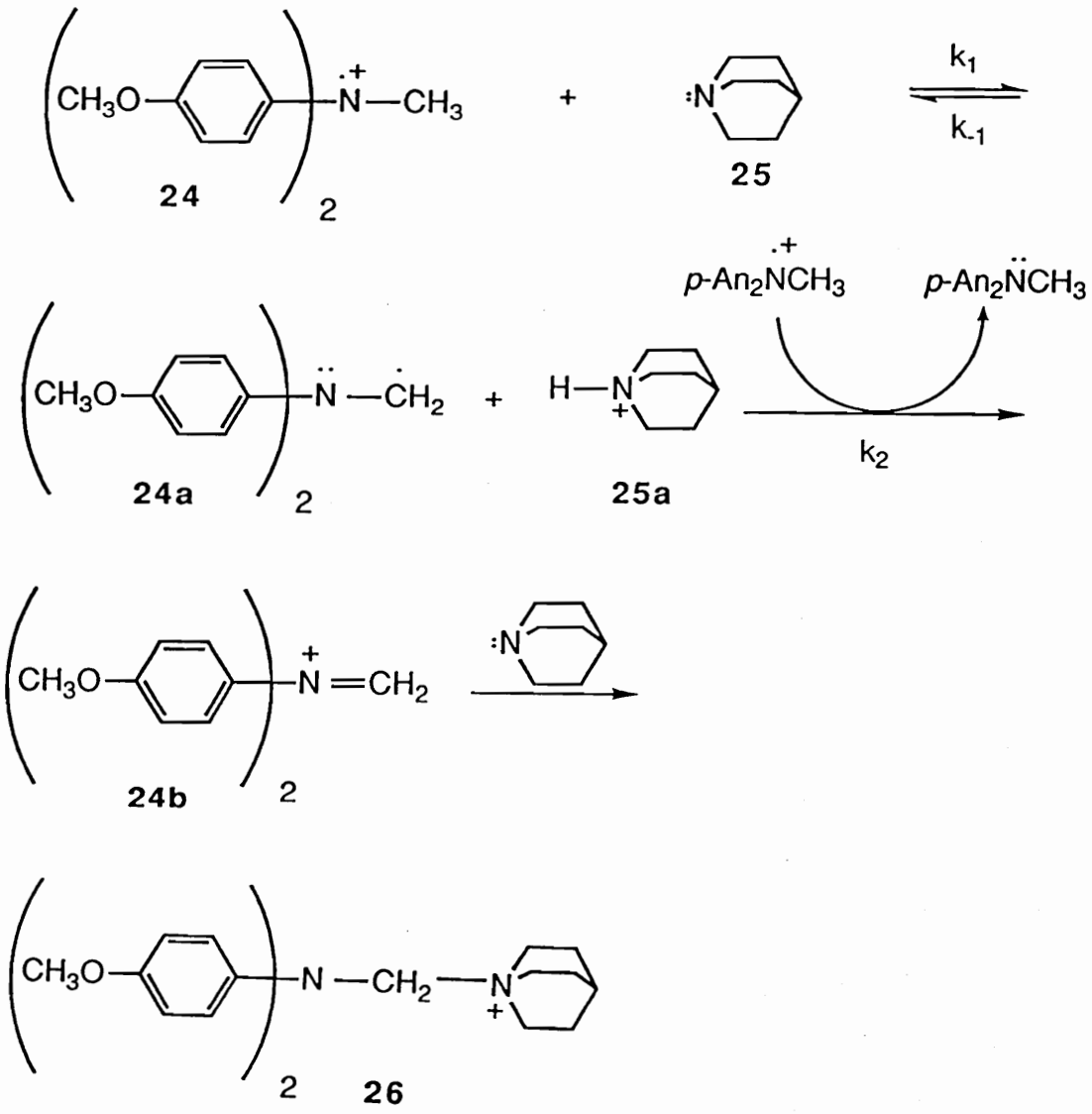

Scheme 5d (Pathway b). Electron Transfer Mechanism.

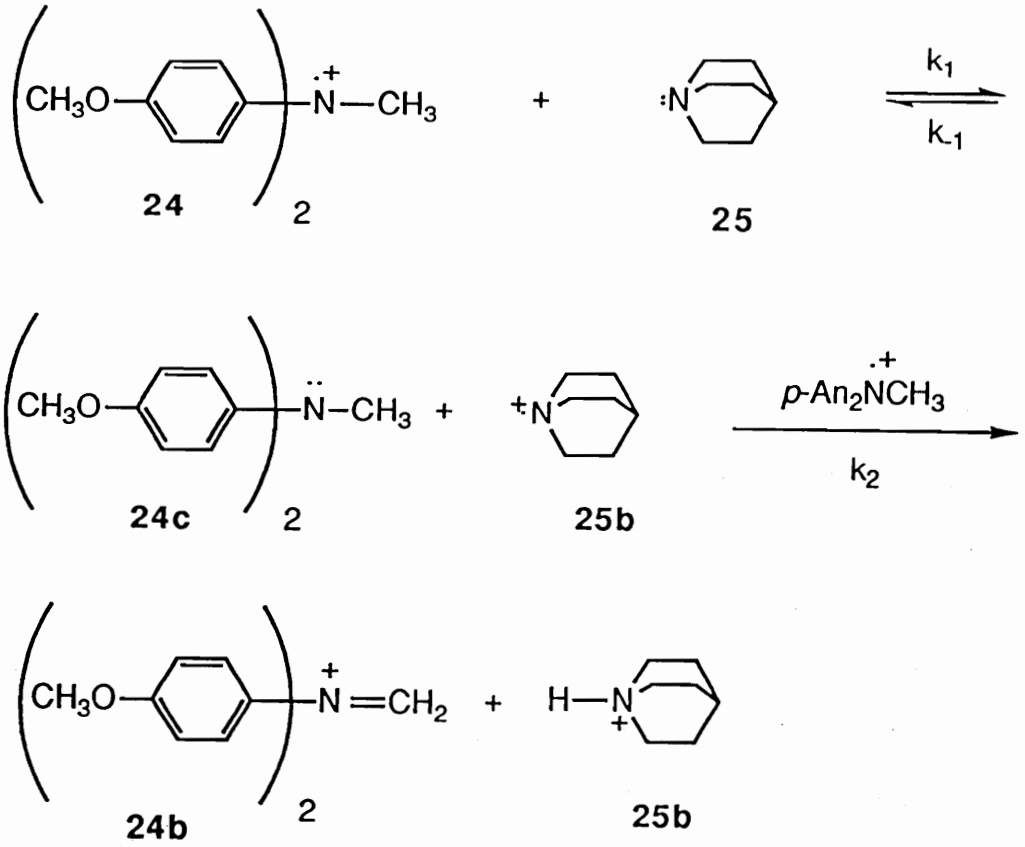

Thus the two mechanisms which were put forward consisted of the deprotonation pathway and the electron transfer pathway. The proton transfer mechanism consisted of deprotonation of **24** (isotope effect of 7.68) to produce a α-amino radical **24a** and the quinuclidinium ion **25a**. The α-amino radical **24a** is strongly reducing and would be expected to be oxidized by **24** to form the iminium ion **24b** and **25**. The iminium ion **24b** is then transformed into **26** by addition of **25** to **24b**. The

susceptibility of **24b** towards nucleophillic attack by **25** to generate **26** was confirmed by reacting synthetic **24b** with **25**. The electron transfer mechanism involves an initial electron transfer from **24** to **25** to generate the corresponding amine **24c** and the quinuclidinium radical cation **25b**. Abstraction of a hydrogen atom by **25b** from the starting material **24** generates **24b**. Alternately this hydrogen atom abstraction can also occur from **24c** to form the same intermediate **24a** as in the deprotonation pathway.

Recently Silverman[62] has provided evidence for a hydrogen atom transfer mechanism or a proton/fast electron transfer mechanism as plausible pathways of deamination by monoamine oxidase. It is known that cyclopropylcarbinyl radicals rearrange to the corresponding 3-butenyl radical at a rate estimated to be 10^8 sec^{-1} or faster.[63a] This rate increases when the cyclopropyl ring is substituted with radical stabilizing groups. For example, the 2-phenylcyclopropylcarbinyl radical opens to the 1-phenyl-3-butenyl radicals at a rate of approximately 10^{11} sec^{-1}.[63b] Silverman argues that such fast rates of ring opening could compete with electron transfer mechanisms and designed the cyclopropyl analog **27** as a test compound to study whether α-deprotonation/electron transfer mechanism (pathway a, Scheme 5b) or hydrogen atom transfer (pathway c, Scheme 5b) operates during the oxidation process. Scheme 5e depicts the above proposal structurally. Monoamine oxidase catalyzed cyclopropyl ring cleavage of **27**, which would lead to inactivation of the enzyme as depicted in pathway c, would be in favour of an α-deprotonation pathway of the intermediate radical cation **27a** leading to

the α-carbon radical **27b**. If no cyclopropyl ring cleavage occurred, it would indicate that either α-carbon radical formation via α-deprotonation does not occur or that second electron transfer from the α-carbon radical occurs faster than does cyclopropyl ring opening (Scheme 5e, pathway a and/or pathway b, pathway c is the proposed enzyme inactivation pathway). Experimental results indicated that incubation of MAO with **27** produced a single product, namely *trans*-2-phenylcyclopropanecarboxaldehyde (**27c**), the oxidation and hydrolysis product without ring cleavage. Kinetic analysis indicated that **27** was a poor substrate of MAO with a turnover number of 22 min^{-1} and a K_m value of 1.41 mM. No inactivation was noticed even at saturating concentrations of 20 mM. These results suggest that either the α-carbon radical is not an intermediate in the oxidation process, or if it is, second electron transfer to the flavin semiquinone occurs at a rate faster than cyclopropyl ring opening. Possible explanations for the lack of ring opening were based on the stability of cyclopropylcarbinyl radicals to which radical stabilizing groups have been attached or steric constraints at the enzymatic active site which may lead to improper overlap between the cyclopropane bond and the carbon radical, thereby slowing the rate of ring opening.

Scheme 5e. Monoamine Oxidase Catalyzed Oxidation of 27.

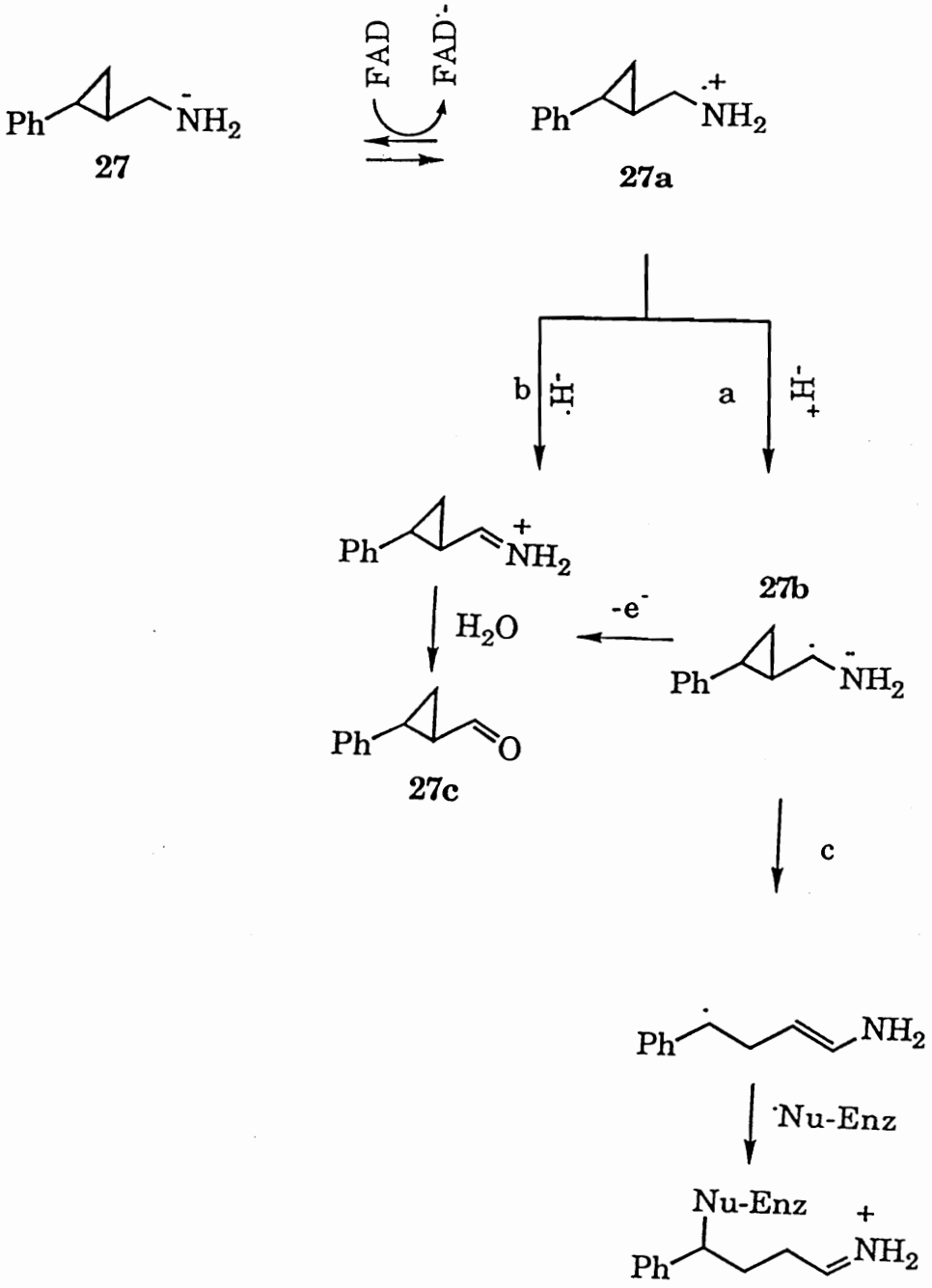

1.3.6. MAO Inhibitors.

Before discussing the chemistry of MAO inhibition it is important to understand some of the general concepts associated with enzyme inhibition. Therfore a brief review of this important aspect of enzymology is provided.

1.4. Enzyme Inhibition.

Enzyme inhibition is a phenomenon of great practical importance as well as a useful probe for characterizing the molecular features of the active site of the enzyme and other factors that influence enzyme activity. The active site of an enzyme represents a small part of the whole enzyme molecule. Characterization of active centers for enzymes for which no X-ray structure is available is dependent on structure activity relationship (SAR) studies including those utilizing specific enzyme inhibitors which may act reversibly or irreversibly. Before proceeding to a discussion of enzyme inhibition it is important to understand how enzymes function as catalysts in the metabolism of substrate molecules in biochemical reactions and therefore a brief description of enzyme catalysis is included.

Enzyme Catalysts.

Enzymes are proteins that catalyze biochemical reactions. Enzymes in general tend to be highly selective for the type of reaction they catalyze. The "catalytic site" on the enzyme contains functionalities that are directly involved in the catalysis. The catalytic site is usually a small, localized region on the enzyme surface. The substrate binding site and the catalytic site are usually in close proximity to each other and frequently overlapping. Together they are referred to as the "active site".

Kinetics of Enzyme Catalyzed Reactions.

As a rule kinetic analysis is done on purified or partially purified enzymes in vitro. Kinetic analysis is a major tool used to investigate the mechanism of enzyme catalysis. One of the main features of kinetic analysis involves the variation in the rate of reaction with substrate concentration. For this purpose a fixed low concentration of the enzyme is used in a series of parallel experiments in which only the substrate concentration is varied. Under these conditions the initial reaction velocity increases until it reaches a maximum value at high substrate concentrations reflecting that all enzyme binding sites are occupied with substrate.

Intially it may be assumed that the reaction between enzyme (E) and substrate (S) proceeds through the formation of an enzyme-substrate complex (ES) and that the (ES) is in equilibrium with the free enzyme (E) and substrate (S). The formation of products proceeds only through the (ES) complex. The steady-state kinetic condition may be introduced to eliminate the requirement that the (ES) complex be in equilibrium with the free enzyme and substrate. The steady state evaluation assumes a fixed level of (ES) complex (Scheme 6). The steady state, which is achieved shortly after mixing enzyme and substrate, constitutes the time interval when the rate of reaction is constant with time. The concentration of the (ES) complex is also a constant during this time period. Usually the substrate is present in much higher molar concentrations than the enzyme. Since the initial period of the reaction only is being examined, the free substrate concentration is approximately

equal to the total substrate added to the reaction mixture.

Scheme 6. Substrate Metabolism to Product by Enzymes.

$$E + S \underset{k_{-1}}{\overset{k_1}{\rightleftharpoons}} E{\cdot}S \xrightarrow{k_2} E + P$$

For the purpose of graphical representation of experimental data in an enzyme catalyzed reaction it is convenient to use the Lineweaver-Burk equation derived using the steady state approximation[64] which states:

$$\frac{1}{V} = \frac{K_m}{V_{max}} \frac{1}{[S]} + \frac{1}{V_{max}}$$

The constant K_m is called the Michaelis constant. One of the important relationships is that between K_m and the substrate concentration (S). K_m can be defined as the concentration of the substrate when the maximum rate of enzyme catalyzed reaction is 50%, i.e. half V_{max}. From the Lineweaver-Burk equation, a plot of 1/V (the reciprocal of the initial rate) vs 1/S (the reciprocal of the substrate concentration) should give a straight line. The slope of that line is K_m/V_{max}, the intercept on the ordinate is $-1/V_{max}$, and the intercept on the abscissa is $-1/K_m$.

Another important aspect of enzyme catalysis is the turnover number of an enzyme (k_{cat}) which is defined as the maximum number of substrate molecules converted to product per active site per unit time. Since the rate limiting step in Scheme 5 is assumed to be the formation of product P from (ES), the initial velocity of the reaction is given by

$$V_i = k_2(ES)$$

The maximum velocity should be obtained when the total enzyme (E_t) is

in the form of the enzyme substrate complex (ES).

$$V_{max} = k_2(E_t) \quad \text{where } E_t = E + ES$$

Thus for the situation represented in Scheme 6, in which there is only one (ES) complex and the conversion of (ES) complex to product is rate-limiting, k_{cat} is equal to the kinetic constant k_2. Thus the turnover number is a direct measure of the catalytic efficiency of the active site of the enzyme.

Reversible Inhibitors.

Reversible inhibitors are compounds that have structures similar to substrates or products of target enzymes, and which bind at the substrate binding sites, thereby blocking substrate binding. They work by a variety of mechanisms that frequently can be distinguished by kinetic analysis. Reversible inhibitors are classified further into competitive and non-competitive reversible inhibitors. In competitive inhibition, the binding of an inhibitor and substrate is mutually exclusive. Usually, but not always, competitive inhibition occurs because the inhibitor structurally resembles the substrate and binds at the active center. In the presence of a competitive inhibitor, the rate of the catalyzed reaction is dependent on the relative concentrations of substrate and inhibitor. Higher concentrations of the substrate overcome the negative effects caused by the inhibitor because both substrate and inhibitor molecules are competing for binding to the same site (Scheme 7a).

Scheme 7a. Enzyme Inhibition by Reversible Inhibitors.

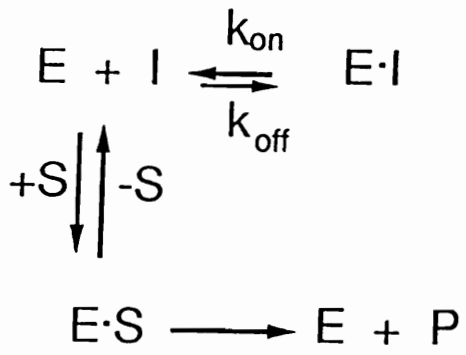

As in the case of the interaction of a substrate with an enzyme the inhibitor can also form a complex with the enzyme (see Scheme 7a). The equilibrium constant K_i (= k_{off}/k_{on}) is the dissociation constant for the breakdown of the E·I (enzyme·inhibitor) complex in Scheme 7a, i.e. K_i = [E] [I]/[E·I]. Therefore, the smaller the value of K_i for I, the better the inhibitor. The equilibrium depends upon the concentrations of the enzyme, the inhibitor, and the substrate. Since the enzyme concentration is low and fixed, the E·I concentration, will principally depend upon the concentrations of the substrate and the inhibitor. The inhibitor may also act as a substrate and may be converted to a metabolically useless product. Interactions of the inhibitor with the enzyme can occur at a site other than the substrate binding site and still result in inhibition of substrate turnover. When this occurs, usually as a result of an inhibitor induced conformational change in the enzyme to give a form of the enzyme that does not bind to the substrate properly, then the inhibitor is known as a non-competitive reversible inhibitor Unless something is known about

this inhibitor-induced change in the enzyme binding site, it is not possible to design non-competitive enzyme inhibitors.

Irreversible Inhibitors.

All competitive and some non-competitive inhibitors are reversible. If the inhibitor concentration is lowered, the enzymatic activity rises. If the inhibitor is removed, the enzyme activity returns to its normal value. In the case of irreversible inhibition, the inhibitor binds so strongly to the enzyme (usually via a covalent bond) that it will not dissociate when the inhibitor concentration is lowered. Irreversible inhibition can occur at the active site or elsewhere. The site of binding of the irreversible inhibitors is best determined by direct chemical methods. Irreversible inhibitors often provide valuable information about the active site of the enzyme. For example, certain amino acid residues that are part of the active site may undergo covalent adduct formation with specific inactivators.

Mechanism-based Enzyme Inactivation.

Mechanism based inactivators generally are relatively unreactive compounds with structural similarities to the substrate or product of a particular enzyme. The normal catalytic mechanism of action converts the inactivator molecule into a species which, without prior release from the active site, binds covalently to that enzyme.

Generally in enzyme catalyzed reactions, an equilibrium is established rapidly between the enzyme bound and free form of the inactivator. The on and off rates for this process are governed by the rate constants k_1 and k_{-1} respectively (Scheme 7b). When an enzyme catalyzes

the conversion of a mechanism-based inactivator into its reactive form there are two processes that can follow. The altered form can be released as product (k_3) or it can react with the enzyme to form a covalent linkage (k_2) as shown in Scheme 7b.

Scheme 7b. Irreversible Mechanism-Based Inactivation.

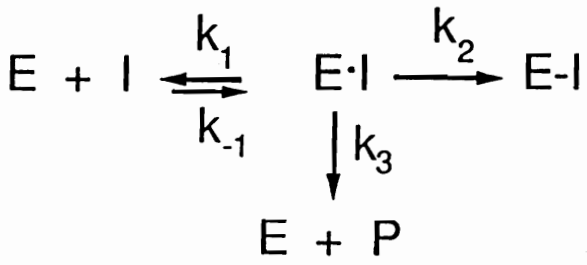

On the assumption that the equilibrium for reversible E·I complex formation is rapid and the rate of dissociation of the E·I complex (k_{-1}) is fast relative to covalent bond formation, then k_2 will be the rate determining step. This reaction scheme (see Scheme 7b) is similar to that for the conversion of substrate to product (see Scheme 6) but instead of a k_{cat}, a catalytic rate constant (turnover number) for product formation, there is a k_{inact}, a first order rate constant for enzyme inactivation. In this case unlike simple reversible inhibition, there will be a time-dependent loss of enzyme activity. The rate of inactivation is proportional to low concentrations of inhibitor but becomes independent at high concentrations.

An important concept related to mechanism-based inactivation is the partition ratio which describes the ratio of the number of latent inactivator molecules converted and released as product relative to each

turnover leading to enzyme inactivation. According to Scheme 6b this ratio would be k_3/k_2. The partition ratio is, therefore, the measure of the efficiency of the inactivator and depends upon the reactivity of the activated intermediate, the rate of diffusion from the active site, and the proximity of an appropriate nucleophile, radical or electrophile on the enzyme for covalent bond formation.

Criteria for Mechanism-based Inactivation.

A set of criteria has evolved for the evaluation of mechanism-based inactivation. In order to characterize unambiguously an inactivator falling into this class, most or all of the criteria should be satisfied. The criteria are as follows:

1) A time dependent loss of enzyme activity is observed.

2) The rate of inactivation is proportional to low concentrations of inhibitor but independent at high concentrations (saturating conditions).

3) The rate of inactivation is slower in the presence of substrate than its absence.

4) Enzyme activity does not return upon dialysis or gel filtration.

5) A 1:1 stoichiometry of radio-labeled inactivator to active site usually results after inactivation followed by dialysis or gel filtration.

Uses and Advantages of the Mechanism-based Enzyme Inactivation Approach.

Mechanism-based enzyme inactivators have proven to be most useful in the study of enzyme mechanisms and in the design of highly specific, low-toxicity drugs.

In enzyme mechanism studies.

The value of these inactivators in the study of enzyme mechanisms is derived from the fact that they are processed by the enzyme by the same catalytic pathway followed in the turnover of a substrate. Acting like a true substrate, they are converted by the catalytic mechanism of the enzyme into products. However, the products of these enzyme mediated reactions are generally reactive species that then become attached covalently to the enzyme. The important event is that the conversion to the activated form is at least initiated by the same catalytic steps involved in the reaction with normal substrates, only the products happen to be more reactive than those generated from normal substrates. Therefore, whatever mechanistic information that can be grasped from inactivation studies is directly linked to the catalytic mechanism of the enzyme.

Studies with mechanism-based inactivators can be a two-way street. Either the inactivators can be designed on the basis of a known mechanism of action of the target enzyme or the mechanism of action of the target enzyme can be elucidated by understanding the inactivation mechanism. Often a combination of the two approaches is taken and a hypothesis regarding the enzyme mechanism is formulated in the design of the inactivator. Then results of the inactivation studies can be used to support or modify the hypothesis.

In drug design.

Many enzyme-inhibitor drugs are specific, reversible, competitive inhibitors where the inhibition arises from the formation of an enzyme-inhibitor complex in preference to an enzyme-substrate complex. The

rational design of mechanism-based inactivators as drugs is a relatively recent approach in drug development. The rational selection of appropriate target enzymes for design of mechanism-based inactivator drugs depends on the desire to deplete the organism of a specific product or to accumulate a substrate of the target enzyme. For example, the therapeutic goal in the inactivation of the enzyme monoamine oxidase leads to potential antidepressant agents/antihypertensive agents/antiparkinsonian agents. The potential of mechanism-based inactivators in drug design is just surfacing. Should these initial efforts prove to be valuable, a much greater incentive to employ this approach in the design of drugs may emerge.

1.5. The discovery of MAO inhibitors.

Historical Aspects.

As observed with many of the chemotherapeutic agents that were the topics of interest in the first half of the 20th century, the discovery of the therapeutic activity of monoamine oxidase inhibitors (MAOIs) was due to the recognition of an important clinical side effect. In this instance a profound mood elevating side effect was observed in tuberculosis patients who had been treated with iproniazid (**28a**), a drug bearing a hydrazine functionality which had been developed to combat tuberculosis. After five years of clinical observations in tuberculosis patients, iproniazid was introduced into clinical medicine as the first antidepressant drug.[65] Biochemical studies indicated that iproniazid was a specific and a potent inhibitor of MAO.[66] Consistent with this view, treatment of rats with tyramine, an MAO substrate, protected the enzyme

against the action of this compound.[67] The discovery that iproniazid is an inhibitor of MAO activity paved the way to the synthesis and pharmacological assessment of inhibitors of the enzyme and also fostered the development of present-day views on the physiological role of MAO.

The early MAOIs were used clinically in the late 1950's to early 1960's for the treatment of depression. MAOIs in the clinic were found to be more effective against "non-endogenous" (neurotic) rather than "endogenous" depression.[68] Many of the MAOIs, particularly those belonging to the hydrazine class, proved to be hepatotoxic. Furthermore the well documented "cheese effect", a phenomenon which gives rise to a hypertensive crisis caused by the tyramine found in certain foodstuffs which remains unmetabolized after MAO inhibition,[69a-b] led to the disuse of MAOIs in the seventies. These side effects have decreased the clinical utilization of MAOIs sharply and only a few drugs, including phenelzine (**28b**), tranylcypromine (**28c**), pargyline (**28d**) and isocarboxazid (**28e**), remain approved for clinical use in certain European countries.

Despite their decline in popularity, there remains a continuing clinical interest in the MAOIs, particularly in the UK and Canada, due to the experience which documented that these substances were well tolerated by patients suffering from neurotic depression for which the traditional tricyclic antidepressants seemed to be less beneficial.

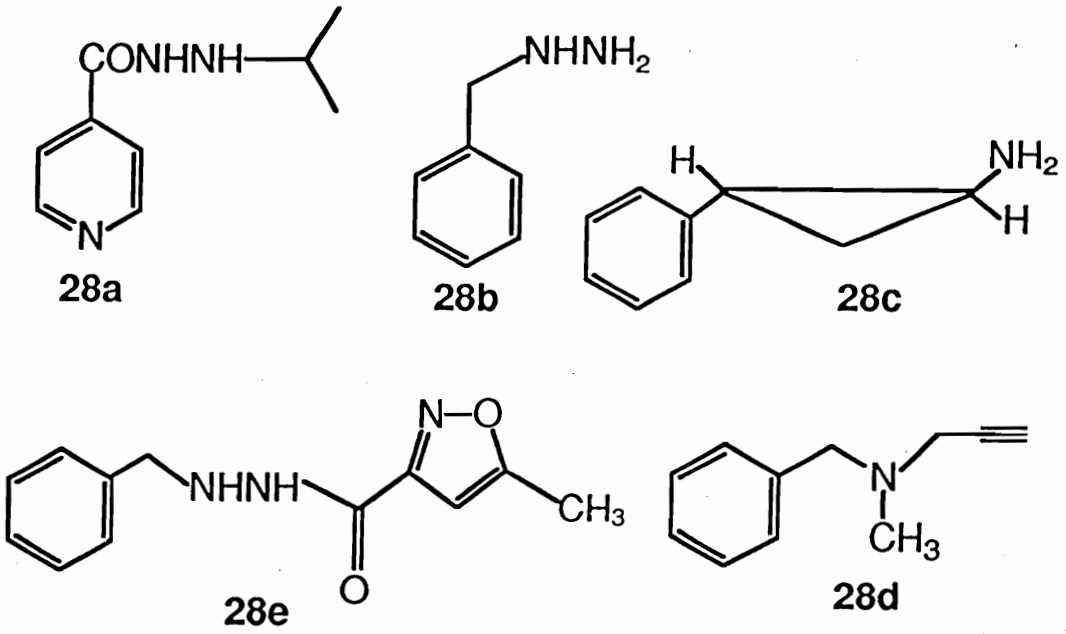

1.6. Irreversible MAO Inhibitors.

The existence of MAO in two different forms opened the opportunity to develop selective inhibitors such as (S)-deprenyl (**15**) and clorgyline (**14**), two of the earliest and best known of these types of drugs. Deprenyl [2-(N-methyl-N-propargylamino)-1-phenylpropane] was developed in 1964 by Knoll and coworkers[70] and was recognized for its unusual spectrum of MAO inhibitory action. Detailed studies[33] revealed that (S)-deprenyl is a selective inhibitor of MAO-B. Clorgyline [1-(N-methyl-N-propargylamino)-3-(2,4-dichlorophenoxypropane)], a compound similar in structure to deprenyl, was developed by Johnston in 1968.[34] A variety of studies established this amine to be a selective inhibitor of MAO-A. In fact the introduction of the terms MAO types A

and B was based on the selective inhibition of MAO-A by clorgyline.

Analysis of the reactivity of MAO-A and MAO-B with irreversible inhibitors provides an opportunity to characterize the structural differences between the two forms. It is well established now that the two enzymes are discrete proteins with very similar molecular weights and subunit composition. Since both MAO-A and -B contain the same covalently bound flavin attached to the same amino acid at the active site, it seems very probable that differences in catalytic activity are due to differences in the structures of the substrate binding sites. This would explain why the two forms differ in substrate and inhibitor specificities. Structure activity studies argue[71a-b] that compounds in which the aromatic nucleus is separated by one or two carbon atoms from the oxidizable nitrogen atom act as preferential substrates for MAO-B. Typical examples include the classical MAO-B substrates benzylamine and phenethylamine. Thus keeping the 1 or 2 carbon distance between the aromatic nucleus and the oxidizable nitrogen atom and making appropriate substitutions on the nitrogen atom generates selective MAO-B inhibitors. Typical examples include S-deprenyl (**15**), pargyline (**28d**), U1424 (**29**), AGN1133 (**30**), AGN1135 (**31**) and tranylcypromine (**28c**) (Table 1).

Table 1. Selective Inactivators of MAO-B.

MAO-B Substrates		TN[a]
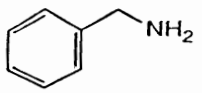 Benzylamine (58)		415
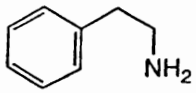 Phenethylamine (16)		132
MAO-B Inactivators		
	pI_{50}	
	MAO-A	MAO-B
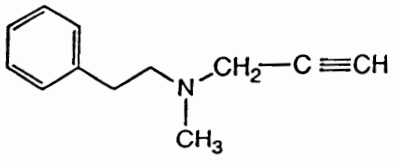 Pargyline (28d)	5.8	7.7[71a]
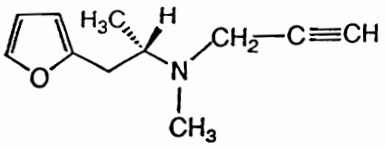 U-1424 (29)	5.7	7.7[71b]
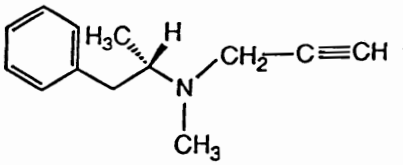 Deprenyl (15)	6.1	7.3[71a]
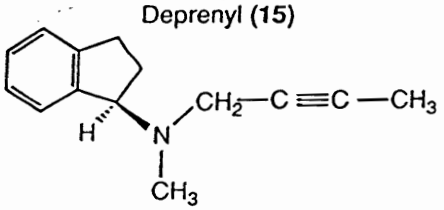 AGN1133 (30)	7.1	7.8[71a]
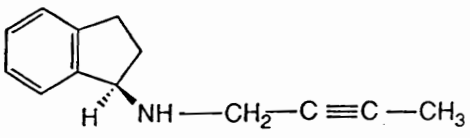 AGN 1135 (31)	4.8	5.8[71c]

[a] micromoles of substrate oxidized per min per micromoles of enzyme.

Table 2. Selective Inactivators of MAO-A.

MAO-A Substrates

	TN
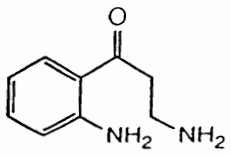 Kynuramine	154
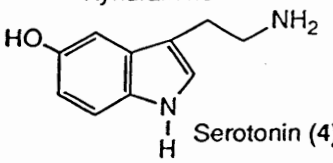 Serotonin (4)	125

MAO-A Inactivators

	pI_{50}	
Acetylenic Compounds	MAO-A	MAO-B[71a]
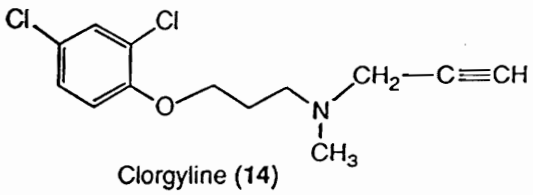 Clorgyline (**14**)	9.7	5.0
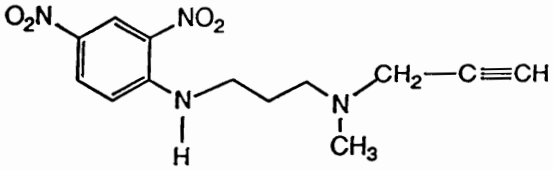 Abbott-21,855 (**32**)	5.3	> 3.0[71b]
Cyclopropylamines		
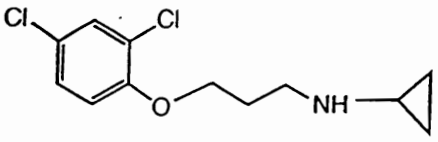 Lilly 51641 (**33**)	8.7	5.4[71c]
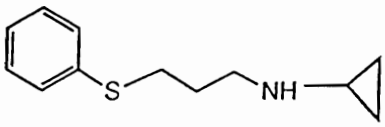 Lilly 49393 (**34**)	8.0	6.0[71c]

pI50 is the negative log of the molar concentration of the drug producing 50% inhibition. Substrate in the experiments was tyramine. MAO source was rat brain.

When the distance between the aromatic nucleus and the nitrogen atom is equivalent to three or more carbon atoms, then the substrate binds selectively to MAO-A. Appropriate substitutions on the nitrogen atom also generates MAO-A inhibitors. Typical examples illustrating this concept include clorgyline (**14**), Abbott-21,855 (**32**), Lilly 51641 (**33**) and Lilly 49393 (**34**) (Table 2).

The information mentioned above serves to suggest that the active sites of the two forms differ by the distance between the binding sites for the nitrogen atom and the aromatic ring. Although a number of MAO inhibitors follow this pattern, this cannot be the only difference in the activity of the two enzymes. Some substrates, such as noradrenaline which has two carbons separating the aromatic ring from the nitrogen, are selective MAO-A substrates.[71c]

The latent alkylating moieties, such as the propargyl or the cyclopropyl functionalities which are attached to the nitrogen atom and which impart the inhibitor properties to the substrate molecule, do not appear to influence the selectivity for inhibition. However other substitutions, particularly on the aromatic ring of the inhibitor molecule, such as a halo or nitro group or an oxygen or sulphur bridge between the aromatic ring and the carbon atoms, contribute to the selectivity of these MAO-A inhibitors. Taken together these observations suggest that MAO-B is less tolerant of steric bulk than MAO-A. Furthermore, the shift in the inhibition selectivity spectrum from MAO-B to MAO-A may involve non-bonding hydrophobic interactions at the substrate binding site of MAO-A. Therefore it is likely that hydrophobic pockets will be

found near the aromatic binding site of MAO-A but not MAO-B which accommodate these aromatic substitutions in MAO-A but which are absent in MAO-B.

1.8. Mechanism of Action of Irreversible MAO Inhibitors.

The irreversible MAO inhibitors can be divided into three structural classes, namely the acetylenes, the cyclopropylamines and the hydrazines. The propargyl, cyclopropyl, and the hydrazine bearing compounds have been shown to inhibit MAO by acting as mechanism-based inhibitors.

(a) Hydrazine Based MAO Inhibitors.

The recognition of the MAO inhibitory properties of iproniazid led to a flurry of studies[72a-b] on the structure-activity relationships of hydrazines in general. These studies attempted to discover the molecular configuration responsible for the observed activity and to gain information concerning the nature of the reactive site of MAO. The results established that neither hydrazine nor acylhydrazides were potent inhibitors of MAO. But introduction of an alkyl or aryl functionality on hydrazine and acylhydrazides led to efficient inhibition. Monosubstitution with alkyl groups on the terminal nitrogen atom of iproniazid was found to produce highly active inactivators of MAO. An increase in the chain length of the alkyl group was accompanied by an increase in the degree of enzyme inhibition which was found to reach a maximum when the alkyl substituent was a butyl functionality. Patek and Hellerman[73] demonstrated that phenylhydrazine (35) was a good inactivator of MAO with the rates of inactivation of 35 being 1.6-2.2 fold

faster than the corresponding rates for alkylhydrazines. Since the inactivation of MAO-B by **35** was found to be irreversible, it was thought that these aromatic hydrazines may be "fitting" the enzyme catalytic center well. Hellerman and Erwin[74] were the first to inquire into the sequence of events leading to inactivation. They proposed that the initial step in the action of phenylhydrazine was dehydrogenation to give the corresponding phenyldiazine (**36**) which might then combine irreversibly with the flavin. They did not attempt to determine the site of attack on the flavin ring or the structure of the inactive adduct.

Kenney[75] in 1979 was able to obtain a labeled flavin containing peptide-adduct from beef liver MAO following inactivation by [^{14}C]-phenylhydrazine. The spectral properties of the adduct (UV characteristics included a shoulder between 326 and 332 nm) were consistent with the flavin moiety bearing a phenyl group at position 4α (**39**). This strongly suggested that the reaction pathway involved initial dehydrogenation of **35** to form the reactive intermediate **36** as predicted by Hellerman. A second step would involve loss of a hydrogen atom from **36** to give **37** which then undergoes homolysis to yield dinitrogen and a phenyl radical (**38**). Radical combination between **38** and FADH· generated by substrate reduction of FAD results in the formation of the adduct **39** (Scheme 8).

Scheme 8. Proposed Mechanism of MAO Inactivation by Phenylhydrazine.

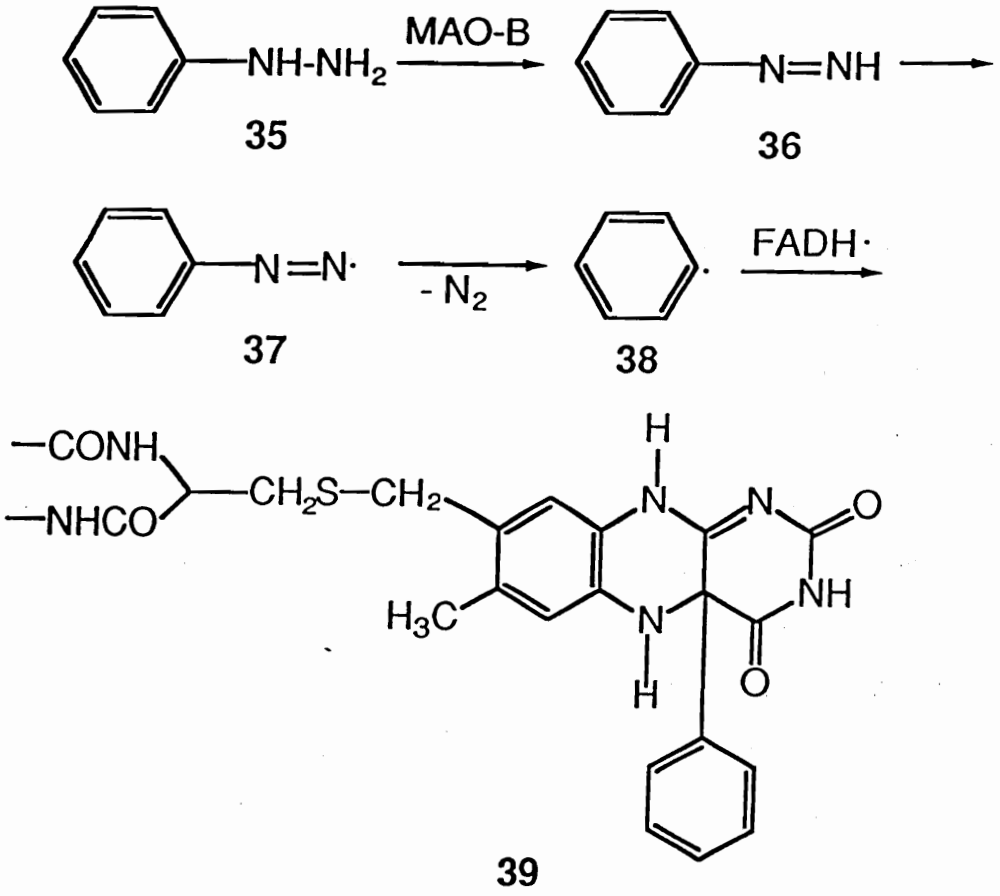

(b) Propargylic amine based MAO inhibitors.

The group that has been studied the most is the acetylenic type of inhibitor. Structure activity relationships have shown that irreversible inhibition is found only when the acetylenic group is β to the amino group in the inhibitor molecule.[76] Therefore these compounds are all propargylamines. This acetylenic group is essential for the irreversible

inhibition found by this series of inhibitors. For example, replacement of the acetylenic group in the MAO-B selective inhibitor N-methyl-N-propargyl-1-aminoindane hydrochloride (**31**) by an olefinic group results in a reversible, non-selective inhibitor.

Rando *et al.*[77] established that the inactivation of MAO by propargylamines consists of two phases: (1) an instantaneous, reversible step which is competitive with the substrate, and (2) a time-dependant, irreversible inactivation step. It was also emphasized in these studies that the irreversible step involves prior oxidation of the amine by the flavin so that the iminium species (see below) is the actual inhibitor. Hellerman and Erwin[78] showed that, on complete inactivation of the bovine kidney enzyme by [^{14}C]-pargyline, one mole of inhibitor becomes bound to one mole of the enzyme. These workers assumed that the irreversible step is due to covalent modification of an amino acid residue. The structure of the resulting adduct was not determined, however.

Abeles, Singer and coworkers studied the inactivation of bovine liver MAO-B with 3-N,N-dimethylaminopropyne (**41**) (Scheme 9a) and assigned the flavocyanine species **43** as the most probable structure of the irreversibly formed adduct between compound **41** and the enzyme **42**.[79] Their conclusion is based on the finding that the electronic spectrum of the inactivated enzyme is very similar to that observed from a photoadduct (**43**, R = H) of **41** with 3-methyllumiflavin (**42**). This product possesses an intense absorption band at 391 nm (ε 25,500, pH 7.0).[80]

Scheme 9a. Inactivation of MAO by Propargylic Amines.

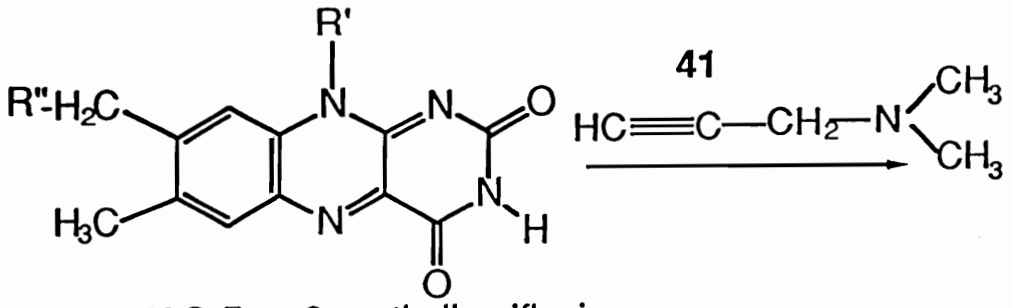

42: MAO-B or 3-methyllumiflavin

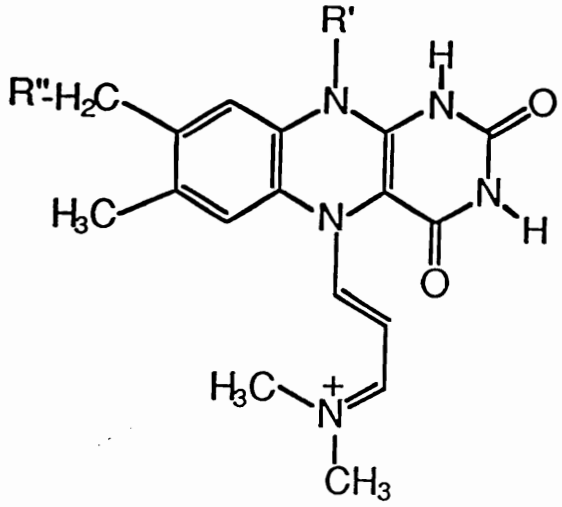

43: R' = CH_3; R" = H

The proposed mechanism (Scheme 9b)[81] views the adduct **43** as the consequence of the union of the reduced flavin (**46**) and the oxidized substrate (**47**). Initial one-electron oxidation leads to the radical cation **44** which loses a proton to form a carbon-centered radical **45**. Loss of a second electron leads to the eyniminium species **47** which combines with

Scheme 9b. Proposed Mechanism of Inactivation of MAO by Propargylic Amines.

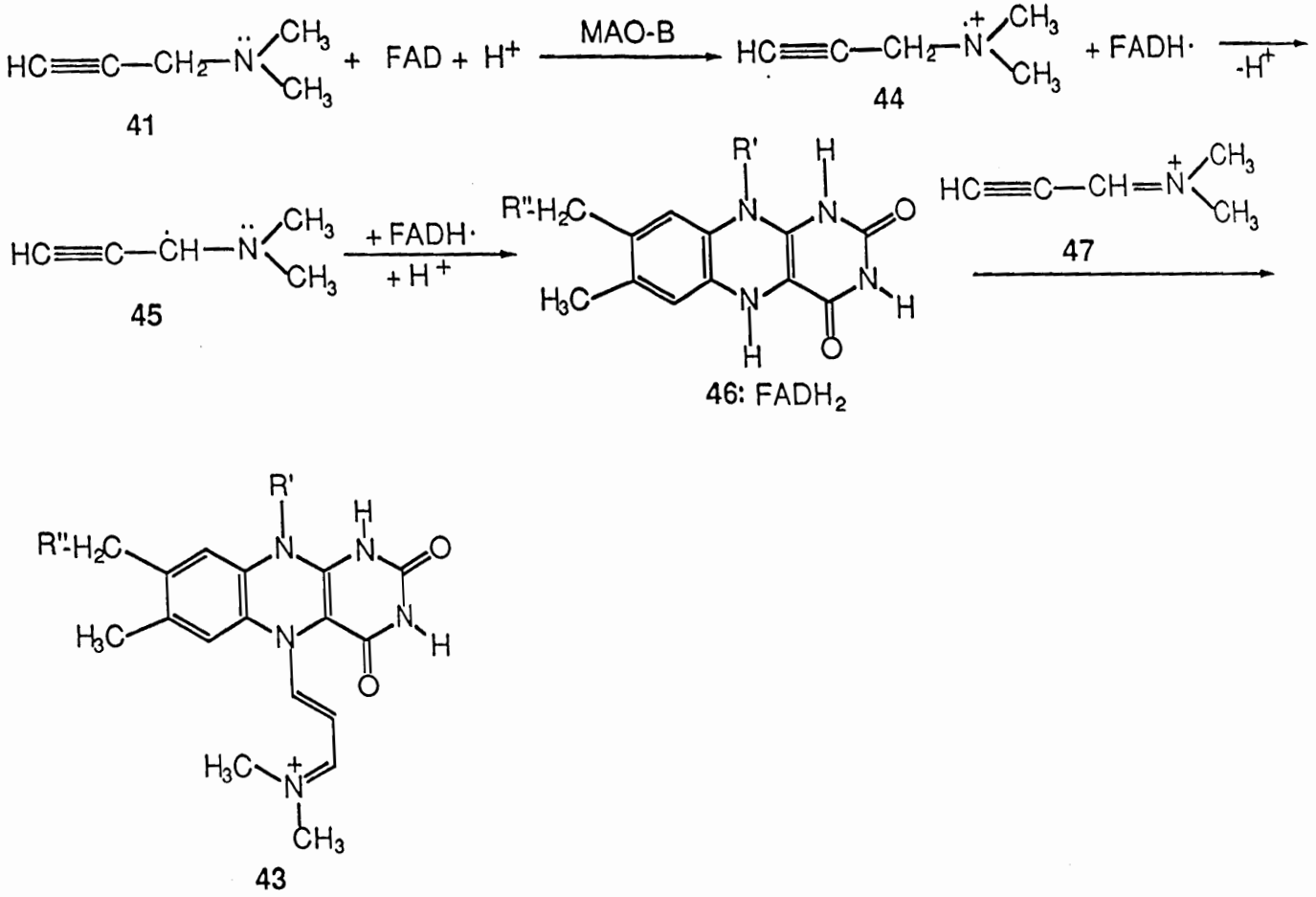

the flavin nitrogen atom to form a covalent bond. Consistent with the proposed mechanistic pathways, other acetylenic amines such as N-but-2-ynyl-N-benzylmethylamine (48)[82] and N-2,3-butadienyl-N-benzylmethylamine (49)[82] were shown to lead to adducts with similar spectral properties, both enzymatically and upon photochemical activation with 3-methyllumiflavin (42).

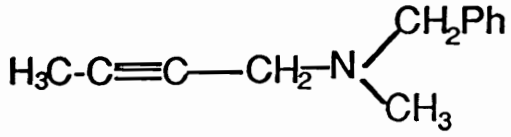

48

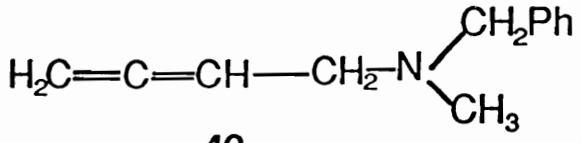

49

(c). Cyclopropyl Based MAO Inhibitors.

During the sixties several new classes of MAO inhibitors were introduced. One of these, tranylcypromine (26), was the first cyclopropylamine used therapeutically. Studies to document the mechanism of the irreversible inhibition by cyclopropylamines were not reported until 1979 when Silverman and Hoffman[83] proposed a suicide inactivation mechanism. Interestingly, it was demonstrated by Hanzlik and co-workers[84] that cyclopropylamines such as 50 also were suicide inactivators of cytochrome P-450. Both groups proposed a mechanism for inhibition that involved oxidation of the amine moiety to a reactive cyclopropylidene species (51) that could react with a nucleophile at the active site to generate 52, thus inactivating the enzyme (Scheme 10a).

In 1984 Silverman and coworkers showed that N-benzyl-1-methylcyclopropylamine (**53**) (see Table 3) also was a time-dependent inactivator of MAO (K_I = 180 μM, k_{inact} = 0.06 min^{-1}).[85]

Scheme 10 a: Earlier Proposed Mechanism for MAO Inactivation by Cyclopropyl Amines.

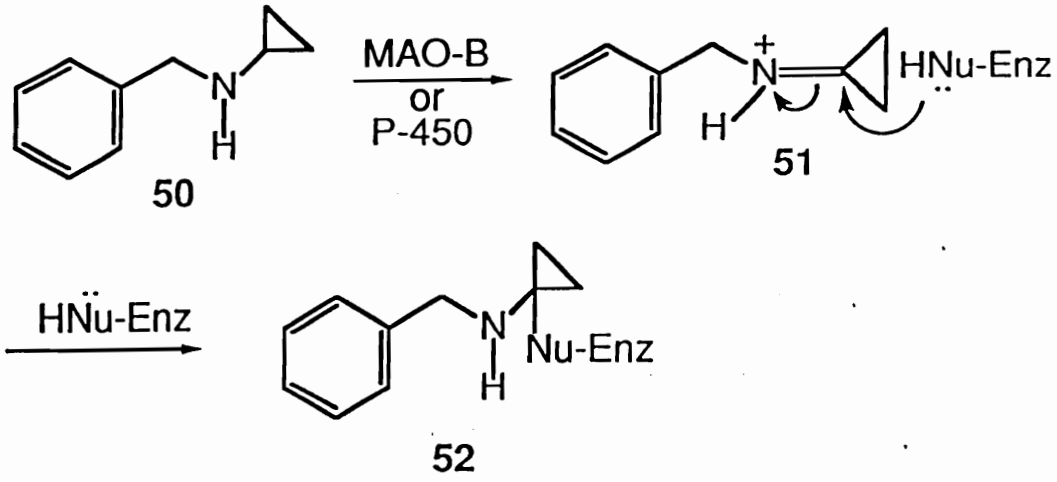

This finding eliminated the mechanism shown in Scheme 10a since the methyl group prevents the formation of a cyclopropylidene species. In 1982 two research groups led by Hanzlik and Macdonald proposed that the mechanism of inhibition of cytochrome P-450 by cyclopropylamines occurred by the mechanism shown in Scheme 10b.[86] A similar mechanism for the inhibition of MAO by cyclopropylamines was later proposed by Silverman[87] based on studies related to the inactivation of MAO by N-benzyl-1-cyclopropylamine (**50**), a potent irreversible inactivator of MAO-B with a k_{inact} of 0.3 min^{-1}. The proposed mechanism of inactivation of MAO and P-450 by cyclopropylamines involves transfer of one electron from **50** to the oxidized flavin to give a cyclopropylamine radical cation (**54**). Then the cyclopropyl ring opens

and the resulting highly reactive primary carbon centered radical **55** is captured by the flavin to give the covalent adduct **56**. The possible hydrolysis products of **56** are benzylamine **57** and the α,β-unsaturated ketone (**58**) derived from the hydrolysis of the covalent adduct **56** (Scheme10b).

Scheme 10b. Revised Mechanism for MAO Inactivation by Cyclopropyl Amines.

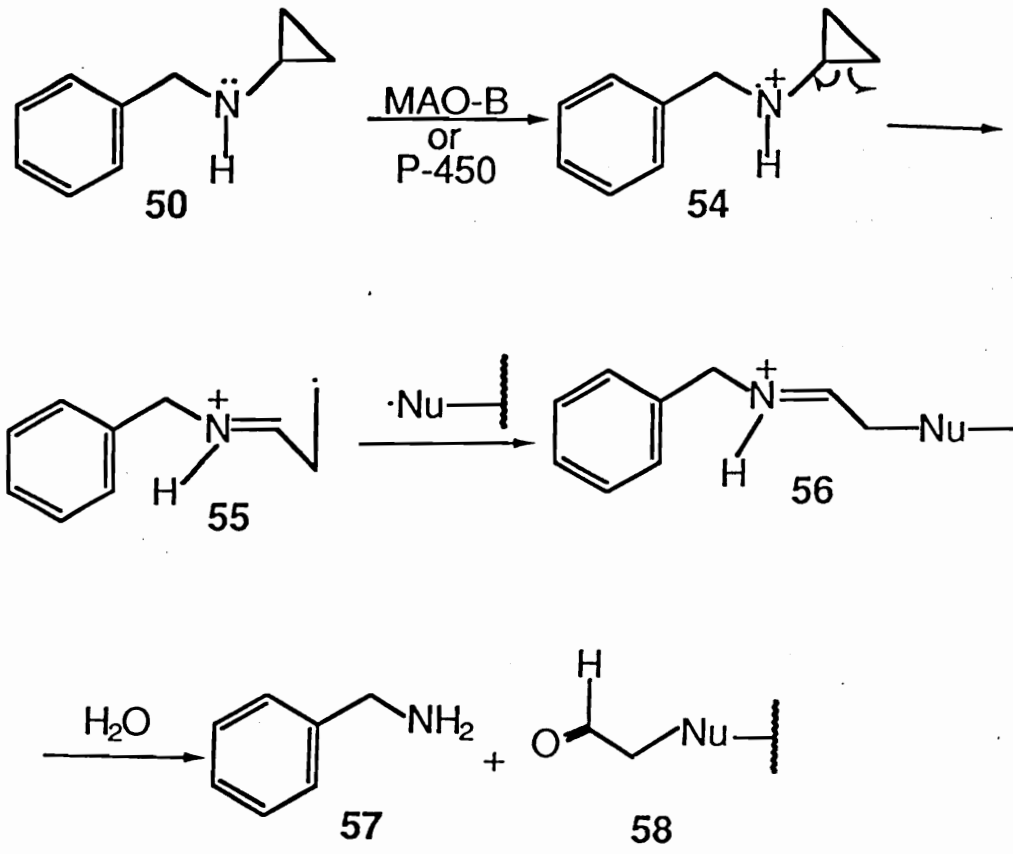

These reports were followed by inactivation studies with cyclopropylamine analogs which generally supported the proposed mechanism. Although the covalent adducts of the type **56** were difficult

to isolate, their structures could be inferred from their spectral and chemical properties. Further, many of the adducts could be released upon treatment of the modified enzyme with base and the structures of the released products were consistent with a radical mechanism for the inactivation of MAO. In an attempt to explore the validity of this pathway, Williams and coworkers[91a] have carried out ESR studies on the radical cation mechanism of the ring opening of cyclopropylamines. The results of these studies provide a firm basis for the ring opening of cyclopropylamine radical cations and furthermore provides a chemical rationale for the proposed inactivation pathway in which a active site nucleophile on the enzyme is bound to the reactive carbon centered radical such as **55**. Table 3 lists several cyclopropylamine derivatives and their appropriate kinetic constants.

Table 3. Cyclopropyl Amines as Irreversible Inactivators of MAO.

compound	K_I (μM)	k_{inact} (min^{-1})	reference
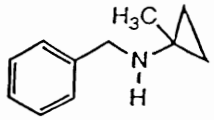 **53**	180	0.06	85
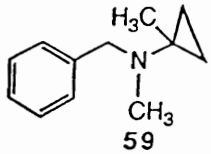 **59**	1750	0.096	88
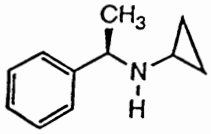 **60**	44	0.25	89
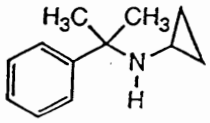 **61**	323	4	89
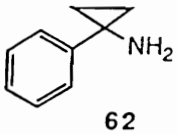 **62**	200	2	90

The 1-phenylcyclobutylamine system **63** also was studied by Silverman.[91b] This compound was shown to be both a substrate and a time dependent irreversible inhibitor of MAO-B. The kinetic parameters indicated a lower K_m value of 110 μM compared to the K_m value of 270 μM displayed by benzylamine the preferred substrate for MAO-B but a poor turnover number of 0.41 min^{-1} versus 270 min^{-1} for benzylamine. A mechanism (Scheme 11) similar to that proposed for cyclopropylamines was proposed for the inhibition process.

Scheme 11. Proposed Mechanism of Inactivation of MAO by 63.

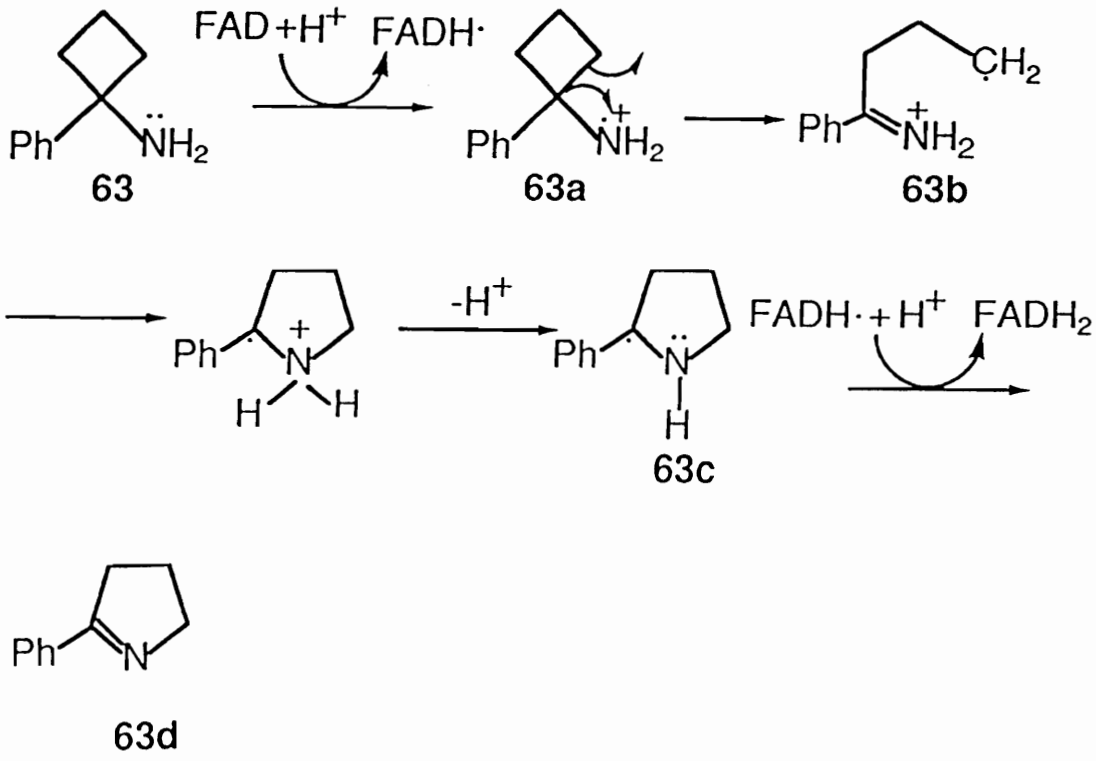

The cyclobutylamine cation radical **63a** was known to undergo homolytic ring cleavage in a manner similar to that of the cyclopropylamine radical, albeit at a much slower rate. Cyclopropylamine

radical cations have been shown to undergo very rapid ring opening with unmeasurable rate constants whereas the first order rate constant for cyclobutylamine radical ring opening has been estimated to be 1.2×10^5 sec^{-1}.[92] These differences in rates of ring opening are associated with the ring strain associated with the small ring systems (cyclobutyl group = 26 Kcal/mole versus cyclopropyl group = 27.5 Kcal/mole).[92] The proposed mechanism was supported by the detection of the pyrroline species **63d** which presumably results from initial ring closure of **63b** (due to the presence of an intramolecular radical trap) to generate the carbon centered radical **63c** followed by loss of an electron. Although so far no flavin radical has been detected during the action of MAO, the radical mechanism (discussed earlier) is strongly supported by the above studies. In the case of the phenylcyclobutylamine system, the product isolated from the reaction is that expected for radical cyclization of the proposed carbon centered radical intermediate.

Mechanistic studies by Silverman[90] also were carried out with 1-phenylcyclopropylamine (PCPA, **62**), a known mechanism-based inhibitor of MAO-B, to identify the active site residue which is covalently modified. It was shown that eight molecules of 1-[phenyl-^{14}C]PCPA were needed to inactivate irreversibly one molecule of the enzyme with the incorporation of one equivalent of radioactivity. An N-5-(3-oxo-3-phenylpropyl)flavin adduct (**65**, Enz-Nu = N_5-Flavin similar to the phenylhydrazine adduct with MAO-B, discussed earlier) was identified as the product of irreversible inactivation. Seven of the eight molecules of the radio-labelled material were shown to form covalent bonds to active

site amino acid residues. However these adducts decomposed with a half-life of 65 minutes to regenerate the active enzyme. This process explains the requirement of 8 labelled molecules per irreversible inactivation event as the rate of irreversible inactivation was found to be seven times slower than the rate of this reversible adduct breakdown. It was thus proposed that this irreversible adduct had the same structure as the reversible ones except that the site of covalent modification was different.

Scheme 12. Identification of the Amino Acid Residue Modified by 62.

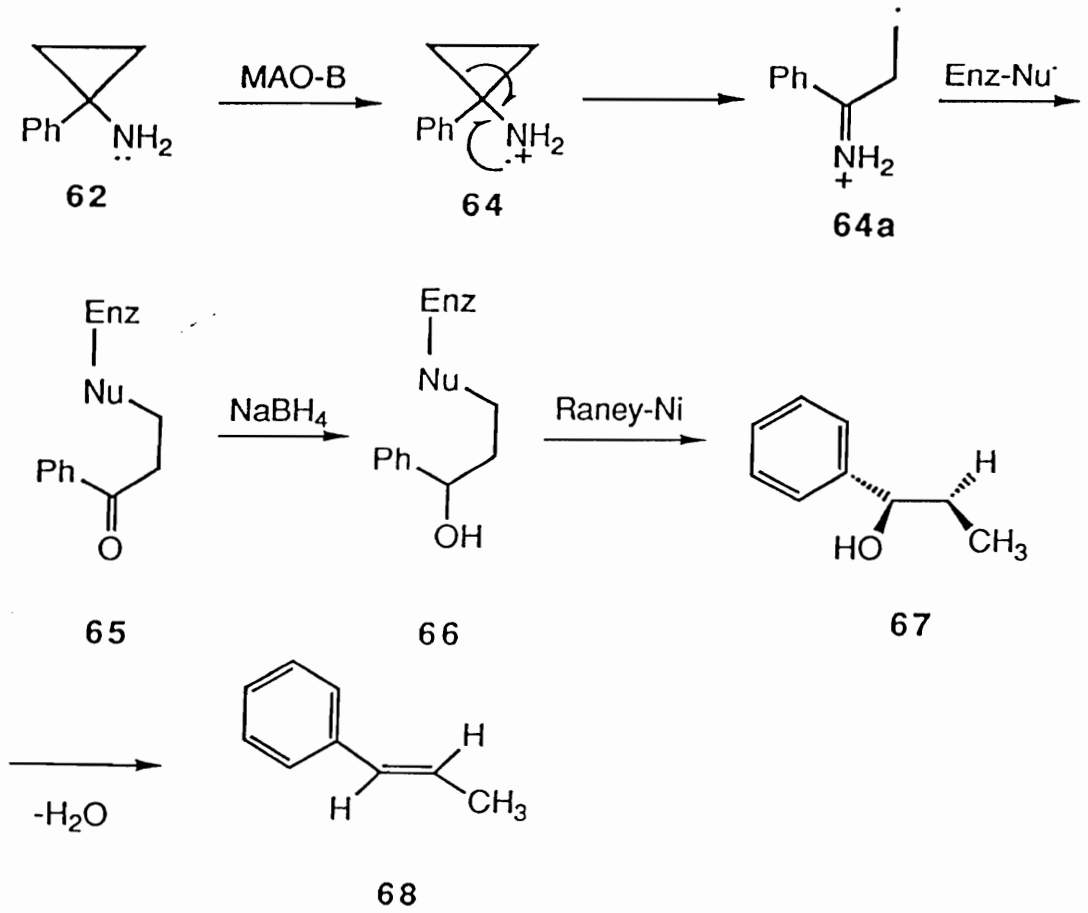

The irreversible adduct was a result of covalent modification at N-5 of the flavin whereas the reversible adducts were the result of covalent modification of amino acid residues. The amino acid was identified as a cysteine residue based on chemical treatment of the inactivated enzyme. Treatment of the inactivated enzyme-inhibitor adduct (**65**, Nu = amino acid, Scheme 12) with $NaBH_4$ led to a stabilized adduct (**66**) and prevented its decomposition (reduction of the keto group to an alcohol). Treatment of **66** with Raney nickel (a specific reagent for the cleavage of carbon-sulphur bonds) led to the formation of a single compound identified as *trans*-β-methylstyrene (**68**) which results from the dehydration of 1-phenylpropanol (**67**), the actual product of raney nickel catalyzed cleavage of **66**. A second experiment consisted of a determination of the effect of the reversible inactivation on the total number of cysteine residues in MAO. Thus in the presence of the cyclopropylamine only 5.2 cysteine residues could be detected whereas in a control experiment with no inhibitor, 6.2 cysteine residues could be detected. These results were found to be consistent with cysteine being the amino acid residue to which PCPA reversibly binds.

1.9. Other Variations to MAO Inhibitors.

a. Trimethylsilyl and Trimethylgermanyl Based Inhibitors of MAO.

Nagahisa and coworkers in 1984, utilizing known organosilicon chemistry, synthesized 20-(2-trimethylsilyl)ethyl-5-pregnen-3-β,20-α-diol

(69) (Scheme 14) and found that the resulting steroid analog was an NADPH dependent and time dependent suicide inhibitor of cytochrome P-450.[93] The proposed rationale behind this inhibition was based on the fact that cytochrome P-450 catalyses the oxidation of cholesterol (70) to pregnaneolone (73),[94a] the first step in the biosynthesis of steroid hormones (Scheme 13).[94b] Three discrete steps have been proposed[94c] to occur within the active site. The first two involve hydroxylations at the C-22 and C-20 positions of **70** to produce 22(R)-hydroxycholesterol (**71**) initially and then (20R,22R)-20,22-dihydroxycholesterol (**72**). This is followed by an oxidative cleavage of the bond between C-20 and C-22 in the last step to afford **73** (Scheme 13). Thus by incorporating a Me_3Si group, these workers had hoped that the cytochrome-P-450 catalyzed oxidation of **69** by P-450 would generate the hydroxylated species **74**. Subsequent generation of the stabilized cation **75** β to the trimethylsilyl group would lead to attack on Si by an active site nucleophile with concomittant cleavage of the C-Si bond and formation of covalent adduct **76** (Scheme 14).

Furthering this rationale, Danzin and co-workers[95] investigated the inactivation by silyl derivatives of amine oxidases such as monoamine oxidase. They designed and synthesized the benzyldimethysilylmethanamine **77** and the two *p*-halogenated analogs **77a** and **77b** and have shown them to be potent and selective irreversible inhibitors of rat brain MAO-B with. The compounds showed time-dependent inhibition with K_I values of 80, 11, and 90 μM for

Scheme 13. Oxidation of Cholesterol by P-450.

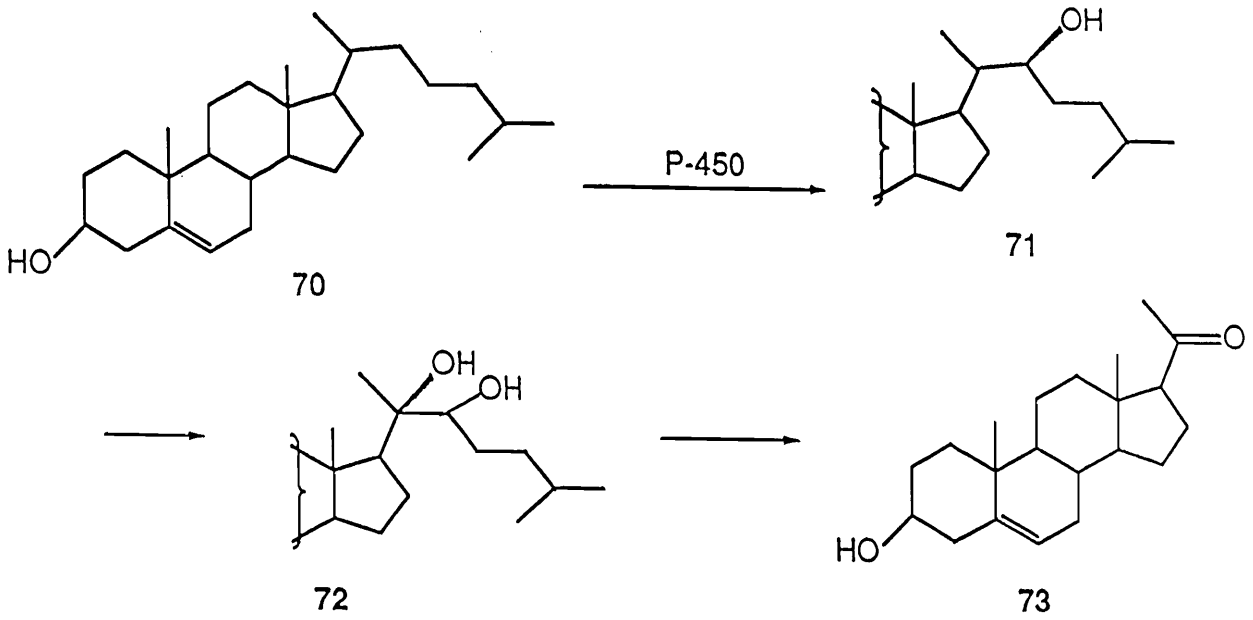

Scheme 14. Proposed Mechanism of Inactivation of P-450 by 69.

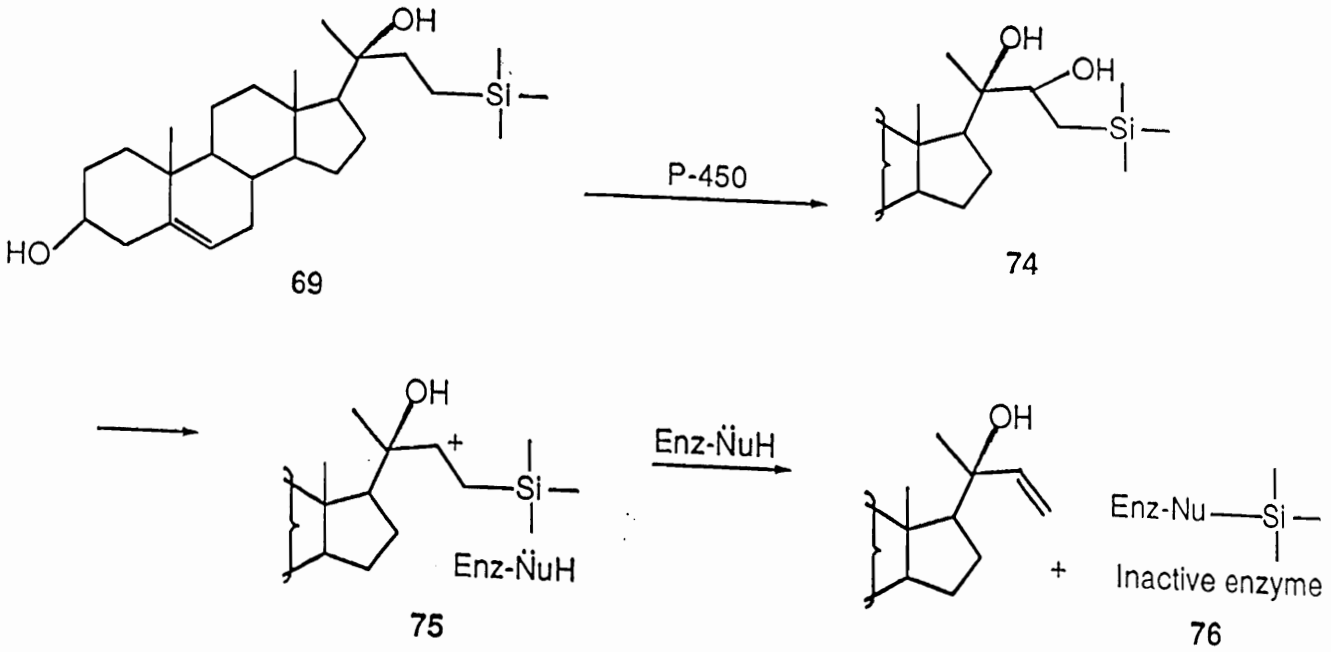

compounds 77, 77a, and 77b respectively and the $t_{1/2}$ values (time required for 50% inactivation of the enzyme at a given concentration of the inhibitor) were determined to be 2.1, 2.3, and 2 minutes for compounds 77, 77a, and 77b respectively.

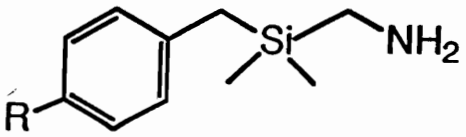

77: R = H
77a: R = F
77b: R = Cl

Silverman extended this idea to generate mechanism-based inactivators of MAO-B using primary amines containing trimethylsilyl and trimethylgermanyl functionalities.[96,97] Three organosilicon derivatives (78-80) were synthesized and investigated as potential MAO-B inactivators.[96] The molecules were found to be irreversible inactivators of MAO-B with k_{inact} values ranging 0.1-0.7 min^{-1} and K_I values ranging from 2-50 mM. Similarly 3 organogermanium derivatives (81-83) were shown to be mechanism-based MAO-B inactivators[97] with k_{inact} values in the range 0.5-4.33 min^{-1} and K_I values ranging from 1-90 mM.

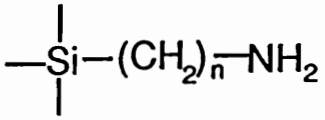

78: n = 1
79: n = 2
80: n = 3

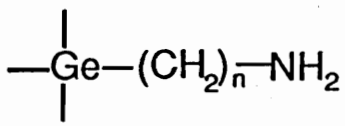

81: n = 1
82: n = 2
83: n = 3

The proposed mechanisms of inactivation for the trimethylsilyl analogs **78, 79,** and **80** are shown in Schemes 15, 16, and 17. One electron transfer from **78** would produce an amine radical cation **78a** which could lead to **78b** following a proton transfer. The iminium ion **78c** obtained from a loss of a second electron from the carbon-centered radical **78b** could potentially inactivate MAO-B to afford the enzyme adduct **78d** (Scheme 15). In the case of **79,** (Scheme 16) the amine radical cation **79a,** following a proton transfer to form **79b** and a further loss of an electron from **79b,** could generate the trimethylsilyliminium species **79c.** An electron deficient iminium species in the β position to the silicon atom activates the trimethylsilyl group to attack by an active site nucleophile which could lead to the trimethylsilylated enzyme **79d.** Similarly for the analog **80,** (Scheme 17) the iminium species **80c,** obtained from **80b,** could potentially inactivate the enzyme via formation of the covalent adduct **80d** and cyclopropylamine. Analogous mechanisms were proposed for the inhibition of MAO-B by the trimethylgermanyl analogs.

Scheme 15. MAO-B Inactivation by Trimethylsilylamine 78.

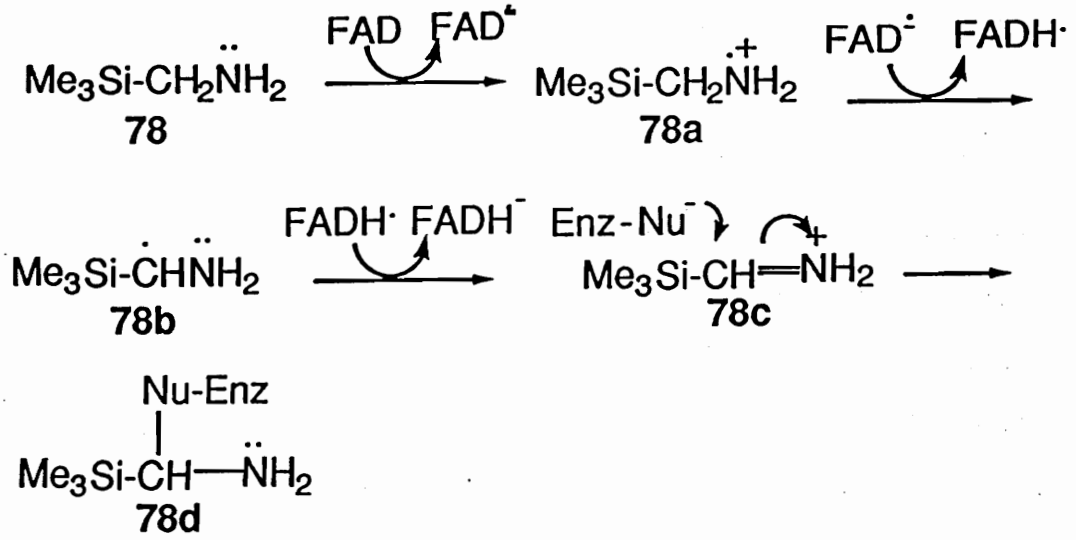

Scheme 16. MAO-B Inactivation by Trimethylsilylamine 79.

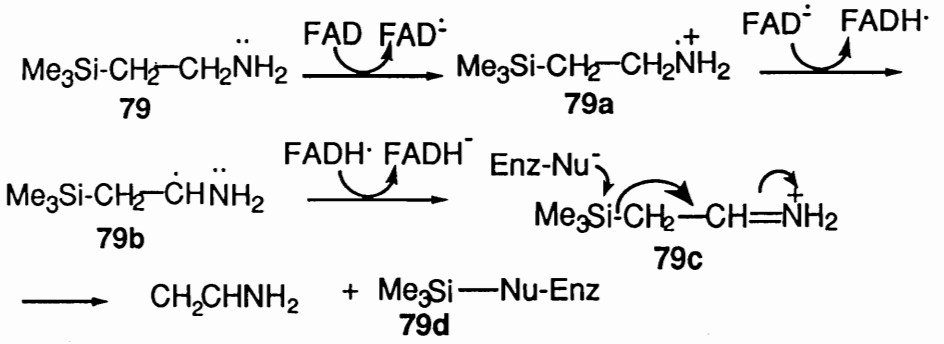

Scheme 17. MAO-B Inactivation by Trimethylsilylamine 80.

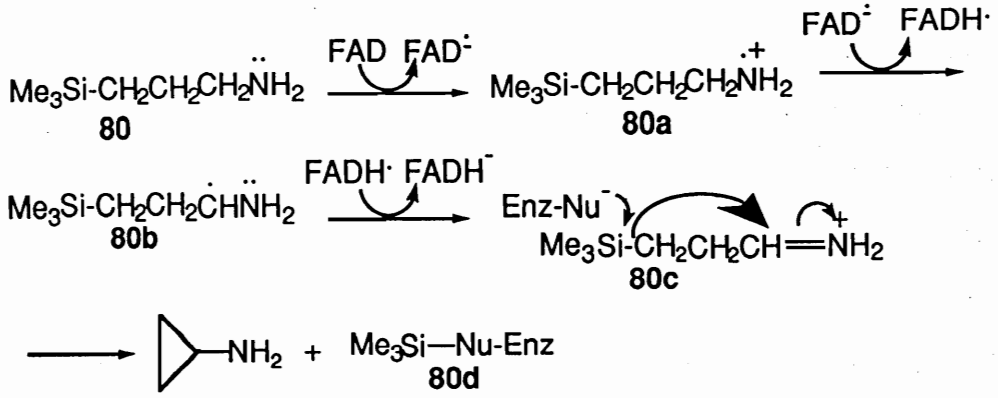

b. 5-(Aminomethyl)-3-aryl-2-oxazolidinones.

One class of inhibitors of MAO that has not received much attention until fairly recently is the oxazolidinones. Structure activity relationship studies[98] of a variety of oxazolidinones uncovered several potent inhibitors of MAO, some of which were MAO-A selective and

some of which were MAO-B selective. The most potent of the MAO-B selective inhibitors was 3-[4-[(3-chlorophenyl)methoxyphenyl]-5-[(methylamino)methyl]-2-oxazolidinone (MD 780236; 84).[99]

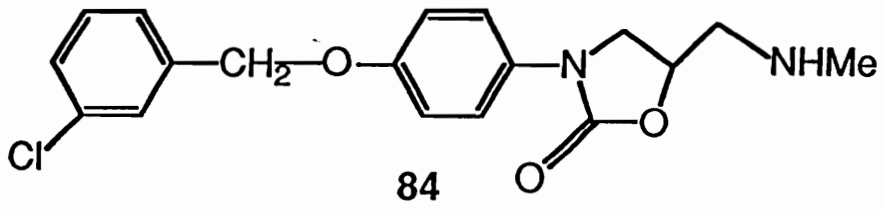

84

It was later shown that 84 also was an irreversible inhibitor of MAO-B. Based on the correlation between irreversible inhibition and mechanism-based inhibition, Silverman and coworkers extended their series on mechanistic aspects of inactivation of MAO-B to studies on 5-(aminomethyl)-3-aryl-2-oxazolidinones such as 85. Both the (R)- and the (S)-isomers of Compound 85 were time-dependent inhibitors of MAO-B.[100a] The kinetic parameters for this inactivation, K_I and k_{inact}, were determined to be 102 μM and 0.011 min^{-1} for the S-isomer, and 399 μM and 0.01 min^{-1} for the R-isomer, respectively. With the aid of chemical model studies, Silverman proposed[100b] two potential mechanisms to account for the inactivation of MAO-B by 85. One-electron oxidation of 85 generates the amine radical cation 86 which loses the α proton to afford the carbon-centered radical 87. The α radical 87 could then inactivate the enzyme via two pathways. Pathway A (Scheme 18) features further oxidation to the iminium system 88 followed by the formation of a covalent adduct 89 by an active site nucleophile. Pathway B (Scheme 19) features a mechanism in which the oxazolidinone ring of the α radical 87 undergoes a radical fragmentation reaction to generate CO_2 and the

resonance stabilized radical cation **90a** and **90b**. Covalent binding would then occur between the carbon centered radical **90b** and a radical (·Nu-Enz, **91**) on the enzyme generated by electron transfer to FADH· to generate adduct **92**. Experimental evidence to support this pathway was the observed liberation of CO_2 during the inactivation of MAO-B (Scheme 19).

Scheme 18. Proposed Mechanism of Inactivation of MAO by 85.

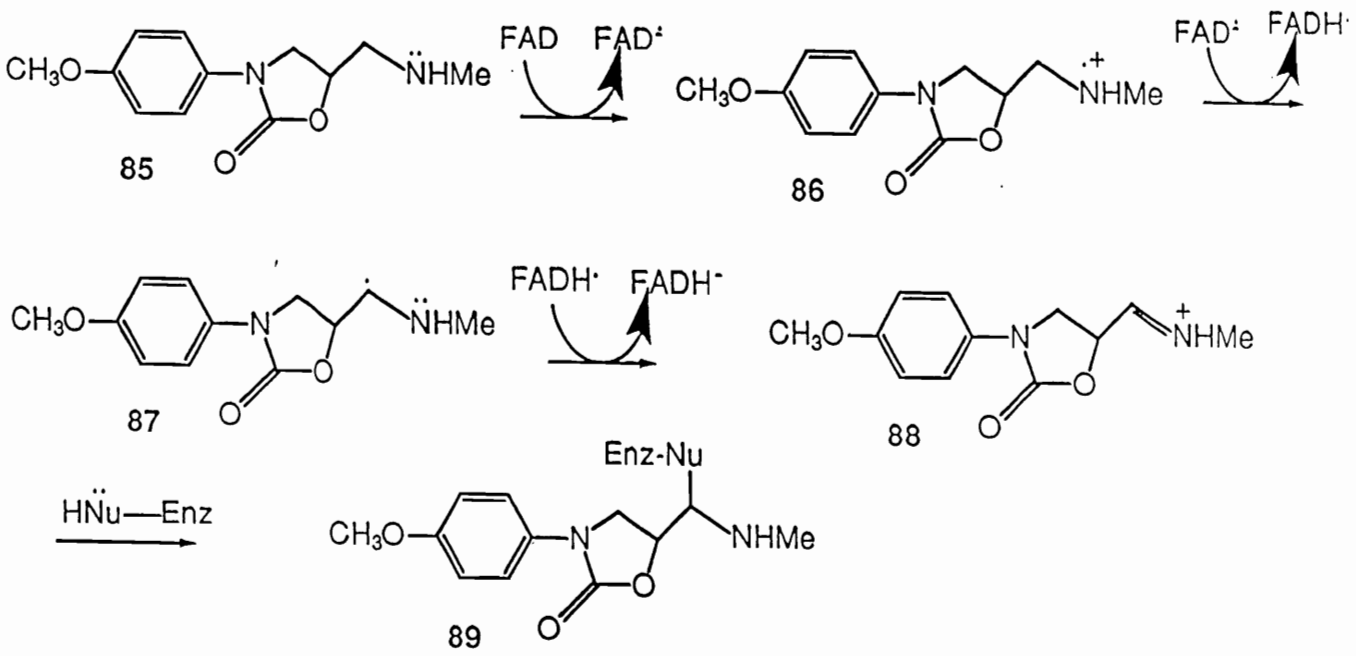

Scheme 19. Another Potential Mechanism of Inactivation of MAO by 85.

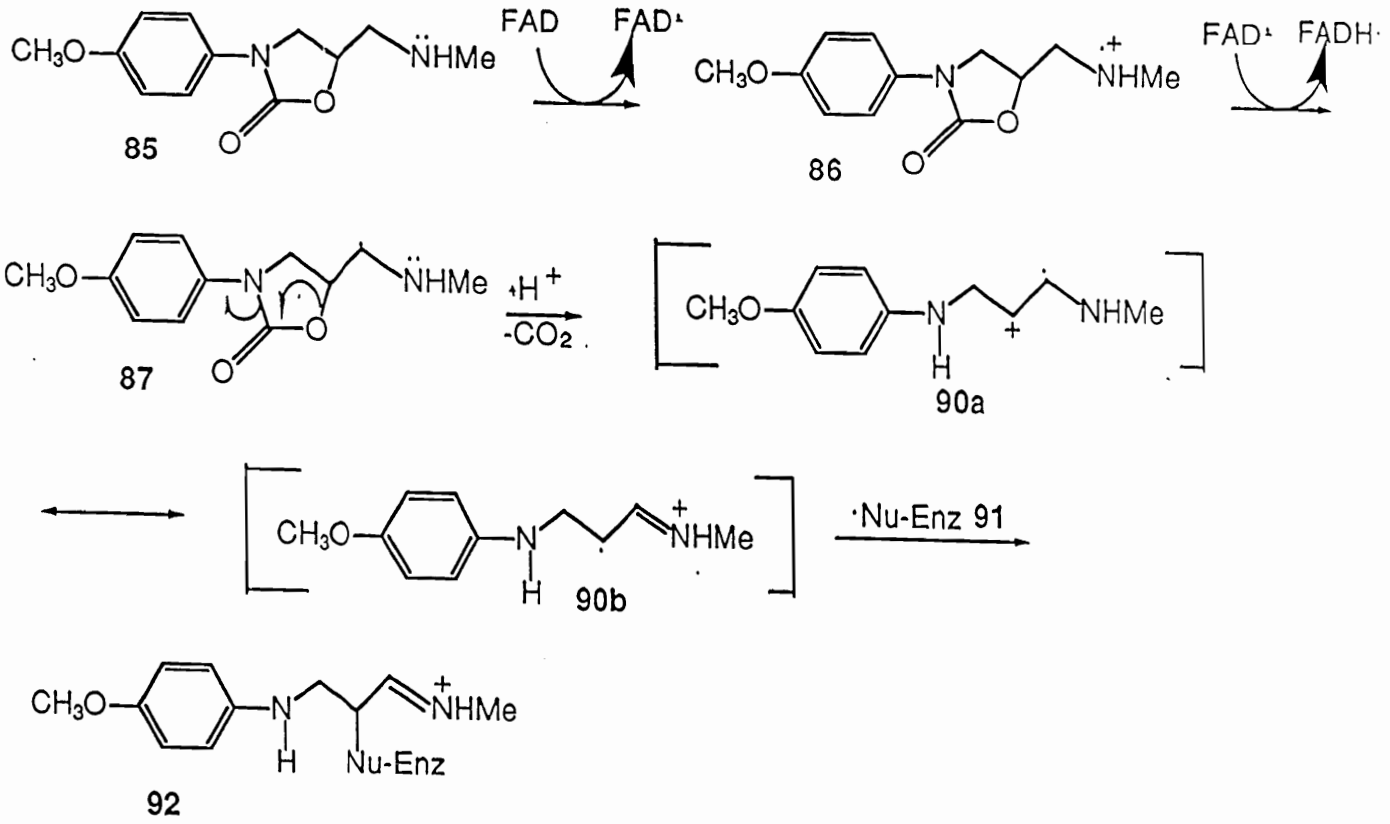

Silverman and coworkers extended this work to 5-(aminomethyl)-3-aryldihydrofuran-2(3H)-one analogs (structures 93 through 96), as a new class of MAO-B inhibitors.[101] These compounds were found to be irreversible inhibitors of MAO-B with k_{inact} values in the range 0.02-0.04 min^{-1} and K_I values in the range from 4-20 mM.

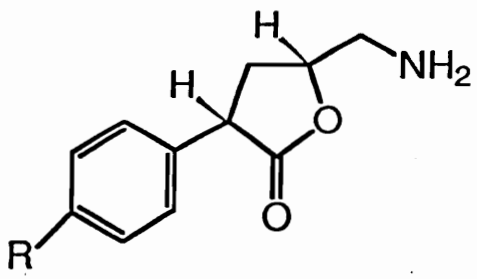

93: R = H
94: R = CH_3O

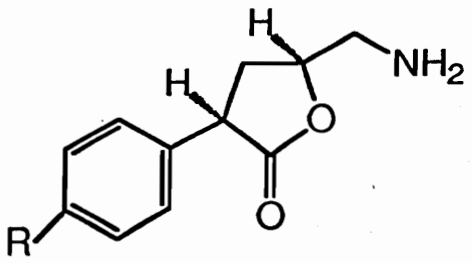

95: R = H
96: R = CH_3O

c. Unusual inhibitors of MAO.

Duffel and co-workers[102] have studied two widely used antitumor agents, vinblastine (VBL) (97) and vincristine (VCR) (98), in terms of inhibition properties with MAO B derived from various sources.

Their interests were stimulated by the substrate/inhibitor properties of MPTP which will be discussed in detail in Chapter 2 of this thesis. Although they are structurally similar, VBL and VCR exhibit different antitumor potencies, clinical applications, metabolic fates, and dose-limiting toxicities. These molecules are extensively metabolized in mammals[103] but little is known regarding the role of metabolism in the mediation of the cytotoxic effects. Furthermore the relationship between anti-tumor and neurotoxic properties[104] is unclear. Previous studies[105a-b] have documented that oxidative biotransformations of the vinca alkaloids involve a one-electron oxidation which leads to the formation

of reactive radicals and iminium intermediates. In a continuing effort to characterize the role of enzymes such as MAO which catalyze one-electron oxidations, preliminary experiments were conducted with rat brain mitochondria. The studies revealed that these vinca alkaloids were more potent inhibitors than some MAO inhibitors like MPTP and its metabolites. Subsequent studies with MAO-B purified from beef liver indicated VCR and VBL to be relatively weak inhibitors of MAO B. The relative inhibitory effects were as follows: MPTP > VBL > VCR. A preliminary evaluation of VBL revealed it to be a competitive inhibitor (K_i = 77 μM) of MAO-B. The inhibition of MAO activity was reversible and not time-dependent. Thus these studies indicated that both VCR and VBL were similar to MPTP in their ability to inhibit MAO-B but, unlike MPTP, they were not substrates for MAO B.

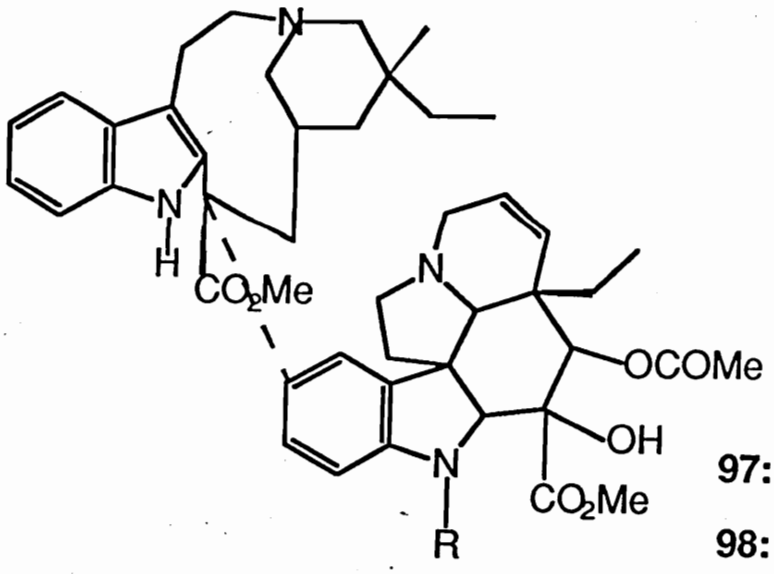

97: R = Me = Vinblastine

98: R = CHO = Vincristine

Recently, studies[106] have led to the identification of a selective, competitive and reversible group of MAO-A inhibitors that do not

contain nitrogen. Thus a group of variously substituted phenoxathiin 10,10-dioxides (**99-102**) were found to be potent inhibitors of MAO and were selective towards MAO-A. A working hypothesis to account for these properties is that the inhibitory activity is due to non-covalent binding to the flavin prosthetic group of the enzyme. Amongst all the derivatives tested, 1-ethylphenoxathiin 10,10-dioxide (**102**) was selected for clinical trial on the basis of in vitro potency (the K_I for competitive inhibition of rat and human MAO-A inhibition was 10 nM) and in vivo inhibition of rat brain MAO-A (ED_{50} = 8 mg/Kg). Furthermore the lack of inhibition of MAO-B, low toxicity in all of the species tested, and lack of significant blood pressure change found in rats ingesting tyramine after pretreatment with the compound (i.e. no cheese effect) make these compounds particularly attractive for clinical trials.

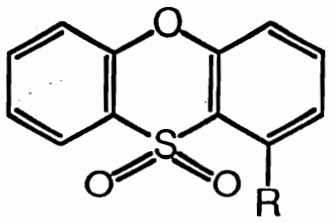

R

99: $CH(OH)CH_2OH$
100: $CH(OH)CH_3$
101: CH_2CH_2OH
102: CH_2CH_3

Recently structure-activity studies[107] by Silverman and co-workers on the anticonvulsant agent Milacemide [2-(n-pentylamino)acetamide (**103**)] and its analogs in relation to substrate and inactivation properties with MAO-B led to the identification of several new mechanism-based inactivators of MAO-B. Milacemide was previously known to be a substrate[108] and a reversible inhibitor[105] of brain MAO-B.

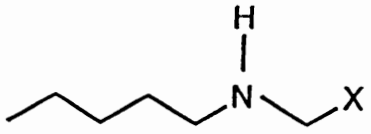

X

103: $CONH_2$ **106:** CO_2H
104: CN **107:** CH_2CN
105: CO_2Et **108:** CF_3

Silverman has found that **103** covalently modifies the enzyme. A series of Milacemide analogs containing different functional groups (**104-108**) subsequently were prepared. The carboxylic acid analog **106** was neither a substrate nor a inactivator of MAO-B. The trifluoro analog **108** could not be tested owing to solubility problems. All of the remaining compounds were substrates and time-dependent irreversible inactivators of MAO-B. Of all the active analogs tested Milacemide was the least efficient with a k_{inact} of 0.0097 min^{-1} and a K_I of 940 μM. The nitrile analog **104** was the most efficient of the series with a k_{inact} of 0.033 min^{-1} and a K_I of 13.99 mM. The ethyl ester analog **105** and the acetonitrile derivative **107** were shown to possess k_{inact} of 0.023 min^{-1} and 0.011 min^{-1} and K_I of 14.22 mM and 5.79 mM respectively. The proposed mechanistic pathway in the case of **103** is illustrated in Scheme 20 and follows the route proposed for other amines, i.e. oxidation of the amine **103** to the radical cation **103a** followed by generation of the reactive carbon-centered radical **103b** which forms the covalent adduct **103c** with the enzyme. The efficiency of inactivation could be related to the

electron-withdrawing ability of the substituent attached to the pentylamino backbone.

Scheme 20. Proposed Mechanism of Inactivation of MAO-B by Milacemide Analogs.

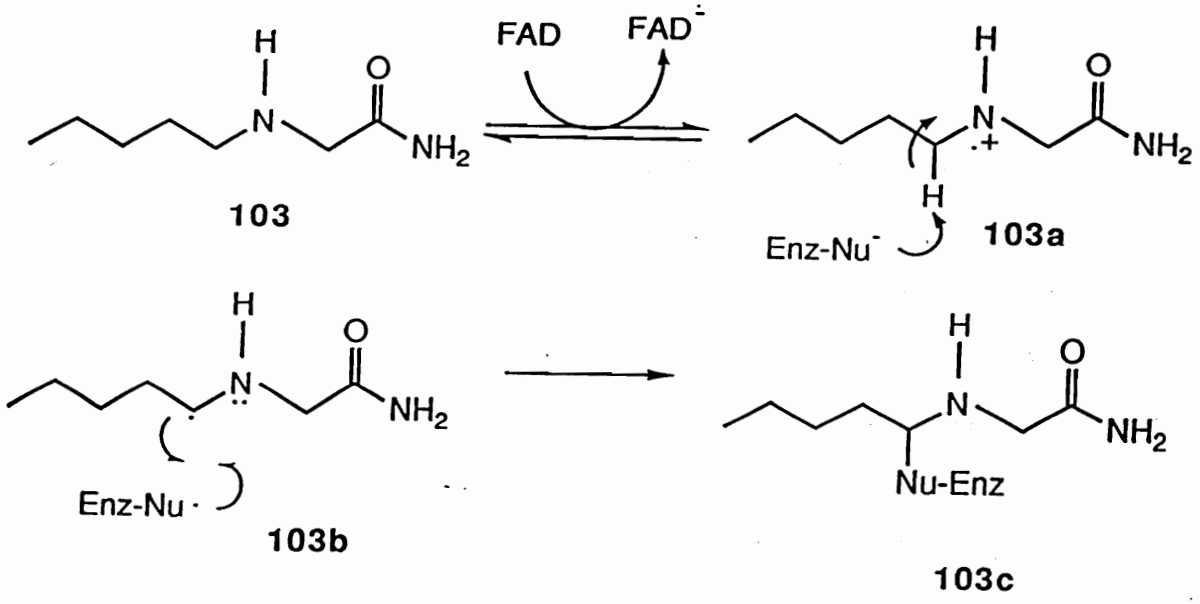

1.10. New Generation of Monoamine Oxidase Inhibitors as Drugs.

Because of the hypertensive effect (cheese effect) and hepatotoxicty associated with MAO inhibitors, there has been a great deal of flux in the introduction and withdrawal of these types of drugs in human therapy. Drugs no longer available include iproniazid, pheniprazine and nialamide. Tranylcypromine (**22**) was withdrawn from the market in 1964 but later became available for patients under close medical observation. At present, the MAO inhibitors which are available for the treatment of depression are phenelzine, tranylcypromine, and isocarboxazid. The realization that multiple forms of MAO exist opened

the possibility of tailoring inhibitors to block selectively monoamine metabolism in such a way as to achieve useful therapeutic goals without the undesirable side effects. For example, if a norepinephrine deficit turns out to be the fundamental lesion in depressive illness, it would be advantageous to inhibit its metabolism while at the same time avoid inhibiting the metabolism of tyramine. Dietary tyramine has been largely responsible for the cheese effect which had brought MAO inhibitor therapy into such disrepute in the sixties. The emergence of clorgyline had provided little encouragement. Although the drug was potent in its inhibitory action, it was also prone to the cheese effect observed with non-selective MAO inhibiting drugs. Renewed interest in the selective inhibition of MAO-B by (S)-deprenyl, also known as selegiline, has emerged recently. (S)-Deprenyl is a powerful, irreversible inhibitor of MAO-B. Pharmacologically (S)-deprenyl appears not to cause the cheese effect.[109] This compound was previously used in the treatment of Parkinson's disease in combination with levodopa (a dopamine precursor). More recently studies have documented (S)-deprenyl's effect at slowing the progression of parkinsonian disability.[110a-d] Such advances in the therapeutics of Parkinson's disease have gained momentum from studies which have revealed that (S)-deprenyl blocks the parkinsonian inducing properties of the neurotoxin MPTP, (see Chapter 2 for details on the role of MPTP, MAO, and Parkinson's disease) by inhibiting its MAO-B catalyzed oxidation to products which mediate the toxic effects. The results from MPTP studies have indicated the role of oxidative mechanisms in the pathogenesis of Parkinson's disease.

Such pathogenesis could conceivably result from a highly selective environmental or endogenous neurotoxin. Such a neurotoxin might also share in some of MPTP's pharmacological properties, such as its need for bioactivation by MAO-B. In retrospect, the discovery that the toxic effects of neurotoxins such as MPTP can be blocked by MAO-B inhibition has shed new light into the underlying mechanisms of neurodegenerative processes and the role that brain enzymes may play in the mediation of these processes.

2. Proposed Research.

2.1. Unusual inactivators of MAO: The MPTP model.

Motor deficits similar to those observed in Parkinson's disease were reported in young drug addicts following self-administration of a street drug that was designed to be 1-methyl-4-phenyl-4-propionoxypiperidine (MPPP, **110**) a meperidine analog. The drug proved to be contaminated with 1-methyl-4-phenyl-1,2,3,6-tetrahydropyridine (MPTP, **111**).[111-115] The formation of **111** from **110** occured from the result of an acidic work-up in the preparation of **110**. It was known that upon heating in acid **110** undergoes elimination of the propionoxy group at the C-4 position to give MPTP **111** (Scheme 21). Subsequent studies involving the administration of **111** to monkeys led to symptoms identical to those observed in humans exposed to **111**. Histopathological evidence confirmed that the parkinsonian syndrome was a consequence of the degeneration of the nigrostriatal dopaminergic neurons.[116,117] The same degeneration was observed in C-57 black mice.[118] Other rodents, however, have been shown to be resistent to the neurodegenerative effects of MPTP.[119,120]

Scheme 21. Conversion of 110 to MPTP in Acid.

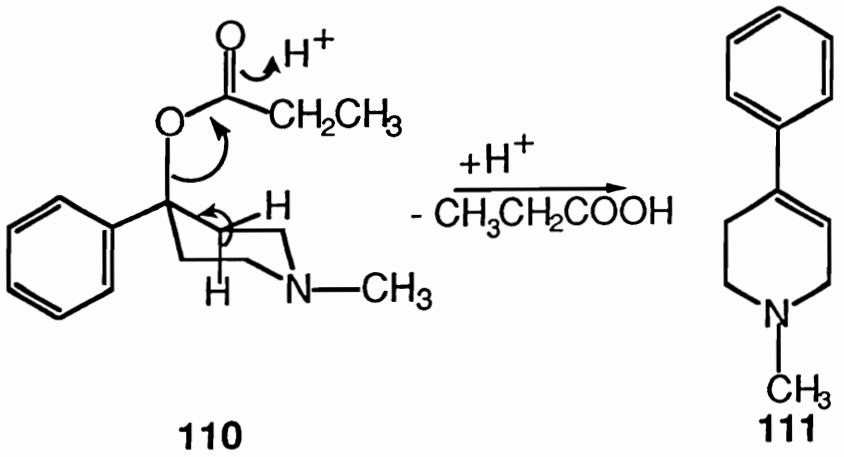

110 111

The molecular basis of MPTP's induced neurotoxic effects on the nigrostriatal system has been studied extensively. The cascade of the events leading to dopaminergic neuronal cell death can be summarized as follows: First, MPTP is oxidized extraneuronally via the dihydropyridinium intermediate (MPDP+, **112**) to the 1-methyl-4-phenylpyridinium species MPP+, (**113**) which is thought to be responsible for cell death (Scheme 22).[121,122,123,124] Second, **113** is actively transported to the dopaminergic neurons by the dopamine uptake system.[125,126] Third, **113** is concentrated in the matrix of the mitochondria[125] where it inhibits NADH dehydrogenase[127,128] and mitochondrial electron transport leading to cessation of oxidative phosphorylation, ATP depletion and neuronal death.[129]

Scheme 22. MAO-B Catalyzed Oxidation of MPTP.

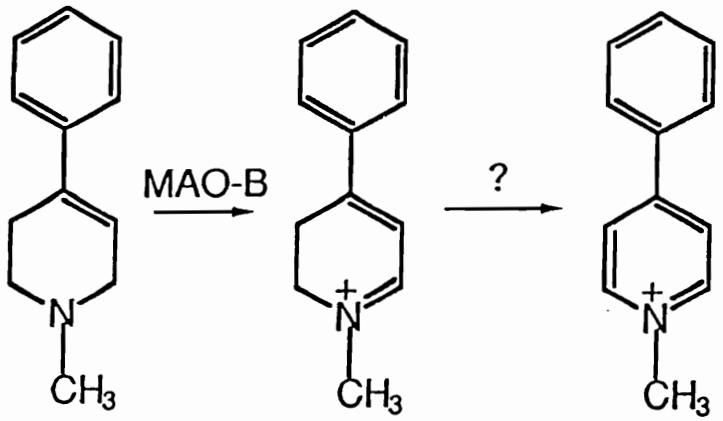

111 112 113

The toxication of MPTP is mediated by monoamine oxidase, principally type B, and to a lesser extent type A. The enzyme catalyses a two electron oxidation of MPTP to the intermediate 2,3-dihydro-1-methyl-4-phenylpyridinium $MPDP^+$ (**112**). $MPDP^+$ was found to be unstable under physiological conditions. It was shown by Chiba[130] and by Peterson and co-workers[131] that MPTP was converted by mitochondrial incubation mixtures prepared in D_2O to the β-monodeuterio analog **113**-d_1. The chemistry of synthetic $MPDP^+$ in D_2O was also analyzed and it was shown that $MPDP^+$ undergoes disproportionation under physiological conditions to form the same **113**-d_1 monodeuterio compound and MPTP which contains no deuterium (Scheme 23). It was proposed[131] that the disproportionation of $MPDP^+$ probably proceeds through a mechanism in which the conjugate base (the 1,2-dihydropyridine species, **114**) of **112** serves as the hydride donor

molecule and the dihydropyridinium species **112** serves as the hydride acceptor molecule. According to this mechanism, the reduction of **112** must involve initial transfer of one of the C-2 protons of **114**, thus resulting in deuterium-free **111** (see Scheme 23). This disproportionation chemistry associated with $MPDP^+$ was shown to be concentration dependent and occured at a measurable rate only at higher concentrations (> 500 μM). At lower concentrations (< 500 μM) **112** undergoes a further two-electron oxidation to **113**. Trevor *et al.*[132] proposed an MAO mediated mechanism for the oxidation of **112** to **113**. The pathway involves conversion of **112** to its conjugate base **114** under physiological conditions. Initial one electron transfer from **114** to the oxidized flavin moiety of the enzyme would result in the amine radical cation **115** which would give rise to the resonance-stabilized carbon-centered radical **116** following a proton loss. Loss of a second electron would yield MPP^+ (Scheme 24).

Scheme 23. Proposed Mechanism for the Disproportionation Reaction of MPDP+.

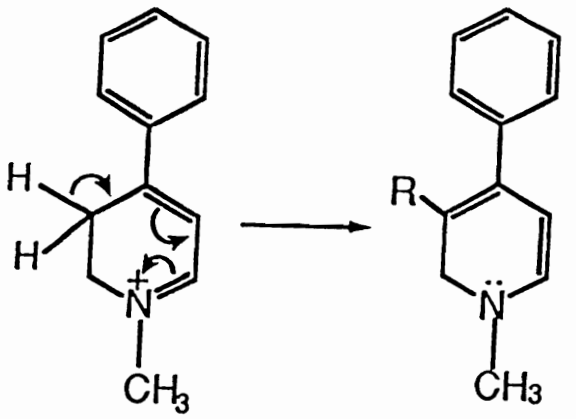

112

114: R = H
114-d_1: R = D

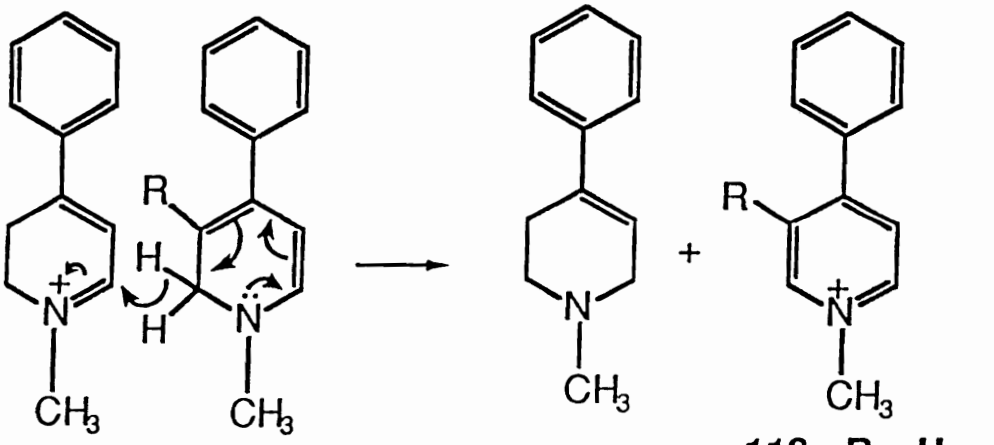

112 114: R = H
114-d_1: R = D

111

113: R = H
113-d_1: R = D

Scheme 24. Proposed Mechanism for Auto-oxidation of $MPDP^+$ to MPP^+.

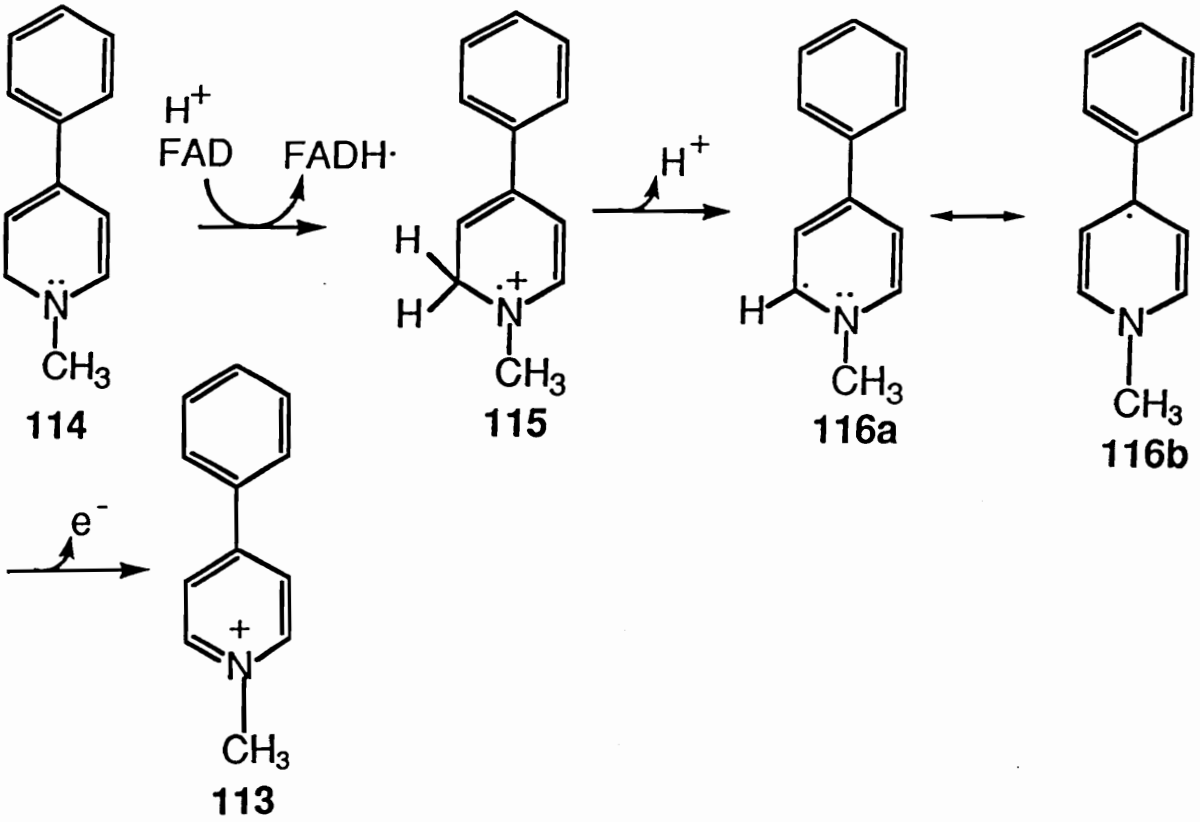

The neurotoxicity of MPTP is blocked by deprenyl (**15**) and pargyline (**28d**) which are potent inhibitors of MAO-B. MAO B purified from beef liver catalyzes the oxidation of MPTP 38% as fast as benzylamine (the preferred MAO-B substrate) with a comparable K_m value.[123] MAO A, isolated from human placenta, catalyzes the oxidation of MPTP to the same dihydropyridinium product at about 12% of the rate of kynuramine, again with a comparable K_m value. This reaction is blocked by the MAO-A selective inhibitor clorgyline (**14**). The rates of oxidation were found to be surprisingly high, considering that tertiary amines are considered to be very poor substrates of MAO. Moreover, it was established[133,134] that the oxidation of MPTP by both forms of MAO was accompanied by their

progressive and irreversible inactivation. The inactivation process followed time-dependent, first order kinetics. Furthermore, the activity of MAO B is not significantly regenerated following gel exclusion chromatography suggesting the formation of a covalent adduct with the enzyme. These results suggest that MPTP follows the criteria associated with a mechanism-based inactivator (see Chapter 1 Section 1.4.). It was reported by Singer *et al.*[135] that MPTP, $MPDP^+$ and MPP^+ are also reversible, competitive inhibitors of both monoamine oxidases A and B, particularly A. The order of inhibition for the A form of the enzyme is $MPDP^+ > MPP^+ >$ MPTP, while for the B form of the enzyme the order shifts to MPTP > $MPDP^+ > MPP^+$. From these studies the first order rate constants were determined for MPTP and its bioactivated products, $MPDP^+$ and MPP^+ as regards their time and concentration dependent inhibition of MAO B (Table 4).

Table 4. First Order Rate Constants for the Inhibition of MAO B.

Compound	Concentration (mM)	k (min^{-1})
MPTP **(111)**	0.5	3.1×10^{-3}
	1	1.1×10^{-2}
	2	1.4×10^{-2}
	3	2.3×10^{-2}
	5	3.4×10^{-2}
$MPDP^+$ **(112)**	2.9	2.2×10^{-2}
MPP^+ **(113)**	5	0

The K_i values for the competitive inhibition of both forms of the enzyme by MPTP, $MPDP^+$ and MPP^+ are shown in Table 5.

Table 5. Inhibition of MAO-A and MAO-B by MPTP and its Metabolites.

		K_i (μM) at 30°		
Enzyme	Substrate	MPTP	$MPDP^+$	MPP^+
MAO A	Kynuramine	18	2.4	3.0
MAO B	Benzylamine	100	200	230

The inactivation data shown in Table 4 indicate that the rates of inactivation are slow compared to the rates of oxidation of MPTP. This suggests a large partition coefficient in favour of substrate turnover and $MPDP^+$ formation. Of the two forms, MAO-B was more sensitive to irreversible inactivation.

Youngster and coworkers[136] investigated the oxidation of MPTP analogs by purified MAO A and B. Several of the tetrahydropyridines and their pyridinium oxidation products inhibited MAO A competitively with low micromolar K_i values. In contrast the pyridinium species inhibited MAO B competitively at only much higher concentrations (> 100 μM). Table 6 lists the K_i values for competitive inhibition of MAO A and B by MPP^+ analogs.

Table 6. K_i Values for Competitive Inhibition of MAO A and MAO B by MPP^+ Analogs.

	K_i	
Compound	MAO A (μM)	MAO B (μM)
MPP^+ **(113)**	3.0	230
2'-MethylMPP^+ **(113a)**	4.8	>100
2'-EthylMPP^+ **(113b)**	4.0	>100
2'-*n* - PropylMPP^+ **(113c)**	ND	500

2'-MethoxyMPP$^+$ **(113d)**	1.6	250
2'-ChloroMPP$^+$ **(113e)**	1.6	ND
3'-MethylMPP$^+$ **(113f)**	1.5	206
3'-FluoroMPP$^+$ **(113g)**	10.3	ND
3'-ChloroMPP$^+$ **(113h)**	4.0	360
3'-BromoMPP$^+$ **(113i)**	2.8	285
3'-MethoxyMPP$^+$ **(113j)**	2.5	ND
4'-MethylMPP$^+$ **(113k)**	1.6	ND
EPP$^+$ **(117)**	6.8	ND
MCP$^+$ **(118)**	7.0	ND
M(4tBu)P$^+$ **(119)**	ND	ND

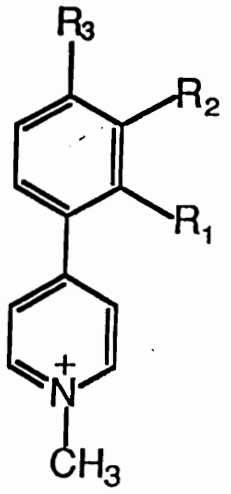

113a: $R_1 = CH_3$, $R_2 = R_3 = H$
113b: $R_1 = CH_2CH_3$, $R_2 = R_3 = H$
113c: $R_1 = CH_2CH_2CH_3$, $R_2 = R_3 = H$
113d: $R_1 = OCH_3$, $R_2 = R_3 = H$
113e: $R_1 = Cl$, $R_2 = R_3 = H$
113f: $R_1 = R_3 = H$, $R_2 = CH_3$
113g: $R_1 = R_3 = H$, $R_2 = F$
113h: $R_1 = R_3 = H$, $R_2 = Cl$
113i: $R_1 = R_3 = H$, $R_2 = Br$
113j: $R_1 = R_3 = H$, $R_2 = OCH_3$
113k: $R_1 = R_2 = H$, $R_3 = CH_3$

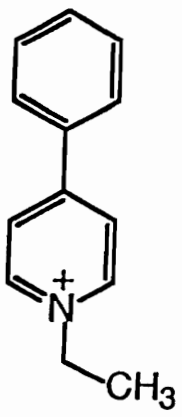

117

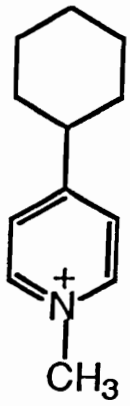

118

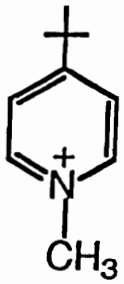

119

Based on these results Singer and co-workers[137] claimed to have identified a new class of powerful inhibitors of human placental MAO A. Derivatives of MPP^+ substituted at the 4' position of the aromatic ring with alkyl groups (**113l-113r**) were found to be more effective reversible inhibitors of MAO A with K_i values of some analogs in the nanomolar range. Inhibition of the B enzyme occured only at much higher concentrations (32-374 mM). Table 7 summarizes the K_i values for the competitive inhibition of MAO A and MAO B by these MPP^+ analogs.

Table 7. K_i Values for Competitive Inhibition of MAO A and B by MPP^+ Analogs.

	K_i (μM)	
Compound	MAO A	MAO B
MPP^+ (**113**)	3.0	230
4'-MethylMPP^+ (**113k**)	1.6	>1000
4'-PropylMPP^+ (**113l**)	0.2	100
4-t-ButylMPP^+ (**113m**)	0.32	35
4'-PentylMPP^+ (**113n**)	0.13	43
4'-HeptylMPP^+ (**113o**)	0.59	32
4'-DecylMPP^+ (**113p**)	3.1	51
4'-AzidoMPP^+ (**113q**)	0.7	374
4'-PentylMPP^+ (**113r**)	0.075	59
4'-Pentyl-4-phenylpyridine (**113s**)	35	38

In conjunction with the inhibition studies on MPTP and its derivatives with MAO, several other studies related to the bioactivation of this tetrahydropyridine have been pursued. It was shown through the use of chemical models such as the 4-phenyl-1,3,3-trimethyl-2,3-dihydropyridinium salt **121** that $MPDP^+$ was unlikely to possess characteristics which could lead to the neurotoxic effects observed with MPTP.[138] Silverman *et al.*[138] demonstrated that 3,3-dimethyl-MPTP (**120**) and 3,3-dimethyl-$MPDP^+$ (**121**) interacted in a similar fashion as MPTP and $MPDP^+$ as regards to the

interaction with MAO. This observation applied to conditions involving the presence of β-mercaptoethanol. In the absence of β-mercaptoethanol, mixed competitive-noncompetitive inhibition kinetics were observed for the two analogs, whereas competitive inhibition kinetics are exhibited by MPTP. Compounds **120** and **121** were found to be time dependent inactivators of MAO and gave identical kinetic parameters (Table 8) as in the case of MPTP and $MPDP^+$.[138] In the presence of β-mercaptoethanol but not glutathione, the rate of inactivation increased dramatically. This suggests that the effect of β-mercaptoethanol towards the inactivation may be to induce a conformational change in the enzyme which reorients an active site nucleophile for attack on the activated species. This argument was supported by the finding that inactivation did not lead to a flavin adduct.

These results were interpreted in terms of two possible mechanisms (Schemes 25 and Schemes 26). MAO-B catalyzed oxidation of **120** would lead to the corresponding dihydropyridinium species **121** which could potentially undergo a 1,2-addition by an active site nucleophile to generate the covalent adduct **122**. Adduct **122** would then give rise to the radical cation **123** following loss of an electron. The carbon-centered radical **124** obtained after a loss of a proton from **123**, would give rise to **125** after subsequent loss of a second electron (Scheme 25). The second interpretation of the inactivation mechanism involves a 1,4-addition by the active site nucleophile on **121** to generate adduct **126**, in equilibrium with the corresponding iminium **127**, which upon hydrolysis would yield aldehyde **128** (Scheme 26).

Scheme 25. Proposed Mechanism of Inactivation of MAO-B by 121.

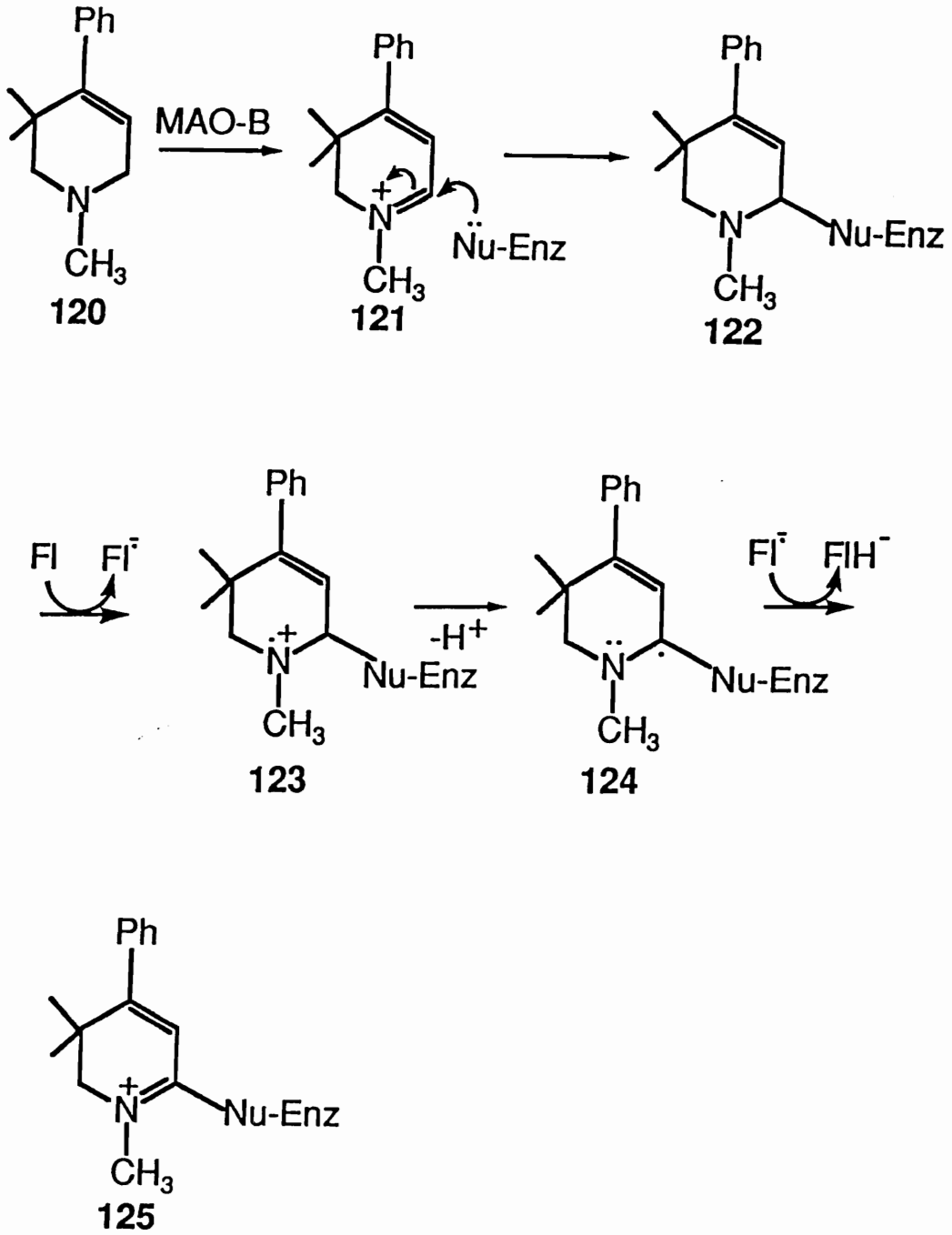

Scheme 26. Another Proposed Mechanism of Inactivation of MAO-B by 121.

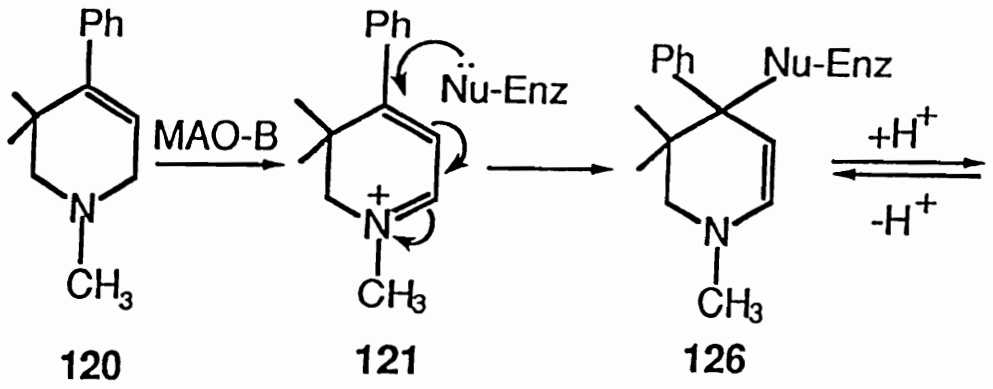

120 121 126

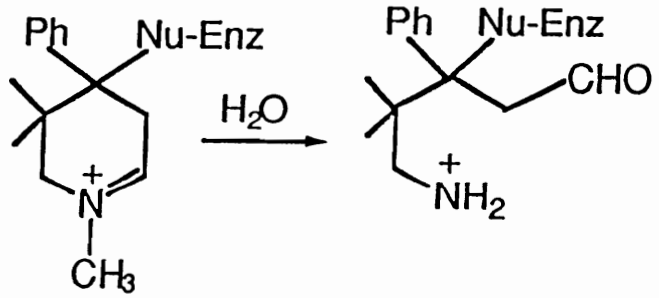

127 128

Table 8 summarizes the kinetic parameters for the 3,3-dimethyl-MPTP and 3,3-dimethyl-$MPDP^+$ analogs.

Table 8. Inactivation Parameters by 3,3-DimethylMPTP analogs 121 and 122.

Compound	K_i (mM)	K_I (mM)	$k_{inact.}$ h^{-1}	PR
120	2.24	2.10	0.16	>50
121	1.4	2.41	0.16	
120 + Thiol	4.95	0.25	1.08	1
121 + Thiol		0.11	1.08	
111	0.28	0.5	2.38	38

These rationales, however were contradictory to the proposal that inactivation of MAO-B by MPTP involves a radical species derived from $MPDP^+$. Isotope effect studies by Ottoboni and coworkers[139,140] established that the rate of inactivation of MAO-B in the presence of the 6,6-dideuterio-MPTP analog **111**-d_2 was the same as that observed with MPTP, even though the ^{D}(Vmax/Km) value for the conversion of MPTP to $MPDP^+$ was 8.01. A kinetic isotope effect of 1.9 for the inactivation of MAO-B by MPTP-2,2,6,6-d_4 **111**-d_4 was also observed. Based on these results, it was postulated that the resonance stabilized carbon-centered radical **116**, derived from $MPDP^+$ might possess the appropriate stability/reactivity characteristics to alkylate and inactivate the enzyme. The reported metabolism dependent covalent binding

of tritium-labelled MPTP[135] is consistent with this proposal as is the recent report that $MPDP^+$ inactivates MAO-B at a faster rate than does MPTP.[141]

2.2. Rationale for proposed research.

The discovery of MPTP as an MAO substrate itself is important since prior to this time no cyclic amine had been reported to be a substrate for this enzyme. These unique structural features of tetrahydropyridines have been examined extensively in terms of the substrate properties of this system.[142,143,144] This thesis is concerned with the possibility of developing novel inactivators of MAO-A and MAO-B by appropriate modifications of the MPTP skeleton to introduce latent electrophilic moieties that, following initial processing by the enzyme, will alkylate an active site nucleophile. Thus, we have elected to examine a series of potential MAO inhibitors that retain some of the basic structural features of MPTP and thereby exploit the unique structural features of this cyclic tertiary allylamine that have been documented by excellent substrate properties. A major effort of this research concerns the synthesis of the targeted potential substrate molecules and the predicted metabolites, namely the dihydropyridinium and the pyridinium species, which may result from the MAO-B catalyzed oxidation of the tetrahydropyridine. A second major effort concerns the characterization of the MAO-B substrate/inhibitor properties of the tetrahydropyridines. In addition to these systematic studies, synthetic and metabolic studies related to the main theme of the thesis also have been pursued.

Initial studies on the design of tetrahydropyridine derivatives with potential MAO inactivating properties focused on the N- and C(4)-cyclopropyl

analogs **129** and **130**, respectively.[145] Based on both theoretical considerations and published experimental results discussed in Chapter 1, the cyclopropyl group was selected as an attractive functionality to mediate the metabolism dependent enzyme inactivation. The results of these experiments established that the C(4)-cyclopropyl analog **130** is a poor inactivator of MAO-B despite the efficiency with which this enzyme catalyzes the conversion of **130** to the dihydropyridinium species **132** via the carbon-centered radical **131**. the intermediate postulated to be required for enzyme inactivation. If one assumes an inactivation pathway proceeding via the stabilized radical **133**, then the poor inactivating properties of compound **130** may be rationalized in terms of the unexpected stability of the dihydropyridinium metabolite **132** which may preclude formation of a reactive radical intermediate **133** (Scheme 27).

Scheme 27. MAO-B Catalyzed Oxidation of C(4)-CyclopropylMPTP Analog.

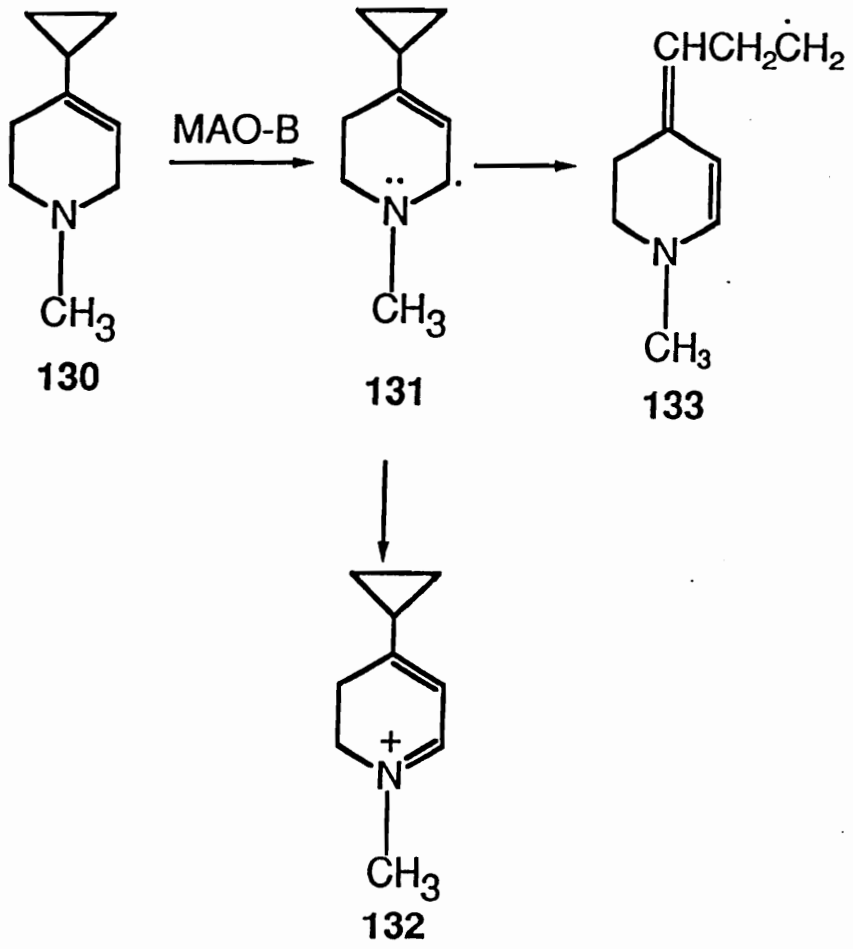

In contrast, the N-cyclopropyl derivative **129** was a very poor substrate but a good concentration and time dependent inhibitor of MAO-B (k_{inact} = 0.7 min^{-1}; K_I = 180 μM vs k_{inact} = 0.03 min^{-1} at 5 mM for MPTP). The efficiency with which compound **129** inactivates MAO-B argues that the N-cyclopropyl group must play an important role in the inactivation process. It seems

reasonable to postulate a radical reaction pathway (Scheme 28) analogous to that proposed by Silverman for other cyclopropylamines, as discussed in Chapter 1. Initial one electron transfer from **129** to the oxidized flavin cofactor would generate the aminium radical **134**. This intermediate would have the option to ring open to the reactive primary radical **135** (pathway leading to inactivation) or lose an α-proton to give the secondary carbon-centered radical **136** which subsequently would undergo a second electron transfer to generate the dihydropyridinium intermediate **137**. In order to study the pathway leading to product formation, an examination of an incubation mixture containing **129** and an excess of MAO-B indicated the formation of an unstable species absorbing at λ_{max} 355 nm (corresponding to the expected λ_{max} for **137**). The chromophore for **137** gradually shifted to λ_{max} 305, the λ_{max} corresponding to the pyridinium species **138** which results as a result of further oxidation of **137**.

Scheme 28. Proposed Mechanism of MAO-B Inactivation by N-CyclopropylMPTPAnalog.

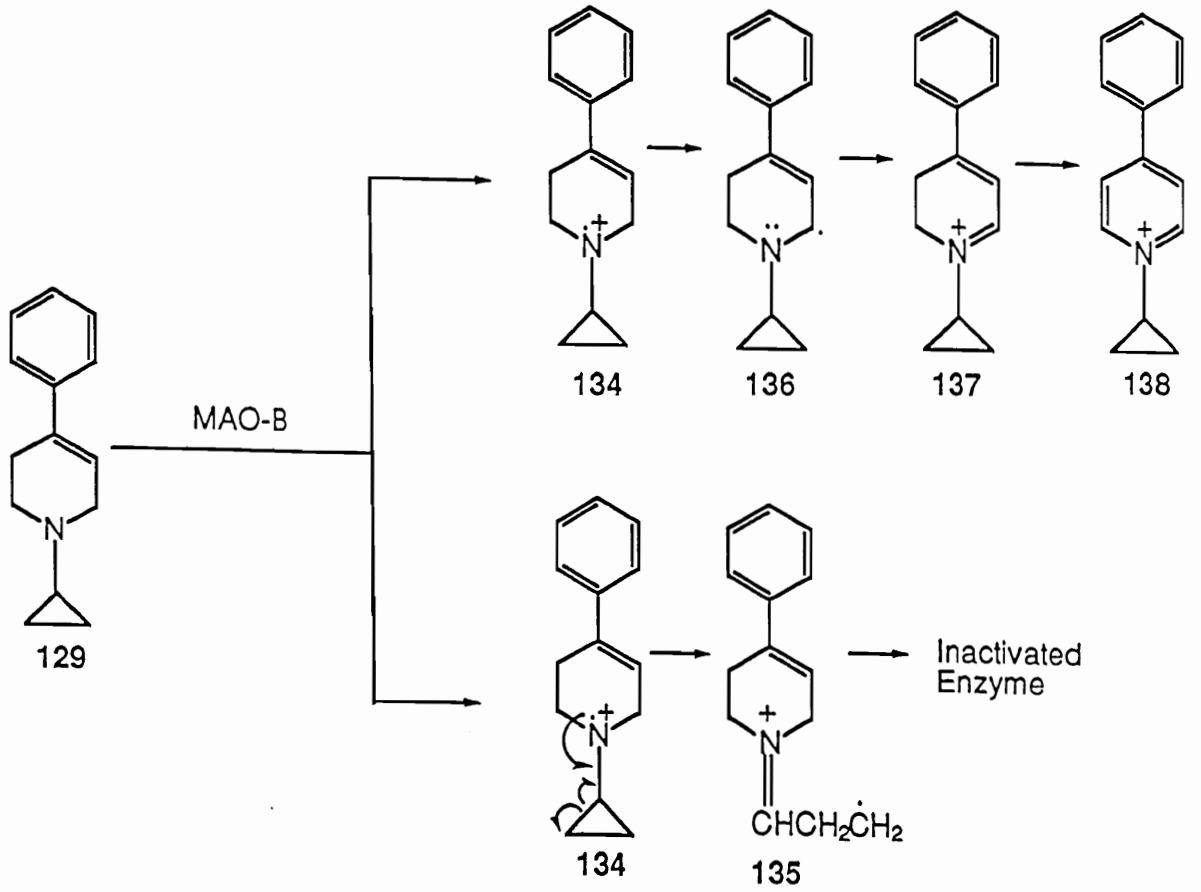

In the present study we have elected to examine the MAO-B substrate and inhibitor properties of a variety of MPTP analogs, the majority of which bear a functional group with the potential to react with a nucleophilic center at the active site following initial processing by the enzyme. A review of the literature underscores the unique structural features of MPTP as an MAO-B substrate. Relatively minor structural modifications (reduction of the piperidiene double bond,[142] substitution of the group on the nitrogen with a substituent larger than methyl[143] or introduction of an additional substituent on the piperidiene ring[144]) lead to MPTP analogs with very poor or non-demonstrable MAO-B substrate properties. On the other hand a variety of 1-methyl-4-substituted-1,2,3,6-tetrahydropyridines are excellent substrates of MAO-B.[142,143,144,145,146] These published structure activity studies have led us to limit the scope of this investigation to 1-substituted-4-phenyl-1,2,3,6-tetrahydropyridine and 1-methyl-4-substituted-1,2,3,6-tetrahydropyridine derivatives. An underlying concept is that good substrate properties, when properly exploited, may lead to good inactivator properties, i.e. the enzyme may catalyze the formation of a reactive intermediate which prior to dissociating to product (like a substrate) could covalently bind to the enzyme (like an inactivator). This concept was demonstrated in the basic structure-activity requirements and mechanism-based inactivation for MAO (see Chapter 1).

The 1-substituted-4-phenyl series includes the N-allyl (**140**) and N-propargyl (**146**) analogs which were considered potential sources for the electrophilic eniminium and yniminium intermediates, **144** and **150** respectively. According to the mechanisms proposed for the inactivation of

MAO by propargylic amines (Chapter 1), compounds **140** and **146** could be processed by MAO to generate the radical cations **141** and **147** which could lose a proton either on the nitrogen substituent to generate carbon-centered radicals **142** and **148**, or the ring α-carbon atom to generate the carbon-centered radicals **143** and **149**. Loss of a second electron from **142** and **148** would lead to the corresponding reactive intermediates **144** and **150**, respectively (enzyme inactivation pathway). On the other hand, loss of an electron from **143** and **149** would lead to the dihydropyridinium intermediates **145** and **151** (Schemes 29a and 29b).

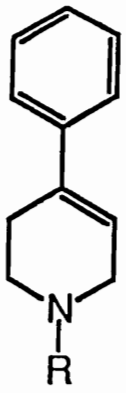

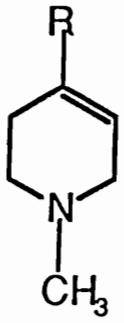

140: R = $CH_2CH{=}CH_2$
146: R = $CH_2C{\equiv}CH$
152: R = $CH_2CH_2CH_3$

153: R =

156: R =

157: R = $CH{=}CH_2$

158: R = $CH{=}CH$

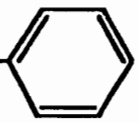

159: R = $C{\equiv}CH$

160: R =

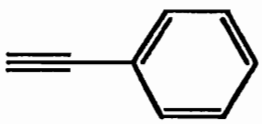

Schemes 29a and 29b. Proposed Mechanisms of MAO Inactivation by the N-Propargyl and the N-AllylMPTP Analogs.

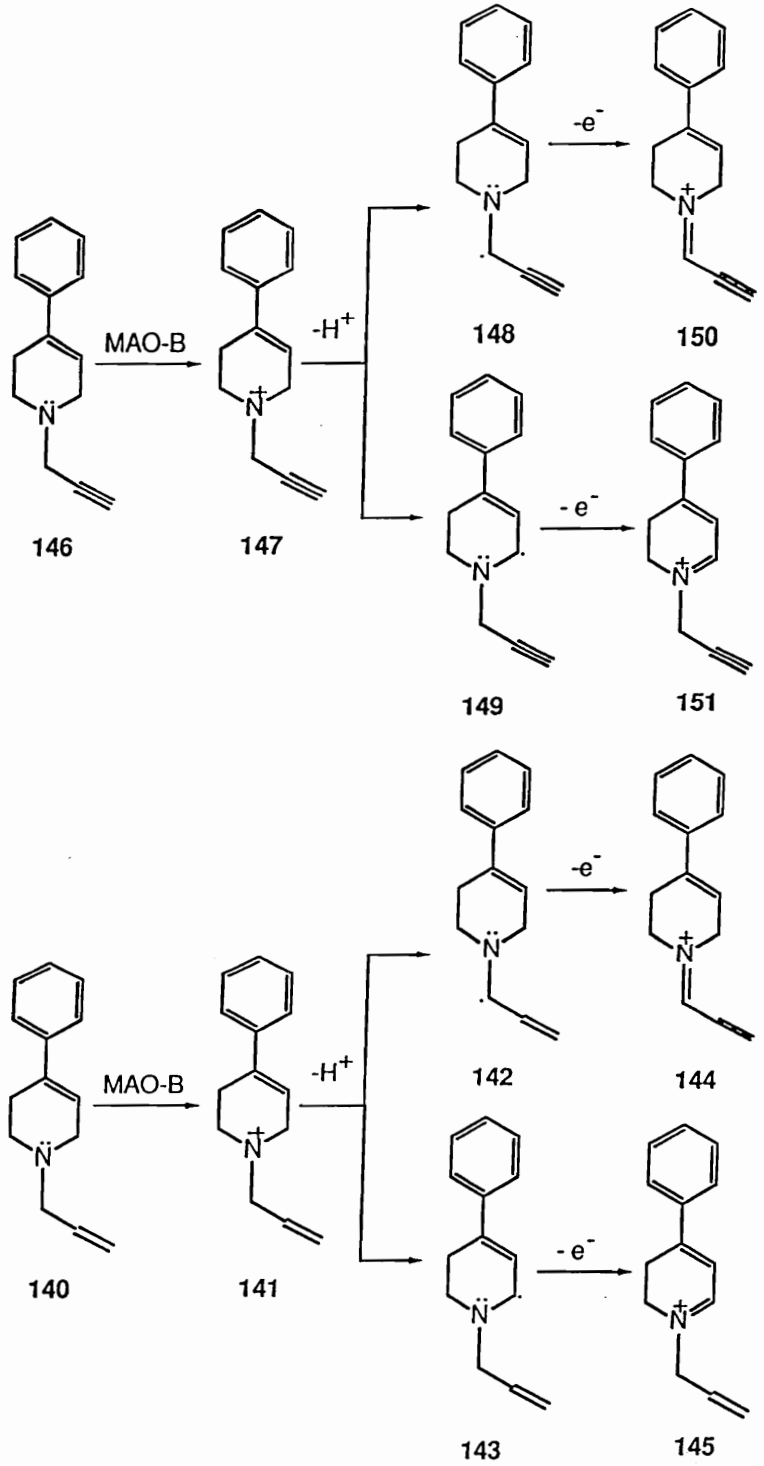

The N-propyl derivative **152** was prepared in an attempt to estimate the rate of the MAO-B catalyzed oxidation of a tetrahydropyridine derivative to the corresponding dihydropyridinium intermediate with a 3-carbon chain attached to the nitrogen atom that would not lead to an analogous electrophilic intermediate. The N-cyclobutyl analog **153** (Scheme 30) was prepared as an extension of our previous studies on the N-cyclopropyl compound **130** with the expectation that its MAO-B catalyzed bioactivation would lead to the aminium radical cation **154**. Due to ring strain energy **154** could generate the ring-opened carbon centered radical **155** analogous to **137**. The N-cyclopentyl derivative **156** was prepared as a strain free cycloalkylamine analog which should not form the corresponding carbon centered radical.

Scheme 30. Proposed Mechanism of MAO Inactivation by the N-cyclobutyl Analog 153.

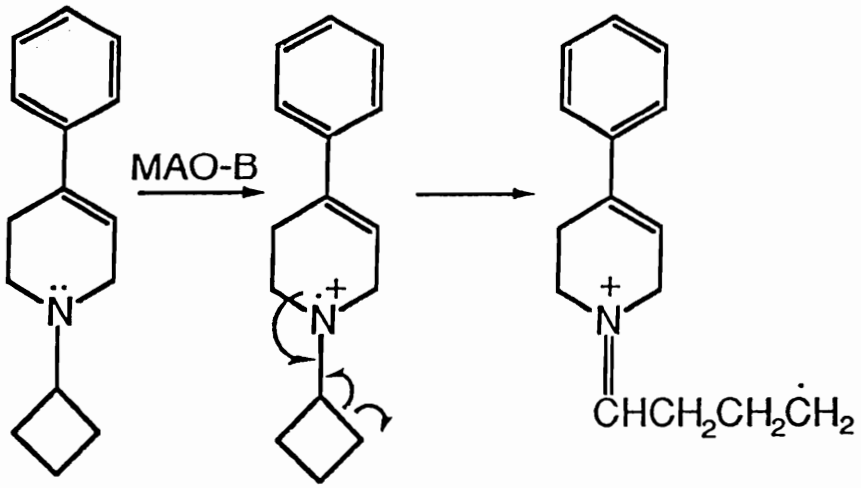

153 **154** **155**

The 4-ethenyl- and 4-ethynyl-1-methyl-1,2,3,6-tetrahydropyridine derivatives **157, 158, 159** and **160** were selected as potential substrates that would generate reactive electrophilic metabolic intermediates with bioalkylating potential positioned at C(4) of the tetrahydropyridine ring. The inactivation pathway was envisioned to proceed via the corresponding dihydropyridinium intermediates. The ethynyl analog **159** was considered particularly attractive since the corresponding dihydropyridinium intermediate **161** could lead to resonance stabilized protein adducts such as **163** via rearrangement of the aminoallene species **162** (Scheme 31).

Scheme 31. Proposed Mechanism of MAO Inactivation by 159.

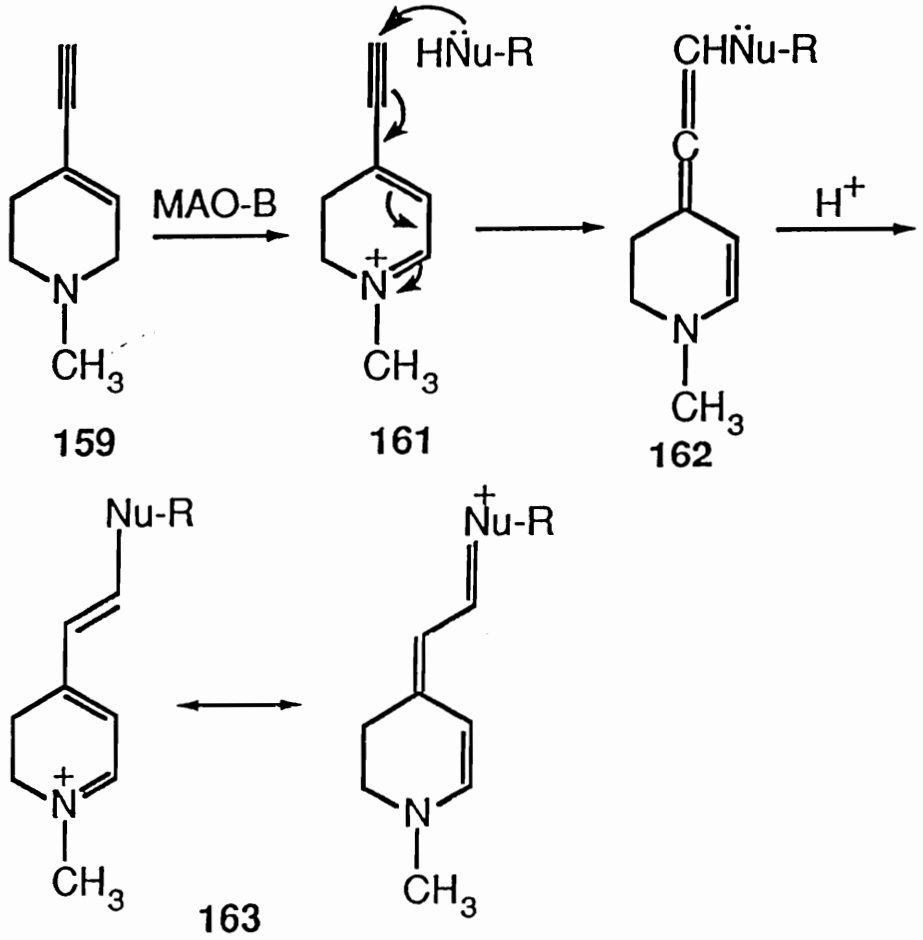

The excellent inactivating properties displayed by the N-cyclopropyl analog prompted us to develop a convenient synthesis of N-cyclopropylpiperidin-4-one (**164**) which could serve as an intermediate in the synthesis of N-cyclopropyl-4-substituted tetrahydropyridines as potential MAO inhibitors.

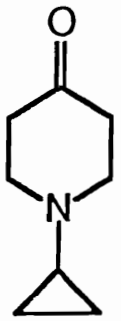

164

Furthermore, we recently have explored the MAO-A and B substrate properties of a variety of other oxygen bearing tetrahydropyridine derivatives. The lead compound was the 1-methyl-4-phenoxy-1,2,3,6-tetrahydropyridine analog **165** which had been synthesized previously to evaluate the substrate properties of tetrahydropyridines bearing heteroatom linked groups at C-4. Unlike the carbon linked analogs the resulting dihydropyridinium metabolite **166** did not undergo further oxidation to the pyridinium species **167** but rather underwent hydrolytic cleavage via the intermediate hemiketal **168** to form the aminoenone **169** and phenol **170** (Scheme 32).

Scheme 32. MAO-B Catalyzed Oxidation of the C(4)-PhenoxyMPTP Analog.

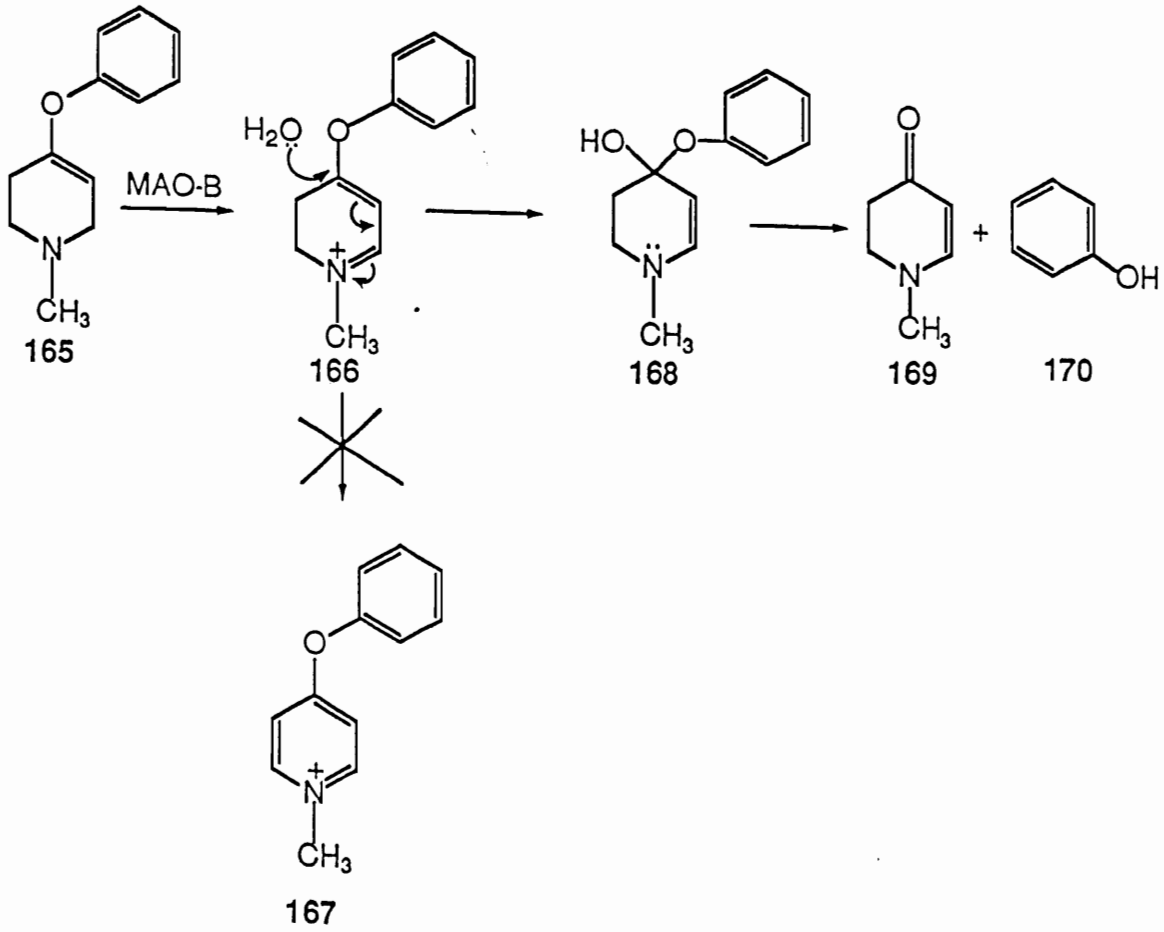

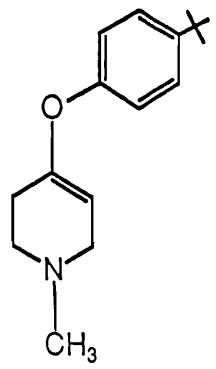

171

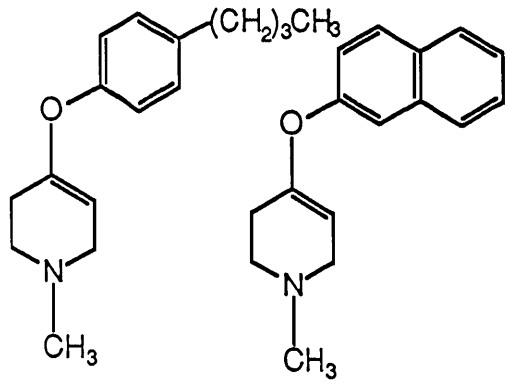

172

173

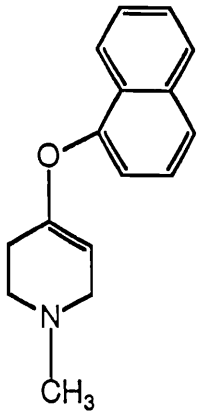

174

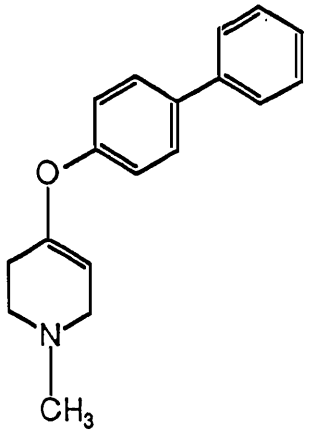

175

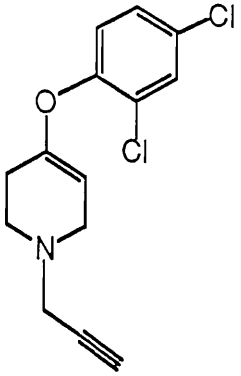

176

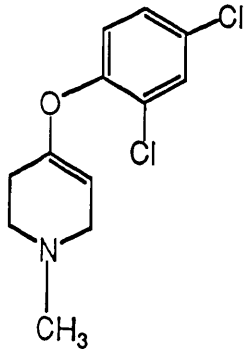

177

This observation has lead to studies designed to explore the possibility of developing novel, nontoxic derivatives of MPTP bearing potential pharmacologically active leaving groups at C-4. The MAO catalyzed oxidation of such substrates **171-175** would result in the formation of unstable dihydropyridinium intermediates which, under physiological conditions, would undergo spontaneous hydrolytic cleavage to generate the aminoenone and the pharmacological group. These efforts have led to the identification of important structural characteristics which are selective for the A and B forms of the enzyme. The results with the aryloxytetrahydropyridines also have focussed our attention on designing selective inhibitors of MAO-A. A combination of experimental results and the potency of clorgyline as a irreversible MAO-A inactivator has led to the possibility of developing an appropriately C(4)- and N-substituted aryloxytetrahydropyridine such as 4-(2,4-dichlorophenoxy)-1-propargyl-1,2,3,6-tetrahydropyridine **176** as a potential MAO-A selective inactivator. Our initial efforts have been targeted towards the synthesis of the corresponding N-methyl analog **177** in an effort to estimate the substrate binding properties exhibited by this molecule towards the two forms of MAO.

3. Results and Discussions.

3.1. Chemistry.

3.1.1. Synthesis of the N-substituted-4-phenyl-1,2,3,6-tetrahydropyridines.

With the exception of the N-cyclobutyl analog **153**, all of the 1-substituted-4-phenyl-1,2,3,6-tetrahydropyridine derivatives were synthesized from 4-phenylpyridine (**178**). N-alkylation of the commercially available **178** with allyl iodide, propargyl bromide, or propyl iodide yielded the pyridinium intermediates **179, 180** and **181** (Scheme 33) as the corresponding halide salts which precipitated out of the reaction mixture and were purified by recrystallization with an appropriate solvent system. The purity of these pyridinium compounds was confirmed by ^{1}H NMR analysis and comparison with the literature melting points.[147] Treatment of the pyridinium intermediates **179, 180,** and **181** with sodium borohydride (see Scheme 33) yielded the desired tetrahydropyridines, **140, 146,** and **152,** respectively, which were isolated and characterized as stable oxalate salts. The GCEI mass spectra of the target tetrahydropyridines gave peaks corresponding to the parent ions at M·$^+$ 199 (Fig. 1), 197 (Fig. 2) and 201 (Fig. 3), respectively. The diagnostic signals in the ^{1}H NMR spectra of the 1-substituted-4-phenyltetrahydropyridine analogs were assigned as follows: The 1-allyl analog **140** (Fig.4) displayed the aromatic proton signals as multiplets in the region δ 7.0-8.0 and the olefinic C-5 proton signal as a broad singlet at δ 6.0. The C-6 methylene protons appeared as a broad singlet centered near δ 3.8. The C-2 methylene proton signals were located as a triplet

centered near δ 3.2 while the upfield broad signal at around δ 2.7 ppm was assigned to the C-3 methylene protons. Other characteristic signals associated with the allyl substituent on nitrogen included the olefinic methylene protons which were observed as a multiplet centered at δ 5.5 and the olefinic CH which centered as a multiplet at δ 5.95. The ^{1}H NMR spectrum for the 1-propargyl analog **146** (Fig. 5) was similar to that of the 1-allyl analog **140**, except that the allyl functionality was replaced by the propargyl substituent. The methylene protons of the propargyl group adjacent to the nitrogen were centered as a multiplet at δ 2.66 and the acetylenic proton appeared alongwith with the C-2 methylenes as a singlet at δ 3.54. The ^{1}H NMR spectrum of the 1-propyl analog **152** (Fig. 6) was consistent with the general features of these systems such as the signals for the aromatic protons and the tetrahydropyridyl moiety also present in the NMR spectra of **140** and **146**. The key diagnostic signals for the propyl functionality included a triplet (δ 0.9) for the terminal methyl group, a multiplet (δ 1.7) for the methylene protons β to the nitrogen atom, and a quartet (δ 3.0) for the methylene protons α to the nitrogen atom. Finally microanalytical data were found to be consistent with the proposed structures.

Attempts to prepare the 1-cyclopentyl-4-phenylpyridinium derivative **182** led to an unexpected result. Reaction of **178** with cyclopentyl bromide in dry acetone under reflux for 72 hours resulted in the precipitation of a crystalline white solid. The ^{1}H NMR spectrum (Fig. 7) of this solid material showed a multliplet at δ 1.8-2.6 which integrated for 8 protons and was assigned to the cyclopentyl methylene protons. A

multiplet at δ 5.5 was assigned to the cyclopentylmethine proton. The phenyl proton signals as usual were observed at δ 7.7. The key diagnostic signals for **182**, the doublets at δ 9.55 and δ 8.22 which are typical of the C-2 and C-6 aromatic proton signals and the C-3 and C-5 protons of the pyridinium ring system, respectively, also were present. Along with these signals, however, were other signals which were typical of the starting material, 4-phenylpyridine (**178**, Fig. 8). Thus the pair of doublets at δ 8.9 and 7.8 correspond to the C-2 and C-6 and the C-3 and C-5 protons of **178**. The multiplet at δ 7.7 assigned to the phenyl protons of **182** also would fit the phenyl protons of **178**. These data suggested a mixture of the expected product, **182**, and the starting 4-phenylpyridine (**178**). The ratio of the product versus the starting material could be estimated by integrating this spectrum and was found to be a 2:1 mixture of the desired pyridinium species **182** and starting material **178**. This "ternary" complex was quite stable to repeated recrystallizations, gave a consistent and sharp melting point (122-4 °C) and could not be separated by tlc. Therefore we elected to use this mixture in the subsequent reduction with sodium borohydride. This ternary complex was reduced with sodium borohydride. The GCEI TIC tracing of the crude reaction mixture showed a 2:1 mixture of the desired 1-cyclopentyltetrahydropyridine **156** (M^+ 227) and **178** (M^+ 155) respectively.

The subsequent process used to purify **156** had been discovered during the synthesis of the N-cyclopropyl-4-phenyltetrahydropyridine derivative **129**. During the purification of **129·HCl** salt, a organic wash using methylene chloride was required and the organic washings were

found to contain predominantly **129·HCl**, presumably because of the lipophilic nature of the MPTP analog. We therefore attempted to purify **156** by treating the crude mixture containing **156** and **178** with dilute acid to convert the two products into their respective hydrochloride salts and subsequently extracting repeatedly with methylene chloride with the hope that the more lipophilic **156·HCl** would be extracted into the organic layer exclusively. The combined organic extracts were concentrated to afford essentially pure **156** as its hydrochloride salt. The GCEI mass spectrum gave a molecular ion at m/z 227 (Fig. 9). The ^{1}H NMR spectrum included the key signals corresponding to a 1-substituted-4-phenyltetrahydropyridine derivative as described above. The upfield multiplet centered at δ 2.0-2.5 was assigned to the cyclopentyl protons and the relatively downfield multiplet at δ 4.2 which integrated for one proton was assigned to the cyclopentylmethine proton (Fig. 10).

Scheme 33. Synthesis of N-Substituted-4-phenyl-1,2,3,6-tetrahydropyridines.

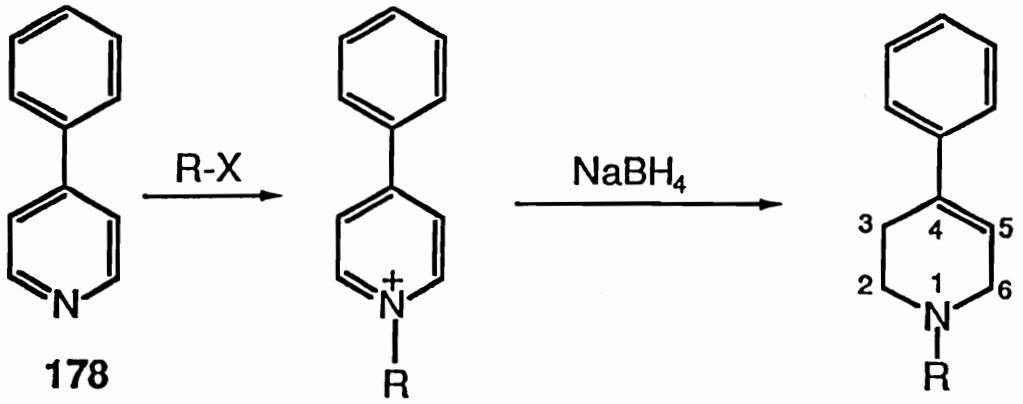

178

	R
179:	CH_2—CH=CH_2
180:	CH_2—C≡CH
181:	$CH_2CH_2CH_3$
183:	
182:	

	R
140:	CH_2—CH=CH_2
146:	CH_2—C≡CH
152:	$CH_2CH_2CH_3$
156:	

Attempted alkylation of **178** with bromocyclobutane under a variety of reaction conditions (room temperature and under reflux in various solvents) failed to yield the corresponding N-

cyclobutylpyridinium species **183**. A similar failure was encountered during the reaction of bromocyclopropane and **178**.[145] Therefore the synthesis of the N-cyclobutyltetrahydropyridine analog **153** was approached via a condensation reaction involving cyclobutylamine, 2-phenylpropene (**184**) and formaldehyde (Scheme 34).[148] It has been reported in the literature[149] that 3-alkyl-6-methyl-6-aryltetrahydro-1,3-oxazines such as **185** and 1-alkyl-4-aryl-4-piperidinols such as **187** are the principal products expected from the reaction of **184**, formaldehyde and primary amine salts. Compounds **185** and **187** can be converted to **153** using hydrochloric acid. The same strategy using cyclopropyl amine, formaldehyde and 2-phenylpropene has been applied successfully in the synthesis of the N-cyclopropyl-4-phenyltetrahydropyridine (**129**) analog. We attempted this same reaction with cyclobutylamine and after 6 hours of heating analysis of a crude reaction mixture by GCMS indicated the presence of the expected 1,3-oxazine **185** (m/z 231, Fig. 11), the isomeric alcohol **187** (m/z 231, Fig. 12) and the desired tetrahydropyridine **153**. The mechanistic pathway probably involves an intramolecular aminomethylation reaction following scission of the tetrahydro-1,3-oxazine ring **185** to carbocation **186** which leads to **153** via intermediates **188** and **189** (Scheme 35). Acid treatment of this mixture afforded the N-cyclobutyl analog **153** which was purified by treatment of the crude product with 0.1N HCl and extraction into methylene chloride to yield essentially pure **153** as the hydrochloride salt. The GCEI mass spectrum of **153** (Fig. 13) displayed the expected molecular ion at m/z 213. The ^{1}H NMR spectrum consisted of the aromatic signals at δ 7.0-7.5 and the C-5

olefinic proton signal at δ 6.0. The upfield region in the NMR spectrum was quite complicated and assignments were made on the basis of the literature spectrum for cyclobutyl amine. The cyclobutylmethine proton signal was assigned to the multiplet centered at δ 4.1. The integration of this multiplet corresponded to 1 proton as required. The upfield signals in the region δ 1.6-2.5 were assigned to the cyclobutyl methylene protons based on the integration pattern and the literature values (Fig. 14). Finally the structure of **153** was confirmed by microanalysis.

Scheme 34. Synthetic route to the N-cyclobutyl analog 153.

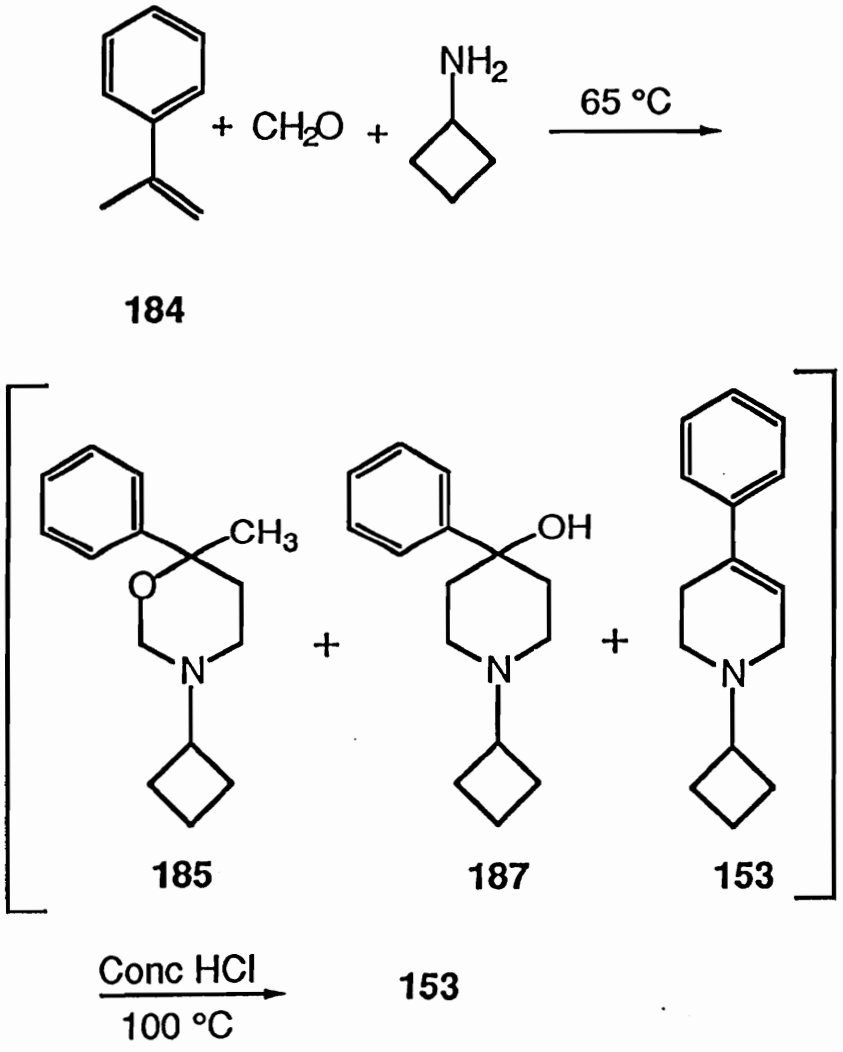

Scheme 35. Proposed Mechanism for the formation of 153 from 185.

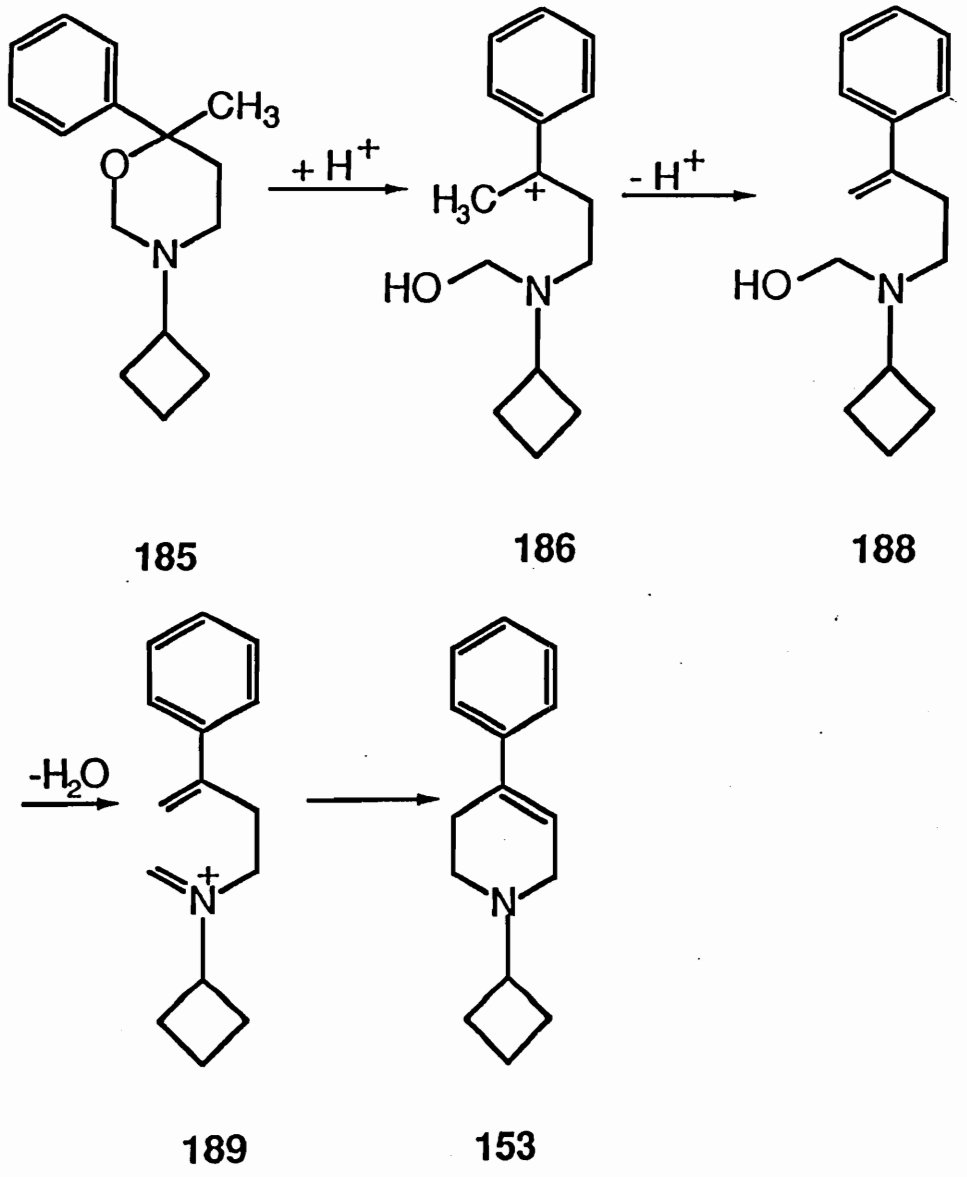

Since our research interests were mainly targeted towards the development of MAO inactivators, we were interested in conducting some preliminary studies on the mechanistic aspects of inactivation of

MAO-B which could provide an insight into the key biomolecular events and active site requirements for inactivation. We chose **146** as the lead compound as it displayed excellent inhibition properties with MAO-B (see Section 3.2.2). We focused our attention on studies directed to measurements of possible deuterium isotope effects which could be estimated from the differences in the rates of inactivation of MAO-B by **146** and **146-d_2**. We therefore required the synthesis of the corresponding deuterio analog of **146-d_2**. We initially approached the synthesis of **146** by synthesizing the amide **191** (Scheme 36) which potentially could be reduced with LAH to afford the desired target molecule. The amide was synthesized by treatment of the corresponding tetrahydropyridine **190** with propiolic acid in the presence of DCC (N,N'-dicyclohexylcarbodiimide) and DMAP (dimethylaminopyridine) to afford a dark brown oil which was composed of the desired amide **191** and DCC as identified by GCMS. Pure **191** was obtained by column chromatography in about 50 % yield. The characterization of **191** included GCMS which showed the molecular ion at m/z 211 (Fig. 15) and ^{1}H NMR (Fig. 16) which was atypical of tetrahydropyridines because of the presence of rotamers **191_a** and **191_b**. However the subsequent reduction of amide **191** with LAH as a model prior to using LAD failed to afford the desired product **146**. GCMS analysis of the crude reaction mixture did not reveal the formation of m/z 197. Instead a m/z 215 corresponding to **192** was observed, which presumably results due to the reduction of the triple bond which is in conjugation with the carbonyl group in **191**. An examination of the literature convinced us that

carbonyl reductions of propargylic amides is not a favored reaction.[150,151]

Scheme 36. Attempted Synthesis of 146 via Amide 191.

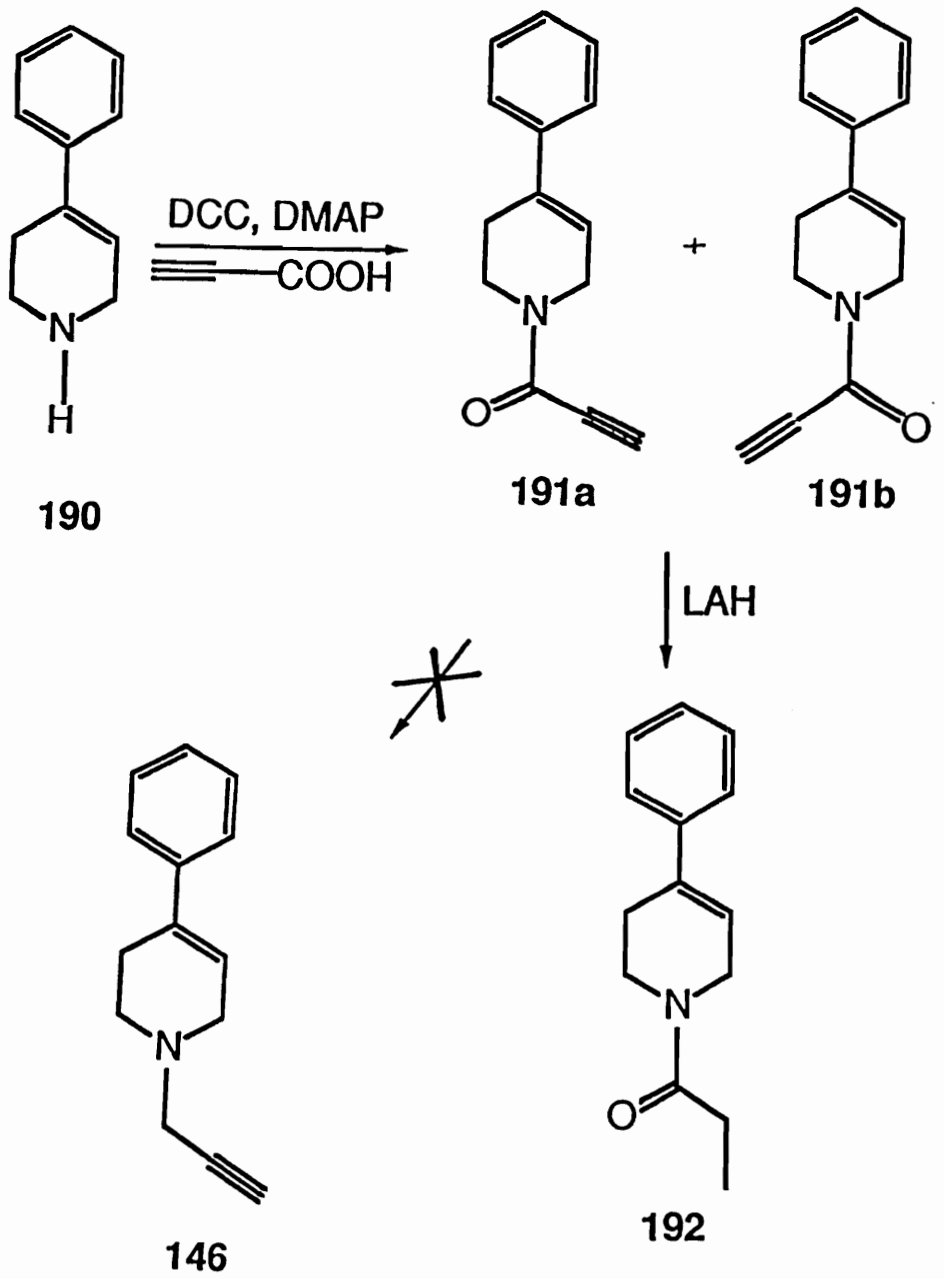

3.1.2. Synthesis of the C(4)-substituted-1-methyl-1,2,3,6-tetrahydropyridine Derivatives.

In the case of the MPTP analogs in the C(4) series, the 4-ethenyl-1-methyl-1,2,3,6-tetrahydropyridine derivative **157** was synthesized by an approach analogous to that previously used in the synthesis of the N-substituted tetrahydropyridines. The reaction involved alkylation of commercially available 4-ethenylpyridine (**193**) with iodomethane (Scheme 37) to generate the corresponding 4-ethenyl-1-methylpyridinium iodide (**194**) which precipitated out of the reaction mixture and was purified by recrystallization and characterized by ^{1}H NMR (Fig. 17). The characteristic signals for **194**, which are also typical of the general structural features of the other C-4 substituted-1-methylpyridinium derivatives,[145] revealed a pair of downfield doublets in the region δ 8.2 and δ 9.0 which were assigned to the C-2 and C-6 and the C-3 and C-5 ring protons. A sharp singlet at δ 4.3 was assigned to the N-CH_3 group. Other structural features for **194** revealed in the NMR spectrum can be explained on the basis of a typical ABX pattern. The doublet of doublets at δ 7.0 ppm was assigned to the olefinic proton H_X because of its closer proximity to the pyridinium ring system and the observed splitting which was due to the coupling of H_X with H_A (J = 18 Hz) and H_B (J = 11 Hz), the two methylene protons of the ethenyl functionality. The doublets at δ 6.6 and 6.0 with coupling constants J = 17 Hz and 11 Hz were assigned to the terminal *trans* olefinic proton H_A (split by H_X) and the terminal *cis* olefinic proton H_B (split by H_X), respectively.

The reduction of **194** initially was attempted using standard

reducing conditions (2 moles of sodium borohydride/MeOH) which had successfully led to the synthesis of the N-substituted tetrahydropyridine derivatives. GCMS analysis of a crude reaction mixture using the above reaction conditions displayed two peaks of almost equal area. The first peak (Fig. 18) showed a molecular ion at m/z 123 as expected for the desired tetrahydropyridine derivative **157**. The second peak (Fig. 19) displayed a molecular ion at m/z 125, consistent with 4-ethyl-1-methyl-1,2,3,6-tetrahydropyridine **195**. The characterization of **195** was based on the fact that all C(4)-substituted tetrahydropyridines show a typical fragment ion at m/z 96 which corresponds to the 1-methyl-1,2,3,6-tetrahydropyridyl radical cation **196** obtained from the loss of the C(4)-substituent.

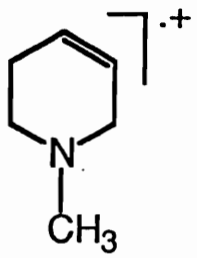

196

The reduction of **194** then was attempted using 1 mole of sodium borohydride (see Scheme 37) and analysis of the crude reaction mixture by GCMS indicated the expected molecular ion at m/z 123 belonging to **157**. The product was isolated and characterized as the oxalate salt. The ^{1}H NMR spectrum (Fig. 20) of **157** displayed the characteristic tetrahydropyridine signals as described earlier for the N-substituted

tetrahydropyridines. Additionally the ethenyl methine proton signal appeared as a doublet of doublets centered at δ 6.4. The signals for the terminal ethenyl [cis (J = 11 Hz and trans (J = 17 Hz) olefinic] protons were observed upfield (δ 5.0-5.4) relative to the corresponding signals for **194**. Finally the N-methyl signal displayed a sharp singlet at δ 2.9.

Scheme 37. Synthetic Pathway to 157.

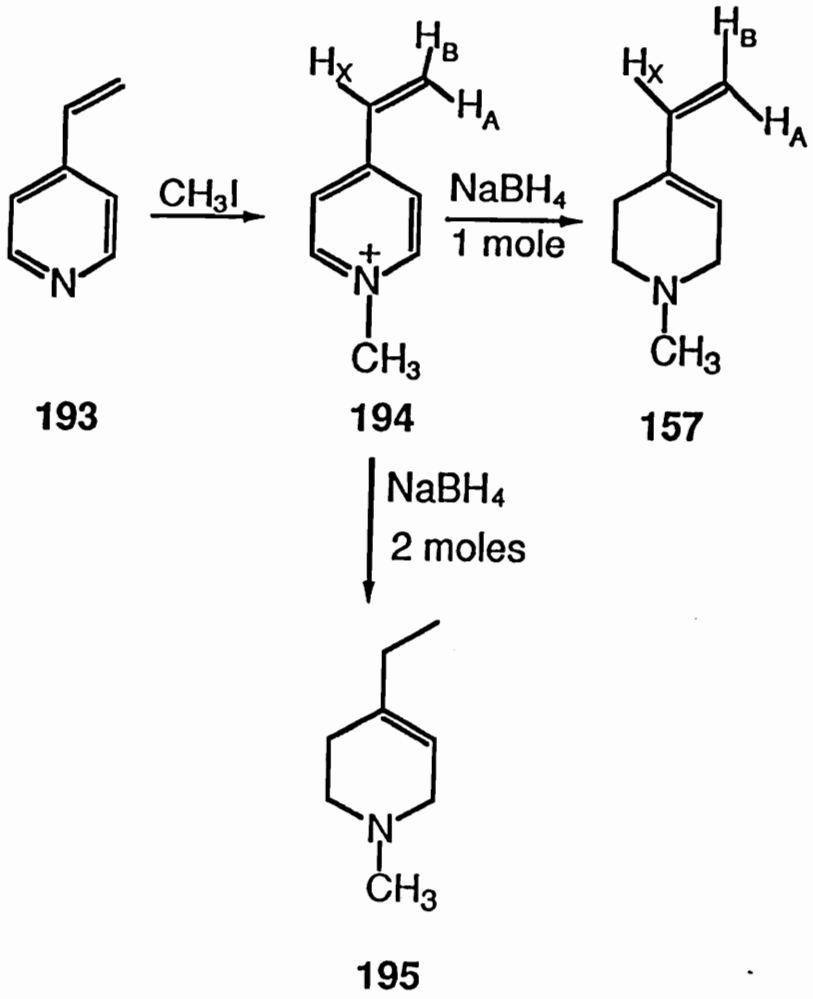

193 **194** **157** **195**

The methodology developed for the synthesis of **158** required (E)-4-(2-phenylethenyl)pyridine (**199**). The synthesis of **199** involved a slight modification of a literature procedure.[152] A reaction mixture containing γ-picoline (**197**) and benzaldehyde (**198**) was heated under reflux in acetic anhydride for 15 hours to generate the desired pyridine **199** (Scheme 38) which was purified by column chromatography on basic alumina to afford a crystalline white solid with a melting point which coincided with the literature report. The GCEI mass spectrum displayed the parent ion at m/z 181 (Fig. 21). The ^{1}H NMR spectrum was in complete agreement with the reported spectrum.[150] The pyridine derivative **199** then was treated with iodomethane to afford the corresponding 1-methyl-(E)-4-(2-phenylethenyl)pyridinium iodide (**200**), the structure of which was confirmed by ^{1}H NMR analysis (Fig. 22). A typical pair of doublets for the C-2 and C-6 and the C-3 and C-5 pyridinium ring protons (δ 8.2-8.9, J = 6 Hz) and the singlet for the N-methyl substituent (δ 4.3) were as expected. Other signals were assigned to the downfield olefinic proton H_A (in closer proximity to the pyridinium moiety) at δ 8.2, the aromatic protons in the region δ 7.2-7.4 and the second olefinic proton H_B which was detected by the integration pattern. The pyridinium species **200** then was easily reduced with sodium borohydride to afford the desired 1-methyl-4-(E)-(2-phenylethenyl)-1,2,3,6-tetrahydropyridine (**158**) in quantitative yield (see Scheme 38). The spectral characterization for **158** involved GCMS analysis which showed the desired molecular ion at m/z 199 (Fig. 23) and ^{1}H NMR analysis (Fig. 24) which showed the characteristic tetrahydropyridine signals and a pair of doublets in the region δ 7.0 and

6.6 which were assigned to the ethenyl protons H_A and H_B, respectively.

Scheme 38. Synthesis of the 4-E-(2-phenylethenyl)tetrahydropyridine analog 158.

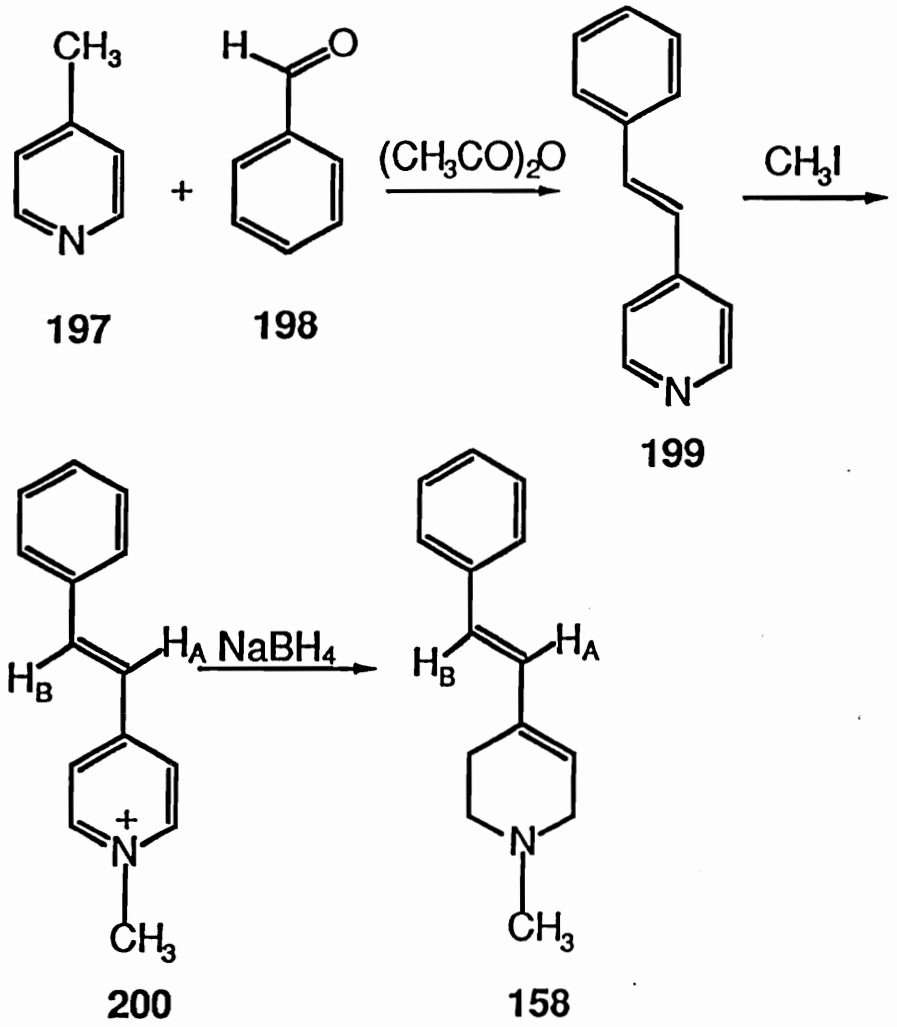

The synthesis of the 4-ethynyltetrahydropyridine analog **159** initially was approached via a dehydration reaction (which has been successfully carried out with related carbinols)[153] of 4-ethynyl-1-methylpiperidin-4-ol (**202**). The synthesis of **202** was carried out in quantitative yield by the reaction between 1-methylpiperidin-4-one (**201**)

and lithium acetylide ethylenediamine complex (Scheme 39).[154,155] The product **202** was isolated and purified as the oxalate salt and characterized by GCMS (Fig. 25) which revealed the parent ion at m/z 139. Other diagnostic mass fragment ions included the species at m/z 122 (**203**) which results from the loss of an OH group from the parent molecule and at m/z 96 (**196**) which results from the loss of the ethynyl substituent and subsequent dehydration. The ^{1}H NMR spectrum (Fig. 26) of **202** was simple to analyze. The acetylenic proton signal appeared as a singlet at δ 3.5, and the C-2 and C-6 methylene proton signals appeared as a broad signal at δ 3.0-3.3. The N-CH_3 protons were located as a sharp singlet at δ 2.75 and the C-3 and C-5 methylene protons appeared as a broad signal at δ 1.9-2.1.

Subsequent attempts to dehydrate **202** with acid catalysts, which included *p*-toluenesulfonic acid, and HCl failed. Starting material only was recovered from these reactions. So we decided to convert **202** to its acetate derivative **204** in an attempt to generate a better leaving group. The synthesis of **204** was attempted by heating **202** under reflux in acetic anhydride (see Scheme 39). This reaction in fact yielded the desired 4-acetoxy-4-ethynyl-1-methylpiperidine (**204**) which was purified by column chromatography and subsequent recrystallization after conversion to the oxalate salt. The characterization of **204** was achieved by GCMS analysis which revealed the molecular ion m/z 181 (Fig. 27). ^{1}H NMR analysis (Fig. 28) showed a spectrum similar to that of **202** except for the presence of a sharp singlet at δ 2.0 which was assigned to the methyl group of the acetoxy substituent. However attempts to induce the elimination

reaction by heating **204** under reflux in dry tetrahydrofuran as well as other conditions, which included heating in the presence of a strong base catalyst such as DBN (1,5-diazabicyclo[4.3.0]non-5-ene)[156] failed.

Scheme 39. Synthesis of intermediates 202 and 204.

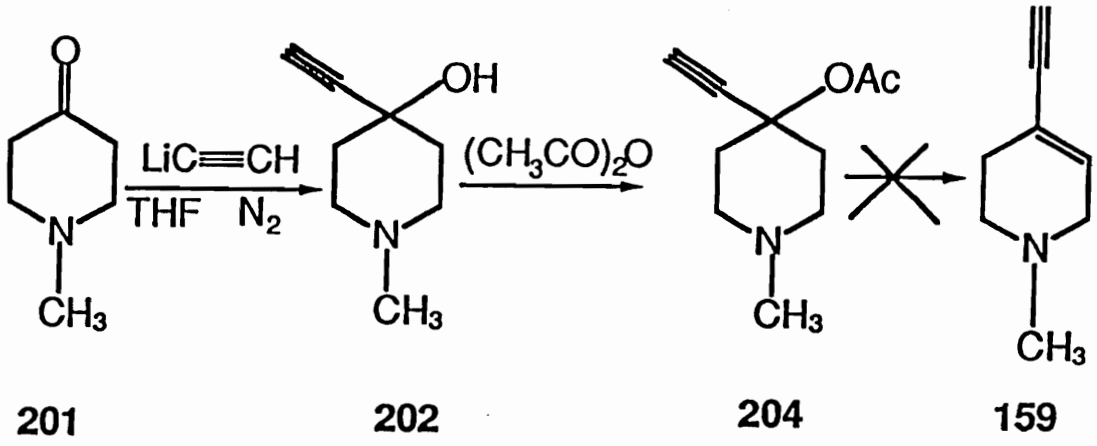

201 **202** **204** **159**

We decided to change the synthetic strategy for **159** altogether and took another approach via 4-ethynylpyridine (**212**) which could be then methylated and reduced to the corresponding tetrahydropyridine **159**. The synthesis of 4-ethynylpyridine has been described in the literature[157,158] but the methods are cumbersome and the overall yields reported are low (3.9% starting from acetylpyridine[155] and 29% from 4-vinylpyridine[156]). However several acetylenic compounds undergo successful coupling with halogen compounds in which halogen is linked to sp^2-carbon (vinylic, allenic, aromatic and heteroaromatic halogen compounds). During the past ten years, considerable progress has been

made with transition metal-mediated organic syntheses. Two important new methods are available for the coupling of acetylenes with the halogen compounds.

a) Reaction of metallated acetylenes, preferably alkynylzinc halides **206**, with the halogen compounds such as **207** in the presence of catalytic amounts of Pd^{II} or Pd^{0} compounds.[182]

b) Reaction of the free acetylene **208** with the halide **209** in the presence of catalytic amounts of Pd^{0} or Pd^{II} compounds, a copper(I)halide and an excess of an amine (to neutralize the hydrogenhalide).

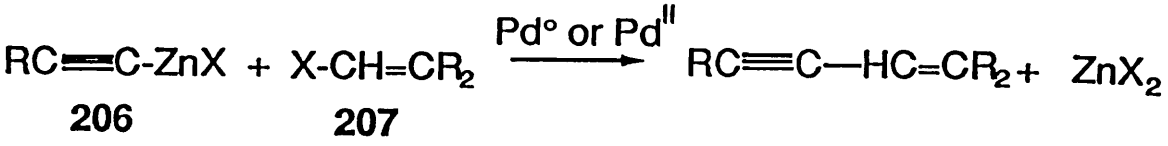

206 **207**

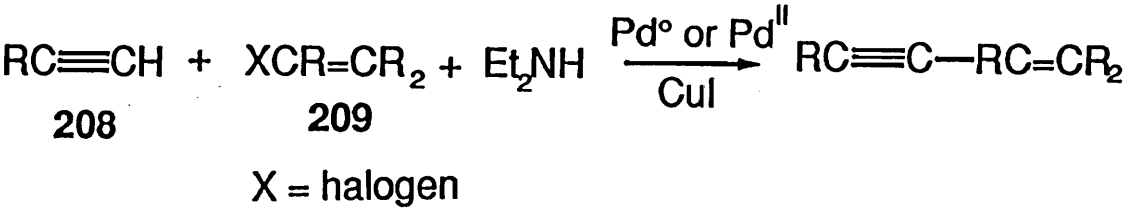

208 **209**

X = halogen

+ $Et_2NH{\cdot}HX$

The reactivity order with respect to the halogen in vinylic halide is I > Br > Cl. The organic halide in the couplings with the alkynylzinc halides is usually an iodide, although vinylic bromides also have been

found to react smoothly.[159] The Pd-catalysts most often used in the reactions decribed above are $Pd(PPh_3)_4$, $PdCl_2(PPh_3)_2$ and $Pd(OAc)_2(PPh_3)_2$. The amount of catalyst preferably is kept as low as possible, for economic reasons, and because palladium residues can give rise to problems during the work-up and the purification of the product.

We therefore elected to utilize a palladium catalyzed cross coupling reaction to synthesize **212** by coupling commercially available 4-bromopyridine (**205**) and ethyne. Since the coupling of ethyne itself to heteroaromatics has not been reported, we chose to use a protected ethyne derivative, since monosubstituted ethynes are known to undergo coupling reactions with a variety of sp^2 centers using Pd^0 or Pd^{II} catalysts.[160,161,162,163] Based on the above reports we chose trimethylsilylethyne (**210**) as the monosubstituted acetylene derivative and employed slight modifications of the methodology reported by Walser *et al.*[164] for the synthesis of arylacetylenes. We anticipated that the coupling reaction between **205** and trimethylsilylethyne in presence of a Pd catalyst would lead to the formation of 4-trimethylsilylpyridine (**211**) which could be subjected to hydrolysis to obtain 4-ethynylpyridine (**212**) (Scheme 40). (The pyridine **212** then could be methylated and reduced to afford **159**). Technically the reaction involved treatment of 4-bromopyridine (**205**) with triphenylphosphine, CuI, acetonitrile, and triethylamine. This mixture was degassed with nitrogen and then $Pd(OAc)_2$ and trimethylsilylethyne (**210**) were added. The reaction mixture was allowed to stir under nitrogen for 6 hours at room temperature at the end of which time GCMS analysis of the crude

reaction mixture indicated complete disappearance of the starting material **205** and formation of **211**. The trimethylsilylethynylpyridine derivative **211** was purified by passing the crude product through a basic alumina column. The purity of the oily **211** was assessed by GCMS which indicated a single product (Fig. 29). The spectrum displayed the expected parent ion at m/z 175. The subsequent hydrolysis of crude **211** was achieved using K_2CO_3 in methanol. This reaction generated in high yield a white solid that was identified as **212** by its melting point which was consistent with the literature report.[166] However treatment of **212** with the standard methylation conditions involving reaction with iodomethane in acetone led to extensive decomposition and the formation of a black solid which could not be identified by the usual spectral methods. Presumably the 4-ethynyl-1-methylpyridinium species was reactive and underwent nucleophilic attack by the iodide counter ion in solution which led to its decomposition. We therefore decided to methylate **211** which would lead to the 1-methyl-4-trimethylsilylpyridinium species **213**. Subsequent reduction of **213** with sodium borohydride potentially could give rise to **159**. Methylation of **211** with iodomethane gave the pyridinium species **213** (see Scheme 40) as a dark yellow solid the structure of which was confirmed by ^1H NMR analysis (Fig. 30). The pair of doublets centered at δ 8.9 and 8.1 were assigned to the pyridinium ring protons C-2 and C-6 and C-3 and C-5, respectively. The sharp singlet at δ 4.2 ppm was assigned to the N-CH_3 group and, as expected the trimethyl functionality arose as a singlet at δ 0.38. Upon standing **213** slowly changed its physical appearance to a

greyish color. However the molecule still retained its ^1H NMR characteristics even after a drastic change in appearance. In addition to the satisfactory ^1H NMR characteristics, the microanalytical data also were consistent with the expected structure. Subsequent attempts at reduction with sodium borohydride afforded alongwith the desired **159**, other products which were identified by GCMS to be the 4-ethenyl-1-methyl- (**157**), and 4-ethyl-1-methyl- (**195**) tetrahydropyridine derivatives and attempts to purify **159** were not successful and this strategy also was abandoned.

Scheme 40. Synthesis of the trimethylsilylethynylpyridinium species 213.

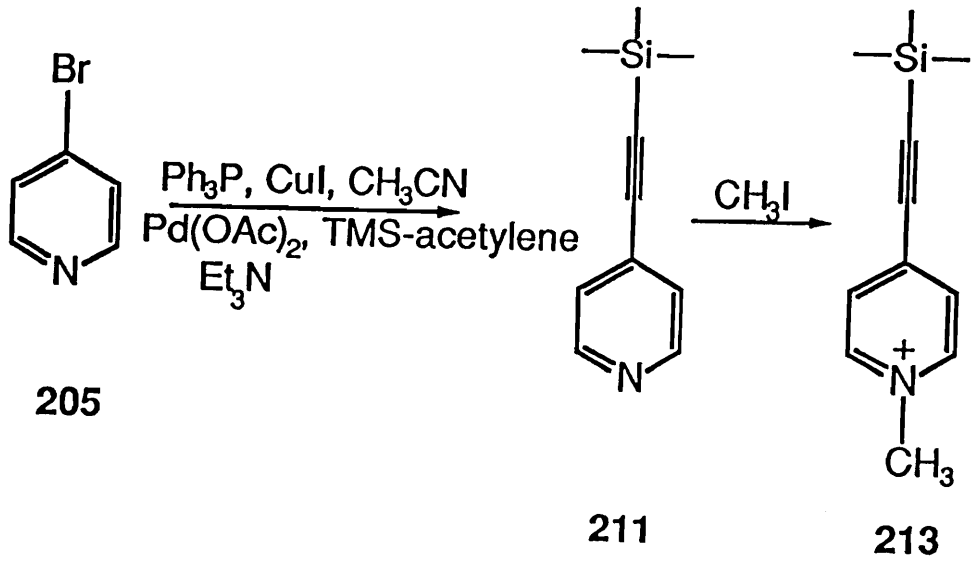

Upon further examination of the literature, an alternative pathway to 4-ethynylpyridine (**212**) involving the palladium catalyzed coupling of commercially available 2,2-dimethyl-3-butyn-2-ol (**214**) with 4-bromopyridine (**205**) became apparent.[166] This reaction is a modification of the Stephans-Castro coupling[167] which involves the coupling of copper(I)arylacetylenes with iodoarenes or iodoalkenes. The disadvantage of the Stephans-Castro coupling is that it requires vigorous reaction conditions and tedious operations in the synthesis of the copperacetylides. In the above synthesis of **212**, catalytic amounts of coupling agents *bis*(triphenylphosphine)palladium dichloride-cuprous iodide in diethylamine are used and the reaction conditions are mild. No coupling occurs at room temperature in the absence of cuprous iodide, indicating that the role of cuprous iodide is important to facilitate the substitution reaction. Although the detailed mechanism of the reaction has yet to be clarified, it is proposed[167] that the substitution occurs through an initial formation of *bis*(triphenylphosphine)dialkynylpalladium (II) species **217** by insertion of the acetylenic compound **216** into the Pd(II) catalyst **215**. The resulting species *bis*(triphenylphosphine)palladium (0) (**218**) is formed through the reductive elimination of 1,4-diphenylbutadiyne (**219**). Subsequent oxidative addition of arylhalide, followed by an alkynylation of the adduct **220** gives an arylalkynyl derivative of palladium **221**. Compound **221** then regenerates the original bis(triphenylphosphine)palladium (0) (**218**) through the reductive elimination of the substitution product **222** (Scheme 41).

Scheme 41. Proposed Mechanism for Pd catalyzed Coupling Reactions.

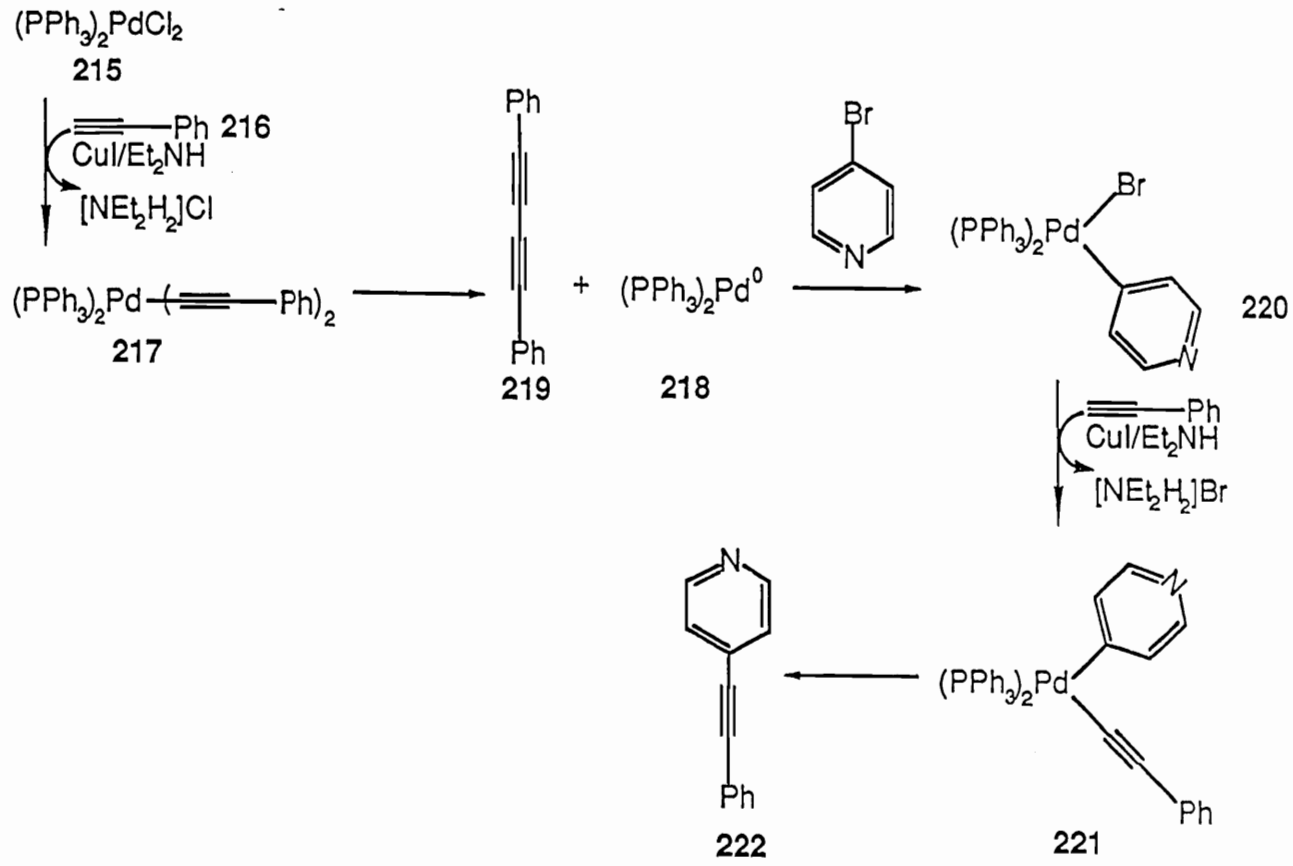

Thus the synthesis of **159** was approached by the condensation of **205** with the protected acetylene **214** in presence of CuI, diethylamine and the commercially available Pd catalyst namely *bis*(triphenylphosphine)Pd(II) dichloride in acetonitrile (Scheme 42). This reaction furnished 2-methyl-4-(4-pyridyl)-3-butyn-2-ol (**223**) in high yield. The product was obtained as a crystalline white solid by basic alumina chromatography. The melting point and ^{1}H NMR spectrum of **223** were in complete agreement with the literature report.[166] GCMS analysis revealed the expected parent ion at m/z 161 (Fig. 31).

Methylation of **223** with iodomethane in dry THF yielded the protected pyridinium product **224** in 89% yield. The structure of **224** was established by ^{1}H NMR analysis (Fig. 32). As expected the pyridinium ring protons, C-2 and C-6 and C-3 and C-5, occurred as doublets at δ 8.95 and 8.1, respectively. The singlet at δ 5.8 was assigned to the OH group and the singlet at δ 4.3 to the N-CH_3 substituent. The sharp singlet at δ 1.5, which corresponded to 6 protons, was assigned to the dimethyl group. Microanalytical data were consistent with the expected structure. The protected pyridinium intermediate **224** was reduced in high yield with sodium borohydride to the protected ethynyltetrahydropyridine derivative **225** which was isolated and characterized as its oxalate salt. Structure confirmation was based on the GCMS data which displayed a parent ion at m/z 179 (Fig. 33) and the ^{1}H NMR spectrum (Fig. 34) which showed a broad signal at δ 5.9 (the C-5 olefinic proton) and a broad signal at δ 3.55, the triplet at δ 3.1, the sharp singlet at δ 2.8 ppm and the broad signal at δ 2.33 all are characteristic of an N-methyltetrahydropyridine

ring system and were assigned in part by analogy to the assignment for **157**. Finally the singlet at δ 1.36 was assigned to the gem-dimethyl group.

Base (NaOH) hydrolysis of **225** in toluene yielded the desired target molecule 4-ethynyl-1-methyltetrahydropyridine (**159**) which was isolated and purified as its oxalate salt. Characterization of the final product included GCMS analysis, which showed the parent ion at m/z 121 (Fig. 35), and ^{1}H NMR analysis (Fig. 36). The spectrum resembled that of **225** except that the signal for the dimethyl group at δ 1.36 had disappeared and a new singlet at δ 4.0 assigned to the acetylenic proton, appeared.

Scheme 42. Synthetic pathway to 159.

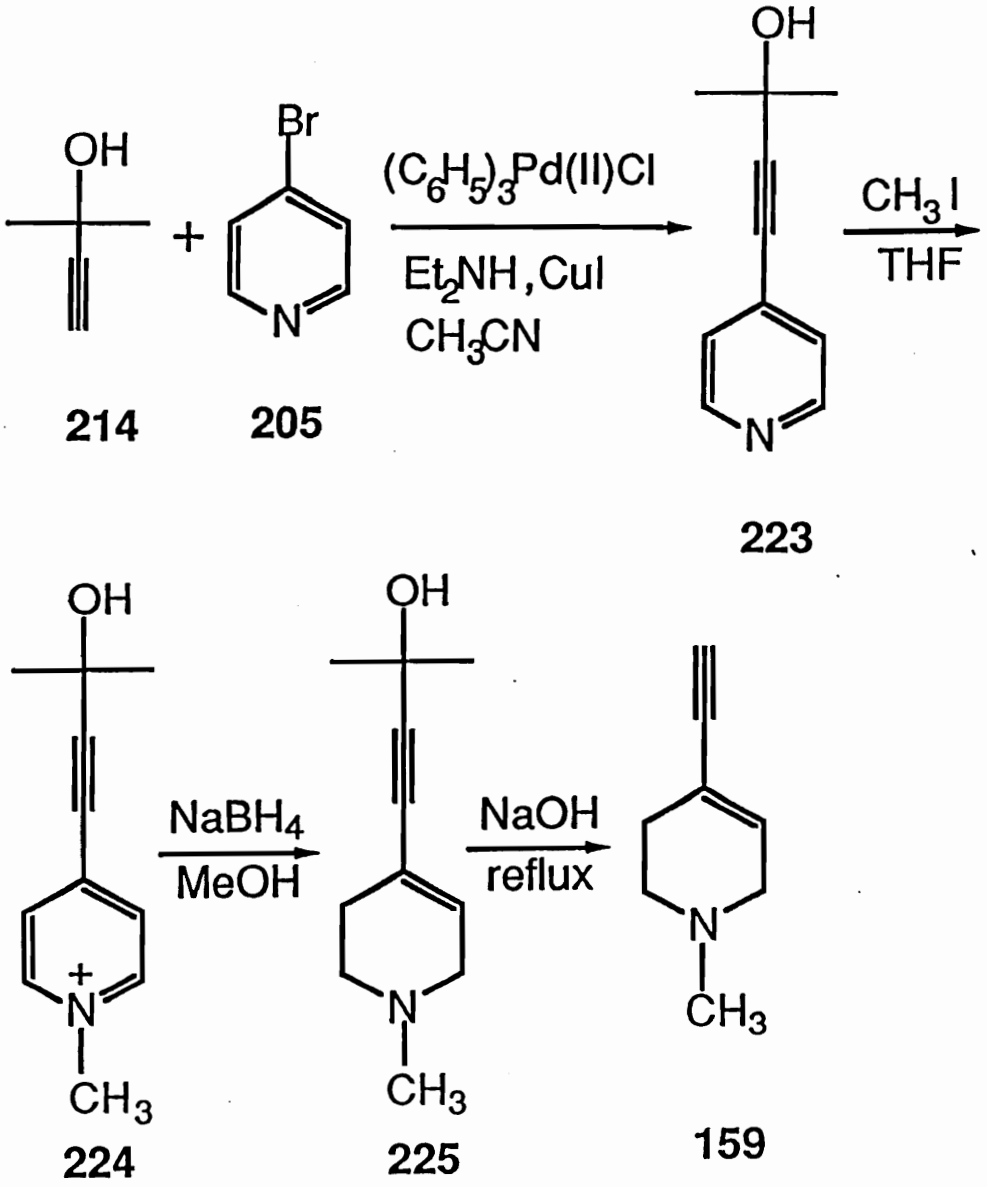

Hydrolysis of **223** under the same conditions (NaOH/toluene) as those used for **225** provided an alternative route to 4-ethynylpyridine (**212**) in excellent yield (Scheme 43). The white crystalline solid possessed the mp and the ^1H NMR features (Fig. 37) of those described in the literature.[166] Subsequent reaction of **212** with iodomethane using dry

THF instead of acetone as solvent led to the successful synthesis of the pyridinium product **226** which precipitated immediately upon formation from the reaction mixture and was characterized by conversion to the perchlorate salt. The success of this reaction (which failed during earlier attempts) was probably due to a change in the solvent system which involved THF instead of acetone. The limited solubility of **226** in THF led to its immediate precipitation which may have precluded its decomposition as observed in acetone. The ^1H NMR spectrum of **226** (Fig. 38) was similar to that **224** except that the signal for the dimethyl group was replaced by a singlet at δ 5.38 ppm which we assigned to the acetylenic proton. We were able to reduce **226** with with 1 mole of sodium borohydride to obtain **159** (see Scheme 43).

Scheme 43. Synthesis of the 4-ethynylpyridinium derivative 226.

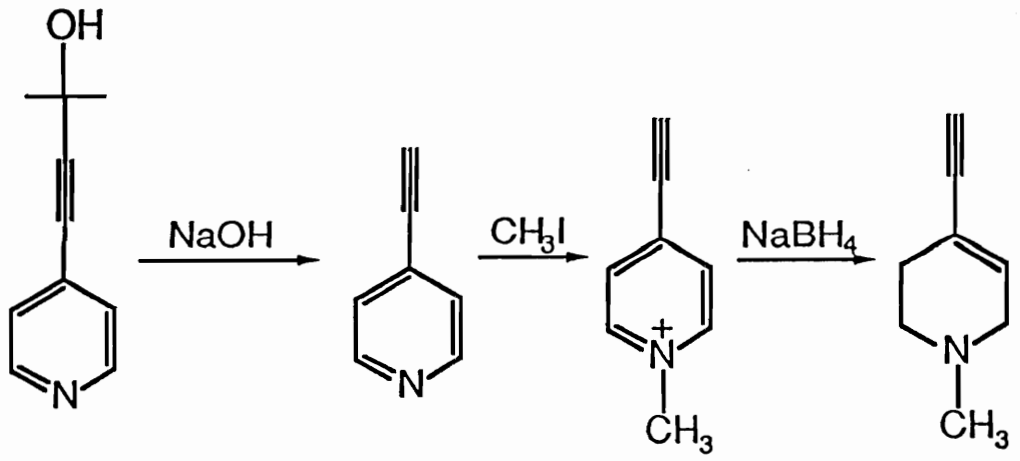

223 **212** **226** **159**

The final target molecule needed for the biological studies with MAO-B was the 1-methyl-4-phenylethynyl-1,2,3,6-tetrahydropyridine derivative **160**. According to a literature search the synthesis of **160** could be approached by two different strategies.[168,169] A literature procedure[168] directed towards the synthesis of ethynylquinolines involved a Pd^0 or Pd^{II} catalyzed coupling of the heteroaromatic system with phenylethyne in the presence of CuI and triethyl amine as solvent. In our case the use of 4-bromopyridine (**205**) could generate the corresponding 4-(2-phenylethynyl)pyridine derivative **222** which subsequently could be methylated and the resulting pyridinium reduced to the desired tetrahydropyridine analog **160**.

An attempt was made to synthesize **222** using catalytic amounts of CuI and the commercially available *tetrakis*triphenylphosphinepalladium ($Pd[PPh_3]_4$) in freshly distilled triethylamine as solvent. The reaction mixture was stirred at room temperature for 24 hours during which time it turned dark brown in color. GCMS analysis displayed a peak with a parent ion at m/z 179 (Fig. 39) confirming the formation of the 4-(2-phenylethynyl)pyridine species **222**. The principal compound detected in the GCMS was the starting material **205**. The reaction was allowed to stir for an additional 48 hours in an effort to improve the overall conversion to the desired product GCMS analysis of this reaction mixture, however still indicated the presence of **205** as the principal component of this reaction mixture. The reaction mixture was worked up to afford a dark brown oil which was treated with an excess of iodomethane which gave after stirring

overnight a brown solid precipitate. The solid was recrystallized from methanol/benzene to afford light brown crystals which were identified as 4-bromo-1-methylpyridinium iodide by NMR analysis. Further concentration of the mother liquor provided dark yellow needles of the 1-methyl-4-(2-phenylethynyl)pyridinium species **228** in about 10 % yield. The formation of **228** was confirmed by ^1H NMR analysis which will be described below.

The second approach to **228** and **160** employed a modified Pd catalyzed cross coupling reaction previously applied to heteroaromatics such as halofurans.[169] The reaction (Scheme 44) consisted of treatment of phenylethyne with *n*-BuLi to generate the lithiated phenylethyne which was treated with anhydrous $ZnCl_2$. This mixture was transferred via a cannula to a flask containing **205** and the Pd catalyst $Pd[(Ph_3P)]_4$. The reaction mixture was heated under reflux overnight. Analysis of this mixture by GCMS showed the presence of a single product which was characterized as the desired **222** by its mass spectrum which displayed the parent ion at m/z 179 (Fig. 39). Subsequent methylation of **222** with iodomethane yielded **228** in high yields. The key diagnostic signals for **228** in the ^1H NMR spectrum (Fig. 40) was the N-CH_3 singlet which ocurred at δ 4.2 ppm, the pyridinium ring protons and the aromatic ring protons which appeared as expected downfield between δ 7.5-9.0 ppm. Reduction of **228** with sodium borohydride gave the desired tetrahydropyridine **160** (see Scheme 44). The phenylethynyltetrahydropyridine was isolated, purified and characterized as its oxalate salt. The GCMS displayed the molecular ion $M^{\cdot+}$ at m/z 197

(Fig. 41). The assignments of the signals in the ^1H NMR spectrum (Fig. 42) included the aromatic protons which, as expected appeared at 7.5 ppm. The remaining proton signals corresponding to the N-methyltetrahydropyridine ring system appeared at chemical shifts corresponding to those observed in the ^1H NMR spectrum for **159**.

Scheme 44. Synthetic Pathway to 1-Methyl-4-phenylethynyl-1,2,3,6-tetrahydropyridine 160.

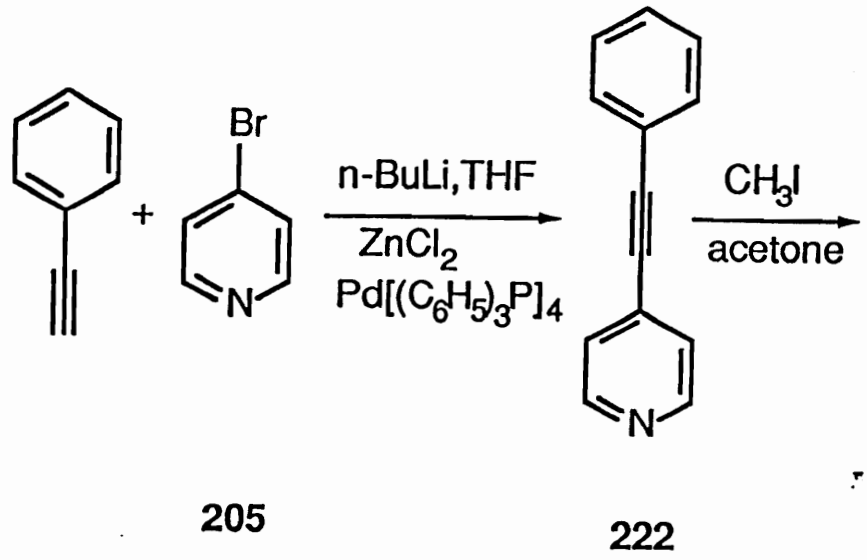

205 222

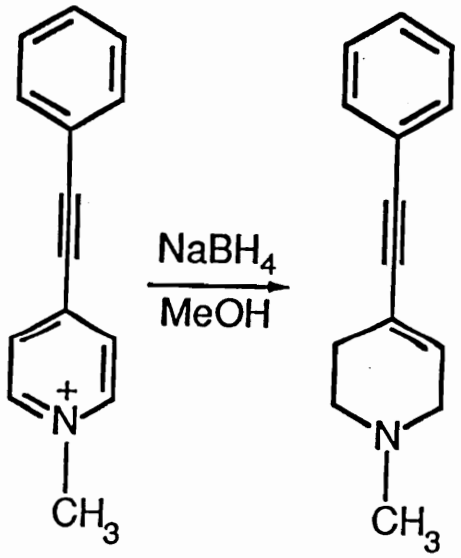

228 160

3.1.3. Synthesis of Dihydropyridinium Metabolites.

Characterization of the MAO-B substrate properties of the tetrahydropyridine derivatives **152, 157, 158** and **159** required the synthesis of the corresponding dihydropyridinium species **233, 234, 235** and **236** (Schemes 45 and 46). We had anticipated, based on the mechanism of bioactivation of MPTP,[123] that these molecules could well be the initial MAO catalyzed oxidation products. Thus the dihydropyridinium derivatives were required for metabolite structure confirmation.

The methodology applied for the synthesis of these dihydropyridinium species was based on the Polonovski reaction which has been utilized successfully in our laboratory[170] and by other workers.[171] The Polonovski reaction involves the α-carbon oxidation of amines to imines. Thus the amine is reacted with hydrogen peroxide to afford the corresponding amine-N-oxide which is then treated with trifluoroacetic anhydride to yield the corresponding iminium species. Three tetrahydropyridine derivatives, **152, 158** and **159**, were treated with *m*CPBA at 0 °C (Scheme 45) to yield the corresponding tetrahydropyridine-N-oxides **229, 231** and **232**, respectively. The N-oxides were isolated and characterized by ^{1}H NMR analysis as their crystalline *meta*-chlorobenzoate salts.

The ^{1}H NMR spectrum of **229** (Fig. 43) displayed a multiplet at δ 7.2-8.0 integrating to 9 protons and were assigned to the 5 aromatic protons of **229** and 4 aromatic protons of the*m*-chlorobenzoic acid moiety. The doublet at δ 6.0 was assigned to the C-5 olefinic proton. The upfield

region of the spectrum (δ 3.5-4.7) displayed a complex multiplet which integrated to 6 protons and was assigned to the C-2 and C-6 tetrahydropyridyl ring methylene protons and the methylene protons of the n-propyl group adjacent to the nitrogen. The multiplet at δ 2.7-3.2 which integrated to 2 protons, was assigned to the C-3 methylene protons of the tetrahydropyridyl ring and the multiplet at δ 2.1 to the methylene protons of the n-propyl substituent β to the nitrogen. Finally the triplet at δ 1.1 was assigned to the terminal methyl group of the n-propyl functionality. The ^{1}H NMR spectrum of **231** (Fig. 44) displayed the aromatic protons (5 ArH belonging to the C(4)-phenylethenyl and 4 ArH belonging to the *m*-chlorobenzoic acid moiety) at δ 7.3-8.0. The doublet at δ 6.7 was assigned to the olefinic proton of the C(4)-substituent which was in closer proximity to the pyridine ring while the doublet at δ 6.5 was assigned to the other olefinic proton of the C(4)-substituent. The C-5 proton signal of the tetrahydropyridine ring system appeared as a singlet at δ 5.7. The multiplets at δ 4.1-4.5 and δ 3.7-3.9 were assigned to the C-6 and the C-2 methylene protons respectively. The N-CH_3 group displayed a sharp singlet at δ 3.5 and the C-3 methylene protons displayed a multiplet relatively upfield at δ 2.7-2.9. The ^{1}H NMR spectrum of **232** (Fig. 45) displayed a multiplet at δ 7.2-7.6 which was assigned to the aromatic protons of the *m*-chlorobenzoic acid. The C-5 olefinic proton appeared as a singlet at δ 6.0. The multiplet centered at δ 3.6-3.9 were assigned to the C-6 and the C-2 methylene protons respectively. The N-CH_3 group appeared as a sharp singlet at δ 3.5 and the singlet at δ 4.1 was assigned to the acetylenic proton. Finally the C-3 methylene protons

displayed a multiplet at δ 2.5-2.8. The structure of the above compounds (**229, 231,** and **232**) were confirmed by microanalysis.

Treatment of the N-oxides **229, 231** and **232** with trifluoroacetic anhydride at 0 °C (see Scheme 45) yielded the desired dihydropyridinium products as their trifluoroacetate salts. Subsequent treatment with 70% methanolic perchloric acid afforded the dihydropyridinium products **233, 235** and **236** as their stable crystalline perchlorate salts in excellent yields. The dihydropyridinium species were characterized by ^{1}H NMR and UV analysis. The NMR spectrum (Fig. 46) for **233** displayed a pair of doublets at δ 8.7 and 7.1 which were assigned to the C-6 proton and C-5 protons. As usual the aromatic protons appeared at δ 7.4-7.6. The multiplet at δ 3.8-4.0, which integrated to 4 protons, was assigned to the C-2 and the n-propyl methylene protons α to the nitrogen. The triplet at δ 3.2 was assigned to the C-3 methylene protons. The multiplet at δ 1.8 and the triplet at δ 1.0 were assigned to the n-propyl methylene protons β to the nitrogen and the terminal-methyl substituent. The UV analysis (MeOH) of **233** (Fig. 47) displayed a chromophore with λ_{max} 343 nm (ε 16,750).

The NMR spectrum of **235** (Fig. 48) displayed the characteristic doublet at δ 8.5 which was assigned to the C-6 proton. The multiplet at δ 7.2-7.7 included the 5 aromatic protons and the olefinic proton (in closer proximity to the nitrogen) on the C(4)-phenylethenyl substituent. The remaining dihydropyridinium ring proton centered as a broad signal at δ 6.6. The triplets at δ 4.0 and δ 3.0 were assigned to the C-2 and C-3 methylene protons. The N-CH_3 substituent appeared as a sharp singlet at δ 3.6. The UV spectrum (MeOH) of **235** (Fig. 49) displayed a chromophore

with λ_{max} 380 nm (ε 24,000).

The NMR spectrum of **236** (Fig. 50) displayed similar characteristics as that of **233**. The C-6 and the C-5 protons centered as broad signals at δ 8.5 and 6.7. The sharp singlets at δ 5.3 and 3.6 were assigned to the acetylenic proton and the N-CH_3 group. The C-2 methylene protons appeared as a triplet at δ 3.7-3.9 and the multiplet at δ 2.7 was assigned to the C-3 methylene protons. The UV spectrum (CH_3CN) of **236** (Fig. 51) showed a chromophore with λ_{max} 308 nm (ε 6000). All of the dihydropyridinium derivatives were characterized by elemental analyses.

The route to the 4-ethenyldihydropyridinium system **234** involved a different starting material, namely 4-ethenyl-1-methylpiperidin-4-ol **(237)**, which was obtained from a Grignard reaction between 1-methyl-4-piperidone **(201)** and vinylmagnesium bromide in high yields (Scheme 46). The carbinol **237** was characterized by GCMS analysis which revealed the parent molecular ion at $M^{\cdot+}$ 141 and subsequently was converted to its oxalate salt and the purity of which was demonstrated by ^1H NMR analysis (Fig. 53). The NMR spectrum consisted of a doublet of doublets at δ 5.9 ppm, which was assigned to the olefinic proton based on the ABX type splitting by the terminal cis and trans olefinic protons (as described in the case of **194**). The doublet at δ 5.2 with a coupling constant J = 18 Hz was assigned to the terminal *trans* olefinic proton and the doublet at δ 5.1 with a coupling constant J = 11 Hz was assigned to the terminal *cis* olefinic proton. The C-2 and the C-6 methylene protons formed a broad multiplet which centered at δ 3.2. The singlet at δ 2.7 was assigned to the N-CH_3 group. Finally a complicated multiplet spanning 1.6-1.9 ppm was

assigned to the C-3 and the C-5 methylene protons. Microanalytical data were consistent with the expected structure. Treatment of **237** under the Polonovski conditions gave the resulting *m*-chlorobenzoate salt of the N-oxide **230** as an oil. All attempts to obtain **230** as a solid failed. The *m*-chlorobenzoate salt of **230** was subjected to basic alumina chromatography which afforded the free N-oxide as a white solid. The ^{1}H NMR spectrum (Fig. 54) of **230** showed a downfield region from δ 6.0-5.1 which was similar to that of **237**. The doublet of doublets at δ 6.0 was assigned to the olefinic proton based on the splitting by the terminal *cis* and *trans* olefinic protons. The pair of doublets at δ 5.3 (J = 17 Hz) and δ 5.1 (J = 11 Hz) was assigned to the terminal *trans* and the *cis* protons, respectively. The OH group centered as a broad signal at δ 4.6. The multiplets at δ 3.6 and 3.1 were assigned to the C-2 and C-6 methylene protons. The N-CH_3 group appeared as a sharp singlet at δ 3.3 and the multiplet spanning δ 1.5-2.5, which integrated to 4 protons, was assigned to the C-3 and C-5 methylene protons. The N-oxide **230** was subsequently treated with trifluoroacetic anhydride (see Scheme 46) to generate the dihydropyridinium species **234**. The pathway of this reaction probably involves the formation of the imnium species **238** which rearranges to the enamine **239** follwed by subsequent elimination to **234**. This product was subsequently converted to the stable perchlorate salt and analyzed by ^{1}H NMR (Fig. 55) and UV (Fig. 56). The NMR spectrum of **234** was typical of that described above. The C-6 and C-5 dihydropyridinium protons appeared at δ 8.6 and 6.5. The olefinic protons on the C(4) positions appeared in the expected regions as described for **230**. The triplets at δ 3.9 and 2.8 corresponded to

the C-2 and C-3 methylenes protons. Finally the N-CH_3 group appeared at δ 3.61. The UV spectrum (MeOH) of **234** displayed a chromophore with λ_{max} 309 nm (ε 6000). Microanalytical data were consistent with the proposed structure.

Scheme 45. Synthesis of the dihydropyridinium intermediates.

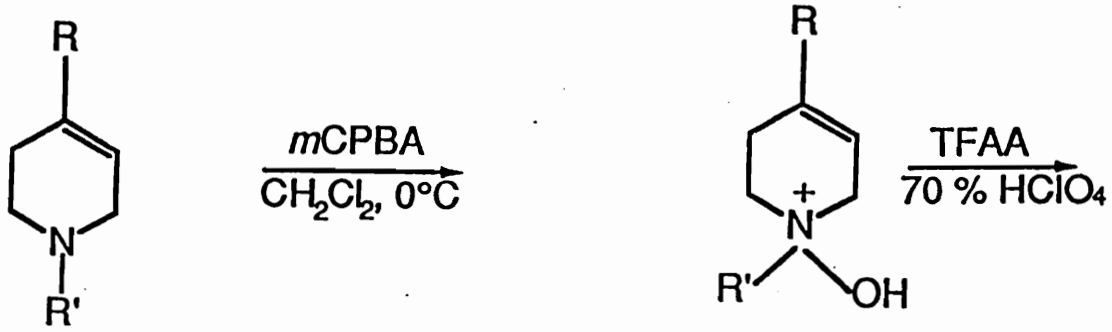

	R	R'	N-oxides
152:	C_6H_5	$CH_2CH_2CH_3$	**229**
158:	$C_6H_5CH{=}CH$	CH_3	**231**
159:	$C{\equiv}CH$	CH_3	**232**

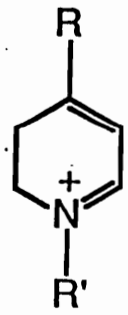

	R	R'
233:	C_6H_5	$CH_2CH_2CH_3$
235:	$C_6H_5CH{=}CH$	CH_3
236:	$C{\equiv}CH$	CH_3

Scheme 46. Synthesis of the ethenyldihydropyridinium system.

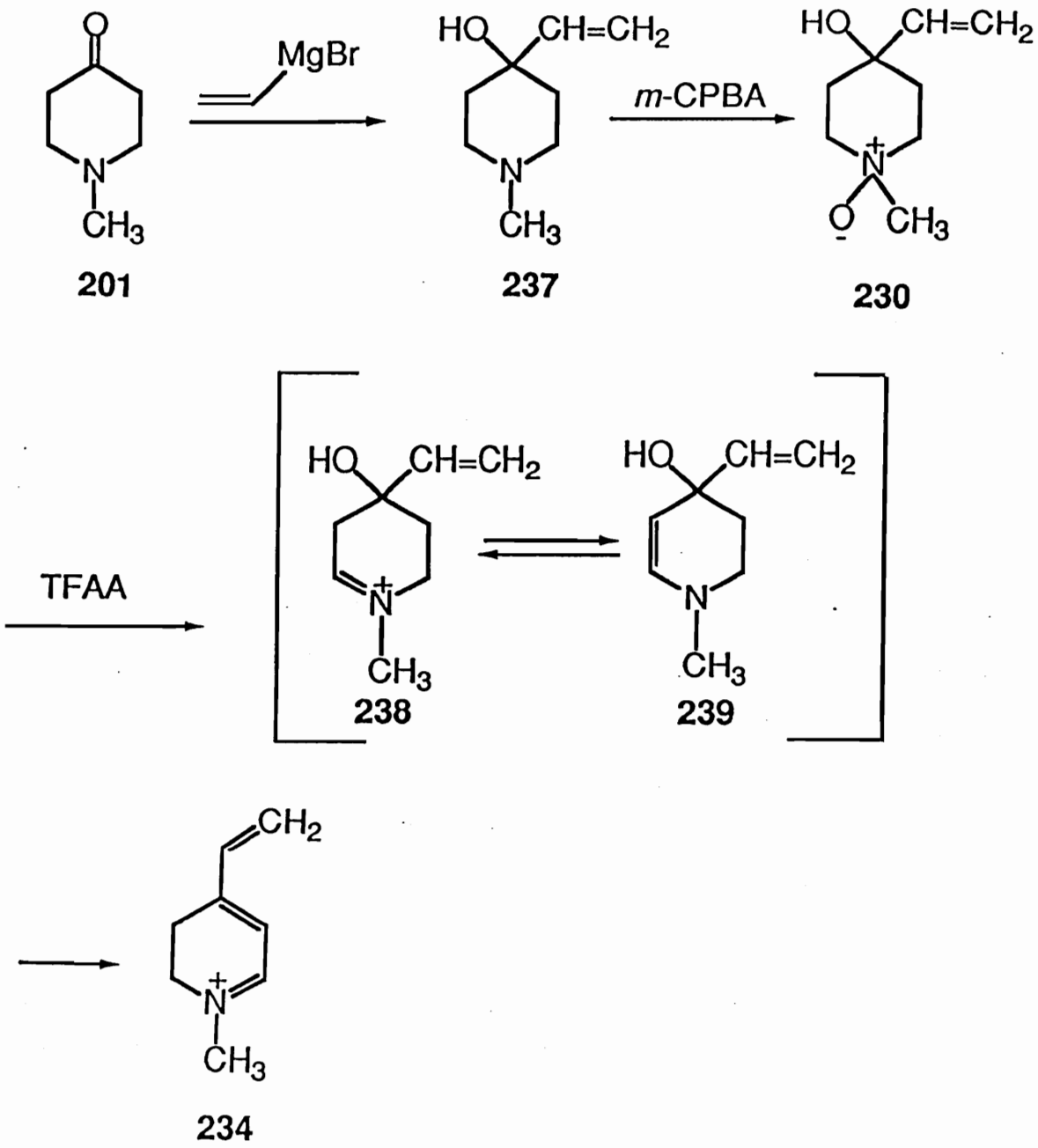

We also required other dihydropyridinium intermediates to estimate their relative rates of autoxidation under physiological conditions to the fully aromatized pyridinium species. These compounds also have been important in attempts to understand the chemical factors which are responsible for the oxidative behavior of the dihydropyridinium intermediates to the putative neurotoxic compounds. The details of these studies are documented in Chapter 3.

The dihydropyridinium species of interest were the 4-(2,6-dimethylphenyl)-, 4-t-butyl- and the 4-thiophenoxydihydropyridinium analogs **246, 247** and **248**, respectively. The compounds were synthesized utilizing the well established Polonovski conditions as described earlier. The typical reactions (Scheme 47) consisted of treatment of the tetrahydropyridine derivatives[172] **240, 241** and **242** with *m*-CPBA to generate the N-oxides **243, 244** and **245**, respectively. The N-oxides **243,** and **245** were characterized by ^{1}H NMR analysis, wheras the N-oxide **244** could not be isolated in a crystalline form and was thus used in the crude form as an oily residue. The NMR spectrum of **243** (Fig. 57) displayed a aromatic region at δ 7.0-7.9 which integrated to 7 protons which were assigned to the 3 aromatic protons on the dimethylphenyl ring and the 4 aromatic protons on the *m*-chlorobenzoic acid moiety. The C-5 olefinic proton centered as a broad signal at δ 5.4. The C-6 and the C-2 methylene protons centered as broad signals at δ 4.4 and 3.9, respectively. The N-CH_3 group appeared as a sharp singlet at δ 3.7 and the C-3 methylene protons displayed a multiplet at δ 2.3-2.9. Finally the singlet at δ 2.3 was assigned to the dimethyl substituent on the aromatic ring.

The ^1H NMR spectrum for **245** (Fig. 58) displayed the aromatic region at δ 7.4-7.9 which corresponded to the 5 aromatic protons on the C(4)-thiophenoxy substituent and the 4 aromatic protons on the *m*-chlorobenzoic acid moiety. The C-5 olefinic proton centered as a broad signal at δ 5.8. The broad signal which centered at δ 4.4 was assigned to the C-6 methylene protons. The C-2 methylene protons appeared as a multiplet at δ 3.8-3.9 and the N-CH_3 group appeared as a sharp singlet at δ 3.5. Finally the C-3 methylene protons appeared as a multiplet at δ 2.3-2.9.

These N-oxides subsequently were treated with trifluoroacetic anhydride to afford the dihydropyridinium products **246, 247** and **248,** respectively, which were characterized as their crystalline perchlorate salts. The dihydropyridinium derivatives were analyzed by ^1H NMR and UV spectroscopy. The NMR analysis of **246** (Fig. 59) revealed characteristics of a typical dihydropyridinium compound with the C-5 and C-6 protons appearing as doublets at δ 6.4 and δ 8.6. The aromatic protons displayed a multiplet at δ 7.1-7.2. The triplets at δ 4.0 and 2.9 corresponded with the C-2 and C-3 methylene protons and the N-CH_3 group appeared as a sharp signal at δ 3.6. Finally the gem-dimethyl substituent resonated at δ 2.22. The UV spectrum (pH 7.4 phosphate buffer, Fig. 60) showed a chromophore at λ_{max} 286 nm (ε 17000). The NMR spectrum of **247** (Fig. 61) was similar in characteristics to that of **246** except for the expected difference in the aromatic region and the replacement of the singlet for the dimethyl substituent by a singlet for the tert-butyl protons which appeared at δ 1.1. The NMR spectrum of **248** (Fig. 62) was also similar to that of **246** except that the signal for the

dimethyl aromatic substituent was missing. The UV spectrum of **248** (pH 7.4 phosphate buffer, Fig. 63) displayed a chromphore with λ_{max} 354 nm (ε 15,200). All of the dihydropyridinium compounds gave consistent microanalytical data.

Scheme 47. Synthesis of dihydropyridinium intermediates 246, 247, 248.

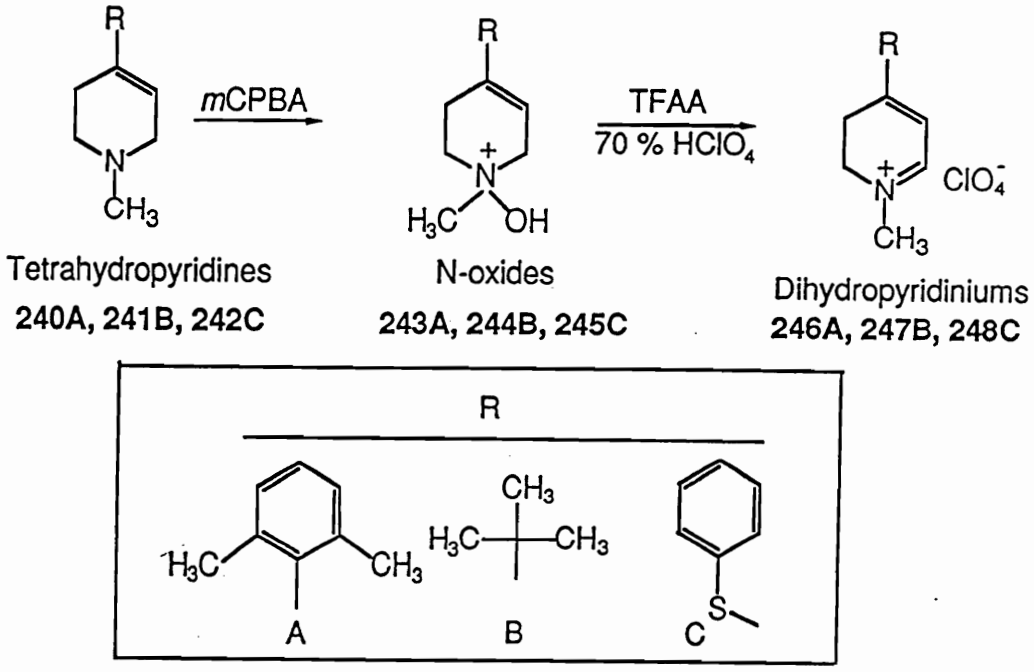

3.1.4. Synthesis of 1-cyclopropylpiperidin-4-one.

As discussed in Chapter 2, the 1-cyclopropyl-4-phenyl-1,2,3,6-tetrahydropyridine analog **130** was a excellent MAO-B inactivator and therefore we were interested in designing a variety of N-cyclopropyl analogs which via selective binding of the C-4 substituent could serve as potential selective inactivators of either form of MAO. We focussed our attention on the synthesis of 1-cyclopropylpiperidin-4-one (**164**) which we anticipated to be a potentially useful synthetic intermediate analogous to 1-methylpiperidin-4-one (**201**) which served as a key intermediate in the synthesis of MPTP[140] and the 4-cyclopropyl analog **131**. The synthesis of **164** was also awarded high priority as the current synthetic pathway to **130** was tedious. The synthetic strategy that developed from a literature survey[173,174] involved reaction of cyclopropylamine with ethyl acrylate (**249**) to give the N,N-*bis*alkylated adduct **250**. Cyclization under Dieckmann conditons should afford β-ketoacid **252** which could be hydrolyzed and decarboxylated to yield **164** (Scheme 48). An initial attempt was made modeled after literature condition[173] in which a 2-fold excess of **249** and cyclopropylamine are heated under reflux. During the course of this 5 hour reaction analysis of the crude mixture by GCMS showed approximately a 2:1 ratio of the monoalkylated product **251** ($M^{\cdot+}$ 157, Fig. 64) and the desired *bis*alkylated product **250** ($M^{\cdot+}$ 257, Fig. 65). Heating for longer periods of time to allow conversion of **251** to **250** failed to improve the yield of the reaction. We then modified the procedure and used a 4-fold excess of **249**. Instead of heating the reaction mixture, the starting materials were stirred under nitrogen at room temperature in

dry ethanol for 72 hours.

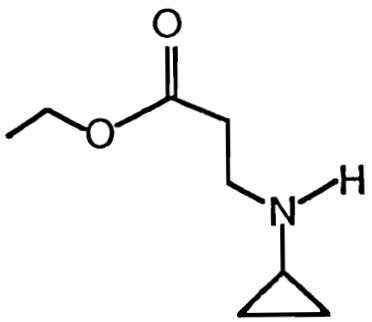

251

GCMS analysis showed complete conversion to the desired product **250** which was obtained as a colorless oil in essentially quantitative yields. Compound **250** was characterized by GCMS which showed a single peak in the total ion current chromatogram and displayed the expected molecular ion at m/z 257 (Fig. 65). The ^{1}H NMR spectrum (Fig. 66) showed a quartet centered at δ 4.1 which integrated for 4 protons and which was assigned to the methylene protons adjacent to the oxygen atom of the ester functionality on each arm of the product. The observed splitting was due to the coupling of the methylene protons with the adjacent methyl group. The signal for the methylene protons α to the nitrogen on each arm appeared as a triplet centered at δ 2.92 ppm. The methylene protons β to the nitrogen on each arm appeared as a triplet centered at δ 2.48 ppm. The multiplet at δ 1.7 was assigned to the cyclopropylmethine proton. The cyclopropyl methylene protons were observed as a multiplet centered at δ 0.44. Finally the methyl protons of

the ester functionality on each arm of **250** showed up at δ 1.25 as a triplet.

The subsequent cyclization reaction involved heating **250** under reflux with NaH in dry THF and catalytic amounts of dry ethanol overnight. GCMS analysis of the crude reaction mixture indicated complete disappearance of the starting material and the appearance of the cyclized product **252** whose spectrum displayed the expected parent ion at m/z 211 (Fig. 67). A second compound with a molecular ion at m/z 139, the molecular weight of the desired final product **164** also was present. The formation of **164** may have ocurred thermally during the GCMS analysis of the sample containing **252** or during the acidic work up of the reaction mixture which may have resulted in hydrolysis and subsequent decarboxylation of β-ketoacid **252** to afford **164**. Since at this point we were interested in **164** we decided to attempt conversion of the crude product to **164** by treatment with 6N HCl for 2 hours under reflux. Compound **164** was obtained in 68% yield starting from **250**. The piperidin-4-one **164** was characterized by GCMS analysis which showed the molecular ion at m/z 139 (Fig. 68). A small amount was converted to the oxalate salt for further characterization. The ^{1}H NMR spectrum of the salt (Fig. 69) displayed triplets centered at δ 3.0 which were assigned to the C-2 and C-6 methylene protons. A second triplet centered at δ 2.4 belonged to the C-3 and C-5 methylene protons. As expected the cyclopropylmethine and the methylene protons showed up at δ 2.1-2.18 and 0.49-0.59, respectively. Finally microanalytical data were consistent with the expected structure.

Scheme 48. Synthesis of N-cyclopropylpiperidin-4-one (164).

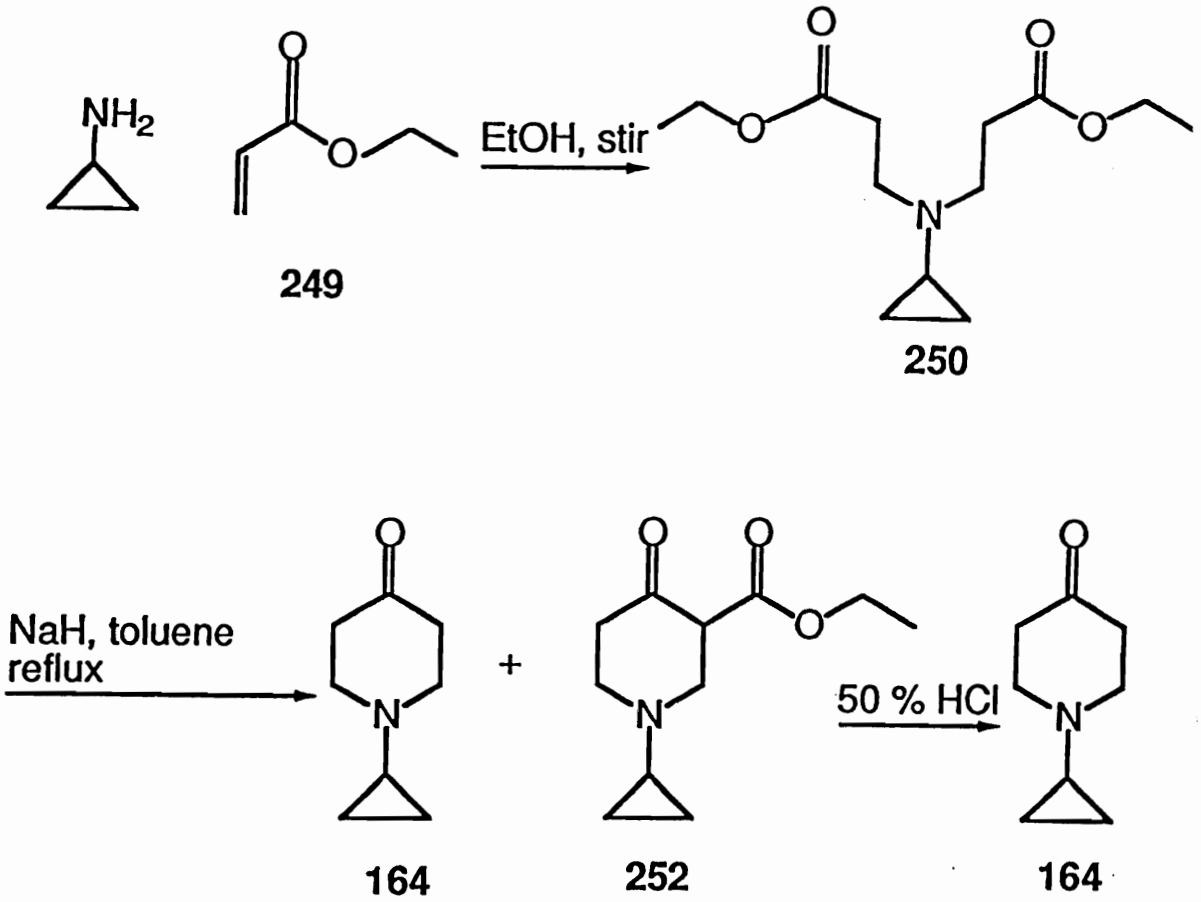

3.1.5. Synthesis of 4-Benzyl-1-propyl-1,2,3,6-tetrahydropyridine.

During our enzyme studies, particularly those related to substrate property analysis of the MPTP analogs with MAO-B, we observed that N-substituents larger then the methyl were poor substrates or non-substrates. The same was true with the N-cyclopropyl (**130**) and the N-propargyl (**146**) analogs which possessed good inactivation properties but were not turned over to the pyridinium metabolites. The N-propyl analog **152** also was a very poor MAO-B substrate with a very low V_{max}

and a high K_M. These characteristics led us to consider exploring the effects of functionalities at the C-4 position of the tetrahydropyridine ring system that might increase molecular flexibility that could potentially lead to a better active site fit and increased substrate affinities with MAO-B. Such an effect had been observed with the 4-benzyl analog **253** which displays better substrate properties than MPTP with MAO-B.[144] This flexibility also might serve to accommodate bulkier N-substituents. The molecule we choose to test this proposal was 4-benzyl-1-propyl-1,2,3,6-tetrahydropyridine (**257**). The molecule was chosen as a prototype as it contained a bulky N-substituent which leads to diminished substrate activity with MAO-B and a C-4 benzyl group which introduces flexibility and better substrate binding properties as observed with the corresponding 4-benzyl-1-methyltetrahydropyridine **253**.[144]

We initially attempted to synthesize **257** by reaction of 4-benzylpyridine (**254**) with an excess of propyl iodide to afford the corresponding pyridinium species **255**. The reaction mixture was stirred at room temperature for 24 hours during which time an orange solid precipitated out. The ^1H NMR spectrum of this solid (Fig. 70) displayed the characteristic signals for the C-2 and C-6 and the C-3 and C-5 pyridinium ring protons at δ 9.3 and 8.4 respectively. The aromatic signals appeared as a multiplet centered at δ 7.7. The triplet at δ 4.8 was assigned to the methylene protons (on the propyl group) adjacent to the nitrogen. The methylene protons β to the nitrogen appeared as a multiplet centered at δ 2.0. The methyl protons appeared as a triplet centered at δ 0.98. The NMR spectrum, however, did not display the

singlet which would correspond to the benzylic protons. GCMS analysis (Fig. 71) of this solid showed a peak bearing a molecular ion at m/z 183. If we had the desired pyridinium species **255** it would show a molecular ion at m/z 169 corresponding to the $M^{\cdot+}$ species of the N-dealkylated product 4-benzylpyridine (**254**). The observed molecular ion resembled that expected for 4-benzoylpyridine that would result from the thermal N-dealkylation of the corresponding benzoylpyridinium compound **256**. The formation of **256** presumably involves air oxidation of the expected pyridinium species **255**. Consequently the reaction was carried out at 0 °C with dropwise addition of the alkylating agent under nitrogen. The pale yellow solid which precipitated from the reaction mixture had similar NMR characteristics (Fig. 72) as **256** however this time the benzylic protons appeared as a sharp singlet at δ 4.8. Analogous behavior for the corresponding N-methyl compound **253**[175] has been reported in the literature. The corresponding pyridinium salt **255** was reduced in high yields to the corresponding tetrahydropyridine **257** (Scheme 49). The tetrahydropyridine **257** was characterized as its oxalate salt by GCMS analysis (Fig. 73) which displayed the desired parent ion at m/z 215 and by ^1H NMR (Fig. 74) which was similar to the 1-propyl-4-phenyltetrahydropyridine (**152**) analog with the additional singlet due to the benzylic protons appearing up at δ 3.5. Finally microanalysis was consistent with the expected structure.

Scheme 49. Synthetic Route to the 4-Benzyl-N-propyl-1,2,3,6-tetrahydropyridine (257).

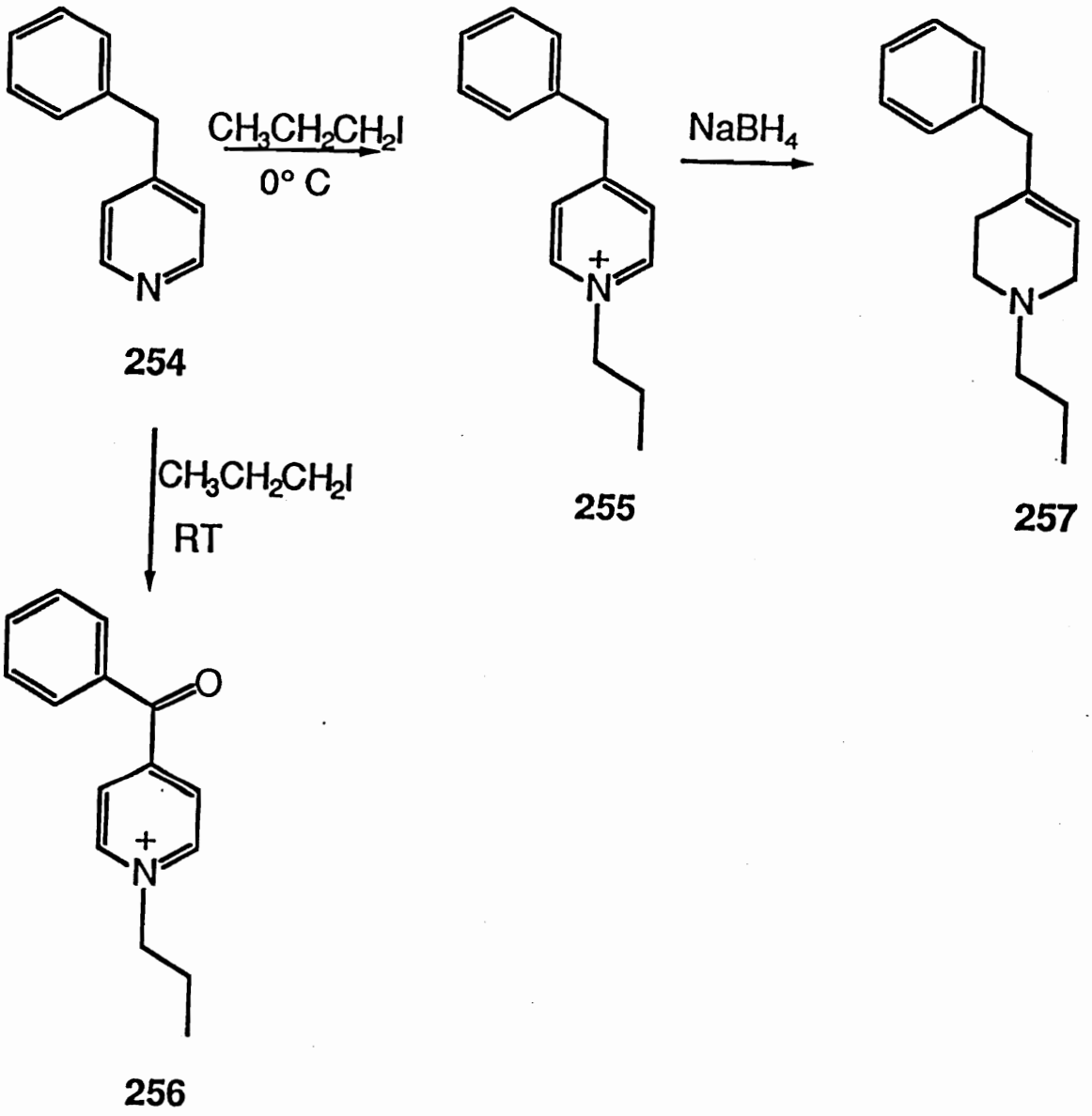

3.1.6 Synthesis of Aryloxytetrahydropyridine Analogs.

As discussed in Chapter 2, the C(4)-phenoxy analog of MPTP **165** was oxidized in a reaction catalyzed by MAO to form the aminoenone **169** and to liberate phenol **170** (see Scheme 32). This behavior of **165** towards MAO led us to focus our attention on the synthesis of several C(4)-substituted aryloxy MPTP analogs. Early results indicated significant differences in the MAO-A (recently available in our laboratory) and MAO-B substrate properties of compounds which were prepared in our laboratory. Such selectivity may play an important role in the future development of MPTP-type inhibitors by increasing the steric bulk on C(4) and including functionalities on the nitrogen capable of inactivating the enzyme. The aryloxy MPTP analogs which we decided to synthesize in an attempt to explore MAO-A and MAO-B structure-activity relationships included analogs **171-175** and **177**. The lead molecule, which was chosen to test the selective MAO-A inactivation proposal, was 4-(2,4-dichlorophenoxy)-1-propargyl-1,2,3,6-tetrahydropyridine **176**. The analog was designed to mimic the structural features of clorgyline which is a highly selective inactivator of MAO-A.

The synthesis of the aryloxy MPTP analogs was achieved by the treatment of the 4-chloro-1-methylpyridinium species **258**[176] with an appropriate phenol in the presence of triethylamine to generate the corresponding aryloxypyridinium derivatives. These then were reduced with sodium borohydride to afford the target aryloxytetrahydropyridine compounds in excellent yields (Scheme 50). The α- and β-naphthoxytetrahydropyridine derivatives **174** and **173** had been

synthesized earlier in our laboratory.[177] Thus **258** was treated with 4-tert-butylphenol (**259**), 4-butylphenol (**260**), 4-phenylphenol (**261**) and 4-(2,4-dichlorophenol) (**262**) in the presence of triethylamine to afford the pyridinium species **263** through **266**. The aryloxypyridinium species were characterized by GCMS analysis each of which displayed the molecular ion corresponding to the thermally demethylated pyridine species at m/z 227 (for pyridinium species **263** and **264**, Figs. 75 and 76), 247 (for pyridinium species **265**, Fig. 77), and 239 (for pyridinium species **266**, Fig. 78). The ^{1}H NMR analysis of the aryloxypyridinium derivatives (Fig. 79-81,83) showed characteristic doublets centered at δ 8.8 related to the C-2 and C-6 pyridinium protons. The other aromatic protons and the C-3 and C-5 pyridinium protons appeared as a multiplet centered at δ 7.5. As expected the N-CH_3 group appeared as a singlet at δ 4.22 ppm. Other characteristic signals for substituents on the aromatic ring at C(4) as in the case of 263 and 264 were as follows: The NMR spectrum for the 4-butylphenoxypyridinium analog **264** (Fig. 79) showed a triplet at δ 2.7 which was assigned to the methylene protons α to the aromatic ring. The methylene protons β to the aromatic ring appeared as a multiplet centered at δ 1.7 and the methylene protons γ to the aromatic ring appeared as a multiplet centered at δ 1.4. Finally the triplet centered at δ 1.0 was assigned to the terminal methyl protons of the butyl chain. The NMR spectrum for the tert-butylphenoxypyridinium derivative **263** (Fig. 80) showed a sharp signal at δ 1.3 in addition to the common features mentioned above. The singlet which integrated to 9 protons was assigned to the tert-butyl group. Finally microanalyses were consistent with the

expected structures in all the cases.

The corresponding tetrahydropyridine derivatives **171, 172, 175,** and **177** were obtained by the sodium borohydride reduction of the above pyridinium derivatives and were characterized by GCMS analysis. The GCEI-mass spectra displayed the molecular ion at m/z 245 (for tetrahydropyridines **171** and **172**, Figs. 82, 84), m/z 257 (for tetrahydropyridine **177**, Fig. 85), m/z 265 (for tetrahydropyridine **175**, Fig. 86). The ^{1}H NMR spectra (Fig. 87-90) of the oxalate salts of these aryloxytetrahydropyridines were similar to that of the 4-(2,4-dichlorophenoxy)tetrahydropyridine (**177**) analog described below.

The NMR spectrum for **177** (Fig. 90) displayed a multiplet centered at δ 7.5 which was assigned to the 3 aromatic protons. The C-5 olefinic proton appeared as a multiplet at centered at δ 4.8. The C-6 methylene protons appeared as a broad signal centered at δ 3.5 and the triplet at δ 3.2 was assigned to the C-2 methylene protons. The N-CH_3 protons and the C-3 methylene protons overlapped as a broad signal at δ 2.7 which integrated to 5 protons. Finally microanalytical data were consistent with the expected structure.

We also required the synthesis of the dihydropyridinium species **268** of the 4-phenylphenoxy MPTP analog **175** for metabolite identification purposes. The synthesis of **268** was achieved in a identical fashion to that described for the other dihydropyridinium derivatives. Compound **175** was treated with *m*-CPBA to afford the corresponding N-oxide **267** as the crystalline *m*-chlorobenzoate salt. This salt was characterized by ^{1}H NMR analysis (Fig. 91). The NMR spectrum showed

a complex aromatic region spanning δ 7.1-8.1 which integrated to the required 13 aromatic protons. The C-5 olefinic proton appeared as a triplet at δ 4.7. The multiplet which centered at δ 4.4 was assigned to the C-6 methylene protons. The multiplet which centered at δ 4.1 was assigned to the C-2 methylene protons. The N-CH_3 protons showed up as a singlet at δ 3.6 and the multiplets which centered at δ 2.7 and 3.2 were assigned to the C-3 methylene protons. Microanalytical data were consistent with the proposed structure. The N-oxide was treated with TFAA to afford the dihydropyridinium compound **268** which was isolated and characterized as its perchlorate salt (Scheme 51). The ^1H NMR spectrum (Fig. 92) for the dihydropyridinium species displayed a doublet at δ 8.3 which corresponds to the C-6 proton. The aromatic region appeared as a complex multiplet spanning δ 7.3-7.8 ppm. The doublet at δ 5.3 was assigned to the remaining C-5 olefinic proton. The triplet centered at δ 4.0 was assigned to the C-2 methylene protons and the N-CH_3 protons appeared as a sharp singlet at δ 3.5. The triplet centered at δ 3.1 was assigned to the C-3 methylene protons. The UV spectrum (pH 7.4 phosphate buffer, Fig. 93) showed a chromophore with a major peak at 313 nm (ε 23,000). Microanalysis was consistent with the proposed structure.

Scheme 50. Synthesis of Aryloxytetrahydropyridines.

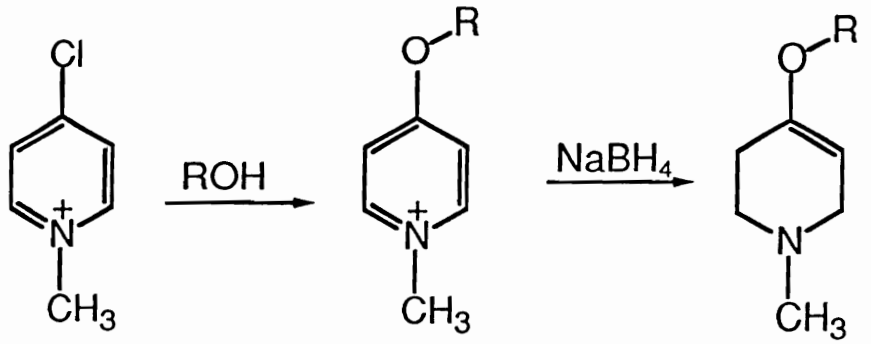

258

R	Phenol	Pyridinium	Tetrahydropyridines
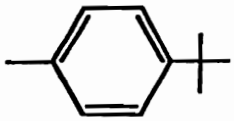	259	263	171
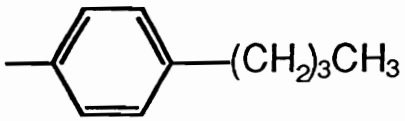	260	264	172
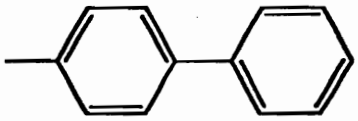	261	265	175
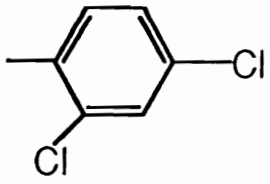	262	266	177

Scheme 51. Synthesis of the 4-Phenylphenoxydihydropyridinium Derivative.

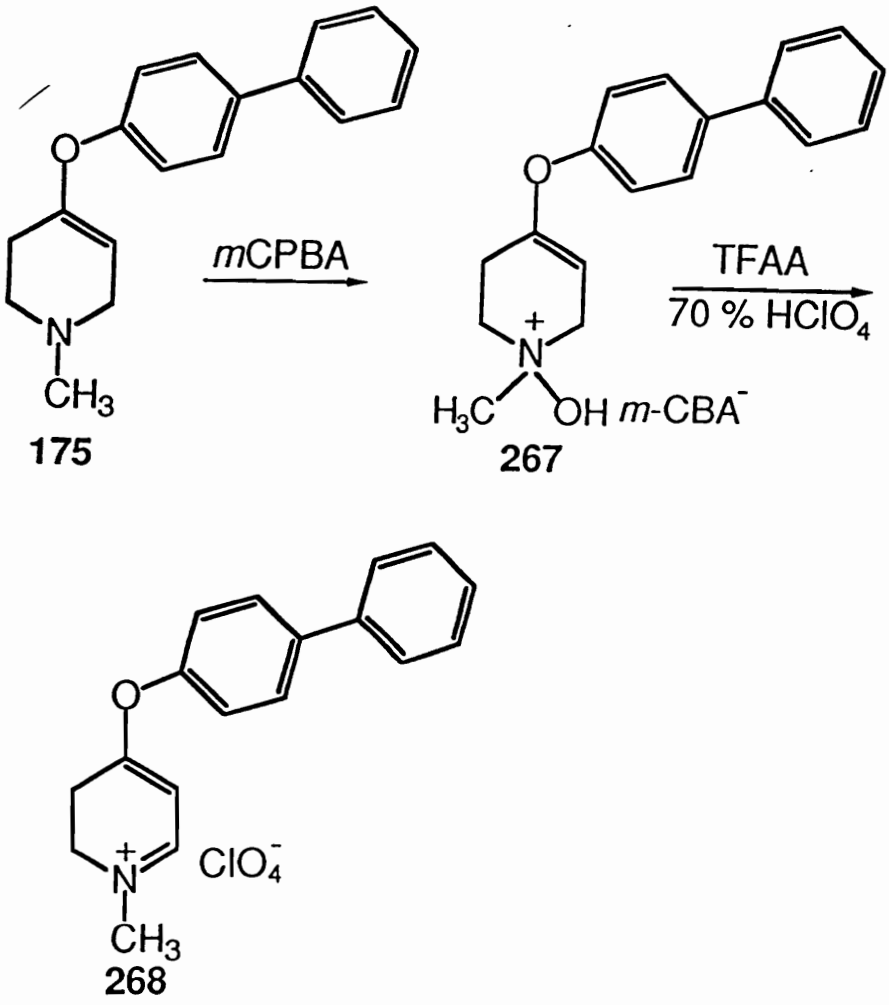

Using the same strategy successfully applied in the synthesis of the aryloxytetrahydropyridines, we tried to synthesize the corresponding 4-(2,4-dichlorophenoxy)-1-propargyltetrahydropyridine analog **176**. The proposed reaction involves the synthesis of 4-bromo-1-propargylpyridinium species **269** which subsequently would be treated

with 2,4-dichlorophenol in the presence of triethylamine to generate the pyridinium species **270**. Compound **270** could be then reduced with sodium borohydride to afford **176**. We were not successful in the synthesis of **269** as a reaction mixture containing 4-bromopyridine (**205**) and excess of propargyl bromide in THF within hours yielded a brown solid material which we tried to analyze by NMR. The solid was sparingly soluble in DMSO-d_6 and the ^{1}H NMR spectrum generated bore no resemblance to the expected product. This reaction was repeated several times, under different reaction conditions (room temperature to 0 °C) without success. We were forced to undertake the synthesis of 4-(2,4-dichlorophenoxy)pyridine (**271**) in the hope that **271** would undergo the required alkylation reaction. The synthesis of **271** was achieved by heating a solution of 4-bromopyridine (**205**), 2,4-dichlorophenol and triethylamine to 150 °C for 48 hours. Analysis of the crude reaction mixture displayed the formation of **271** (m/z 239, Fig. 95) and the disappearance of **205**. The components of the reaction mixture were subjected to column chromatography using silica gel to afford the pyridine **271** in about 30% yield. Compound **271** was characterized by ^{1}H NMR (Fig. 94). Subsequent attempts at the alkylation of **271** with propargyl bromide in dry THF at 0 °C afforded the desired pyridinium compound **270** as a white solid in about 20% yield. The compound was characterized by ^{1}H NMR (Fig. 96) which indicated a doublet at δ 8.2 which was assigned to the C-2 and C-6 pyridinium ring protons. The singlet at δ 7.2 was assigned to the C'-3 aromatic proton. The multiplet which centered at δ 6.9 and integrated to 4 protons consisted of the C-3

and C-5 pyridinium ring protons and the two remaining aromatic protons. The propargylic methylene appeared as a singlet at δ 4.7 and the acetylenic proton displayed a singlet at δ 3.2. The pyridinium compound **270** should be synthesized in large quantities which subsequently would be converted to the target tetrahydropyridine **176** following reduction with sodium borohydride.

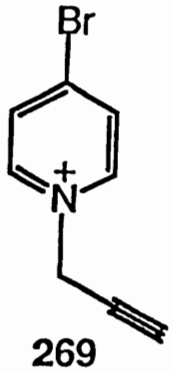

269

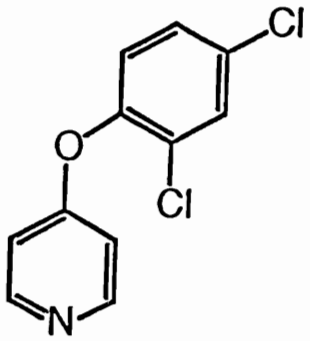

271

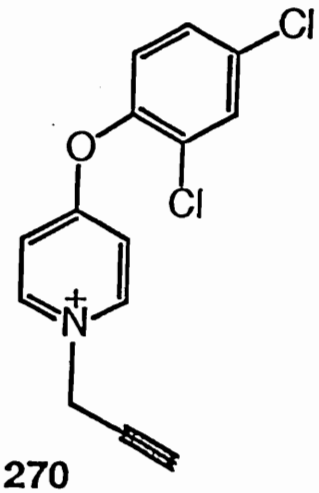

270

3.2. Enzymology.

3.2.1. Substrate studies with MAO-B.

The substrate properties of the candidate compounds were examined with purified beef liver MAO-B (the complete details of the isolation and purification of MAO-B are described in the Experimental Section). We first screened these molecules for their general substrate properties by performing repeated 400 to 200 nm scans of incubation mixtures containing 2 mM solutions (in pH 7.4 sodium phosphate buffer, 100 mM) of each compound in the presence of 0.02 units of MAO-B at 37 °C over a period of 1 hour. MPTP (**111**) was included as a reference compound against which to compare the properties of the test compounds. Under these conditions **111** undergoes rapid oxidation to the corresponding dihydropyridinium species $MPDP^+$ (**112**, λ_{max} 343 nm) which is converted slowly to the pyridinium metabolite MPP^+ (**113**, λ_{max} 290 nm).[121] Except for the N-propyl-4-phenyltetrahydropyridine analog **152**, all of the remaining N-substituted-4-phenyltetrahydropyridine derivatives were non-MAO-B subtrates, that is none of these compounds showed the formation of a chromophore which corresponded to that of a dihydropyridinium species upon incubation with MAO-B. Furthermore, addition of MPTP after a 1 hour incubation with each substrate gave rise to $MPDP^+$, demonstrating that the lack of oxidation of these compounds was not due to inhibition of the enzyme. The N-propyl analog **152** was a weak MAO-B substrate. It underwent the standard two electron oxidation to form the dihydropyridinium species **233** which absorbed maximally at 342 nm. This dihydropyridinium intermediate also underwent further

oxidation to the pyridinium species **181** (λ_{max} 294 nm) (see Scheme 52a). The structures of the metabolites **233** and **181** were confirmed by comparison of the chromophores of the enzyme generated species with those of the synthetic standards. On the other the corresponding 4-benzyl-1-propyl MPTP analog **257** displayed much better substrate properties with MAO-B (V_{max} = 330 nmols/min/unit MAO-B, and K_m = 1.6 mM). The rate of oxidation of **257** was 50 fold greater than 152 however the binding affinity for the enzyme was about the same probably due to the bulky propyl side chain.

The kinetic parameters for the MAO-B catalyzed oxidation of **152** were calculated from the Lineweaver-Burke plot (Fig. 97) constructed from the data obtained by incubating several concentrations of **152** with MAO-B and measuring the initial rate of formation to the dihydropyridinium species. The V_{max} and K_M values for **152** turned out to be 7 nmols/min-unit MAO-B and 2 mM, respectively. The high K_M and the low V_{max} values relative to MPTP document its poor MAO-B substrate properties. Nevertheless, based on these results, previous reports (see Chapter 2 for structure-activity requirements for MPTP analogs) suggesting the lack of substrate properties of MPTP analogs bearing N-substituents larger than an ethyl group must be viewed with caution. Since the N-allyl (**140**) and the N-propargyl (**146**) derivatives appeared to be completely stable under the incubation conditions that led to a measurable rate of oxidation of **152**, we speculate that electronic factors may contribute to the nature of the interactions of these tetrahydropyridine derivatives with MAO-B.

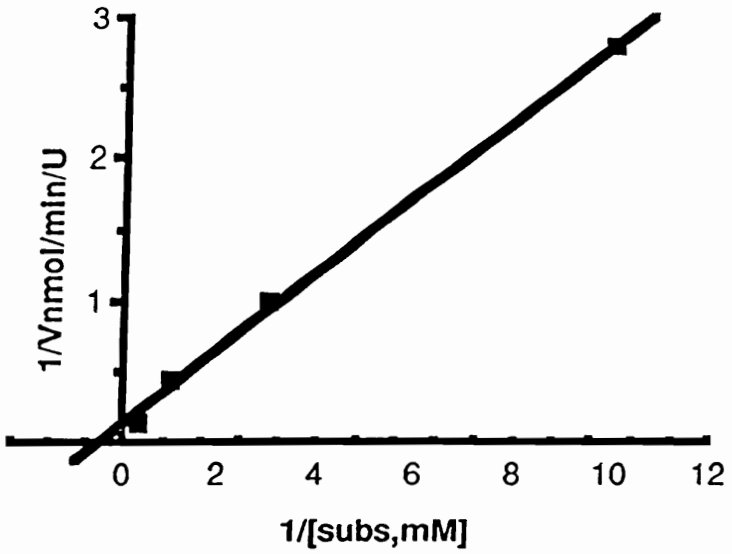

Fig. 97. Lineweaver Burke Plot for MAO-B Catalyzed Oxidation of the 4-Phenyl-1-propyl-1,2,3,6-tetrahydropyridine.

Scheme 52a. MAO-B Catalyzed Oxidation of N-Propyl MPTP Analog.

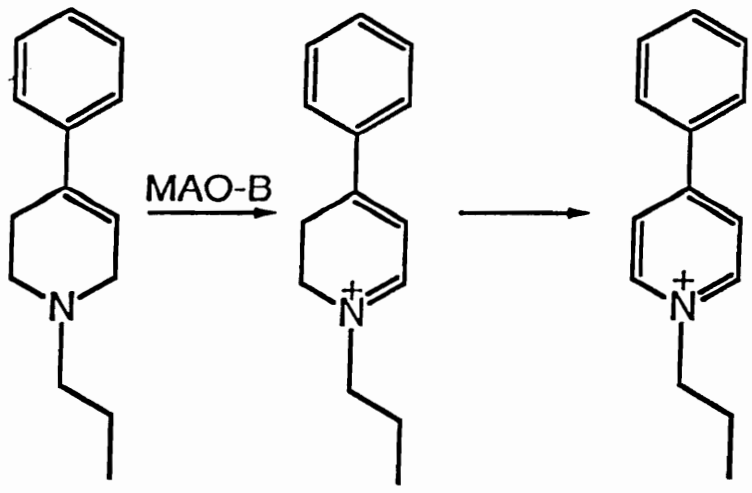

Scheme 52b. MAO-B Catalyzed Oxidation of C-4-Substituted MPTP Analogs.

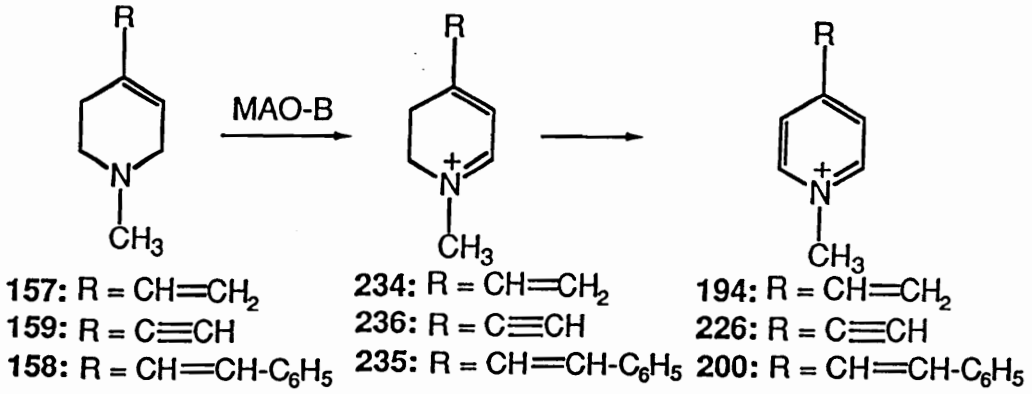

The C-4 substituted tetrahydropyridines, the 4-ethenyl (**157**) and the 4-ethynyl (**159**) analogs, underwent rapid MAO-B oxidation to generate the corresponding dihydropyridinium species **234** (λ_{max} 309) (Fig. 98a, 98b and 98c) and **236** (λ_{max} 308), respectively (Scheme 52b). Once again, the metabolic products were identified by comparison of their spectral properties with those of synthetic standards. These enzymatically generated dihydropyridinium species namely, the 4-ethenyl-1-methyl-2,3-dihydropyridinium **234** and the ethynyl derivative **236** behaved like $MPDP^+$ and underwent slow oxidation to the respective pyridinium products **194** and **226** (λ_{max} 264). The synthetic dihydropyridinium species **234** and **236** when incubated in pH 7.4 phosphate buffer at 37 °C behaved

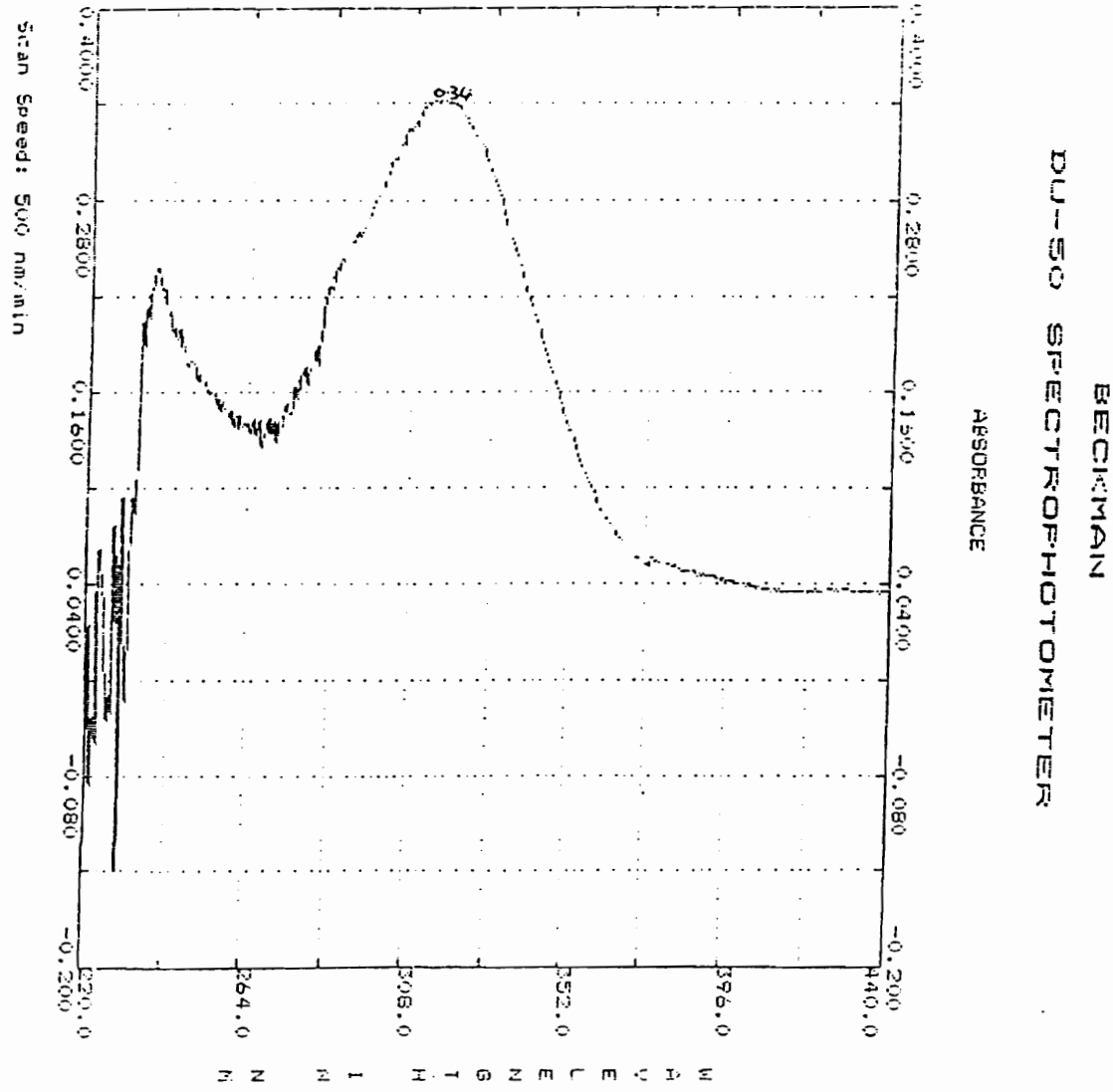

Figure 98a. UV Spectrum of MAO-B Catalyzed Oxidation of 2 mM 4-Ethenyl-1-methyltetrahydropyridine at T = 0 minutes.

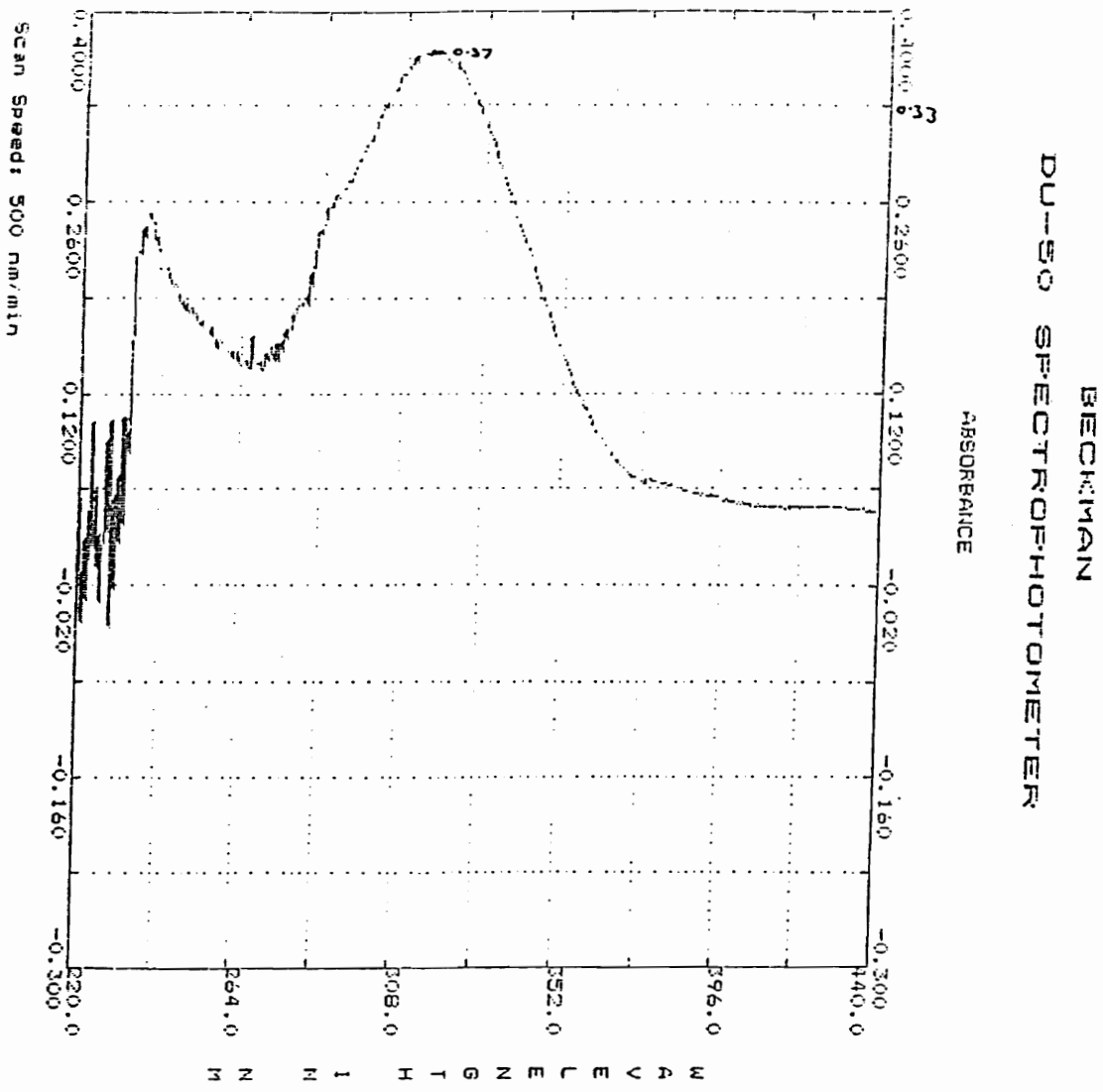

Figure 98b. UV Spectrum of MAO-B Catalyzed Oxidation of 2 mM 4-Ethenyl-1-methyltetrahydropyridine at T = 10 minutes.

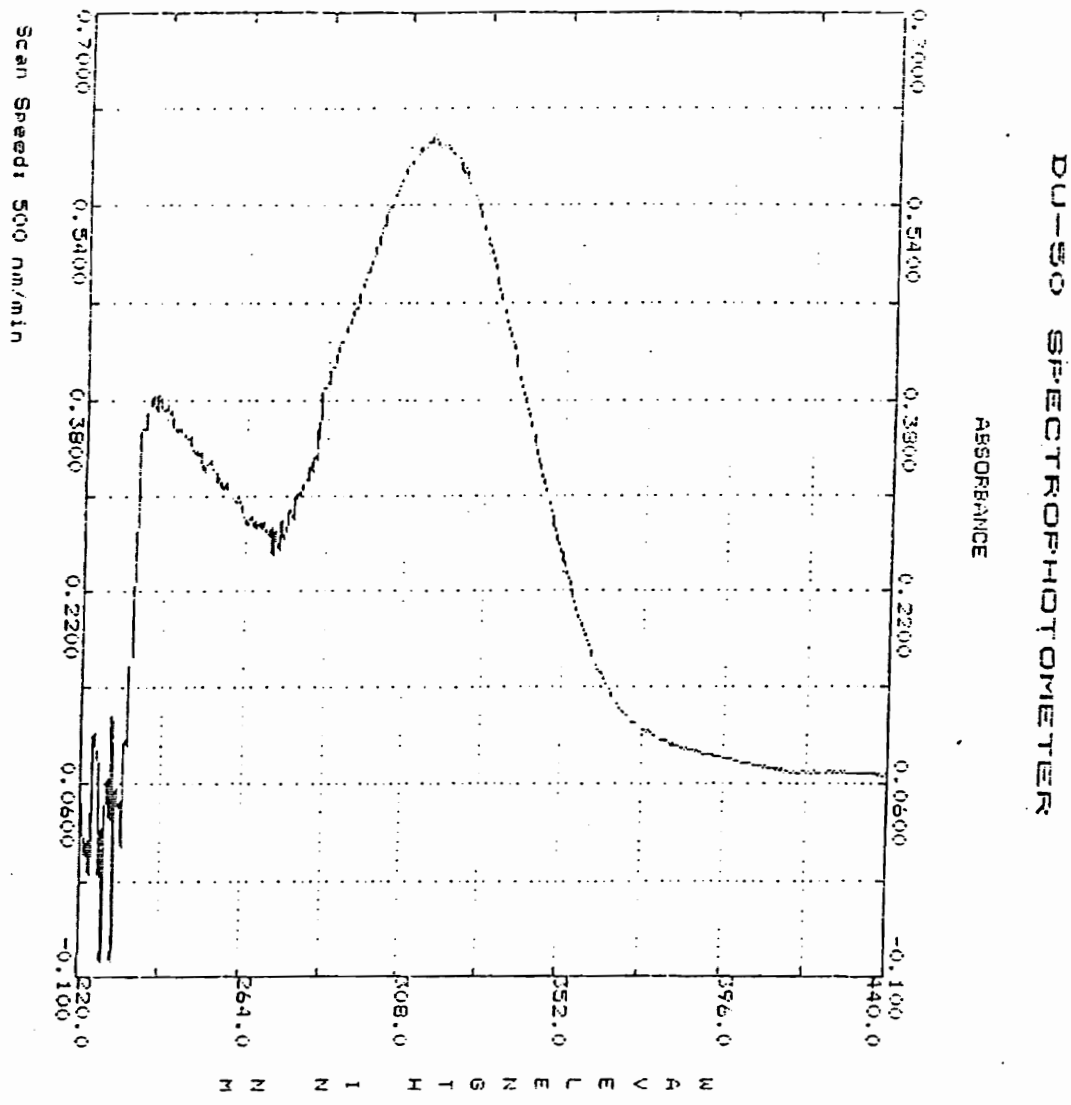

Figure 98c. UV Spectrum of MAO-B Catalyzed Oxidation of 2 mM 4-Ethenyl-1-methyltetrahydropyridine at T = 20 minutes.

in a fashion identical to that of the metabolically generated dihydropyridinium species. Furthermore, contrary to reports on MPDP+,[123] the rate of this oxidation was not affected by MAO-B, suggesting that the conversion of **236** to **226** is an autoxidative process.

In addition to the ethynylpyridinium species, a second product with λ_{max} 375 nm was observed in the UV scans of the MAO-B incubation mixture with compound **159**. When incubated under these conditions but without the enzyme, the synthetic dihydropyridinium compound also displayed the same chromophore. Although we have no direct evidence, one possible structure for this product is the aldehyde derivative **273**.

Scheme 53. Proposed Conversion of the Ethynyldihydropyridinium Metabolite 236 to Aldehyde 273.

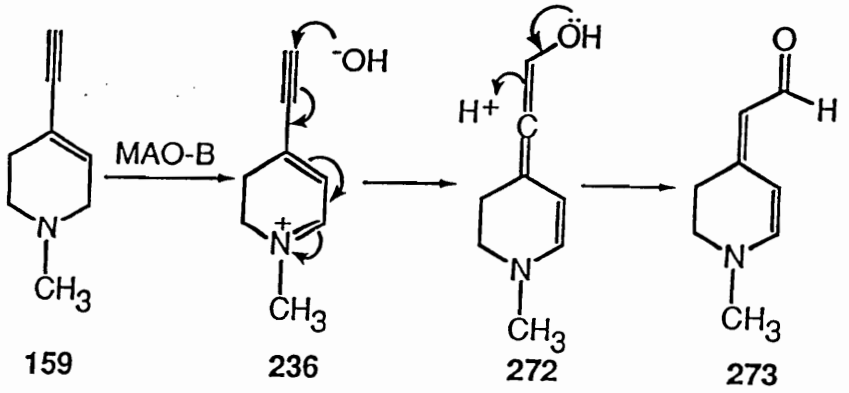

The proposed pathway leading to the formation of the **273** involves nucleophilic attack by water on the reactive ethynyldihydropyridinium system **236** to generate the allene intermediate **272** followed by rearrangement to the aldehyde **273** (Scheme 53). This is analogous to the Schuster-Meyer rearrangement[178] which involves hydration of a propargylic cation intermediate **274** followed by rearrangement of the resulting allenol **275** to yield an acrolein derivative **276** (Scheme 54).

Scheme 54. Schuster-Meyer Rearrangement.

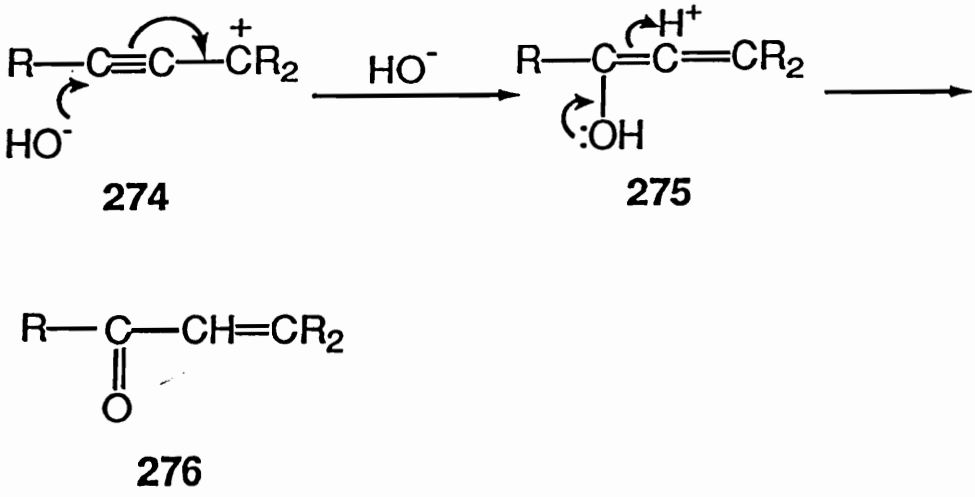

Kinetic data were obtained for the two analogs **157** and **159** by examining the dependence of oxidation rates on substrate concentration. We performed detailed kinetic studies using several concentrations of the two analogs with MAO-B. The values for V_{max} and K_M that were obtained from the Lineweaver Burke plot analyses (Fig. 99 and 100, respectively) were 190 nmols/min/unit MAO-B and 80 μM for the ethenyl derivative **157** and 684 nmols/min/unit MAO-B and 861 μM for

the ethynyl analog **159**, respectively. Based on the V_{max}/K_M ratio for these two compounds, it is evident that their MAO-B substrate properties are comparable to those of MPTP.

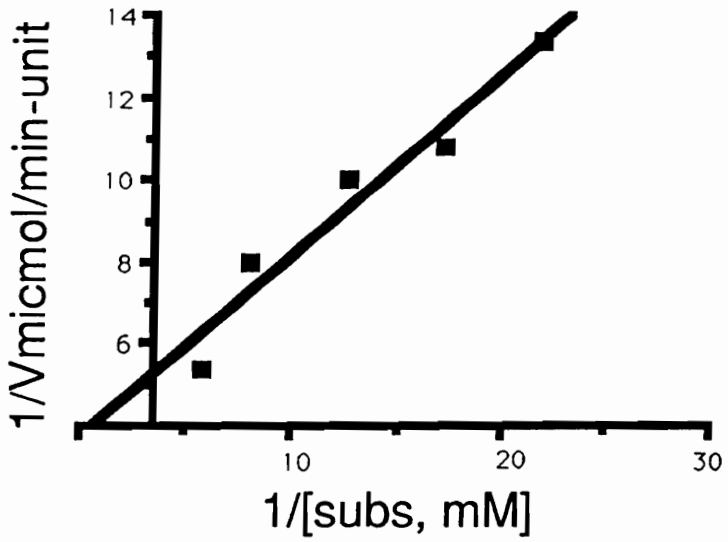

Fig 99. MAO-B Catalyzed Oxidation of 4-Ethenyl-1-methyltetrahydropyridine.

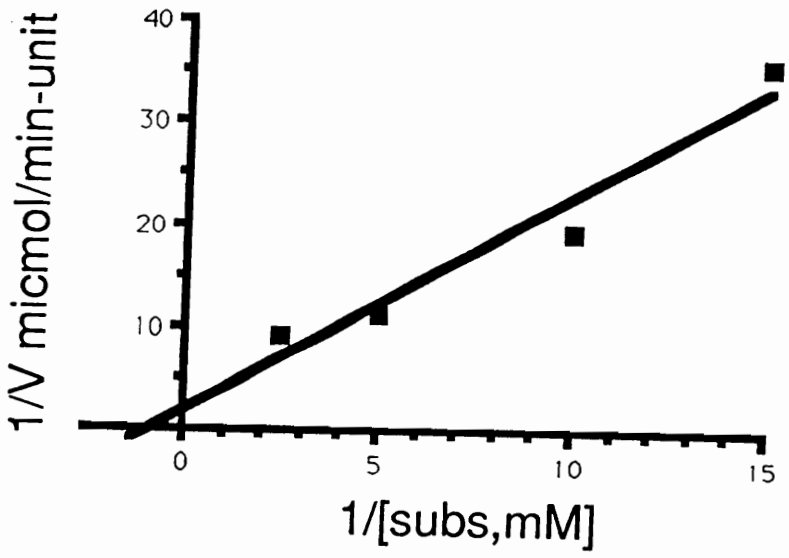

Fig 100. MAO-B Catalyzed Oxidation of 4-Ethynyl-1-methyltetrahydropyridine.

Of the remaining compounds tested as MAO-B substrates, only the phenylethenyl derivative **158** showed any significant turnover under these incubation conditions. Scans of **158** clearly showed the formation of a metabolite with λ_{max} 375 nm corresponding to the synthetic dihydropyridinium derivative **235**. Upon standing, the absorption maximum shifted to 350 nm which corresponds to the spectrum of the synthetic pyridinium species **200** (see Scheme 52). An earlier report[144] that the phenylethenyl compound **158** is not a substrate for MAO-B may be due to the use of a mitochondrial enzyme preparation instead of the purified enzyme studied here. Linear semilog plots of initial rates vs concentration provided data which were analyzed by a double reciprocal

plot. The V_{max} and K_M values were found to be 10 nmols/min-unit MAO-B and 954 μM. The phenylethynyl derivative **160** was an extremely poor MAO-B substrate with undetermined kinetic parameters. The results of our kinetic studies are summarized in Table 9.

The 4-ethenyl **157** and the 4-ethynyl **159** compounds displayed substrate properties comparable to those of MPTP while the phenylethenyl analog **158** proved to be a weak substrate and the phenylethynyl analog **160**, an extremely weak substrate. The good substrate properties of the ethenyl and the ethynyl analogs relative to the phenylethenyl and the phenylethynyl derivatives are likely to reflect unfavored steric interactions in the MAO-B active site of the larger C-4 substituted analogs. The excellent substrate properties of the previously reported 4-benzyl and the 4-(2-phenylethyl) analogs emphasize the importance of geometry in this region of the substrate molecules. The observation that significant bulk is tolerated at the *meta*- but not the *para*-position of the phenyl group of MPTP is suggestive of a hydrophobic region which may accomodate the 4-benzyl and the 4-(2-phenylethyl) groups but not the more rigid phenyl substituted ethenyl and ethynyl substituents.[144]

Some structural features influencing the binding to the MAO active site have been postulated on the basis of conformational analyses utilizing a large number of MPTP analogs. A rudimentary model of the substrate binding sites of both MAO-B and MAO-A was proposed.[179] The salient features of the model include the possibility of assigning substrate binding sites to two major regions: (i) the amine-binding region; and (ii)

the bulky (C)-4 substituent region. For both MAO-A and MAO-B, the optimum substrate length measured along the main axis (N-C-4-C-1'-C-4') of the MPTP analogs is about 8.5 A°. This measurement represents the distance between the C4' on the phenyl ring and the carbon atom on the N-methyl group in MPTP. Thus the phenyl group in the (C)-4-benzyl analog deviates from this main axis by 71°, leading to a significant increase in substrate activity.

Table 9. Kinetic Parameters for the MAO-B Catalyzed Oxidation of MPTP and Analogs

Compd.	V_{max}[a]	K_M[b]	V_{max}/K[c]
MPTP (**111**)	755	390×10^3	1935×10^{-6}
152	7	2000×10^3	3.5×10^{-6}
157	190	80×10^3	2370×10^{-6}
158	10	954×10^3	10×10^{-6}
159	684	861×10^3	790×10^{-6}

[a]nmol/min/Unit MAO-B. [b]nM. [c]L/min/Unit MAO-B

During the preliminary substrate studies, we observed that some of the dihydropyridinium metabolites were unstable under physiological conditions and underwent a second two electron oxidation to generate the potentially neurotoxic pyridinium species. This phenomenon also is observed with the MAO-B generated metabolic species $MPDP^+$ (from MPTP) which undergoes further oxidation to the pyridinium species MPP^+, the ultimate putitive neurotoxin.[124] Literature reports[122] state that the conversion of $MPDP^+$ to MPP^+ is MAO-B mediated. However other pathways which are non-enzyme mediated may account for the

oxidation to the neurotoxic pyridinium species. These include autoxidation by molecular oxygen,[132] disproportionation[131] and cycloaddition chemistry.[180] Disproportionation of MPDP+ to generate the pyridinium and tetrahydropyridine species, however, occurs at a significant rate only at concentrations higher than 500 μM.[131]

In an attempt to characterize structural features that influence the rate of autoxidation of dihydropyridinium species to the pyridinium species, we incubated 125 μM solutions of a variety of synthetic dihydropyridinium species in pH 7.4 phosphate buffer at 37 °C and monitored the disappearance of the dihydropyridinium chromophore and the appearance of the chromophore due to the pyridinium species spectrophotometrically. The formation of the pyridinium species was confirmed by comparing the chromophores with the synthetic standards. The 125 μM concentration was chosen to focuss on autoxidation and to avoid the bimolecular disproportionation and Diels-Alder reactions. A similar study was performed on MPDP+ as a reference.

Under these conditions, the ethenyl (**234**) and the ethynyl (**236**) dihydropyridinium species underwent autoxidation to the pyridinium species **194** and **226**, respectively at rates faster than that observed with MPDP+ ($t_{1/2}$ = 330 minutes). The ethynyldihydropyridinium species **236** was converted at a much faster rate to the pyridinium species ($t_{1/2}$ = 40 minutes) than the ethenyl derivative **234** ($t_{1/2}$ = 156 minutes). The rate of disappearance of the ethenyldihydropyridinium vs time due to autoxidation to the corresponding pyridinium is shown in Fig. 101. The N-propyl-4-phenyldihydropyridinium species **233** and the 4-(E)-(2-

phenylethenyl)dihydropyridinium species **235** had $t_{1/2}$ oxidation values in the range of 600-720 minutes. The 4-(2,6-dimethyl)- and the 4-thiophenoxydihydropyridinium analogs **246** and **248** were quite stable under these incubation conditions. Detectable levels of the corresponding pyridinium species were observed only after a period of 24 hours. On the other hand the 4-t-butyldihydropyridinium analog **247** was completely stable to autoxidation at pH 7.4 as seen in Fig. 102 which shows a slight decrease in concentration of the dihydropyridinium. However when **247** was incubated in pH 9.0 buffer, there was a steady increase in pyrdinium formation with respect to time with the half-life of oxidation being 5 hours. This differential behavior of the dihydropyridinium compounds in pH 7.4 may be explained to a certain degree by considering the proposed mechanism for the conversion of the dihydropyridinium to the pyridinium by the oxidation of the intermediate 1,2-dihydropyridine (Scheme 55).[139] These studies clearly indicate that the autoxidation of dihydropyridinium species to the neurotoxic pyridinium is dependent on the pH of the system. These results argue against an enzyme mediated oxidation to the potentially neurotoxic pyridinium species. Physiological conditions (pH 7.4) may not be a basic enough system for the abstraction of the C-3 proton from the dihydropyridinium species to form the free base, i.e. the corresponding 1,2-dihydropyridine. Furthermore the substituents present on C-4 of the dihydropyridinium system also could sterically hinder proton abstraction. This is consistent with the result that the tert-butyldihydropyridinium species **247** and the 2,6-dimethylphenyldihydropyridinium **246** are stable

to autoxidation at pH 7.4, i.e. steric hindrence by the bulky tert-butyl group and the 2,6-dimethyl groups prevents formation of the free base and therefore oxidation to the corresponding pyridinium compound.

Scheme 55. Autoxidation of Dihydropyridiniums in pH 7.4 Phosphate Buffer.

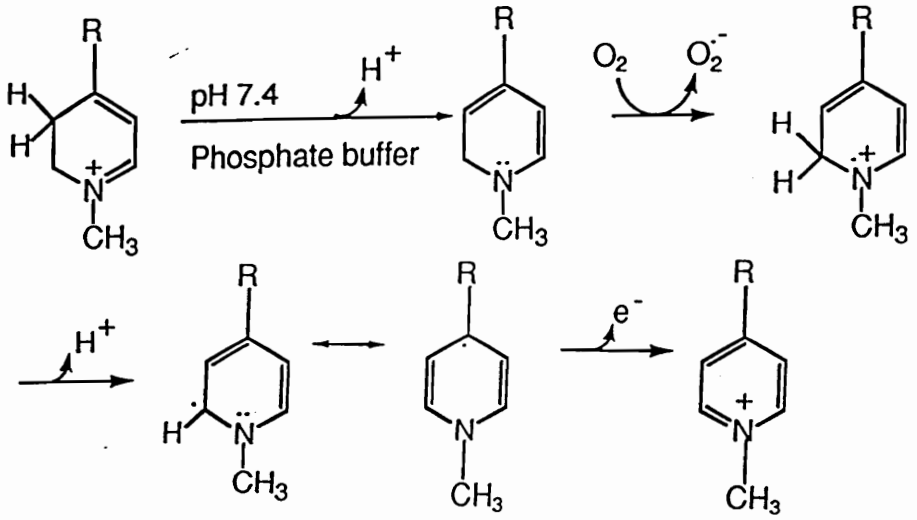

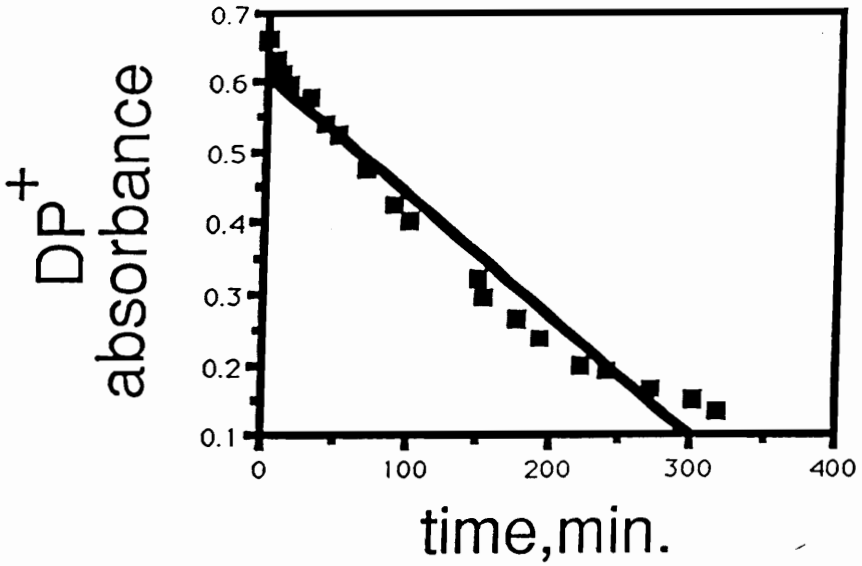

Fig. 101. Autoxidation Studies on 4-Ethenyl-1-methyldihydropyridinium System.

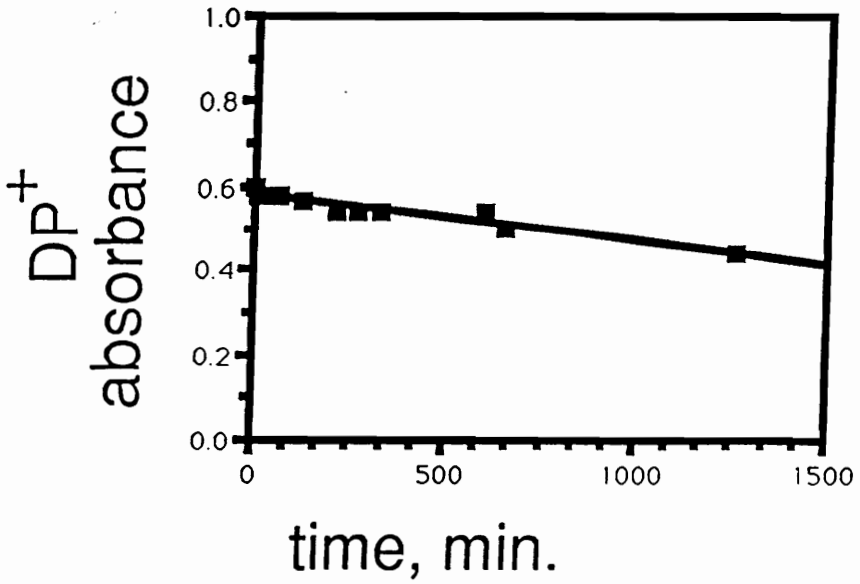

Fig. 102. Autoxidation Studies on 4-t-Butyl-1-methyldihydropyridinium System.

3.2.2. Inhibition studies with MAO-B.

The MAO-B inhibiting properties of the tetrahydropyridine derivatives prepared in these studies were investigated by assessing the rate of loss of enzyme activity (as measured by the initial rate of oxidation of 5 mM MPTP) vs time at several concentrations of the potential inhibitor. Linear semilog plots were obtained for those compounds displaying significant inhibitor properties. Figure 103a presents data for 4-phenyl-1-propargyl-1,2,3,6-tetrahydropyridine (**146**) which are typical of these plots and from which the observed rate of loss of enzyme activity (k_{obs}) could be calculated for each concentration of inhibitor. It is clear from the plot that the rate of inactivation increases with increasing concentration of **146** and the rate of inactivation is time dependent. These characteristics of time and concentration dependent inhibition of enzyme activity are typical of those associated with mechanism based inactivators that irreversibly inhibit enzyme activity by alkylating an active site functionality essential for substrate turnover. The double reciprocal plot of $1/k_{obs}$ vs 1/inhibitor concentration (Figure 103b) provided estimates of k_{inact} (maximum rate of inactivation) and K_I (the concentration of inhibitor at which the rate of oxidation of MPTP was 50% of its maximal rate).

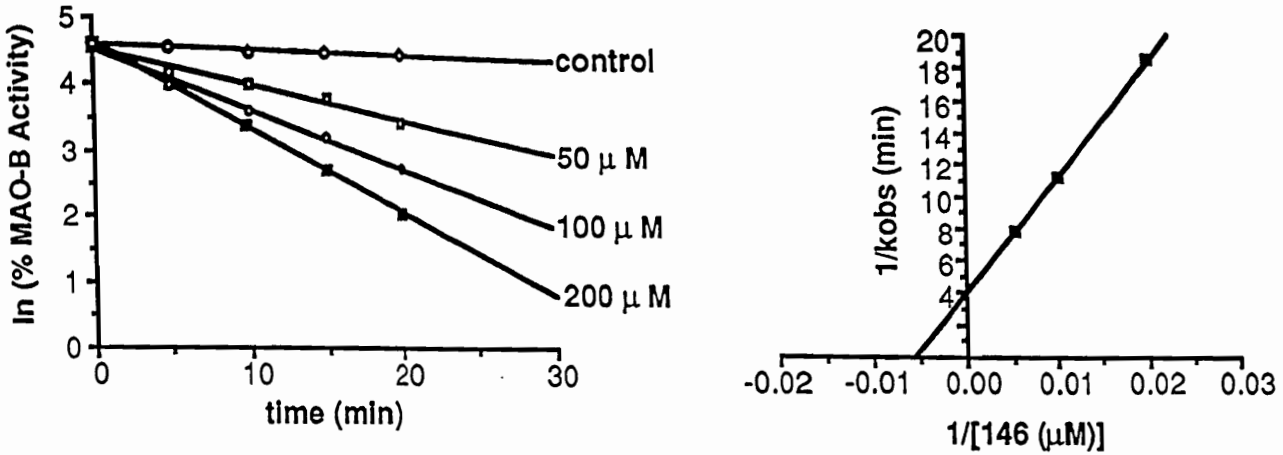

Figure 103. Kinetic studies on the inactivation of MAO-B by 4-phenyl-1-propargyl-1,2,3,6-tetrahydropyridine. Fig. 103a (left panel) shows the time and concentration dependent inactivation curves. Fig. 103b (right panel) is a double reciprocal plot constructed from the linear semilog plots shown in Fig. 103a.

The most efficient inhibitor of MAO-B in this series is the propargyl derivative **146**. Based on published evidence for the inactivation pathway associated with other propargylamines, (See Chapter 1) compound **146** presumably inactivates MAO-B via the pathway shown in Scheme 56. Initial one-electron transfer generates the aminium radical species **147** which then loses a proton from the methylene group of the propargyl moiety (pathway a) to form the carbon centered radical **148**. A second one-electron transfer leads to the highly electrophilic ethynyliminium species **150** which presumably inactivates the enzyme by reacting with an active site nucleophilic group. This pathway is analogous (see Chapter 1, Section 1.2) to the previously proposed mechanism by which other tertiary propargylic amines, via covalent binding of the ethynyliminium intermediate with the flavin prosthetic group to form a flavocyanine, are thought to inactivate MAO. In the present case, one might expect that the aminium radical **147** also would yield the ring allylic carbon centered radical **149** and hence the dihydropyridinium intermediate **151**. However, no evidence for the formation of **151** under standard conditions of incubation as well as in the presence of a forty fold increase in the enzyme concentration could be obtained. The fact that the N-propyl analog **152** undergoes ring α-carbon oxidation to yield the expected dihydropyridinium metabolite **233** at a measurable rate demonstrates the feasibility of such a pathway with a 3 carbon group attached to nitrogen.

Scheme 56. Proposed Inactivation Pathway of MAO-B by 146.

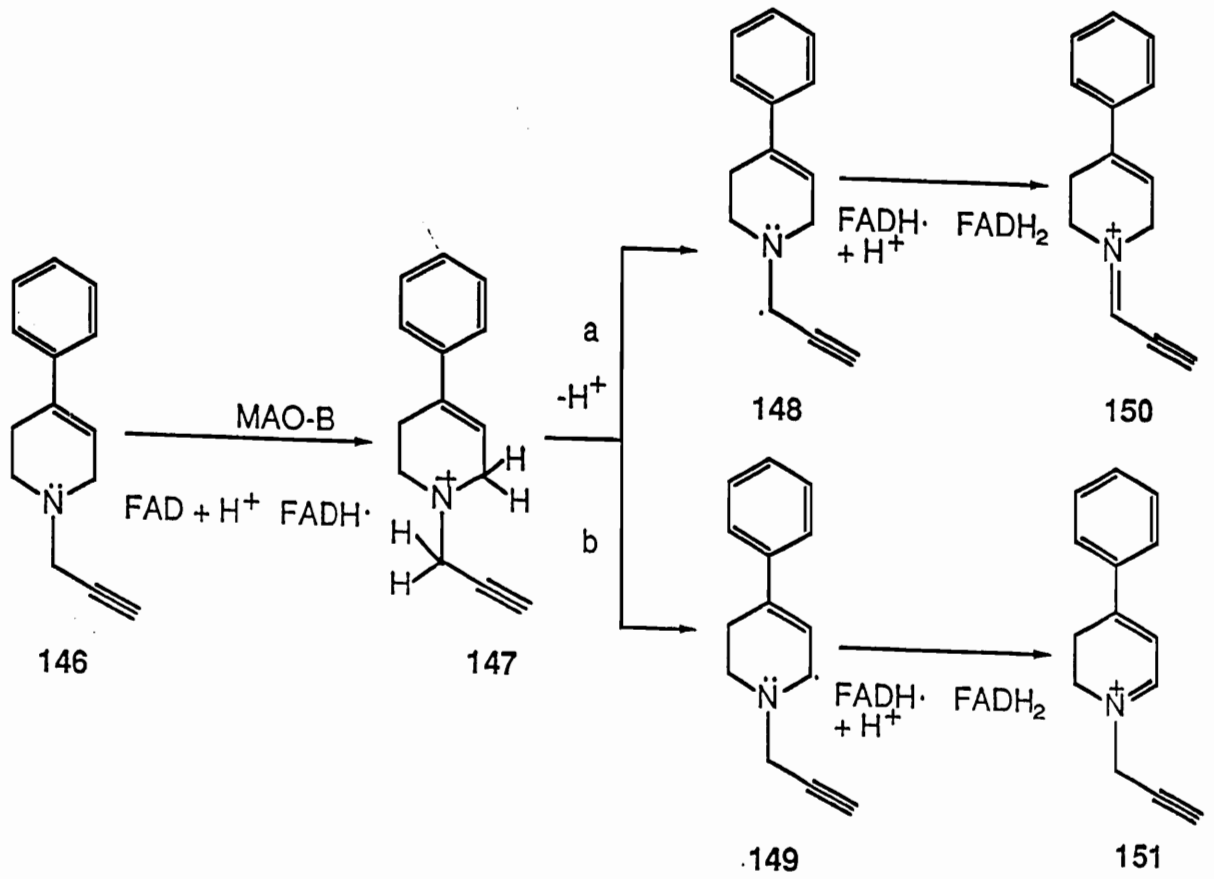

Although many of the other candidate compounds in these two series were found to be time and concentration dependent inhibitors of MAO-B, none of them proved to be very efficient. In view of the moderately effective inactivating properties of the N-propargyl derivative, the weak inactivating properties of the N-allyl analog **140** were somewhat surprising. Although some allylamines are also inhibitors of MAO[181] they require considerably higher concentrations than their acetylenic analogs to effect the same change in MAO activity. One distinction that can be drawn between the allylic and the propargylic inhibitors that may account for the greater reactivity of the latter is the acidity of their α protons.

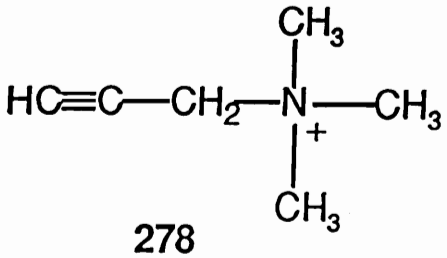

278

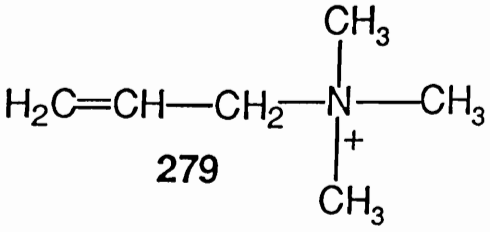

279

Krantz and workers[182] evaluated the ease of removal of propargyl and allylic protons by measuring the rates of deuterium exchange of the quaternary ammonium salts **278** and **279** which crudely represent the

tertiary amine radical cation **147** at the active site of MAO. Whereas **278** undergoes exchange of its propargylic protons in 1 M NaOD-D_2O with a half life of 5 minutes at 25 °C, the allyltrimethylammonium ion **279** under the same conditions shows little evidence of exchange even after six months. At 70 °C, **279** has a half life of about 60 hours in 1 M $NaOCD_3$-CD_3OD.

In contrast with the corresponding N-cyclopropyl derivative **130**, the N-cyclobutyl analog **153** showed no significant activity at 200 μM. This may be attributed to the poor fit of **153** due to the bulky N-substituent in the MAO-B active site which leads to absence of MAO-B substrate properties and no inactivation (see Table 10). The limited solubility of **153** precluded a more definitive characterization of its interactions with MAO-B.

Despite their good substrate properties and the potential electrophilic reactivity of the corresponding dihydropyridinium metabolic intermediates, neither the ethenyl (**157**) nor the ethynyl (**159**) analog displayed significant inhibitor properties. The fact that the ethenyl (**157**) and the ethynyl (**159**) analogs did not display significant inactivation of MAO-B was surprising. We expected the electrophilic dihydropyridinium metabolites generated from **157** and **159** would be susceptable to nucleophilic attack by an active site nucleophile on MAO-B. Although the tetrahydropyridine proved to be a good MAO-B substrate, it appeared that covalent bond formation leading to inactivation was not taking place. This suggested to us the possibility that either the metabolically generated Michael acceptor (the

ethynyldihydropyridinium species **236**) was not reactive enough or there was no active site nucleophile in the C-4 region of the molecule was present.

We decided to assess the reactivity of the synthetic ethynyldihydropyridinium system by monitoring its reactivity towards several model nucleophiles. We examined the susceptibility of **236** to attack with N-acetylcysteine (**281**) and benzylamine (**282**). When treated with **281** or **282** at room temperature, the UV chromophore of **236** (λ_{max} 308 nm) was replaced by chromophores with λ_{max} 414 nm for **281** (Fig. 104) and λ_{max} 451 nm for **282** (Fig. 105). These spectral characteristics are consistent with the adducts **285** and **286** that would result from nucleophilic attack by the sulfhydryl and the amino functionalities on the ethynyldihydropyridinium system to generate the reactive aminoallene **283** and **284** which could stabilize via resonance structures as adducts **285** and **286** respectively as shown in Scheme 57. This pathway is analogous to the one proposed in Scheme 54 for the hydrolysis of **236**.

This reaction pathway was studied in a greater detail using N-methylaniline (**287**) as the nucleophile. The reaction was monitored by ^{1}H NMR using 0.5 M **236** and **287** in CD_3CN. Evidence of reaction (loss of the characteristic downfield signals of **236**) was immediate. Upon work-up a fluffy orange solid was isolated which was characterized by ^{1}H NMR (Fig 106), fast atom bombardment mass spectrometry (M^+ 227) and elemental analysis as 4-(2-N-methylanilinoethenyl)-1-methyl-2,3-dihydropyridinium perchlorate (**289**). The UV spectral characteristics of **289** (λ_{max} 464 nm, ε 51,000, Fig. 107) are comparable to those of structurally

related cyanines such as **290** and **291**.[184,185] The pathway (Scheme 58) to **289** may involve initial formation of the highly reactive aminoallene **288** which could rearrange to the resonance stabilized product **289a** and **289b**.

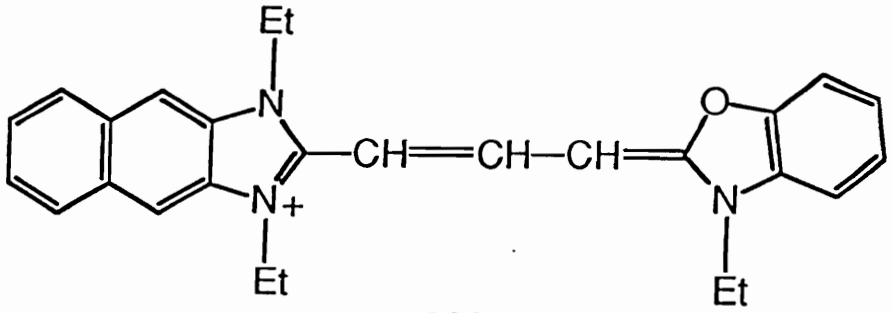

290

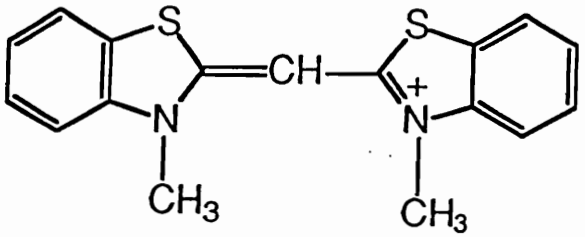

291

Scheme 57. Reactivity Studies on the Ethynyldihydropyridinium System.

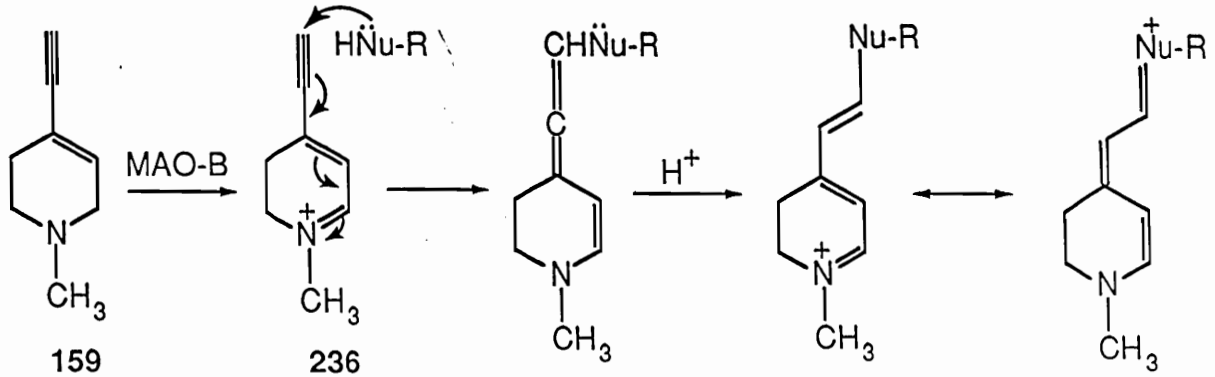

Scheme 58. Reaction of N-methylaniline with the Ethynyldihydropyridinium System.

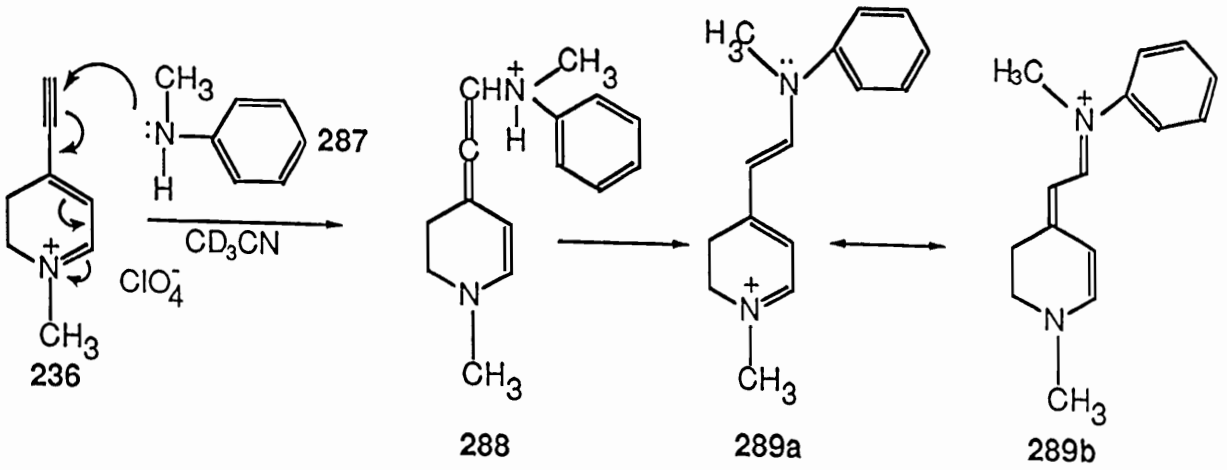

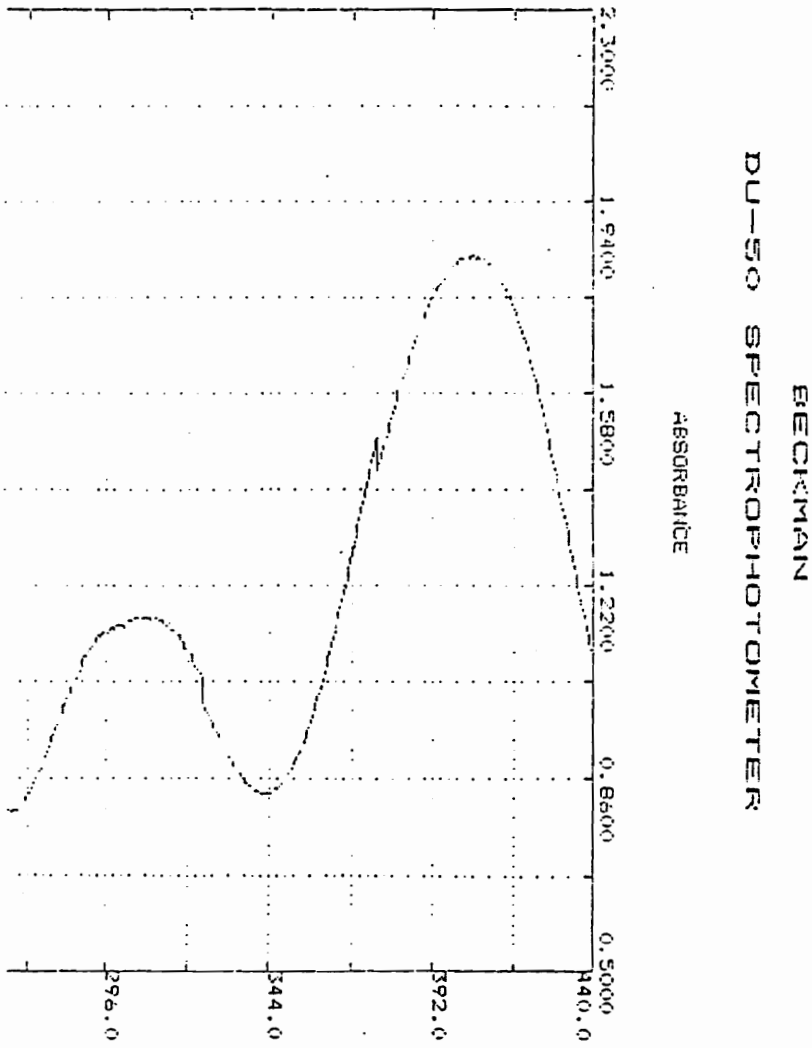

Figure 104. UV Spectrum of the Product Derived From the Reaction of 125 μM 4-Ethynyldihydropyridinium and N-Acetylcysteine.

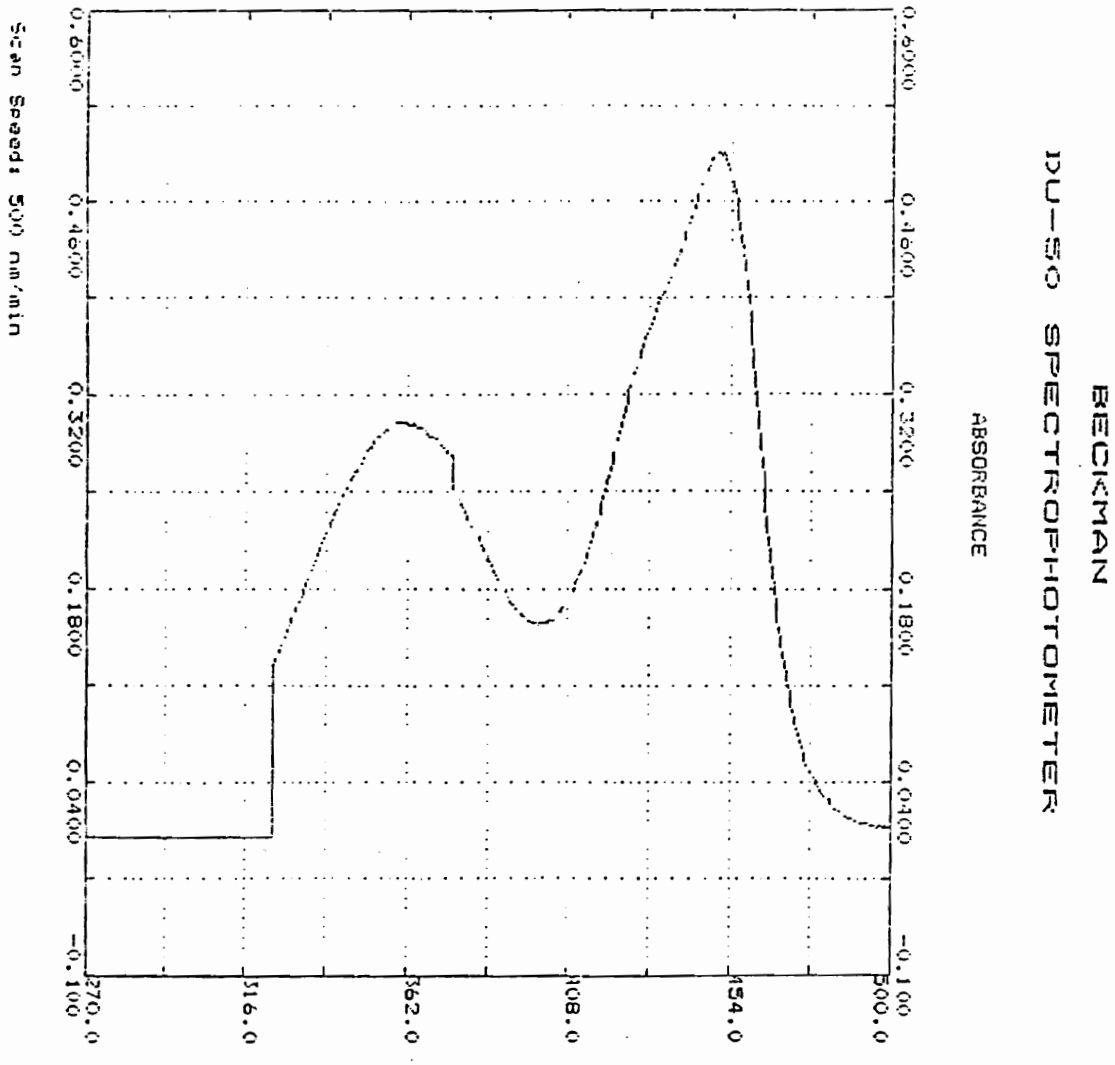

Figure 105. UV Spectrum of the Product Derived From the Reaction of 125 μM 4-Ethynyldihydropyridinium and Benzylamine.

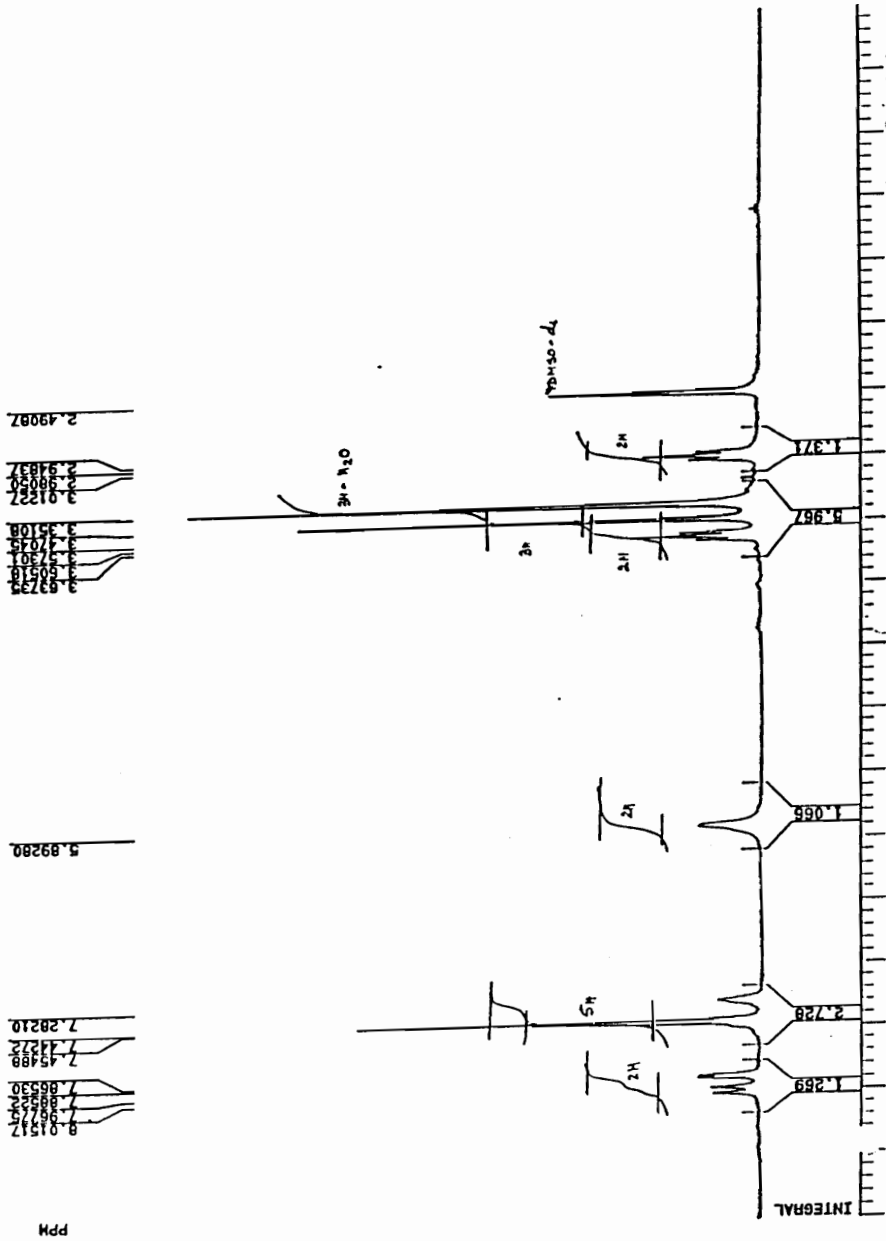

Figure 106. ^{1}H NMR (DMSO-d_6) of the Product Derived From the Reaction of 4-Ethynyldihydropyridinium and N-Methylaniline.

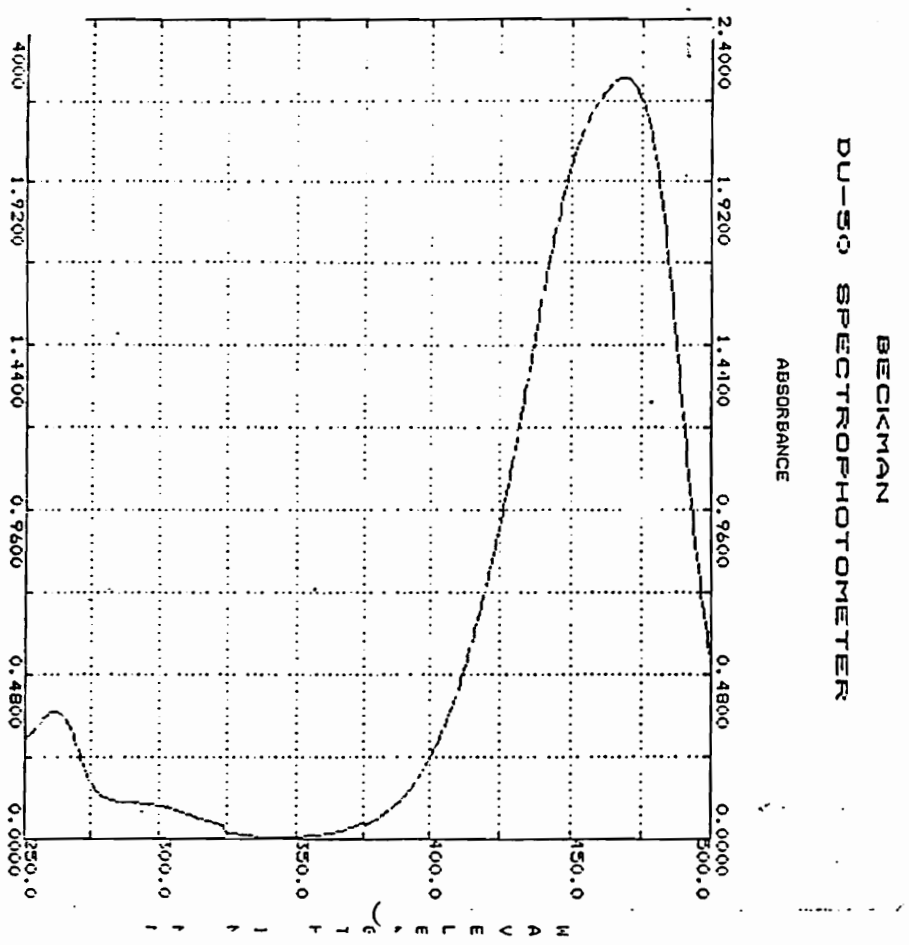

Figure 107. UV Spectrum of the Product Derived From the Reaction of 125 μM 4-Ethynyldihydropyridinium and N-Methylaniline.

Table 10. MAO-B Inactivation Properties of N- and C(4)-substituted MPTP Analogues.[a]

Compd	k_{inact} (min^{-1})	K_I (μM)
MPTP (**111**)	0.034	5000
140	0.029	268
146	0.24	172
152	0.06	5000
153	Not active[b]	---------
156	0.045	173
157	0.08	330
158	0.05	312
159	0.05	154
160	0.32	820

[a]The kinetics of inactivation were determined as described in the Experimental Section. The inhibitor concentrations used in these experiments depended on the activity of the individual compound and ranged from 50-100 μM for **146** to 300-1500 μM for **152**. [b]The limited solubility of **153** precluded a thorough study of its inhibitor properties.

4. Evaluation of Tetrahydropyridines as MAO-A Substrates.

As presented in the previous Chapter, the MAO-B characteristics of a variety of tetrahydropyridine derivatives have been demonstrated in terms of both their substrate and inhibitor properties. Except for the N-propyl-4-phenyltetrahydropyridine (**152**) analog which revealed weak substrate properties, none of the other N-substituted-4-phenyl-1,2,3,6-tetrahydropyridines showed any substrate properties with MAO-B. On the other hand tetrahydropyridines substituted at C-4 such as the 4-ethenyl (**157**) and the 4-ethynyl (**159**) analogs demonstrated much better substrate properties with MAO-B. During the course of these studies, a crude preparation of MAO-A became available to us. Consequently we have carried out preliminary studies with this crude preparation to obtain a qualitative assessment of the substrate properties of these compounds with MAO-A. This chapter summarizes the results of these experiments.

Preliminary experiments to study the MAO-A substrate properties of these derivatives were conducted following protocol similar to that used with MAO-B. In order to determine the metabolic fate of the tetrahydropyridine derivatives with MAO-A an incubation mixture containing a fixed concentration (500 μM) of the potential substrate (i.e. tetrahydropyridines prepared in this study) in pH 7.2 sodium phosphate buffer with 0.01 units of MAO-A was scanned for 1 hour spectrophotometrically at 37 °C.

4.1. Substrate Studies with N-and (C)-4-substituted Tetrahydropyridines.

We observed some dramatic differences in the characteristics of the

oxidative process catalyzed by the two isozymes. In the case of the N-substituted tetrahydropyridine derivatives, the N-propargyl and the N-allyl analogs **146** and **140**, which were non-MAO-B substrates, turned out to be moderately good substrates for MAO-A (Scheme 59). The N-propargyl analog **146** upon incubation with MAO-A was converted to a product which absorbed maximally at 344 nm and which was assigned the dihydropyridinium structure **151**. Under the given incubation conditions the dihydropyridinium intermediate was unstable and underwent further oxidation to the pyridinium species **180** (λ_{max} at 292 nm) (Fig. 108 and Fig. 109). At this point we do not have the synthetic dihydropyridinium standard **151**, but the confirmation of the second product of the MAO-A catalyzed oxidation, namely the pyridinium species **180** was based on the comparison with the synthetic pyridinium standard. The N-allyl analog **140** upon incubation with MAO-A was converted to a product which displayed a chromophore with λ_{max} 343 nm and which we have tentatively assigned to the dihydropyridinium species **145**. This dihydropyridinium metabolite also underwent further oxidation to the pyridinium species **179** (λ_{max} at 294 nm) (Figs. 110 and 111). The N-propyl analog **152** also turned out to be a substrate for MAO-A. Once again the intermediate dihydropyridinium species **233** (λmax 343 nm) underwent further oxidation to the stable pyridinium product **181** (λ_{max} 292 nm) (Fig. 112). The other N-substituted tetrahydropyridine derivatives, the N-cyclopropyl (**129**), N-cyclobutyl (**153**), and the N-cyclopentyl (**156**) analogs, showed no evidence of turnover under these incubation conditions with MAO-A.

Utilizing the same incubation conditions as in the case of the N-substituted tetrahydropyridine analogs, we studied the substrate properties of the C-4 substituted MPTP analogs with MAO-A. We also were surprised to discover that the C-4 substituted ethenyl (**157**) and the ethynyl (**159**) analogs, which were good MAO-B substrates, turned out to be non-MAO-A substrates. On the other hand the C-4 phenylethenyl derivative **158**, which was a weak MAO-B substrate, demonstrated moderately good substrate properties with MAO-A. The metabolic species formed in the MAO-A catalyzed oxidation of the C-4 phenylethenyl analog **158** was the dihydropyridinium species **235** (λ_{max} 375 nm) which underwent slow oxidation to the pyridinium species **200** as observed with the MAO-B experiment. Finally the C-4 phenylethynyl analog **160** was a extremely weak MAO-A substrate as well. The results of these qualitative studies are summarized in Table 11. The data in Table 11 are preliminary results due to the crudeness of the MAO-A preparation. Furthermore this "impure" MAO-A preparation resulted in turbid incubation mixtures of substrate and enzyme which also resulted in poor UV scans of the metabolic products of oxidation (shown throughout this section). This did not distract the qualitative information gathered from the data but prevented generation of reliable quantitative data.

Table 11. Comparison of the MAO-B vs MAO-A Substrate Properties of the N- and C-4 substituted MPTP Analogs.

Compd	MAO-B Substrate	MAO-A Substrate
MPTP	+++	+
129	-	-
140	-	+
146	-	+
152	+	+
153	-	-
156	-	-
157	++	-
158	++	-
159	+	++
160	-	-

- = not a substrate. + = moderate substrate properties. ++ = good substrate. +++ = extremely good substrate. MAO-A data based on qualitative analysis only. Wheras MAO-B data is based on kinetic analysis and estimation of Michaelis-Menton constants.

Scheme 59. MAO-A Catalyzed Oxidation of N-Substituted-4-phenyl-tetrahydropyridines.

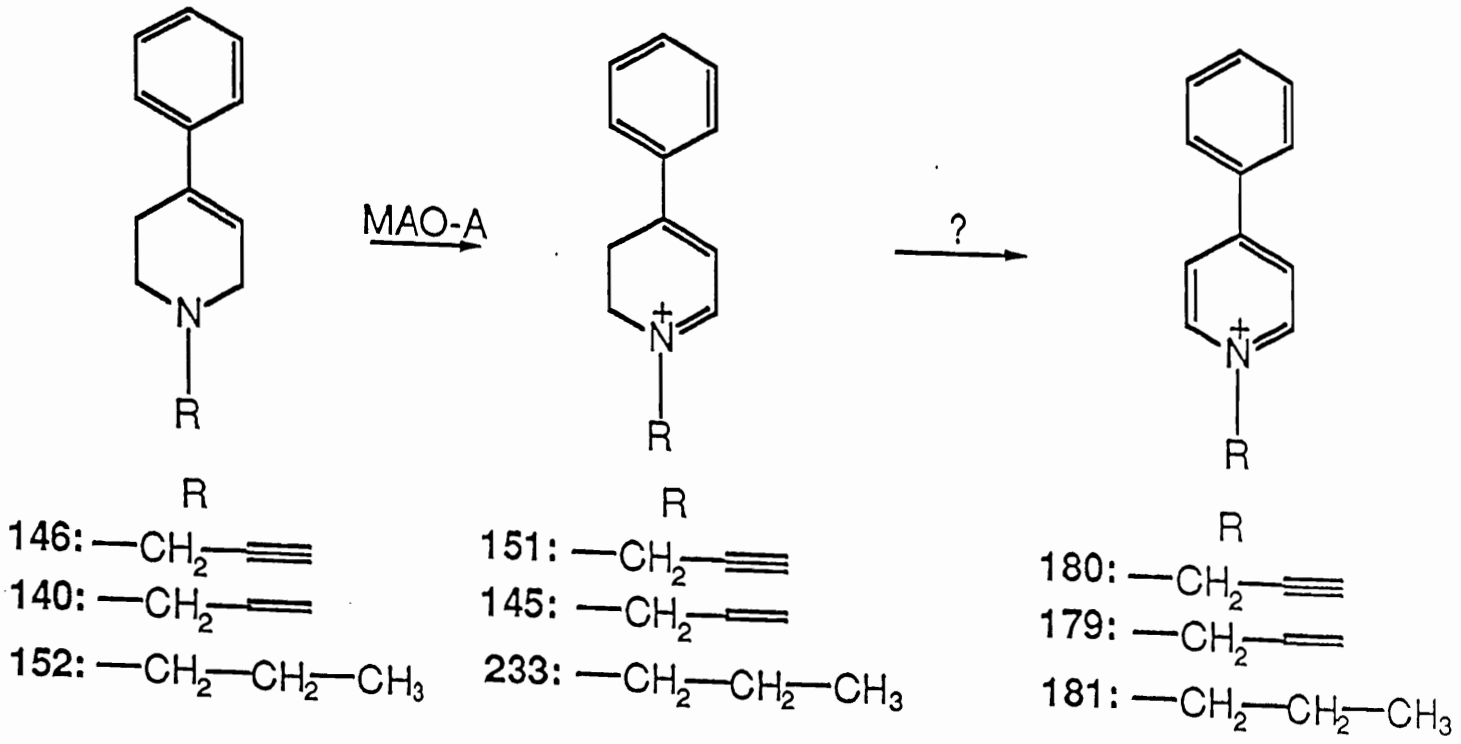

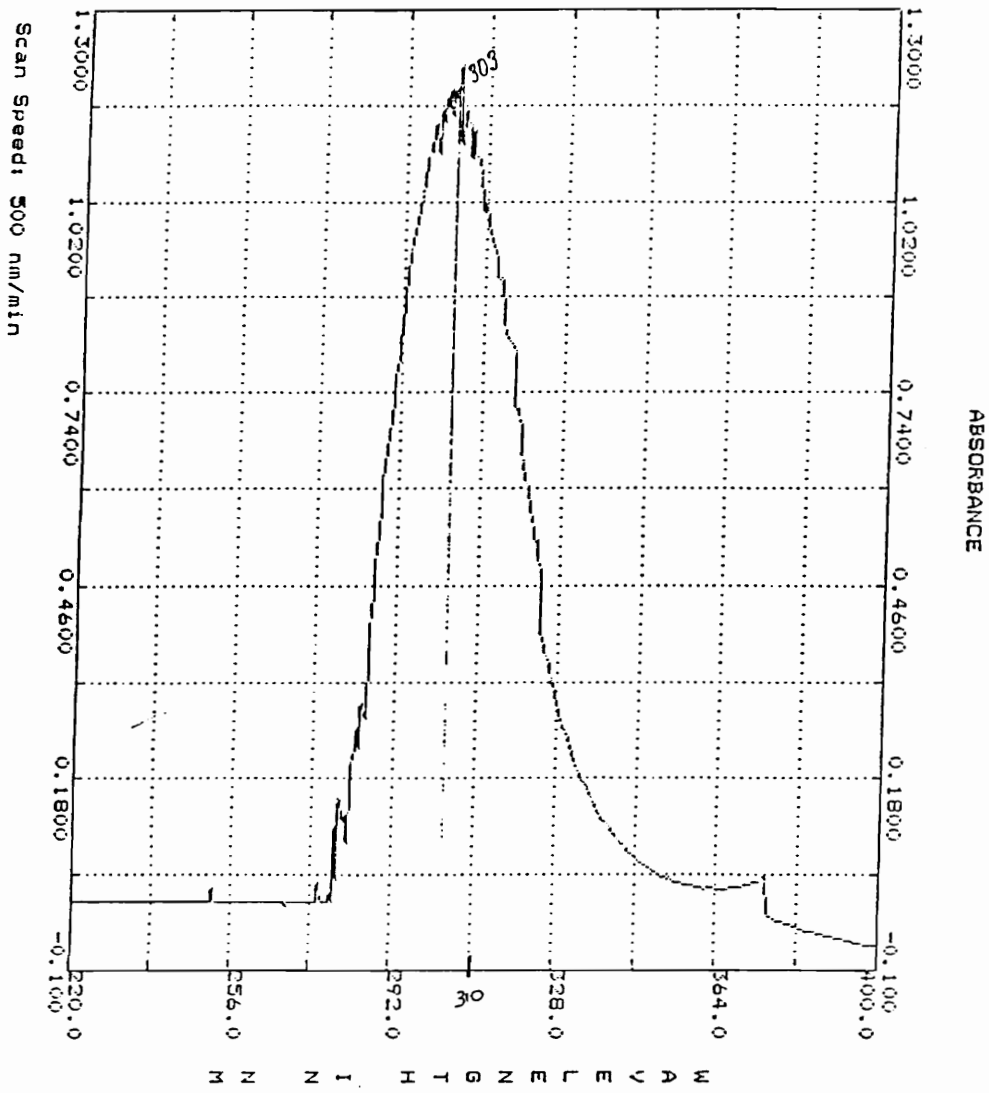

Figure 109. UV Spectrum of MAO-B Catalyzed Oxidation of 0.5 mM 4-Phenyl-1-propargyltetrahydropyridine at T = 40 minutes.

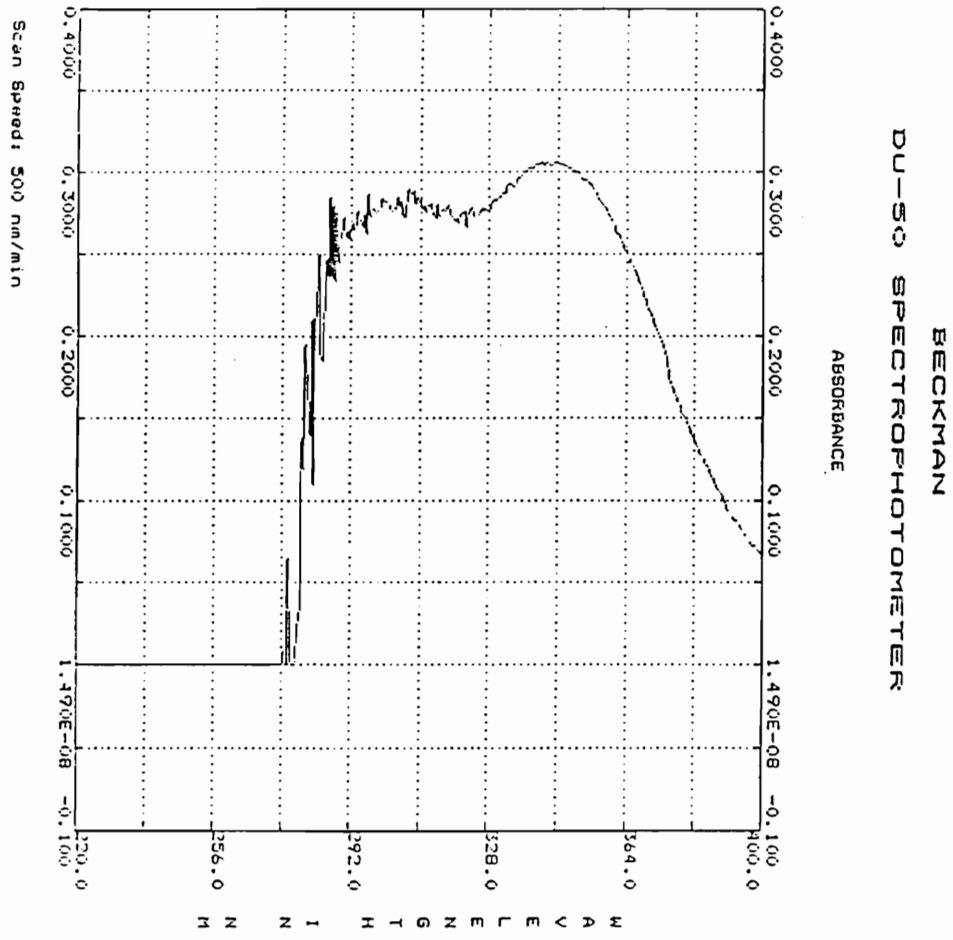

Figure 110. UV Spectrum of MAO-B Catalyzed Oxidation of 0.5 mM 1-Allyl-4-phenyltetrahydropyridine at T = 10 minutes.

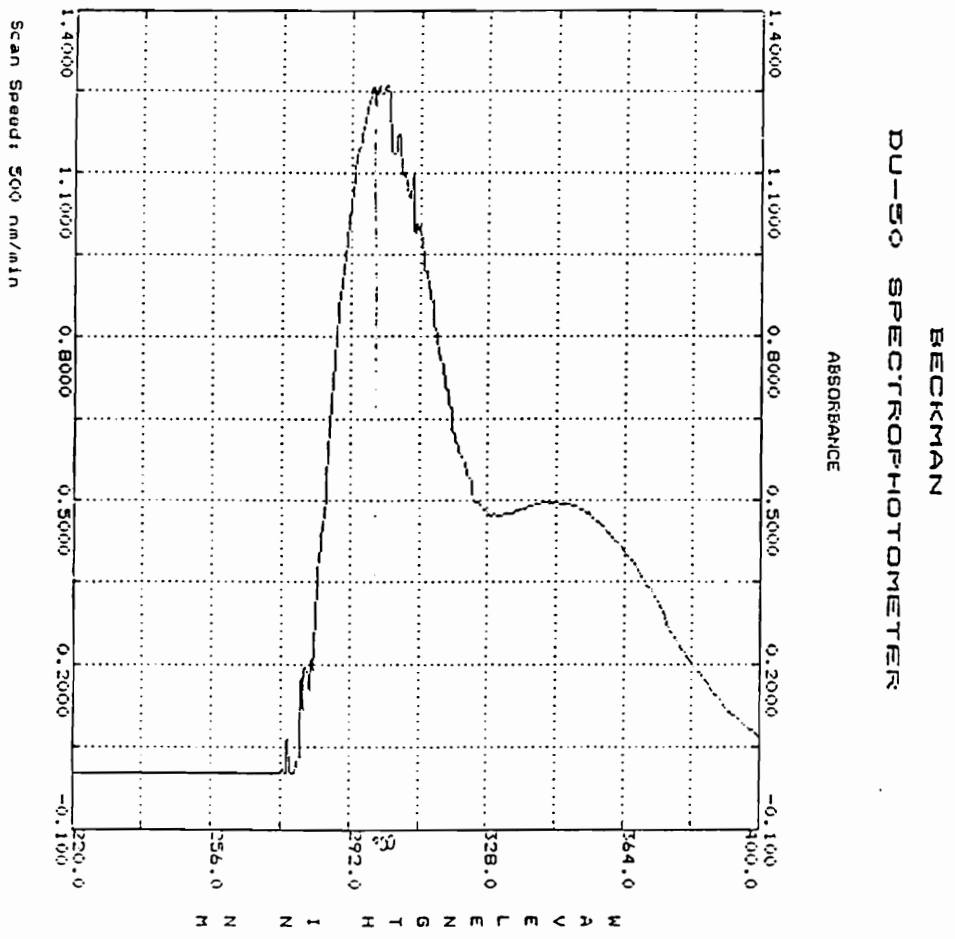

Figure 111. UV Spectrum of MAO-B Catalyzed Oxidation of 0.5 mM 1-Allyl-4-phenyltetrahydropyridine at T = 40 minutes.

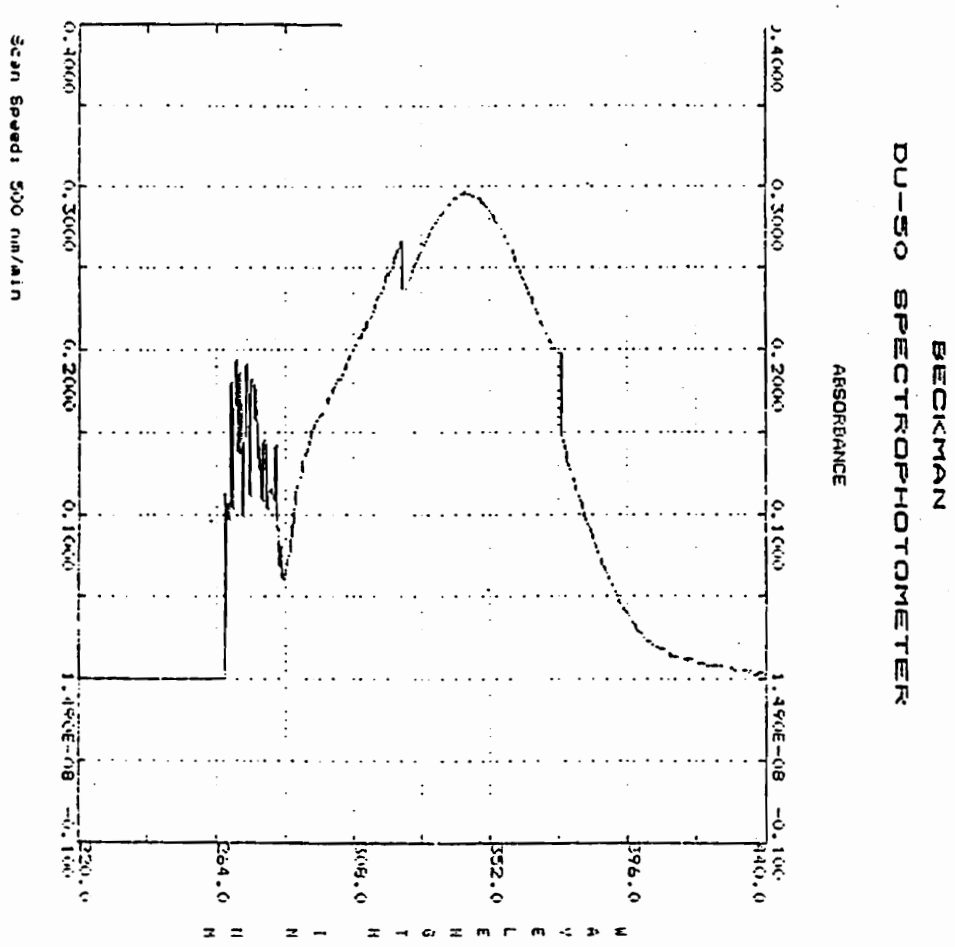

Figure 112. UV Spectrum of MAO-B Catalyzed Oxidation of 0.5 mM 4-phenyl-1-propyltetrahydropyridine at T = 20 minutes.

4.2. MAO-B and -A Substrate Studies with the C-4-Aryloxy -MPTP Derivatives.

As described earlier in Chapter 2, pg 96, MAO-B substrate studies on the MPTP derivative, N-methyl-4-phenoxy-1,2,3,6-tetrahydropyridine (**165**) led to a rapid formation of a compound with λ_{max} of 324 nm which was tentatively assigned to the expected dihydropyridinium species **166** (the initial metabolite of MAO-B catalyzed oxidation of **165**). The λ_{max} of the synthetic dihydropyridinium compound was found to be 316 nm and upon standing, however, this value shifted to 324 nm, the same absorbance observed in the MAO-B incubation mixture of **165**. A close examination of an MAO-B incubation mixture containing **165** revealed the formation of the dihydropyridinium metabolite at 316 nm and its rapid shift to the 324 nm absorbing species. A consideration of its potential reactivity suggested the possibility that **166** was undergoing hydrolytic cleavage via the hemiketal **168** to yield the corresponding aminoenone **169** and phenol **170** (See Chapter 2, Scheme 32, pg 97). This proposal was documented fully by GC-EI mass spectral analysis of an extract of an incubation mixture which revealed molecular ions corresponding to phenol **170** and the aminoenone **169**. Independent mass spectral analysis of synthetic **169** revealed a molecular ion $M^{\cdot+}$ 111 which coincided with the molecular ion obtained from the incubation mixture.

The excellent substrate properties of **165** (see Table 12) and the susceptibility of the dihydropyridinium metabolite to hydrolytic cleavage suggested the possibility of designing prodrugs in which a pharmacologically active moiety is attached to the C-4 of the 1,2,3,6-

tetrahydropyridine system via a heteroatom. Subsequent MAO catalyzed oxidation would result in liberation of this pharmacophore via hydrolytic cleavage as observed with **165** as depicted in Scheme 60. In order to assess the scope of this prodrug concept we have extended our studies to design a series of C-4-aryloxyMPTP derivatives **171-175, 177**. Furthermore the recent availability of MAO-A provided us with a opportunity to study the substrate selectivity of these aryloxyMPTP analogs towards MAO-A or MAO-B.

Scheme 60. The Prodrug Concept.

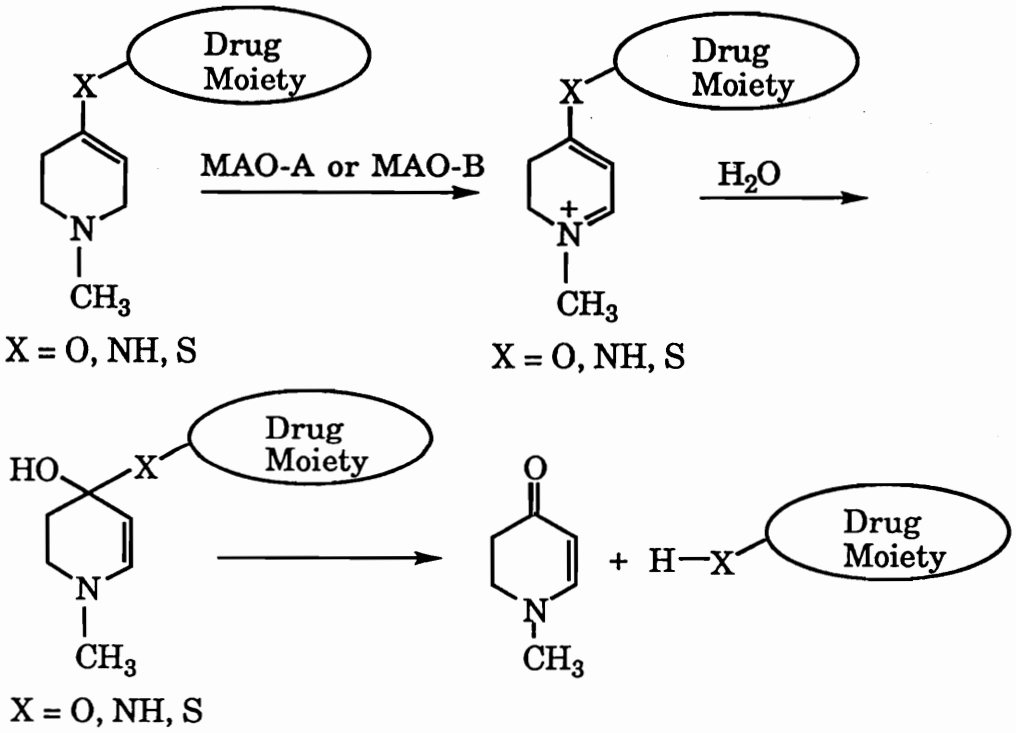

Substrate Studies with MAO-B.

The substrate properties of the candidate compounds were examined with MAO-B purified from beef liver. We first screened these

molecules for their general substrate properties by performing repeated 400 to 200 nm scans of incubation mixtures containing 500 μM solution of each compound in pH 7.4 100 mM sodium phosphate buffer in the presence of 0.05 units of MAO-B at 37 °C over a period of 30 minutes. Under these conditions all of the aryloxyMPTP analogs were rapidly metabolized via the dihydropyridinium intermediates to the aminoenone species at λ_{max} 324 nm. As a representative case, the UV tracings of the MAO-A catalyzed oxidation of 4-(2,4-dichlorophenoxy)-1-methyltetrahydropyridine analog **177** is shown in Fig. 113a. Some dihydropyridinium intermediates appeared to undergo hydrolysis much faster than others. Our initial attempts to generate quantitative kinetic data on the rates of oxidation were complicated by the fact that all of the dihydropyridinium species generated as the initial products of oxidation of the aryloxyMPTP analogs appeared to absorb at a similar wavelength (λ_{max} 324 nm) as that of the hydrolysis product, the aminoenone. So we elected to use the λ_{max} 324 nm absorption to monitor the initial rates of oxidation of the aryloxyMPTP analogs and have used ε 15000 in our calculations of the V_{max} and K_M. This assumptions were justified when the metabolic dihydropyridinium species **268** which results from the MAO-B catalyzed oxidation of **175** was synthesized and revealed λ_{max} at 315 nm with a ε value similar to the aminoenone. The kinetic parameters for the MAO-B catalyzed oxidation of the aryloxyMPTP analogs were calculated from the lineweaver-Burke plot constructed from the data obtained by incubating several concentrations of a given tetrahydropyridine with MAO-B and measuring the initial rates of

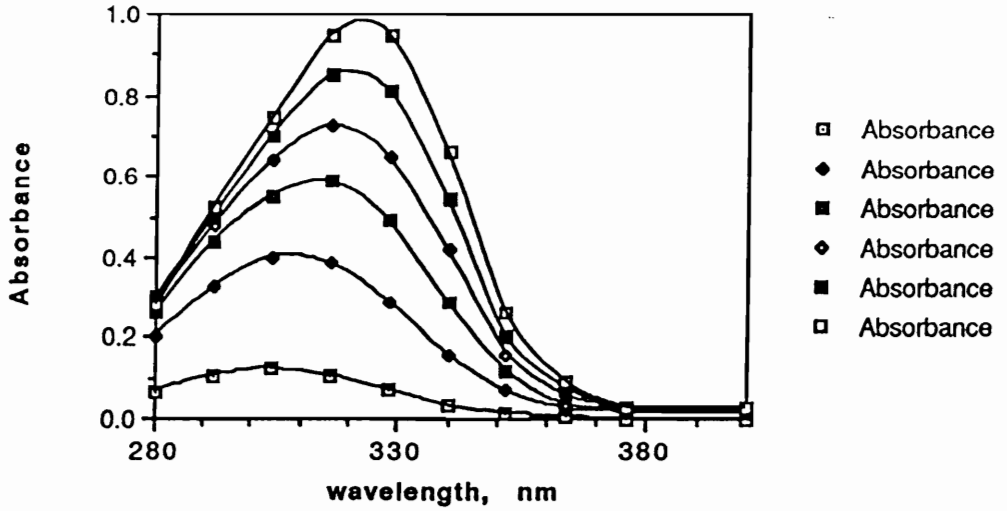

Fig. 113a. MAO-A Catalyzed Oxidation of 4-(2,4-Dichlorophenoxy)-1-methyl-1,2,3,6-tetrahydropyridine (177).

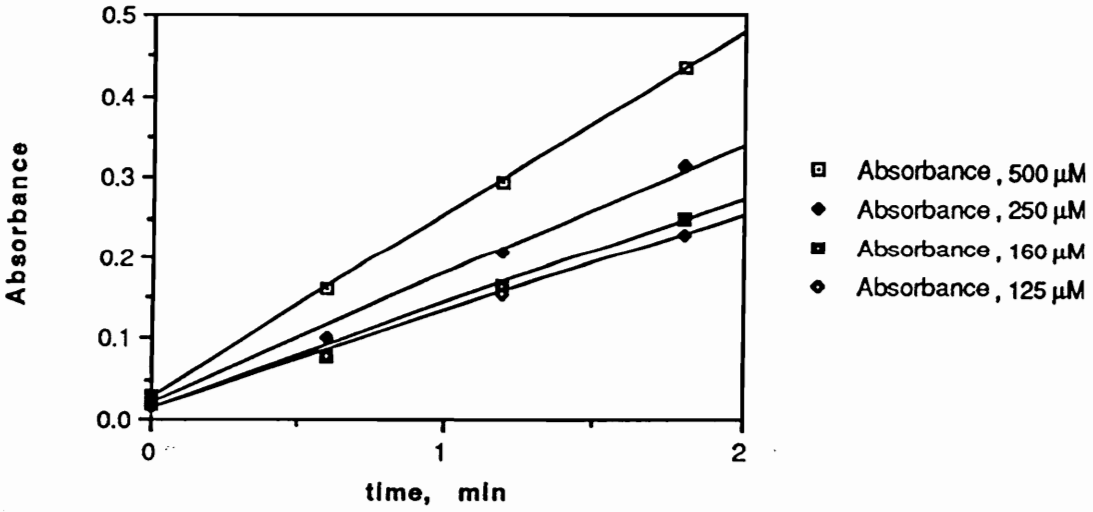

Fig. 113b. Initial Rates of MAO-A Catalyzed Oxidation of 177.

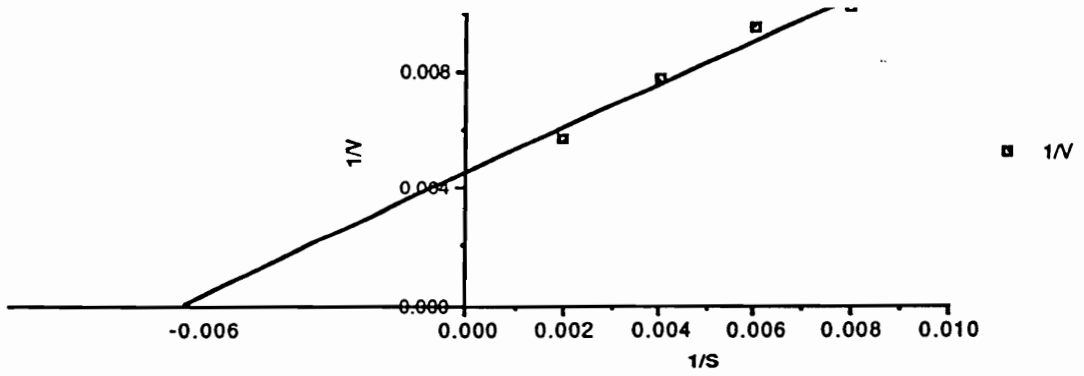

Fig. 113c. Lineweaver-Burke Plot for the MAO-A Catalyzed Oxidation of Substrate Studies with MAO-A. 177.

Qualitative MAO-A substrate studies (under incubation conditions similar to those described for the N- and C-4-MPTP derivatives) with the C(4)-aryloxyMPTP analogs **171-175,177** were carried out to gain additional information on possible differences between MAO-B and MAO-A. As in the case with MAO-B, the aryloxy analogs **171-175,** and **177** upon incubation with MAO-A revealed the initial formation of products bearing chromophores in the range of 315-320 nm (dihyropyridinium species) which rapidly underwent hydrolysis to the aminoenone as shown in the case of the 4-phenylphenoxy-1-methyltetrahydropyridine derivative **175** (Fig 114a). Quantitative data was obtained by measuring the initial rates of oxidation of a series of concentrations of the tetrahydropyridine derivatives with MAO-A at 324 nm (Fig 114b: in the case of the aryloxy analog **175**) which were then utilized in the determination of the kinetic parameters V_{max} and K_M from the Lineweaver-Burke plot (Fig. 114c: in the case of the aryloxy analog **175**).

The results of these experiments is summarized in Table 12.

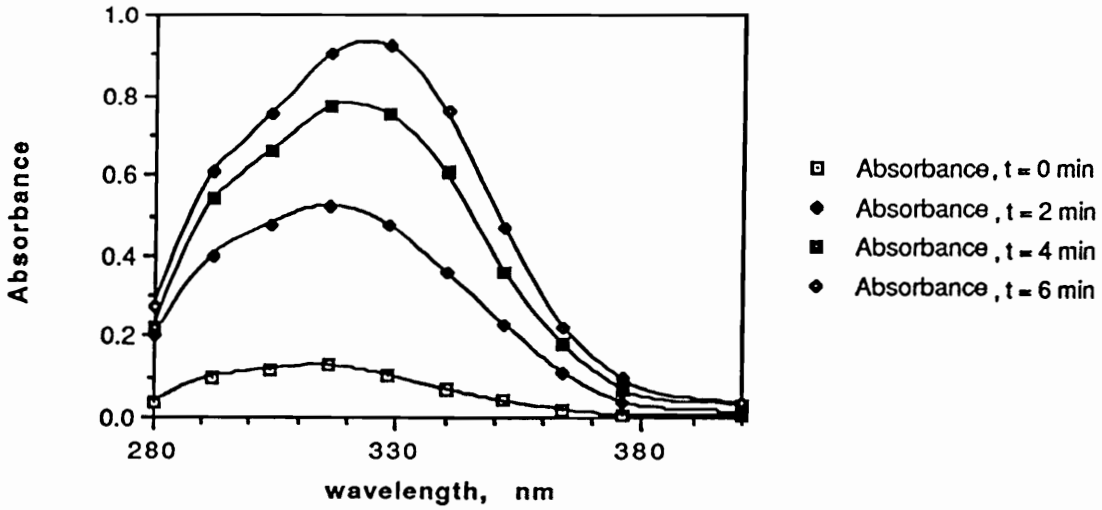

Fig. 114a. MAO-A Catalyzed Oxidation of 4-(Phenylphenoxy)-1-methyl-1,2,3,6-tetrahydropyridine (175).

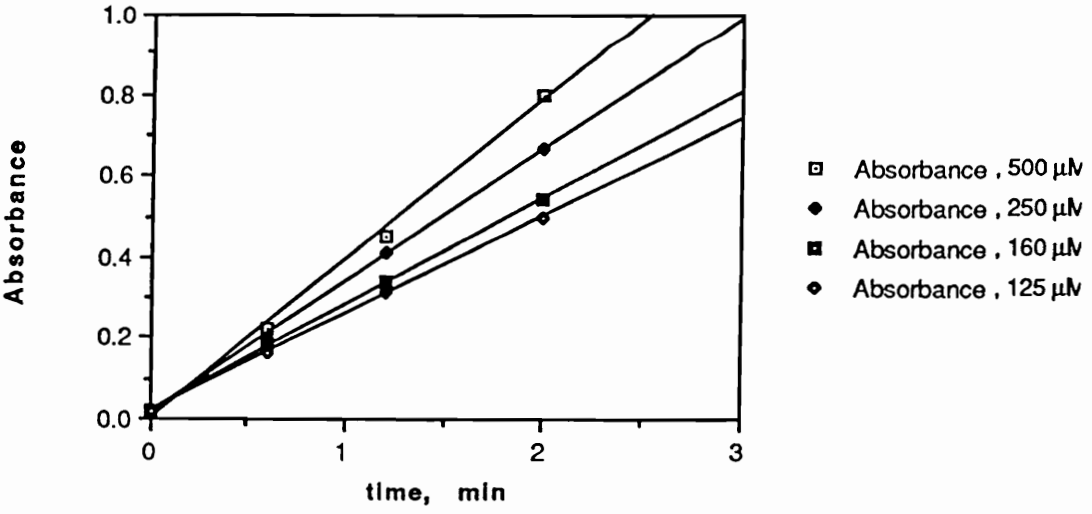

Fig. 114b. Initial Rates of MAO-A Catalyzed Oxidation of 175.

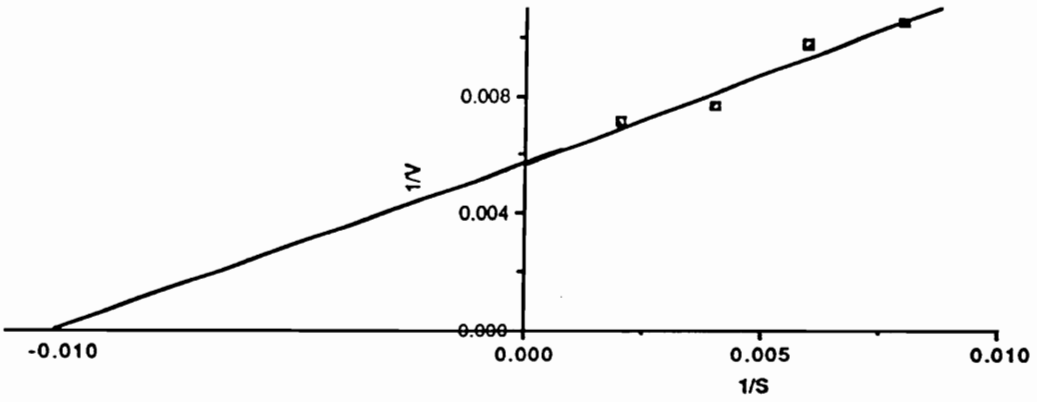

Fig. 114c. Lineweaver-Burke Plot for the MAO-A Catalyzed Oxidation of 175.

Table 12. Oxidation of AryloxyMPTP Analogs by Monoamine Oxidase (MAO).

Michaelis-Menten Kinetic Parameters for Oxidation by MAO-A and MAO-B				
	MAO-A		MAO-B	
Compd	V_{max}[a]	K_m[b]	V_{max}	K_m
165	1040	55	241	58
171	888	130	81	56
172	680	51	340	84
173	1656	77	1232	274
174	1816	144	300	143
175	1384	101	381	284
177	760	29	825	167

[a]nmol/min/Unit MAO-A. [b]μM.

5. Conclusions.

Analysis of MPTP Analogs as MAO-A and MAO-B Substrates. One of the objectives of this exercise was to characterize the features of MAO which play a role in the metabolism of MPTP and its analogs. It was shown earlier in our laboratory[186] and by others[187] that introduction of a methylene bridge between the tetrahydropyridine ring and the phenyl group of MPTP results in MPTP analog **292** which demonstrates a two fold increase in MAO-B substrate activity than MPTP, presumably because of increased flexibility of the C-4 substituent. The kinetic parameters for the MAO-A and MAO-B catalyzed oxidation of **292** are as follows: V_{max} = 74 nmols/min/unit MAO-A and K_M = 66 μM; V_{max} = 714 nmols/min/unit MAO-B and K_m = 154 μM wheras the corresponding parameters for MPTP are V_{max} = 160 nmols/min/unit MAO-A and K_m = 140 μM; V_{max} = 755 nmols/min/unit MAO-B and K_m = 390 μM. This result is in excellent agreement with our studies (Chapter 3, Section 3.2.) on the corresponding MAO-B substrate properties of 4-benzyl-1-propyl-1,2,3,6-tetrahydropyridine (**257**) and the 4-phenyl-1-propyl-1,2,3,6-tetrahydropyridine (**152**) analogs. Incorporation of a methylene group into the rigid structure of **152** to generate **257** resulted in a MPTP analog with increased flexibility as demonstrated by the corresponding kinetic parameters of MAO-B catalyzed oxidation of the rigid **152** (V_{max} = 7 nmols/min/unit MAO-B, K_m = 2 mM) versus the more flexible **257** (V_{max} = 330 nmols/min/unit MAO-B, K_m = 1.6 mM). For reasons which remain unclear, both the 4-benzyl-1-propyl and the 4-benzyl-1-methyl MPTP analogs **257** and **292** display poor MAO-A properties, albeit only qualitative data is available for **257** due to the poor quality of our MAO-A preparation. Also

consistent with this result, the phenethyl MPTP analog **293** has been shown to be a much better substrate of MAO-A than MAO-B (V_{max} = 1096 nmols/min/unit MAO-A and K_m = 120 μM; V_{max} = 225 nmols/min/unit MAO-B and K_m = 54 μM). However introduction of rigidity at the C-4 position of **293** proved detrimental for MAO-B substrate activity as observed in the case of the corresponding phenylethenyl (**158**) and the phenylethynyl (**160**) derivatives. These derivatives however, displayed, slightly enhanced MAO-A substrate properties and no quantitative data is yet available.

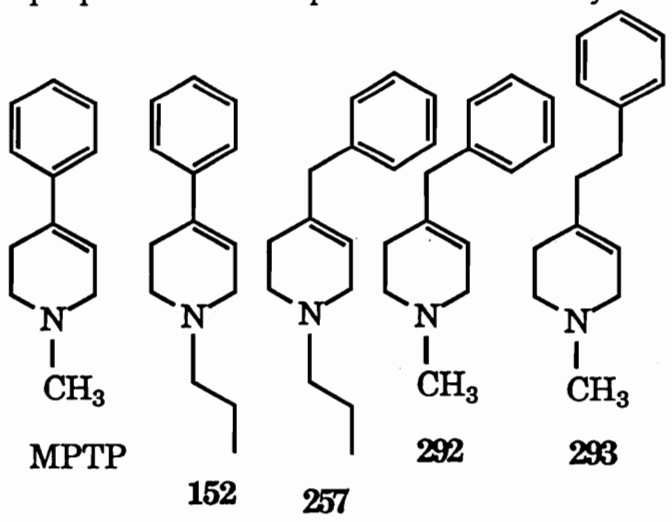

The *de novo* C-4 ethenyl (**157**) and the ethynyl (**159**) MPTP analogs displayed a remarkable selectivity pattern with the two forms of the enzyme. Both the MPTP analogs were found to be good MAO-B substrates and virtually displayed no substrate properties with MAO-A (only qualitative data available on MAO-A substrate properties). These results point out to important differences in the active site of the two forms of MAO, particularly in the region which binds the C-4 substituent of these tetrahydropyridines.

The subsequent MAO studies on the substrate properties of the N-substituted -4-phenyl MPTP analogs led to some very interesting findings.

The lack of MAO-B substrate properties previously documented for the 4-phenyl-1-propyl MPTP analog (**152**) was shown to be contradictory to the subsequent results obtained in our laboratory. Based on these results, previous reports (see Chapter 2 for structure-activity requirements for MPTP analogs) suggesting the lack of substrate properties of MPTP analogs bearing nitrogen substituents larger than methyl must be viewed with caution. None of the remaining N-substituted-4-phenyl MPTP analogs displayed any substrate properties. The corresponding substrate studies with MAO-A revealed a totally different profile. The N-propargyl (**146**), N-allyl (**140**) which had shown no affinity for MAO-B turned out to be moderate MAO-A substrates and underwent MPTP-like oxidation to the corresponding dihydropyridinium species which was eventually oxidized further to the pyridinium species. No quantitative data is yet available and subsequent studies to estimate their rates of oxidation is in progress. Once again these results do not support the generalization based on conformational and molecular determinants[179,142] that good MAO-A substrates required a methyl substituent on the nitrogen atom of MPTP.

Studies on the substrate properties of the C-4 aryloxytetrahydropyridine analogs with MAO indicated that almost all of the derivatives were good to excellent substrates for both MAO-A and MAO-B. A majority of the compounds were as good or better MAO-A substrates than kynuramine, the generally accepted preferred substrate for this form of the enzyme. Of particular interest, was the low Km value (29 μM) for the 2,4-dichlorophenoxy analog (**177**) which was designed to share some of the structural features of the highly selective and potent MAO-A inactivator clorgyline (**14**). These data

would argue that the corresponding N-Propargyl derivative (**176**) might display interesting inactivator properties as well. These results also indicate that seperation of the phenyl and tetrahydropyridyl ring by an oxygen atom leads to a dramatic improvement in the overall substrate properties particularly in terms of the turnover characteristics. Thus while the V_{max} value for MPTP is only 160 nmols/min/unit MAO-A, the aryloxy compounds display high V_{max} values ranging from 766 nmols/min/unit MAO-A for the 2,4-dichlorophenoxy analog to 1816 nmols/min/unit for the α-napthoxy derivative **174**. The introduction of butyl and *tert*-butyl groups at the 4-position alters the binding and turnover characteristics to a small extent relative to the unsubstituted compound **165**, but overall these groups appear to be well tolerated by MAO-A. The excellent MAO-A substrate properties of the 4-(4-phenylphenoxy) and the two napthoxy compounds are consistent with the results obtained by Efange and co-workers[187] who obtained similar values for the corresponding α- and β-napthylmethyl derivatives **294** and **295** respectively.

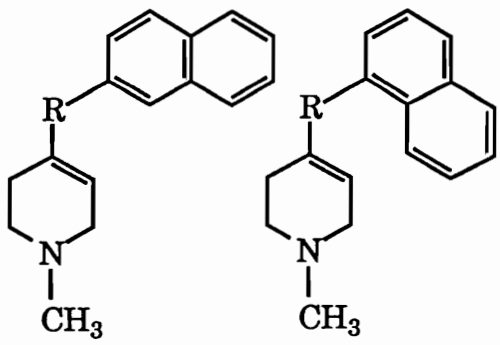

173: R = O **174:** R = O
294: R = CH_2 **295:** R = CH_2

What is puzzling, however, is the difference in the substrate properties of the 4-benzyltetrahydropyridine (**292**) versus the 4-

phenoxytetrahydropyridine (**165**) (V_{max} for **292** = 92 nmols/min/unit MAO-A vs V_{max} for **165** = 1040 nmols/min/unit MAO-A). It appears that relatively subtle changes in the arrangement of the phenyl group at C-4 can influence the nature of the interactions at the active site.

The aryloxy compounds also turned out to be excellent MAO-B substrates. Vmax values ranged from 81 nmols/min/unit MAO-B for *tert*-butyl analog **171** to 1232 for β-napthoxy analog **173**. The majority of these analogs are much better MAO-B substrates than previously studied MPTP analogs and some are better substrates than benzylamine, the preferred MAO-B substrate. Athough it is possible to discern some general trends when comparing the MAO-A vs MAO-B substrate properties of these compounds, no well defined generalizations can be reached in terms of selectivity for one form of the enzyme over the other. This outcome is not consistent with the recent report on a series of 4-arylmethyl-1-methyl-1,2,3,6-tetrahydropyridine derivatives[187] which display a distinct selectivity in terms of substrate properties, which was not seen with the corresponding aryloxy derivatives. It is clear that in contrast to the results obtained with MAO-B, the A form of the enzyme tolerates well the larger groups at C-4. In the case of the aryloxy compounds this distinct seperation between the two forms of the enzyme was not observed. Thus the comparison between the arylmethyl and the aryloxy derivatives was inconsistent. Although the Km values were similar the turnover numbers of the aryloxy compounds were considerably lower. The previous claim that MAO-B prefers smaller analogs while MAO-A shows preference for bulkier substituents does not hold true in this series of compounds and must be viewed with caution.

Analysis of MPTP Analogs as Inactivators.

The effectiveness of the N-cyclopropyl (**130**) and the N-propargyl (**146**) MPTP analogs as MAO-B inactivators had shown promise. However larger substituents (latent alkylating groups) on nitrogen did not lead to significant inactivation, although some of them showed time-dependent inactivation, probably because of increased steric bulk on nitrogen leading to poor binding characteristics at the active sites of MAO-B, as illustrated by the lack of substrate properties by the N-cycloutyl analog **153** and the large K_m value for the N-propyl derivative **152**. In view of the moderately effectiveness of **146**, the failure of the corresponding N-allyl (**140**) analog as a MAO-B inactivator was somewhat surprising. Although it is known that allylamines are also inhibitors of MAO-B[181] they require much higher concentrations than the corresponding propargylicamines (pKa differences: see Chapter 3, Section 3.2.) to effect the same change in MAO activity. One of interesting aspects of further work would be to study the mechanism of inactivation of MAO-B by the N-propargyl analog **146**. Attempts were made to synthesize the corresponding deuterium-labelled analog **146-d_2** for isotope effect study, but we have been unsuccessful in the synthesis so far.

The failure of the C-4 ethenyl (**157**) and ethynyl (**159**) analogs was surprising. These molecules had been designed to generate more electrophilic dihydropyridinium species upon initial enzyme processing. These manipulations were carried out due to the surprising stability of the 4-cyclopropyl-2,3-dihydropyridinium species (see Chapter 2). The compounds turned out be good MAO-B substrates but poor inactivators and an estimate of the partition ratio favours dissociation of the substrate from the active site of

the enzyme into product. Subsequent synthesis and chemical reactivity studies on the 4-ethynyl-2,3-dihydropyridinium system **236** with various nucleophiles demonstrated the high electrophilicity of this system and the general conclusion from the failure of this molecule as an inactivator could be attributed to the absence of a active site nucleophile in the C-4 region of the tetrahydropyridyl moiety.

In view of the unexpected MAO-A substrate properties demonstrated by the N-propargyl (**146**) and the N-allyl (**140**) analogs, it remains to be seen whether these compounds inactivate MAO-A significantly. Similarly the lack of MAO-A substrate properties by the C-4 ethenyl and the ethynyl analogs **157** and **159** could be an indication of potent inactivation of the enzyme (the N-cyclopropyl (**130**) and the N-propargyl (**146**) derivatives were non MAO-B substrates but efficent inactivators of the enzyme) and these studies should be deemed as high priority.

With the synthesis of the N-cyclopropyl-4-piperidin-4-one (see Chapter 3, Section 3.1. for synthesis of this intermediate) in large quantities Dr. Simon Kuttab, in our group has been able to synthesize various N-cyclopropyl--substituted analogs of MPTP and subsequent substrate/inactivation studies have also been carried out with both the forms of the enzyme. The following paragraph will attempt to summarize the results of that study and the potential mechanistic significance to MAO catalyzed oxidations in general.

As revealed earlier[145] the N-cyclopropyl-4-phenyl MPTP analog **130** was an extremely poor substrate but a good time- and concentration-dependent inactivator of MAO-B (k_{inact} = 0.7 min^{-1} and K_I = 182 μM). It was also shown to display moderate inactivation properties with MAO-A (k_{inact} =

0.04 min^{-1}, K_I = 0.93 μM). The poor substrate properties are consistent with the general lack of turnover of MPTP derivatives with bulkier N-alkyl groups and the inactivation properties are also consistent with the proposed role of the cyclopropyl group in being enzymatically activated and reacting with an active site functionality. The poor MAO-B inactivation properties of MPTP supports these data.

In conjunction with the enhanced MAO-B substrate properties displayed by the 4-benzyltetrahydropyridine analog **292**, the corresponding 4-benzyl-1-cyclopropyl-1,2,3,6-tetrahydropyridine (**296**) derivative was synthesized as a potential selective MAO-B inactivator. The compound was found to be a MAO-B substrate with a V_{max} value of 2356 nmols/min/unit MAO-B and a K_m of 414 μM. The overally affinity of **296** for MAO-B (V_{max}/K_m) indicates that it is a weaker substrate than its methyl analog **292**. Furthermore **296** was also shown to display inactivation properties with MAO-B (k_{inact} = 0.11 min^{-1} and K_I = 75 μM). The low K_I value indicates increased binding affinity for MAO-B due to the incorporation of a methylene bridge at C-4 (K_I for the corresponding 4-phenyl-1-cyclopropyl analog **130** = 182 μM). Substrate studies with MAO-A did not reveal any MAO-A substrate properties with **296** which is also consistent with the corresponding N-methyl and the N-propyl analogs **292** and **257** which lack MAO-A substrate properties. On the other hand, **296** turned out to be a potent inactivator of MAO-A with undetermined kinetic parameters due to severe inactivation at higher concentrations (satuarting conditions). At lower concentrations **296** displayed a time- and concentration-dependent profile characteristic of a mechanism-based inactivator.

Scheme 61. Proposed Mechanism of Inactivation of MAO by 296.

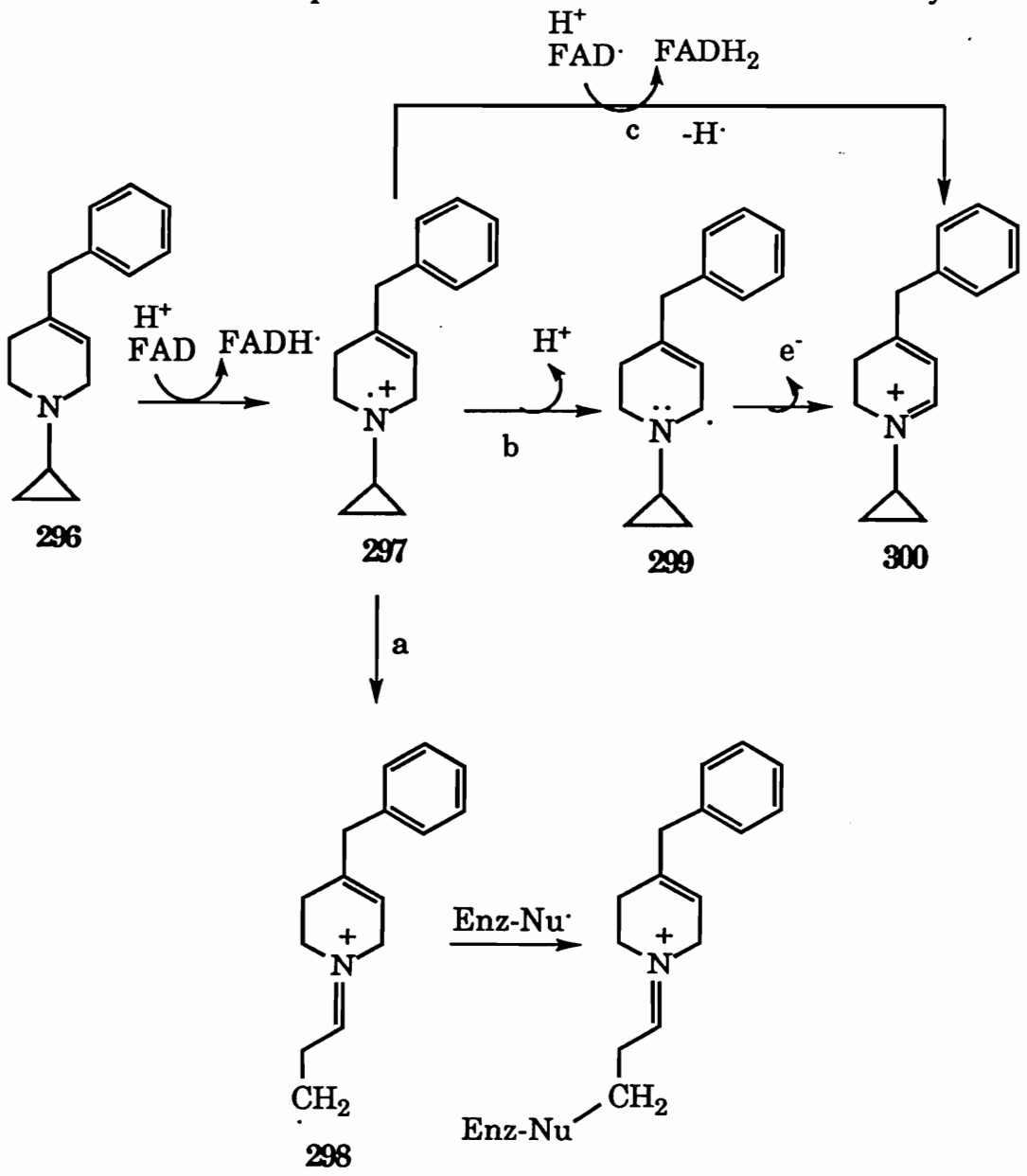

If the general mechanism of inactivation of MAO by cyclopropylamines holds true (Chapter 1), then cyclopropylamine radical cation **297** generated by the MAO-B catalyzed oxidation of **296** should be very reactive and must undergo spontaneous ring opening to the carbon-centered radical **298** which could then inactivate MAO-B by covalent modification of a active site nucleophile. In our case the data with MAO-B indicates a partitioning of the amine radical cation **297** between the proposed cyclopropyl ring opening (inactivation pathway, pathway a) and α-proton abstraction to give secondary carbon-centered radical **299** which undergoes a second one-electron loss (pathway b) to generate the dihydropyridinium intermediate **300,** or an hydrogen atom abstraction (pathway c) to directly generate **300** (Scheme 61). This observation presents convincing evidence for the operation of a partitioning situation between two pathways in the enzyme environment. While the amine radical cation formation **297** is the initial mandatory step, it may be envisaged that steric hinderence in the transition state and constraints at the active site of the enzyme may influence the proper positioning and overlap between the p-orbital of the amine radical cation and the cyclopropyl ring bonds thus imparting some stability to the amine radical cation and slowing the rate of ring cleavage in favour of α-hydrogen deprotonation or hydrogen atom abstraction. Another possible explaination is that there is a nucleophilic or radical center on the active site which may be in juxtaposition to the α-proton in the case of MAO-B allowing pathway b to partially proceed. In this respect it may be said that the active site of MAO-B plays a different role than the active site of MAO-A in the interaction and orientation of the

molecule resulting in partitioning between substrate and inactivation pathways.

A recent report by Silverman[190] indicates that the ring opening of 1-phenylcyclopropylamine by MAO-B is stereoselective and thus influenced by the enzyme active site and asymmetry. This actually suggests that the rate of ring opening of the amine radical cation 297 may be modified by the enzyme environment and may not be as fast as predicted in the laboratory. Thus the original proposal of a partitioning mechanism in MAO oxidations via a cyclopropyliminium species (see Chapter 1) may still be a valid option depending on the structure of the compound under investigation.

6. Experimental.

6.1. Chemistry.

Melting points were determined using a Thomas-Hoover melting point apparatus and are uncorrected. Unless stated otherwise reagents were obtained from commercial sources and were used directly. Reactions were conducted under a dry nitrogen atmosphere. THF and diethyl ether were distilled from $LiAlH_4$. UV-vis spectra were recorded on a Beckman DU Series 50 spectrophotometer using a path length of 1 cm. ^1H NMR spectra were recorded on either a Bruker 270 MHz or 200 MHz spectrometer; chemical shifts are reported in parts per million (ppm) relative to internal TMS except where noted. The following abbreviations are used to describe peak patterns when appropriate: b = broad, s = singlet, d = doublet, t = triplet, q = quartet, m = multiplet, db = doublet of doublets. Gas chromatography/mass spectrometry (GCMS) was performed using an Hewlett Packard (HP) 5890 capillary GC coupled to an HP 59970 MS chem station. The capillary column used in all the cases was an HP-1 (12.5 m x 200 μm x 0.33 mm film thickness). FAB (using p-nitrobenzyl alcohol as matrix) were obtained on a VG 7070 HF instrument and capillary column (HP-1) from the Dept. of Biochemistry, Virginia Tech, Blacksburg, VA. Elemental analyses, performed by Atlantic Microlab, Inc., Norcross, GA, were within 0.4 % of the theoretical values calculated for C, H, and N.

The N-alkyl-4-phenylpyridinium halides **179·I, 180·Br, 181·I** were prepared as described previously.[147]

General Procedure for the Synthesis of the Oxalate Salts of N-

Substituted-4-phenyl-1,2,3,6-tetrahydropyridine Derivatives 140, 146 and 152. Sodium borohydride (5.52 mmol) was added in portions to a stirred solution of the appropriate N-alkyl-4-phenylpyridinium halide (2.76 mmol) in 30 mL dry methanol at 0 °C. The mixture was stirred for an additional 60 minutes at room temperature and the solvent was subsequently removed under reduced pressure. The residue was taken up in 15 mL H_2O and the solution extracted with diethyl ether (3 x 50 mL). The combined organic layers were dried (Na_2SO_4), filtered, and concentrated to 50 % of the original volume. Treatment with oxalic acid (2.76 mmol) in 10 mL of diethyl ether precipitated the crude oxalate salt which was recrystallized from the appropriate solvent to afford a white crystalline solid.

Oxalate Salt of 1-Allyl-4-phenyl-1,2,3,6-tetrahydropyridine (140). The product was obtained in 80% yield and recrystallized from ethanol: mp 174-6 °C; ^1H NMR (DMSO-d_6) δ 2.8 (m, 2 H, C-3 CH_2), 3.45 (m, 2 H, C-2 CH_2), 3.7 (m, 4 H, CH_2), 5.5 (m, 2 H, olefinic CH_2), 5.95 (m, 1 H, olefinic CH), 6.35 (bs, 1 H, C-5 olefinic H), 7.45 (m, 5 H, ArH); GCMS (temperature program: 100 °C for 1 minute followed by a ramp of 20 °C/min for 8 minutes) showed a single peak (R_t = 5.35 minute) M^+ 199. Anal. Calcd for $C_{16}H_{19}NO_4 \cdot 0.25\ H_2O$: C 65.41, H 6.69, N 4.77. Found: C 65.73, H 6.56, N 4.78.

Oxalate Salt of 4-Phenyl-1-propargyl-1, 2, 3, 6-tetrahydropyridine (146). The product was obtained in 85% yield and recrystallized from ethanol: mp 143-5 °C; ^1H NMR (DMSO-d_6) δ 2.56 (m, 2 H, CH_2), 3.04 (m, 2 H, C-3 H CH_2), 3.54 (s, 1 H, acetylenic H), 3.6 (m, 2 H, C-2 CH_2), 3.8 (m, 2 H,

C-6 CH_2), 6.23 (bs, 1 H, olefinic H), 7.36 (m, 5 H, ArH); GCMS (temperature program: 100 °C for 1 minute followed by a ramp of 25 °C/min) showed a single peak (R_t = 5.5 minutes) M^+ 197. Anal. Calcd for $C_{16}H_{17}NO_4 \cdot 0.25\ H_2O$: C 65.85, H 6.04, N 4.8. Found: C 66.24, H 6.01, N 4.79.

Oxalate Salt of 4-Phenyl-1-propyl-1,2,3,6-tetrahydropyridine (152). The product was obtained in 86% yield and recrystallized from 2-propanol: mp 174-5 °C; ^1H NMR (DMSO-d_6) δ 1.0 (t, 3 H, CH_3), 1.8 (m, 2 H, CH_2), 2.8 (bd, 2 H, C-3 CH_2), 3.0 (q, 2 H, CH_2), 3.4 (m, 2 H, C-2 CH_2), 3.8 (m, 2 H, C-6 CH_2), 6.2 (bs, 1 H, C-5 olefinic H), 7-3-7.5 (m, 5 H, ArH); GCMS (temperature program: 100 °C for 1 minute followed by a ramp of 20 °C/min) showed a single peak (R_t = 4.93 minutes) M^+201. Anal. Calcd for $C_{16}H_{21}NO_4$: C 65.96, H 7.27, N 4.81. Found: C 65.88, H 7.30, N 4.79.

1-Cyclobutyl-4-phenyl-1,2,3,6-tetrahydropyridine Hydrochloride (153·HCl). A solution containing cyclobutylamine (1.0 g, 14.06 mmol), acidified with 50% HCl to pH 6, and 37% aqueous formaldehyde (2.32 g, 77.6 mmol) was heated to 65 °C for 10 minutes at which time 2-phenylpropene (**184**, 0.832 g, 7.0 mmol) was added. After Heating at 65 °C for an additional 6 hours, methanol (50 mL) was added and the reaction mixture was allowed to stir at room temperature overnight. The methanol was removed under reduced pressure to afford a yellow oil which, according to GCMS analysis, was composed of a mixture of the 1,3-oxazine **185** ($M^{\cdot+}$ 231), the isomeric alcohol **187** ($M^{\cdot+}$ 231) and the desired tetrahydropyridine **153** (M^+ 213). This oil was heated at 100 °C for 1 hour in 15 mL of concentrated HCl. The excess acid was removed under

reduced pressure and the resulting yellow oil in 0.1 N HCl was extracted with CH_2Cl_2 (3 x 15 mL). The combined organic extracts were dried ($MgSO_4$), filtered, and the solvent removed under reduced pressure to yield 0.81 g of a yellow solid which was recrystallized from acetonitrile/diethyl ether to afford 0.7 g (42%) of **153·HCl** as an off-white crystalline solid: mp 214-217 °C (dec); ^{1}H NMR ($CDCl_3$) δ 2.0-2.3 (m, 6 H, CH_2), 2.85 (m, 2 H, C-3 CH_2), 3.5 (m, 4 H, C-2 and C-6 CH_2), 4.1 (m, 1 H, cyclobutylmethine), 6.0 (bs, 1 H, C-5 olefinic H), 7.5 (m, 5 H, ArH), 8.4 (bs, 1 H, NH); GCMS (temperature program: 100 °C for 1 min followed by a ramp of 25 °C/min) showed a single peak (R_t = 6.3 minutes) M^+ 213. Anal. Calcd for $C_{15}H_{20}NCl·0.75\ H_2O$: C 70.40, H 8.14, N 5.48. Found: C 70.41, H 7.96, N 5.75.

1-Cyclopentyl-4-phenyl-1,2,3,6-tetrahydropyridine Hydrochloride (156·HCl). A solution of 4-phenylpyridine (**178**, 1.0 g, 6.4 mmol) and bromocyclopentane (3.8 g, 26 mmol) in acetone (50 mL) was heated under reflux for 72 hours and the resulting precipitated white solid (1.75 g) was filtered and recrystallized from acetone/diethyl ether. This product was shown by ^{1}H NMR to be a 2:1 mixture of the pyridinium species **182** and the starting 4-phenylpyridine (**178**): mp 122-4 °C; ^{1}H NMR ($CDCl_3$) δ 1.8-2.6 (m, 8 H, cyclopentyl H), 5.5 (m, 1 H, cyclopentylmethine), 7.6 (m, 5 H, ArH), 8.22 (d, 2 H, C-2 and C-6 H), 9.55 (d, 2 H, C-3 and C-5 H), 7.7 (m, ArH related to **178**), 7.8 (d, C-2 and C-6 H related to **178**), 8.9 (d, C-3 and C-5 H related to **178**). To this solid (0.75 g, 2.4 mmol) in methanol (25 mL) was added portionwise sodium borohydride (0.18 g, 4.8 mmol) with stirring at 0 °C. The reaction mixture was stirred at room temperature for 1 hour

following which the methanol was removed under reduced pressure. An aqueous solution of the residue was extracted with diethyl ether (3 x 20 mL) and the combined organic layers were extracted with 1 N HCl (2 x 10 mL). This aqueous solution was extracted with CH_2Cl_2 (2 x 15 mL) and the organic extract was dried ($MgSO_4$), filtered, and evaporated to yield a white solid which was recrystallized from ethanol to yield 0.21 g (38%) of **156·HCl** as a white crystalline solid: mp 255-256 °C; ^{1}H NMR ($CDCl_3$) δ 1.6-2.2 (m, 8 H, cyclopentylmethylenes), 2.6 (m, 2 H, C-3 CH_2), 3.1-3.6 (m, 4 H, C-2 and C-6 CH_2), 4.2 (m, 1 H, cyclopentylmethine), 5.99 (d, 1 H, C-5 olefinic H), 7.28-7.3 (m, 5 H, ArH); GCMS (temperature program: 50 °C for 1 min. followed by a ramp of 25 °C/min. for 10 minutes) showed a single peak (R_t = 6.92 minutes) M^+ 227. Anal. Calcd for $C_{16}H_{22}ClN$: C 72.85, H 8.41, N 5.31. Found: C 72.72, H 8.42, N 5.28.

4-Ethenyl-1-methylpyridinium Iodide (194). A mixture of iodomethane (5.06 g, 35.6 mmol) and commercially available 4-ethenylpyridine (**193**, 2.5 g, 23.7 mmol) in acetone (30 mL) was stirred at room temperature for 30 minutes. The precipitated bright yellow solid was recrystallized from hot acetone to yield 5.28 g (90%) of shiny yellow crystals: mp 148-149 °C; UV (MeOH) λ_{max} 265 nm (ε 1.53 x 10^4); ^{1}H NMR ($CDCl_3$) δ 4.6 (s, 3 H, CH_3), 6.0 (db, 1 H, J = 17 Hz), 6.4 (db, 1 H, J = 11 Hz), 6.9 (m, 1 H, vinylic H), 8.15 (d, 2 H, C-3, C-5 H), 9.35 (d, 2 H, C-2, C-6 H). Anal. Calcd for $C_{18}H_{10}NI·0.5\ H_2O$: C 37.52, H 4.33, N 5.47. Found: C 37.47, H 3.90, N 5.33.

Oxalate Salt of 4-Ethenyl-1-methyl-1,2,3,6-tetrahydropyridine (157). To a solution of 4-ethenyl-1-methylpyridinium iodide (**194**, 0.7 g, 2.8

mmol) in 30 mL of methanol was added sodium borohydride (0.105 g, 2.8 mmol) portionwise at 0 °C with stirring. The reaction mixture was stirred at 0 °C for 30 minutes following which the methanol was removed under reduced pressure. The residue was treated with water (10 mL) and extracted with diethyl ether (2 x 30 mL). The combined organic extracts were dried ($MgSO_4$), filtered and oxalic acid (0.2 g, 2.2 mmol) in diethyl ether (10 mL) was added to precipitate the oxalate salt of **157** as a white solid which was recrystallized from 2-propanol to yield 0.28 g (47%) of white fluffy crystals: mp 147-149 °C; ^1H NMR (DMSO-d_6) δ 2.4 (bd, 2 H, C-3 CH_2), 3.0 (s, 3 H, CH_3), 3.5 (m, 2 H, C-2 CH_2), 3.7 (m, 2 H, C-6 CH_2), 5.4 (d, 1 H, J = 17 Hz), 5.5 (d, 1H, J = 11 Hz), 6.0 (bs, 1 H, C-5 olefinic H), 6.6 (dd, 1 H, vinylic H); GCMS (temperature program: 50 °C for 1 min followed by a ramp of 25 °C/min) for 10 minutes showed a single peak (R_t = 2.06 minutes) M^+123. Anal. Calcd for $C_{10}H_{15}NO_4 \cdot 0.5\ H_2O$: C 54.05, H 7.26, N 6.30. Found: C 53.97, H 6.97, N 6.24.

1-Methyl-(E)-4-(2-phenylethenyl)pyridinium iodide (200·I). A reaction mixture containing benzaldehyde (**198**, 5.83 g, 55 mol) and γ-picoline (**197**, 4.65 g, 50 mmol) in 50 mL acetic anhydride was heated under reflux for 15 hours. The reaction mixture was cooled and poured into crushed ice and acidified to pH 2 with 50% HCl. The aqueous solution was extracted with CH_2Cl_2 (4 x 100 mL) and the organic wash was discarded. The aqueous layer was treated with 1N NaOH to obtain a pH of 11 and then was extracted with CH_2Cl_2 (5 x 100 mL). The combined organic layers were dried (Na_2SO_4), filtered and the solvent was evaporated under reduced pressure. The residue was applied to a basic

alumina column and eluted with CH_2Cl_2 to afford the pyridine **199** as a white crystalline solid in 60% yield: mp 126-7 °C (lit.[152] mp 127-128 °C); GCMS (temperature program 50 °C for 1 min followed by a temperature ramp of 25 °C/min for 10 min) showed a single peak at R_t = 6.0 min M^+181. A solution containing **199** (1.25 g, 6.9 mmol) and iodomethane (3.9 g, 27.6 mmol) in 25 mL of dry acetone was stirred at room temperature for 2 hours and the crystalline yellow solid which precipitated out of this reaction was collected by filtration and recrystallized from MeOH/diethyl ether to afford yellow needles of the pyridinium derivative **200** (1.8 g, 81%): mp 214-215 °C (Lit.[152] mp 214-215 °C); ^{1}H NMR (DMSO-d_6) δ 8.9 (d, 2 H, C-2 & C-6 H), 8.26 (d, 2 H, C-3 & C-5 H), 8.2 (d, 1 H, olefinic H), 7.3-7.5 (m, 6 H, 5 ArH and 1 olefinic H), 4.3 (s, 3 H, CH_3).

Oxalate Salt of (E)-1-Methyl-4-(2-phenylethenyl)-1,2,3,6-tetrahydropyridine (158). Sodium borohydride (0.095 g, 2.52 mmol) was added portionwise to a solution of (E)-1-methyl-4-(2-phenylethenyl)pyridinium iodide (**200·I**, 0.41 g, 1.26 mmol) in methanol (25 mL) at 0 °C with stirring. The reaction mixture was allowed to stir at room temperature for 30 minutes following which the methanol was removed under reduced pressure. The residue was treated with water (10 mL) and extracted with diethyl ether (3 x 15 mL). The combined organic extracts were dried ($MgSO_4$), filtered, and oxalic acid (0.11 g, 1.22 mmol) in diethyl ether (10 mL) was added to precipitate the oxalate salt of **158** which was recrystallized from methanol to afford 0.26 g (72%) of a white crystalline solid: mp 222-224 °C; GCMS (temperature program: 50 °C for

1min followed by a temperature gradient of 25 °C/min for 10 minutes) showed a single peak (R_t = 6.2 minutes) M^+199; ^1H NMR (DMSO-d_6) δ 2.6 (bd, 2 H, C-3 CH_2), 2.8 (s, 3 H, CH_3), 3.3 (m, 2 H, C-2 CH_2), 3.75 (bs, 2 H, C-6 CH_2), 5.9 (bs, 1 H, C-5 olefinic H), 6.6 (d, 1 H, J = 16 Hz), 7.0 (d, 1 H, J = 16 Hz), 7.3-7.5 (m, 5 H, ArH). Anal. Calcd for $C_{16}H_{19}NO_4$: C 66.42, H 6.62, N 4.84. Found: C 66.36, H 6.62, N 4.83.

Oxalate Salt of 4-Ethynyl-1-methylpiperidin-4-ol (202). A solution of N-methylpiperidin-4-one (**201**, 1.77 g, 15.6 mmol) in 40 mL of dry diethyl ether was added to a suspension of lithiumacetylide ethylenediamine complex (10.23 g, 111 mmol) in 40 mL of dry diethyl ether under nitrogen. The resulting reaction mixture was allowed to stir at room temperature for 4 hours. The reaction was quenched with water and the resulting mixture was extracted into diethyl ether (2 x 75 mL). The combined organic layers were dried (Na_2SO_4), filtered and oxalic acid (1.2 g, 13 .3 mmol) in 15 mL of ether was added to the organic layers to precipitate the product as the oxalate salt which was recrystallized from hot acetone to afford 2.1 g (60%) of pure product: mp 142-4 °C; ^1H NMR (DMSO-d_6) δ 3.45 (s, 1 H, acetylenic H), 3.1-3.3 (bs, 4 H, C-2 & C-6 H), 2.75 (s, 3 H, CH_3), 1.9-2.1 (bs, 4 H, C-3 & C-5 H); GCMS (temperature program: 50 °C for 1 min followed by a temperature ramp of 25 °C/min for 10 minutes showed a single peak at R_t = 2.6 minutes M^+ 139. Anal. Calcd for $C_{10}H_{15}NO_5$: C 52.40, H 6.40, N 6.11. Found: C 52.28, H 6.57, N 6.06.

Oxalate Salt of 4-Acetoxy-4-ethynyl-1-methylpiperidine (204). A reaction mixture containing **202** free base (0.3 g, 2.15 mmol) and acetic anhydride (25 mL) was heated under reflux for 4 hours. The reaction

mixture was cooled and extracted into diethyl ether (2 x 15 mL). The combined organic layers were dried (Na_2SO_4), filtered and oxalic acid (89 mg, 0.98 mmol) in diethyl ether was added to the organic extract to precipitate the product as the oxalate salt which was recrystallized from MeOH/diethyl ether to afford a white crystalline solid in 55% yield: mp 172-4 °C; ^1H NMR (DMSO-d_6) δ 3.7 (s, 1 H, acetylenic H), 3.2-3.4 (bs, 4 H, C-2 & C-6 H), 2.7 (s, 3 H, CH_3), 2.3 (bs, 4 H, C-3 & C-5 H), 2.0 (s, 3 H, OAc); GCMS (temperature program: 50 °C for 1 min followed by a temperature ramp of 25 °C/min for 10 minutes) showed a single peak at R_t = 4.2 minutes M^+181.

1-Methyl-4-trimethylsilylethynylpyridinium Iodide (213·I). A mixture of **205** (2.5 g, 13.3 mmol), triphenylphosphine (0.524 g, 2 mmol), cuprous iodide (0.126 g, 0.66 mmol), triethylamine (7 mL) and acetonitrile (70 mL) was degassed with argon for 15 minutes. (Trimethylsilyl)ethyne (2.61 g, 26.6 mmol) was added followed by palladium acetate (0.149 g, 0.66 mmol). The mixture was stirred under argon for 6 hours at room temperature and the residue obtained after evaporating the solvent was partitioned between water and CH_2Cl_2. The organic layer was dried (Na_2SO_4) and evaporated and the residue was chromatographed on basic alumina using CH_2Cl_2 to afford 1.1 g (47 %) of **211** as a yellow oil. The crude product was treated with iodomethane (2.2 g, 16 mmol) to yield the corresponding pyridinium salt (**213**) as fine yellow crystals (1.8 g, 45%): mp 180-182 °C; ^1H NMR (DMSO-d_6) δ 0.38 (s, 9 H, TMS-H), 4.29 (s, 3 H, CH_3), 8.15 (d, 2 H, C-2 and C-6 H), 8.9 (d, 2 H, C-3 and C-5 H). Anal. Calcd for $C_{11}H_{16}INSi$: C 41.65, H 5.08, N 4.42. Found: C 41.87, H 5.20, N 4.50.

2-Methyl-4-(4'-pyridyl)-3-butyn-2-ol (223). *Bis*(triphenylphosphine)palladium dichloride (0.35 g) and CuI (50 mg) were added sequentially to 4-bromopyridine hydrochloride (**205**·HCl, 9.7 g, 50 mmol) in 100 mL freshly distilled diethylamine and 2-methyl-3-butyn-2-ol (5 g, 60 mmol) under nitrogen at room temperature. The reaction mixture was stirred for 4 hours and was treated subsequently with water. The aqueous solution was extracted with diethyl ether (3 x 150 mL) and the combined organic layers were dried (Na_2SO_4) and filtered. The solvent was concentrated and the residue was applied to a basic alumina column and eluted with CH_2Cl_2 to afford the desired product as a crystalline white solid which was recrystallized from EtOAc/hexanes to afford 4.9 g (61%) of product: mp 108-110 °C (lit[166] mp 108-110 °C); ^1H NMR ($CDCl_3$) δ 8.5 (d, 2 H, C-2 & C-6 H), 7.2 (d, 2 H, C-3 & C-5 H), 3.5 (bs, 1 H, OH), 1.5 (s, 6 H, dimethyl H); GCMS (temperature program 50 °C for 1 minute followed by a temperature ramp of 25 °C/min for 10 min showed a single peak at R_t = 5.3 minutes M^+ 161.

4-(4-But-3-yn-2-methyl-2-ol)-1-methylpyridinium Iodide (224·I). A mixture of iodomethane (5.27 g, 37.2 mmol) and 2-methyl-4-(4-pyridyl)-3-butyn-2-ol (**223**, 2 g, 12.4 mmol) in dry THF (20 mL) was stirred overnight under nitrogen. Recrystallization of the resulting precipitate from methanol/diethyl ether afforded 3.3 g (89%) of product: mp 114-118 °C; ^1H NMR (DMSO-d_6) δ 1.51 (s, 6 H, $(CH_3)_2$), 4.32 (s, 3 H, CH_3),5.8 (s, 1 H, acetylenic H), 8.0-8.1 (d, 2 H, J = 17 Hz), 8.95-8.97 (d, 2 H, (J = 17 Hz); UV(MeOH) λ_{max} 264 (ε 1.22 x 10^4). Anal. Calcd for $C_{11}H_{14}NOI$: C 43.58, H 4.66, N 4.62. Found: C 43.48, H 4.67, N 4.57.

Oxalate Salt of 4-(4-But-3-yn-2-methyl-2-ol)-1-methyl-1,2,3,6-tetrahydropyridine (225). To a solution of **224** (0.2 g, 0.66 mmol) in MeOH (20 mL) was added sodium borohydride (49 mg, 1.32 mmol) at 0 °C. After stirring at 0 °C for 40 minutes the solvent was removed under reduced pressure, the residue was dissolved in water (10 mL) and was extracted with diethyl ether (3 x 15 mL). The combined organic layers were dried (Na_2SO_4), filtered, and oxalic acid (65 mg, 0.67 mmol) in diethyl ether (5 mL) was added to precipitate the oxalate salt which was recrystallized from methanol/diethyl ether to afford 90 mg (75%) of the desired product: mp 158-9 °C; GCMS (temperature program: 50 °C for 1 min followed by a temperature ramp of 25 °C/min) showed a single peak at (R_t = 4.5 minutes) M^+ 179. ^1H NMR (DMSO-d_6) δ 1.36 (s, 6 H, $(CH_3)_2$), 2.33 (bs, 2 H, C-3 CH_2), 2.8 (s, 3 H, CH_3), 3.0-3.1 (t, 2 H, C-2 CH_2), 3.55 (bs, 2 H, C-6 CH_2), 5.9 (bs, 1 H, C-5 olefinic H). Anal. Calcd for $C_{13}H_{19}NO_5$: C 57.98, H 7.11, N 5.2. Found: C 57.87, H 7.16, N 5.23.

Oxalate Salt of 4-Ethynyl-1-methyl-1,2,3,6-tetrahydropyridine (159). A mixture of NaOH (0.3 g, 7.6 mmol) and **225** (1.37 g, 7.6 mmol) in dry toluene (40 mL) was heated under reflux for 2.5 hours. After cooling water (10 mL) was added and the resulting mixture was acidified with 0.1 N HCl. The toluene layer was discarded and the aqueous solution was neutralized with aqueous K_2CO_3 and then extracted with diethyl ether (2 x 25 mL). The combined organic extracts were dried (Na_2SO_4), filtered, and oxalic acid (0.68 g, 7.6 mmol) was added to the solution to precipitate the oxalate salt which was recrystallized from methanol/diethyl ether to afford 0.92 g (59%) of the desired product: mp 159-161°C; GCMS

(temperature program: 50 °C for 1 min followed by a temperature ramp of 25 °C/min. for 10 minutes) showed a single peak (R_t = 3.1 minutes) M^+ 121; ^1H NMR (DMSO-d_6) δ 2.39 (bs, 2 H, C-3 CH_2), 2.71 (s, 3 H, CH_3), 3.1 (t, 2 H, C-2 CH_2), 3.63 (bs, 2 H, C-6 CH_2), 4.0 (s, 1 H, acetylenic H), 6.08 (bs, 1 H, C-5 olefinic H), 9.0 (bs, 2 H, oxalate H). Anal. Calcd for $C_{10}H_{13}NO_4$: C 56.87, H 6.2, N 6.63. Found: C 56.68, H 6.24, N 6.66.

4-Ethynylpyridine (212). A mixture of NaOH (0.476 g, 11.9 mmol) and **223** (1.9 g, 11.9 mmol) in dry toluene (50 mL) was heated under reflux for 2 hours. The reaction mixture was cooled and acidified with 0.1 N HCl. The aqueous solution was separated and neutralized with aqueous K_2CO_3 and extracted with diethyl ether (3 x 15 mL). The combined organic extracts were dried (Na_2SO_4), filtered, and the solvent was removed under reduced pressure to afford a light brown solid which was recrystallized from ethyl acetate/diethyl ether to yield 0.8 g (65%) of **212**: mp 94-96 °C (lit.[166] mp 95-96 °C).

4-Ethynyl-1-methylpyridinium Perchlorate (226·ClO_4). A solution of **212** (0.4 g, 3.8 mmol) and iodomethane (1.6 g, 11.4 mmol) in dry THF (15 mL) was stirred at room temperature for 6 hours during which time the methiodide of **226** precipitated as a dark brown solid. This material (0.43 g, 50%) was treated with 0.7 mL of 70% ethanolic perchloric acid to afford **226** as the perchlorate salt in an overall yield of 40%: mp 161-3 °C; ^1H NMR (DMSO-δ_6) δ 4.5 (s, 3 H, CH_3), 5.38 (s, 1 H, acetylenic H), 8.18-8.21 (d, 2 H, C-3 and C-5 H), 8.98-9.01 (d, 2 H, C-2 and C-6 H); UV(MeOH) λ_{max} 264 (ε 1.22 x 10^4). Anal. Calcd for $C_8H_8NClO_4$: C 44.16, H 3.71, N 6.44. Found: C 44.11, H 3.72, N 6.37.

1-Methyl-4-(-1-phenylethynyl)pyridinium Iodide (228·I). n-Butyllithium (15.63 mL of a 1.6 M solution in hexane, 25 mmol) was added to a solution of phenylethyne (2.4 g, 23.6 mmol) in 25 mL of freshly distilled, dry THF at 0 °C. After stirring the reaction mixture for 2 hours, the contents of the flask were added to a solution of anhydrous zinc chloride (3.4 g, 25 mmol) in 25 mL of dry THF. After stirring for 1 hour the phenylacetylide-zinc chloride complex was added dropwise to a solution of 4-bromopyridine free base [obtained from 4-bromopyridine hydrochloride (**205·HCl**, 1.166 g, 5.9 mmol)] in 40 mL of dry THF containing palladium *tetrakis*triphenylphosphine (50 mg, 0.05 mole). The resulting reaction mixture was heated under reflux overnight and after cooling the reaction was quenched by the addition of 200 mL of saturated aqueous ammonium chloride. The organic layer was separated, washed with water (3 x 100 mL) and extracted with 1.0 M HCl (3 x 100 mL). After washing with $CHCl_3$ (100 mL) the pH of the aqueous extract was adjusted to 11 with 1.0 M NaOH and the resulting solution was extracted with diethyl ether (2 x 100 mL). The organic extract was dried ($MgSO_4$), filtered, and the solvent was removed under reduced pressure to afford a yellow oil 0.89 g (84%). Treatment of this oil in 20 mL of acetone with iodomethane (8.41 g, 59.2 mmol) gave a yellow solid precipitate which was recrystallized from 2-propanol to yield 1.35 g (71%) of **228·I** as yellow crystals: mp 151-53 °C; ^1H NMR (DMSO-d_6) δ 4.3 (s, 3 H, CH_3), 7.5-7.7 (m, 5 H, ArH), 8.3 (d, 2 H, J = 6.64 Hz), 9.01 (d, 2 H, J = 6.71 Hz); UV (H_2O) λ_{max} 328 (ε 1.70 x 10^4). Anal. Calcd for $C_{14}H_{12}NI \cdot 0.89\ H_2O$: C 49.82, H 4.08, N 4.15. Found: C 49.65, H 3.67, N 4.19.

Oxalate Salt of 1-Methyl-4-(1-phenylethynyl)-1,2,3,6-tetrahydropyridine (160). To a solution of 1-methyl-4-(1-phenylethynyl)pyridinium iodide (**228·I**, 0.7 g, 2.1 mmol) in methanol (20 mL) was added sodium borohydride (0.158 g, 4.2 mmol) portionwise at 0 °C with stirring. The reaction mixture was stirred at room temperature for 1 hour and then the solvent was removed under reduced pressure. The residue was taken up in water (15 mL) and extracted with diethyl ether (3 x 20 mL). The organic extract was dried ($MgSO_4$), filtered, and oxalic acid (0.175 g, 1.9 mmol) in diethyl ether (5 mL) was added to precipitate the oxalate salt of **160** which was recrystallized from hot 2-propanol to afford 0.46 g (76%) of fine white crystals: mp 202-204 °C; ^1H NMR (DMSO-d_6) δ 2.5 (bd, 2 H, C-3 CH_2), 2.7 (s, 3 H, CH_3), 3.2 (m, 2 H, C-2 CH_2), 3.7 (m, 2 H, C-6 CH_2), 6.2 (bs, 1 H, C-5 olefinic H), 7.5 (m, 5 H, ArH); GCMS (temperature program: 50 °C for 1 min followed by a ramp of 25 °C/min for 10 minutes) showed a single peak at (R_t = 6.3 minutes) M^+197. Anal. Calcd for $C_{16}H_{17}NO_4 \cdot 0.75\ H_2O$: C 65.52, H 6.07, N 4.78. Found: C 65.46, H 5.99, N 4.93.

***m*-CBA Salt of 4-Phenyl-1-propyl-1,2,3,6-tetrahydropyridine-N-oxide (229).** To a solution of 4-phenyl-1-propyl-1,2,3,6-tetrahydropyridine free base (**152**) [obtained from the corresponding oxalate salt (0.4 g, 1.37 mmol)] in 20 mL CH_2Cl_2 was added 60% *m*-CPBA (0.26 g, 1.5 mmol) at 0 °C. After stirring for 2 hours at 0 °C, the solvent was removed under reduced pressure to afford 0.29 g (64%) of the white crystalline N-oxide as its *m*-CBA salt. The analytical sample was obtained by recrystallization from acetone/diethyl ether: mp 92-93 °C ; ^1H NMR ($CDCl_3$) δ 2.1 (m, 2 H,

CH_2), 2.6-3.2 (m, 2 H, C-3 CH_2), 3.7-4.6 (m, 5 H, C-2, C-6 and N-propyl CH_2), 6.0 (d, 1 H, C-5 olefinic H), 7.3-8.0 (complex m, 8 H, ArH). Anal. Calcd for $C_{21}H_{24}ClNO_3$: C 67.46, H 6.47, N 3.75. Found: C 67.39, H 6.49, N 3.76.

***m*-CBA Salt of 4-Ethynyl-1-methyl-1,2,3,6-tetrahydropyridine-N-oxide (232).** A solution of the tetrahydropyridine free base **159** obtained from the corresponding oxalate salt (0.41 g, 1.94 mmol) and 60% *m*-CPBA (0.365 g, 2.1 mmol) was stirred at 0 °C for 1 hour. Removal of the solvent under reduced pressure gave a yellow oil which was stirred in diethyl ether to yield the desired product as a crystalline *m*-CBA salt in 61% yield: mp 77-78 °C; ^{1}H NMR ($CDCl_3$). δ 7.2-8.0 (m, 4 H, ArH), 6.0 (s, 1 H, C-5 H), 3.9-4.5 (dd, 2 H, C-6 H), 3.6-3.9 (m, 2 H, C-2 H), 3.5 (s, 3 H, NCH_3), 3.1 (s, 1 H, acetylenic H), 2.5-3.0 (m, 2 H, C-3 H). Anal. Calcd for $C_{16}H_{17}ClNO_3$: C 61.33, H 5.49, N 4.77. Found: C 61.39, H 5.52, N 4.80.

***m*-CBA Salt of (E)-1-Methyl-4-(2-phenylethenyl)-1, 2, 3, 6-tetrahydropyridine-N-oxide (231).** This compound was obtained in an identical fashion in 74% yield: mp 114-116 °C; ^{1}H NMR ($CDCl_3$) δ 7.26-8.0 (m, 9 H, ArH), 6.7-6.8 (d, 1 H, olefinic H), 6.5-6.6 (d, 1 H, olefinic H), 5.74 (s, 1 H, C-5 olefinic H), 4.1-4.58 (m, 2 H, C-6 CH_2), 3.7-3.9 (m, 2 H, C-2 CH_2), 3.5 (s, 3 H, CH_3), 2.7-2.95 (m, 2 H, C-3 CH_2). Anal. Calcd for $C_{21}H_{22}ClNO_3$: C 67.83, H 5.96, N 3.77. Found: C 67.67, H 5.99, N 3.74.

***m*-CBA Salt of 4-(2,6-Dimethylphenyl)-1-methyl-1, 2, 3, 6-tetrahydropyridine-N-oxide (243).** This compound was obtained in a similar manner in 47% yield: mp 89-90 °C (lit. mp 90-91 °C); ^{1}H NMR ($CDCl_3$) δ 7.2-7.9 (m, 7 H, ArH), 5.4 (bs, 1H, C-5 H), 4.4 (m, 2 H, C-6 H), 3.7 (m, 2H, C-2 H), 3.6 (s, 3 H, CH_3), 2.7 (m, 2 H, C-3 H), 2.2 (s, 6 H, $ArCH_3$).

m-CBA Salt of **1-Methyl-4-thiophenoxy-1, 2, 3, 6-tetrahydropyridine-N-oxide (245)**. This compound was obtained in a similar manner in 51% yield: mp 90-92 °C; ^{1}H NMR (DMSO-d_6) δ 7.4-8.0 (m, 7 H, ArH), 5.7 (bs, 1 H, C-5 H), 4.4 (bs, 2 H, C-6 H), 3.5 (m, 2 H, C-2 H), 3.5 (s, 3 H, CH_3), 2.2-2.6 (m, 2 H, C-3 H). Anal. Calcd for $C_{19}H_{20}ClNO_3S$: C 60.39, H 5.33, N 3.71. Found: C 60.21, H 5.41, N 3.75.

4-Phenyl-1-propyl-2,3-dihydropyridinium perchlorate (233·ClO_4). The above N-oxide free base (**229**, 0.27 g, 0.72 mmol) in CH_2Cl_2 was applied to a basic alumina column which was eluted with CH_2Cl_2. The solvent was removed under reduced pressure and the resulting N-oxide free base in CH_2Cl_2 (15 mL) was treated at 0 °C with trifluroacetic anhydride (0.89 g, 3.9 mmol) in 5 mL of CH_2Cl_2. After stirring at 0 °C for 1 hour the solvent was removed and the resultant yellow oil (0.43 g) was crystallized from methanol (15 mL) containing 0.11 mL 70% perchloric acid to yield 100 mg (45%) of shiny yellow crystals: mp 96-98 °C; UV (MeOH) λ_{max} 343 nm (ε 1.68 x 10^4); ^{1}H NMR (DMSO-d_6) δ 1.1 (t, 3 H, CH_2), 1.8 (m, 2 H, CH_2), 3.2 (t, 2 H, C-3 CH_2), 3.8-4.0 (m, 4 H, C-2 and N-propyl CH_2), 7.1 (d, 1 H, C-5 H), 7.4-7.6 (m, 5 H, ArH), 8.7 (d, 1 H, C-6 H). Anal. Calcd for $C_{14}H_{18}ClNO_4$: C 56.10, H 6.05, N 4.67. Found: C 56.16, H 6.07, N 4.65.

4-Ethynyl-1-methyl-2,3-dihydropyridinium Perchlorate (236·ClO_4): This compound was obtained in 61 % yield following the procedure for the preparation of **233·ClO_4**: mp 112 °C (dec); UV (CH_3CN) λ_{max} 308 (ε 6.0 x 10^3); ^{1}H NMR (DMSO-δ_6) δ 8.57 (bs, 1 H, C-6 H), 6.77 (bs, , 1 H, C-5 H), 5.34 (s,1 H, acetylenic H), 3.8-3.9 (t, 2 H, C-2 CH_2), 3.62 (s, 3 H, CH_3), 2.77-

2.84 (t, 2 H, C-3 CH_2). Anal. Calcd for $C_8H_{10}ClNO_4 \cdot 0.5H_2O$: C 41.99, H 4.81, N 6.12. Found: C 41.90, H 4.45, N 6.03.

(E)-1-Methyl-4-(2-phenylethenyl)-2,3-dihydropyridinium Perchlorate (235·ClO_4). This compound was obtained in 82% yield following the procedure for the preparation of **233·ClO_4**: mp 172-4 °C; UV (MeOH) λ_{max} 364 (ε 2.4 x 10^4); ^1H NMR (DMSO-d_6) δ 8.5 (d, 1 H, C-6 H), 7.2-7.7 (m, 7 H, ArH and olefinic H), 6.6 (bs, 1 H, C-5 H), 4.0 (t, 2 H, C-2 CH_2), 3.6 (s, 3 H, CH_3), 3.0 (t, 2 H, C-3 CH_2). Anal. Calcd for $C_{14}H_{16}ClNO_4$: C 56.48, H 5.42, N 4.70. Found: C 56.26, H 5.44, N 4.68.

4-Ethenyl-1-methylpiperidin-4-ol Oxalate (237). A solution of 1-methyl-4-piperidone (**201**, 2.26 g, 20 mmol) in diethyl ether (50 mL) treated with vinyl magnesium bromide (30 mL, 1.0 M solution in THF, 30 mmol) was heated under reflux for 1.5 hours. The reaction was quenched with 1.0 M NaOH and the resulting mixture was extracted with diethyl ether (2 x 75 mL). The combined organic extracts were dried ($MgSO_4$), filtered and oxalic acid (1.7 g, 18.8 mmol) in diethyl ether (15 mL) was added to precipitate a colorless oil which solidified upon standing to afford 2.4 g (52 %) of the desired product. An analytical sample was prepared by recrystallization from acetone/diethyl ether: mp 125-127 °C; ^1H NMR (CD_3OD) δ 1.6-1.9 (bd, 4 H, C-3 and C-5 CH_2), 2.8 (s, 3 H, CH_3), 3.2 (m, 4 H, C-2 and C-6 CH_2), 5.1 (d, 1 H (J = 11 Hz), 5.2 (d, 1 H, (J = 18 Hz), 5.9 (m, 1 H, olefinic H); GCMS (temperature program: 50 °C for 1 min followed by a temperature ramp of 25 °C/min for 10 minutes) showed a single peak (R_t = 2.6 minutes) M^+ 141. Anal. Calcd for $C_{10}H_{17}NO_5$: C 51.94, H 7.41, N 6.06. Found: C 51.87, H 7.45, N 6.03.

4-Ethenyl-1-methyl-2,3-dihydropyridinium Perchlorate (234·ClO_4). A solution of 60% *m*-CPBA (0.4 g, 2.33 mmol) and the free base of **237** (0.3 g, 2.2 mmol) was stirred at 0 °C for 1 hour. The solvent was removed under reduced pressure and the oily residue was chromatographed on basic alumina with CH_2Cl_2/MeOH (90:10) to yield the N-oxide **230** as an oil (0.22 g, 68%): ^1H NMR ($CDCl_3$) δ 5.9-6.0 (dd, 1 H, C-5 H), 5.3 (dd, 1 H, (J = 17 Hz), 5.1 (dd, 1 H, (J = 10 Hz), 4.6 (bs, 1 H, OH), 3.6 (m, 2 H, C-6 CH_2), 3.3 (s.,3 H, CH_3), 3.1 (m, 2 H, C-2 CH_2), 1.5-2.5 (m, 4 H, C-3 and C-5 CH_2). TFAA (1.33 g, 6.35 mmol) was added dropwise to a CH_2Cl_2 solution of **230** (0.2 g, 1.27 mmol) under a nitrogen atmosphere at 0 °C. After stirring the reaction mixture at 0 °C for 1 hour the solvent was removed under reduced pressure and the residue was treated with 0.2 mL of 70 % methanolic perchloric acid solution to afford **234** as the perchlorate salt in 67% yield: mp 95-95°C; ^1H NMR (DMSO-d_6) δ 2.89 (t, 2 H, C-3 CH_2), 3.61 (s, 3 H, CH_3), 3.9 (t, 2 H, CH_2), 5.8 (d, 1 H, (J = 10 Hz), 6.09 (d, 1 H, (J = 17 Hz), 6.5 (d, 1 H, C-5 H), 6.7-6.8 (dd, 1 H, olefinic H), 8.6 (d, 1 H, C-6 H); UV (H_2O) λ_{max} 309 (ε 6.0 x 10^3). Anal. Calcd for $C_8H_{12}ClNO_4$·0.25 H_2O: C 41.66, H 5.68, N 6.07. Found: C 41.86, H 5.28, N 6.03.

4-(2,6-Dimethylphenyl)-1-methyl-2,3-dihydropyridinium Perchlorate (246·ClO_4). This intermediate was synthesized in a fashion identical to **235** in 67% yield: mp 145-7 °C (lit. mp 144-5 °C); ^1H NMR (DMSO-d_6) δ 8.62 (d, 1 H, C-6 H), 7.1-7.2 (m, 3 H, ArH), 6.4 (d, 1 H, C-5 H), 4.0 (t, 2 H, C-2 H), 3.7 (s, 3 H, CH_3), 2.9 (t, 2 H, C-3 H), 2.22 (s, 6 H, $ArCH_3$).

4-t-Butyl-1-methyl-2,3-dihydropyridinium Perchlorate (247·ClO_4). This compound was prepared in a manner identical to **235** in 43 % yield

except that the crude N-oxide, which could not be obtained in a solid form, was used: mp 114-115 °C; ^{1}H NMR (DMSO-d_6) δ 8.5 (d, 1 H, C-6 H), 6.3 (d, 1H, C-5 H), 3.8 (t, 2 H, C-2 H), 3.6 (s, 3 H, CH_3), 2.7 (t, 2 H, C-3 H), 1.2 (s, 9 H, t-butyl H). Anal. Calcd for $C_{10}H_{18}ClNO_4$: C 47.72, H 7.21, N 5.56. Found: C 47.59, H 7.25, N 5.51.

1-Methyl-4-thiophenoxy-2,3-dihydropyridinium Perchlorate (248·ClO_4). This compound was generated in a manner similar to that for **235** in 71% yield: mp 98-100 °C; ^{1}H NMR (DMSO-d_6) δ 8.2 (bs, 1 H, C-6 H), 7.6 (m, 5 H, ArH), 5.6 (d, 1 H, C-5 H), 3.9 (t, 2 H, C-2 H), 3.6 (s, 3 H, CH_3), 3.0 (t, 2 H, C-3 H); UV (pH 7.4 phosphate buffer) λ_{max} 353 (ε 1.52 x 10^4). Anal. Calcd for $C_{12}H_{14}ClNO_4S$: C 47.75, H 4.65, N 4.61. Found: C 47.49, H 4.69, N 4.57.

N,N-*Bis*ethylpropionate-N-cyclopropylamine (250). To a solution of ethyl acrylate (76 mL, 700 mmol) in 200 mL of absolute ethanol was added cyclopropylamine (10 g, 175 mmol). The reaction mixture was stirred under nitrogen for 72 hours. Evaporation of the solvent under reduced pressure yielded (40 mL, 86%) of the desired product as a colorless oil. This material (1 g) was converted to its oxalate salt for characterization: mp 101-102°C; GCMS (temperature program: 125°C for a min. followed by a temperature ramp of 20°C/min for 15 minutes) showed a single peak at (R_t = 10.7 minutes) M^+ 257; ^{1}H NMR ($CDCl_3$) (free base) δ 4.07-4.15 (q, CH_2 adjacent to CO, 4H), 2.89-2.94 (t, NCH_2, 4H), 2.47-2.52 (t, CH_2, 4H), 1.7-1.75 (m, cyclopropyl methine, 1H), 1.2-1.22 (t, CH_3, 6H), 0.39-0.47 (m, cyclopropyl CH_2, 4H). Anal. calcd for $C_{13}H_{23}NO_4$: C 60.66, H 9.01, N 5.45. Found: C 60.56, H8.97, N 5.49.

1-Cyclopropylpiperidin-4-one (164): To a suspension of NaH (0.7 g, 17.4 mmol) (60 % dispersion in mineral oil) in freshly distilled THF (60 mL) placed in a flame dried 250 ml round-bottomed flask fitted with a addition funnel was added **250** (3 g, 14 mmol) in THF dropwise followed by 3 mL of absolute ethanol. The reaction mixture was stirred under reflux overnight. The reaction mixture was cooled and the solvent was removed under vacuo. A solution of 5% acetic acid was added dropwise to obtain a pH of 7 and this aqueous solution was extracted with ethyl acetate. The combined organic layers were dried (Na_2SO_4), filtered, and the solvent was removed under vacuo. The resultant oil was heated under reflux in 50% HCl for 3 hours. The reaction mixture was cooled and washed with 50 mL of THF (the THF layer was discarded) and then treated with 1M NaOH to obtain a pH of 11. The resultant solution was extracted with ethyl acetate. The combined organic layers were dried, filtered and the solvent was removed under reduced pressure to afford a yellow oil (1.1 g, 68 %). A small quantity of the product was converted to its oxalate salt for characterization: mp 122-5 °C; GCMS (temperature program: 70°C for 1 min. followed by a temperature ramp of 20°C/min for 15 minutes) showed a single peak at (R_t = 9.3 minutes) M^+ 139; ^1H NMR ($CDCl_3$) (free base) δ 2.8-2.9 (t, NCH_2, 4H), 2.36-2.41 (t, CH_2, 4H), 1.66-1.74 (m, cyclopropyl methine, 1H), 0.41-0.53 (m, cyclopropyl CH_2, 4H). Anal. Calcd for $C_9H_{15}NO_5 \cdot H_2O$: C 48.58, H 6.93, N 5.66. Found: C 48.97, H 6.61, N 5.87.

Oxalate Salt of 4-Benzyl-1-propyl-1,2,3,6-tetrahydropyridine (257). Iodopropane (7.8 mL, 80 mmol) was added dropwise at 0 °C to a solution

containing 4-benzylpyridine (**254**, 5 g, 30 mmol) in dry acetone (10 mL) and the resulting reaction mixture was stirred for 16 hours. The solid which precipitated was filtered and washed with acetone to afford essentially pure pyridinium product as a crystalline yellow solid (5.1 g, 50%): mp 77-79 °C; ^{1}H NMR (DMSO-d_6) δ 9.5 (d, 2 H, C-2 & C-6 H), 8.5 (d, 2 H, C-3 & C-5 H), 7.7 (m, 5 H, ArH), 5.0 (t, 2 H, NCH_2), 4.8 (s, 2 H, benzylic H), 2.3 (m, 2 H, CH_2), 1.4 (t, 3 H, CH_3). Sodium borohydride (0.2 g, 5.35 mmol) was added to a solution of the crude pyridinium salt **255** (1.4 g, 4.12 mmol) in 20 mL MeOH at 0 °C and the reaction mixture was stirred for 1 hour. The solvent was concentrated and the residue was treated with water and extracted with diethyl ether (3 x 25 mL). The combined ether extracts were dried (Na_2SO_4), filtered and oxalic acid (0.37 g, 4.12 mmol) in diethyl ether was added to the organic extracts to precipitate the product as its oxalate salt which was recrystallized from MeOH/diethyl ether to afford white crystals (0.51 g, 43 %): mp 154-6 °C; ^{1}H NMR (DMSO-d_6) δ 7.3 (m, 5 H, ArH), 5.4 (bs, 1 H, C-5 H), 3.6 (bs, 2 H, C-6 H), 3.3 (s, 2 H, benzylic H), 3.1 (t, 2 H, C-2 H), 2.9 (m, 2 H, NCH_2), 2.2 (bs, 2 H, C-3 H), 1.7 (m, 2 H, CH_2), 0.9 (t, 3 H, CH_3); GCMS (temperature program: 50 °C for 1 min followed by a temperature ramp at 25 °C/min for 10 minutes) showed a single peak at R_t = 6.5 minutes M^+ 215. Anal. Calcd for $C_{17}H_{23}NO_4$: C 66.86, H 7.59, N 4.59. Found: C 66.68, H 7.59, N 4.53.

General Procedure for the Synthesis of the Pyridinium Iodide Salts of the C-(4)-Phenoxy Substituted MPTP Analogs 263, 264, 265, 266. A solution containing phenol (2 mmol), freshly distilled triethylamine (3 mmol) and 4-choro-1-methylpyridinium iodide (2 mmol) in 25 mL dry

acetone was stirred under nitrogen overnight. The solvent was concentrated and the residue was treated with sat $NaHCO_3$. The aqueous solution was extracted with CH_2Cl_2 (2 x 25 mL) and the combined organic extracts were dried (Na_2SO_4), filtered and diethyl ether was added dropwise to this solution to afford the essentially pure pyridinium methiodide salt which was recystallized from the appropriate solvent.

4-(4'-Butylphenoxy)-1-methylpyridinium iodide (264·I). Compound **264·I** was obtained in 50 % yield and recrystallized from CH_2Cl_2/diethyl ether: mp 98-100 °C; ^1H NMR ($CDCl_3$) δ 9.3 (d, 2 H, C-2 & C-6 H), 7.0-7.4 (m, 6 H, C-3 & C-5 H and ArH), 4.5 (s, 3 H, N-CH_3), 2.8 (m, 2 H, butyl CH_2), 1.7 (m, 2 H, butyl CH_2), 1.4 (m, 2 H, butyl CH_2), 1.0 (m, 3 H, butyl CH_3); GCMS (temperature program: 50 °C for 1 min followed by a temperature ramp of 25 °C/minutes showed a single peak (Rt = 7.3 minutes) M-15 227. Anal. Calcd for $C_{16}H_{20}NOI$: C 52.02, H 5.46, N 3.79. Found: C 51.96, H 5.49, N 3.73.

4-(4'-t-Butylphenoxy)-1-methylpyridinium iodide (263·I). This product was obtained in 53 % yield and recrystallized from CH_2Cl_2/diethyl ether: mp 187-189 °C; ^1H NMR ($CDCl_3$) δ 9.2 (d, 2 H, C-2 & C-6 H), 7.0-7.6 (m, 6 H, C-3 & C-5 H and ArH), 4.5 (s, 3 H, N-CH_3), 1.4 (s, 9 H, t-butyl H); UV (ethanol) λ_{max} 243 nm (ε 1.53 x 10^4); GCMS (temperature program: 50 °C for 1 min followed by a temperature ramp of 25 °C/min for 10 minutes showed a single peak (Rt = 6.9 minutes) M-15 227. Anal. Calcd for $C_{16}H_{20}NOI$: C 52.02, H 5.46, N 3.79. Found: C 51.86, H 5.49, N 3.77.

1-Methyl-4-(4'-phenylphenoxy)pyridinium iodide (265·I). This

product was obtained in 62 % yield and recrystallized from methanol/diethyl ether: mp 258-260 °C; ^{1}H NMR (DMSO-d_6) δ 8.9 (d, 2 H, C-2 & C-6 H), 7.4-8.0 (m, C-3 & C-5 H and ArH), 4.3 (s, 3 H, NCH_3); UV (pH 7.4 sodiumphosphate buffer) λ_{max} 250 nm (ε 2.21 x 10^4). Anal. Calcd for $C_{18}H_{16}NOI$: C 55.52, H 4.14, N 3.60. Found: C 55.24, H 4.17, N 3.56.

4-(2,4-Dichlorophenoxy)-1-methylpyridinium iodide (266·I). This product was obtained in 64 % yield and recrystallized from CH_2Cl_2/diethyl ether: mp 184-185 °C; ^{1}H NMR (DMSO-d_6) δ 8.8 (d, 2 H, C-2 & C-6 H), 7.6-8.0 (m, 5 H, C-3 & C-5 H and ArH), 4.3 (s, 3 H, NCH_3); GCMS (temperature program: 50 °C/min for 1 min followed by a temperature ramp of 25 °C/min for 10 minutes showed a single peak (R_t = 6.9 minutes) M-15 239. Anal. Calcd for $C_{12}H_{10}Cl_2NOI$: C 37.73, H 2.64, N 3.67. Found: C 37.79, H 2.69, N 3.62.

General Procedure for the Synthesis of the Oxalate Salts of the 4-Aryloxy-1-methyl-1,2,3,6-tetrahydropyridine Derivatives. Sodium borohydride (0.93 mmol) was added in portions to a stirred solution of the appropriate 4-aryloxy-1-methylpyridinium iodide (0.78 mmol) in 15 mL dry methanol at 0 °C. The mixture was stirred for an additional 30 minutes and the solvent was subsequently removed under reduced pressure. The residue was taken up in 10 mL water and the solution extracted with diethyl ether (3 x 20 mL). The combined ether layers were dried (Na_2SO_4), filtered, and concentrated to 50 % of the original volume. Treatment with oxalic acid (0.77 mmol) in 5 mL of diethyl ether precipitated the crude oxalate salt which was recrystallized from the appropriate solvent to afford a crystalline white solid.

Oxalate Salt of 4-(4'-Butylphenoxy)-1-methyl-1,2,3,6-tetrahydropyridine (172). This product was obtained in 74% yield and recrystallized from methanol/diethyl ether: mp 113-115 °C; ^{1}H NMR (CD_3OD) δ 7.0-7.4 (d, 4 H, ArH), 4.7 (s, 1 H, C-5 H), 3.8 (s, 2 H, C-6 H), 3.6 (m, 2 H, C-2 H), 3.0 (s, 3 H, NCH_3), 2.6-2.9 (m, 4 H, C-3 H & butyl CH_2), 1.7 (m, 2 H, butyl CH_2), 1.4 (m, 2 H, butyl CH_2), 1.0 (t, 3 H, butyl CH_3); UV (MeOH) λ_{max} 220 nm (ε 9.0 x 10^3) GCMS (temperature program: 40 °C for 1 min followed by a temperature ramp of 25 °C/min for 10 minutes showed a single peak at (Rt = 7.4 minutes) M^+ 245. Anal. Calcd for $C_{18}H_{25}NO_5$: C 64.44, H 7.52, N 4.18. Found: C 64.32, H 7.62, N 4.14.

Oxalate Salt of 4-(4'-tert-Butylphenoxy)-1-methyl-1,2,3,6-tetrahydropyridine (171). This product was obtained in 51% yield and recrystallized from methanol/diethyl ether: mp 149-151 °C; ^{1}H NMR (DMSO-d_6) δ 7.0-7.5 (m, 4 H, ArH), 4.7 (s, 1 H, C-5 H), 3.6 (d, 2 H, C-6 H), 3.3 (t, 2 H, C-2 H), 2.7 (s, 3 H, NCH_3), 1.7 (s, 9 H, t-butyl CH_2); UV(MeOH) λ_{max} 220 (ε 6.3 x 10^3) GCMS (temperature Program: 50 °C for 1 min followed by a temperature ramp of 25 °C/min for 10 minutes showed a single peak (R_t = 7.1 minutes) M^+ 245. Anal. Calcd for $C_{18}H_{25}NO_5$: C 64.44, H 7.52, N 4.18. Found: C 64.34, H 7.61, N 4.11.

Oxalate Salt of 1-Methyl-4-(4'-phenylphenoxy)-1,2,3,6-tetrahydropyridine (175). This product was obtained in 61% yield and recrystallized from methanol/diethyl ether: mp 241-242 °C; ^{1}H NMR (DMSO-d_6) δ 7.1-7.7 (m, 9 H, ArH), 4.9 (s, 1 H, C-5 H), 3.6 (s, 2 H, C-6 H), 3.3 (t, 2 H, C-2 H), 2.7 (s, 3 H, NCH_3), 2.5 (s, 2 H, C-3 H); UV (MeOH) λ_{max} 252 nm (ε 1.08 x 10^4). Anal. Calcd for $C_{20}H_{21}O_5N \cdot 0.5H_2O$: C 66.67, H 5.69, N

3.88. Found: C 66.89, H 6.03, N 3.88.

Oxalate Salt of 4-(2,4-dichlorophenoxy)-1-methyl-1,2,3,6-tetrahydropyridine (177). This product was obtained in 74% yield and recrystallized from methanol/diethyl ether: mp 150-152 °C; ^{1}H NMR (DMSO-d_6) δ 7.2-7.8 (m, 3 H, ArH), 4.8 (s, 1 H, C-5 H), 3.6 (s, 2 H, C-6 H), 3.4 (t, 2 H, C-2 H), 2.8 (s, 3 H, NCH3), 2.5 (s, 2 H, C-3 H); GCMS (temperature program: 50 °C for 1min followed by a temperature ramp of 25 °C/min for 10 minutes showed a single peak (R_t = 7.1 minutes) M^+ 257. Anal. Calcd for $C_{14}H_{15}Cl_2NO_5$: C 48.29, H 4.34, N 4.02. Found: C 48.40, H 4.39, N 4.06.

***m*-CBA Salt of 1-Methyl-4-(4'-phenylphenoxy)-1,2,3,6-tetrahydropyridine-N-oxide (267).** A solution of the tetrahydropyridine free base **175** obtained from the corresponding oxalate salt (0.4 g, 1.1 mmol) was stirred with *m*-chloroperoxybenzoic acid (0.208 g, 1.2 mmol) in 10 mL of CH_2Cl_2 at 0 °C for 1 hour. Upon evaporation of the solvent, the residue in diethyl ether gave a white solid which was recrystallized from CH_2Cl_2/diethyl ether to afford **267** as the *m*-CBA salt in 56 % yield: mp 110-111 °C; ^{1}H NMR ($CDCl_3$) δ 7.0-8.0 (m, 13 H, ArH), 4.67 (t, 1 H, C-5 H), 3.7-4.3 (complex m, 4 H, C-6 & C-2 H), 3.6 (s, 3 H, NCH_3), 2.6-3.2 (m, 2 H, C-3 H). Anal. Calcd for $C_{25}H_{24}ClNO_4$: C 68.57, H 5.52, N 3.2. Found: C 68.48, H 5.56, N 3.22.

1-Methyl-4-(4'-phenylphenoxy)-2,3-dihydropyridinium perchlorate (268·ClO_4). Triflouroacetic anhydride (0.31 mL, 2.25 mmol) was added dropwise to a solution of **267** (0.2 g, 0.45 mmol) in 10 mL CH_2Cl_2 at 0 °C and the reaction mixture was stirred at 0 °C for 30 minutes. The solvent

was evaporated and the residue was treated with 70% methanolic perchloric acid (0.1 mL) to afford crude **268·ClO_4** which was recrystallized from methanol/diethyl ether to afford orange needles in 75 % yield: mp 145-147 °C; ^{1}H NMR (DMSO-d_6) δ 8.3 (d, 1 H, C-6 H), 7.3-7.9 (m, 9 H, ArH), 5.4 (d, 1 H, C-5 H), 4.0 (t, 2 H, C-2 H), 3.5 (s, 3 H, NCH_3), 3.0 (t, 2 H, C-3 H); UV (MeOH) λ_{max} 278 nm (ε 1.55 x 10^4), 310 nm (ε 8.5 x 10^3). Anal. calcd for $C_{18}H_{18}ClNO_5$: C 59.43, H 4.99, N 3.85. Found: C 59.49, H 4.99, N 3.79.

4-Phenyl-1-(ethynylcarbonyl)-1,2,3,6-tetrahydropyridine (190). An aqueous solution of 4-phenyl-1,2,3,6-tetrahydropyridine HCl salt (**190**, 1.2 g, 6.1 mmol) was treated with K_2CO_3 to obtain a pH of about 8-9 and was extracted with CH_2Cl_2. The combined organic extracts were dried (Na_2SO_4), filtered and DCC (2.51 g, 12.2 mmol), 4-dimethylaminopyridine (60 mg) and propiolyic acid (0.85 g, 12.2 mmol) were added to the filtrate. The resulting mixture was stirred under nitrogen overnight. The reaction was quenched with water and the resulting mixture was washed with 1N HCl (50 mL). The aqueous solution was extracted with ethyl acetate (3 x 30 mL). The combined organic layers were dried (Na_2SO_4) and filtered. The solvent was evaporated under reduced pressure and the residue was chromatographed on a silica gel column with ethyl acetate: hexanes 1:1. The fractions containing only the desired product (from tlc) were combined and evaporated to afford **190** in 51% yield as a pale yellow solid: mp 100-102 °C; ^{1}H NMR ($CDCl_3$) δ 7.4 (m, 5 H, ArH), 6.0 (m, 1 H, C-5 H), 4.3-4.5 (m, 2 H, C-6 H), 3.9-4.0 (t, 2 H, C-2 H), 3.2 (d, 1 H, acetylenic H), 2.6 (m, 2 H, C-3 H); GCMS (temperature program: 50 °C for 1 min followed by a temperature ramp of 25 °C/min for 10 minutes) recorded a

single peak at R_t = 8.07 minutes M^+211.

4-(2-N-Methylanilinoethenyl)-1-methyl-2,3-dihydropyridinium Perchlorate (289·ClO_4). A reaction mixture containing the 4-ethynyldihydropyridinium product **236**·ClO_4 (0.1 g, 0.45 mmol) and N-methylaniline (**287**, 48 μL, 0.45 mmol) in CD_3CN (1 mL) was allowed to stand for six hours at room temperature following which the solvent was removed under reduced pressure and the residue was crystallized from CH_2Cl_2/diethyl ether to afford 60 mg (41%) of a fluffy red solid: mp 147-8 °C; UV (CH_3CN) λ_{max} 464 nm (ε 5.10 x 10^4); ^1H NMR (DMSO-d_6) δ 2.9 (t, 2H, C-3 H), 3.3 (s, 3H, CH_3), 3.5 (s, 3H, CH_3), 3.6 (t, 2 H, C-2 H), 5.9 (bs, 2 H, olefinic H), 7.5 (m, 5 H, ArH), 8.0 (dd, 2 H, olefinic H); FABMS (M^+ 227). Anal. Calcd for $C_{15}H_{19}ClN_2O_4$: C 55.13, H 5.86, N 8.57. Found: C 55.02, H 5.89, N 8.54.

6.2. Enzymology.

6.2.1 Preparation of Beef liver MAO-B.

Isolation of the mitochondria:

The isolation procedure was adapted from that utilized by Salach *et al* .[190] Fresh beef liver was obtained from the slaughter house and was transported packed on ice. Initial isolation procedures were carried out at 4 °C in the cold room facilities. Beef liver (1.5-2.0 Kg) was cut with a knife into roughly 8 portions of 250 g each and these portions were minced through a meat grinder since a Foley mill was not available. The minced paste so obtained was pressed through a coarse strainer (a cheese cloth will suffice for this operation) and diluted to 25% (w/v from the original value) with 250 mM sucrose buffer containing 10 mM phosphate and 0.5 mM EDTA at pH 7.2. The tissue suspension was mixed and homogenized with a motor driven loose fitting glass/teflon homogenizer on ice with at least 3 vertical passes or until a homogeneous solution was obtained. The homogenization step requires manual force as the tissue has a lot of fat and the teflon pestle cannot flow easily through the glass mortar and therefore the following two steps could save some labor. The liver is to be minced into a paste making sure that no chunks remain and secondly a motor driven homogenizer should be used which could provide sufficient power for homogenization. Failure to adhere closely to this step may result in grief at later stages as the chunks of liver not properly homogenized, contain precious amounts of protein and would be wasted. The homogenized solution was further diluted with about 700 mL (1:1) of the sucrose/EDTA buffer (pH 7.4, 100 mM) and centrifuged at

400 g for 15 min. The supernatant solution was carefully decanted, filtered through cheese cloth (one must avoid connective tissue spilling into the solution) and centrifuged at 10,500 g for 15 min. The pellet obtained after the centrifugation was resuspended in a small volume of sucrose buffer (100 mM, pH 7.4) without EDTA and homogenized. This homogenized solution was diluted further to about one liter in the same buffer and centrifuged at 7,500 g for 15 min. The supernatant was discarded and the pellet was homogenized in a buffer containing 150 mM KCl and 10 mM phosphate (pH 7.2) to give roughly about 10% of the volume used in the initial centrifugation. This suspension was centrifuged at 15,000 g for 20 minutes. The speed was increased because we were advised that greater speed would provide more tissue. The supernatant was discarded and the pellets were stored at -20 °C in plastic bottles. Attempted short-cuts, such as mincing the beef liver by passing through polytron rotors, will definitely save time but will result in appreciable loss in enzyme activity. The procedure for the isolation of the mitochondria described above is easy to follow but is tedious and time consuming, therefore it is recommended to reserve the rotors and the centrifuges which are going to be used in advance and to notify the owners of the laboratory regarding the usage of their facilities.

In order to proceed to the next step it is highly advisable to obtain a rough estimate of enzyme activity, even though this may be difficult due to the low specific activity of the crude preparation (For the assay used to measure enzyme activity, the reader is directed towards the end of this procedure, where the procedure is described in detail). It is mandatory to

measure the protein content of the mitochondria as the subsequent purification step requires accurate estimation of the protein concentration. The protein concentration can be measured using the Sigma diagnostic protein assay and the detailed procedure described therein (This kit is available from Ms Usuki). In our case we estimated the protein content of our preparation from the standard calibration curve to be 29.6 mg/mL.

Purification of Phospholipase A from Naja Naja Venom.

In order to proceed to the next purification step it is required to purify Phospholipase A from Naja naja venom (See ref and references sited within) Suitable eye-wear, face mask, lab coat and at least double pair of gloves must be used while handling the snake venom. Exposure of lyophillised venom on broken skin could result in death (Read instructions on venom container). It is highly recommended to carry out this procedure in a well ventilated hood with one worker constantly in charge of disposal of toxic waste.

A 10 % (w/v) aqueous solution of venom (400 mg in 4 mL of deionized water for about 2 kg liver) was brought to pH 3.6 with 1 N H_2SO_4 at room temperature and the pH of this solution was maintained at 3.6 in a boiling water bath for 5-10 minutes. After cooling sufficient 1 M K_2HPO_4 was added to yield a 50 mM phosphate concentration. During the course of the experiment we calculated that 400 mg of venom would require about 3.7 mL of phosphate buffer to afford approximately a 50 mM phosphate concentration. The pH of this solution was adjusted to 7.6 with 3M NH_4OH and the precipitated proteins were removed by

centrifugation in Eppendorf tubes at 12,000 g for 15 min at 0 °C. The tubes were stored at 0 °C until required.

It has been found that Sigma Chemicals sells Phospholipase A_2 (partially purified from Naja Naja venom) and during the purification of MAO-A which will be described later, the commercially available phospholipase A_2 (partially purified from Naja Naja venom) was used. This saves the workers from carrying out the purification process of phospholipase A from snake venom and furthermore we do not have the assay established to measure Phopholipase A_2 and it is recommended to use the commercially available material.

Purification of MAO-B.

The following steps will describe an overview on the purification. A detailed description will follow next.

1. The pellet (mitochondria) was homogenized with cold deionized water.
2. The resulting homogenate was centrifuged at 100,000 g for 15 minutes.
3. The supernatant was discarded and the pellet was homogenized in TEA buffer.
4. The protein content was adjusted to 30 mg/mL.
5. Phospholipase A_2, Phospholipase C and $CaCl_2$ were added.
6. The solution was digested for 1 hour, with continuous stirring, the pH was maintained at 7.3.
7. The digested mitochondria were centrifuged at 100,000 g for 15 minutes.
8. The supernatant was discarded and the pellet was homogenized in

TEA buffer.

9. The protein content was adjusted to 15 mg/mL.

10. Triton X-100, commercially available from Fisher (20% W/V) was added to the above homogenate and the solution was homogenized in a Warring blender.

11. The homogenized solution was stirred for an additional 25 minutes.

12. The homogenate was centrifuged at 100,000 g for 15 minutes.

13. The supernatant was retained (stored overnight on ice) and the pellet was discarded.

14. Required amounts of ficoll, dextran, PEG and water were stirred overnight at room temperature to ensure homogeniety.

15. The supernatant from step 13 was treated with the above solution and stirred for 5 minutes.

16. The resulting emulsions were poured into centrifuge tubes and allowed to stand for 30 minutes.

17. The emulsion was centrifuged in a swinging bucket centrifuge at 10,000 g for 20 minutes.

18. The upper and the lower solutions were carefully aspirated.

19. The middle solid layer was homogenized in TEA buffer.

20. The protein content was adjusted to 10 mg/mL.

21. The homogenate was centrifuged at 41,000 g for 20 minutes.

22. The pellet was discarded and the supernatant was stored overnight at 0 °C.

23. The supernatant was centrifuged at 41,000 g for 20 minutes.

24. The pellet was discarded and the supernatant was retained.

25. The supernatant was centrifuged at 252,000 g for 90 minutes.

26. The supernatant was discarded and the yellow pellet was homogenized in Na phosphate buffer containing 50% glycerol (w/v).

27. The enzyme activity was assayed.

The procedure which will be described in the following paragraphs is based on the purification of one bottle (which contains a pellet from the last centrifuge step described in the isolation step. In other words we were following exactly $1/10^{th}$ additions and dilutions as described in Salach's procedure). The mitochondria from one bottle was thawed overnight prior to the purification and suspended in 100 mL of cold, deionized nanopure water. The suspension was homogenized with a motor driven glass/teflon homogenizer, further diluted with 250 mL of water and centrifuged at 100,000 g at 4 °C for 15 min.

The following steps may be carried out at room temperature. The washed mitochondria (pellet), resuspended in 60 mL of 0.1 M triethanolamine (TEA) (pH of the triethanolamine was adjusted to 7.2) was homogenized as before. The resulting mixture was diluted further with 100 mL of 0.1 M TEA buffer in a beaker which was placed on a Dubnoff incubator at 30 °C. The protein content was measured at this stage. The solution was diluted further with TEA buffer to obtain a protein concentration of 30 mg/mL. $CaCl_2$ (1M) was added to this suspension to afford a solution 25 mM in calcium, followed by 30 mg of phospholipase A_2 (commercially available from Sigma) or the crude preparation from venom stored in Eppendorf tubes and 1.0 mg of phospholipase C (commercially available from Sigma) per 500 mg of

protein. The mixture was then incubated for 1 hour at 30 °C with stirring and constant maintenance of the pH at 7.3 with 2 M NH_4OH. The digested mitochondria were centrifuged at 100,000 g for 15 min at 4 °C and the resulting pellet was homogenized in 100 mL of TEA buffer. The total volume at the end of this step was 120 mL. The protein concentration of this solution was adjusted to 15 mg/mL with Triton X-100 (10-20%, w/v stock solution). Thus 1 mg of a 20% triton X-100 solution in deionized water was added per each 3 mg of protein (so if the biological extract contained 15 mg/mL of protein, 5 mg of 20% triton solution is to be added). This suspension was homogenized 20-30 seconds in a Warring blender. The mixture was stirred an additional 25 minutes and centrifuged at 100,000 g for 15 minutes at 4 °C. The supernatant was retained and stored overnight on ice (total volume at the end of this operation was 270 mL).

For each mL of the Triton extract the following materials were added: dextran (110 mg or 110 x total prep. volume 270 mL = 29.7 g), ficoll (120 mg or 120 x total prep. volume 270 mL = 32.4 mg), PEG (80 mg or 80 x total prep. volume 270 mL = 21.6 mL) and water (0.19 g or 0.19 x total prep volume 270 mL = 51 mL). A mixture of the above materials was stirred overnight on the previous evening to ensure a homogeneous solution. The triton extract was treated with 200 mL of 0.1 M TEA buffer and to this solution was added the stirred polymers. This solution was stirred for an additional 5 minutes. The total volume at the end of this step was about 400 mL. The emulsion was poured into polycarbonate centrifuge tubes and allowed to stand for 20-30 min to allow further equilibration. This

was centrifuged in a SW 28 swinging bucket rotor at 10,000 g (which could be obtained at 7500 rpm) for 15 minutes at 20 °C. It is extremely important to allow the rotor to come to a complete stop without the use of brakes. The enzyme was now distributed in the compact interphase. The upper and lower phases were carefully aspirated and the interfacial solids (the thin wafer like layer) was resuspended in 60 mL of TEA buffer (all these operations were carried out in a ice bath) and centrifuged at 41,000 g for 20 minutes at 4 °C. A small white pellet of $Ca(OH)_2$ similar to that observed by Salach was seen at the bottom of the centrifuge tube and this pellet was discarded. The clear supernatant solution was centrifuged at 252,000 g (50,000 rpm) for 90 min in an Beckman 60 Ti rotor following which the supernatant solution was drained off and the yellow pellet was suspended in 6-10 mL of Na Phosphate buffer, pH 7.2 containing 50% glycerol (w/v). We used about 11 mL of this buffer and so our total volume at the end was 15 mL. Extreme caution regarding the capability of the polycarbonate tubes to withstand the high g's should be taken. Before attempting the 252,000 g centrifugation the tubes should be checked for cracks. It is recommended to use new tubes. The enzyme activity in 15 mL was determined to be 16.4 units based on benzylamine. One unit of MAO-B is defined as the quantity of enzyme required to oxidize 1 μmol of benzylamine per minute.

Determination of enzyme activity.

The activity of MAO-B was calculated by the following procedure.

1. The Beckman DU-50 UV spectrophotometer was started and program # 6 (kinetic pac module) was entered. The wavelength was locked on 342 nm (this is the wavelength at which the MAO-B catalyzed oxidation product of MPTP, $MPDP^+$ absorbs maximally) and the initial rate measurements were set to be recorded, every 2 seconds for 180 seconds.

2. A 4 mM solution of MPTP hydrochloride in pH 7.2 phosphate buffer was prepared.

3. The activity of MAO-B catalyzed oxidation of MPTP to $MPDP^+$ was confirmed in a preliminary experiment (400-220 nm) by repeated scanning of an incubation mixture containing 1600 µL of 4 mM MPTP and 40 µL of MAO-B. We observed almost immediate formation of a chromophore which absorbed at 342 nm and increased in OD with respect to time.

4. We then determined the initial rate for this transformation by monitoring the formation of $MPDP^+$ kinetically as described in step 1. An incubation mixture containing 1600 µL of MPTP (4 mM) was placed in a UV cell and allowed to equilibrate at 37 °C for 30 seconds. MAO-B (40 µL) was then added to this incubation mixture with all the required parameters adjusted as in step 1 and initial rate measurements were noted.

5. Calculation of # of units of MAO-B in 15 mL solution.

The rate measurement obtained from the above experiment was

0.15 Absorption units/min. In order to convert to concentration units we make use of the Beer-Lambert law, i.e. $A = \varepsilon bc$

where A = absorbance, ε = molar extinction coefficient, c = concentration and b = pathway of the cell.

or $c = A/\varepsilon b$- - - - - - - (1)

Since 40 µL of MAO-B was used in the experiment to determine the initial rate of oxidation of MPTP (0.15 abs.units/minute), the initial rate of oxidation of MPTP catalyzed by 15 mL (15,000 µL) of MAO-B is:

Substituting the value of A in equation (1), we have

$c = 0.15\ min^{-1}/\ 18{,}000\ cm^{-1}.\ mmol^{-1}$ ($\varepsilon = 18000\ cm^{-1}.M^{-1}$ for $MPDP^+$ and b = 1 cm)

i.e. $c = 15 \times 10^{-2}/1.8 \times 10^4$ mmoles $min^{-1}mL^{-1}$

$c = 8.3 \times 10^{-6}$ mmoles $min^{-1}\ mL^{-1}$

therefore for the entire preparation (15,000 µL)

$c = 8.3 \times 10^{-6} \times 15000\ \mu L/40\ \mu L$

$c = 3.1 \times 10^{-3}$ mmoles $min^{-1}\ mL^{-1}$

Turnover number for MPTP = $2.0 \times 10^2\ min^{-1}$

$c = 3.1 \times 10^{-3}$ mmoles $min^{-1}\ mL^{-1}/2.0 \times 10^2\ min^{-1}$

$c = 1.5 \times 10^{-5}$ mmoles

Since total volume in the cuvette was 2 mL

$c = 3.0 \times 10^{-5}$ mmoles

now 1 unit of MAO-B corresponds to 3.7 nmoles.

c = 30 nmoles/3.7 nmoles

c = 8.2 units of MAO-B.

6.2.2. Preparation of MAO-A.

Isolation of mitochondria from human placenta.

The source of human placenta was the Montgomery Regional Hospital. The isolation must be initiated within 45 min after delivery due to the proteolytic activity which destroys MAO-A activity. The placenta was placed on ice immediately after delivery and was freed from the umbical cord and other connective tissue. The connective tissue free placenta was cut into small pieces with surgical scissors and passed through a coarse strainer (cheese cloth) directly into 1.5 liters of 0.25 M sucrose pH 7.2 at 0 °C, containing 10 mM phosphate, 0.5 mM EDTA and 15 mL of phenylmethylsulfonyl fluoride (50 mM in absolute ethanol). The tissue slurry was homogenized in a Waring blender equipped with polytron blades (a regular blender will suffice) and centrifuged at 1250 g for 15 min. The supernatant was carefully decanted and centrifuged at 26,000 g for 15 min. The pellet from this centrifugation was washed by resuspension by hand homogenization in 500 mL of the buffer used earlier using a loose-fitting glass/teflon homogenizer and centrifuged at 26,000 g for 15 min. The mitochondria (pellet) was washed again by homogenizing the pellet in 70-100 mL of KCl buffer (0.15 M) containing tris-phosphate 10 mM, pH 7.0-7.2 at 0 °C and 0.5 mM EDTA and centrifugation at 40,000 g for 20 min. The pellets at the end of this centrifugation can be stored at -70 °C for several months.

It is necessary to know the potential health risks which are involved in this preparation and only qualified individuals must attempt this preparation. A full and detailed safety program offered by the

university regarding precautionary measures to be followed during this preparation must be taken prior to participation .

Purification of MAO-A.

The purification of MAO-A follows the same operations and principles as described in the purification of MAO-B which follows the literature procedure of Salach. Mitochondria from 7 placentas are removed from the -70 °C freezer, pooled together and thawed overnight at 0 °C. The mitochondrial pellets are suspended in 0.1 M triethanolamine buffer pH 7.2 by hand homogenization and the protein content of this solution is measured and adjusted to 20 mg/mL. At this stage we had a total volume of 340 mL, and the protein determination of this solution revealed 10,200 mg of protein. In order to adjust the protein concentration to 20 mg/mL, a 2/3 dilution was carried out (170 mL of TEA was added) to afford a final volume of 510 mL. $CaCl_2$ (1M) was added to give a solution 25 mM in calcium. The suspension was placed in a 25 °C water bath and 670 units of phospholipase A_2 (partially purified from Naja Naja venom and commercially available from Sigma), 1.0 mg of phospholipase C (commercially available from Sigma), respectively for each 500 mg of protein present were added. Since we had 10,200 mg of protein we added 13,668 units of phospholipase A_2 and 20.4 mg of phospholipase C. This solution was digested with continuous stirring for 1 hour and the pH of this solution was maintained at 7.3 with 2 M ammonia. The digest was centrifuged at 45,000 g (19,000 rpm) on a JA-20 rotor for 15 minutes. The pellet was washed again by homogenizing in 0.1 M TEA buffer and repeating the centrifugation. The washed pellet

was again homogenized in the same buffer and the protein concentration was adjusted to 15 mg/mL. The enzyme was then extracted into Triton X-100 (20% solution in deionized water) to afford 1 mg of Triton per 3 mg of protein. Thus hypothetically if 5266 mg of protein is present, then 1755 mg of Triton must be added to afford 1 mg of Triton per 3 mg of protein. Since Triton is a 20% solution therefore 20 gm are contained in 100 mL solution or 20,000 mg are contained in 100 mL, so in order to add 1755 mg of Triton, we need to add 8.7 mL of 20% Triton solution. After the addition of Triton, the solution was homogenized in a glass teflon homogenizer, and the mixture was stirred at 25 °C for 30 minutes. The suspension was centrifuged as before and the supernatant recentrifuged to minimize turbidity. This supernatant may be stored at 0 °C overnight. For each 8 mL of the Triton extract (we had 350 mL of this extract) the following chemicals were added. Dextran (0.5 g/8 mL or 21.87 g/350 mL) and PEG (0.4 g/8 mL or 17.5 g/350 mL). The solids are dissolved by stirring the mixture for 30 minutes at 25 °C. The solution is centrifuged in a swinging bucket rotor at 9,500 g (8,500 rpm) rotor SW-27. The rotor is allowed to stop without braking. (This centrifugation is carried out in the department of Biochemistry). A two phase system with an interphase results in which the enzyme is present in the upper layer. The enzyme layer is carefully withdrawn with a pasteur pipette. PEG is then added to achieve a PEG concentration of 25% w/v and the mixture is stirred at 20 °C for 30 minutes. This mixture is centrifuged at 17,000 g (JA-20 rotor) at 4 °C for 10 minutes. The pellet is homogenized in pH 7.2 Na phosphate buffer (20 mM) containing 20% glycerol. From our purification attempt

on 7 placentas we were successful in obtaining 8 units of MAO-A activity based on the kynuramine assay. One unit of MAO-A is defined as the amount of enzyme required to oxidize 1 μmol of kynuramine in 1 minute. The activity determination was exactly the same as the procedure described for MAO-B except that kynuramine was used as a substrate for MAO-A instead of MPTP. The oxidation of kynuramine was monitored at 314 nm (the wavelength at which the oxidation product of kynuramine, namely 6-hydroxyquinoline absorbs). So far we have attempted no further purification on MAO-A due to lack of facilities and equipment and we are currently in the process of preparing for this purification.

6.2.3. Enzymology Studies.

The activity of the enzyme MAO-B was determined spectrophotometrically at 345 nm ($MPDP^+$) using MPTP (4 mM) or 250 nm (benzaldehyde) using benzylamine (2 mM) as substrate on a Beckman DU 50 spectrophotometer using initial rate measurements (30-120 seconds). The activity of MAO-A was determined in a identical fashion using 1 mM kynuramine as substrate and measuring the formation of 6-hydroxyquinoline at 314 nm. A unit of activity (equivalent to 3.7 nmol protein) is defined as the amount of enzyme required to convert 1 μmol of benzylamine to benzaldehyde or 1 μmol of kynuramine to 6-hydroxyquinoline in 1 minute.

Substrate and Inactivation Studies with MAO B.

General Methods. All UV spectral data were obtained on a Beckman DU-50 spectrophotometer.

Stock solutions of the test compounds were prepared in phosphate buffer (100 mM, pH 7.4) and diluted with the same buffer to give concentrations of 0.05, 0.067, 0.10, 0.20, 1.0, and 2.5 mM. A 480 μL aliquot of each solution was added to a sample cuvette which then was placed in a spectrophotometer that was maintained at 37 °C. After a 2 minute equilibration period, 0.05 units of MAO-B in 20 μL buffer were added and the rates of oxidation were determined by monitoring the increment in absorbance of the corresponding dihydropyridinium product formed during the enzyme catalyzed reaction. Initial rates were estimated from product yield over 30-180 sec time period. The V_{max} and K_M values were determined by the Lineweaver Burk plot.

The following steps constitute the key points during the substrate analysis.

(1). The tetrahydropyridine was incubated with MAO-B at 37 °C and the incubation mixture was scanned spectrophotometrically to determine whether the compound was an MAO-B substrate. It will be useful if the synthetic dihydropyridinium species which is the initial metabolic product of oxidation is available for comparison purposes.

(2). If the compound was an MAO-B substrate, then the Michaelis Menton kinetic parameters were determined. The following steps attempt to illustrate the experiment to determine initial rates of oxidation using the kinetic package available on the Beckmann DU-50 UV

spectrophotometer.

a. The UV spectrophotometer was started and using the program and the step key, the instrument was set at program 6, which contained the kinetic mode. The R/S key can be used to set the desired parameters, toggling with the enter key each time a question is answered. The total time for each run was set at 2 min and the wavelength was set at the λ_{max} of the dihyropyridinium species formed in the initial incubation (see step (1)). The instrument was calibrated with pH 7.4 phosphate buffer in a 1 mL quartz cuvette. When the calibration proceeds correctly, the screen on the instrument will read "insert sample, R/S to read".

b. The enzyme was placed on ice during use.

c. A 500 µL aliquot of a given concentration of the tetrahydropyridine was placed in the cuvette and allowed to equilibrate at 37 °C. MAO-B (0.05 units, 10 µL) was added and the incubation mixture was allowed to equilibrate for 15-20 seconds (this was indicated by a rapid rise in the absorbance at the set wavelength). The R/S key was pressed to monitor the initial rate of oxidation at this stage. The instrument records absorbance increase of the product in the set period of time. At the end of the run, the printer plotted the absorbance vs time data, after which the screen read 0 = edit, 1 = run sample. It is absolutely critical to not touch 0 or 1 but instead, press the enter key several times after which the printer records the initial rate. After the rate has been recorded on the plotter, step c may be repeated.

d. A series of concentrations in an increasing order, of a given tetrahydropyridine (if it is a MAO-B substrate) with MAO-B provides

initial rates which then are converted in terms of concentration units prior to plotting the double reciprocal plot to determine V_{max} and K_M.

MAO-B inhibition studies were conducted as follows: A 250 mM stock solution of the test compound in 100 mM sodium phosphate buffer (pH = 7.4) was diluted with buffer to obtain solutions of 0.1 to 2 mM. MAO-B (0.5 units) was added and incubations were carried out with gentle agitation in a water bath incubator at 37 °C. A 50 μL aliquot was removed at 0, 5, 10, 15, and 20 minutes and was added to a sample cuvette containing 5 mM MPTP in phosphate buffer (450 mL, pH = 7.4). The rate of $MPDP^+$ formation was determined by monitoring the absorbance at 343 nm every 3 seconds for 2 minutes in kinetic program # 6 available on the UV spectrophotometer. A control experiment was done in an exactly same manner as described above with the exception that the potential inactivator was not included. The rates which were generated from the UV spectrophotometer were converted to percentage enzyme activity values by dividing the slopes by the slope at time t = 0 based on the assumption that at t= 0, presumably no inactivation takes place. The % enzyme activity values were converted to their natural logarithms and plotted vs time to generate k_{obs} which is the pseudo-first order rate constant for inactivation at that concentration and is obtained as the slope of the plot of ln(% enzyme activity remaining) vs time. In some cases the observed rate constant k_{obs} has to be corrected for the natural loss in enzyme activity that could occurs during incubations. This correction can be obtained by subtracting the slope obtained for the control (i.e. no substrate) from the k_{obs} to get a corrected rate constant (k_{corr}). The

reciprocal of the inhibitor concentration vs the reciprocal of k_{obs} is then plotted to obtain the rate of inactivation k_{inact} (from 1/y intercept) and the concentration at which this rate is 50% i.e. K_I (from slope/k_{inact}). The program 6 which applies to the kinetic mode was used in this study and key steps are the same as noted in the substrate studies.

Substrate studies with MAO-A.

General methods. All preliminary incubations were performed at a fixed concentration of the substrate (500 μM). A typical study involved UV spectrophotometric scanning from 200-440 nm of a incubation mixture containing 480 μL of potential substrate (500 μM with pH 7.3 phosphate buffer) at 37 °C with 0.01 units of MAO-A. In the case of good MAO-A substrates complete kinetic analysis using various concentrations of substrates and 0.01 units of MAO-A was carried out as described in the substrate studies with MAO-B and the kinetic parameters were determined in a fashion identical to that described with MAO-B substrates.

7. References.

1. Vogt, W. Naturally Occurring Lipid-Soluble Acids of Pharmacological Interest. *Pharmac. Rev.* **1958**, *10*, 407-436.

2. Blaschko, H. Amine Oxidase and Amine Metabolism. *Pharmacol. Rev.* **1952**, *4*, 415-458.

3a. Dahlstrom, A.; Fuxek, K. Evidence for the Existence of Monoamine Containing Neurons in the CNS. I. Demonstration of Monoamines in the Cell Bodies of Brain Stem Neurons. *Acta. Physiologica. Scandinavica., Suppl.* **1964**, *232*, 1-55.

3b. Ahtee, L.; Sharman, D.; Vogt, M. Acid Metabolites of Monoamines in the Avain Brain. *Brit. J. Pharmacol.* **1970**, *38*, 72.

3c. Weissbach, H.; Redfield, B. G.; Axelrod, J. The Enzymatic Acetylation of Serotonin and Other Naturally Occuring Amines. *Biochem. Biophys. Acta.* **1961**, *54*, 190.

3d. Bloom, F. E. The Fine Structural Localization of Biogenic Monoamines in Nervous Tissue. *Int. Rev. Neurobiol.* **1970**, *13*, 27.

4. Euler, U. S. von. A Specific Sympathomimetic Ergone in Adrenergic Nerve Fibres (Sympathin) and its Relations to Adrenaline and Noradrenaline. *Acta. Physiol. Scand.* **1946**, *12*, 73-97.

5. Holtz, P.; Heise, R.; Ludtke, K. Fermentativer Abbau Von l-Dioxyphenylalanine (DOPA) Durch Niere. *Arch. Exp. Path. Pharmak.* **1938**, *191*, 87-118.

6. Burn, J. H.; Rand, M. J. Sympathetic Postganglionic Mechanism. *Nature* (London) **1959**, *184*, 163-165.

7. Carlsson, A.; Falck, B.; Hillarp, N-A. Cellular Localization of Brain Monoamines. *Acta. Physiol. Scand.* **1962**, *56* (suppl. 196), 1-27.

8. Carlsson, A. The Occurrence, Distribution and Physiological Role of Catecholamines in the Nervous System. *Pharmac. Rev.* **1959**, *11*, 233-566.

9. Glover, V.; Sandler, M.; Owen, F. Dopamine is a Monoamine Oxidase B Substrate in Man. *Nature* **1977**, *265*, 80-81.

10. Hornykiewicz, O. Dopamine (3-Hydroxytyramine) and Brain Function. *Pharmac. Rev.* **1966**, *18*, 925-964.

11. Jarrott, B.; Iverson, L. L. Noradrenaline Metabolizing Enzymes in Normal and Sympathetically Denervated Vas Deferens. *J. Neurochem.* **1971**, *18*, 1-6.

12. Neff, N. H.; Yang, H-Y, T.; Goridiss, C. Degradation of the Transmitter Amines by Specific Types of MAOs. In *Frontiers of Catecholamine Research.* (Snyder, S. H.; Usdin, E., Eds.) **1973**, pp 133-137, Permagon Press, London and New York.

13. Kopin, I. J. Biosynthesis and Metabolism of Catecholamines. *Anesthesiology* **1968**, *29*, 654-660.

14. Blaschko, H. The Specific Action of l-Dopa Decarboxylase. *J. Physiol. Lond.* **1939**, *96*, 50P-51P.

15. Gurin, S.; Delluva, A. The Biological Synthesis of Radioactive Adrenalin From Phenylalanine. *J. Biol. Chem.* **1947**, *170*, 545-550.

16. Levin, E. Y.; Levenberg, B.; Kaufman, S. The Enzymatic Conversion of 3,4-Dihydroxyphenylethylamine to Norepinephrine. *J. Biol. Chem.* **1960**, *235*, 2080-2086.

17. Celada, P.; Sarrias, M. J.; Artigas, F. Serotonin and 5-Hydroxyindoleacetic Acid in Plasma. Potential Use as Peripheral Measures of MAO-A Activity. *J. Neural Transm.* **1990**, Suppl 32, 149-154.

18. Aghajanian, G. K.; Bloom, F. Localization of Tritiated Serotonin in Rat Brain by Electron-Microscopic Autoradiography. *J. Pharmacol. Exp. Ther.* **1967**, *156:23*, 188-196.

19. Udenfriend, S.; Titus, E.; Weissbach, H.; Peterson, R. Biogenesis and Metabolism of 5-Hydroxyindole Compounds. *J. Biol. Chem.* **1956**, *219*, 335.

20. Wurtman, R. J.; Fernstrom, J. D. L-Tryptophan, L-Tyrosine, and the Control of Brain Monoamine Biosynthesis. In *Perspectives in Neuropharmacology*. (Snyder, S. H., Ed.) Oxford University Press **1972**, pp 143-148.

21. Axelrod, J. Methylation Reactions in the Formation and Metabolism of Catecholamines and Other Biogenic Amines: the Enzymatic Conversion of Norepinephrine (NE) to Epinephrine (E). *Pharmac. Rev.* **1966**, *18*, 95-113.

22. Barwell, C. J.; Basma, C. A.; Canham, A. N.; Williams, C. Evaluation of N,N-Dimethylphenethylamine and N,N-Dimethyltyramine as Substrates for Monoamine Oxidase B. *Pharm. Res. Commun.* **1988**, *20*, 101-102.

23. Malmstrom, B. G.; Andreasson, L-E.; Reinhammar, B. Copper-Containing Oxidases and Superoxide Dismutex. In *The Enzymes*. Boyer, P. D., Ed., Academic Press, New York, 1975, 12, pp 507.

24. Gorkin, V. Z.; Tatyanenko, L. V. Transformation of Mitochondrial Monoamine Oxidase Into a Diamine Oxidase-Like Enzyme in Vitro. *Biochem. Biophys. res. Commun.* **1967**, *27*, 613.

25. Zeller, E. A. Diamine Oxidase. *Adv. Enzymol.* **1942**, *2*, 93.

26. Malmstrom, B. G.; Andreasson, L-E.; Reinhammar, B. Copper-Containing Oxidases and Superoxide Dismutex. In *The Enzymes*. Boyer, P. D., Ed., Academic Press, New York, 1975, 12, pp 507.

27. Yamada, H.; Adachi, O. Amine Oxidase. In *Methods in Enzymology*. Tabor, H.; Tabor, C. W., Eds., Academic Press, New York, 1971, Vol. 17B, pp 705.

28. Zeller, E. A. Classification and Nomenclature of Monoamine Oxidases and Other Amine Oxidases. In *Monoamine Oxidase: Structure and Altered Functions*. Singer, T. P.; Korff, R. W.; Murphy, D. L., Eds., Academic Press, New York, 1979, 531.

29. Hare, M. L. C. Tyramine Oxidase I. A New Enzyme System In Liver. *Biochem. J.* **1928**, *22*, 968-972.

30. Zeller, E. A. Oxidation of Amines. In *The Enzymes*. Summer, J. B.; Myrback, K., Eds., Academic Press, New York, 1951, Vol. 2 (Part 1) pp 536.

31. Zeller E. A. *Classification and Nomemclature of Monoamine Oxidases and Other Amine Oxidases: Structure, Function and Altered Functions*. Singer, T. P.; Korff, R. W.; Murphy, D. L. Eds., Academic Press New York, 1979, pp 531.

32. Green, A. R.; Mitchell, B.; Tordoff, A.; Youdim, M. B. H. Evidence of Dopamine Deamination by Both Type A and B Monoamine Oxidase in Rat Brain in Vivo and for Degree of Inhibition of Enzyme Necessary for Increased Functional Activity of Dopamine and 5-Hydroxytryptamine. *Br. J. Pharmacol.*. **1977**, *60*, 343.

33. Knoll, J.; Magyar, K. Some Puzzling Pharmacological Effects of Monoamine Oxidase Inhibitors. *Adv. Biochem. Psychopharmacol.* **1972**, *5*, 393.

34. Neff, N. H.; Fuentes, J. A. The Use of Selective Monoamine Oxidase Inhibitor Drugs for Evaluating Pharmacological and Physiological Mechanisms. In *Monoamine Oxidase and its Inhibition.* Ciba Foundation Symposium No. 39, Elsevier, Amsterdam, 1976, 163.

35. Pearce, L. B.; Roth, J. A. Human Brain Monoamine Oxidase Type B: Mechanism of Deamination as Probed by Steady State Methods. *Biochemistry* **1985**, *24*, 1821-1826.

36. Denney, R. M.; Fritz, R. R.; Patel, N. T.; Abell, C. W. Human Liver MAO-A and MAO-B Seperated by Immunoaffinity Chromatography with MAO-B Specific Monoclonal Antibody. *Science* **1982**, *215*, 1400-1403.

37. Denney, R. M.; Denney, C. B. An Update on the Identity Crisis of Monoamine Oxidase: New and Old Evidence for the Independence of MAO-A and MAO-B. *Pharmac. Ther.* **1985**, *30*, 227-259.

38. Huang, R. Lipid-Protein Interactions in the Multiple Forms of Monoamine Oxidase. Enzymatic and ESR Studies with Purified Intact Rat Brain Mitochondria. *Molec. Pharmac.* **1980**, *17*, 192-198.

39. Hsu, Y-P. P.; Weyler, W.; Chen, S.; Sims, K. B.; Rinehart, W. B.; Utterback, M.; Powell, J. K.; Breakefield, X. O. Structural Features of Human Monoamine Oxidase A Elucidated from cDNA and Peptide Sequences. *J. Neurochem.* **1988**, *51*, 1321-1324.

40. Kearney, E. B.; Salach, J. I.; Walker, W. H.; Seng, R. L.; Kenney, W.; Zeszotek, E.; Singer, T. P. The Covalently Bound Flavin of Hepatic

Monoamine Oxidase. Isolation and Sequence of a Flavin Peptide and Evidence for Binding at the 8-Alpha Position. *Eur. J. Biochem.* **1971**, *24*, 321-327.

41. Billett, E. E.; Mayer, R. J. Monoclonal Antibodies to Monoamine Oxidase B and Other Mitochondrial Protein From Human Liver. *Biochem. J.* **1986**, *235*, 257-263.

42. Hsu, Y-P. P.; Powell, J. F.; Sims, K. B.; Breakefield, X. O. Molecular Genetics of the Monoamine Oxidases. *J. Neurochem.* **1989**, *53*, 12-18.

43a. Weyler, W.; Salach, J. I. Purification and Properties of Mitochondrial Monoamine Oxidase Type A from Human Placenta. *J. Biol. Chem.* **1985**, *260*, 13199-13207.

43b. Kochersperger, L. M.; Parker, E. L.; Siciliano, M.; Darlington, G. J.; Denney, R. M. Assignment of Genes for Human Monoamine Oxidases A and B to the X-Chromosome. *J. Neurosci. Res.* **1986**, *16*, 601-616.

44. Levitt, P.; Pintar, J. E.; Breakefield, X. O. Immunocytochemical Demonstration of Monoamine Oxidase B in Brain Astrocytes and Serotonergic Neurons. *Proc. Natl. Acad. Sci. U. S. A.* **1982**, *79*, 6385-6389.

45. Weyler, W.; Salach, J. I. Iron Content and Spectral Properties of Highly Purified Bovine Liver Monoamine Oxidase. *Archs Biochem. Biophys.* **1981**, *212*, 147-153.

46. Carmichael, S. W.; Pfeiffer, G. L. Histochemical Localization of Monoamine Oxidases Types A and B in the Adrenal Gland. *Histochem. J.* **1985**, *17*, 1289-1298.

47. Donnez, J.; Goenen, E.; Casanas, F.; Caprasse, J.; Ferin, J.; Thomas, K. Monoamine Oxidase Reactivity in the Human Fallopian Tube. *Fertil. Steril.* **1985,** *43,* 121-138.

48. Minamiura, N.; Yasunobu, K. T. Bovine Liver Monoamine Oxidase. A Modified Purification Procedure and Preliminary Evidence for Two Subunits and One FAD. *Archs Biochem. Biophys.* **1978,** *189,* 481-489.

49. Westlund, K. N.; Denney, R. M.; Kochersperger, L. M.; Rose, R. M.; Abell, C. W. Distinct Monoamine Oxidase A and B Populations in Primate Brain. *Science* **1985,** *230,* 181-183.

50. Weyler, W. Monoamine Oxidase A from Human Placenta and Monoamine Oxidase from Bovine Liver Both Have One FAD Per Subunit. An Important Revision. *Biochem. J.* **1989,** *260,* 726-729.

51. Ito, A.; Kuwahara, T.; Inadome, S.; Sagara, Y. Molecular Cloning of a cDNA for Rat Liver Monoamine Oxidase. *Biochem. Biophys. Res. Commun.* **1988,** *157,* 970-976.

52. Waldmeier, P. C. Amine Oxidases and Their Endogenous Substrates (With Special Refernce to Monoamine Oxidase and Brain). *J. Neural Transm.* **1987,** *23* (suppl.), 55-72.

53a. Blaschko, H. Oxidation of Tertiary Amines by MAO. *J. Pharm. Pharmacol.* **1989,** *41,* 664.

53b. Benedetti, S.; Sontag, N.; Boucher, T.; Kan, J-P. in Function and Regulation of Monoamine Enzymes. (Usdin, E.; Weiner, N.; Youdim, M. B. H., eds.), **1981,** pp 527-538, Macmillan, London.

54. Williams, C. H.; Lawson, J.; Backwell, F. R. C. Oxidation of 3-Amino-1-phenylprop-1-enes by MAO and their Use in a Continuous Assay of the Enzyme. *Biochem. J.* **1988**, *256*, 911-915.

55a. Yu, P. H.; Davis, B. A. Stereospecific deuterium Substitution at the α-Carbon Position of Dopamine and its Effect on Oxidative Deamination Catalyzed by MAO-A and MAO-B from Different Tissues. *Biochem. Pharmacol.* **1986**, *35*, 1027-1036.

55b. Fuller, R. W.; Hemrick-Lueke, S. K. Influence of Ring and Side-Chain Substituents on the Selectivity of Amphetamine as a Monoamine Oxidase Inhibitor. *Res. Commun. Substances Abuse.* **1982**, *3*, 159.

55c. Robinson, J. B. Stereoselectivity and Isoenzyme Selectivity of Monoamine Oxidase Inhibitors. *Biochem. Pharmacol.* **1985**, *34*, 4105-4108.

55d. Arai, Y.; Toyoshima, Y.; Kinemuchi, I. Studies of Monoamine Oxidase and Semicarbazide-Sensitive Amine Oxidase II. Inhibition by α-Methylated Substrate Analog Monoamines, α-Methyltryptamine, α-Methylbenzylamine, and Two Enantiomers of α-Methylbenzylamine. *Jpn. J. Pharmacol.* **1986**, *41*, 191-197.

55e. Williams, C. H. β-Phenylethanolamine as a Substrate for MAO. *Biochem. Soc. Trans.* **1977**, *5*, 1770-1771.

McEwen, C. M., Jr.; Sasaki, G.; Lenz, W. R. Human Liver Monoamine Oxidase. I. Kinetic Studies of Model Interactions. *J. Biol. Chem.* **1968**, *243*, 5217-5225.

56a. Yelekci, K.; Lu, X.; Silverman, R. B. Electron Spin Resonance Studies of Monoamine Oxidase B. First Direct Evidence for a Substrate Radical Intermediate. *J. Am. Chem. Soc.* **1989**, *111*, 1138-1140.

56b. Tan, A.; Glantz, M. D.; Piette, H. L.; Yasunobo, K. T. ESR Analysis of the FAD in Bovine Liver Monoamine Oxidase. *Biochem. Biophys. Res. Commun.* **1983**, *117*, 517-523.

57a. Chow, Y. L.; Danen, W. C.; Nelson, S. F.; Rosenblatt, D. H. Nonaromatic Aminium Radicals. *Chem. Rev.* **1978**, *78*, 243.

57b. Weinberg, N. L.; Weinberg, H. R. Electrochemical Oxidation of Organic Compounds. *Chem. Rev.* **1968**, *68*, 449.

58. Mann, C. K.; Barnes, K. K. In *Electrochemical Reactions in Nonaqueous Systems*; Marcel Dekker: New York, 1970; Chapter 9.

59a. Burka, L. T.; Guengerich, F. P.; Willard, R. J.; Macdonald, T. L. Mechanism of Cytochrome P-450 Catalysis. Mechanism of N-Dealkylation and Amine Oxide Deoxygenation. *J. Am. Chem. Soc.* **1985**, *107*, 2549.

59b. Wimalsena, K.; May, S. W. Mechanistic Studies on Dopamine-β-monooxygenase Catalysis: N-Dealkylation and Mechanism-Based Inhibition by Benzylic-Nitrogen Containing Compounds. Evidence for Single Electron Transfer. *J. Am. Chem. Soc.* **1987**, *109*, 4036.

60. Nelson, S. F.; Ippoliti, J. T. On the Deprotonation of Trialkylamine Cation Radicals by Amines. *J. Am. Chem. Soc.* **1986**, *108*, 4879-4881.

61. Dinnocenzo, J. P.; Banach, T. E. Deprotonation of Tertiary Amine Cation Radicals. A Direct Experimental Approach. *J. Am. Chem. Soc.* **1989**, *111*, 8643-8653.

62. Silverman, R. B.; Zelechonok, Y. Evidence for a Hydrogen Atom Transfer Mechanism or a Proton/Fast Electron Transfer Mechanism for Monoamine Oxidase. *J. Org. Chem.* **1992**, *57*, 6373-6374.

63a. Newcomb, M.; Glen, A. G. A Convenient Method for Kinetic Studies of Fast Radical Rearrangements. Rate Constants and Arrhenius functions for the Cyclopropylcarbinyl Radical Ring Opening. *J. Am. Chem. Soc.* **1989,** *111,* 275-277.

63b. Newcomb, M.; Manek, M. B. Picosecond Radical Kinetics. Benzeneselenol as a Fast Radical Trapping Agent and Rate Constants for Ring Opening of the *Trans*-(2-phenylcyclopropyl)carbinyl Radical. *J. Am. Chem. Soc.* **1990,** *112,* 9662-9663.

64. Kitz, R.; Wilson, I. B. Esters of Methanesulfonic Acid as Irreversible Inhibitors of Acetylcholinesterases. *J. Biol. Chem.* **1962,** *237,* 3245-3249.

65. Zeller, E. A.; Barsky, J.; Fouts, J. E.; Kirchheimer, W. E.; Van Orden, L. Influence of Isonicotonic Acid Hydrazide and *l*-Isonicotinic-2-isopropyl Hydrazide on Bacterial and Mammalian Enzymes. *Experientia* **1952,** *8,* 349-350.

66. Youdim, M. B. H.; Finberg, J. P. M. Monoamine Oxidase Inhibitors. In *Psychopharmacology. Part I, Preclinical Psychopharmacology* (Eds. Graham-Smith, D. G.; Cowen, P. E.), 1983, Excerpta Medica, Amsterdam, pp 37-51.

67. Tyrer, P. *psychopharmacology of Affective Disorders.* Paykel, E. S.; Coppen, A., Eds., Oxford University Press, Oxford, 1979, pp 159.

68. Baldessarini, R. J. In *Goodman and Gilman's 'The Pharmacological Basis of Therapeutics'*; Gilman, A. G., Goodman, L. S.; Rall, T. W.; Murad, F., Eds., Macmillan, New York, 1985, 7th ed., pp 391.

69a. Goodman and Gilman's *'The Pharmacological Basis of Therapeutics'*; Gilman, A. G., Goodman, L. S.; Rall, T. W.; Murad, F., Eds., Macmillan, New York, 1985, 7th ed., pp 423.

69b. Youdim, M. B. H. Tyramine and Psychiatric Disorders. In Neuroregulators and Psychiatric Disorders (Eds. Usdin, E.; Hamburg, D.; barchas, D. J.) 1976, Oxford University Press, New york, 1976.

70. Knoll, J.; Magyar, K. Some Puzzling Pharmacological Effects of Monoamine Inhibitors. *Adv. Biochem. Psychopharmacol.* **1972,** *5,* 393-408.

71a. Kalir, A.; Sabbach, Y.; Youdim, M. B. H. *Br. J. Pharmacol.* **1981,** *73,* 55.

71b. Murphy, D. L.; Donnelly, C. H.; Richelson, E.; Fuller, R. W. N-Substituted Cyclopropylamines as Inhibitors of MAO-A and MAO-B. *Biochem. Pharmacol.* **1978,** *27,* 1767-1769.

71c. Mills, J.; Kattau, R.; Slater, I. H.; Fuller, R. W. N-Substituted Cyclopropylamines as Monoamine Oxidase Inhibitors. Structure-Activity Relationships. Dopa Potentiation in Mice and In Vitro Inhibition of Kynuramine Oxidation. *J. Med. Chem.* **1968,** *11,* 95-98.

72a. Barsky, J.; Pacha, W. L.; Sarkar, S.; Zeller, A. E. Amine Oxidases: XVII. Mode of Action of 1-Isonicotinyl-2-isopropylhydrazine on Monoamine Oxidase. *J. Biol. Chem.* **1962,** *234,* 389-391.

72b. Zeller, A. E.; Sarkar, S. Amine Oxidases: XIX. Inihibition of Monoamine Oxidase by Phenylcyclopropylamines and Iproniazid. *J. Biol. Chem.* **1962,** *237,* 2333-2336.

73. Patek, D.; Hellerman, L. Mitochondrial Monoamine Oxidase: Mechanism of Inhibition by Phenylhydrazine and Araalkylhydrazines. Role of Enzymatic Oxidation. *J. Biol. Chem.* **1974,** *249,* 2373-2380.

74. Hellerman, L.; Erwin, V. G. Mitochondrial Monoamine Oxidase II. Action of Various Inhibitors on the Bovine Kidney Enzyme. Catalytic Mechanism. *J. Biol. Chem.* **1968,** *243,* 5234-5243.

75. Kenney, W, C.; Nagy, J.; Salach, J. I.; Singer, T. P. Structure of the Phenylhydrazine Adduct of Monoamine Oxidase, in *Monoamine Oxidase: Structure, Function, and Altered Functions*, Singer, T. P., Von Korff, R. W.; Murphy, D. L. Eds., Academic Press, New York, **1979**, 25.

76. Gartner, B.; Hemmerich, P. Inhibition of Monoamine Oxidase by Propargylamine: Structure of the Inhibition Complex. *Angew. Chem. Internat. Edit.* **1975**, *14*, 110-111.

77. Rando, R. R. in *Methods of Enzymology* (Jacoby, W. B. and Wilchek, M., Eds.), *Vol. 46*, pp 158-171, Academic Press, New York.

78. Hellerman, L.; Erwin, E. V. Mitochondrial Monoamine Oxidase I. Purification and Characterization of the Bovine Kidney Enzyme. *J. Biol. Chem.* **1967**, *242*, 4230.

79. Maycock, A. L.; Abeles, R. H.; Salach, J. I.; Singer, T. P. The Structure of the Covalent Adduct Formed by the Interaction of 3-Dimethylamino-1-propyne and the Flavine of Mitochondrial Monoamine Oxidase. *Biochem.* **1976**, *15*, 114-125.

80. Maycock, A. L. Structure of a Flavoprotein-Inactivator Model Compound. *J. Am. Chem. Soc.* **1975**, *97*, 790-792.

81. Singer, T. P. Active Site Directed, Irreversible Inhibitors of Monoamine Oxidase. In Monoamine Oxidase: Structure, Function and Altered Functions. (Von Korff, R. W., eds) pp 7-23.

82. Krantz, A.; Lipkowitz, G. S. Studies of Mitochondrial Monoamine Oxidase. Inactivation of the Enzyme by Isomeric Acetylenic and Allenic Amines Yielding Mutually Exclusive Products. *J. Am. Chem. Soc.* **1977**, *99*, 4156-4159.

83. Silverman, R. B.; Hoffman, S. J. Mechanism of Inactivation of Mitochondrial Monoamine Oxidase by N-Cyclopropyl-N-arylalkyl Amines. *J. Am. Chem. Soc.* **1980**, *102*, 884-886.

84. Hanzlik, R. P.; Tullman, R. H. Suicidal Inactivation of Cytochrome P-450 Enzymes by Cyclopropylamines. Evidence for Cation-Radical Intermediates. *J. Am. Chem. Soc.* **1982**, *104*, 2048.

85. Silverman, R. B.; Yamasaki, R. B. Mechanism-Based Inactivation of Mitochondrial Monoamine Oxidase by N-(1-Methylcyclopropyl)benzylamine. *Biochemistry* **1984**, *23*, 1322-1332.

86. Hanzlik, R. P.; Tullman, R. H.; Kishore, V. Inactivation of Cytochrome P-450 Enzymes by Cyclopropylamines. in *Microsomes, Drug Oxidations and Chemical Carcinogenesis* (Coon, M. J.; Conney, A. H.; Estabrook, W.; Gelboin, H. V.; Gillette, J. R.; O'Brien, P. J. Eds.) pp 327-330, Academic Press, New York.

87. Vazquez, M.; Silverman, R. B. Revised Mechanism for Inactivation of Mitochondrial Monoamine Oxidase by N-Cyclopropylbenzylamine. *Biochemistry* **1985**, *24*, 6538-6543.

88. Silverman, R. B.; Zieske, P. A. Mechanism of Inactivation of Monoamine Oxidase by 1-Phenylcyclopropylamine. *Biochemistry* **1985**, *24*, 2128-2138.

89. Silverman, R. B.; Hoffman, S. J. N-(1-Methyl)-cyclopropylbenzylamine: A Novel Inactivator of Mitochondrial Monoamine Oxidase. *Biochem. Biophys. Res. Commun.* **1981**, *101*, 1396-1401.

90. Silverman, R. B.; Zeiske, P. Identification of the Amino Acid Bound to the Labile Adduct Formed During Inactivation of Monoamine Oxidase by 1-

Phenylcyclopropylamine. *Biochem. Biophys. Res. Commun.* **1986,** *136,* 154-159.

91a. Qin, X-Z.; Williams, F. ESR Studies on the Radical Cation Mechanism of the Ring Opening of Cyclopropylamines. *J. Am. Chem. Soc.* **1987,** *109,* 595-597.

91b. Silverman, R. B.; Zeiske, P. A. 1-Phenylcyclobutylamine, the First in a New Class of Monoamine Oxidase Inactivators. Further Evidence for a Radical Intermediate. *Biochemistry* **1986,** *25,* 341-346.

92. Y. Maeda, Ingold, K. U. Kinetic Applications of Electron Paramagnetic Resonance Spectroscopy. 35. The Search for a Dialkylaminyl Rearrangement. Ring Opening of N-Cyclobutyl-N-n-propylaminyl. *J. Am. Chem. Soc.* **1980,** *102,* 328-331.

93. Nagahisa, A.; Orme-Johnson, W. H. Silicon-Mediated Suicide Inhibition: An Efficient Mechanism-Based Inhibitor of Cytochrome P-450_{scc} Oxidation of Cholesterol. *J. Am. Chem. Soc.* **1984,** *106,* 1166-11647.

94a. Constantopoulos, G.; Satoh, P. S.; Tchen, T. T. Cytochrome P-450 Catalyzed Oxidation of Cholesterol. *Biochem. Biophys. Res. Commun.* **1962,** *8,* 50.

94b. Burstein, S.; Gut, M. Intermediates in the Conversion of Cholesterol to Pregnenolone: Kinetics and Mechanism. *Steroids* **1976,** *28,* 115-131.

94c. Duque, C.; Morisaki, M.; Ikekawa, N.; Shikita, M. The Enzyme Activity of Bovine Adrenocortical Cytochrome P-450 Producing Pregnenolone From Cholesterol: Kinetics and Electrophoresis Studies on the Reactivity of Hydroxylation Intermediates. *Biochem. Biophys. Res. Commun.* **1978,** *82,* 179-187.

95. Danzin, C.; Collard, J, N.; Marchal, P.; Schirlin, D. Selective Inactivation of MAO-B by Benzyldimethylsilylmethanamines in Vitro. *Biochem. Biophys. Res. Commun.* **1989**, *160*, 540-544.

96. Silverman, R. B.; Banik, G. M. (Aminoalkyl)trimethylsilanes. A New Class of Monoamine Oxidase Inactivators. *J. Am. Chem. Soc.* **1987**, *109*, 2219-2220.

97. Vadnere, M. K.; Silverman, R. B. (Aminoalkyl)trimethylgermanes. The First Organogermanium Mechanism-Based Enzyme Inactivators: A New Class of Monoamine Oxidase Inactivators. *Bioorg. Chem.* **1987**, *15*, 328-332.

98. Dostert, P.; Benedetti, S. M.; Jalfre, M. In *Monoamine Oxidase: Basic and Clinical Frontiers;* Kamujo, K., Ed.; Excerpta Medica: Amsterdam, 1982; pp 155-163.

99. Ancher, J. F. *Drugs Future* **1984**, *9*, 585-586.

100a. Gates, K. S.; Silverman, R. B. 5-(Aminomethyl)-3-aryl-2-oxazolidinones. A Novel Class of Mechanism-Based Inactivators of Monoamine Oxidase B. *J. Am. Chem. Soc.* **1990**, *112*, 9364-9372.

100b. Gates, K. S.; Silverman, R. B. Model Studies for the Mechanism of Inactivation of Monoamine Oxidase by 5-(Aminomethyl)-3-aryl-2-oxazolidinones. *J. Am. Chem. Soc.* **1989**, *111*, 8891-8895.

101. Ding, Z.; Silverman, R. B. 5-(Aminomethyl)-3-aryldihydrofuran-2(3H)-ones, A New Class of Monoamine Oxidase Inactivators. *J. Med. Chem.* **1992**, *35*, 885-889.

102. Son, J. K.; Rosazza, J. P. N.; Duffel, M. W. Vinblastine and Vincristine are Inhibitors of Monoamine Oxidase B. *J. Med. Chem.* **1990**, *33*, 1845-1848.

103. *Chemistry and Pharmacology of Drugs, Volume 3; Antineoplastic Agents;* Remers, W. A., Lednicer, D., Eds.; John Wiley & Sons: New York, 1984; pp 210-212.

104. Goswami, A.; Schaumberg, J. P.; Duffel, M. W.; Rosazza, J. P. N. Enzymatic and Chemical Oxidations of Leurosine to 5'-Hydroxyleurosine. *J. Org. Chem.* **1987**, *52*, 1500.

105. Goswami, A.; Macdonald, T. L.; Hubbard, C.; Duffel, M. W.; Rosazza, J. P. N. Leurosine Biotransformations: An Unusual Ring-Fission Reaction Catalyzed by Peroxidase. *Chem. Res. Toxicol.* **1988**, *1*, 238.

106. Harfenist, M.; McGee, D. P. C.; White, H. L. A Selective, Reversible, Competitive Inihibitor of Monoamine Oxidase A Containing No Nitrogen, with Negligible Potentiation of Tyramine-Induced Blood Pressure Rise. *J. Med. Chem.* **1991**, *34*, 2931-2933.

107. Nishimura, K.; Lu, X.; Silverman, R. B. Inactivation of Monoamine Oxidase B by Analogs of the Anticonvulsant Agent Milacemide (2-(*n*-Pentylaminoacetamide). *J. Med. Chem.* **1993**, *36*, 446-448.

108a. Janssens de Verbeke, P.; Cavalier, R.; David-Remacle, M.; Youdim, M. B. H. Formation of the Neurotransmitter Glycine from the Anticonvulsant Milacemide is Mediated by Brain Monoamine Oxidase B. *J. Neurochem.* **1988**, *50*, 1011-1016.

108b. Janssens de Verbeke, P.; Pauwels, G.; Buyse, C.; David-Remacle, M.; DeMay, J.; Roba, J.; Youdim, M. B. H. The Novel Neuropsychotropic Agent Milacemide is a Specific Enzyme-Activated Inhibitor of Brain Monoamine Oxidase B. *J. Neurochem.* **1989**, *53*, 1109-1116.

109. Cohen, G.; Pasik, P.; Cohen, B.; Leist, A.; Mytilineou, C.; Yahr, M. D. Pargyline and Deprenyl Prevent the Neurotoxicity of 1-Methyl-4-phenyl-1,2,3,6-tetrahydropyridine (MPTP) in Monkeys. *Eur. J. Pharmacol.* **1984**, *106*, 209-210.

110a. USA PSG Effect of Deprenyl on the Progression of Disability in Early Parkinson's disease. *N. Engl. J. Med.* **1989**, *321*, 1364-1371.

110b. Tatton, W. G.; Greenwood, C. E. Rescue of Dying Neurons: A New Action for Deprenyl in MPTP Parkinsonism. *J. Neurosci. Res.* **1991**, *30*, 666-672.

110c. LeWitt, P. A. Deprenyl's Effect at Slowing Progression of Parkinsonian Disability: The DATATOP Study. *Acta. Neurol. Scand.* **1991**, *84*, 79-86.

110d. Salo, P. T.; Tatton, W. G. Deprenyl Reduces the Death of Motorneurons Caused by Axotomy. *J. Neurosci. Res.* **1992**, *31*, 394-400.

111. Heikkila, R. E.; Hess, A.; Duvoism, R. C. Dopaminergic Neurotoxicity of 1-Methyl-4-phenyl-1,2,3,6-tetrahydropyridine in Mice. *Science* **1984**, *224*, 1451-1453.

112. Langston, J. W.; Forno, L. S.; Rebert, C. S.; Irwin, I. Selective Nigral Toxicity After Systemic Administration of MPTP in the Squirrel Monkey. *Brain Res.* **1984**, *292*, 390-394.

113. Burns, R. C.; Chieuh, C. C.; Markey, S. P.; Ebert, M. H. E.; Jacobowitz, D. M.; Kopin, I. J. A primate Model of Parkinsonism. *Proc. Natl. Acad. Sci.* U. S. A. **1984**, *80*, 4546-4550.

114. Sundstrom, S.; Jonsson, G. Pharmacological Interference with the Neurotoxic Action of 1-Methyl-4-phenyl-1,2,3,6-tetrahydropyridine (MPTP) on Central Catecholamine Neurons. *Eur. J. Pharmacol.* **1985**, *116*, 179.

115. Cashman, J. R.; Zeigler, D. M. Contribution of N-Oxygenation to the Metabolism of MPTP (1-Methyl-4-phenyl-1,2,3,6-tetrahydropyridine) by Various Liver Preparations. *Mol. Pharmacol.* **1986,** *29,* 163.

116. Chiba, K.; Trevor, A. J.; Castagnoli, N., Jr. Metabolism of the Neurotoxic Tertiary Amine MPTP by Brain Monoamine Oxidase. *Biochem. Biophys. Res. Commun.* **1984,** *120,* 574-578.

117. Castagnoli, N., Jr.; Chiba, K.; Trevor, A. J. Potential Bioactivation Pathways for the Neurotoxin 1-Methyl-4-phenyl-1,2,3,6-tetrahydropyridine (MPTP). *Life Sci.* **1985,** *36,* 225-230.

118. Fuller, R. W.; Hemricke-Luecke, S. K.; Kindt, M. V.; Heikkila, R. E. Different Effects of Monoamine Oxidase Inhibition on MPTP Depletion of Heart and Brain Catecholamines in Mice. *Life Sci.* **1988,** *42,* 263-271.

119. Langston, J. W.; Irwin, I.; Langston, E. B.; Forno, L. S. 1-Methyl-4-phenylpyridinium ion (MPP^+): Identification of a Metabolite of MPTP, a Toxin Selective to the Substantia Nigra. *Neurosci. Lett.* **1984,** *48,* 87-92.

120. Langston, J. W.; Irwin, I.; Langston, E. B.; Forno, L. S. Pargyline Prevents MPTP-Induced Parkinsonism in Primates. *Science* **1984,** *225,* 1480-1482.

121. Chiba, K.; Trevor, A. J.; Castagnoli, N., Jr. Metabolism of the Neurotoxic Tertiary Amine MPTP by Brain Monoamine Oxidase. *Biochem. Biophys. Res. Commun.* **1984,** *120,* 547-578.

122. Chiba, K.; Peterson, L. A.; Castagnoli,, K.; Trevor, A. J.; Castagnoli, N., Jr. Studies on the Molecular Mechanism of Bioactivation of the Selective Nigrostriatal Neurotoxin 1-Methyl-4-phenyl-1,2,3,6-tetrahydropyridine. *Drug Metab. Dispos.* **1985,** *13,* 342-347.

123. Salach, J. I.; Singer, T. P.; Castagnoli, N., Jr.; Trevor, A. J. Oxidation of the Neurotoxic Amine 1-Methyl-4-phenyl-1,2,3,6-tetrahydropyridine (MPTP) by Monoamine Oxidases A and B and Suicide Inactivation of the Enzymes by MPTP. *Biochem. Biophys. Res. Commun.* **1984**, *125*, 831-835.

124. Trevor, A. J.; Castagnoli, N., Jr.; Caldera, P. S.; Ramsay, R. R.; Singer, T. P. Bioactivation of MPTP: Reactive Metabolites and Possible Biochemical Sequelae. *Life Sci.* **1987**, *40*, 713.

125. Javitch, J. A.; D'Amata, R. J.; Strittmatter, S. M.; Snyder, S. H. Parkinsonism-Inducing Neurotoxin 1-Methyl-4-phenyl-1,2,3,6-tetrahydropyridine: Uptake of the Metabolite N-Methylpyridine by Dopaminergic Neurons Explains Selective Toxicity. *Proc. Natl. Acad. Sci.* U. S. A. **1985**, *82*, 2173-2177.

126. Chiba, K.; Trevor, A. J.; Castagnoli, N., Jr. Active Uptake of MPP^+, a Metabolite of MPTP by Brain Synaptosomes. *Biochem. Biophys. Res. Commun.* **1985**, *128*, 1228-1232.

127. Nicklas, W. J.; Vyas, I.; Heikkila, R. E. Inhibition of NADH-Linked Oxidation in Brain Mitochondria by 1-Methyl-4-phenyl-1,2,3,6-tetrahydropyridine. *Life Sci.* **1985**, *36*, 2503-2508.

128. Vyas, I.; Heikkila, R. E.; Nicklas, W. J. Studies on the Neurotoxicity of 1-Methyl-4-phenyl-1,2,3,6-tetrahydropyridine: Inhibition of NAD-Linked Substrate Oxidation by its Metabolite, 1-Methyl-4-phenylpyridinium. *J. Neurochem.* **1986**, *46*, 1501-1507.

129. Ramsay, R. R.; Salach, J. I.; Singer, T. P. Uptake of the Neurotoxin 1-Methyl-4-phenylpyridine (MPP^+) by Mitochondria and its Relation to the

inhibition of the Mitochondrial Oxidation of NAD+-Linked Substrates by MPP+. *Biochem. Biophys. Res. Commun.* **1986,** *134,* 743-748.

130. Chiba, K.; Peterson, L. A.; Castagnoli, K. P.; Trevor, A. J.; Castagnoli, N., Jr. Studies on the Molecular Mechanism of Bioactivation of the Selective Nigrostriatal Neurotoxin 1-Methyl-4-phenyl-1,2,3,6-tetrahydropyridine. *Drug Metabolism and Disposition* **1985,** *13,* 342-347.

131. Peterson, L. A.; Caldera, P. S.; Trevor, A. J.; Chiba, K.; Castagnoli, N., Jr. Studies on the 1-Methyl-4-phenyl-2,3,-dihydropyridinium Species 2,3-MPDP+, the Monoamine Oxidase Catalyzed Oxidation Product of the Nigrostriatal Toxin 1-Methyl-4-phenyl-1,2,3,6-tetrahydropyridine. *J. Med. Chem.* **1985,** *28,* 1432-1436.

132. Trevor, A. J.; Castagnoli, N., Jr.; Singer, T. P. The Formation of reactive Intermediates in the MAO-Catalyzed Oxidation of the Nigrostriatal Toxin 1-Methyl-4-phenyl-1,2,3,6-tetrahydropyridine. *Toxicology* **1988,** *49,* 513-519.

133. Singer, T. P.; Salach, J. I.; Castagnoli, N., Jr.; Trevor, A. J. Interactions of the Neurotoxic Amine 1-Methyl-4-phenyl-1,2,3,6-tetrahydropyridine with Monoamine Oxidases. *Biochem. J.* **1986,** *235,* 785-789.

134. Krueger, M. J.; McKeown, K.; Ramsay, R. R.; Youngster, S.; Singer, T. P. Meachanism-Based Inactivation of Monoamine Oxidases A and B by Tetrahydropyridines and Dihydropyridines. *Biochem. J.* **1990,** *268,* 219-224.

135. Singer, T. P.; Salach, J. I.; Crabtree, D. Reversible Inhibition and Mechanism-Based Irreversible Inactivation of Monoamine Oxidases by 1-Methyl-4-phenyl-1,2,3,6-tetrahydropyridine. *Biochem. Biophys. Res. Commun.* **1985,** *127,* 707-712.

136. Youngster, S. K.; McKeown, K. A.; Jin, Y. Z.; Ramsay, R. R.; Heikkila, R. E.; Singer, T. P. Oxidation of Analogs of 1-Methyl-4-phenyl-1,2,3,6-tetrahydropyridine by Monoamine Oxidases A and B and the Inhibition of Monoamine Oxidases by the Oxidation Products. *J. Neurochem.* **1987**, *53*, 1837-1842.

137. Jin, Y. Z.; Ramsay, R. R.; Youngster, S. K.; Singer, T. P. A New Class of Powerful Inhibitors of Monoamine Oxidase A. *Biochem. Biophys. Res. Commun.* **1990**, *172*, 1338-1341.

138. Heibert, C. K.; Sayre, L. M.; Silverman, R. B. Inactivation of Monoamine Oxidase of 3,3-Dimethyl Analogues of 1-Methyl-4-phenyl-1,2,3,6-tetrahydropyridine and 1-Methyl-4-phenyl-2,3-dihydropyridine Ion. *J. Biol. Chem.* **1989**, *36*, 21516-21521.

139. Ottoboni, S.; Carlson, T. J.; Trager, W. F.; Castagnoli, K.; Castagnoli, N., Jr. Studies on the Cytochrome P-450 Catalyzed Ring α-Carbon Oxidation of the Nigrostriatal Toxin 1-Methyl-4-phenyl-1,2,3,6-tetrahydropyridine (MPTP). *Chem. Res. Toxico.* **1990**, *3*, 423-427.

140. Ottoboni, S.; Caldera, P.; Trevor, A. J.; Castagnoli, N., Jr. Deuterium Isotope Effect Measurements on the Interactions of the Neurotoxin 1-Methyl-4-phenyl-1,2,3,6-tetrahydropyridine with Monoamine Oxidase B. *J. Biol. Chem.* **1989**, *264*, 13684-13688.

141. Singer, T. P.; Ramsay, R. R. The Interaction of Monoamine Oxidases and Tertiary Amines. *Biochem. Soc. Trans.* **1991**, *19*, 211-215.

142. Maret, G.; Testa, B.; Jenner, P.; El Tayar, N.; Carrupt, P-A. The MPTP Story: MAO Activates Tetrahydropyridine Derivatives to Toxins Causing Parkinsonism. *Drug Metab. Rev.* **1990**, *22*, 291-332.

143. Brossi, A.; Gessner, W.; Fritz, R. R.; Bembenek, M. E.; Abell, C. W. Interaction of Monoamine Oxidase B with Analogues of 1-Methyl-4-phenyl-1,2,3,6-tetrahydropyridine Derived from Prodine-Type Analgesics. *J. Med. Chem.* **1986**, *29*, 444-445.

144. Efange, S. M. N.; Michelson, R. H.; Remmel, R. P.; Boudreau, R. J.; Dutta, A. K.; Freshler, A. Flexible N-Methyl-4-phenyl-1,2,3,6-tetrahydropyridine Analogues: Synthesis and Monoamine Oxidase Catalyzed Bioactivation. *J. Med. Chem.* **1990**, *33*, 3133-3138.

145. Hall, L.; Murray, S.; Castagnoli, K.; Castagnoli, N., Jr. Studies on 1,2,3,6-Tetrahydropyridine Derivatives as Potential Monoamine Oxidase Inactivators. *Chem. Res. Toxico.* **1992**, *5*, 625-633.

146. Altomore, C.; Carrupt, P-A.; Gaillard, P.; Tayar, N. E.; Testa, B.; Carotti, A. Quantitative Structure-Metabolism Relationship Analyses of MAO-Mediated Toxication of 1-Methyl-4-phenyl-1,2,3,6-tetrahydropyridine and Analogues. *Chem. Res. Toxico.* **1992**, *5*, 366-375.

147. Rollema, H.; Johnson, E. A.; Booth, R. G.; Caldera, P.; Lampen, P.; Youngster, S. K.; Trevor, A. J.; Naiman, N.; Castagnoli, N., Jr. In Vitro Intracellular Microdialysis Studies in Rats of MPP^+ Analogues and Related Charged Species. *J. Med. Chem.* **1990**, *33*, 2221-2230.

148. Schmidle, C. J.; Mansfield, R. C. The Aminomethylation of Olefins. A New Synthesis of 4-Phenylpyridine and Related Compounds. *J. Am. Chem. Soc.* **1954**, *78*, 1702-1706.

149. Schmidle, C. J.; Mansfield, R. C. *ibid.*, **1956**, *78*, 425-428.

150. Borch, R. F. A New Method for the Reduction of Secondary and Tertiary Amides. *Tetrahedron Lett.* **1968**, *21*, 2915-2916.

151. Brettle, R.; Shibib, S. M. The Selective Reduction of α,β-Olefinic Amides. *Tetrahedron Lett.* **1980**, *101*, 5690-5691.

152. Efange, S. M. N.; Michelson, R. H.; Remmel, R. P.; Boudreau, R. J.; Dutta, A. K.; Freshler, A. Flexible N-Methyl-4-phenyl-1,2,3,6-tetrahydropyridine Analogues: Synthesis and Monoamine Oxidase Catalyzed Bioactivation. *J. Med. Chem.* **1990**, *33*, 3133-3138.

153. Schmidt, C. A Synthesis of Homosafranic Acid and Related Compounds. *Can. J. Chem.* **1976**, *54*, 2310.

154. Beumel, O. F.; Harris, R. F. The Reaction of Lithium Acetylide-Ethylenediamine with Ketones. *J. Org. Chem.* **1964**, *29*, 1872-1876.

155. Midland, M. M. The Preparation of Monolithium Acetylide in Tetrahydrofuran. Reaction with Aldehydes and Ketones. *J. Org. Chem.* **1975**, *40*, 2250-2252.

156. Rossi, R.; Carpita, A.; Quirici, M. G.; Gaudenzi, M. L. Insect Sex Pheromones: Palladium-Catalyzed Synthesis of Aliphatic 1,3-Enynes by Reaction of 1-Alkynes with Alkenyl Halides under Phase Transfer Conditions. *Tetrahedron* **1982**, *38*, 631-637.

157. Corey, E. J.; Fuchs, P. L. A Synthetic Method for Formyl to Ethynyl Conversion. *Tetrahedron Lett.* **1972**, *36*, 3769-3772.

158. Gray, A. P.; Kraus, H.; Heitmeier, D. E.; Shiley, R. H. Cyclopropylpyridines. Interaction with Acid and Hydrogen. The Synthesis of Cyclopropanes "Ring-Opened" Analogs. *J. Org. Chem.* **1968**, *33*, 3007-3014.

159. Jeffery-Luong, T.; Linstrumelle, G. Palladium-Catalyzed Arylation and Vinylation of Alkenyllithium Reagents; A Route to Arylallenes, 1,2,4-Alkatrienes, and 1-Alkenylketones. *Synthesis* **1982**, 738-740.

160. Pelter, A.; Rowlands, M. The Conversion of Furans to 2(3H)-Butenolides. *Tetrahedron Lett.* **1987**, *28*, 1203-1206.

161. Sonogashira, K.; Tohda, Y.; Hagihara, N. A Convenient Synthesis of Acetylenes: Catalytic Substitutions of Acetylenic Hydrogen with Bromoalkenes, Iodoarenes, and Bromopyridines. *Tetrahedron Lett.* **1975**, *50*, 4467-4470.

162. Lee, G. C. M.; Tobias, B.; Holmes, J. L.; Harcourt, D. A.; Garst, M. E. A New Synthesis of Fulvenes. *J. Am. Chem. Soc.* **1990**, *112*, 9330-9336.

163. Dang, H. P.; Linstrumelle, G. An Efficient Stereospecific Synthesis of Olefins by the Palladium-Catalyzed Reaction of Grignard Reagents with Alkenyl Iodides. *Tetrahedron Lett.* **1978**, *2*, 191-194.

164. Walser, A.; Flynn, T.; Mason, C.; Crowley, H.; Maresca, C.; O'Donell, M. Thienotriazolodiazepines as Platelet-Activating factor Antagonists. Steric Limitations for the Substituent in Position 2. *J. Med. Chem.* **1991**, *34*, 1440-1446.

166. Cianna, L. D.; Haim, A. A Synthesis of 1,4-Bis(4-pyridyl)butadiyne. *J. Heterocycl. Chem.* **1984**, *21*, 607-608.

167. Dieck, H. A.; Heck, F. R. Palladium Catalyzed Synthesis of Aryl, Heterocyclic and Vinylic Acetylene Derivatives. *J. Organomettalic Chem.* **1975**, *93*, 259-263.

168. Sakamoto, T.; Shiraiwa, M.; Kondo, Y.; Yamanaka, H. A Facile Synthesis of Ethynyl-Substituted Six-Membered N-Heteroaromatic Compounds. *Synthesis* **1983**, 312-314.

169. Pelter, A.; Rowlands, M.; Clements, G. Cross Coupling Reactions for the Preparation of 2-Arylfurans, 2-Benzylfuran and 2-Cinnamylfuran. *Synthesis* **1987**, 51-53.

170. Subramanyam, B.; Woolf, T.; Castagnoli, N., Jr. Studies on the In Vitro Conversion of Haloperidol to a Potentially Neurotoxic Pyridinium Metabolite. *Chem. Res. Toxicol.* **1991**, *4*, 123-128.

171. Gessner, W.; Brossi, A.; Shen, R.; Fritz, R. R.; Abell, C. W. Conversion of 1-Methyl-4-phenyl-1,2,3,6-tetrahydropyridine and its 5-Methyl Analog into Pyridinium Salts. *Helv. Chim. Acta.* **1984**, *67*, 2037-2042.

172. These tetrahydropyridines were obtained from previous workers in our laboratory and were recrystallized prior to use.

173. Morosawa, S. Studies on Seven-Membered Heterocyclic Compounds Containing Nitrogen. II. An Improved Synthesis of 1-Azacycloheptan-4-one and its Related Compounds. *Bull. Chem. Soc. Japan.* **1958**, *31*, 418-422.

174. McElvain, S. M.; Stork, G. Piperidine Derivatives. XV. The Preparation of 1-Benzoyl-3-carbethoxy-4-piperidone. A Synthesis of Guvacine. *J. Am. Chem. Soc.* **1946**, *68*, 1049-1053.

175. Procter, G. R.; Smith, F. J. Bridged-Ring Nitrogen Compounds. Part 5. Synthesis of 2,6-Methano-3-benzazonine Ring Systems. *J. Chem. Soc. Perkin Trans.* **1981**, 1754-1762.

176. Sprague, R. H.; Brooker, L. G. S. Studies in the Cyanine Dye Series. IX. 4,4'-Pyridocyanines and 4-Pyrido-4'-cyanines. *J. Am. Chem. Soc.* **1937**, 2697-2699.

177. Unpublished Results by Naiman, N.; and Castagnoli, N., Jr. Compounds were recrystallized prior to use.

178. Swaminathan, S.; Narayan, K. V. The Rupe and Meyer-Schuster Rearrangement. *Chem. Rev.* **1971**, *71*, 429-438.

179. Efange, S. M. N.; Boudreau, R. J. Molecular Determinants in the Bioactivation of the Dopaminergic Neurotoxin N-Methyl-4-phenyl-1,2,3,6-tetrahydropyridine (MPTP). *J. Comp-Aided Mol. Des.* **1991**, *5*, 405-417.

180. Leung, L.; Ottoboni, S.; Oppenheimer, N.; Castagnoli, N., Jr. Characterization of a Product Derived from the 1-Methyl-2,3-dihydropyridinium Ion, a Metabolite of the Nigrostriatal Toxin, 1-Methyl-4-phenyl-1,2,3,6-tetrahydropyridine. *J. Org. Chem.* **1989**, *54*, 1052-1055.

181. Swett, L. R.; Martin, W. B.; Taylor, J. D.; Everett, G. M.; Wykes, A. A.; Gladish, Y. C. Allyl amine-an MAO-B Inihibitor. *Ann. N. Y. Acad. Sci.* **1963**, *107*, 891.

182. Krantz, A.; Lipkowitz, G. S. Studies on the Mitochondrial Monoamine Oxidase. Inactivation of the Enzyme by Isomeric Acetylenic and Allenic Amines Yielding Mutually Exclusive Products. *J. Am. Chem. Soc.* **1977**, *99*, 4156-4159.

183. Dinnocenzo, J. P.; Bauach, T. E. Deprotonation of tertiary Amine Cation Radicals. A Direct Experimental Approach. *J. am. Chem. Soc.* **1989**, *111*, 8646-8653.

184. Sprague, R. H. Cyanine Dyes. I. Absorption of Cyanines Derived from Pyranothiazole and Thiopyranothiazoles. *J. Am. Chem. Soc.* **1959**, *79*, 2275-2281.

185. Sprague, R. H.; De Stevens, G. Cyanine Dyes. II. Absorption of Cyanines Derived from 2-Methyl-8H-indeno[1,2-d]thiazole. *J. Am. Chem. Soc.* **1959**, *79*, 3095-3098.

186. Naiman, N.; Rollema, H.; Johnson, E.; Castagnoli, N., Jr. Studies on 4-Benzyl-1-methyl-1,2,3,6-tetrahydropyridine, a Nonneurotoxic Analogue of the Parkinsonian Inducing Agent 1-Methyl-4-phenyl-1,2,3,6-tetrahydropyridine. *Chem. Res. Toxicol.* **1990**, *3*, 133-138.

187. Efange, S. M. N.; Michelson, R. H.; Tan, A. K.; Krueger, M. J.; Singer, T. P. Molecular Size and Flexibility as Determinants of Selectivity in the Oxidation of N-Methyl-4-phenyl-1,2,3,6-tetrahydropyridine Analogs by Monoamine Oxidase A and B. *J. Med. Chem.* **1993**, *36*, 884-890.

188. Kruger, M. J.; Efange, S. M. N.; Michelson, R. H.; Singer, T. P. Interaction of Flexible Analogs of N-Methyl-4-phenyl-1,2,3,6-tetrahydropyridine and N-Methyl4-phenylpyridinium with Highly Purified Monoamine Oxidase A and B. *Biochemistry* **1992**, *31*, 5611-5615.

189. Tan, A. K.; Weyler, W.; Salach, J. I.; Singer, T. P. Differences in Substrate Specificities of Monoamine Oxidase A from Human Liver and Placenta. *Biochem. Biophys. Res. Commun.* **1991**, *181*, 1084-1088.

190. Salach, J. I.; Weyler, W. Preparation of the Flavin-Containing Aromatic Amine Oxidases of Human Placenta and Beef Liver. In *Methods in Enzymology*; Kaukfman, S., Ed.; Academic Press: London, 1987; Vol. 142, pp 627-637.

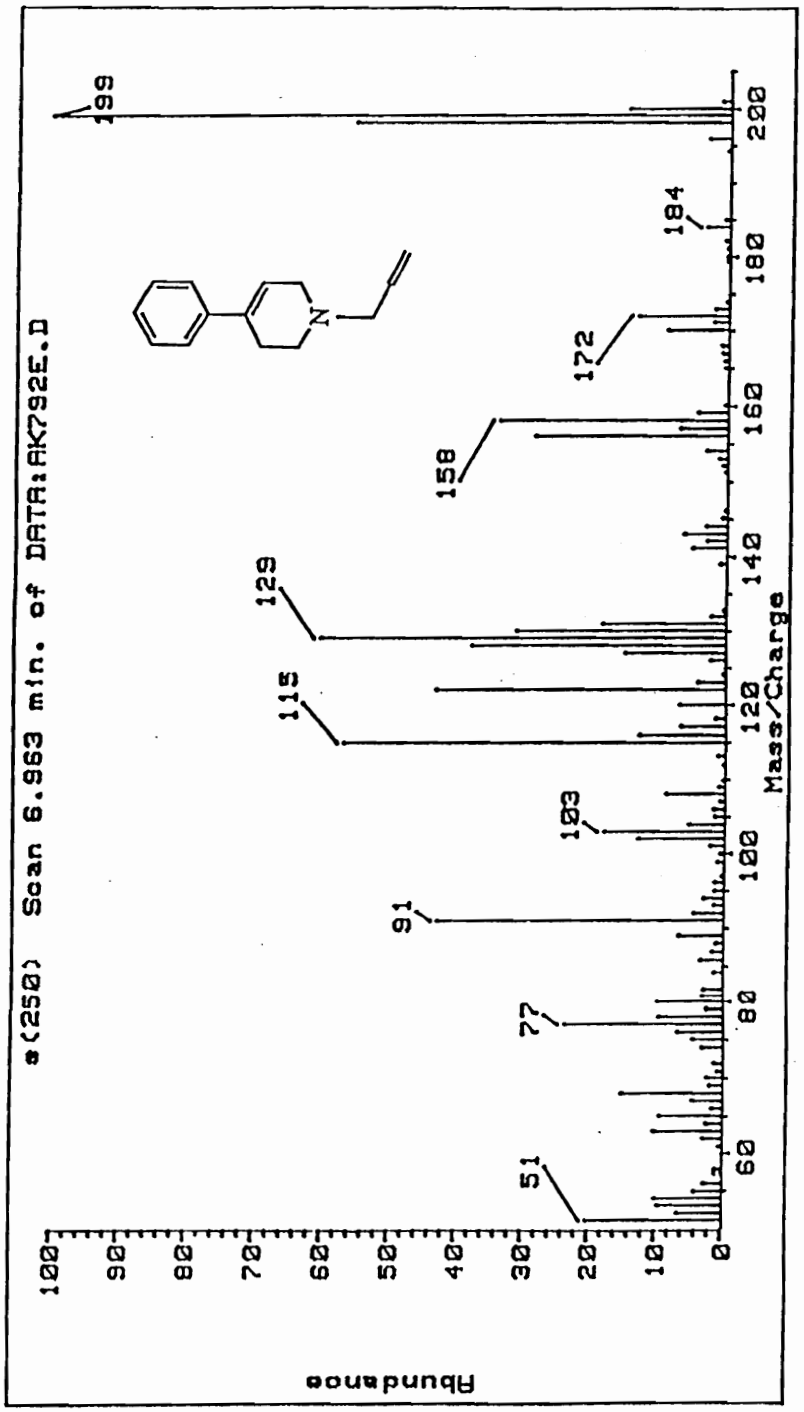

Figure. 1. GC/EIMS of 1-Allyl-4-phenyl-1,2,3,6-tetrahydropyridine.

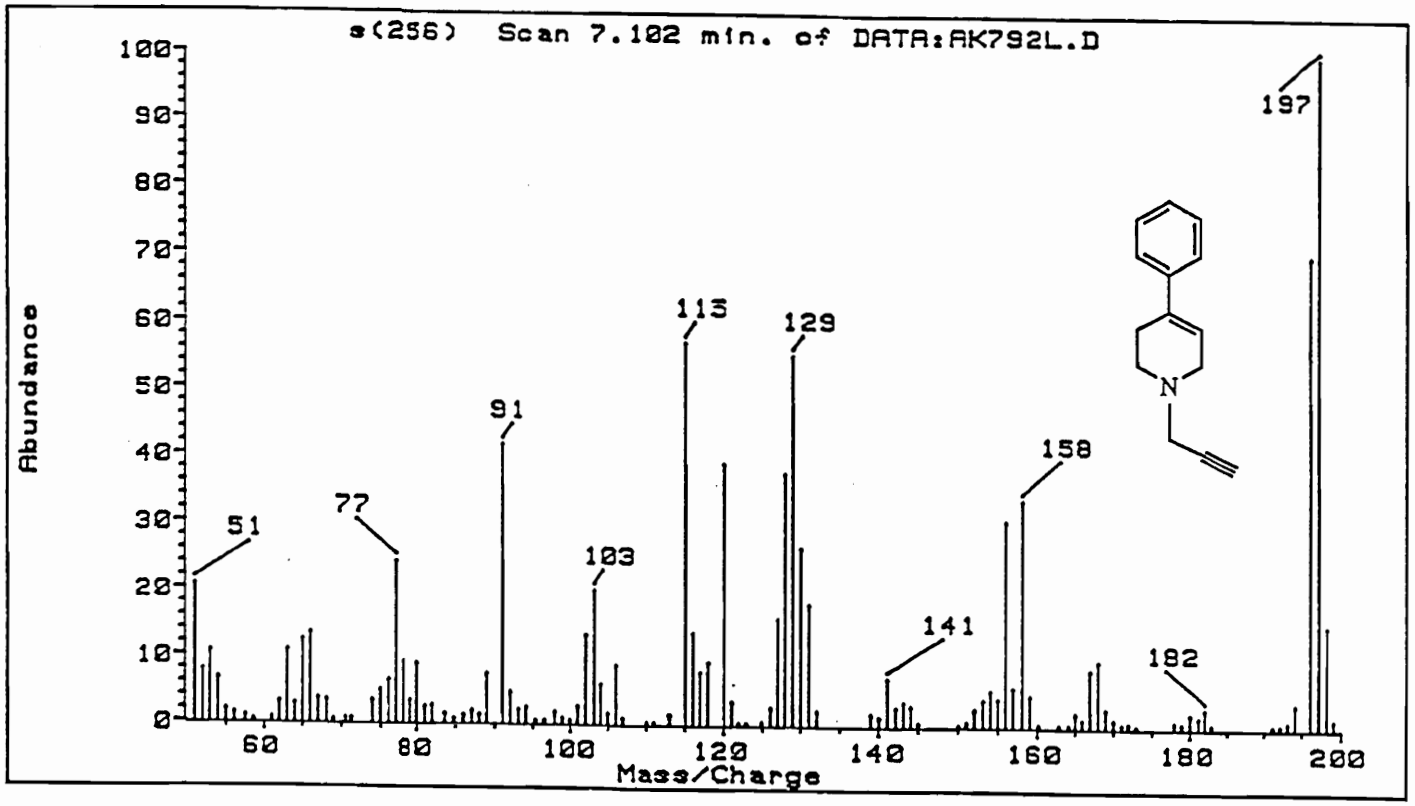

Figure. 2. GC/EIMS of 4-Phenyl-1-propargyl-1,2,3,6-tetrahydropyridine.

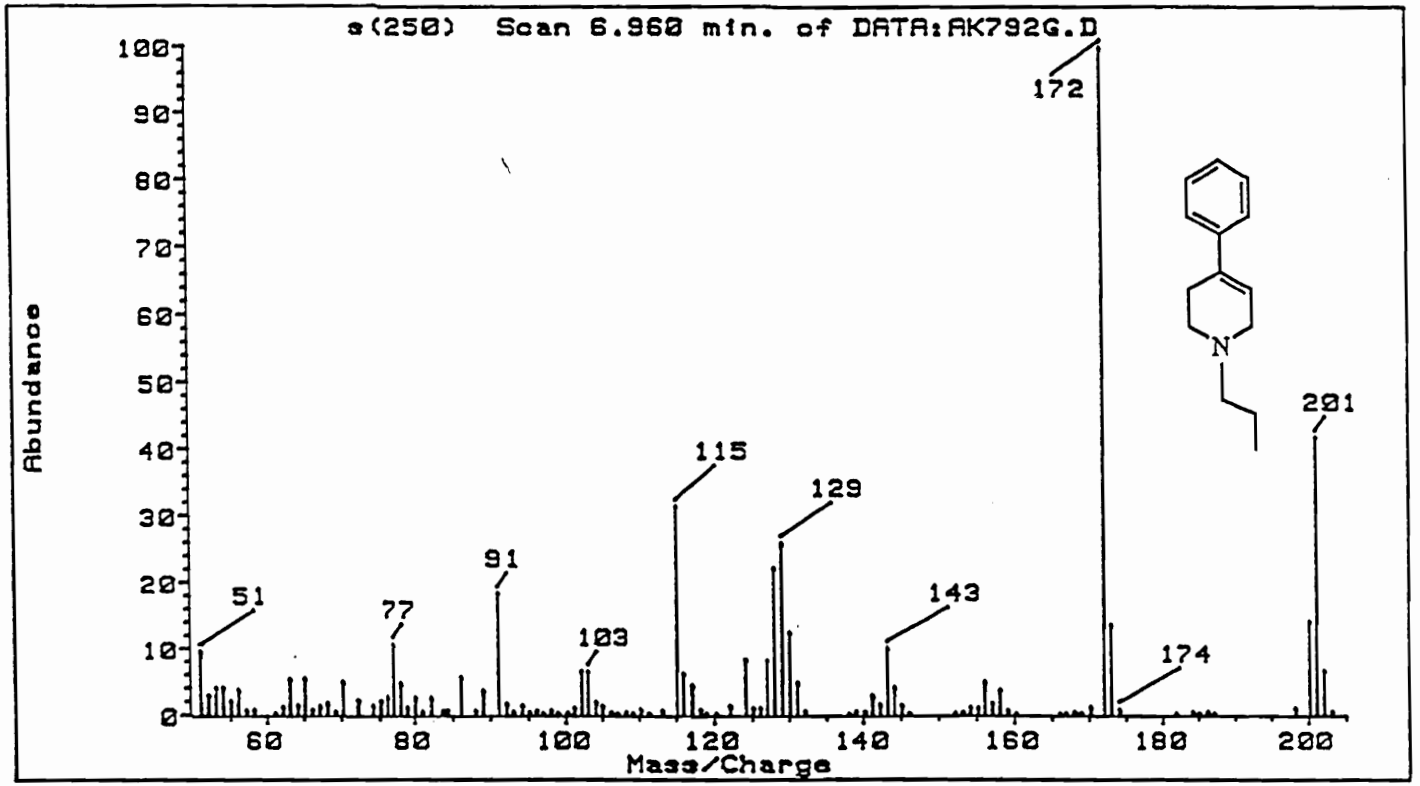

Figure. 3. GC/EIMS of 4-Phenyl-1-propyl-1,2,3,6-tetrahydropyridine.

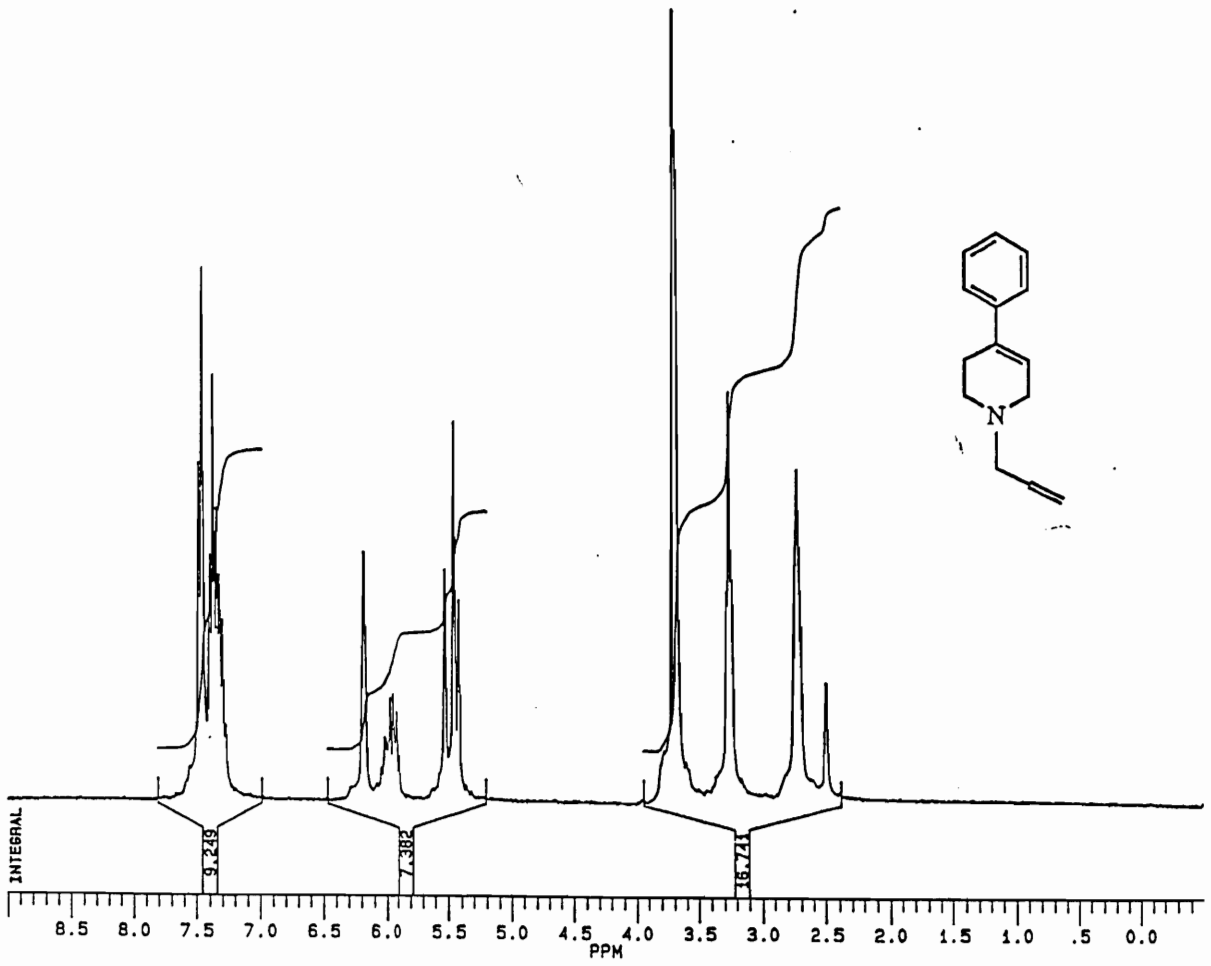

Figure. 4. ^{1}H NMR Spectrum (DMSO-d_6) of 1-Allyl-4-phenyl-1,2,3,6-tetrahydropyridine.

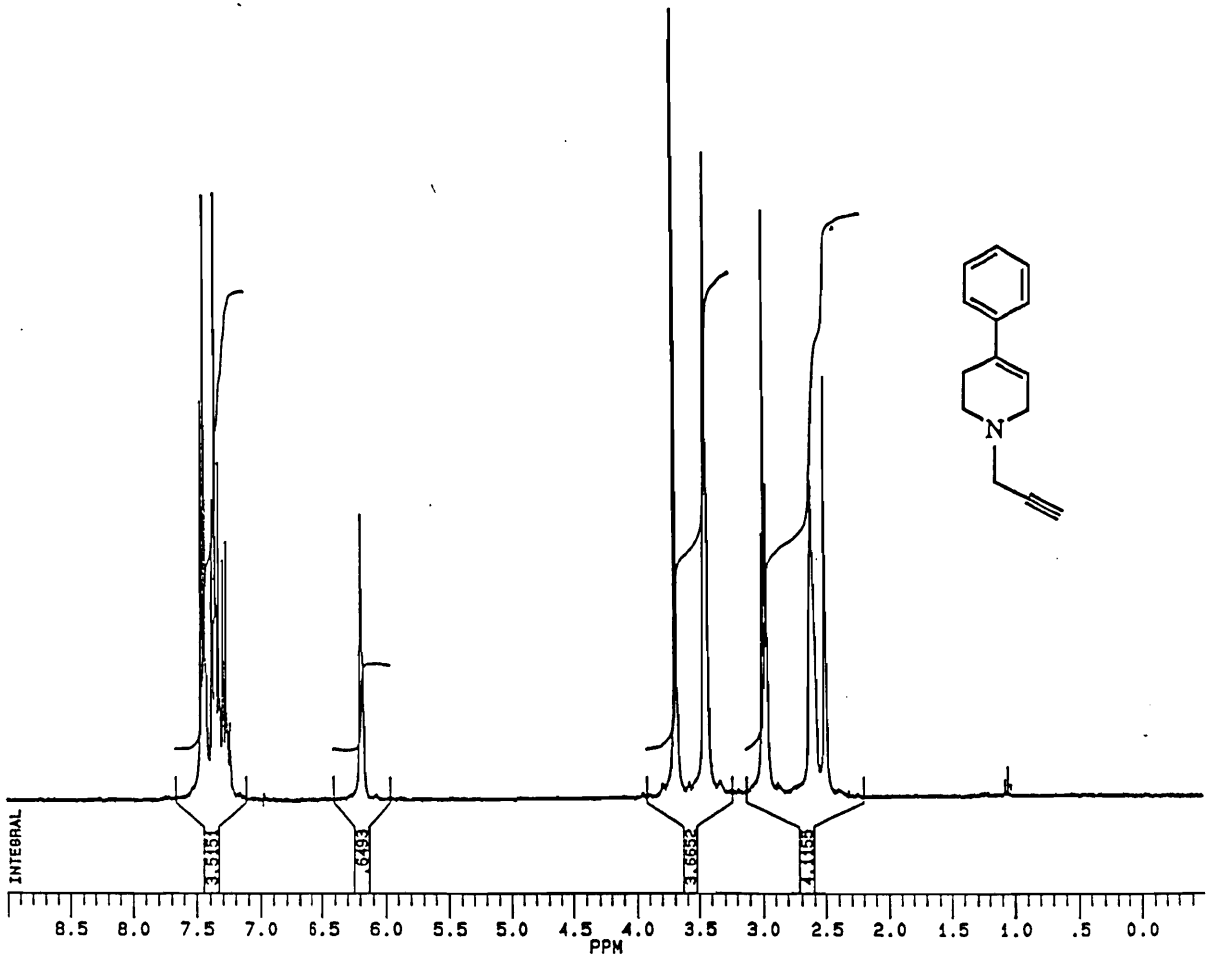

Figure. 5. ^{1}H NMR Spectrum (DMSO-d_6) of 4-Phenyl-1-propargyl-1,2,3,6-tetrahydropyridine.

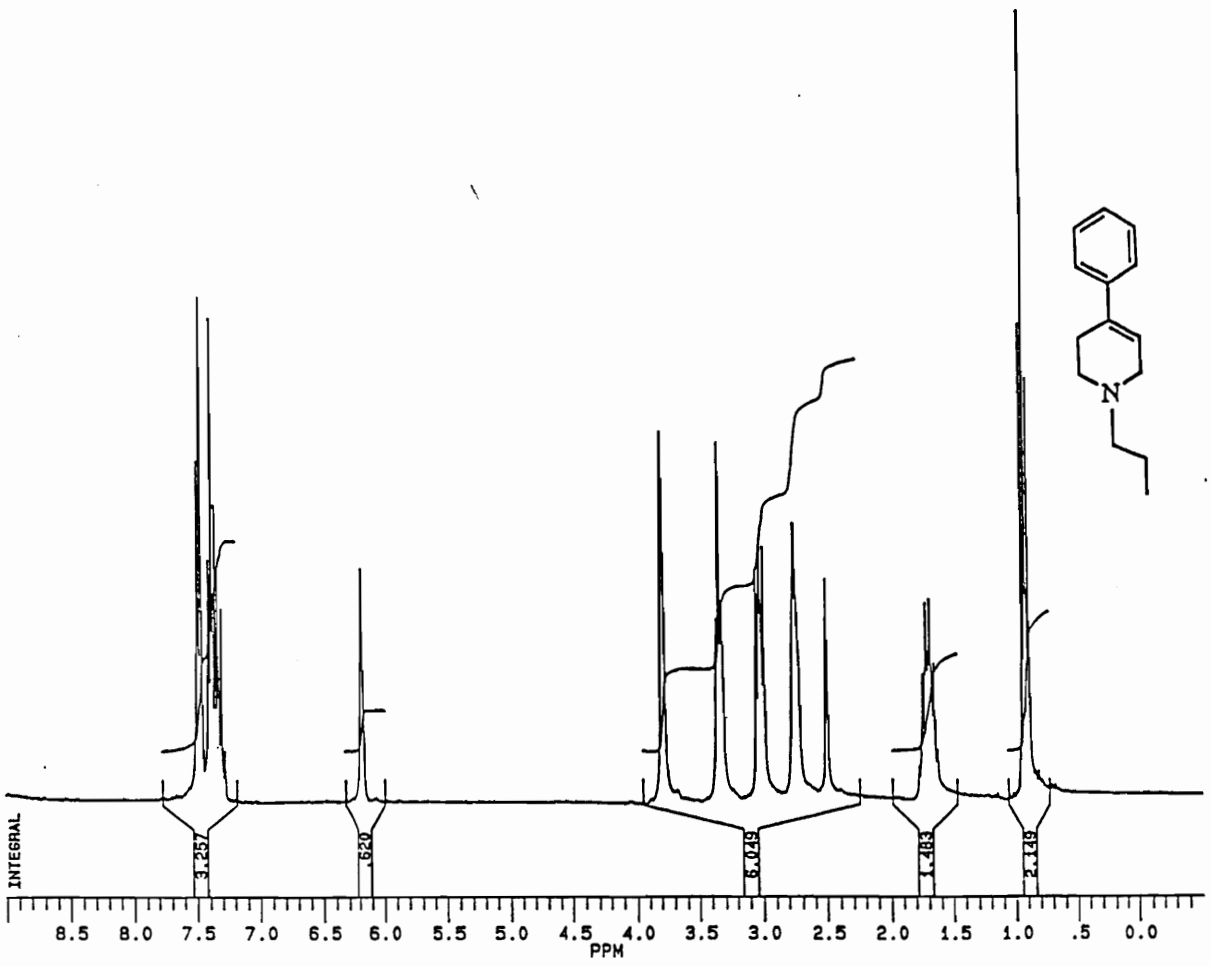

Figure. 6. ^{1}H NMR Spectrum (DMSO-d_6) of 4-Phenyl-1-propyl-1,2,3,6-tetrahydropyridine.

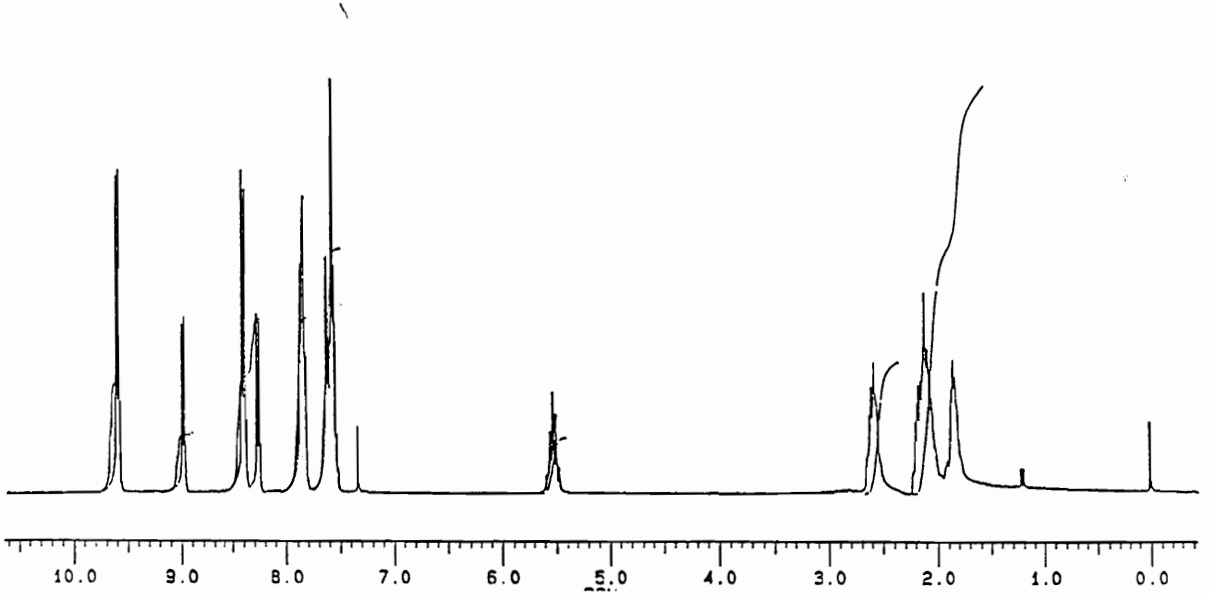

Figure. 7. ^{1}H NMR Spectrum ($CDCl_3$) of the "Ternary Complex".

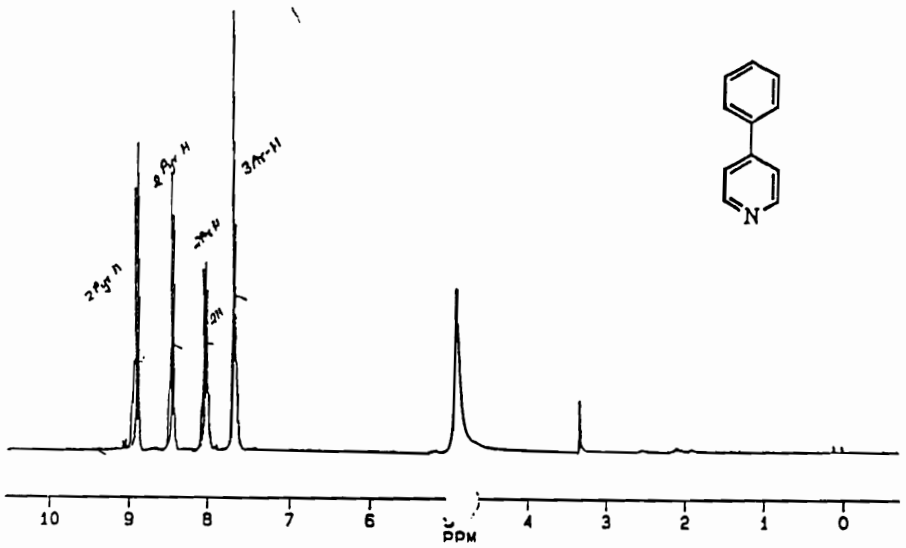

Figure. 8. ^{1}H NMR Spectrum ($CDCl_3$) of 4-Phenylpyridine.

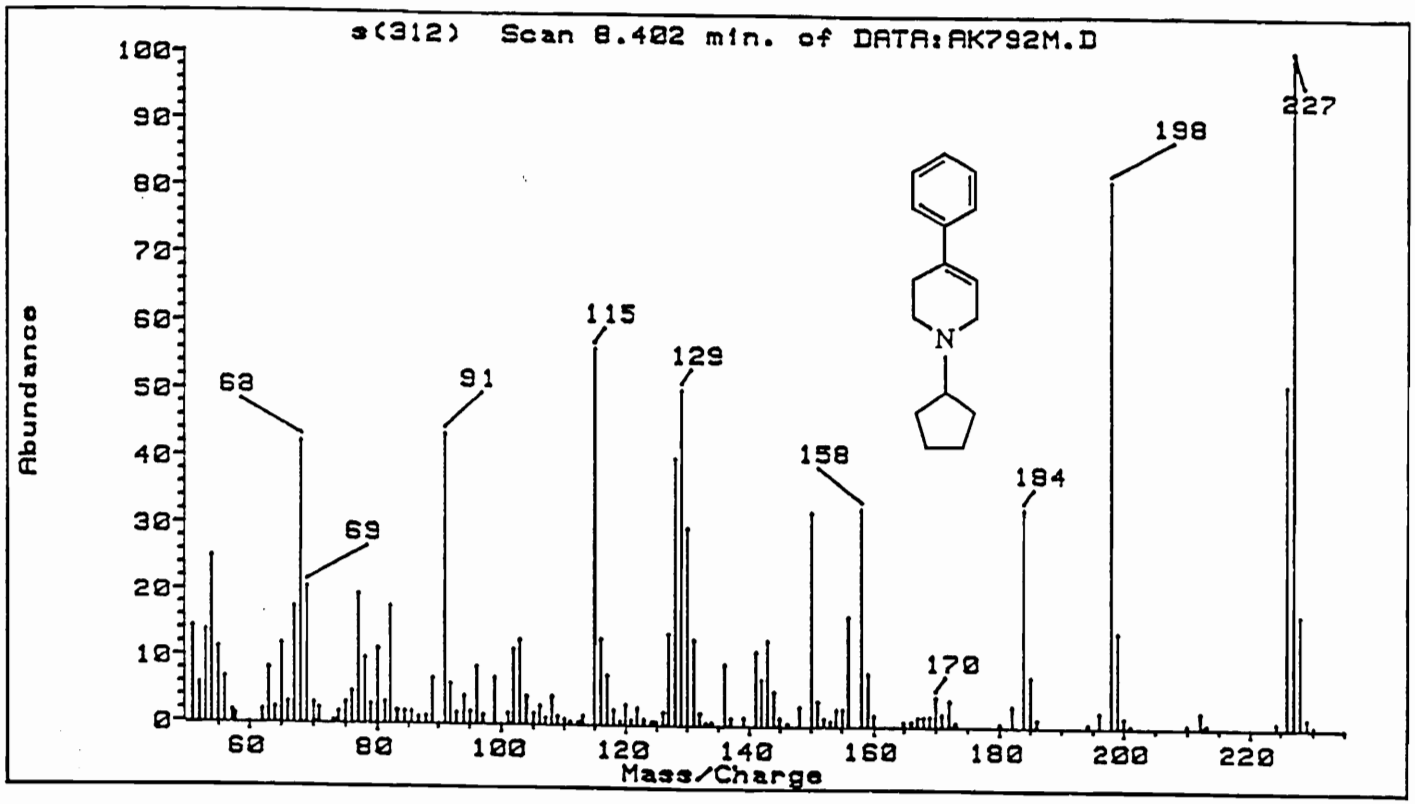

Figure. 9. GC/EIMS of 1-Cyclopentyl-4-phenyl-1,2,3,6-tetrahydropyridine.

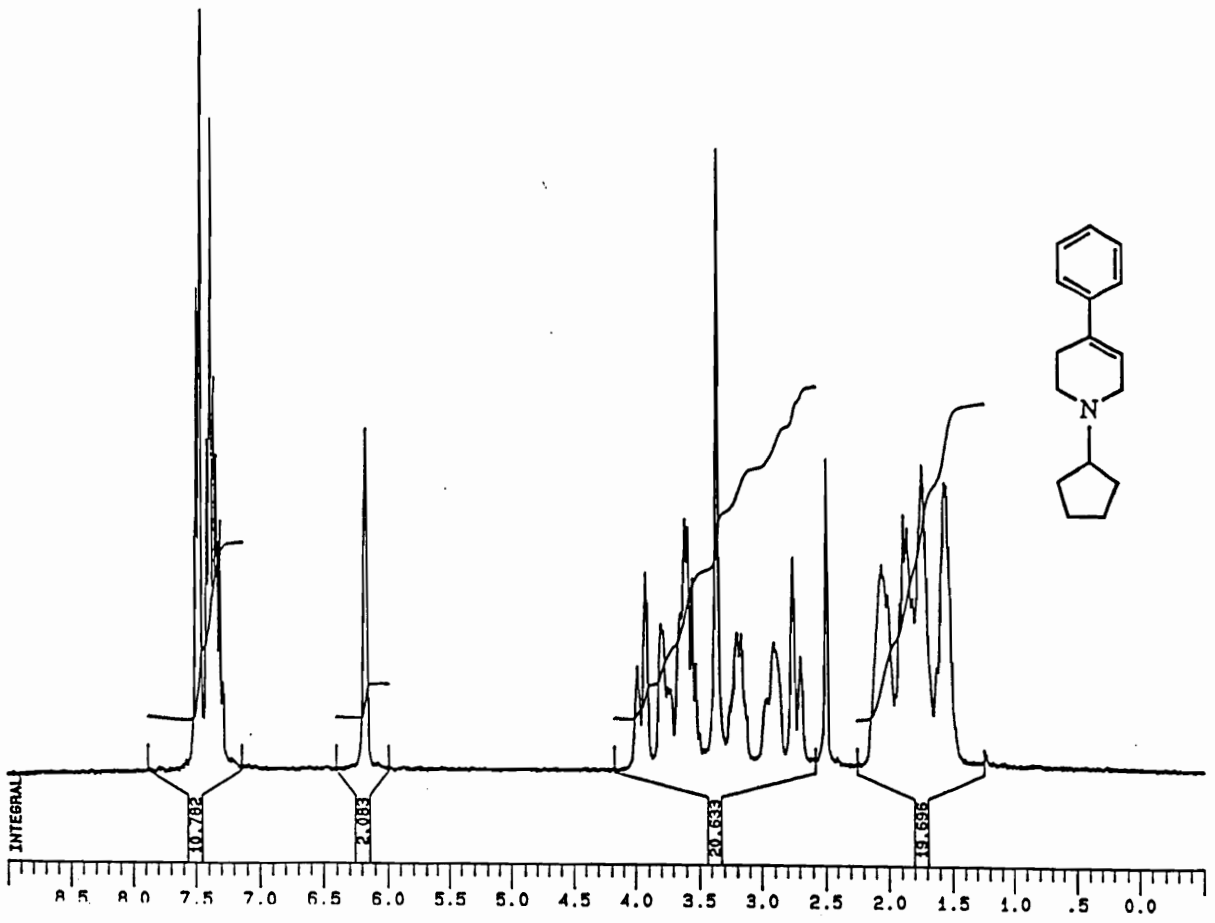

Figure. 10. ^{1}H NMR Spectrum ($CDCl_3$) of 1-Cyclopentyl-4-phenyl-1,2,3,6-tetrahydropyridine.

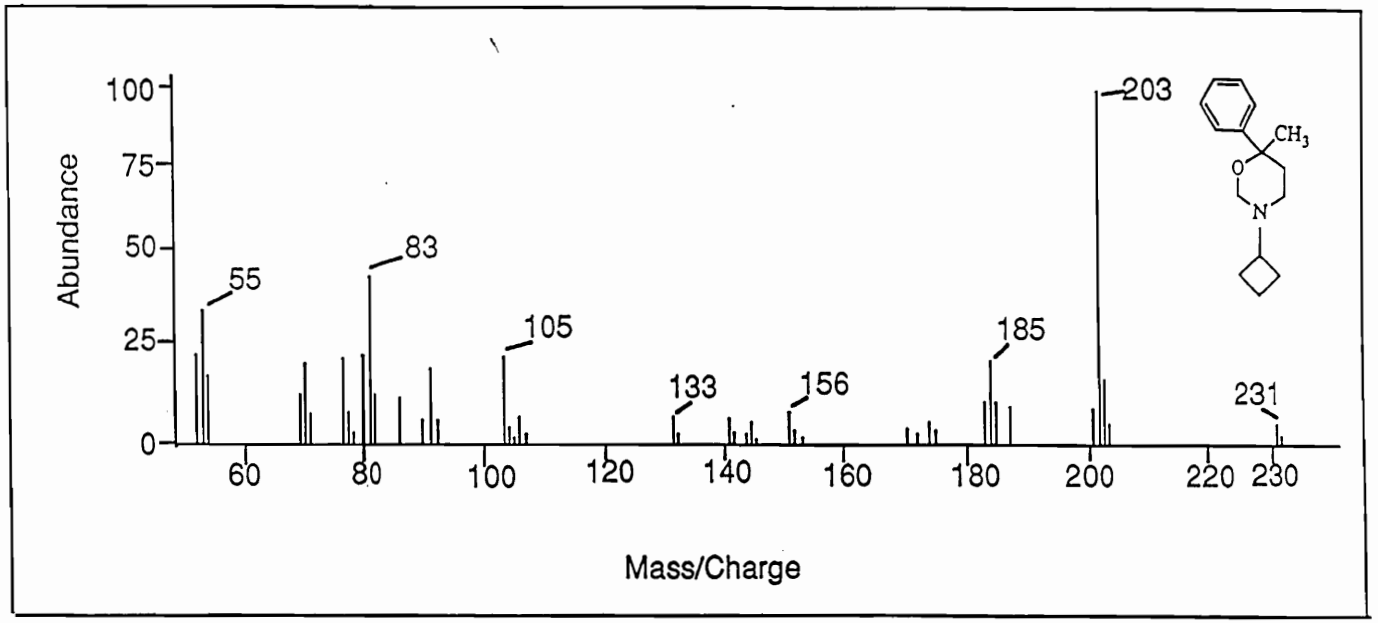

Figure. 11. GC/EIMS of 1-Cyclobutyl-4-methyl-4-phenyl-1,3-oxazine.

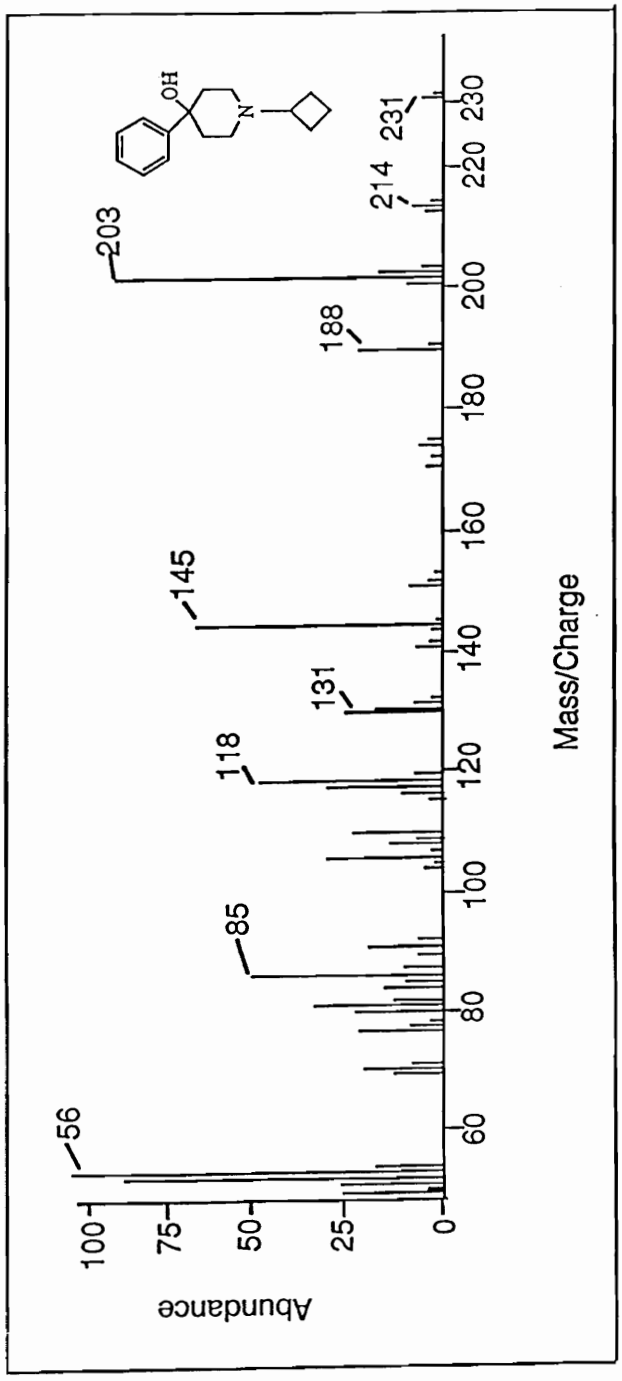

Figure. 12. GC/EIMS of 1-Cyclobutyl-4-phenylpiperidin-4-ol.

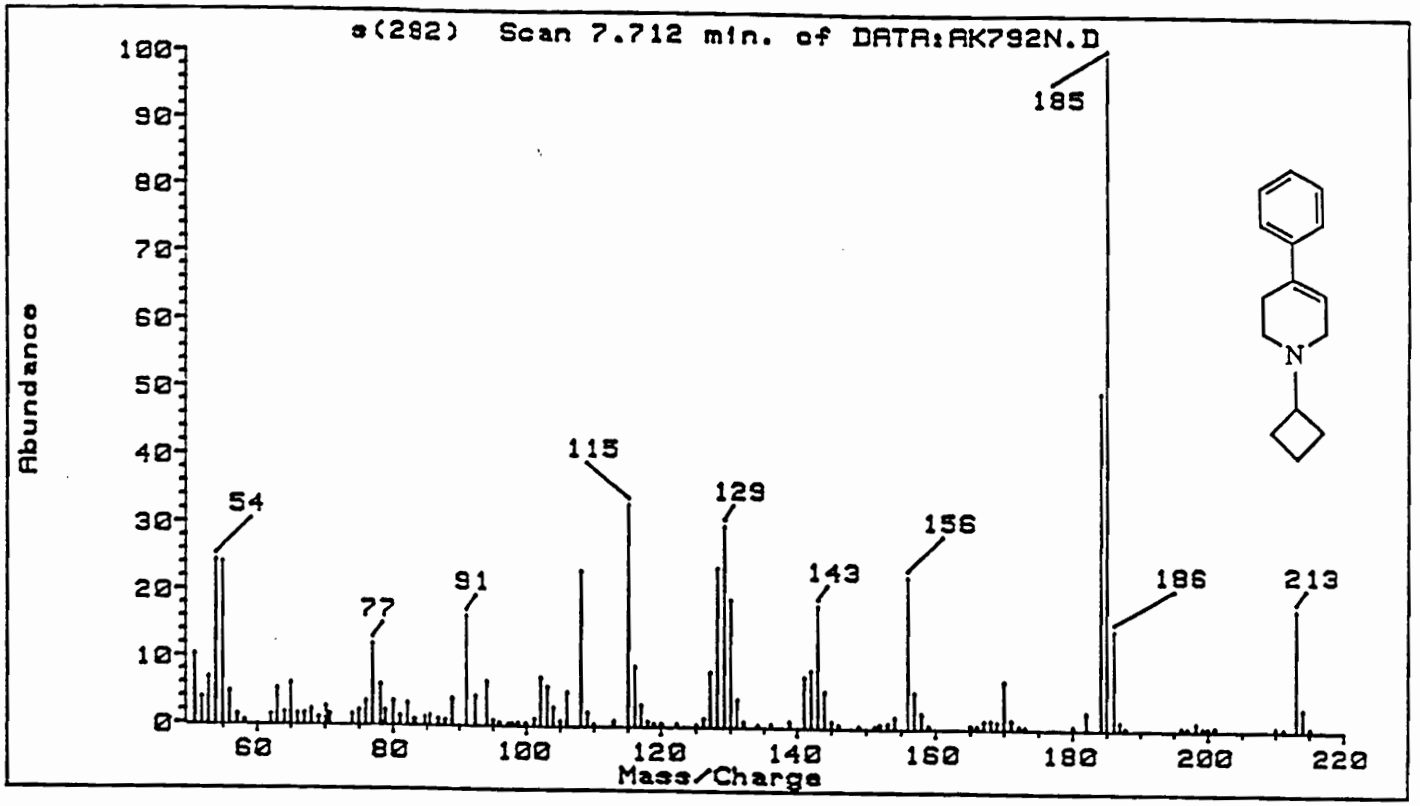

Figure. 13. GC/EIMS of 1-Cyclobutyl-4-phenyl-1,2,3,6-tetrahydropyridine.

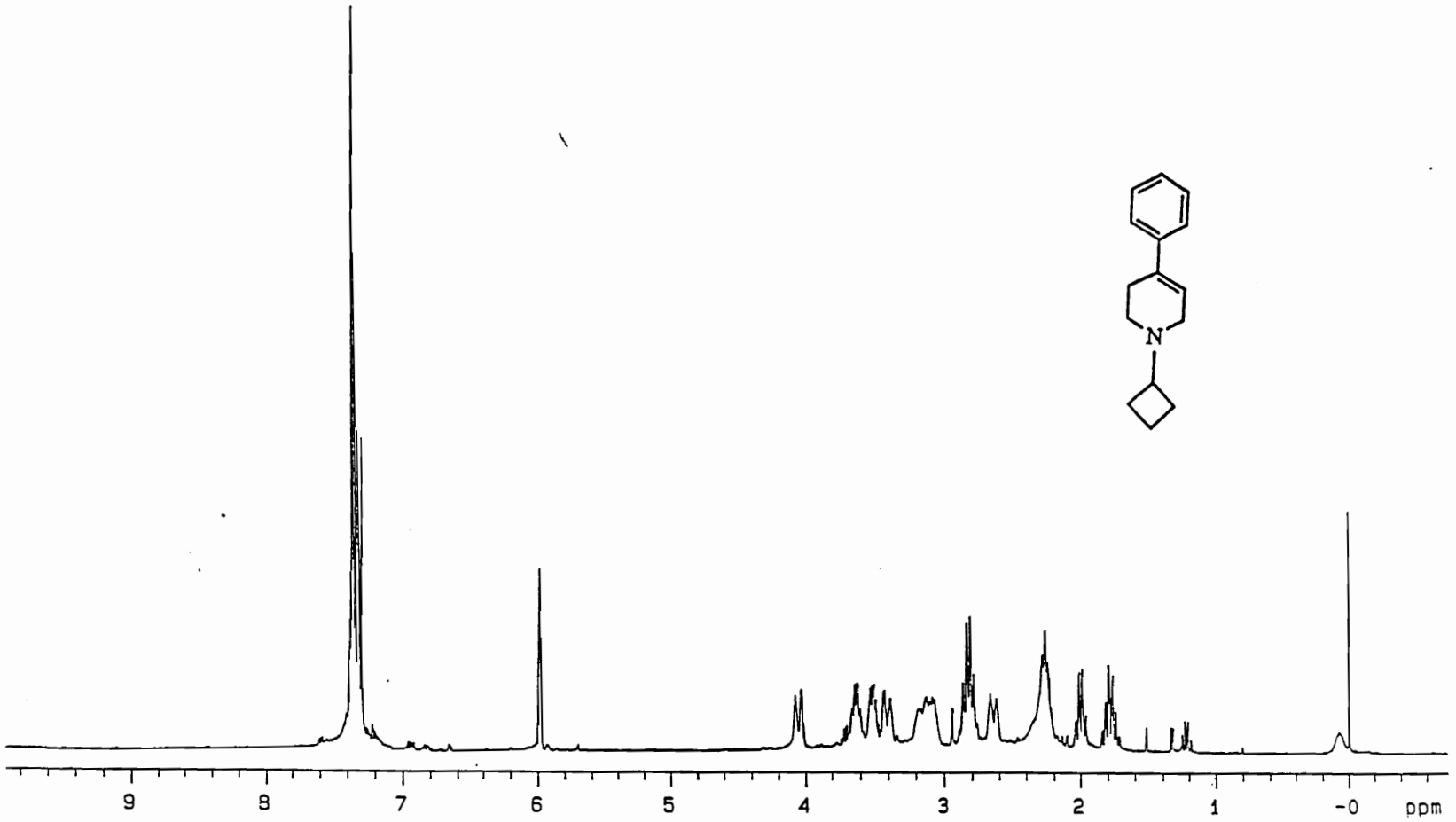

Figure. 14. ^{1}H NMR Spectrum ($CDCl_3$) of 1-Cyclobutyl-4-phenyl-1,2,3,6-tetrahydropyridine.

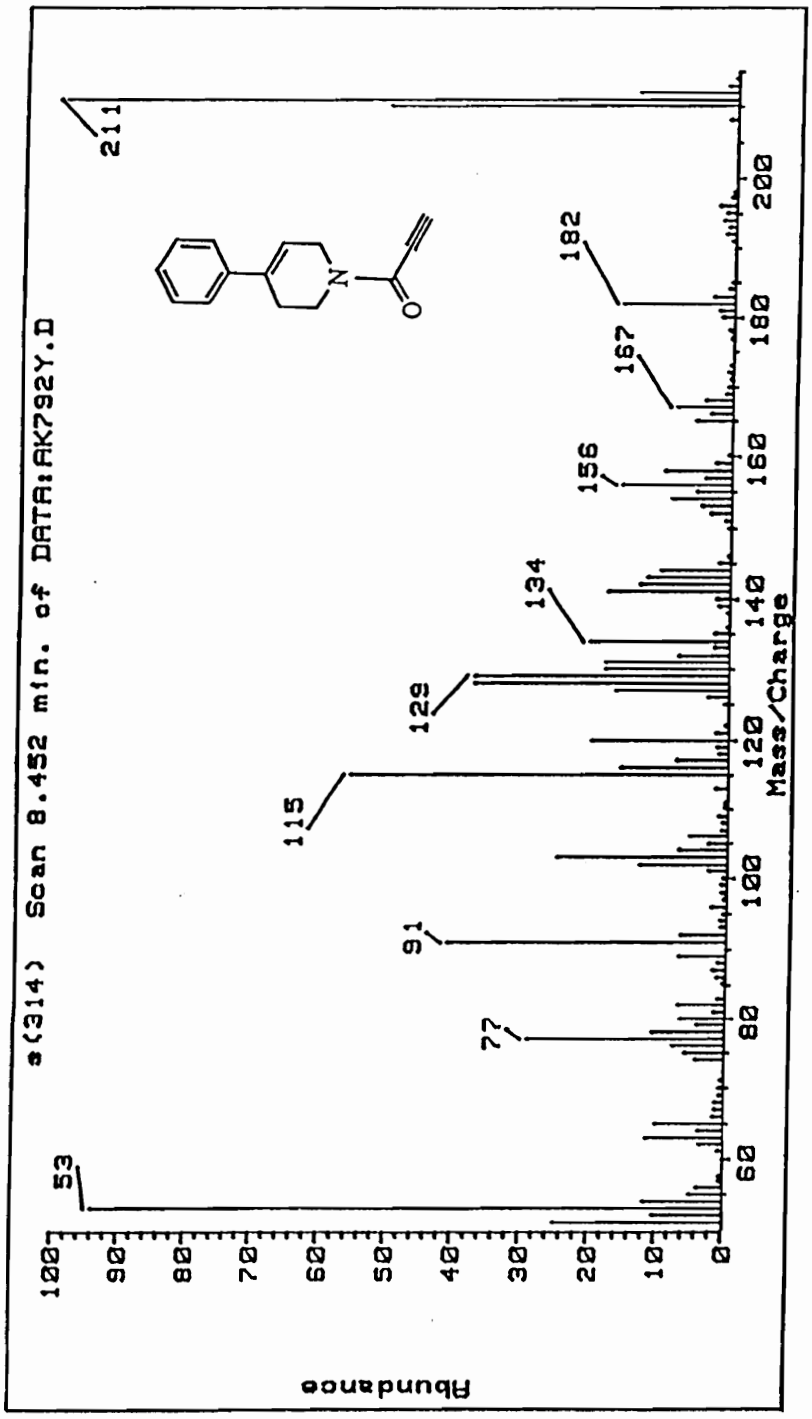

Figure. 15. GC/EIMS of 191.

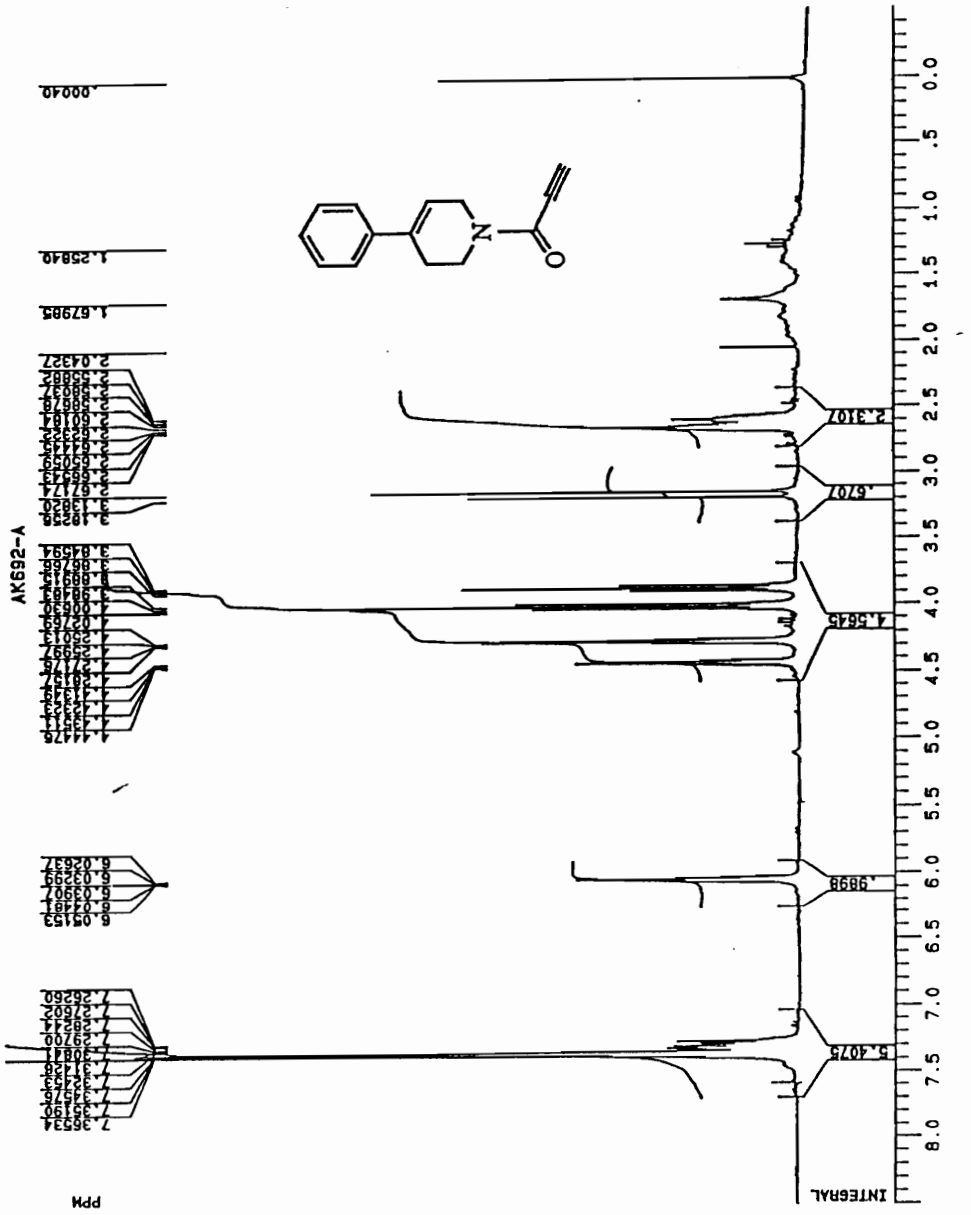

Figure. 16. ^{1}H NMR Spectrum ($CDCl_3$) of Amide 191.

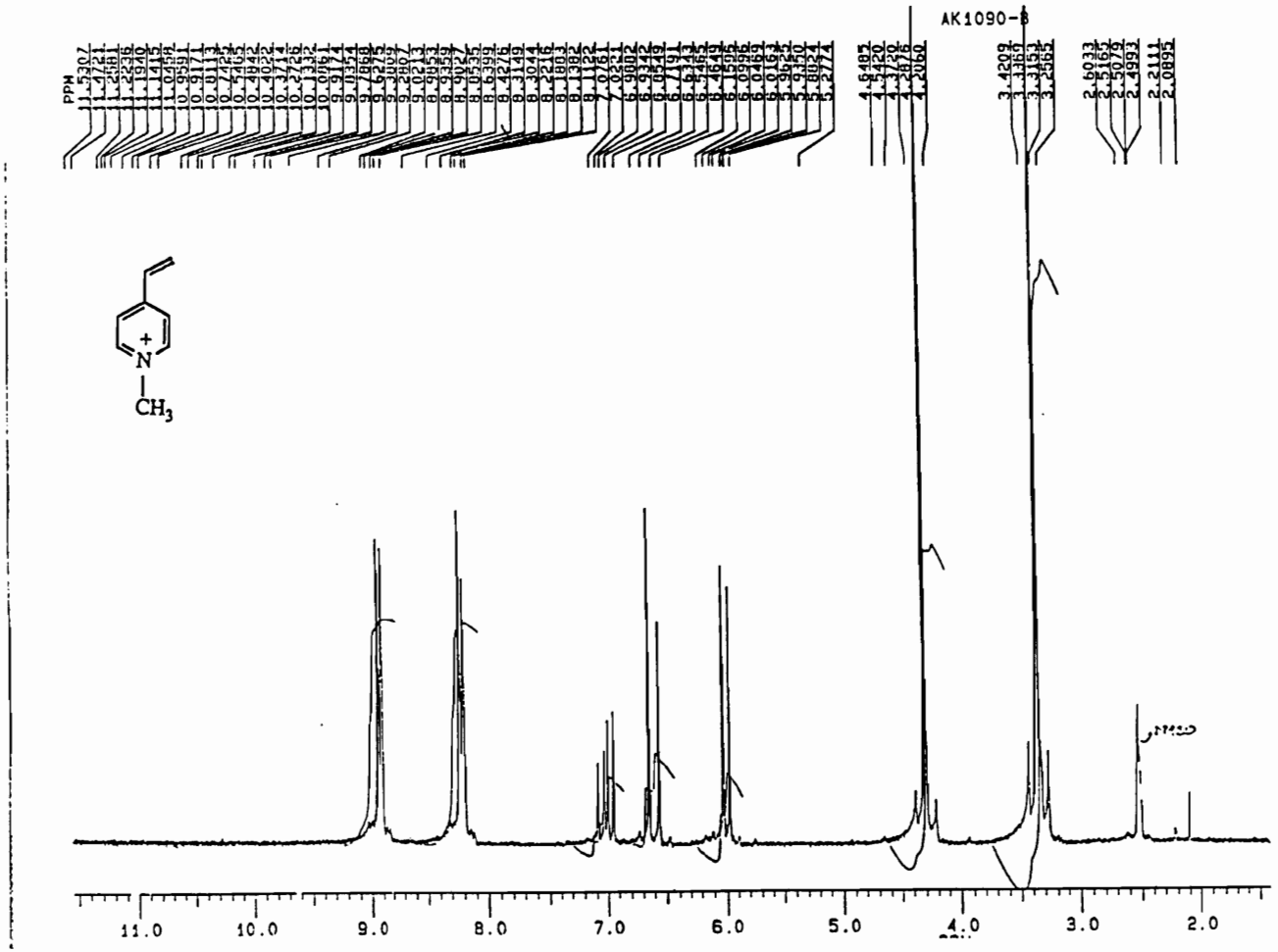

Figure. 17. ^{1}H NMR Spectrum (DMSO-d_6) of 4-Ethenyl-1-methylpyridinium Iodide.

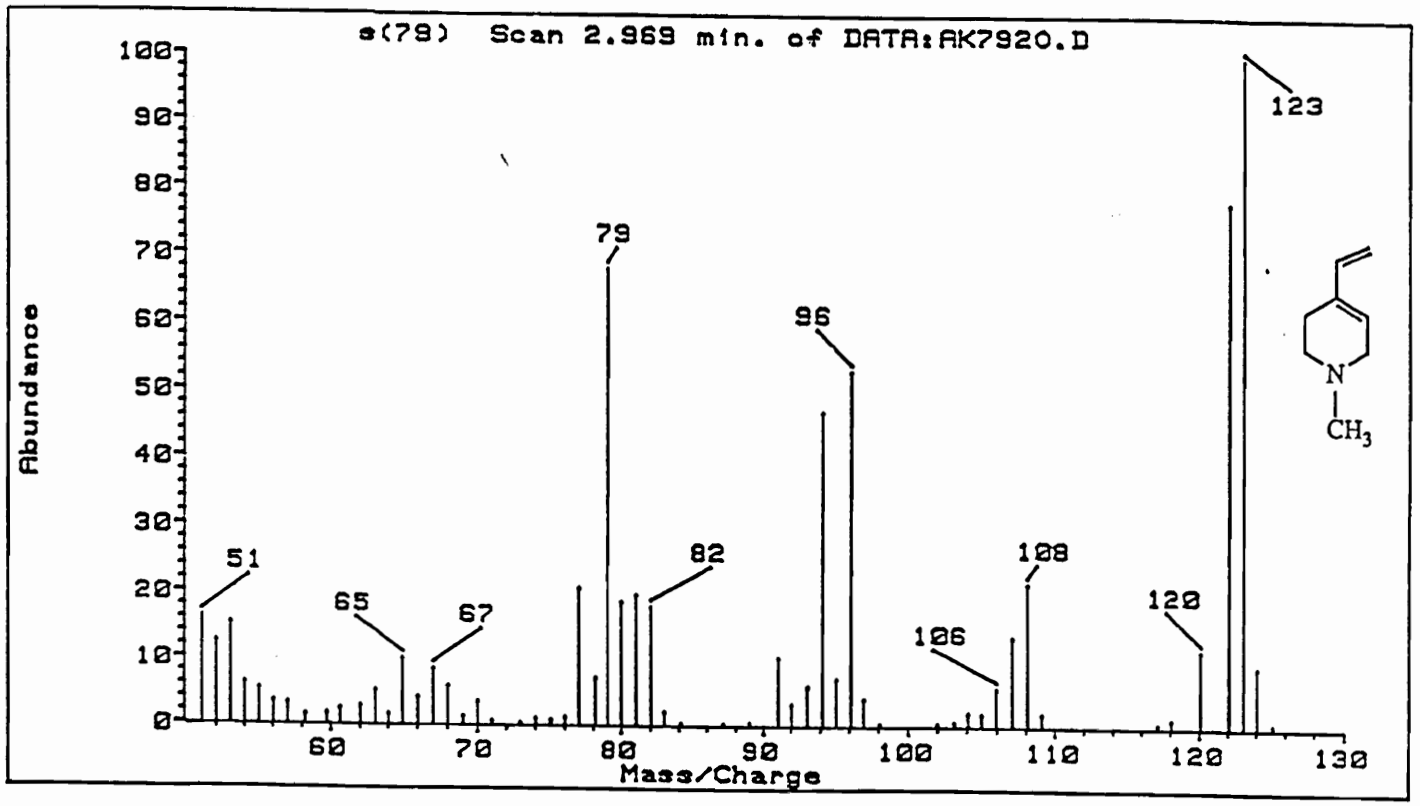

Figure. 18. GC/EIMS of 4-Ethenyl-1-methyl-1,2,3,6-tetrahydropyridine.

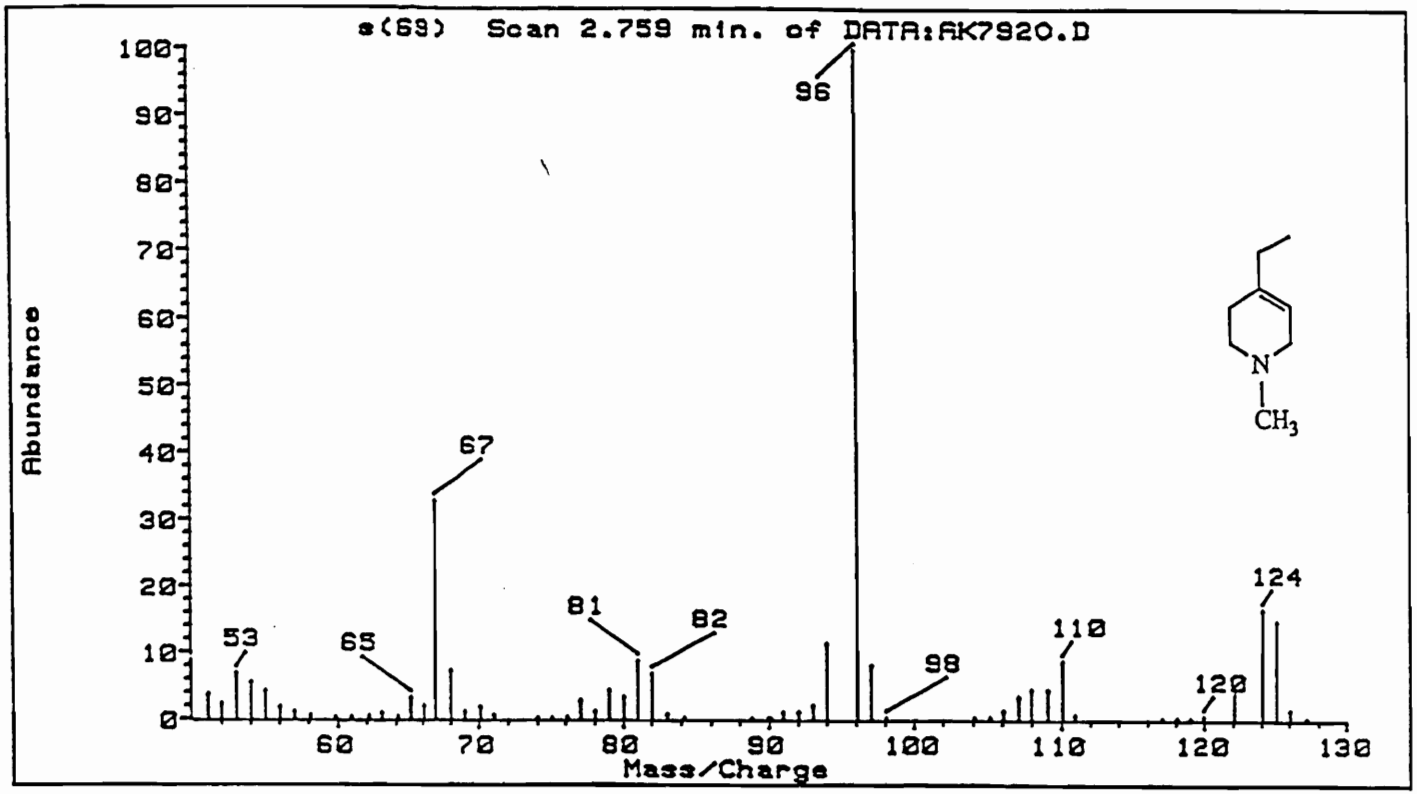

Figure. 19. GC/EIMS of 4-Ethyl-1-methyl-1,2,3,6-tetrahydropyridine.

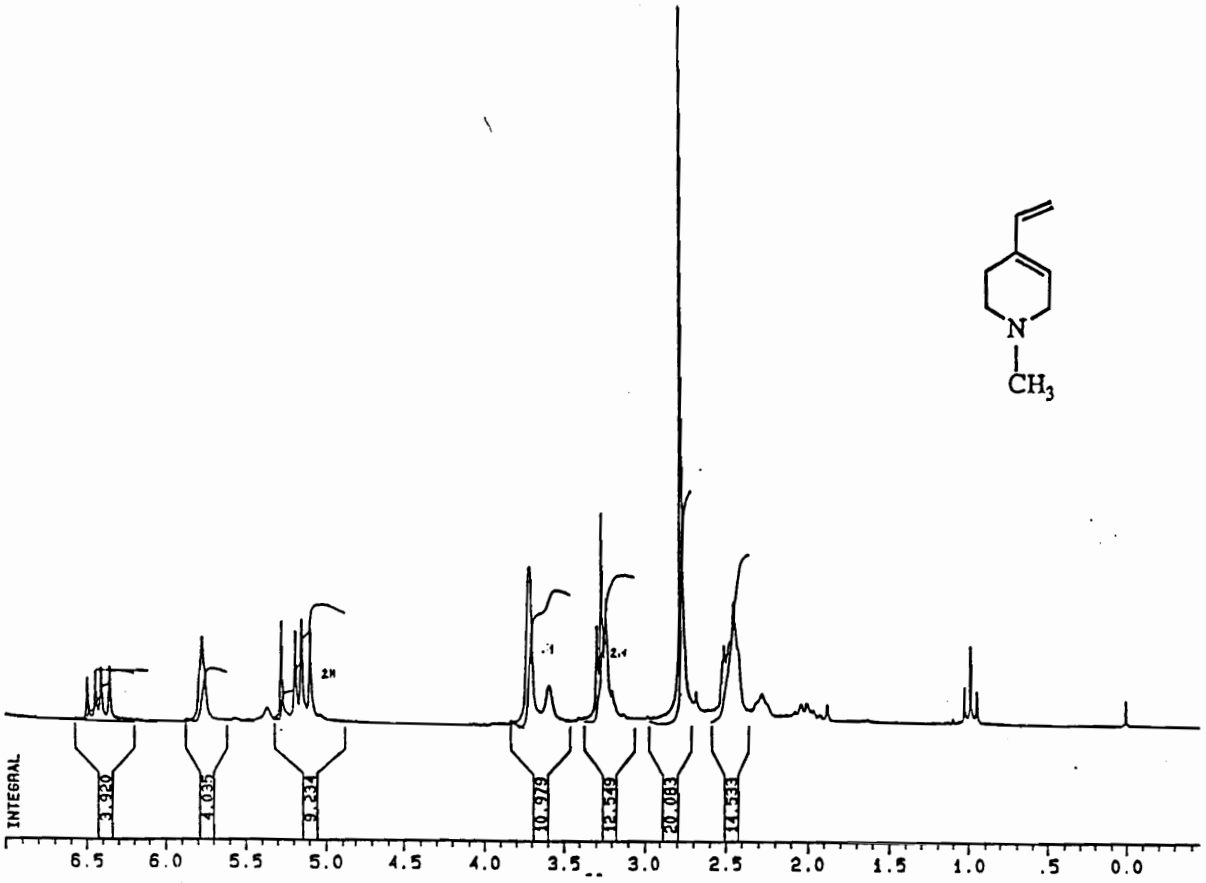

Figure. 20. ^{1}H NMR Spectrum (DMSO-d_6) of 4-Ethenyl-1-methyl-1,2,3,6-tetrahydropyridine.

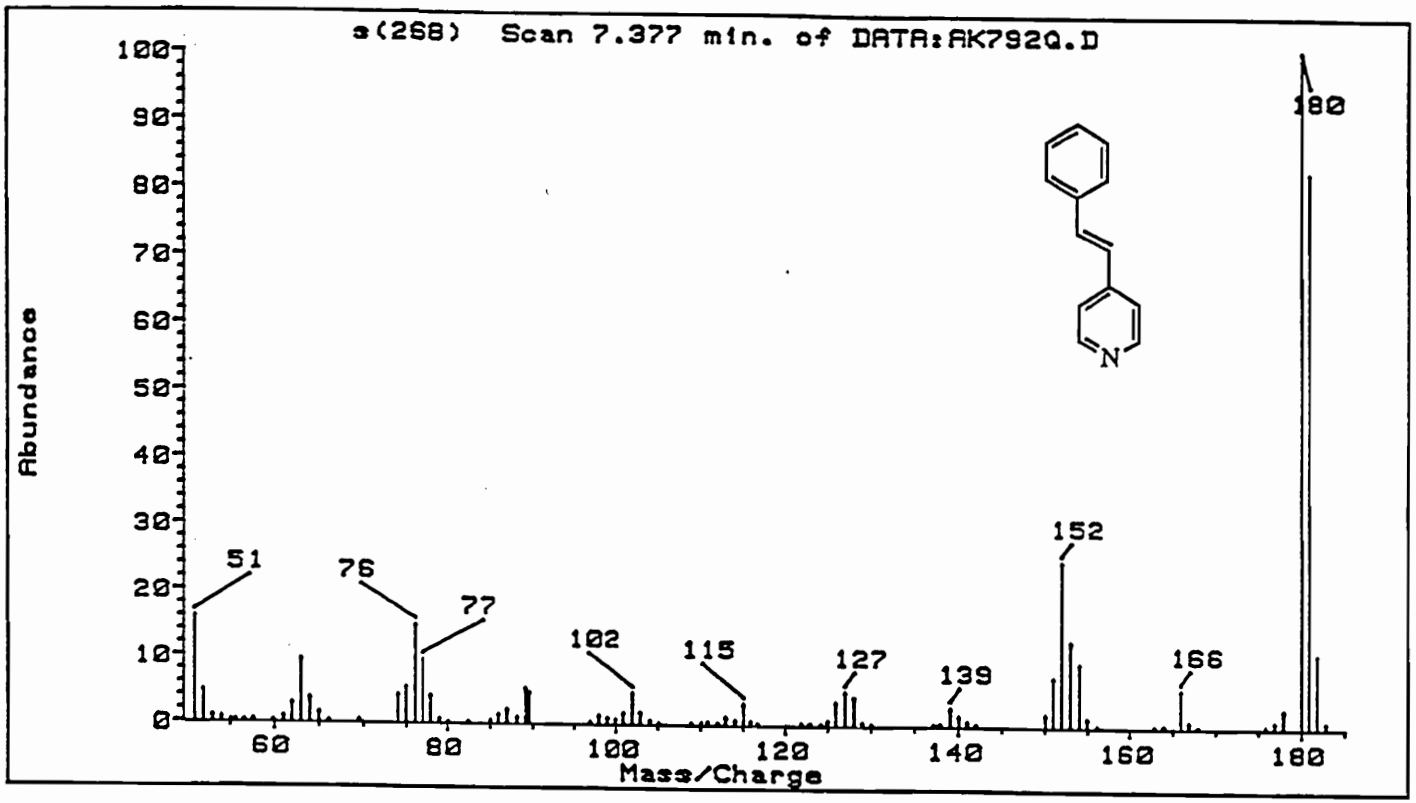

Figure. 21. GC/EIMS of (E)-4-(2-Phenylethenyl)pyridine.

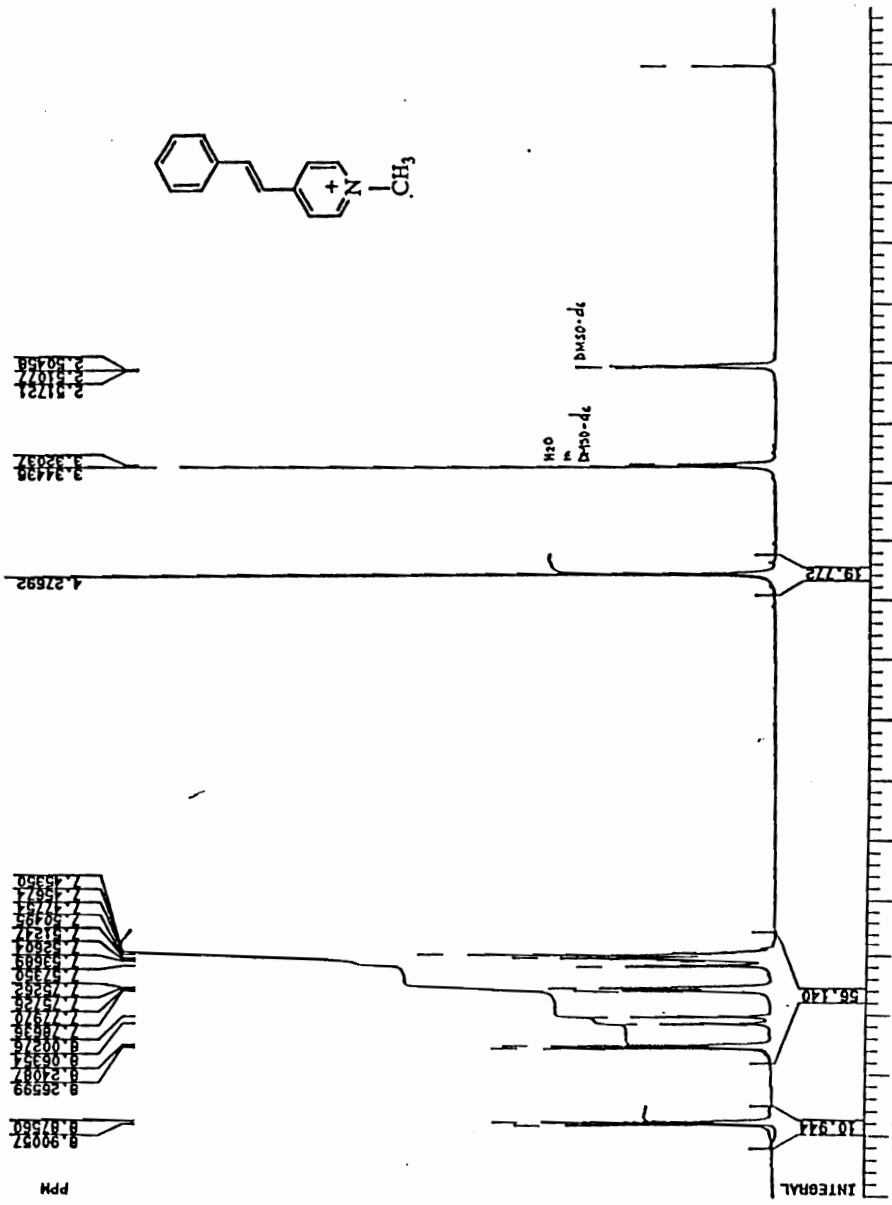

Figure. 22. ^{1}H NMR Spectrum (DMSO-d_6) of 1-Methyl-4-(E)-(2-phenylethenyl)pyridinium Iodide.

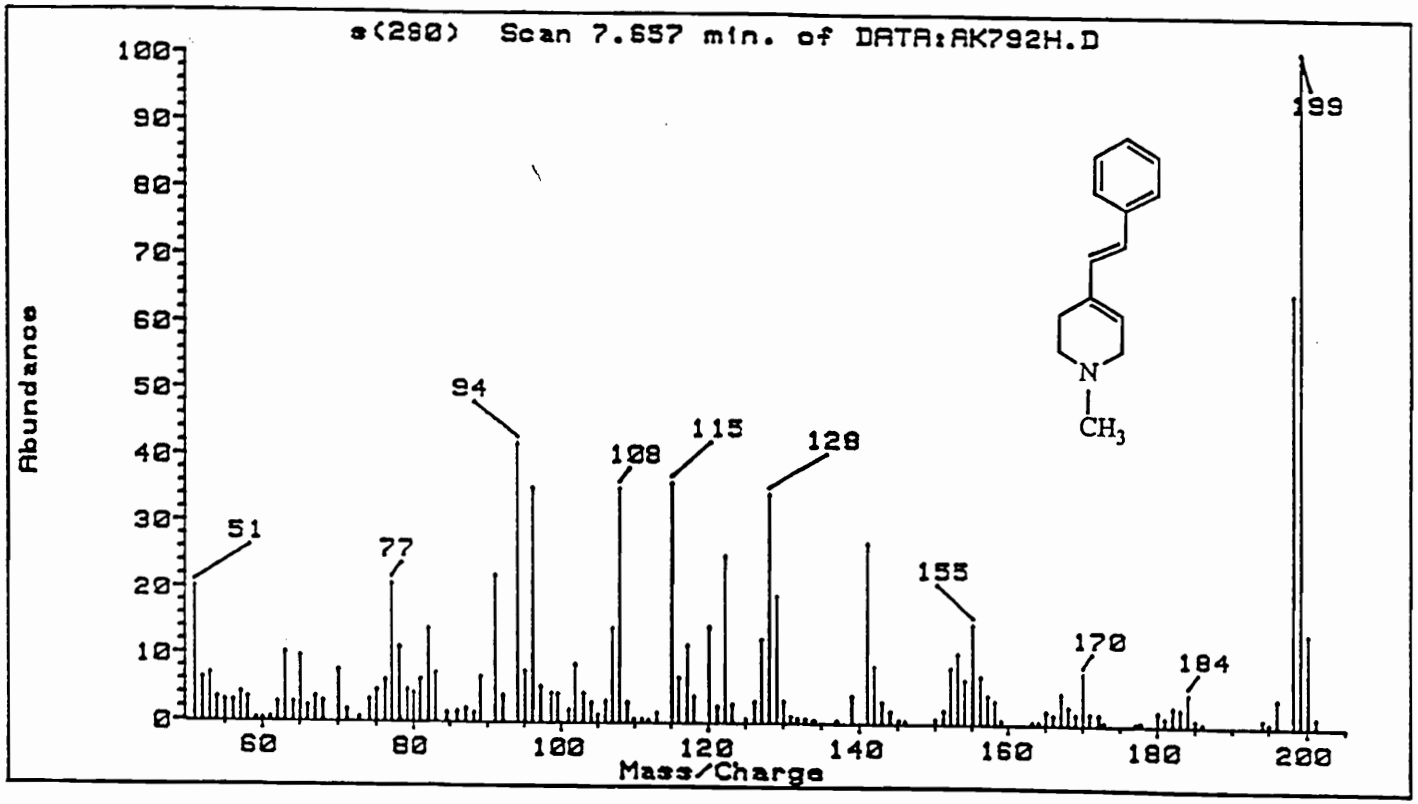

Figure. 23. GC/EIMS of 1-Methyl-4-(E)-(2-phenylethenyl)-1,2,3,6-tetrahydropyridine.

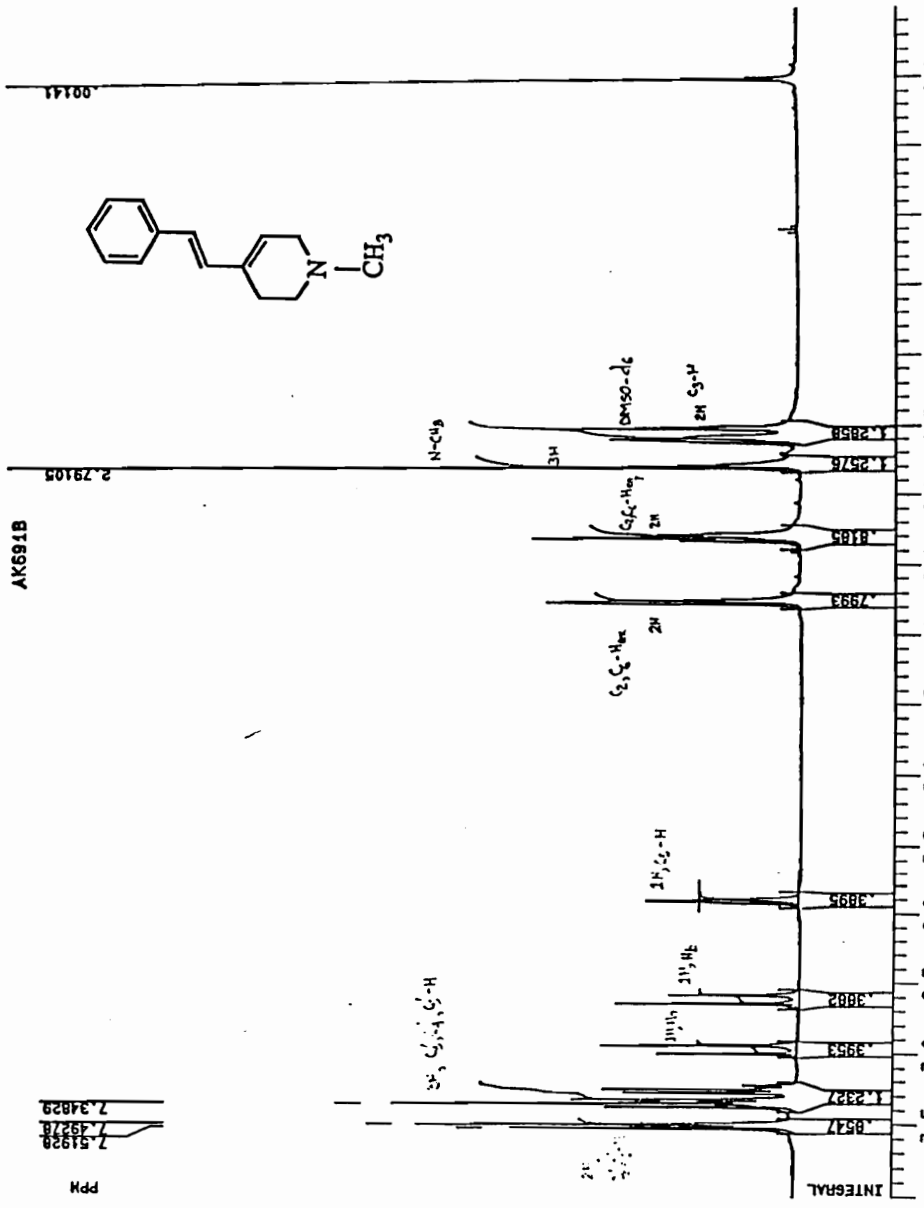

Figure. 24. 1H NMR Spectrum (DMSO-d_6) of 1-Methyl-4-(E)-(2-phenylethenyl)-1,2,3,6-tetrahydropyridine.

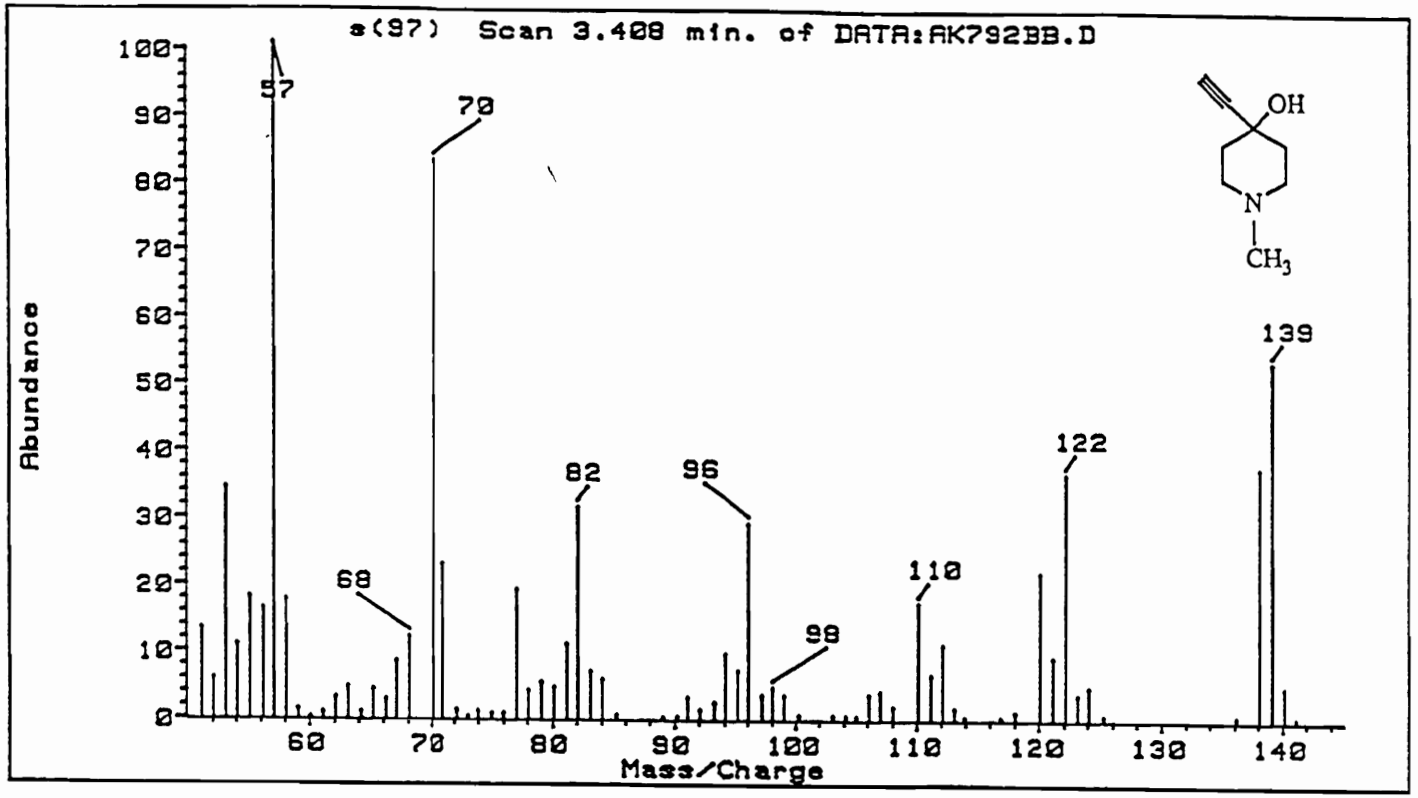

Figure. 25. GC/EIMS of 4-Ethynyl-1-methylpiperidin-4-ol.

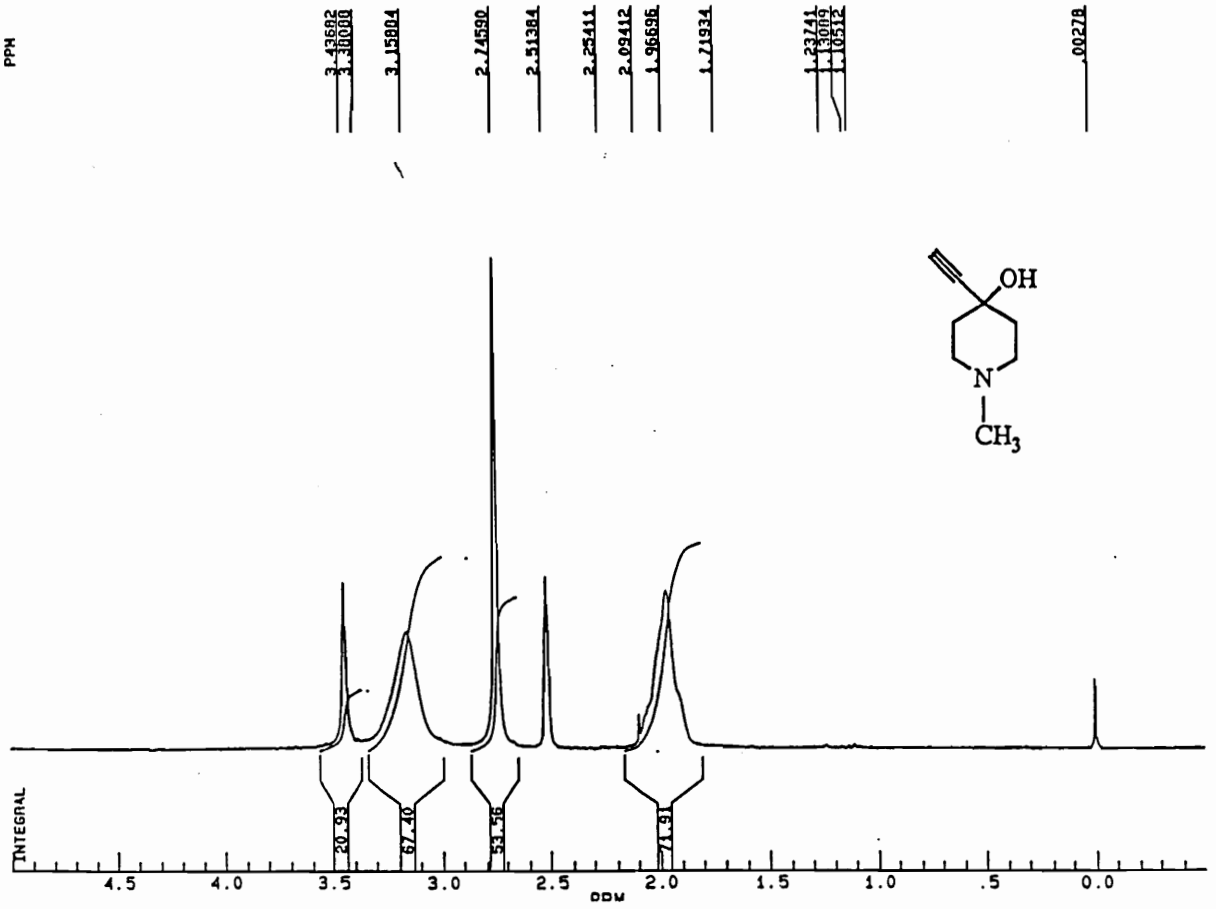

Figure. 26. ^{1}H NMR Spectrum (DMSO-d_6) of 4-Ethynyl-1-methylpiperidin-4-ol.

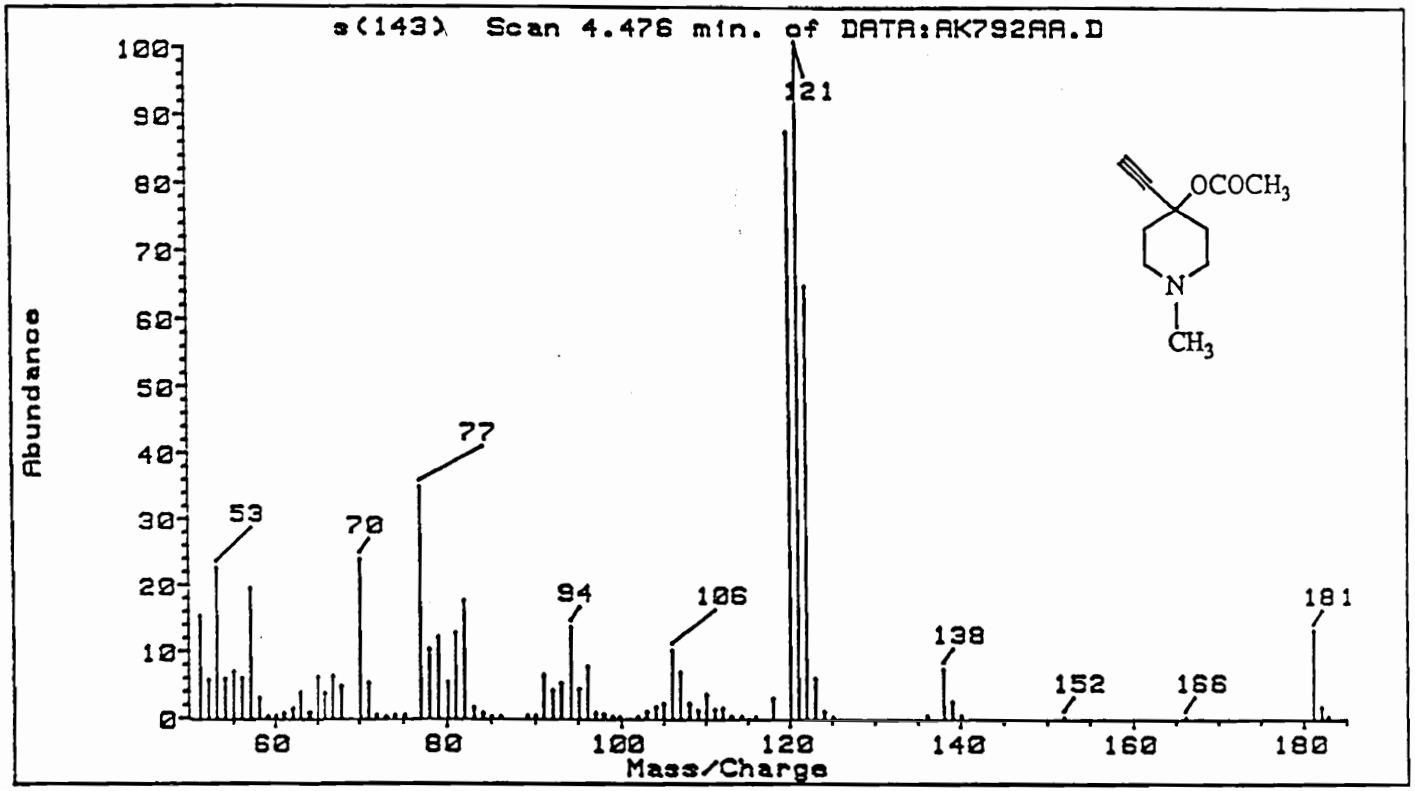

Figure. 27. GC/EIMS of 4-Acetoxy-4-ethynyl-1-methylpiperidine.

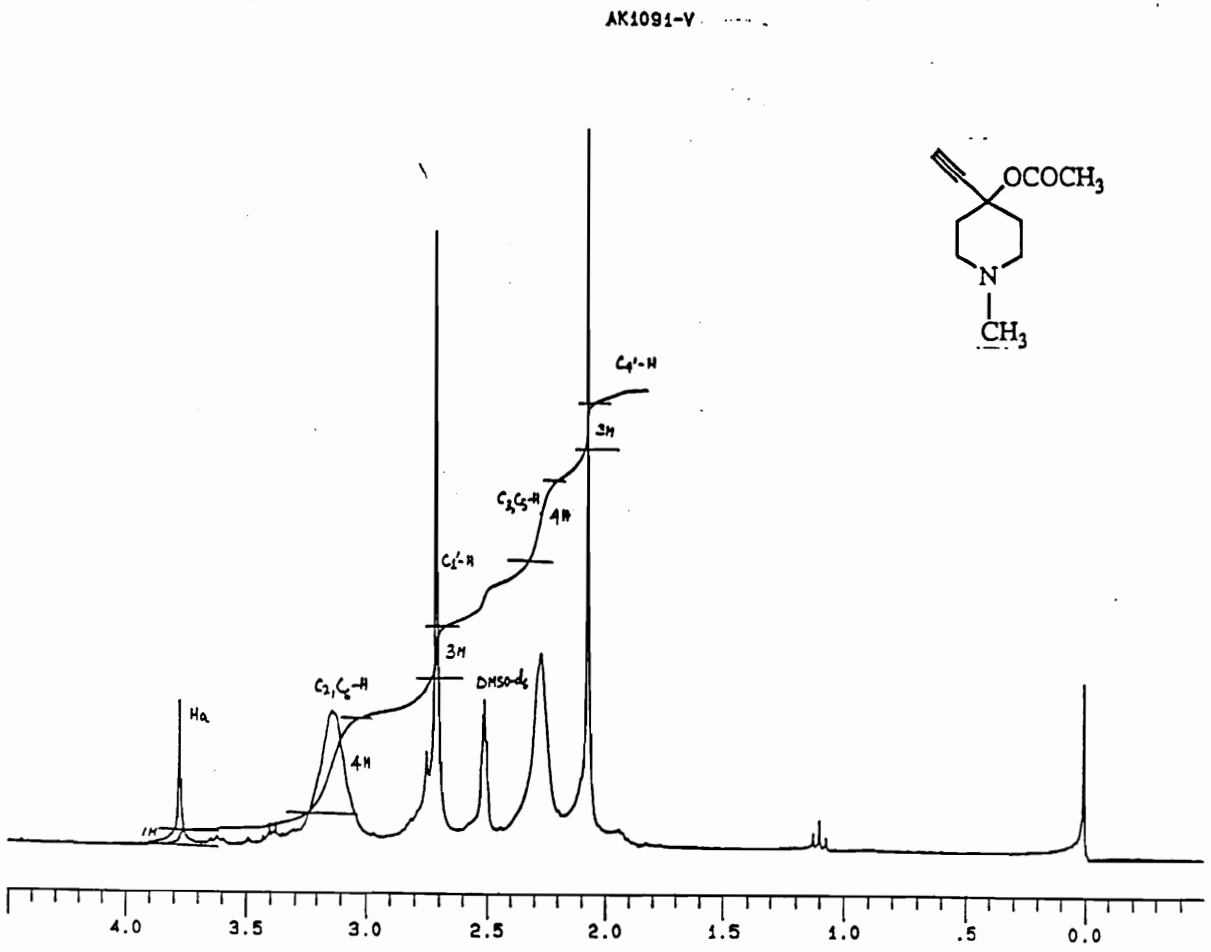

Figure. 28. ^{1}H NMR Spectrum (DMSO-d_6) of 4-Acetoxy-4-ethynyl-1-methylpiperidine.

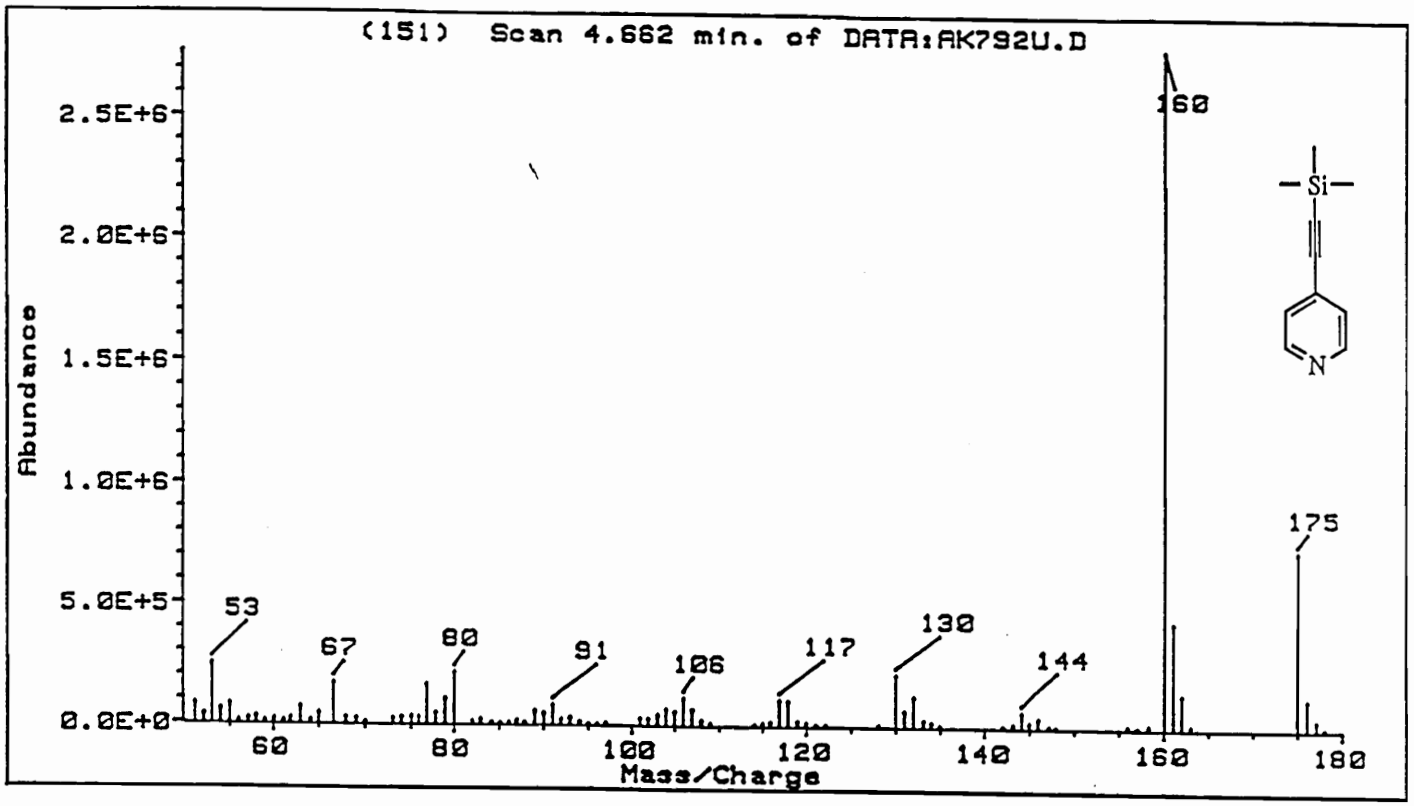

Figure. 29. GC/EIMS of 4-Trimethylsilylethynylpyridine.

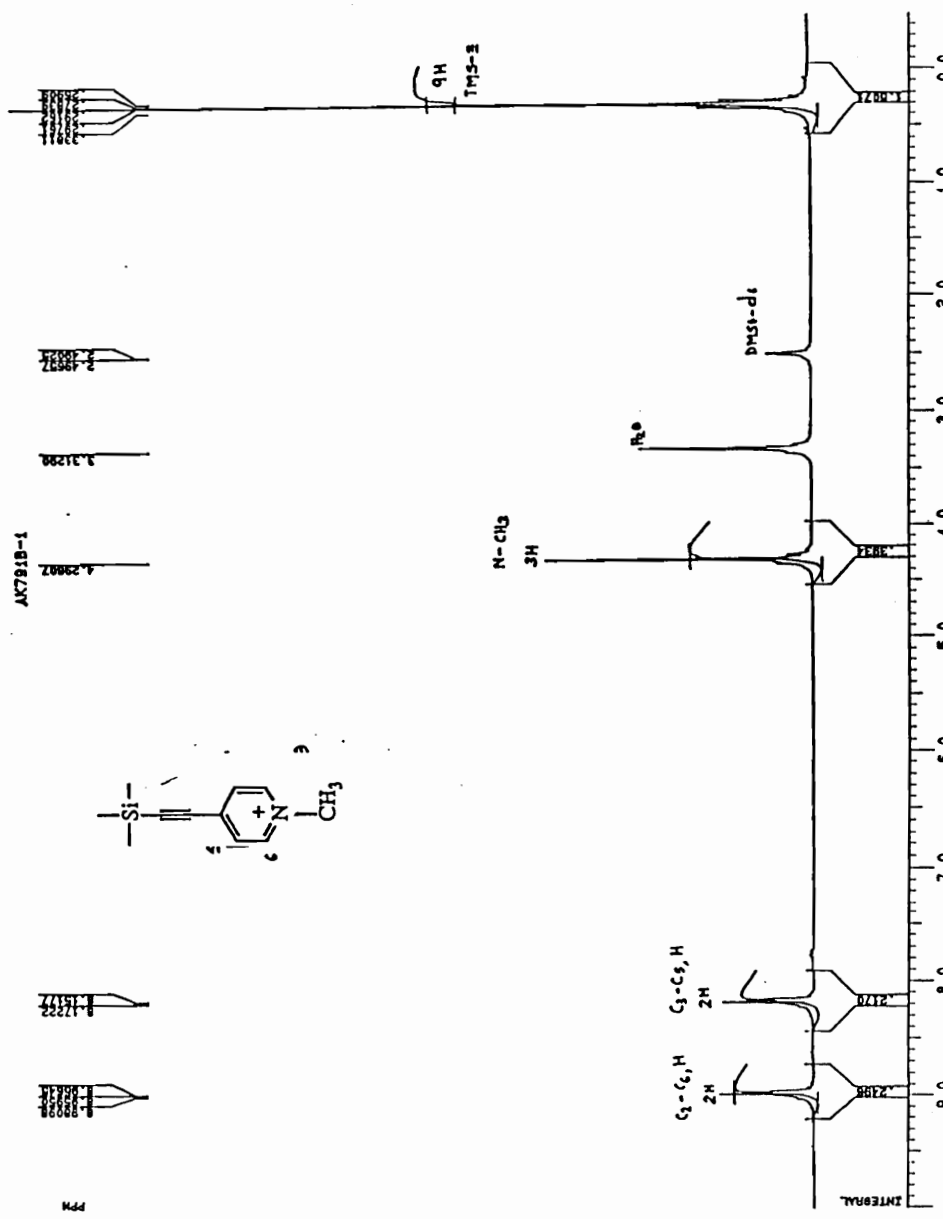

Figure. 30. ^{1}H NMR Spectrum (DMSO-d_6) of 1-Methyl-4-trimethylsilylpyridinium Iodide.

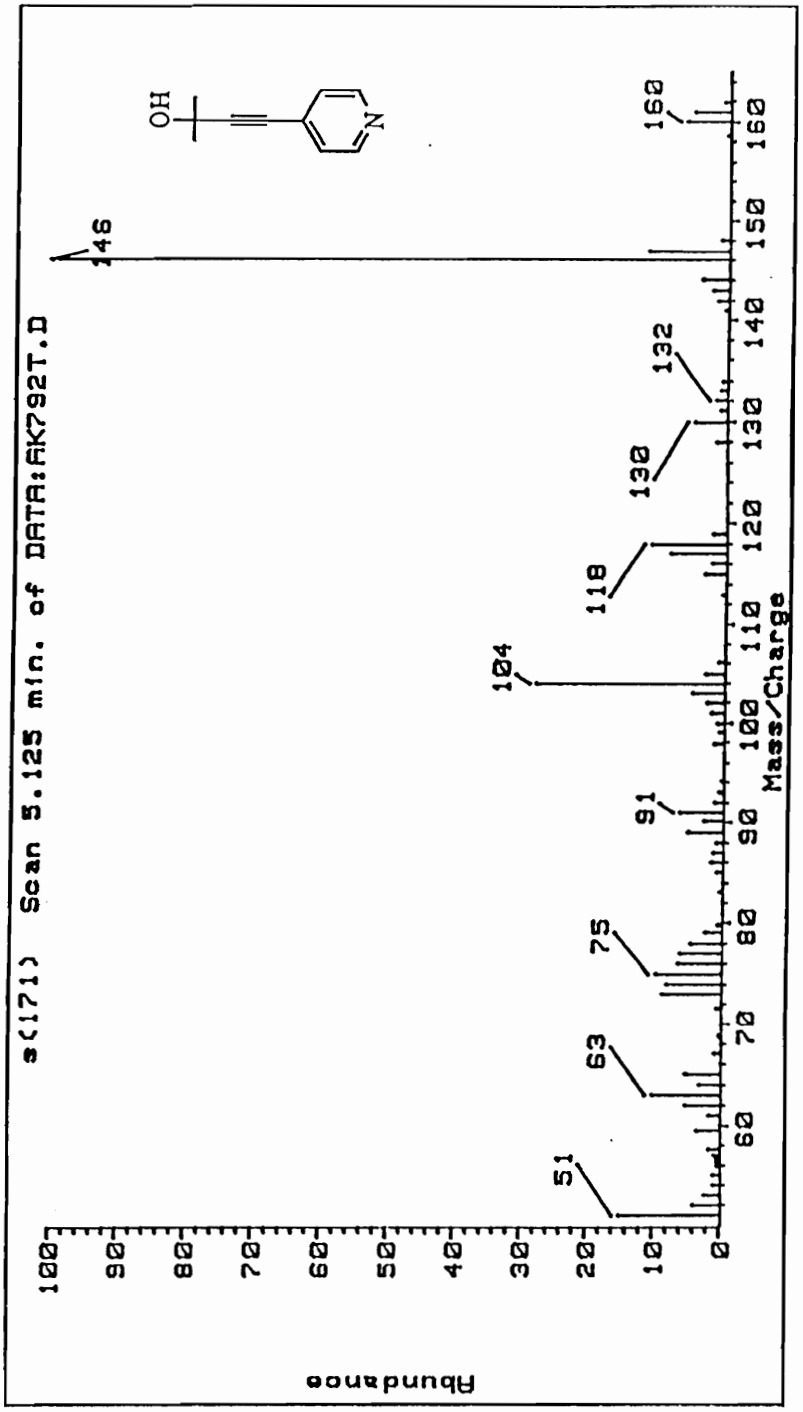

Figure. 31. GC/EIMS of 2-Methyl-4-(4-pyridyl)-3-butyn-2-ol.

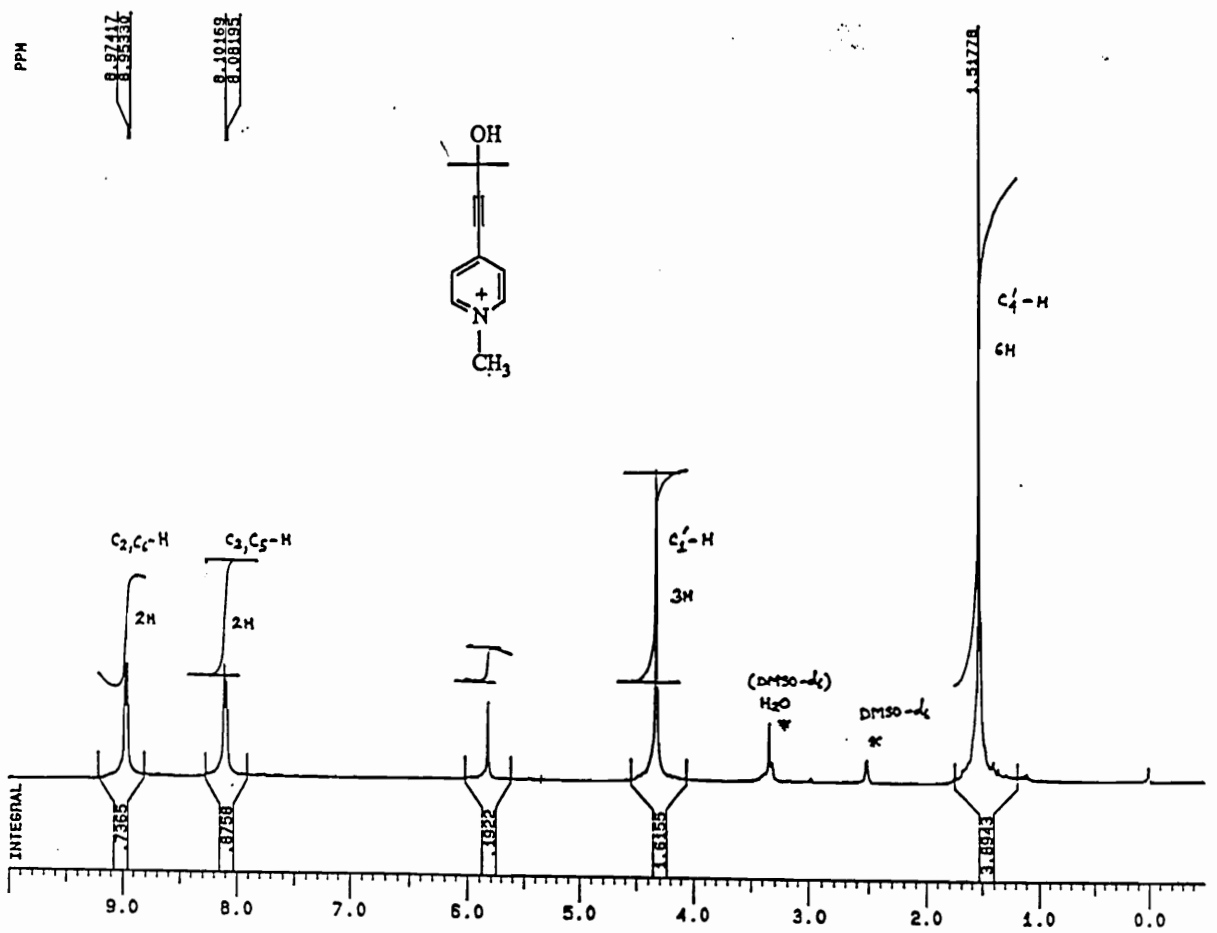

Figure. 32. ^{1}H NMR Spectrum (DMSO-d$_6$) of 2-Methyl-4-(4-(N-methylpyridyl)-3-butyn-2-ol Iodide.

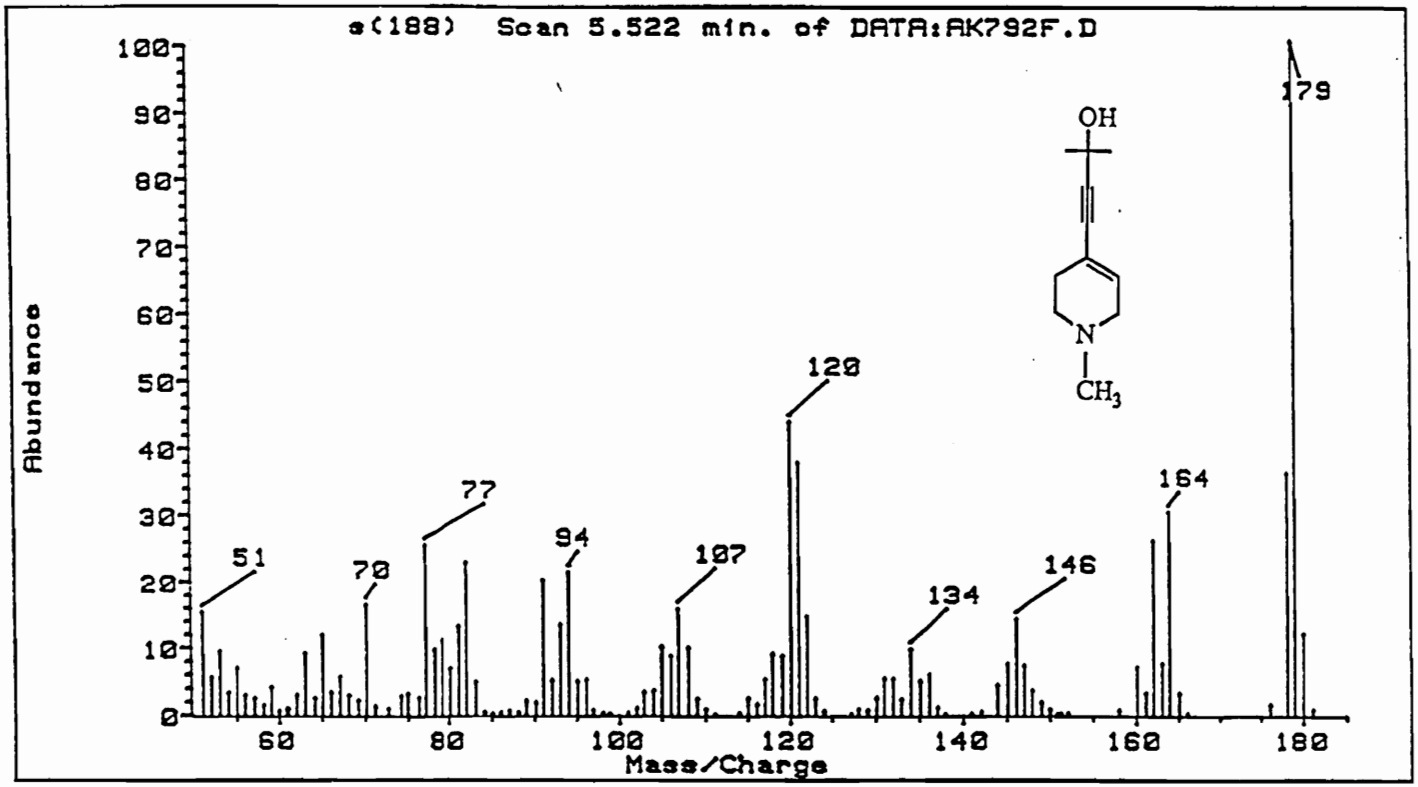

Figure. 33. GC/EIMS of
2-Methyl-4-(4-(N-methyltetrahydropyridyl)-3-butyn-2-ol.

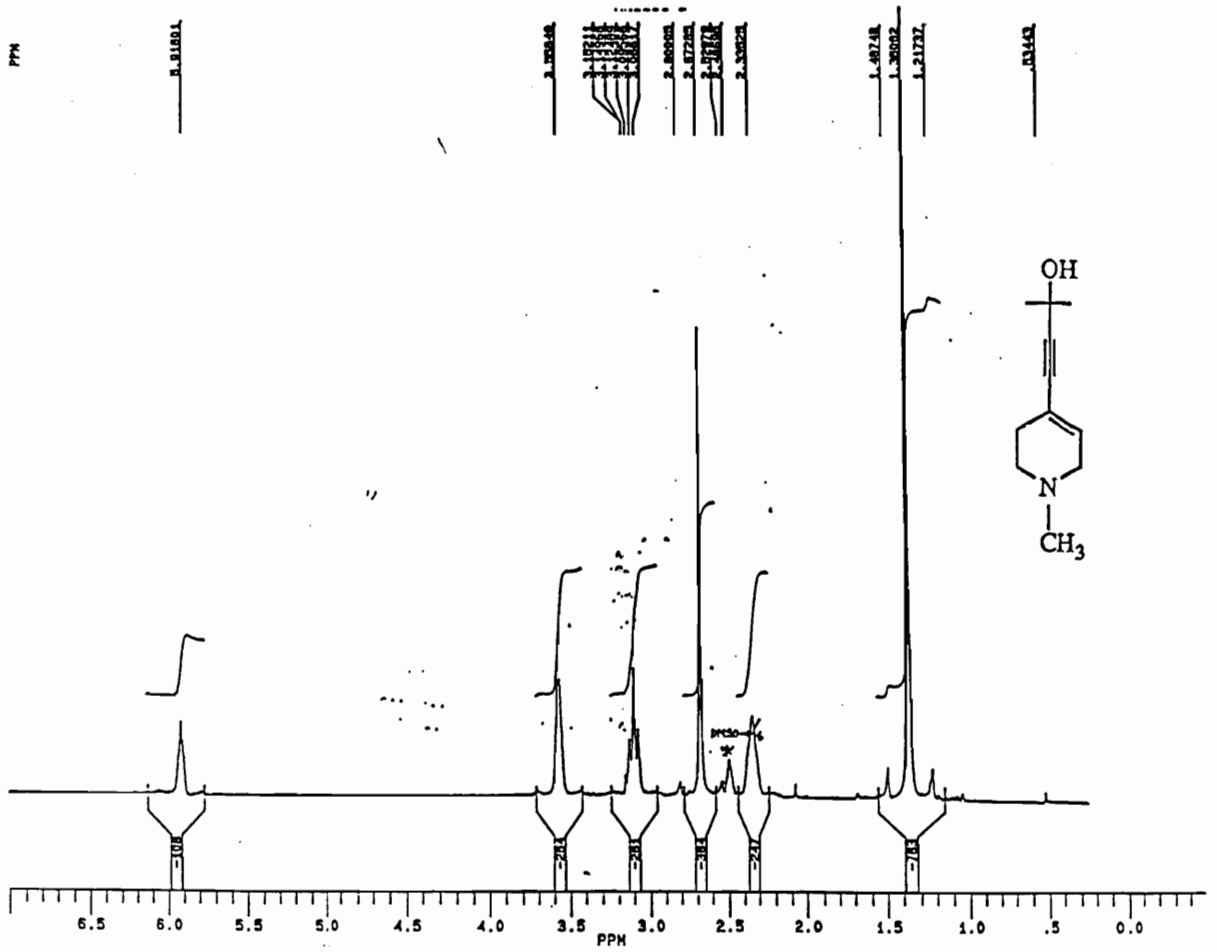

Figure. 34. ^{1}H NMR Spectrum (DMSO-d_6) of
2-Methyl-4-(4-(N-methyltetrahydropyridyl)-3-butyn-2-ol.

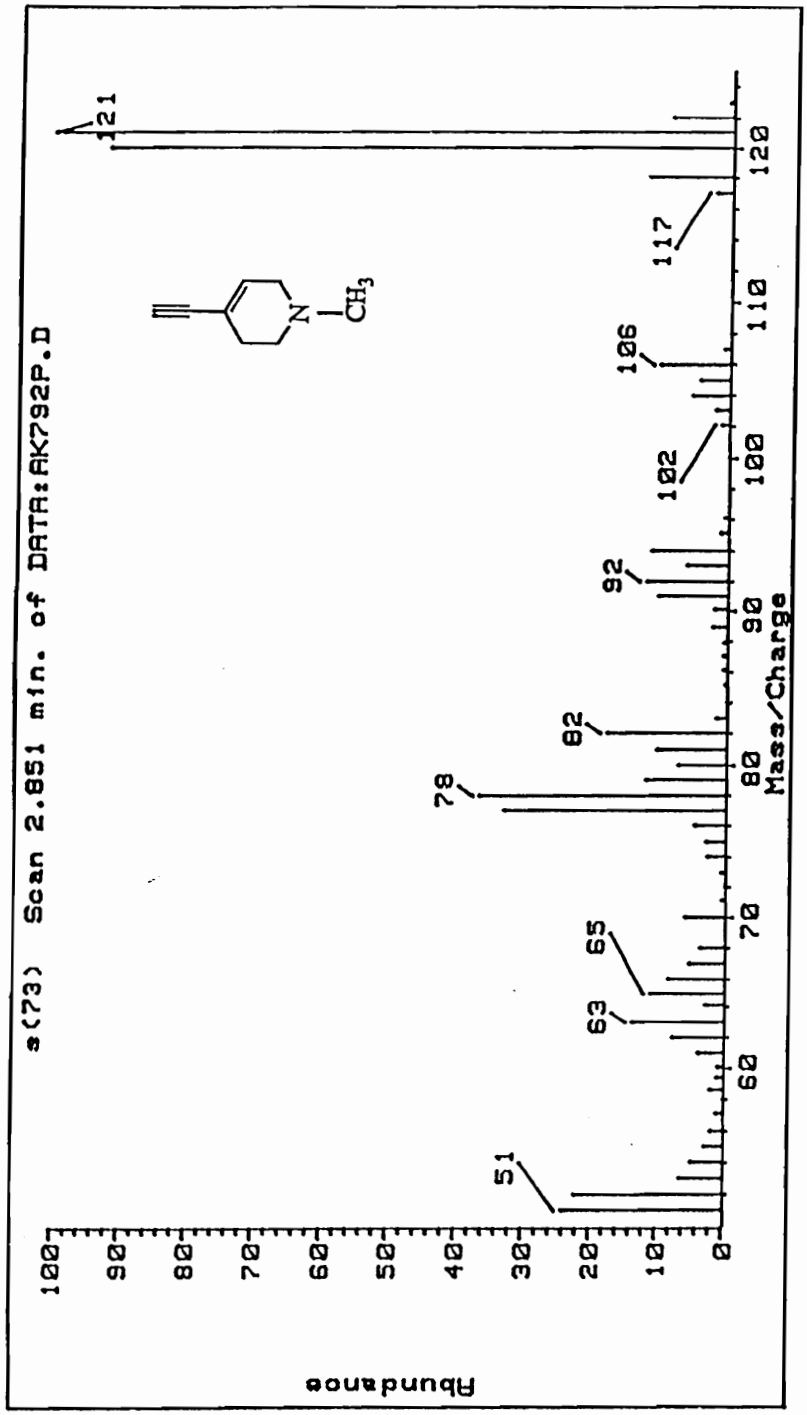

Figure. 35. GC/EIMS of 4-Ethynyl-1-methyl-1,2,3,6-tetrahydropyridine.

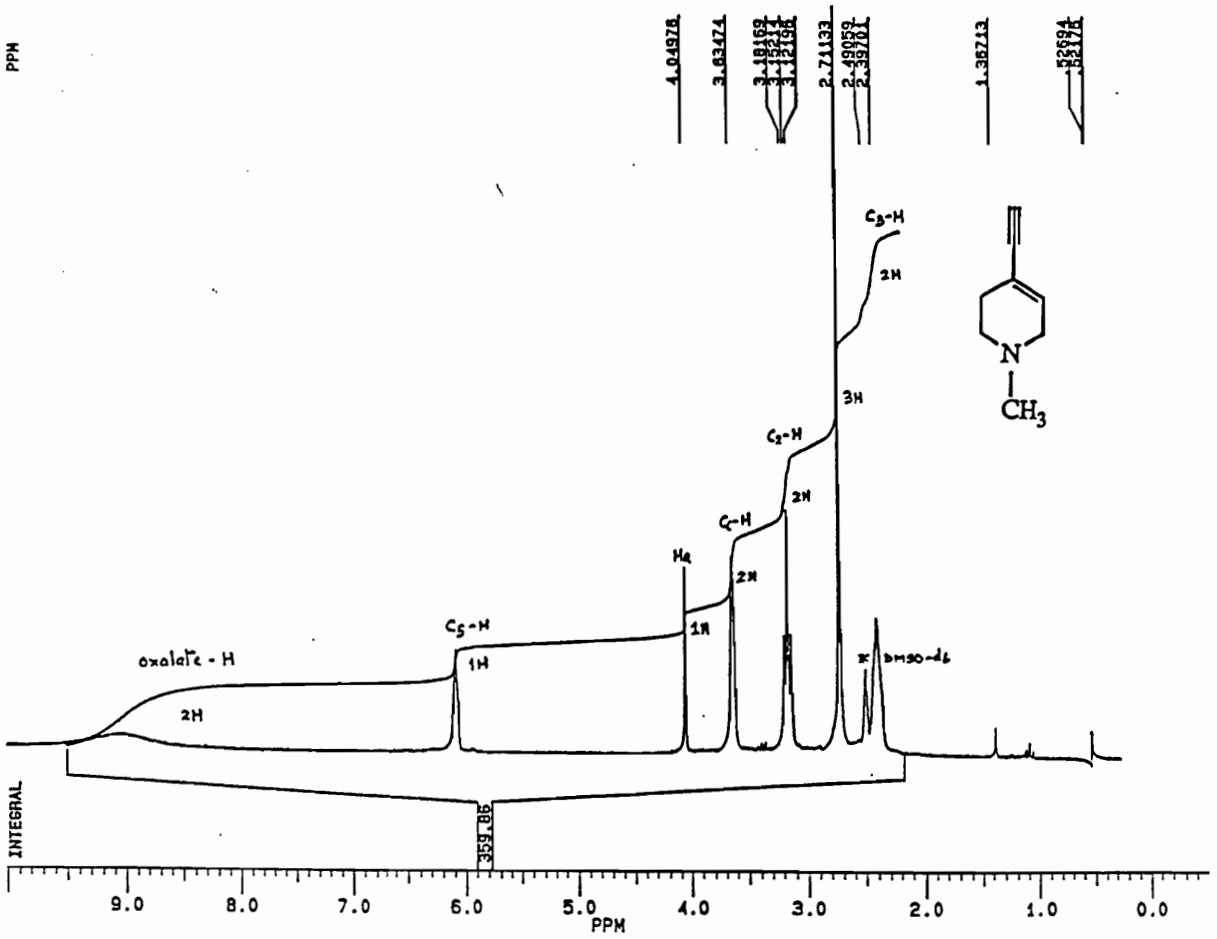

Figure. 36. ^{1}H NMR Spectrum (DMSO-d_6) of 4-Ethynyl-1-methyl-1,2,3,6-tetrahydropyridine.

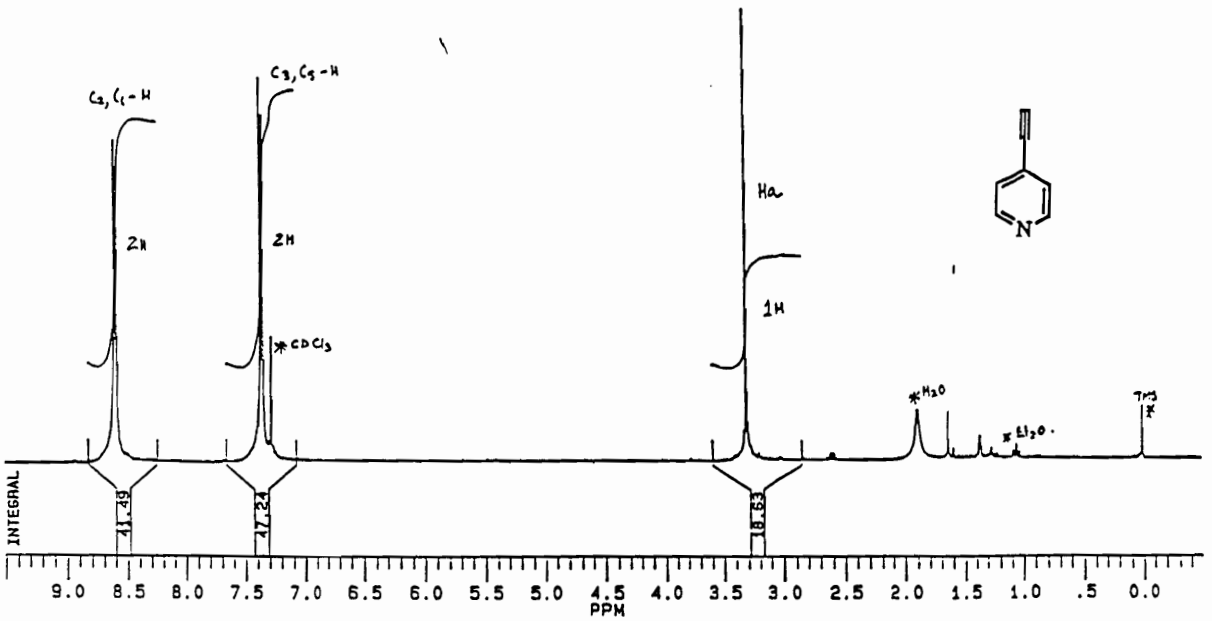

Figure. 37. ^{1}H NMR Spectrum ($CDCl_3$) of 4-Ethynylpyridine.

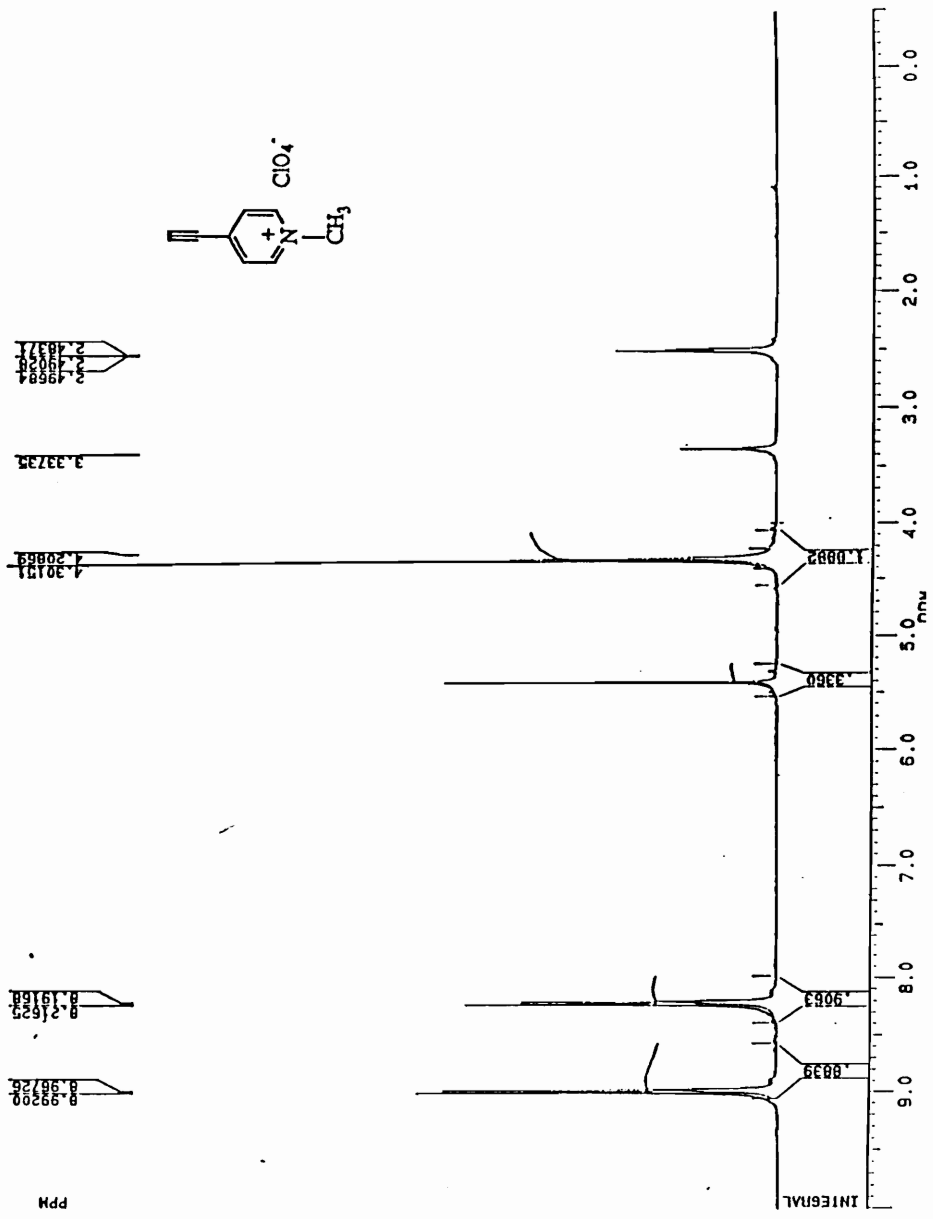

Figure. 38. ^{1}H NMR Spectrum (DMSO-d_6) of 4-Ethynyl-1-methylpyridinium Perchlorate.

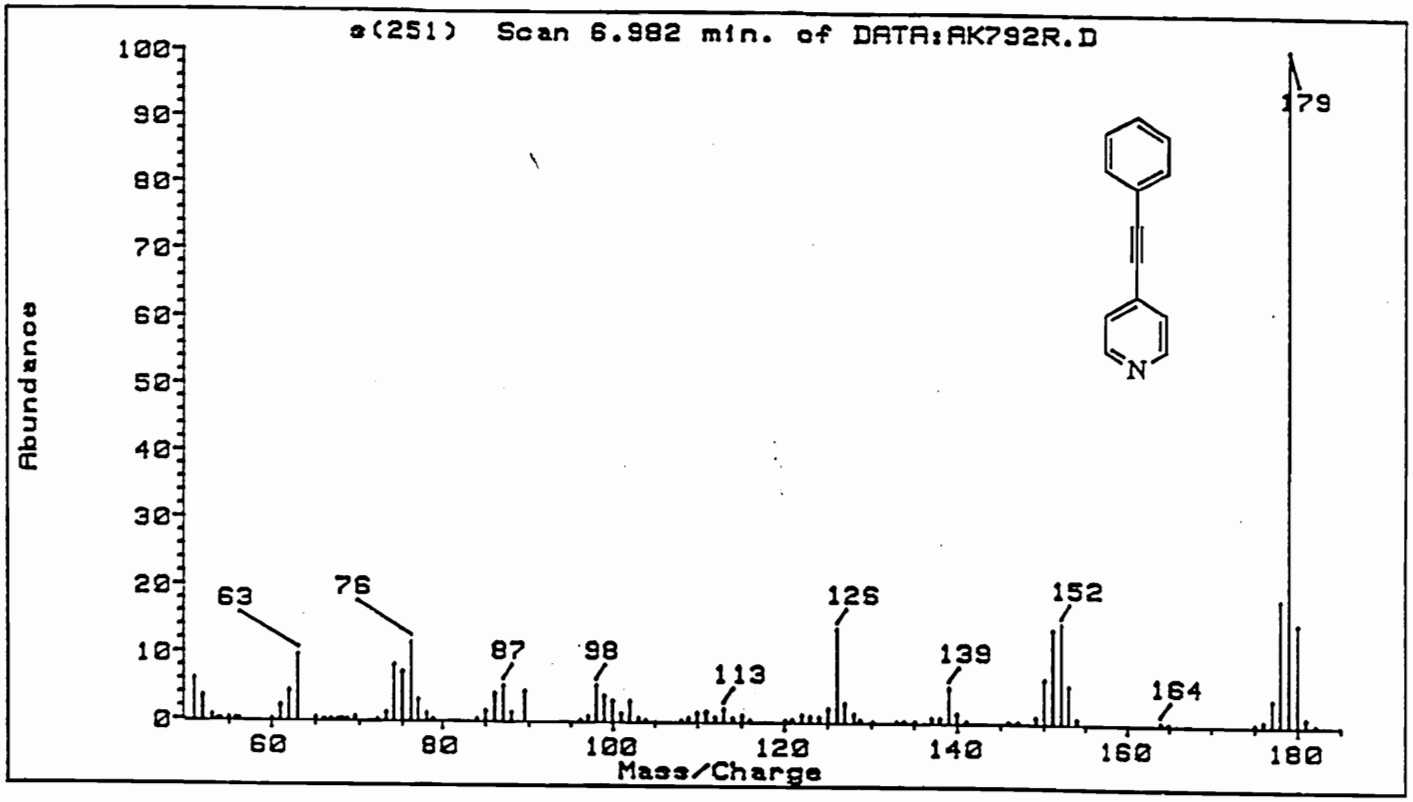

Figure. 39. GC/EIMS of 4-(2-Phenylethynyl)pyridine.

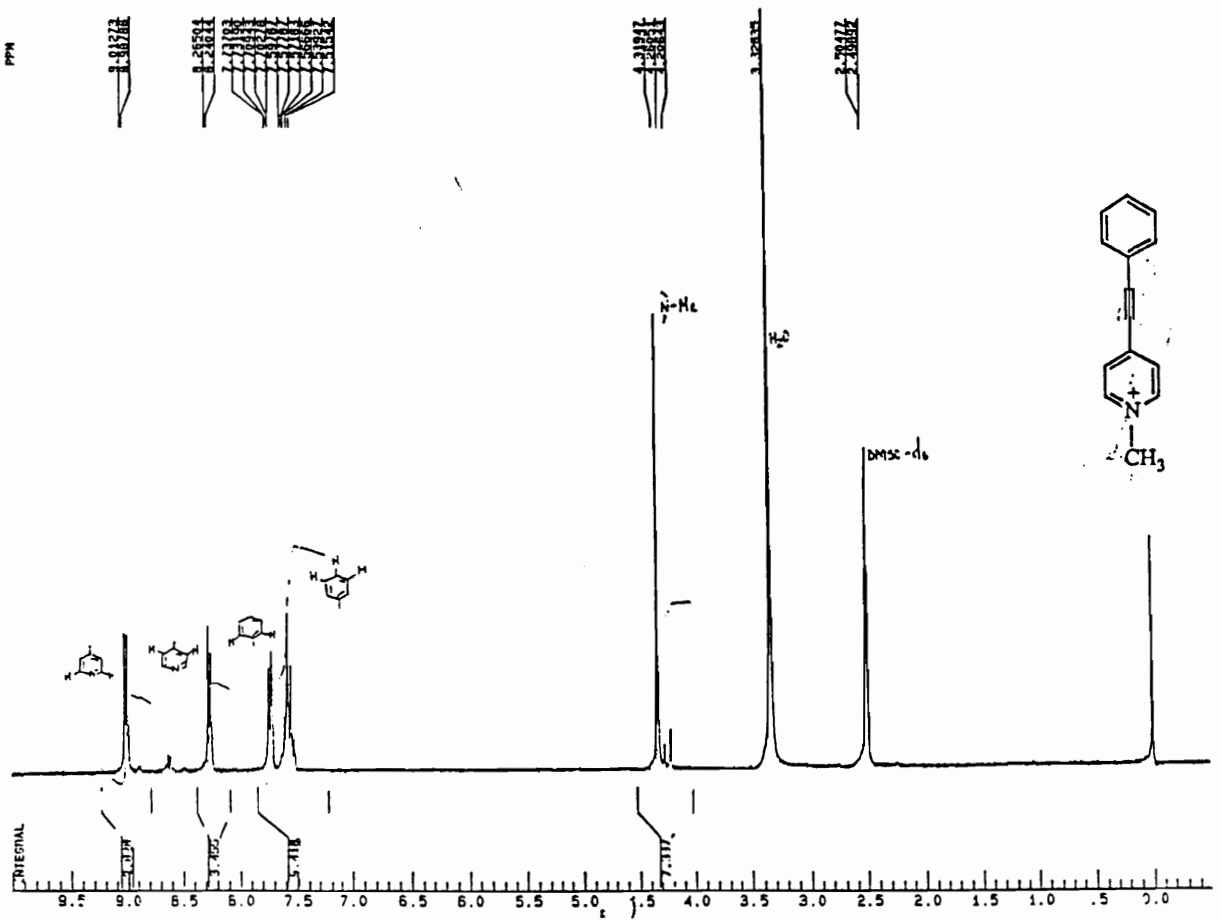

Figure. 40. ^{1}H NMR Spectrum (DMSO-d_6) of 1-Methyl-4-phenylethynylpyridinium Iodide.

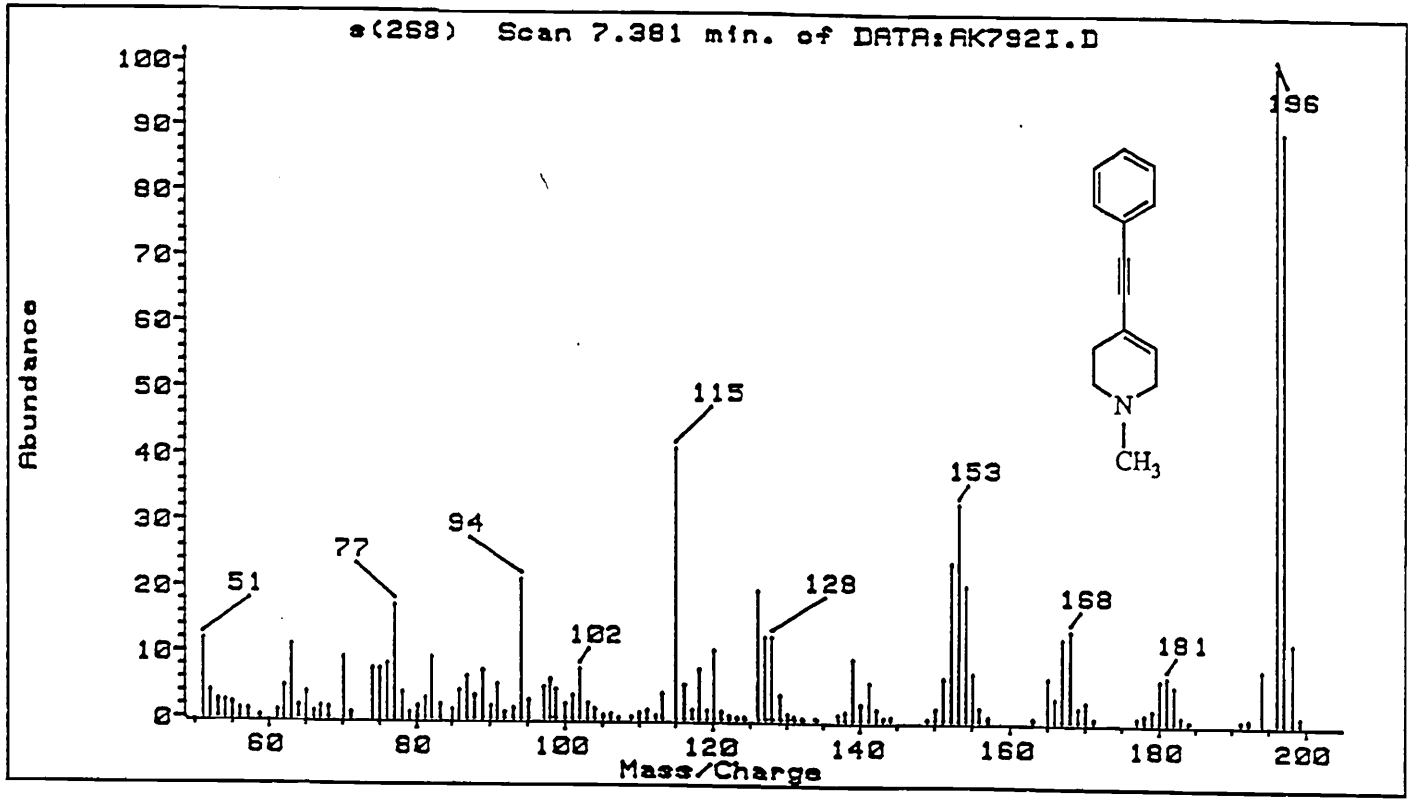

Figure. 41. GC/EIMS of 1-Methyl-4-(2-Phenylethynyl)-1,2,3,6-tetrahydropyridine.

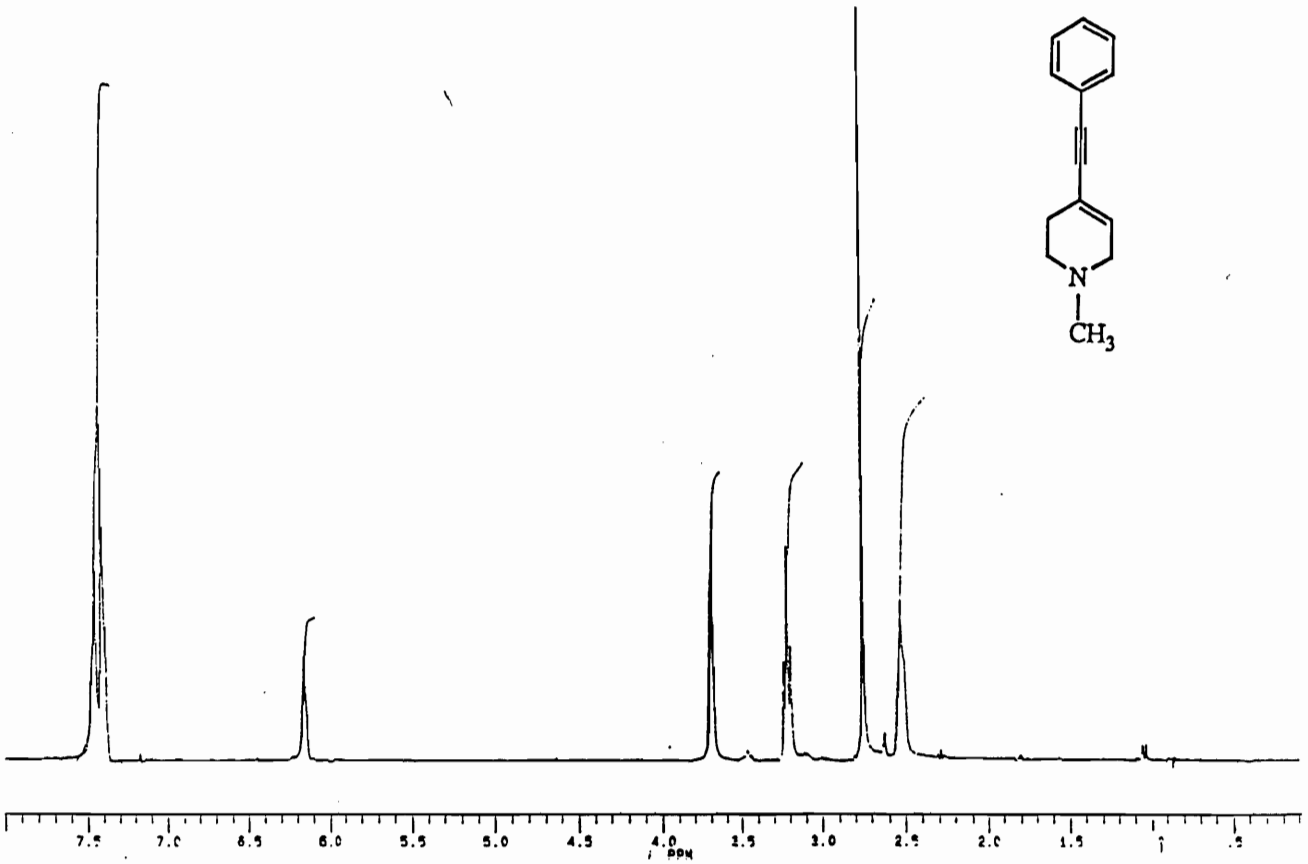

Figure. 42. ^{1}H NMR Spectrum (DMSO-d_6) of 1-Methyl-4-phenylethynyl-1,2,3,6-tetrahydropyridine.

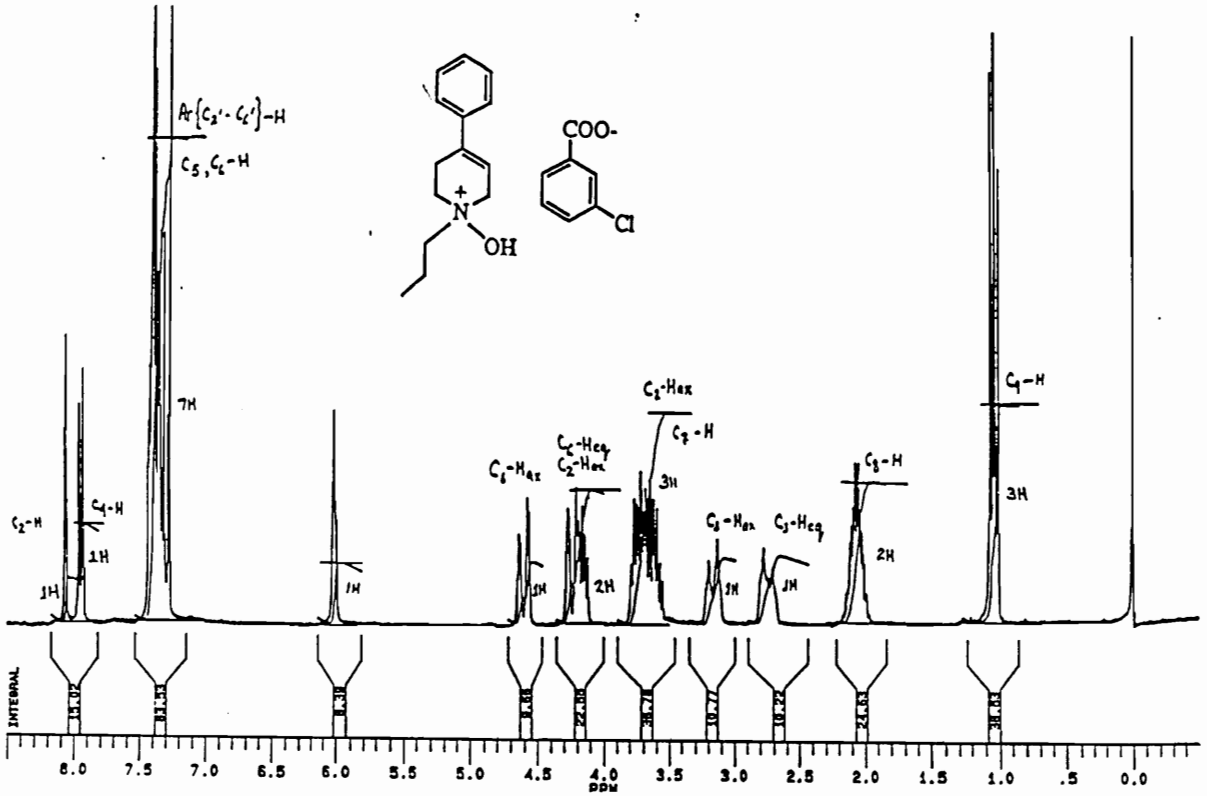

Figure. 43. ^{1}H NMR Spectrum ($CDCl_3$) of the *m*CBA Salt of the N-Oxide of 4-Phenyl-1-propyl-1,2,3,6-tetrahydropyridine.

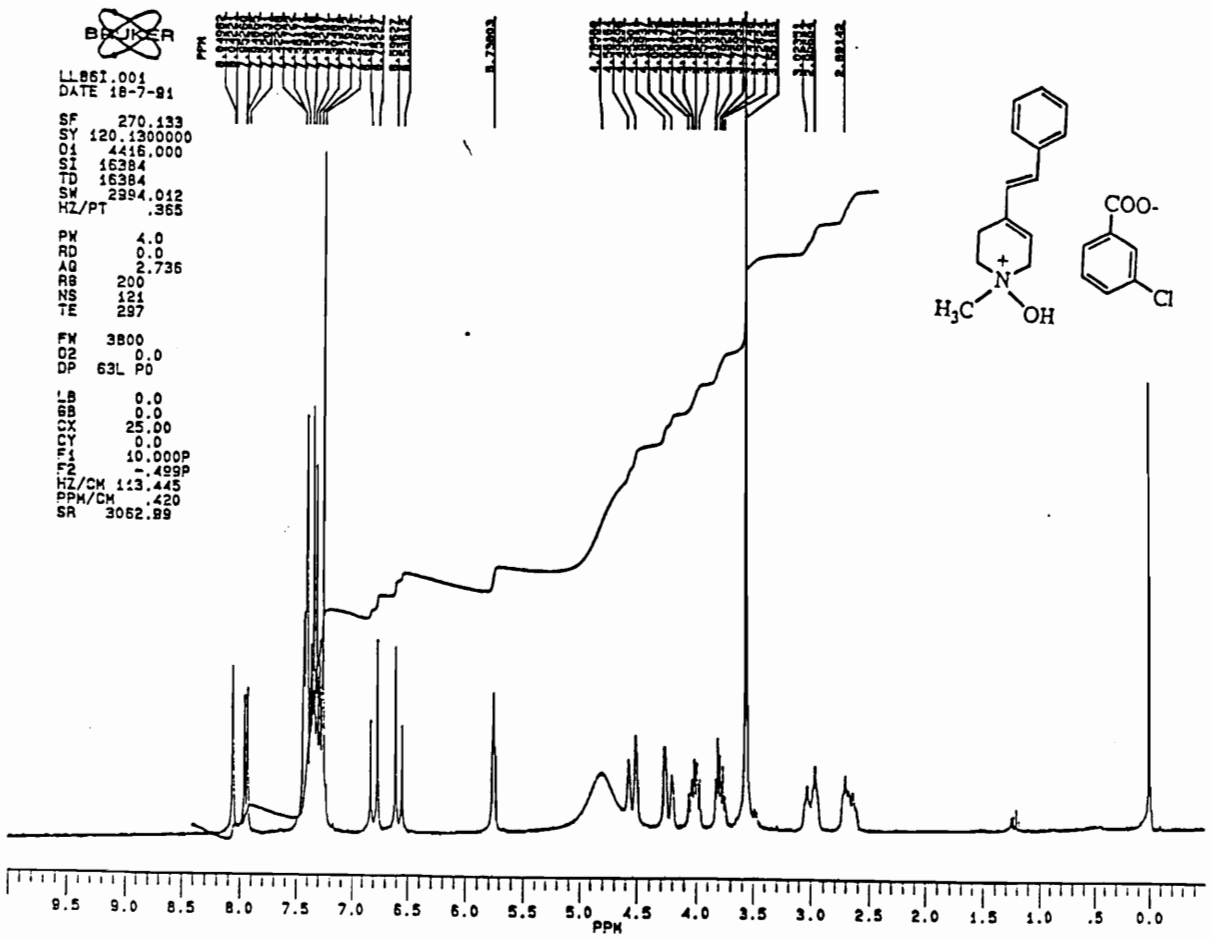

Figure. 44. ^{1}H NMR Spectrum ($CDCl_3$) of the *m*CBA Salt of the N-Oxide of 1-Methyl-4-(E)-(2-phenylethenyl)-1,2,3,6-tetrahydropyridine.

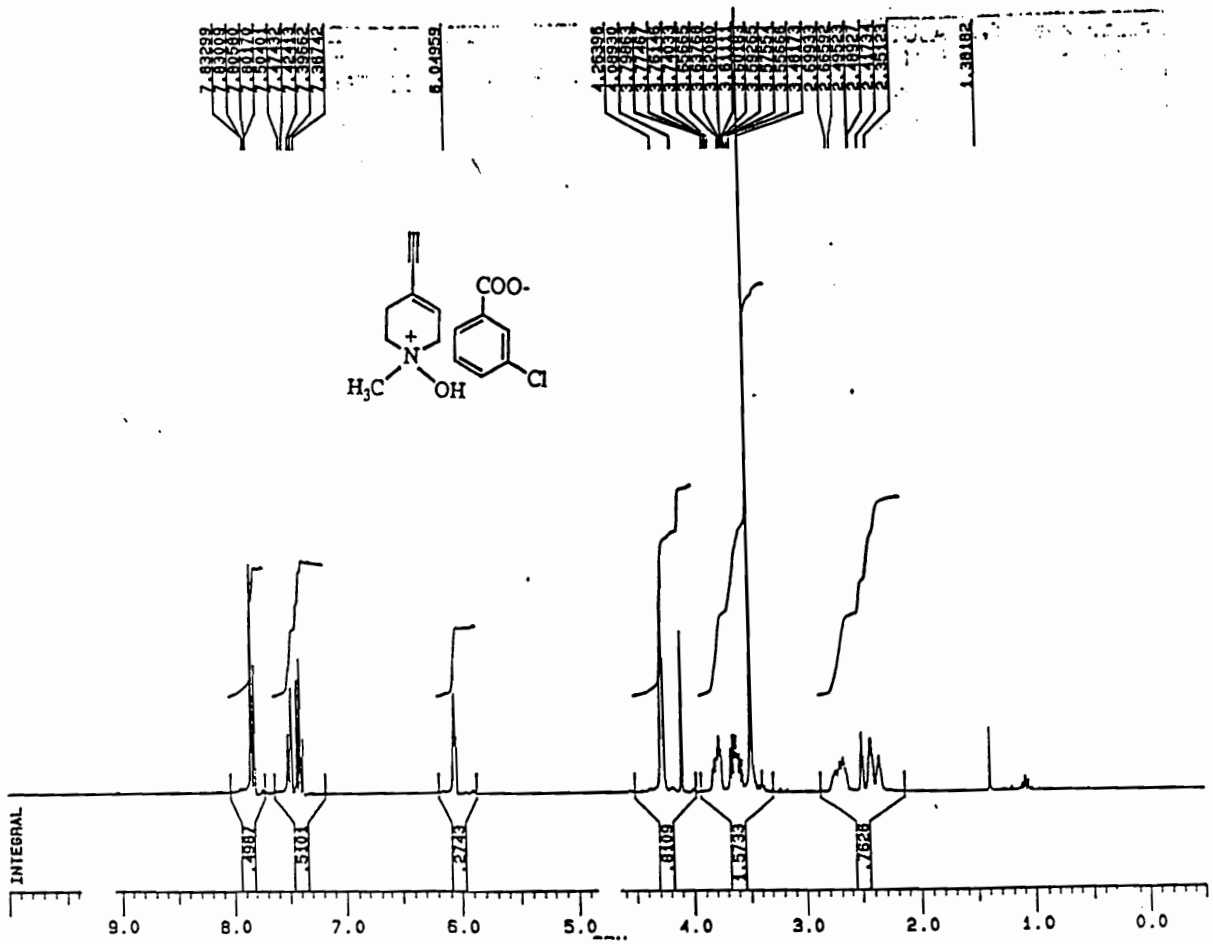

Figure. 45. ^{1}H NMR Spectrum ($CDCl_3$) of the *m*CBA Salt of the N-Oxide of 4-Ethynyl-1-methyl-1,2,3,6-tetrahydropyridine.

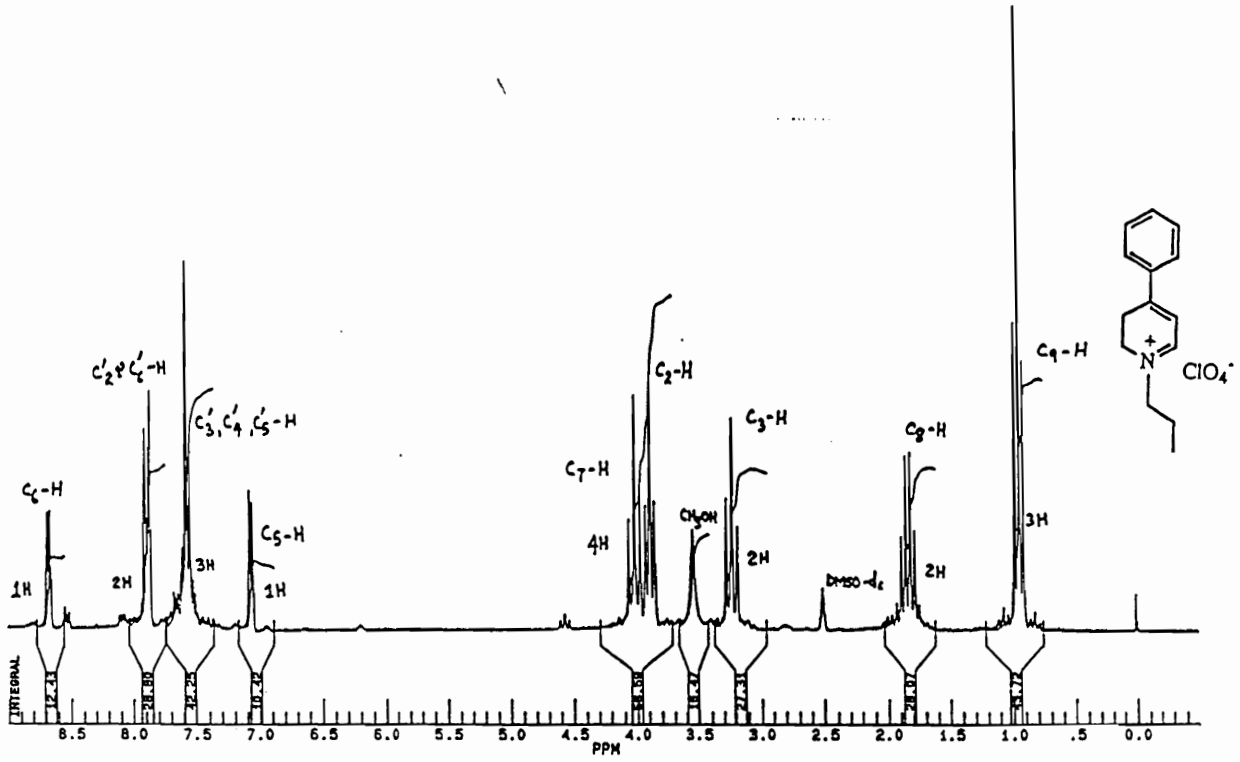

Figure. 46. ^{1}H NMR Spectrum (DMSO-d$_6$) of 4-Phenyl-1-propyl-2,3-dihydropyridinium Perchlorate.

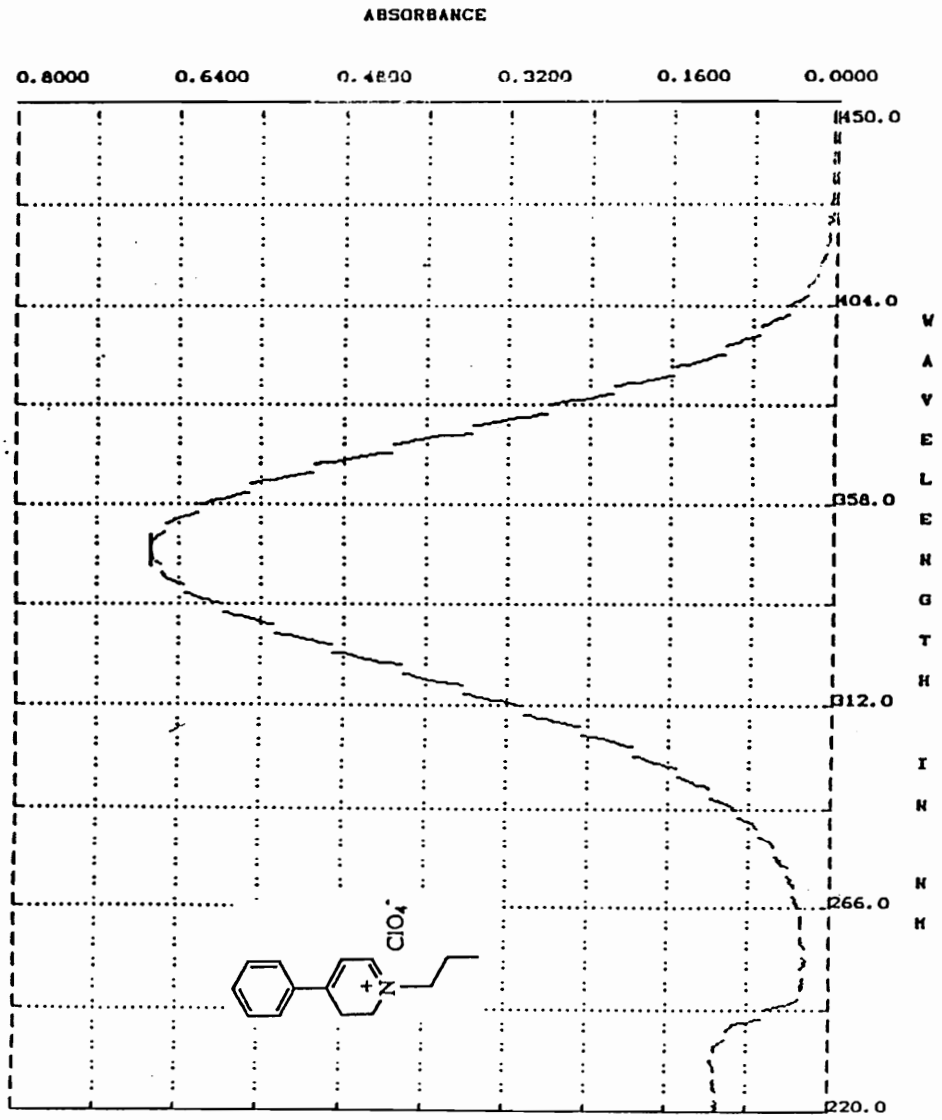

Figure. 47. UV Spectrum of 40 μM
4-Phenyl-1-propyl-2,3-dihydropyridinium Perchlorate in MeOH.

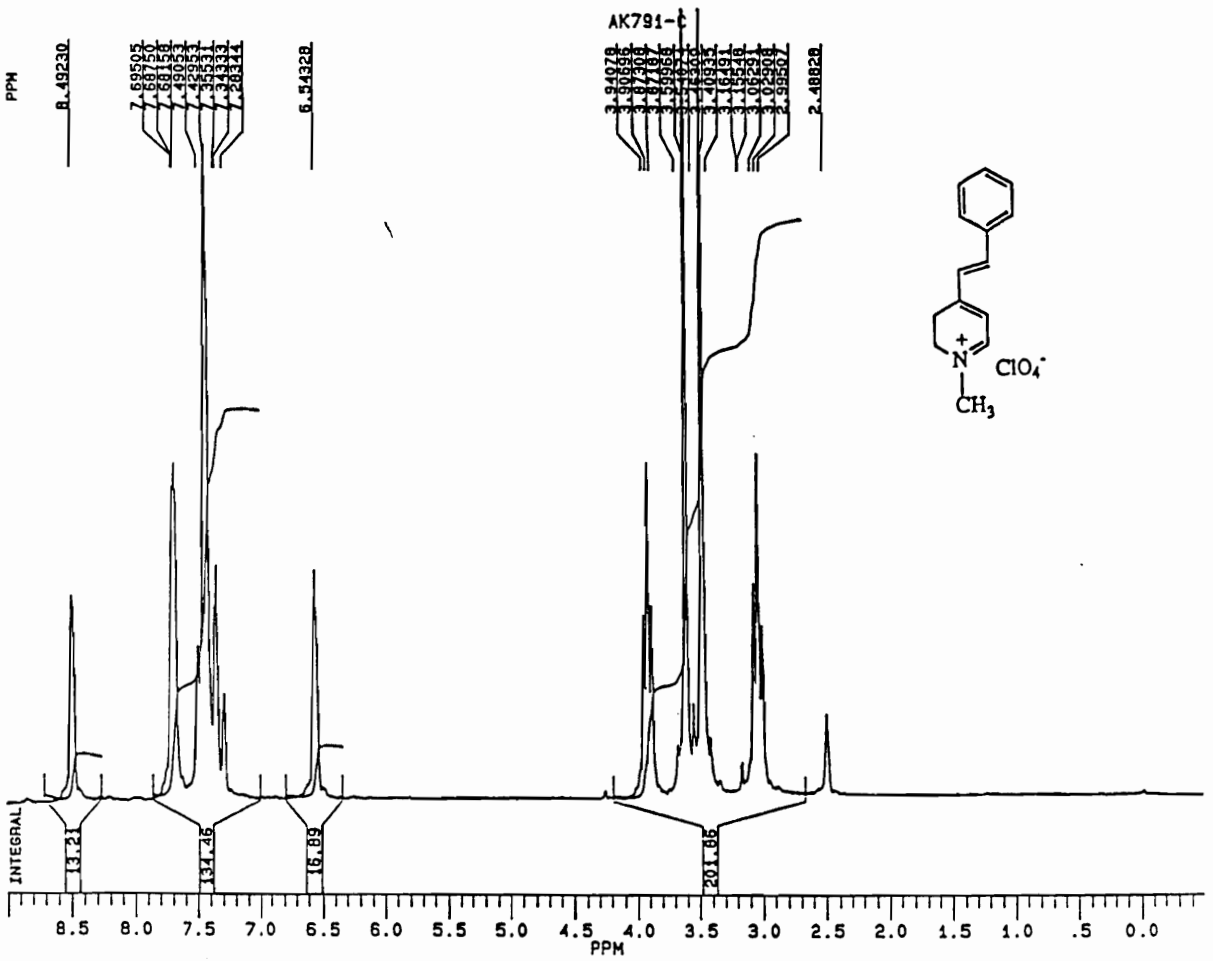

Figure. 48. ^{1}H NMR Spectrum (DMSO-d_6) of 1-Methyl-4-(E)-(2-phenylethenyl)-2,3-dihydropyridinium Perchlorate.

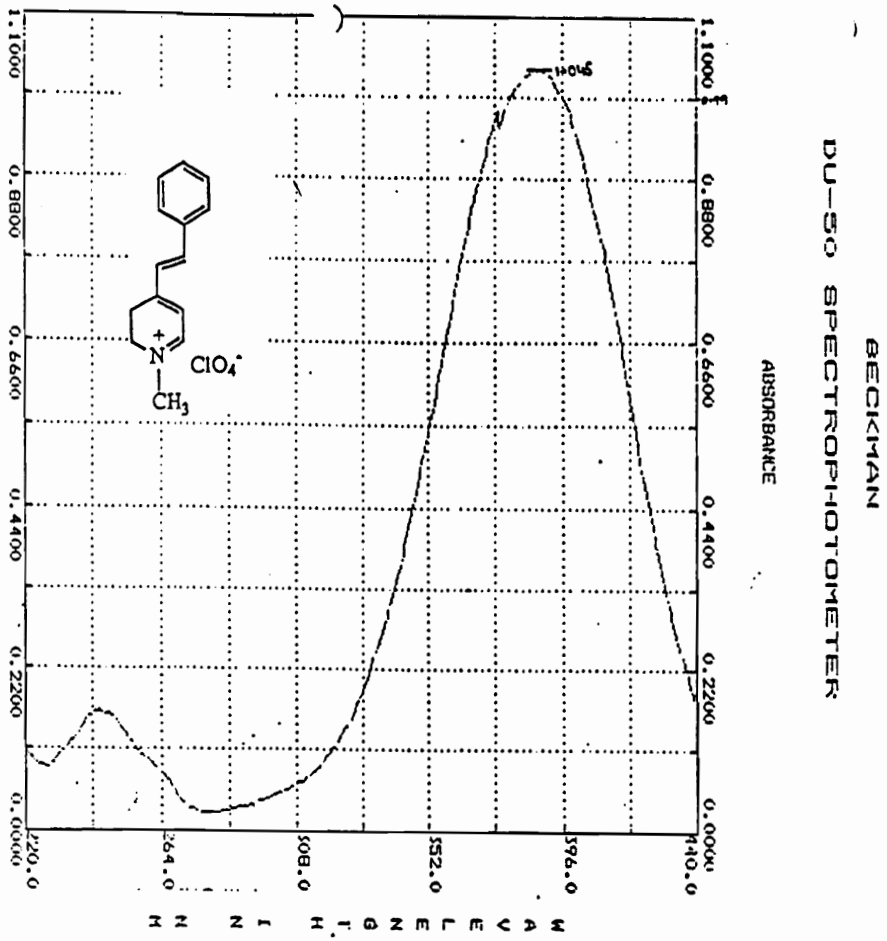

Figure. 49. UV Spectrum of 40 μM (in MeOH)
1-Methyl-4-(E)-2-(phenylethenyl)-2,3-dihydropyridinium Perchlorate.

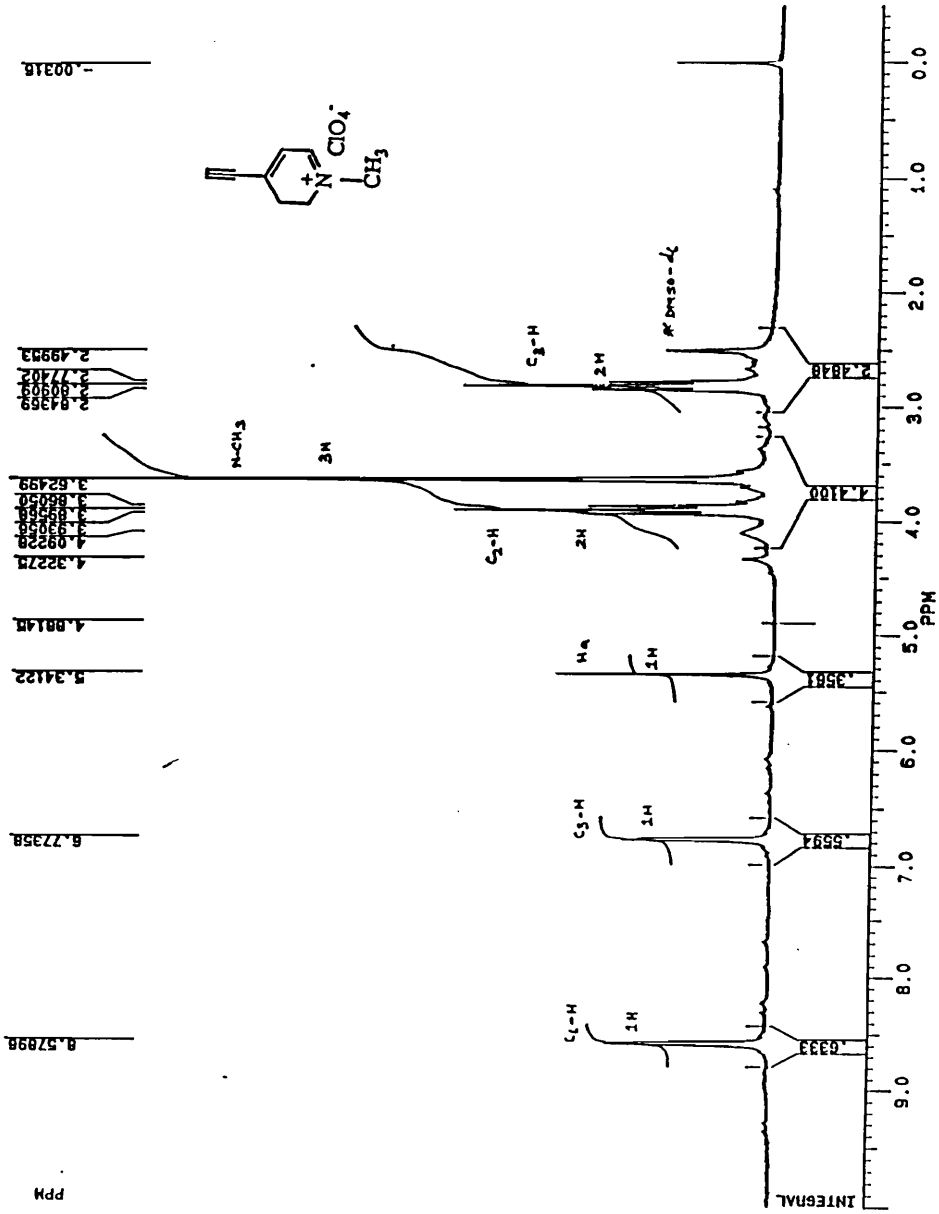

Figure. 50. ^{1}H NMR Spectrum (DMSO-d6) of 4-Ethynyl-1-methyl-2,3-dihydropyridinium Perchlorate.

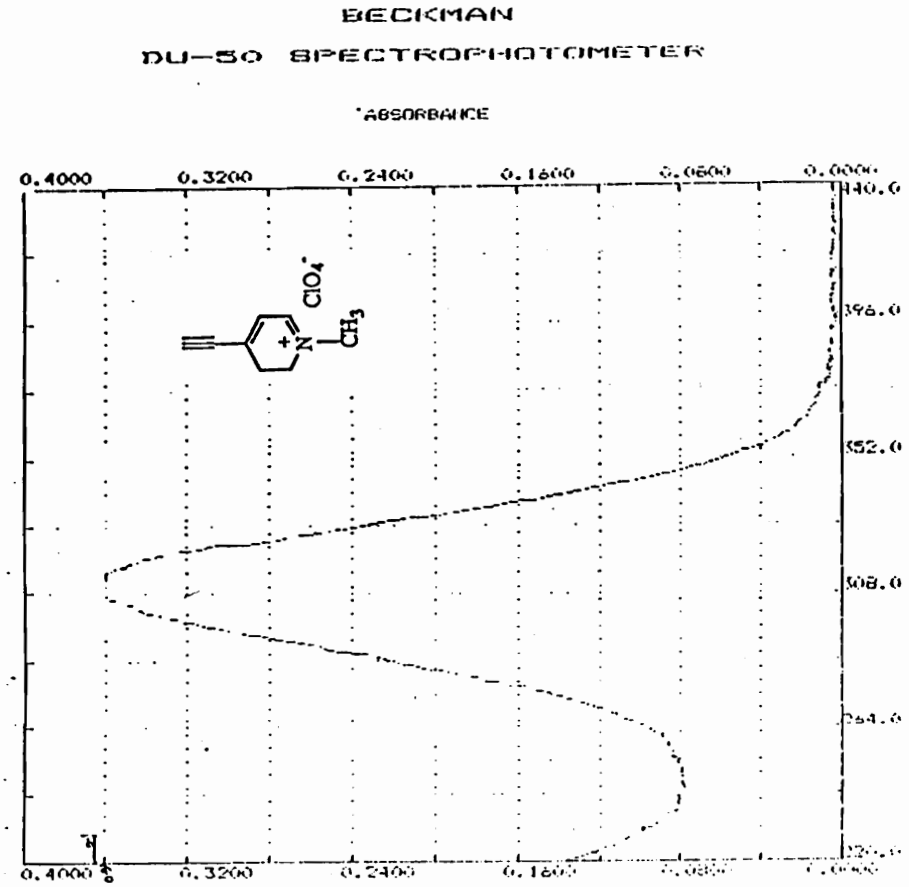

Figure. 51. UV Spectrum of 40 µM (in Acetonitrile) 4-Ethynyl-1-methyl-2,3-dihydropyridinium Perchlorate.

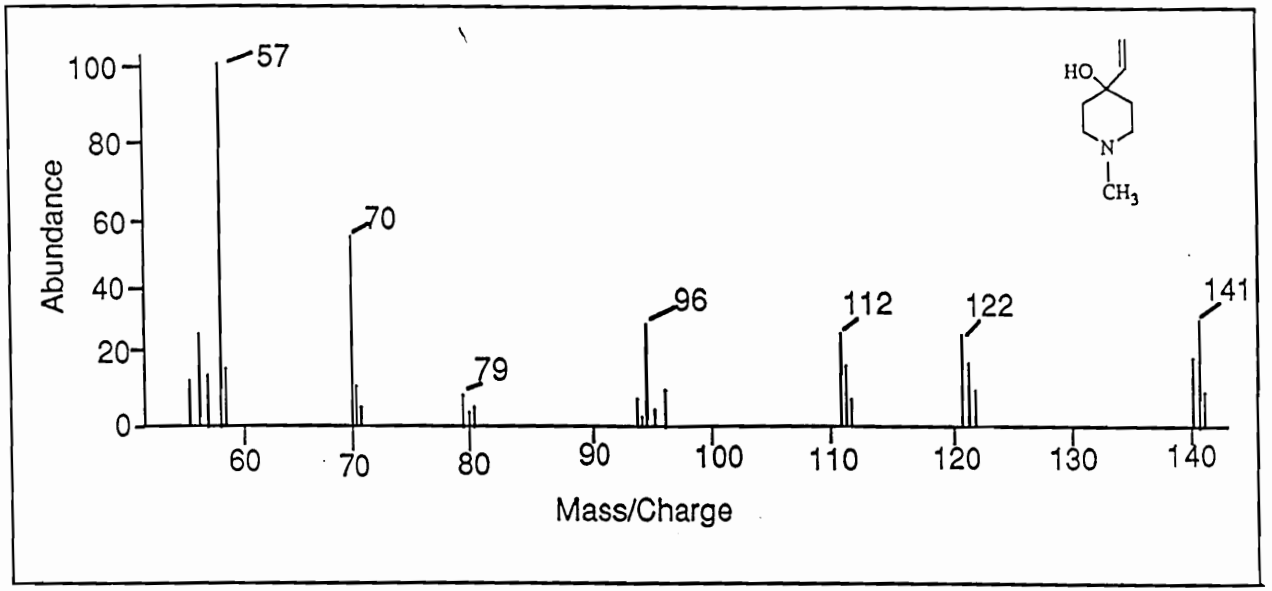

Figure. 52. GC/EIMS of 4-Ethenyl-1-methylpiperidin-4-ol.

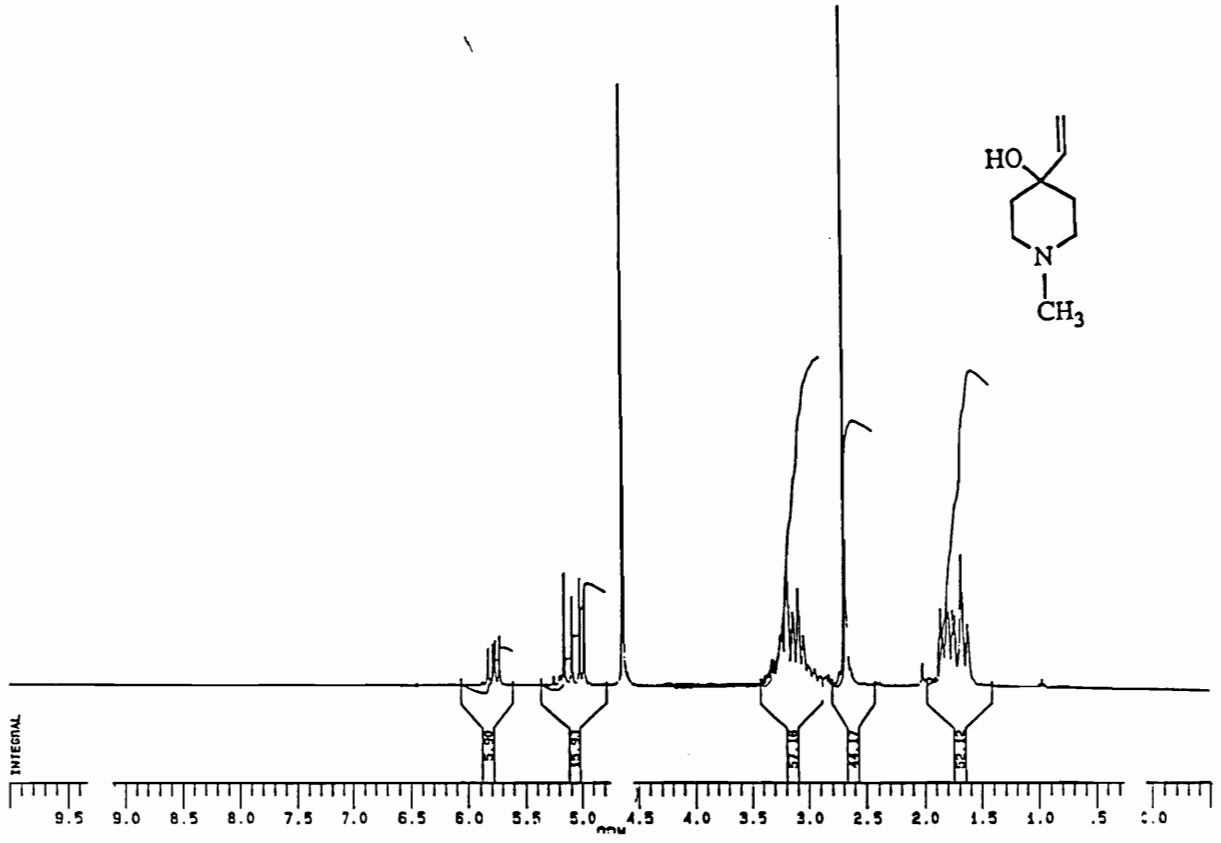

Figure. 53. ^{1}H NMR Spectrum (DMSO-d_6) of 4-Ethenyl-1-methylpiperidin-4-ol.

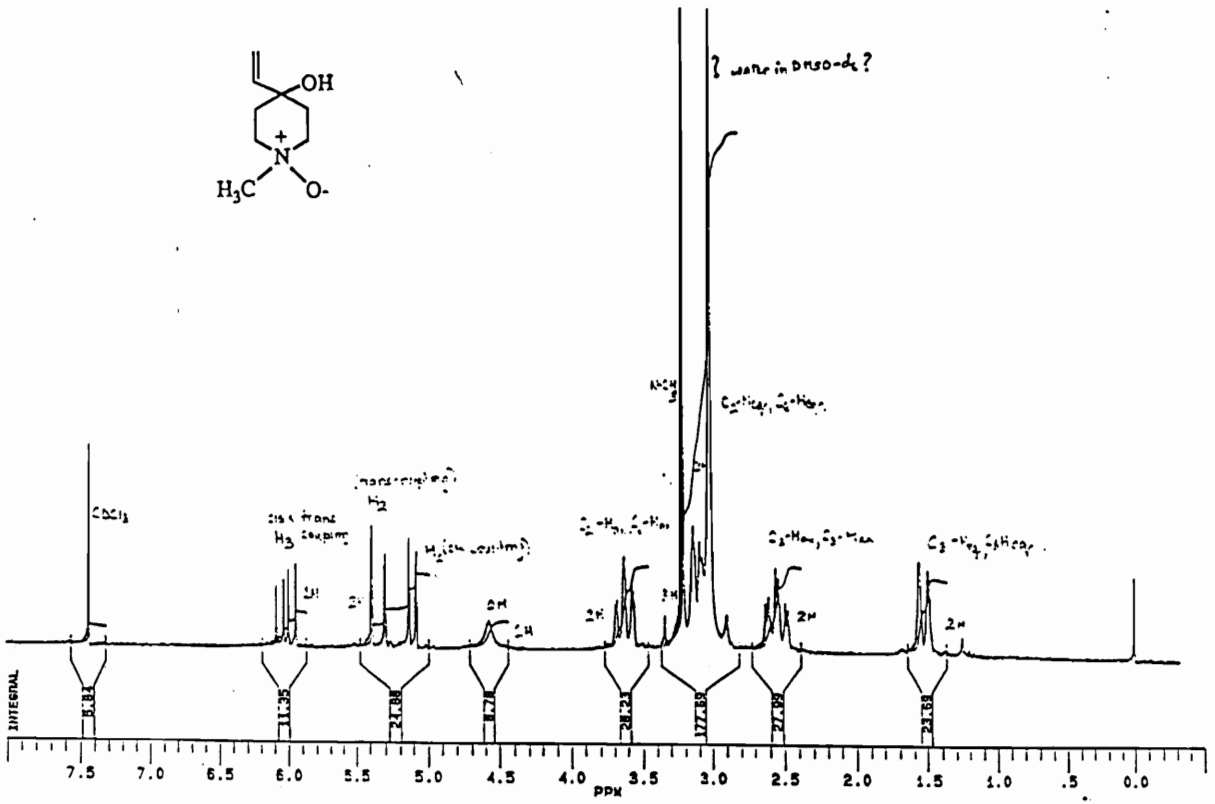

Figure. 54. ^{1}H NMR Spectrum ($CDCl_3$) of the N-Oxide of 4-Ethenyl-1-methylpiperidin-4-ol.

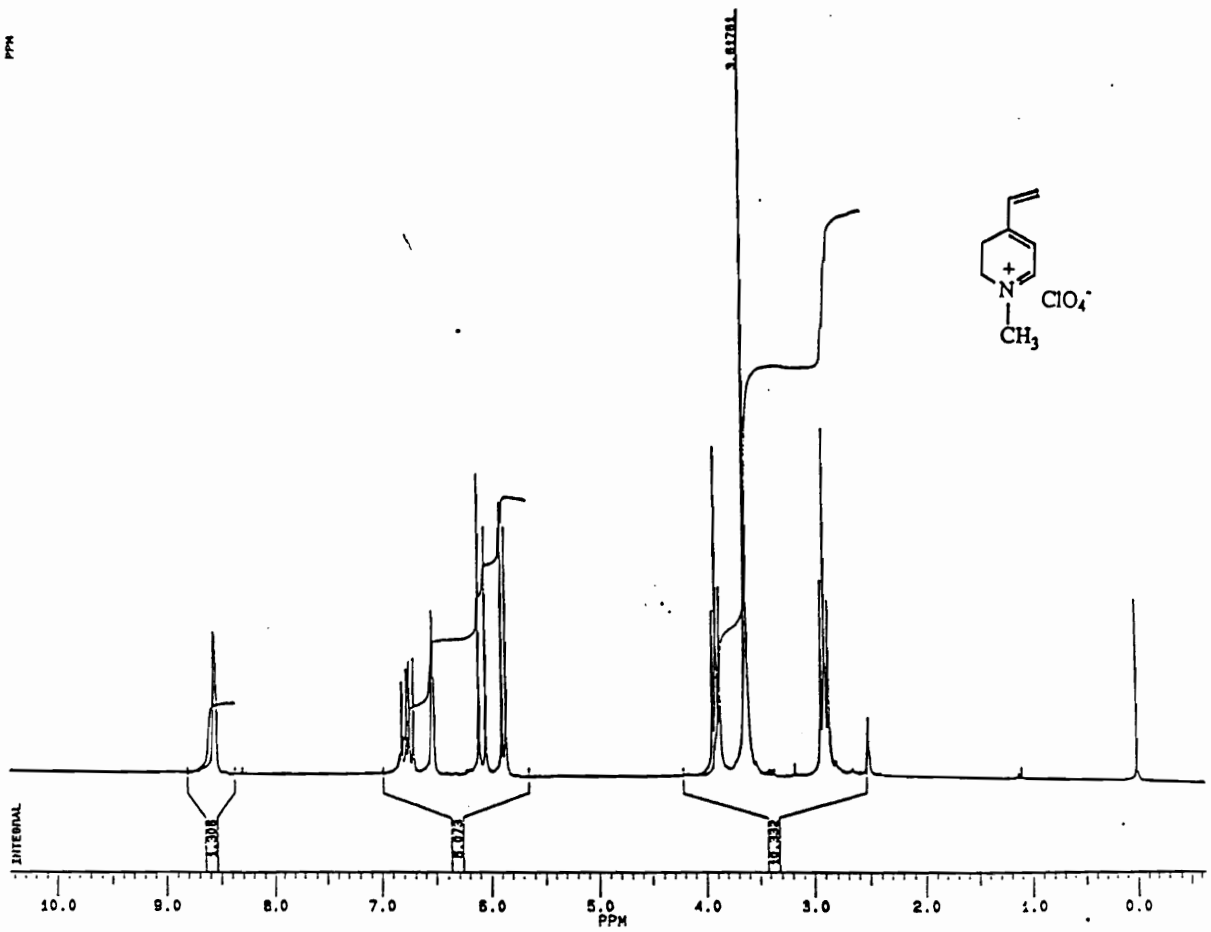

Figure. 55. ^{1}H NMR Spectrum (DMSO-d_6) of 4-Ethenyl-1-methyl-2,3-dihydropyridinium Perchlorate.

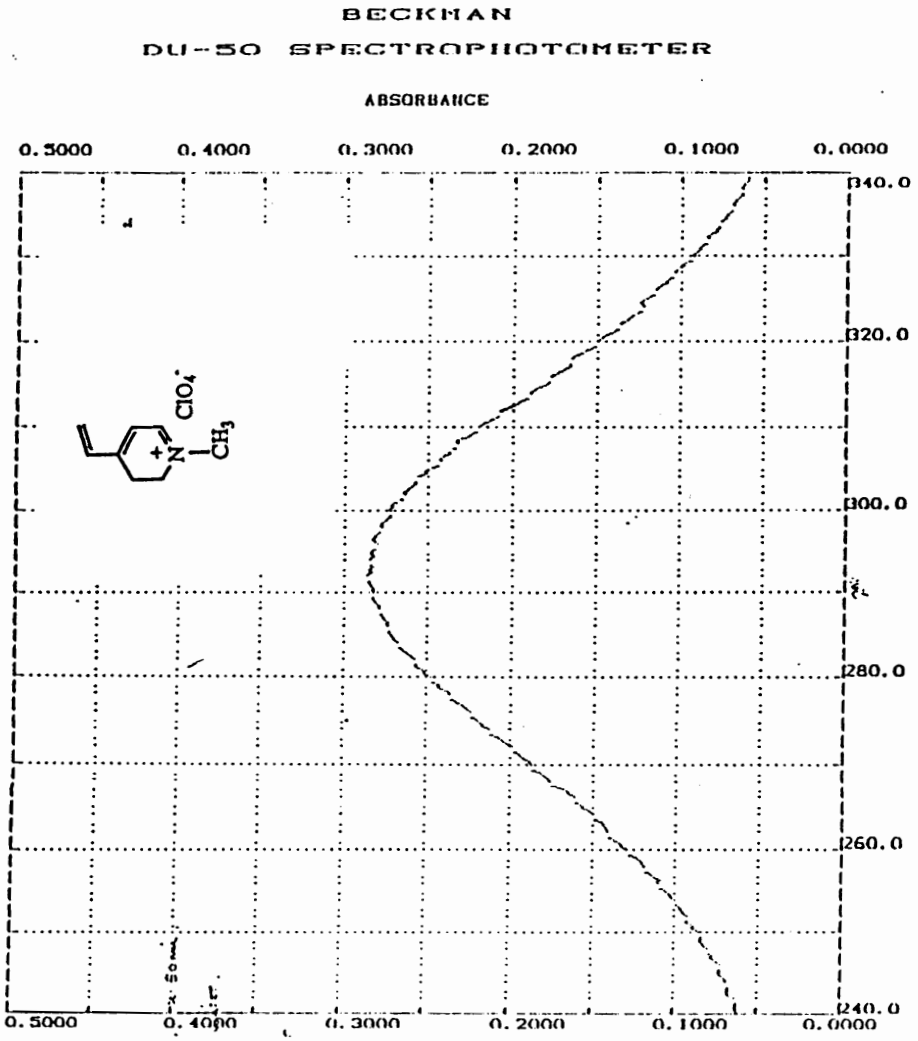

Figure. 56. UV Spectrum of 40 μM (in MeOH) 4-Ethenyl-1-methyl-2,3-dihydropyridinium Perchlorate.

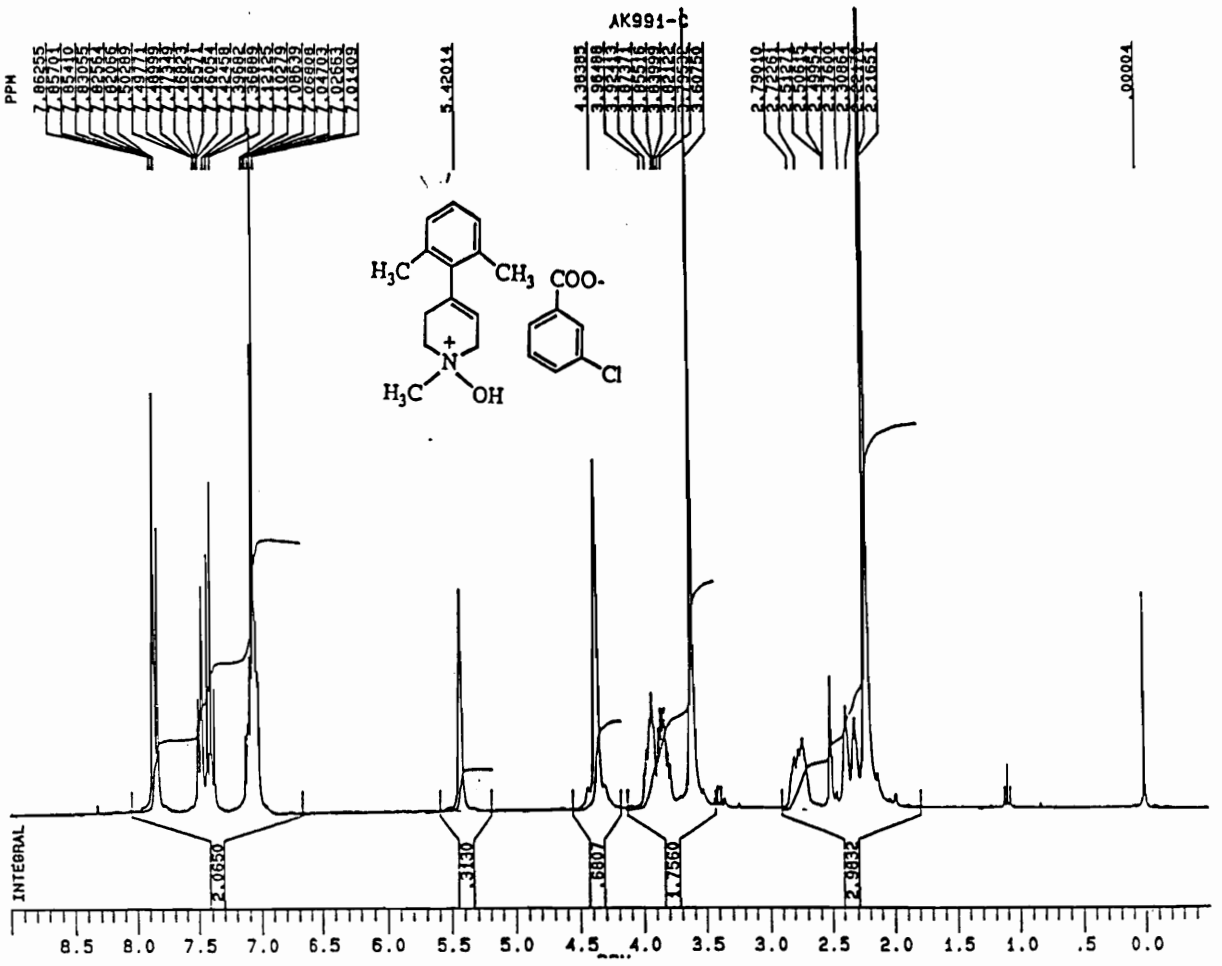

Figure. 57. ^{1}H NMR Spectrum ($CDCl_3$) of the *m*CBA Salt of the N-Oxide of 4-(2,6-Dimethyl)phenyl-1-methyl-1,2,3,6-tetrahydropyridine.

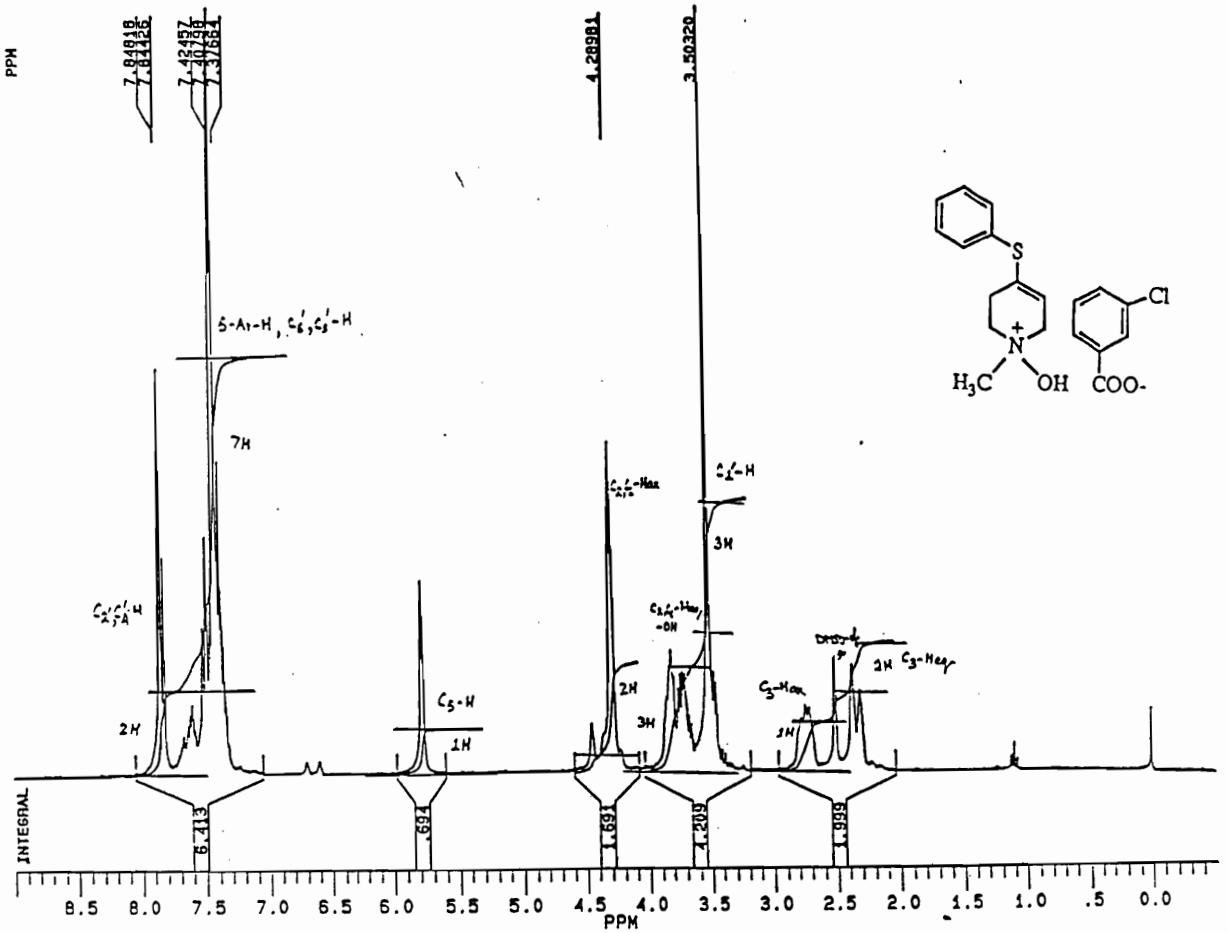

Figure. 58. ^{1}H NMR Spectrum ($CDCl_3$) of the *m*CBA Salt of the N-Oxide of 4-Thiophenoxy-1-methyl-1,2,3,6-tetrahydropyridine.

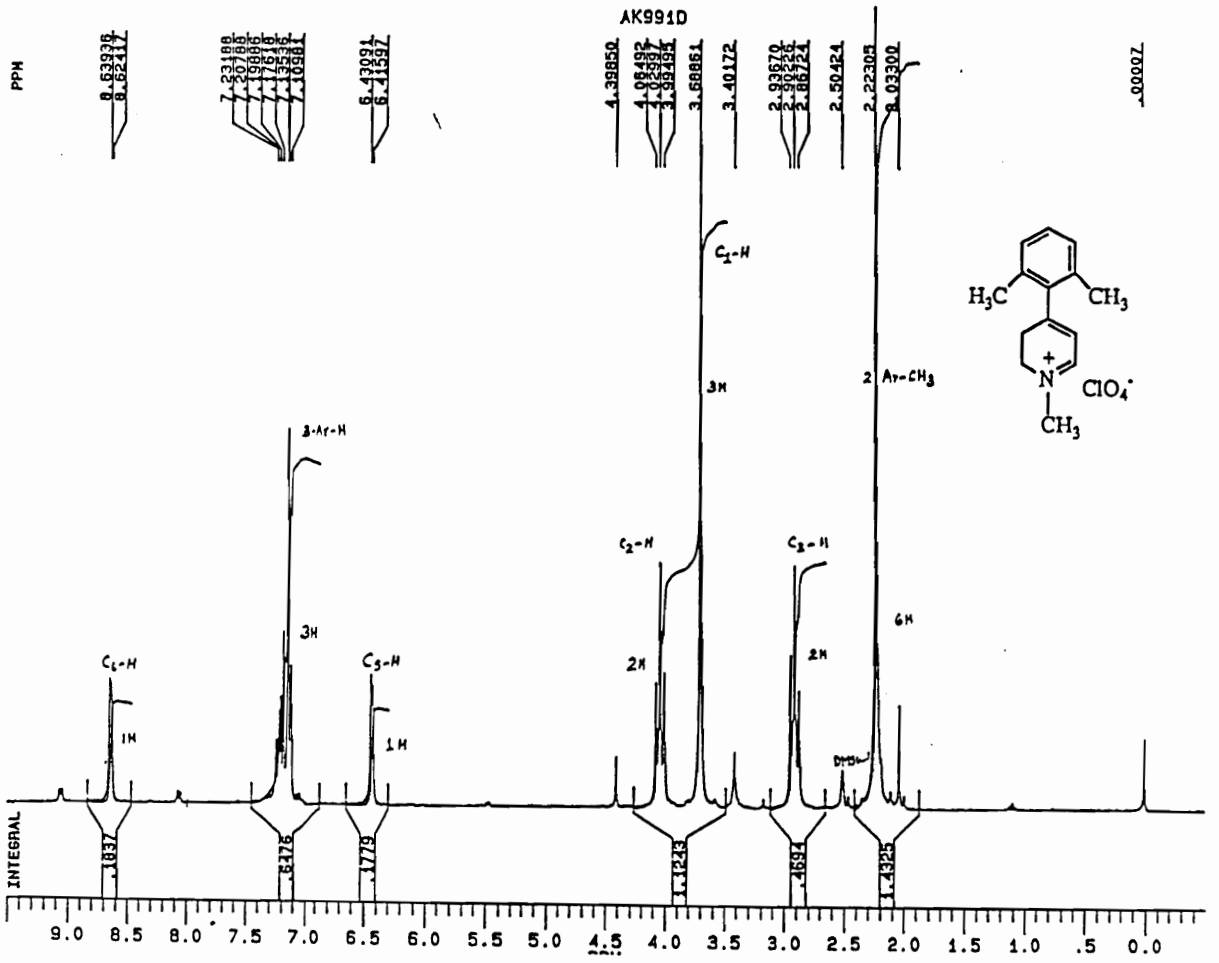

Figure. 59. ^1H NMR Spectrum (DMSO-d_6) of 4-(2,6-Dimethyl)-1-methyl-2,3-dihydropyridinium Perchlorate.

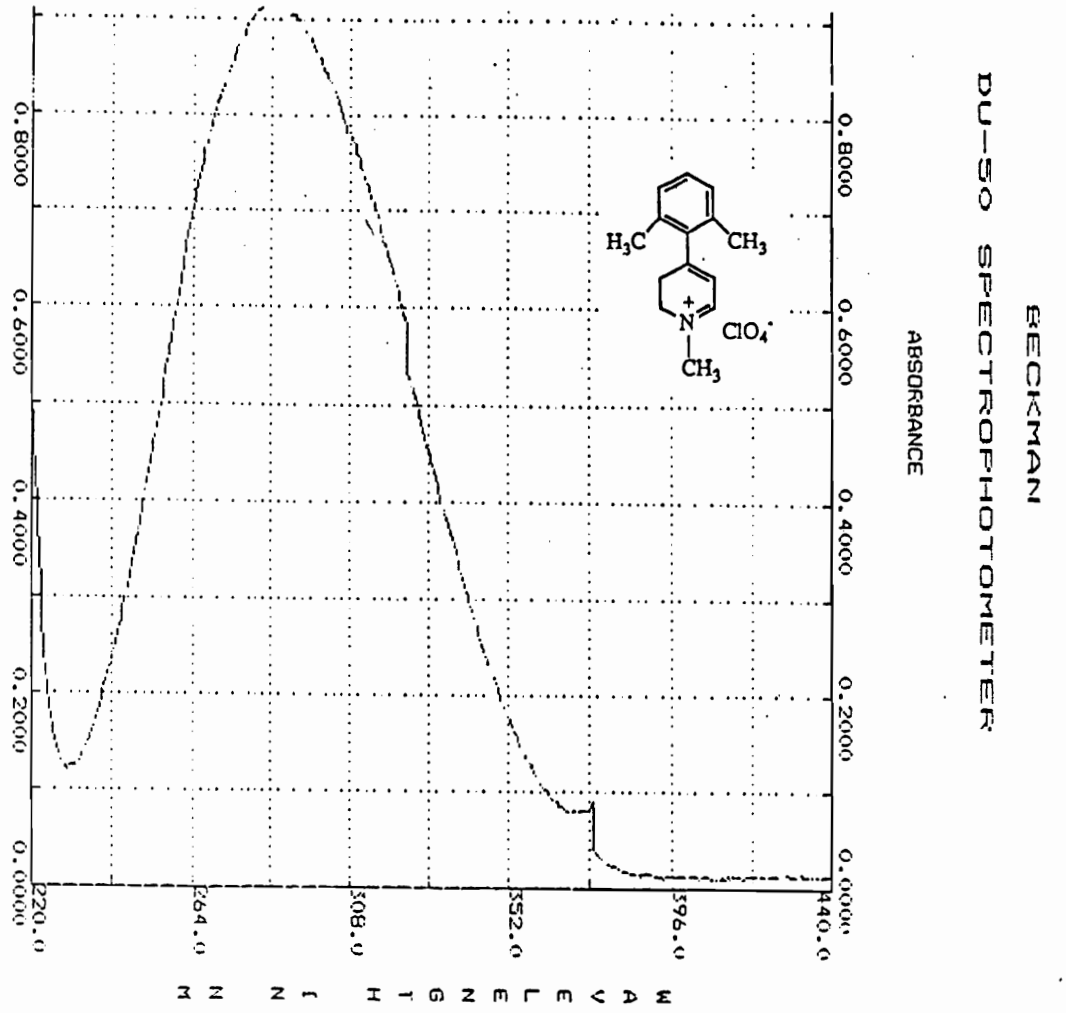

Figure. 60. UV Spectrum of 125 μM (in pH 7.4 Phosphate Buffer) 4-(2,6-Dimethylphenyl)-1-methyl-2,3-dihydropyridinium Perchlorate.

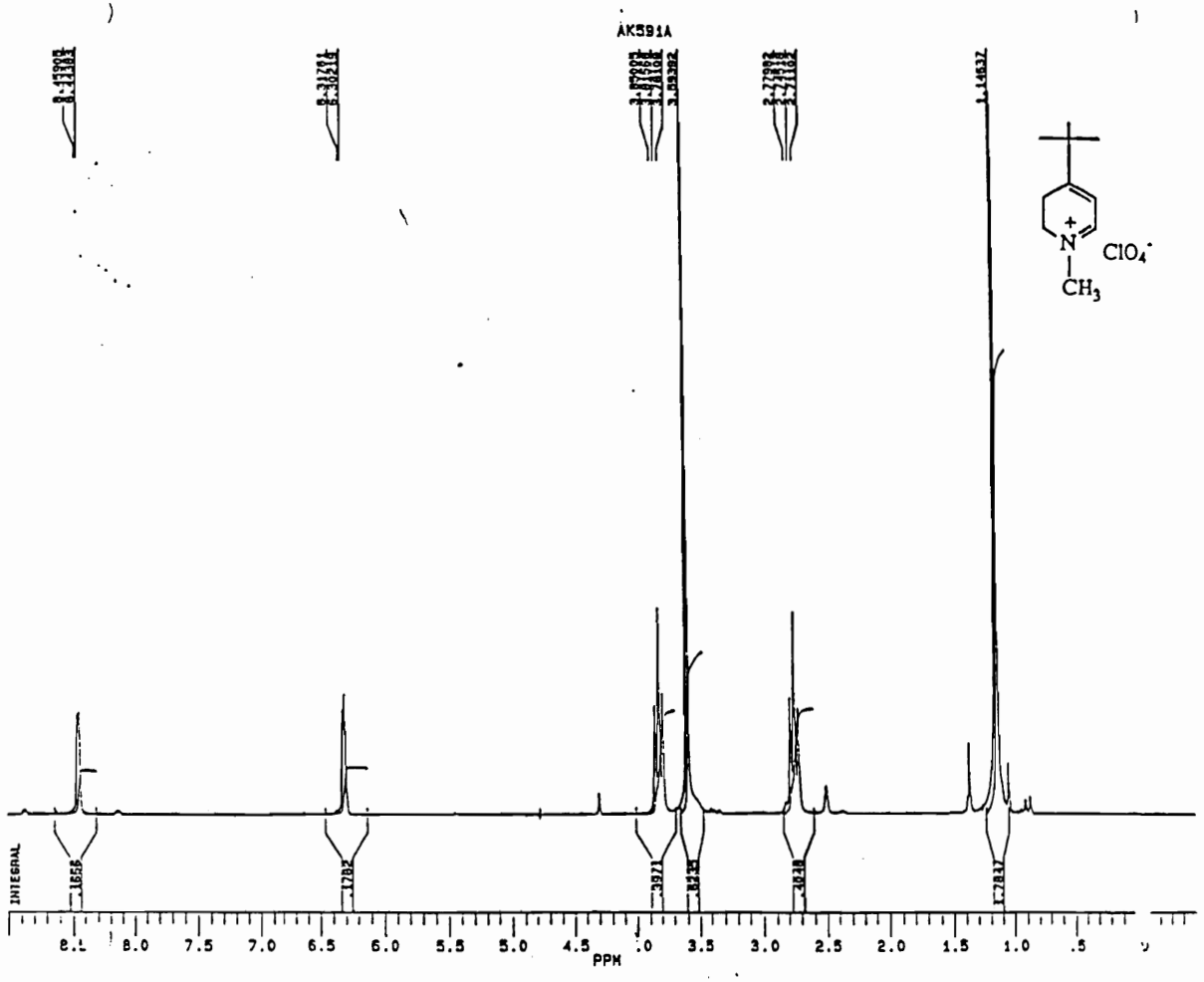

Figure. 61. ^{1}H NMR Spectrum (DMSO-d_6) of 4-*tert*-Butyl-1-methyl-2,3-dihydropyridinium Perchlorate.

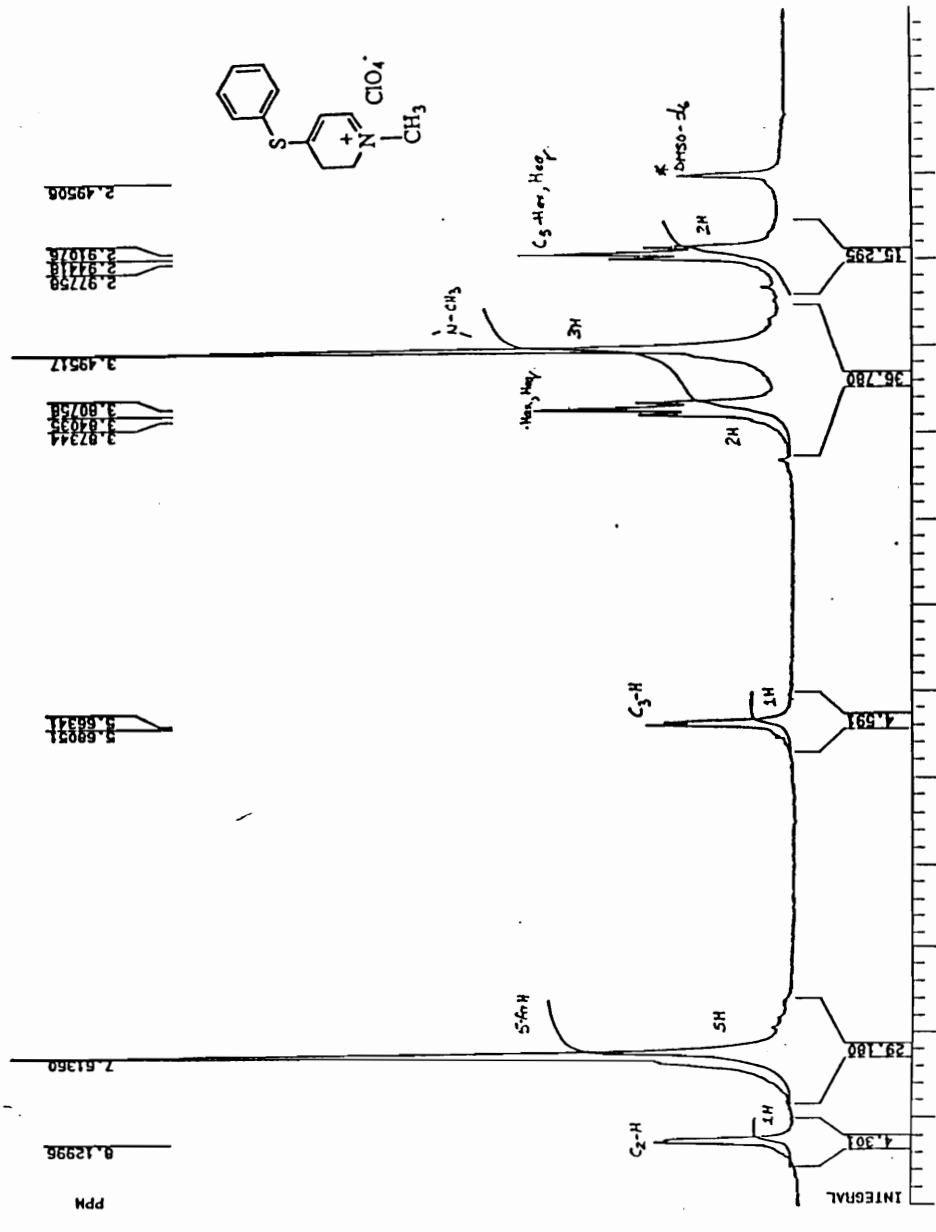

Figure. 62. ^{1}H NMR Spectrum (DMSO-d_6) of 4-Thiophenoxy-1-methyl-2,3-dihydropyridinium Perchlorate.

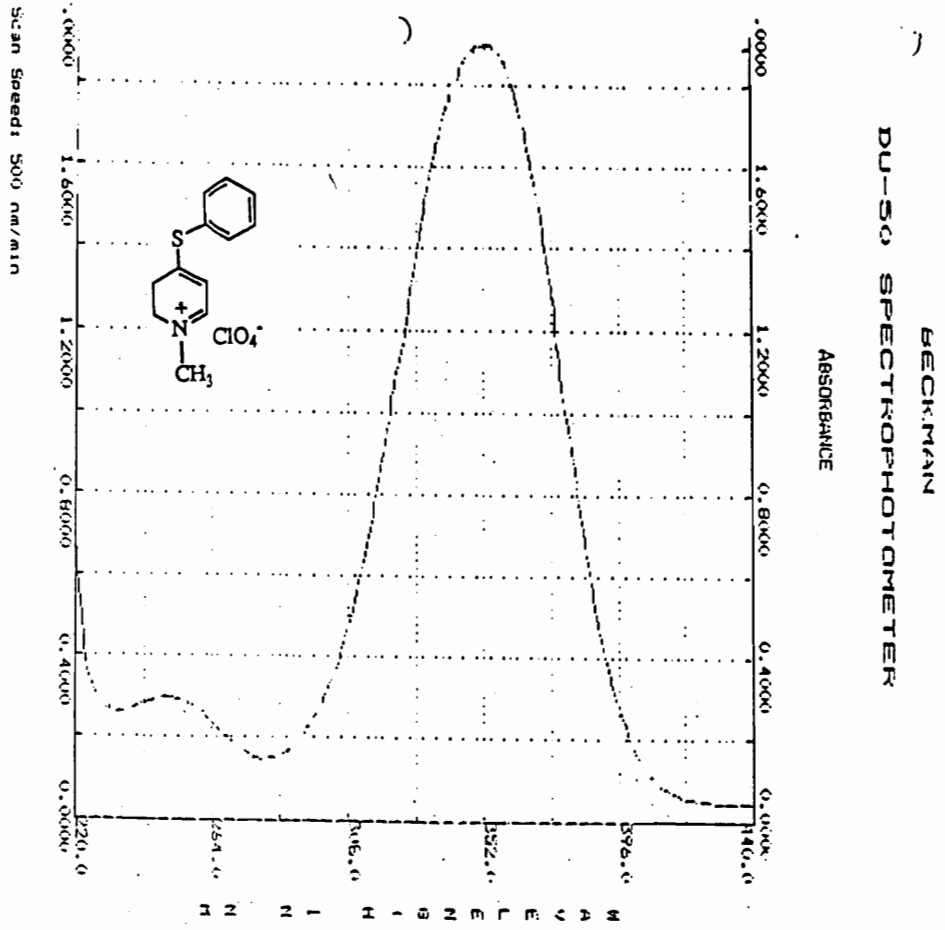

Figure. 63. UV Spectrum of 125 μM (in pH 7.4 Phosphate Buffer) 4-Thiophenoxy-1-methyl-2,3-dihydropyridinium Perchlorate.

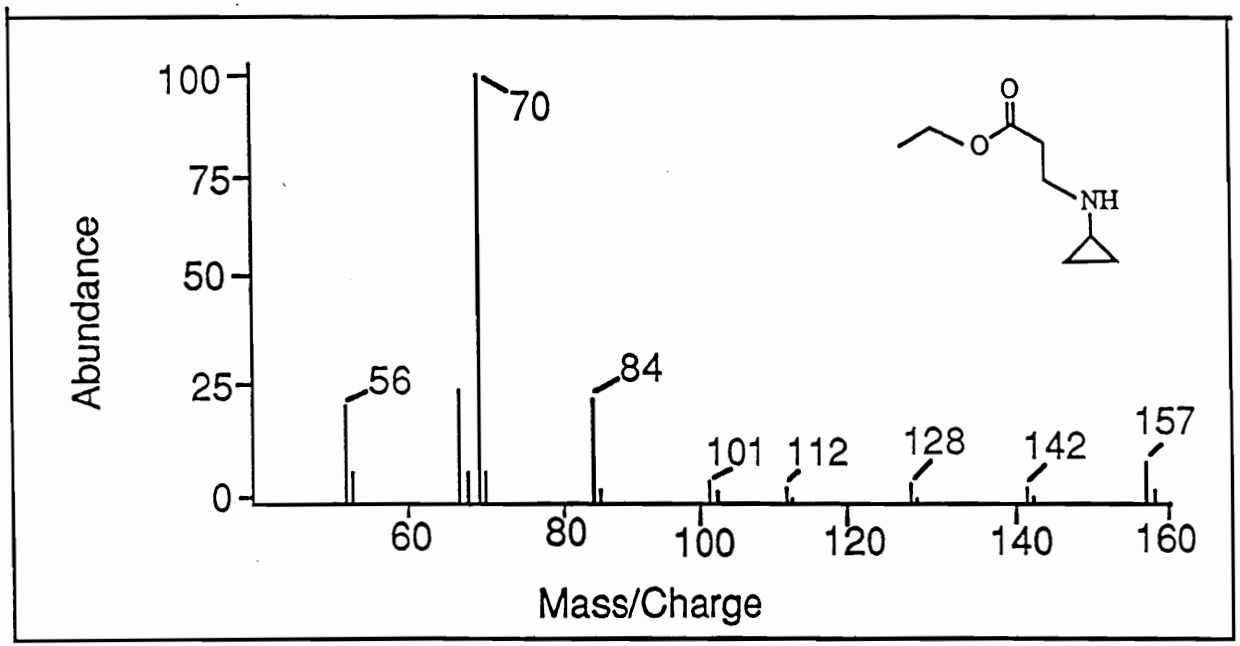

Figure. 64. GC/EIMS of the Monoalkylated Product 251.

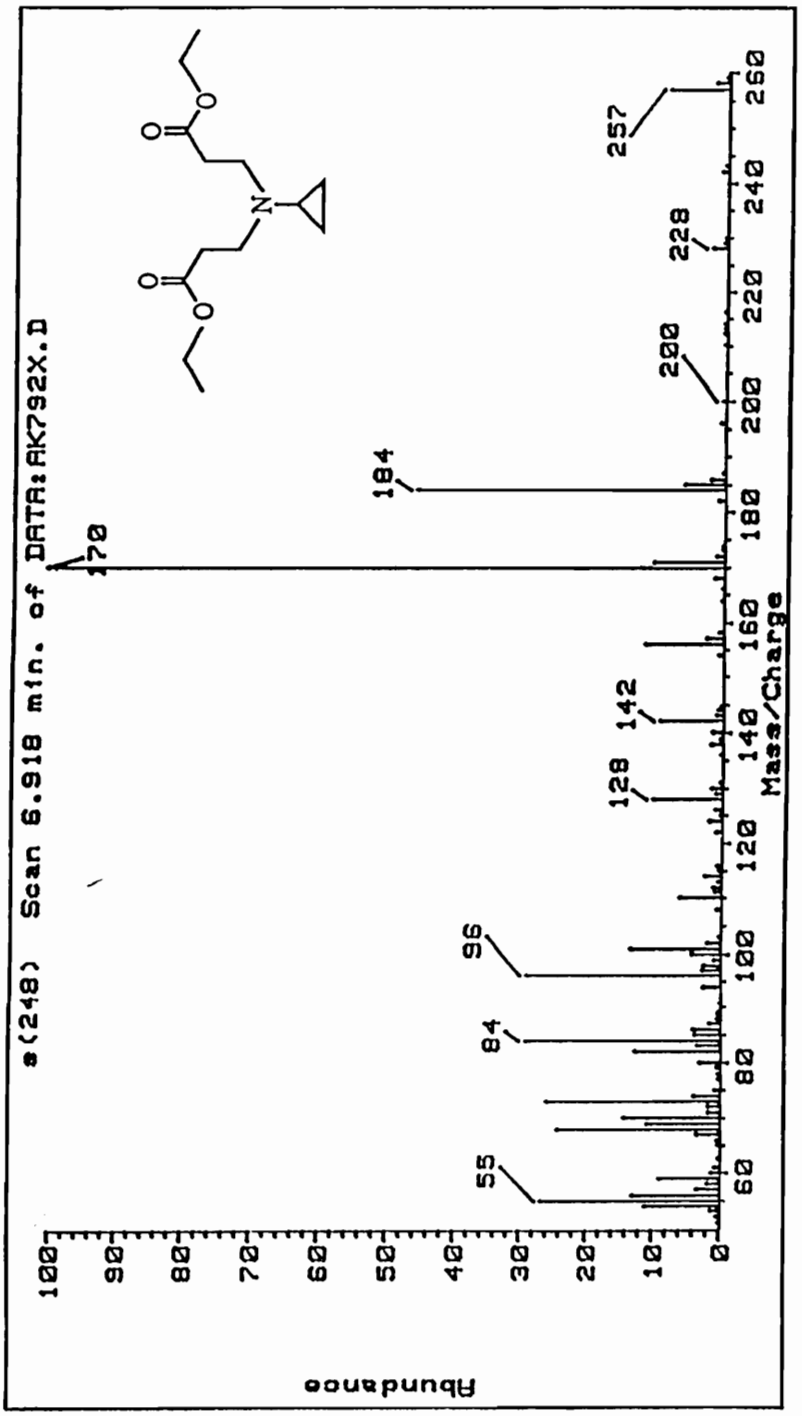

Figure. 65. GC/EIMS of the Bisalkylated Product 250.

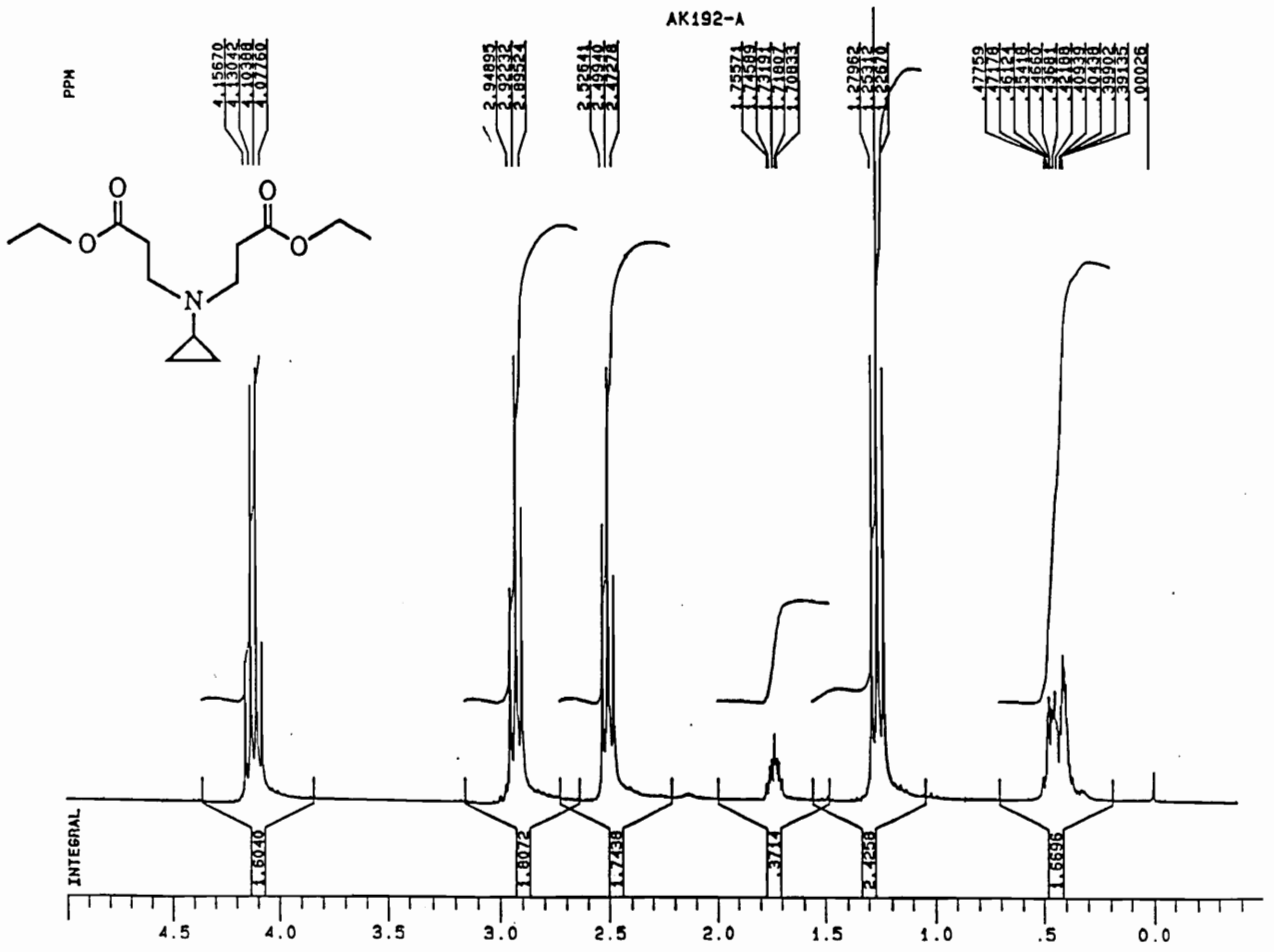

Figure. 66. ^{1}H NMR Spectrum ($CDCl_3$) of the Bisalkylated Product 250.

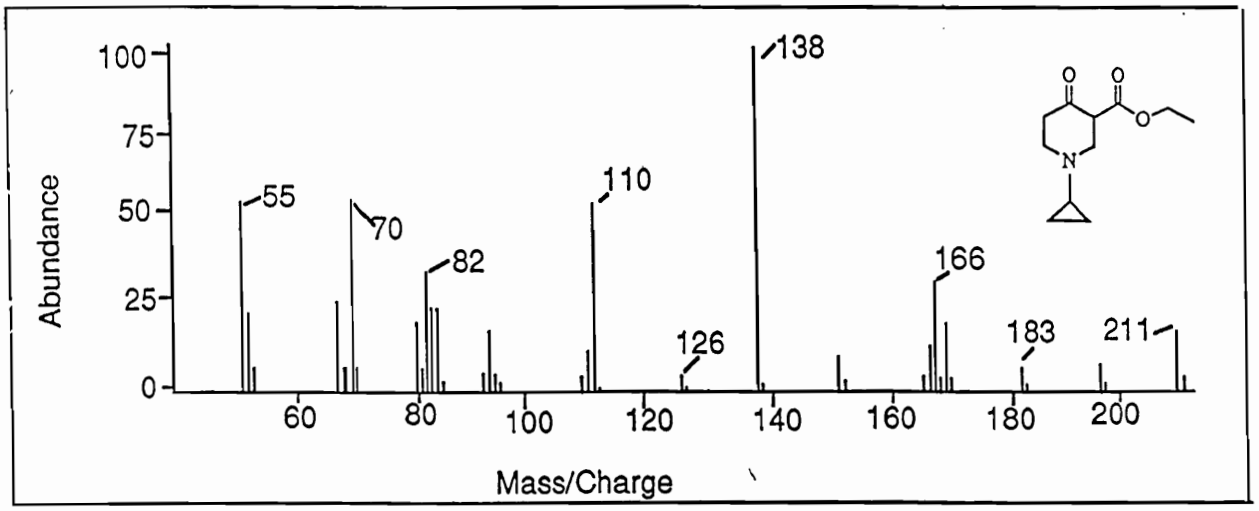

Figure. 67. GC/EIMS of the Cyclized Product 252.

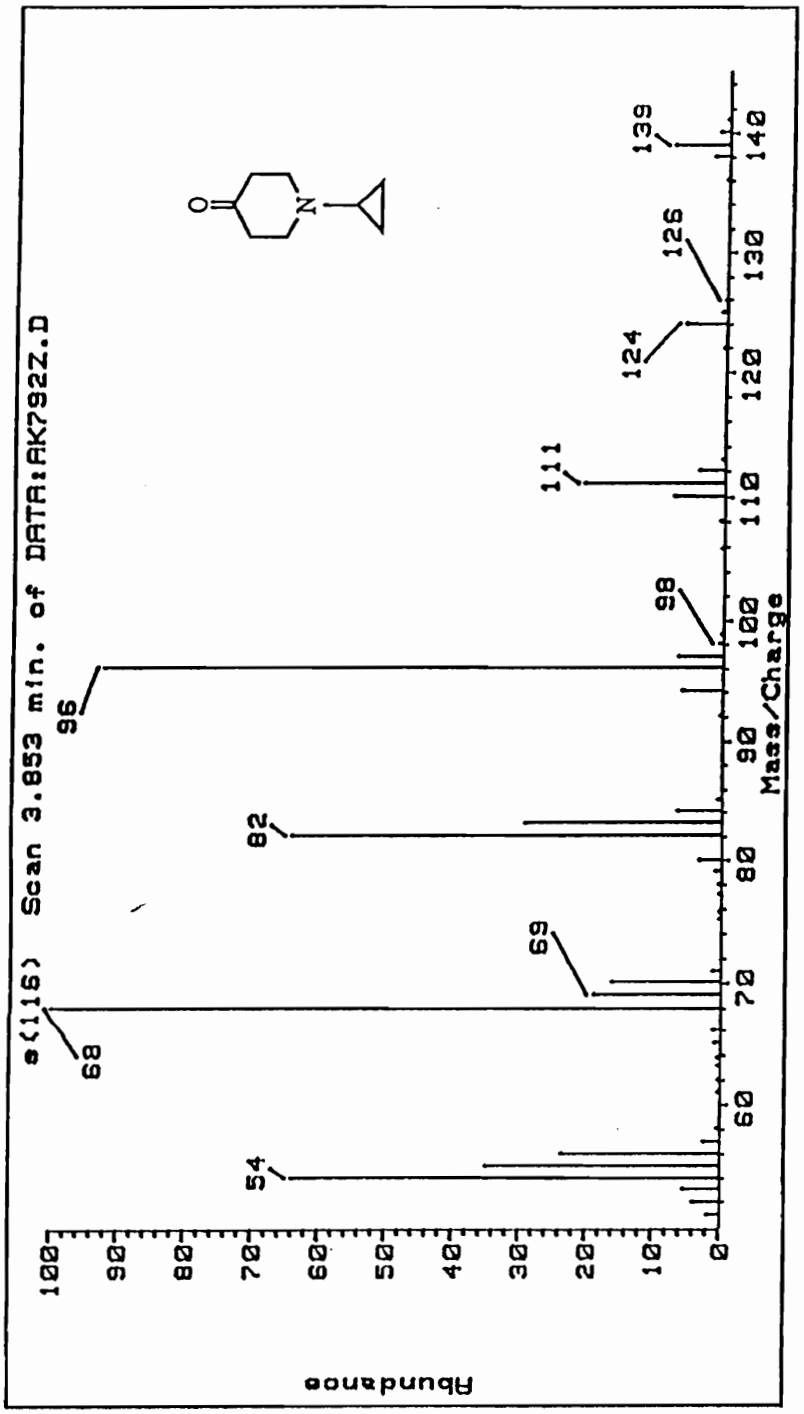

Figure. 68. GC/EIMS of 1-Cyclopropylpiperidin-4-one.

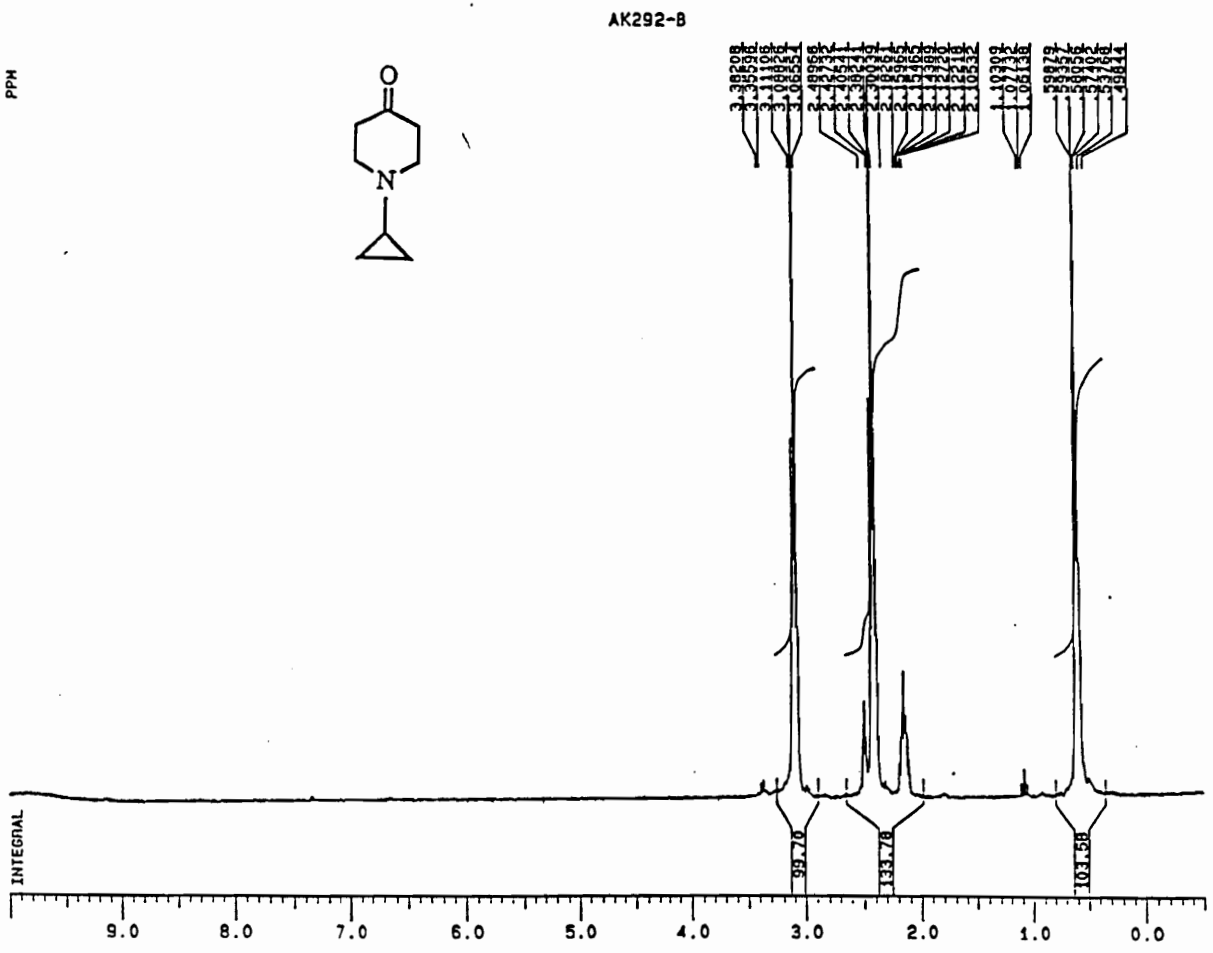

Figure. 69. ^{1}H NMR Spectrum (DMSO-d_6) of 1-Cyclopropylpiperidin-4-one.

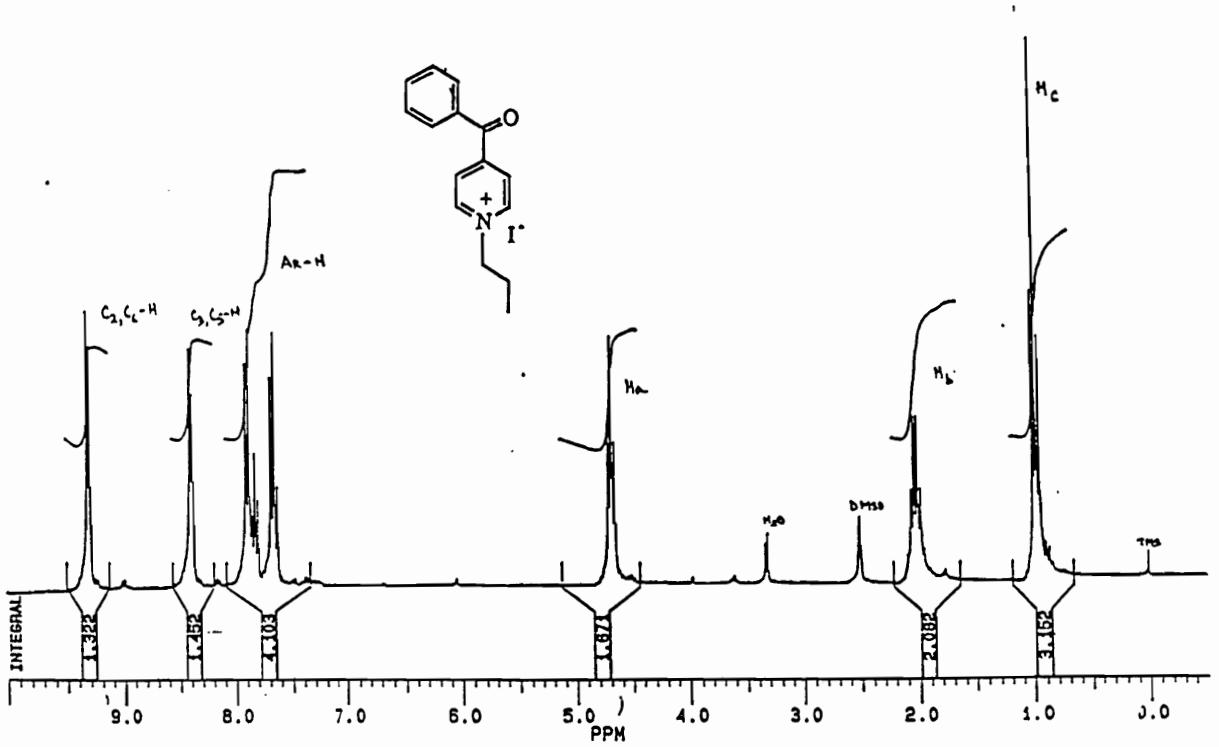

Figure. 70. ^{1}H NMR Spectrum (DMSO-d_6) of 4-Benzoyl-1-propylpyridinium Iodide (256).

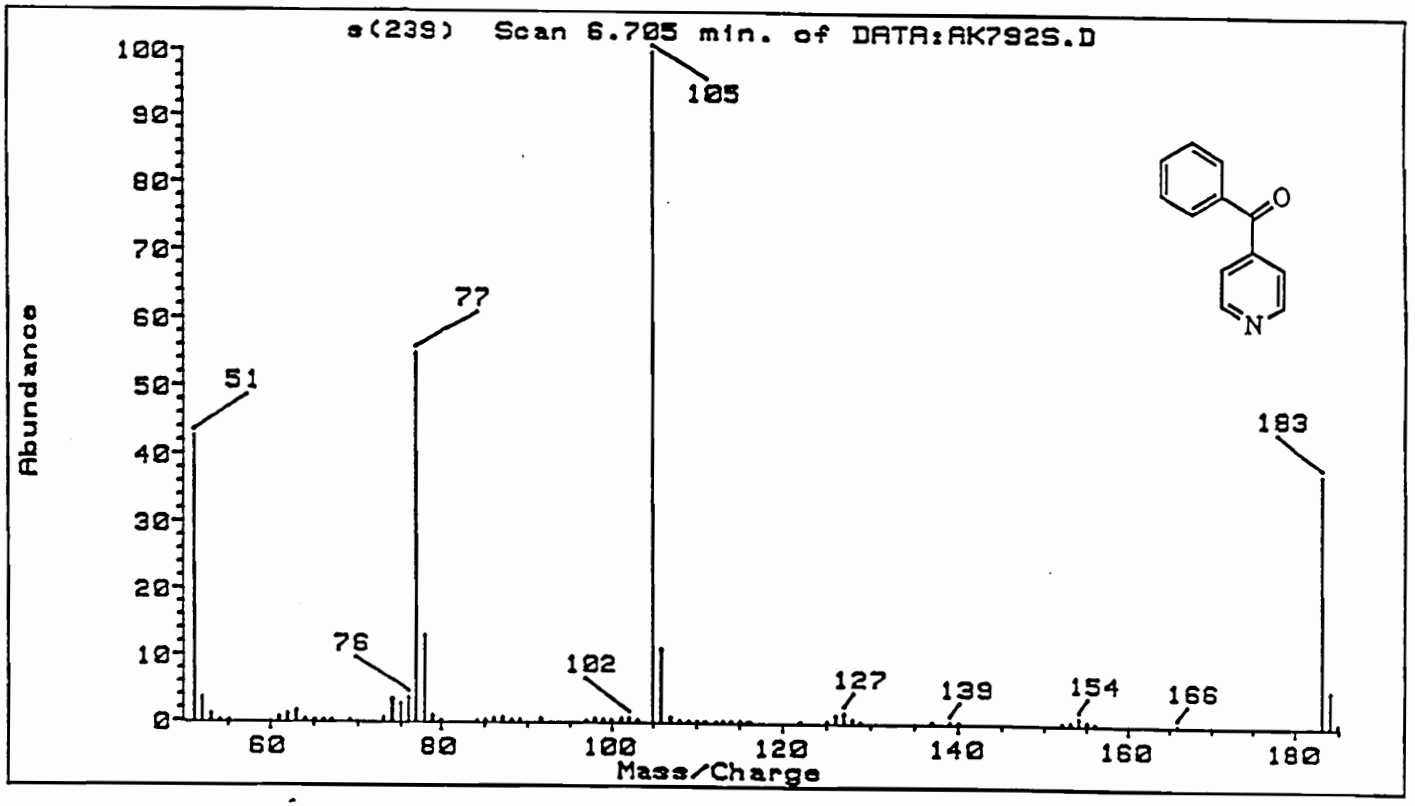

Figure. 71. GC/EIMS of the Thermally Dealkylated Product from 256.

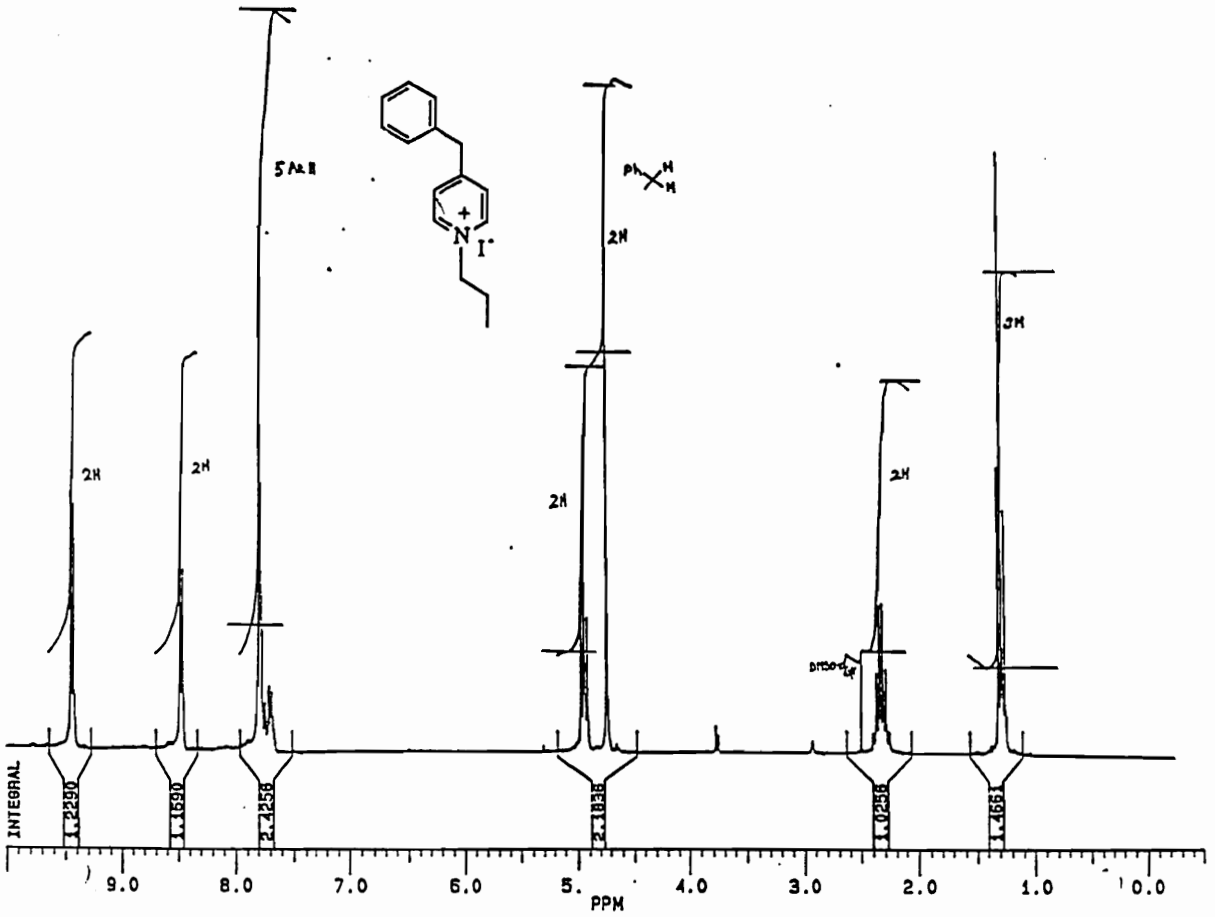

Figure. 72. ^{1}H NMR Spectrum (DMSO-d_6) of 4-Benzyl-1-propylpyridinium Iodide.

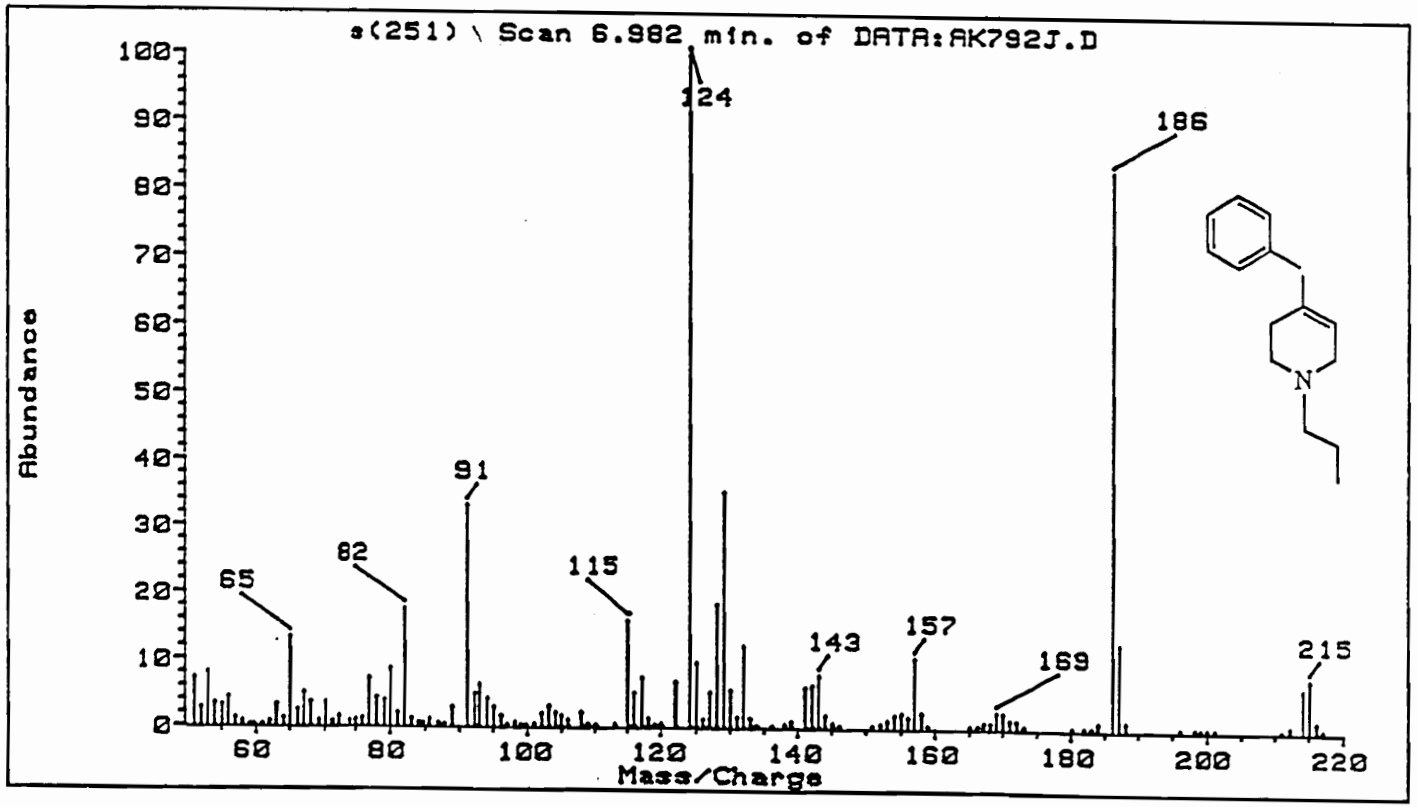

Figure. 73. GC/EIMS of 4-Benzyl-1-propyl-1,2,3,6-tetrahydropyridine.

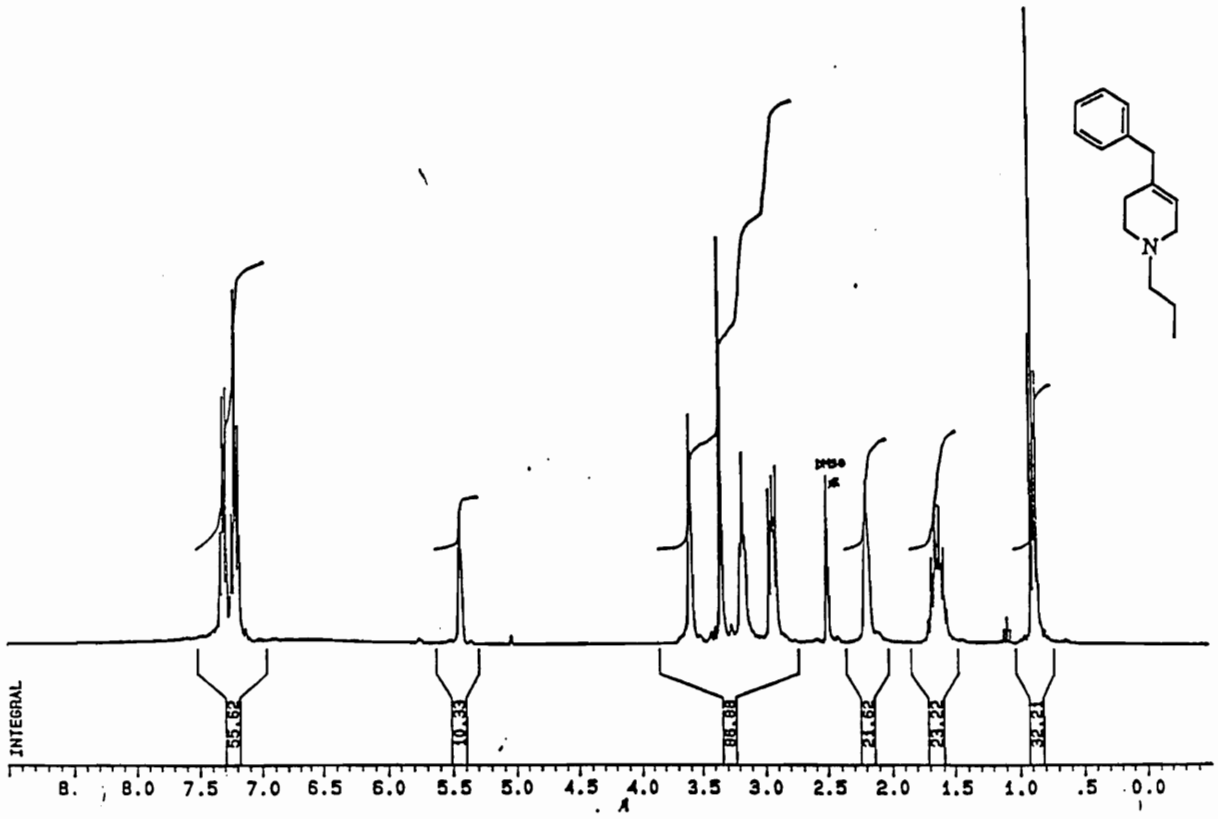

Figure. 74. ^{1}H NMR Spectrum (DMSO-d_6) of 4-Benzyl-1-propyl-1,2,3,6-tetrahydropyridine.

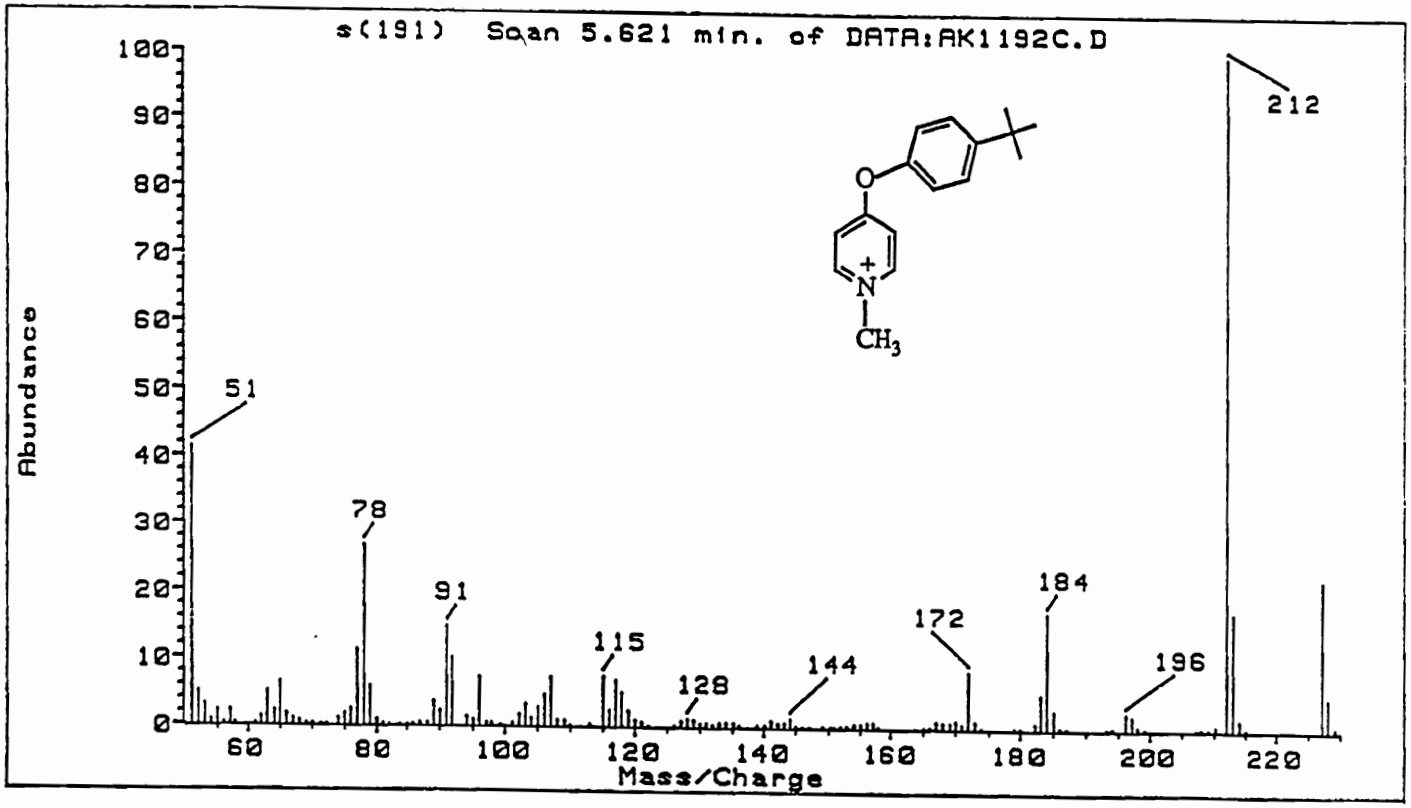

Figure. 75. GC/EIMS of 4-*tert*-Butylphenoxy-1-methylpyridinium iodide.

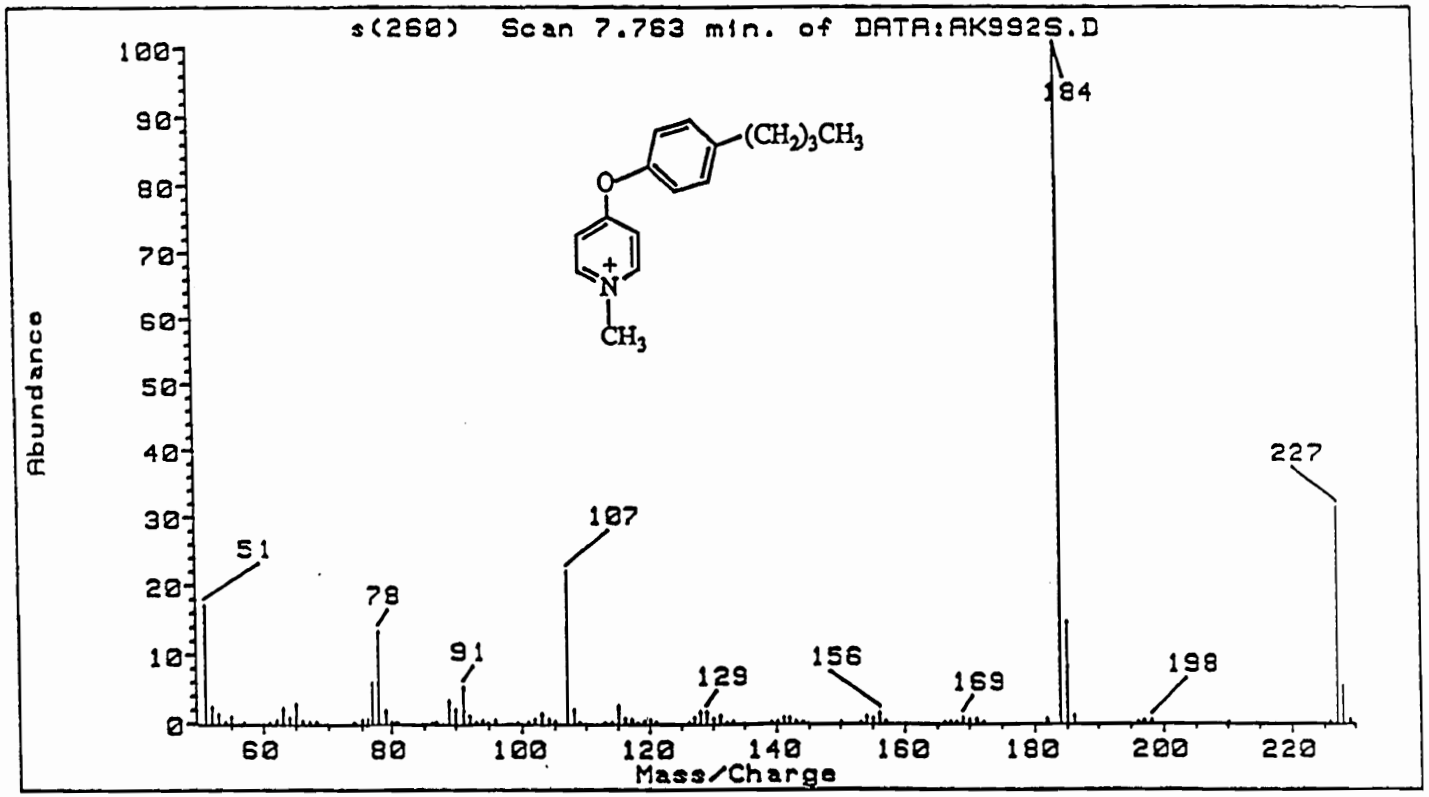

Figure. 76. GC/EIMS of 4-Butylphenoxy-1-methylpyridinium iodide.

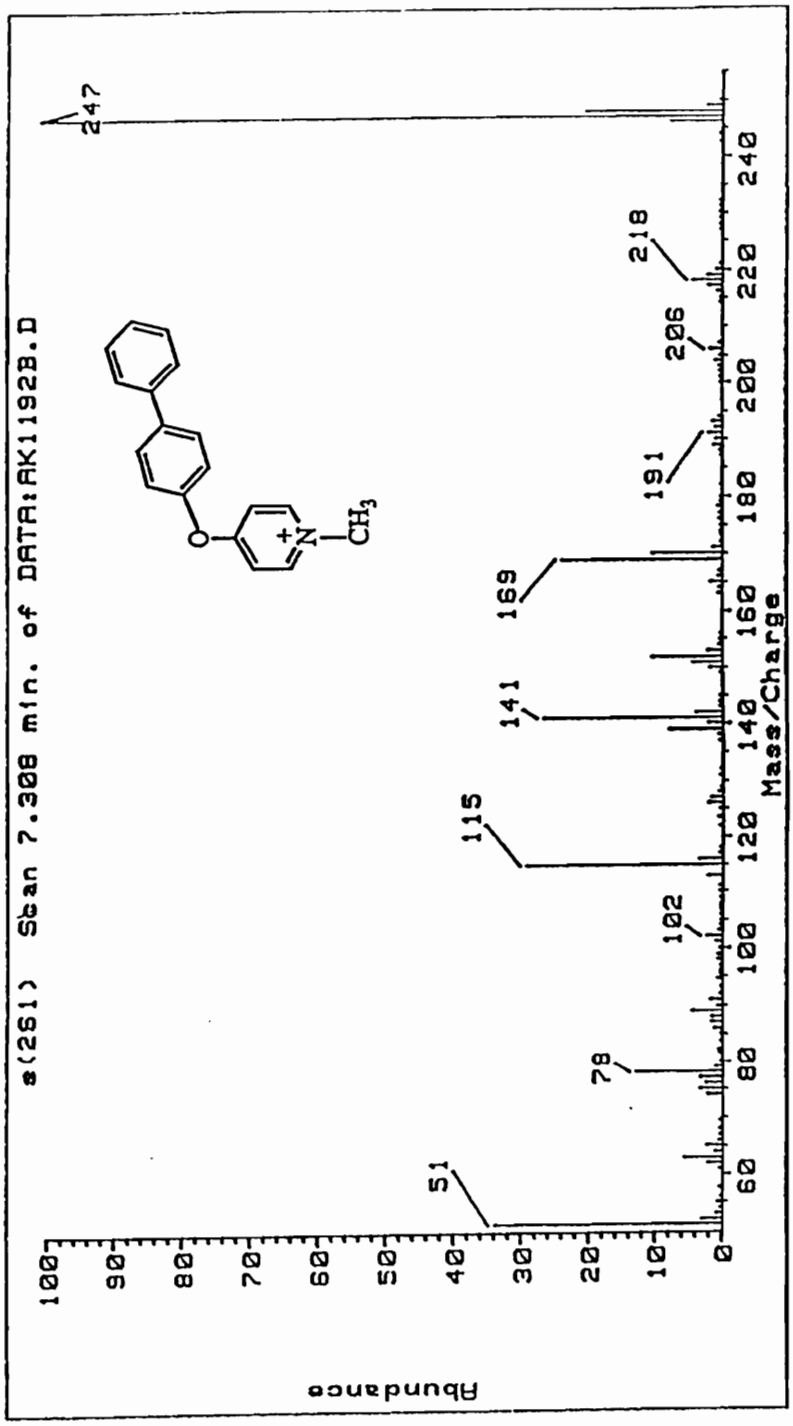

Figure. 77. GC/EIMS of 4-Phenylphenoxy-1-methylpyridinium iodide.

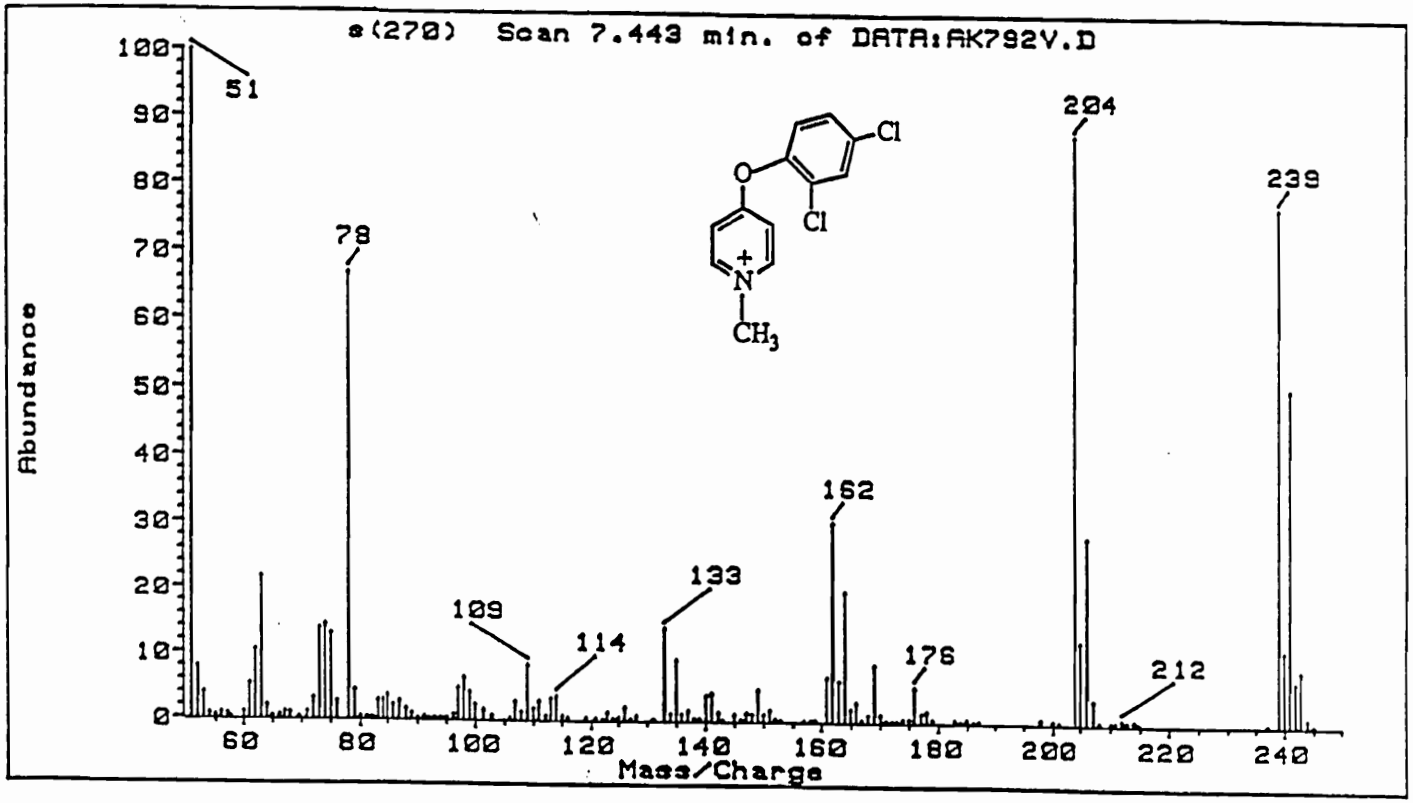

Figure. 78. GC/EIMS of 4-(2,4-Dichlorophenoxy)-1-methylpyridinium iodide.

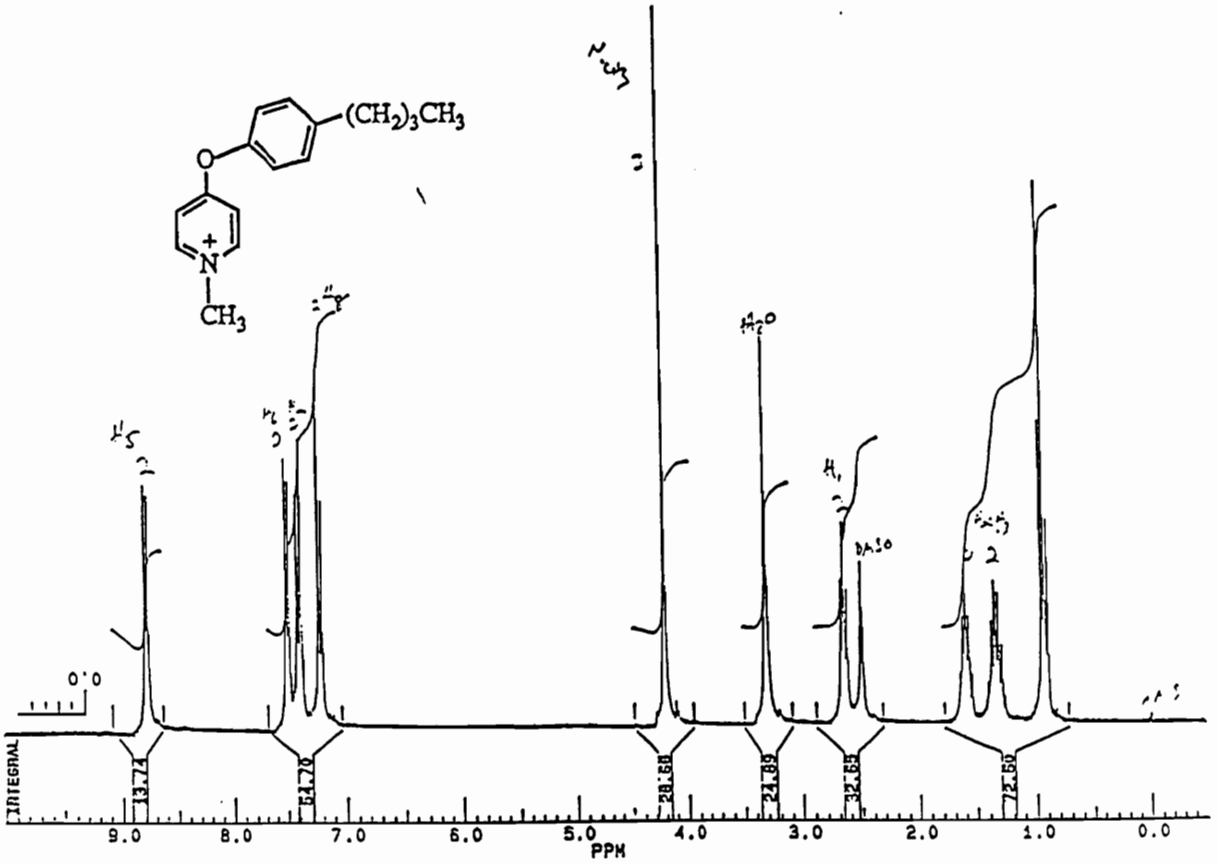

Figure. 79. ^{1}H NMR Spectrum (DMSO-d_6) of 4-Butylphenoxy-1-methylpyridinium Iodide.

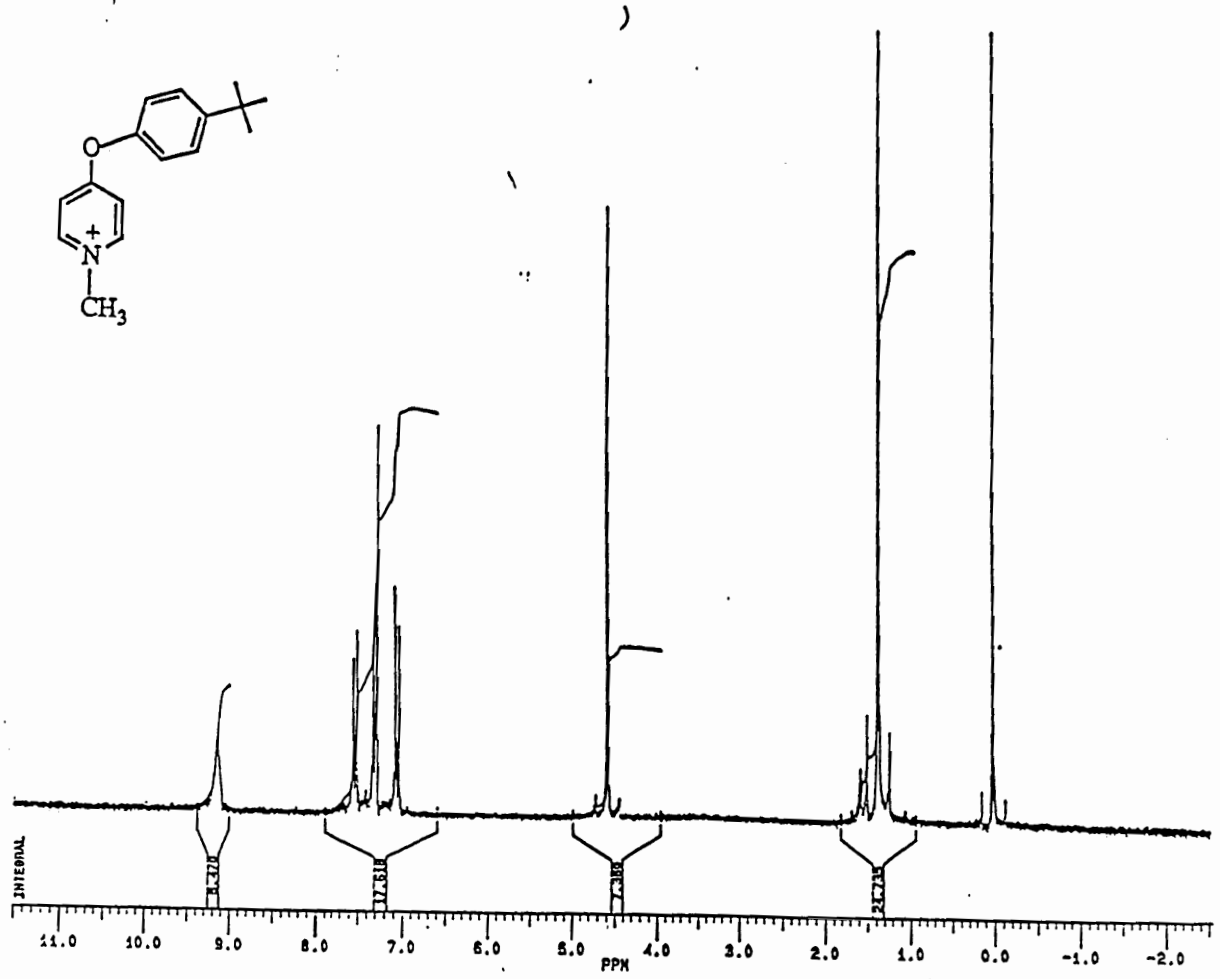

Figure. 80. ^{1}H NMR Spectrum (DMSO-d$_6$) of 4-*tert*-Butylphenoxy-1-methylpyridinium Iodide.

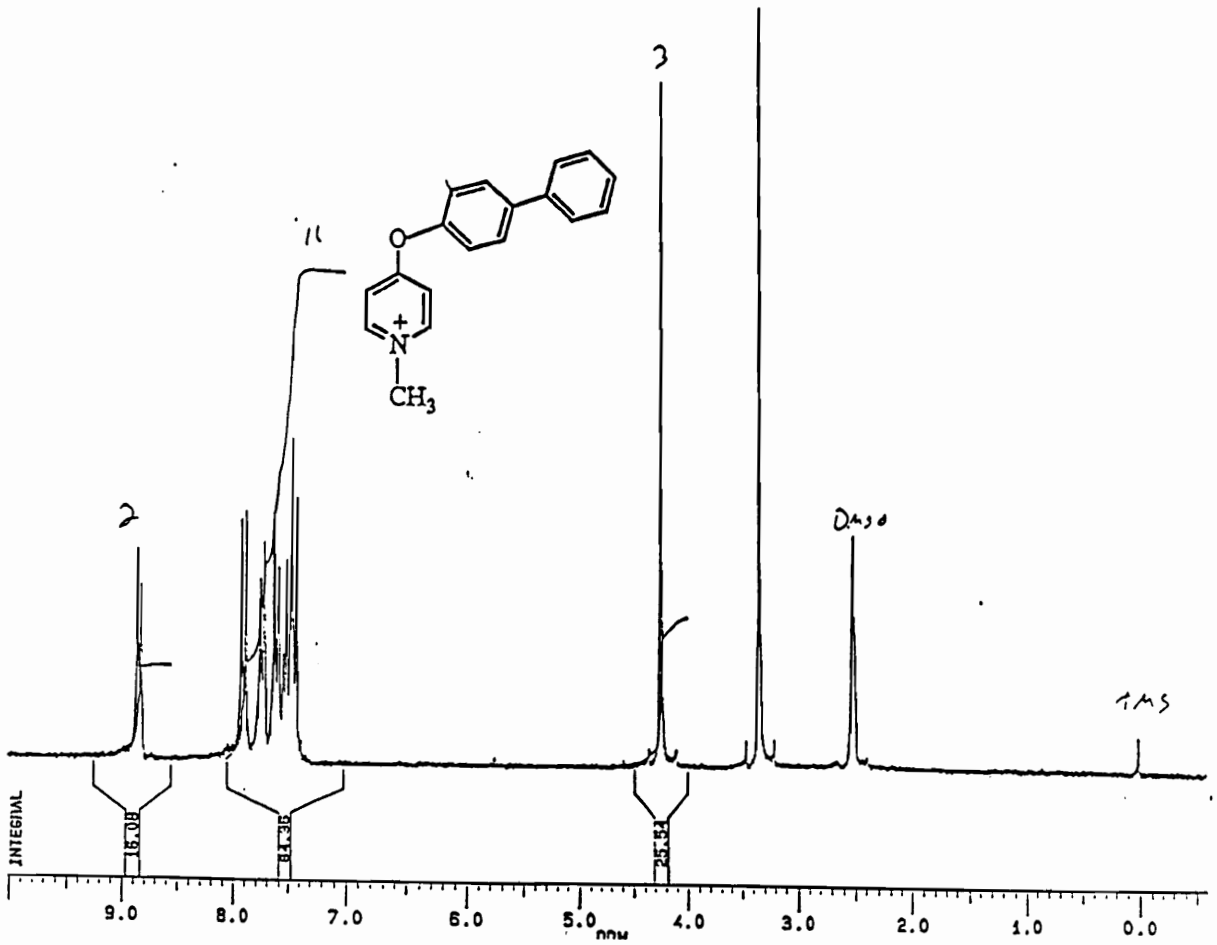

Figure. 81. ^{1}H NMR Spectrum (DMSO-d_6) of 1-Methyl-4-phenylphenoxypyridinium Iodide.

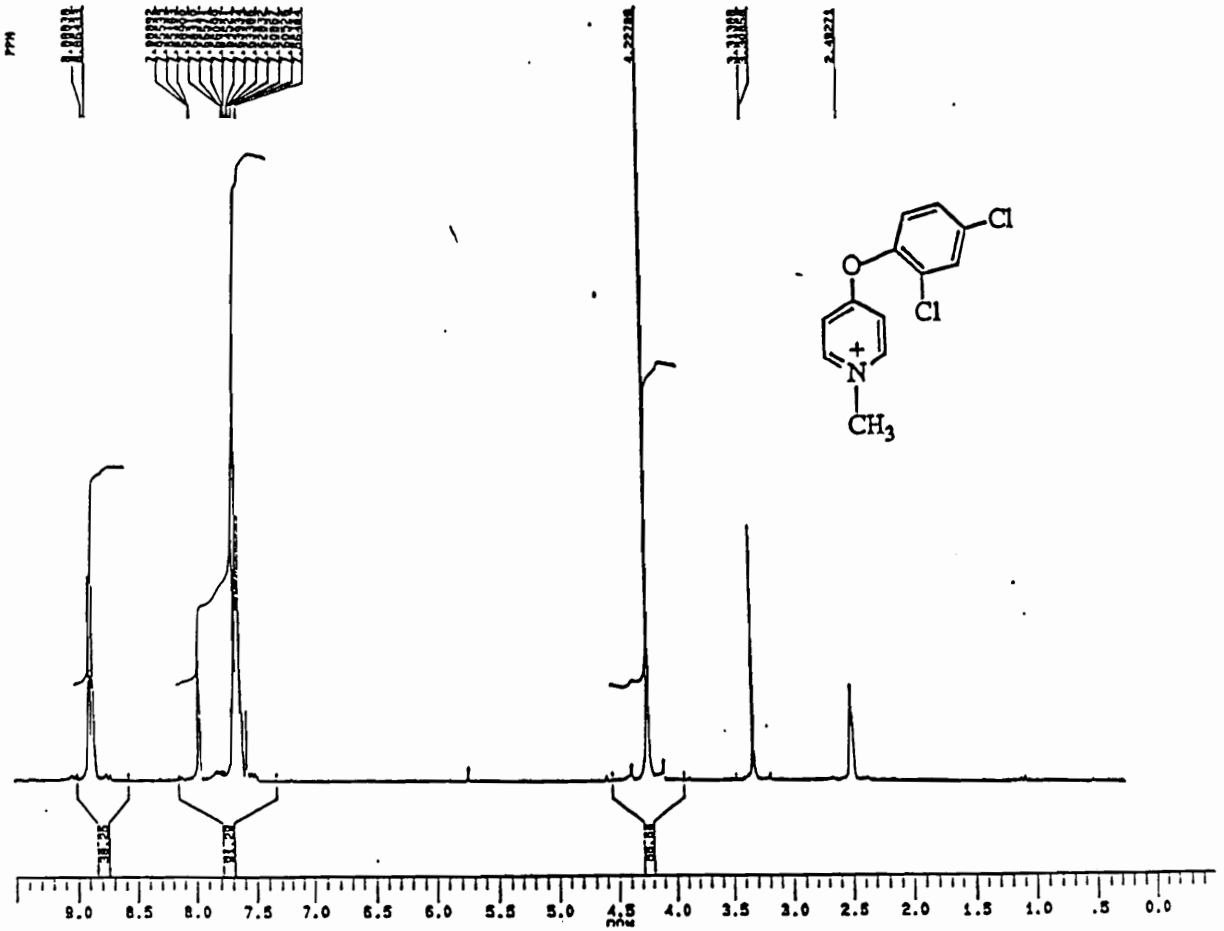

Figure. 83. ^{1}H NMR Spectrum (DMSO-d_6) of 4-(2,4-Dichlorophenoxy)-1-methylpyridinium Iodide.

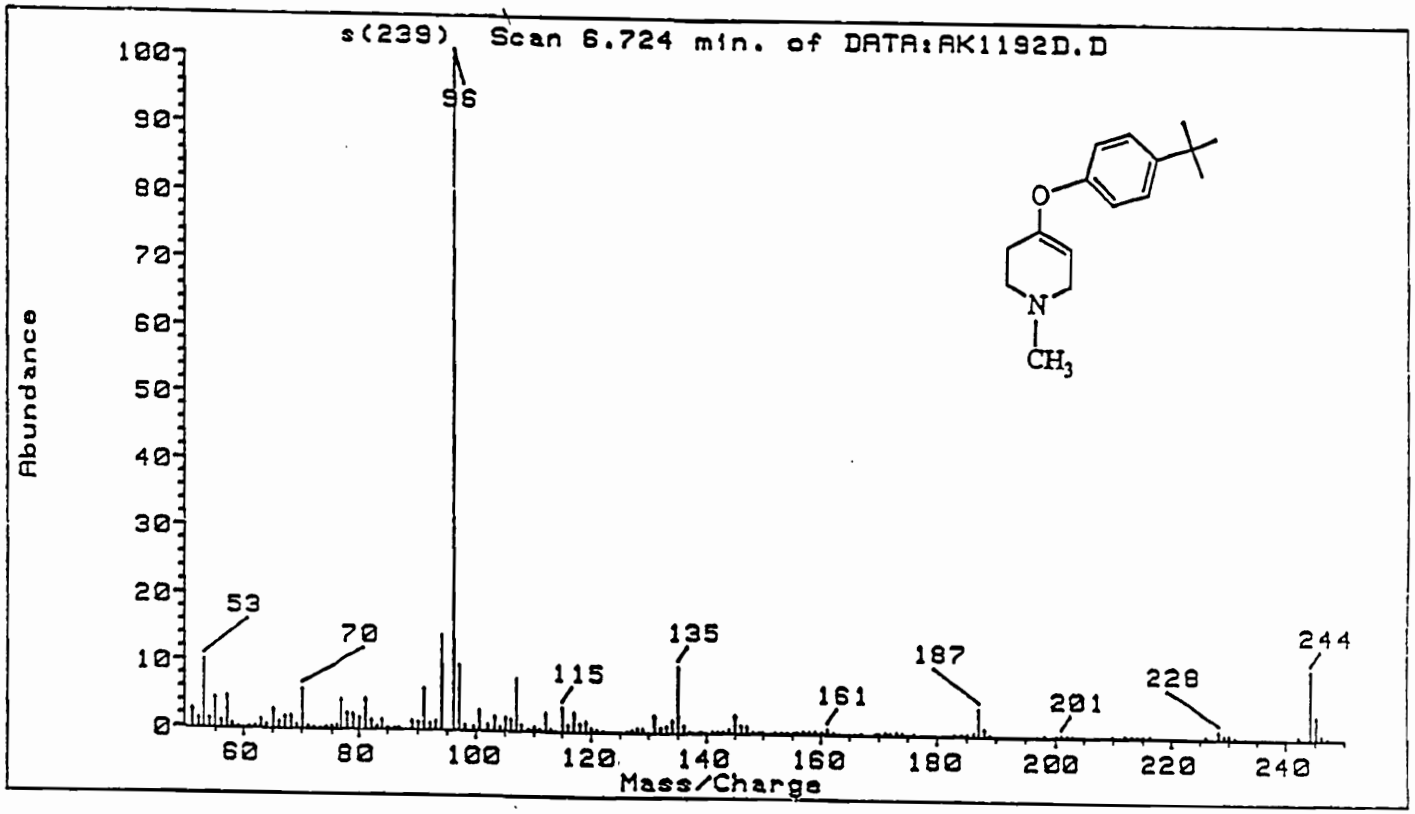

Figure. 82. GC/EIMS of 4-*tert*-Butylphenoxy-1-methyl-1,2,3,6-tetrahydropyridine.

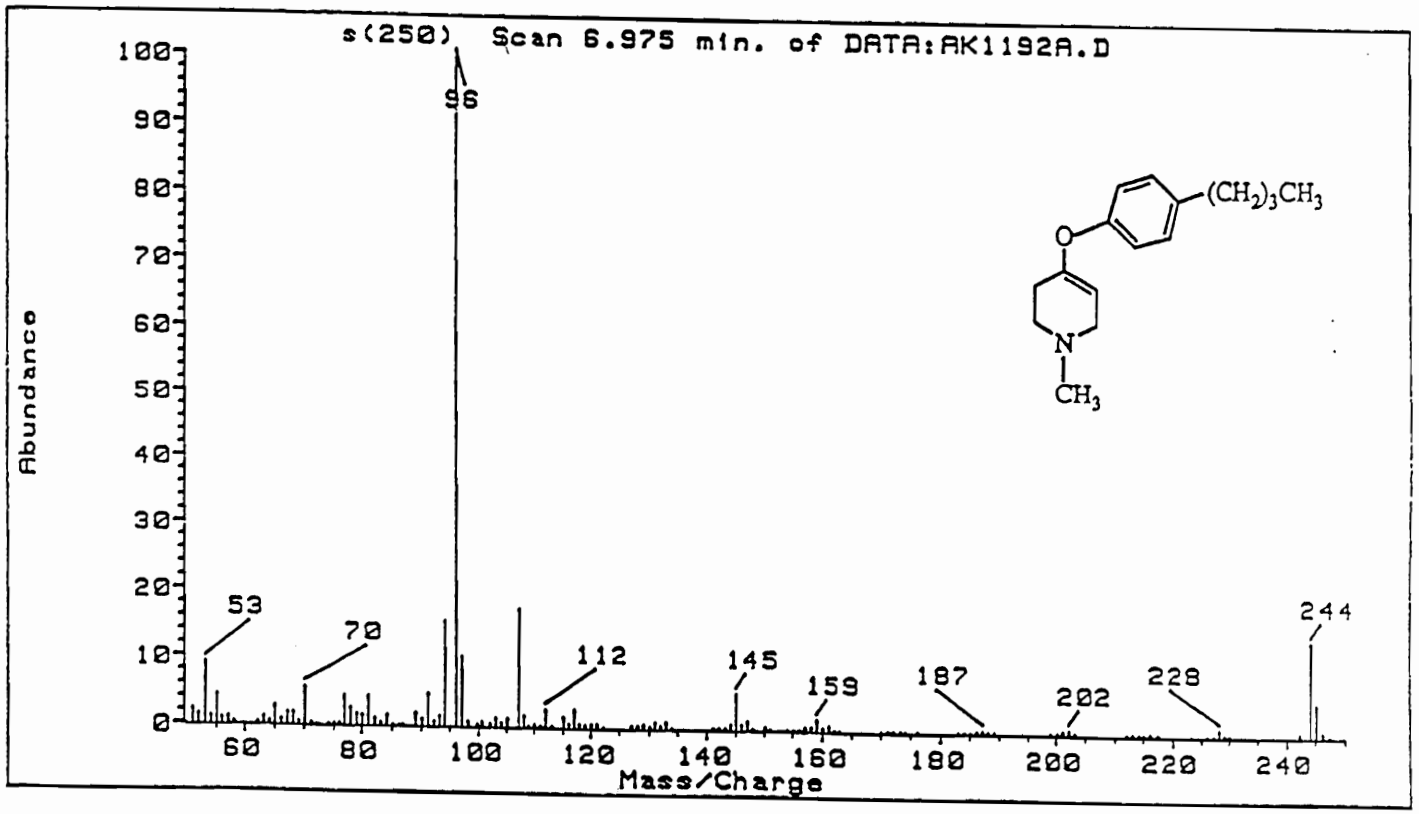

Figure. 84. GC/EIMS of 4-Butylphenoxy-1-methyl-1,2,3,6-tetrahydropyridine.

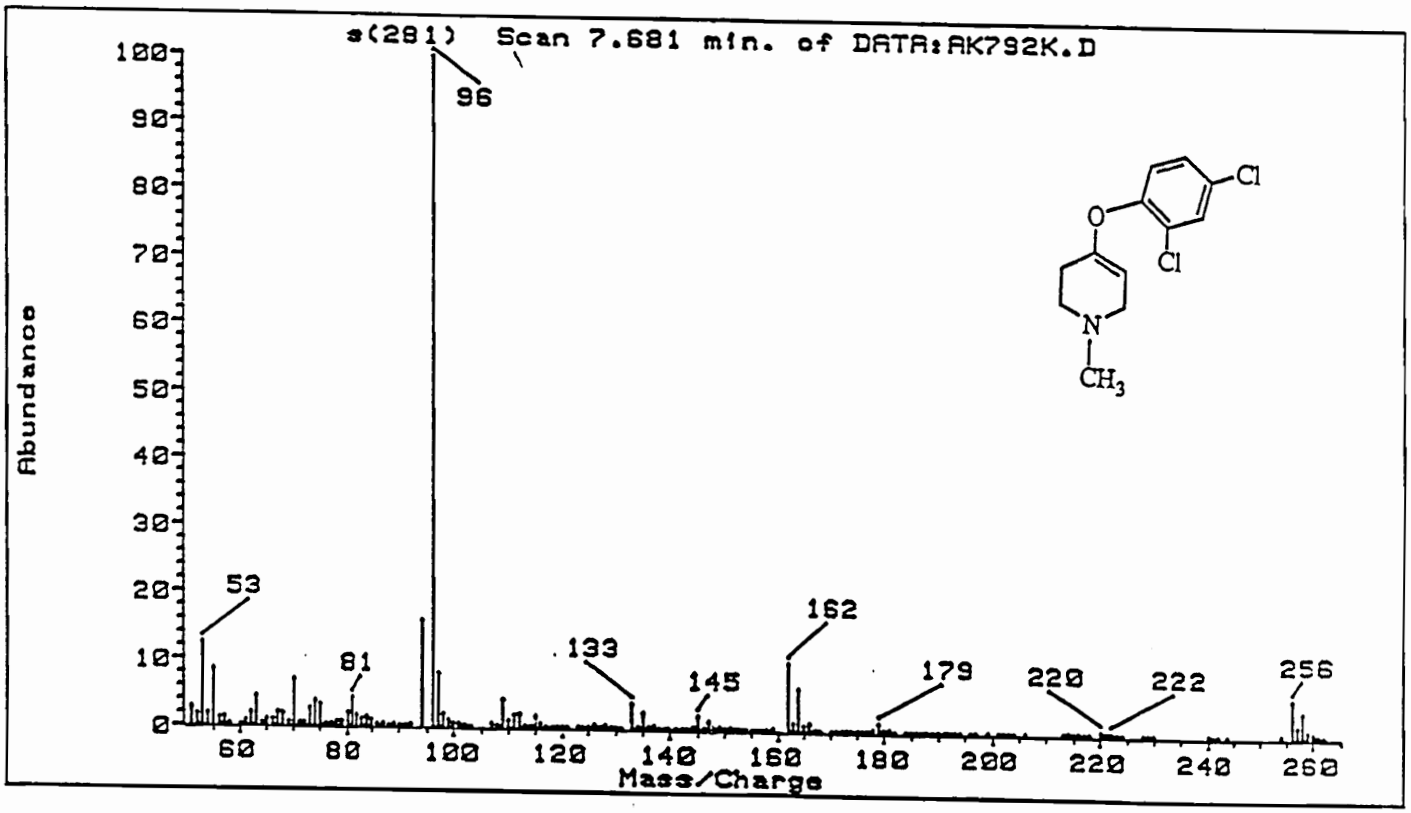

Figure. 85. GC/EIMS of 4-(2,4-Dichlorophenoxy)-1-methyl-1,2,3,6-tetrahydropyridine.

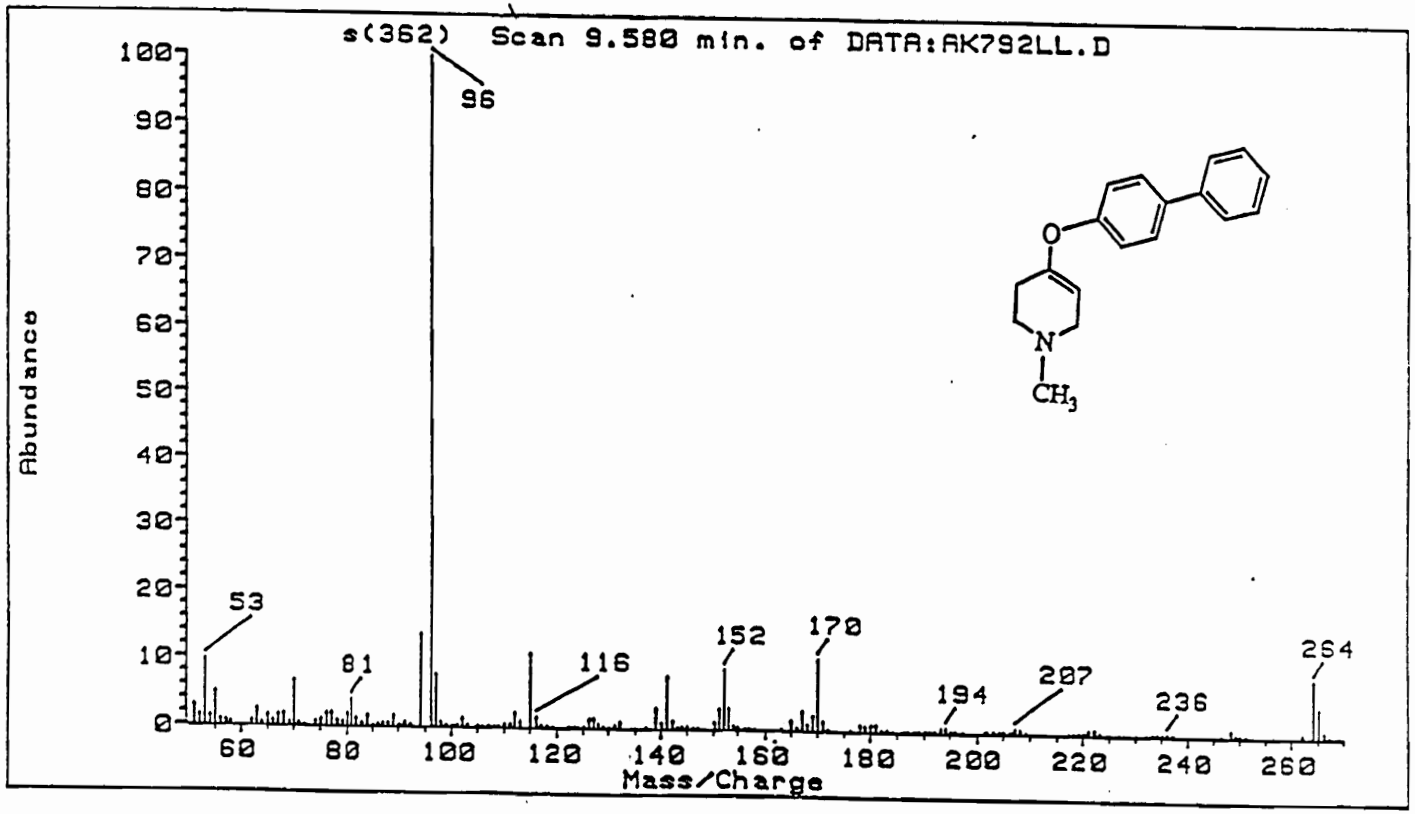

Figure. 86. GC/EIMS of 4-(Phenylphenoxy)-1-methyl-1,2,3,6-tetrahydropyridine.

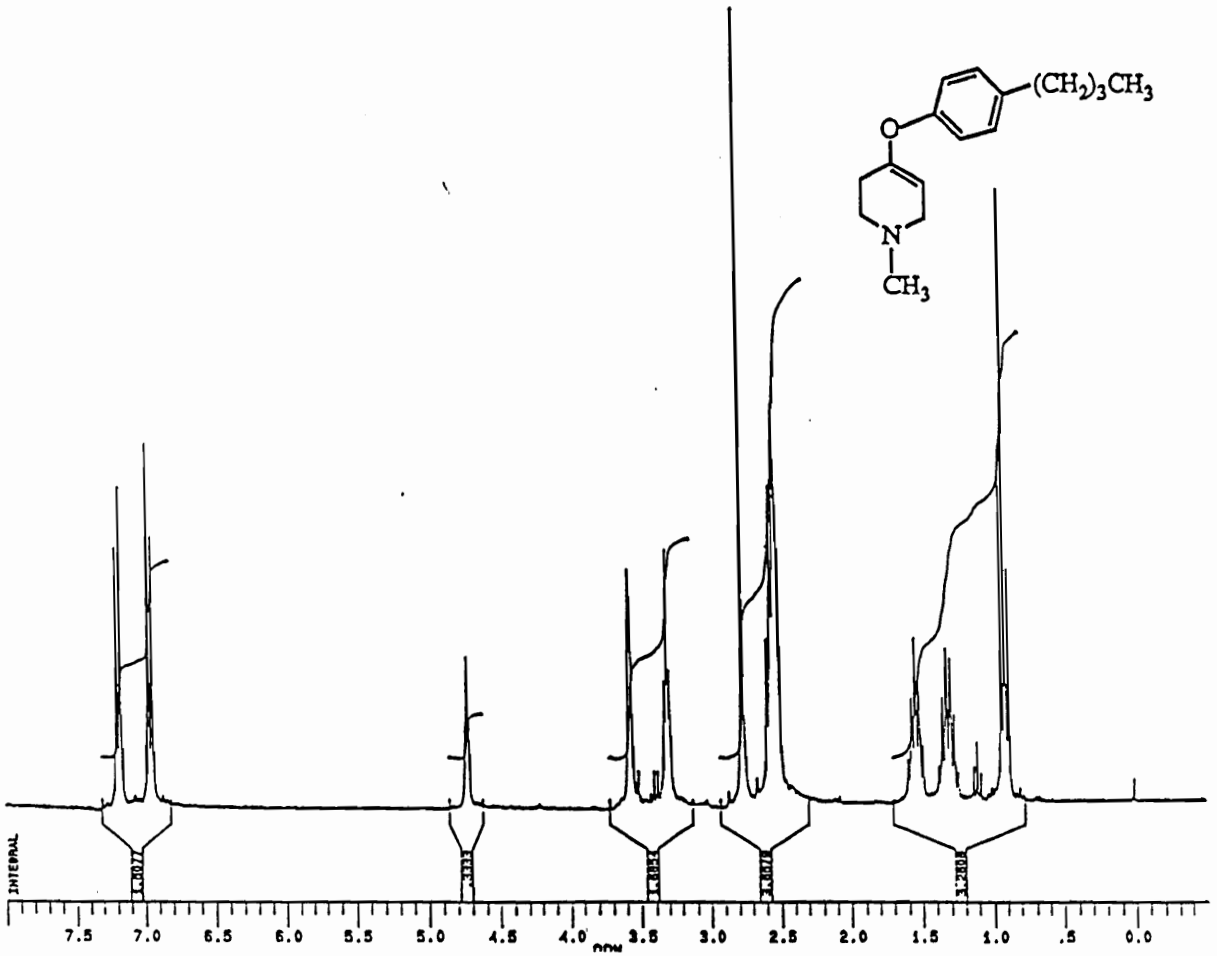

Figure. 87. ^{1}H NMR Spectrum (DMSO-d$_6$) of 4-Butylphenoxy-1-methyl-1,2,3,6-tetrahydropyridine.

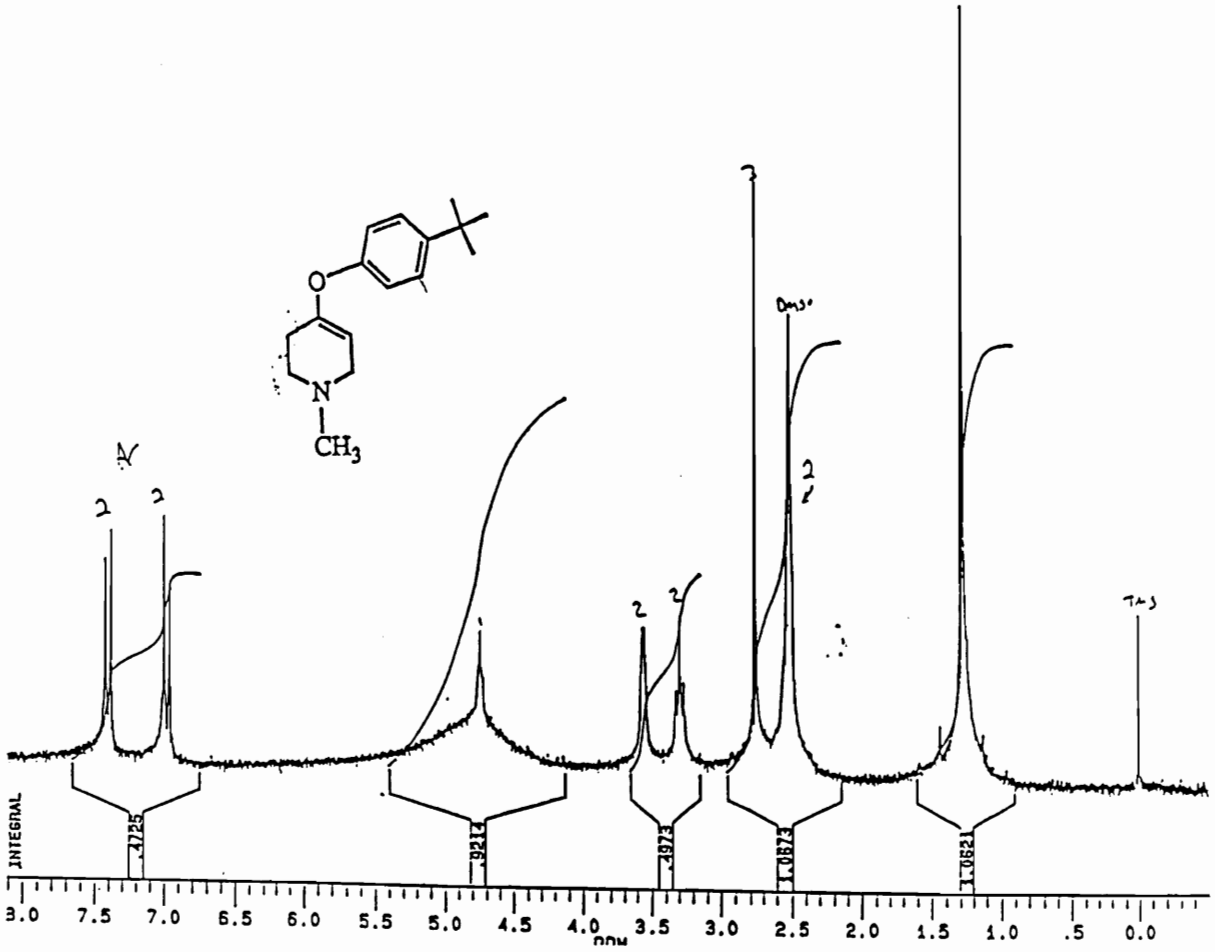

Figure. 88. ^{1}H NMR Spectrum (DMSO-d_6) of 4-*tert*-Butylphenoxy-1-methyl-1,2,3,6-tetrahydropyridine.

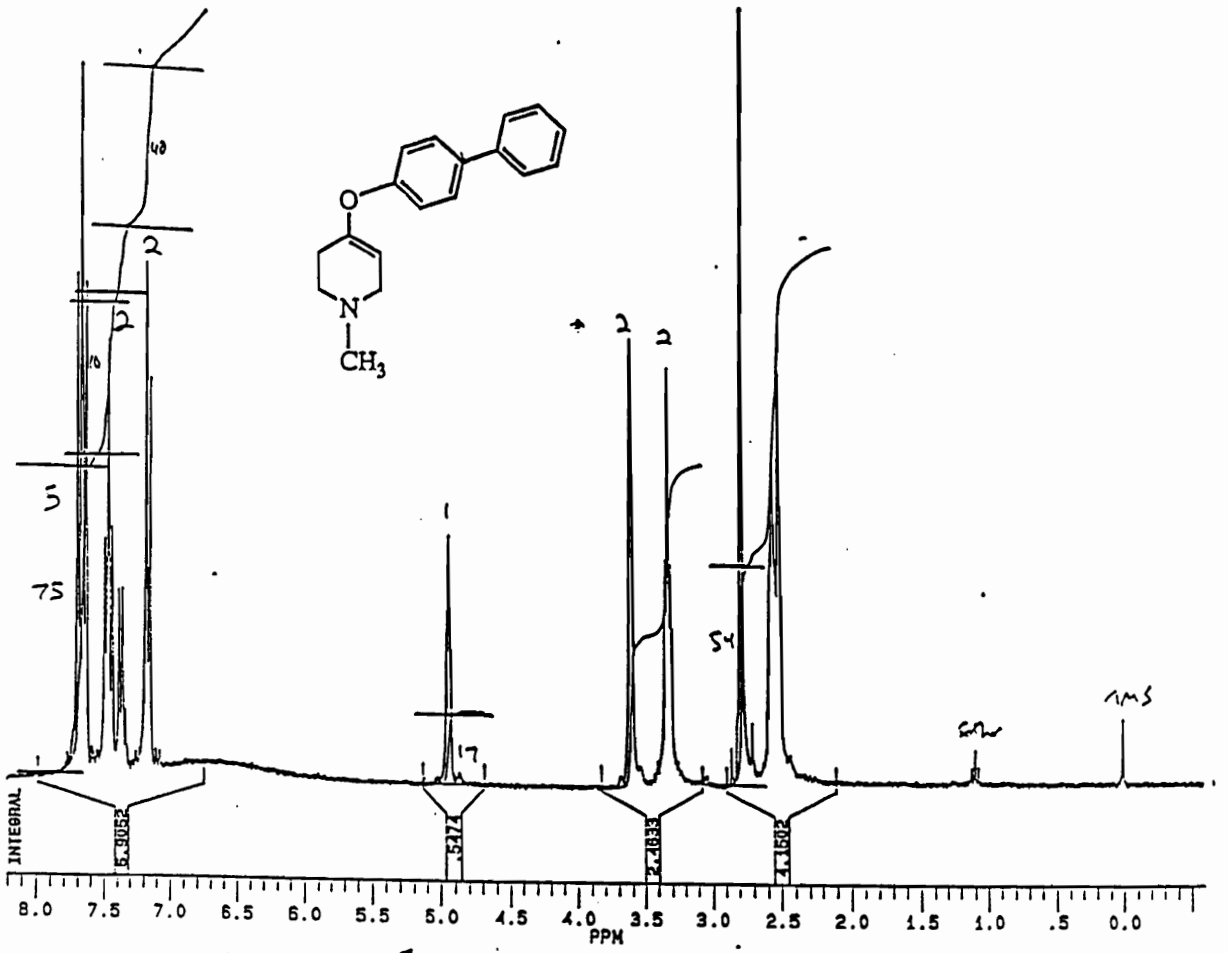

Figure. 89. ^{1}H NMR Spectrum (DMSO-d_6) of
1-Methyl-4-phenylphenoxy-1,2,3,6-tetrahydropyridine.

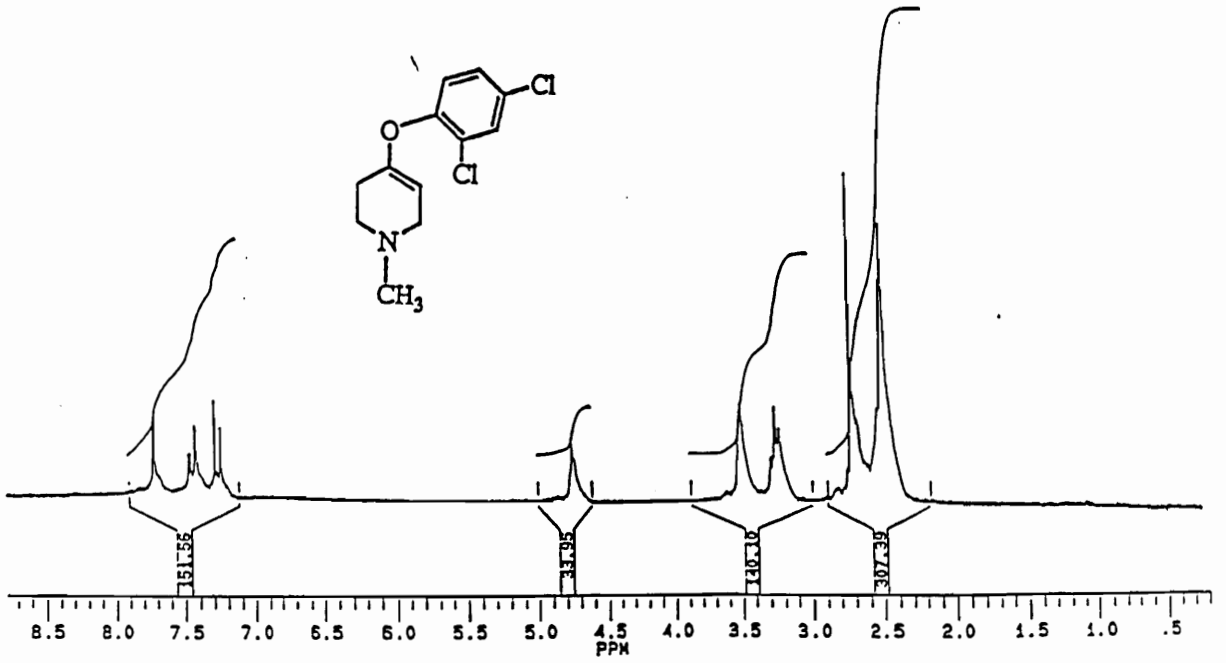

Figure. 90. ^{1}H NMR Spectrum (DMSO-d_6) of 4-(2,4-Dichlorophenoxy)-1-methyl-1,2,3,6-tetrahydropyridine.

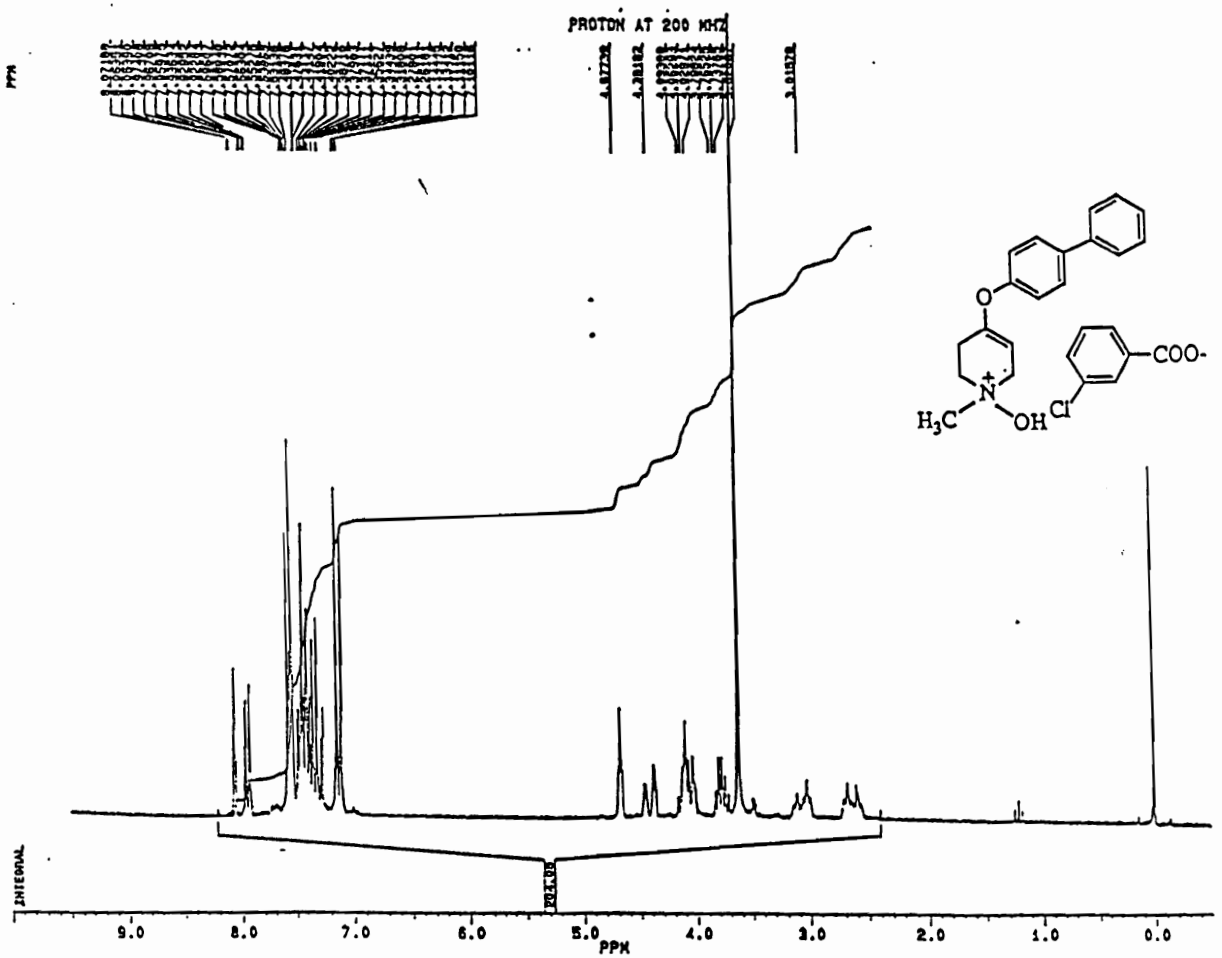

Figure. 91. ^{1}H NMR Spectrum ($CDCl_3$) of the *m*CBA Salt of the N-Oxide of 1-Methyl-4-phenylphenoxy-1,2,3,6-tetrahydropyridine.

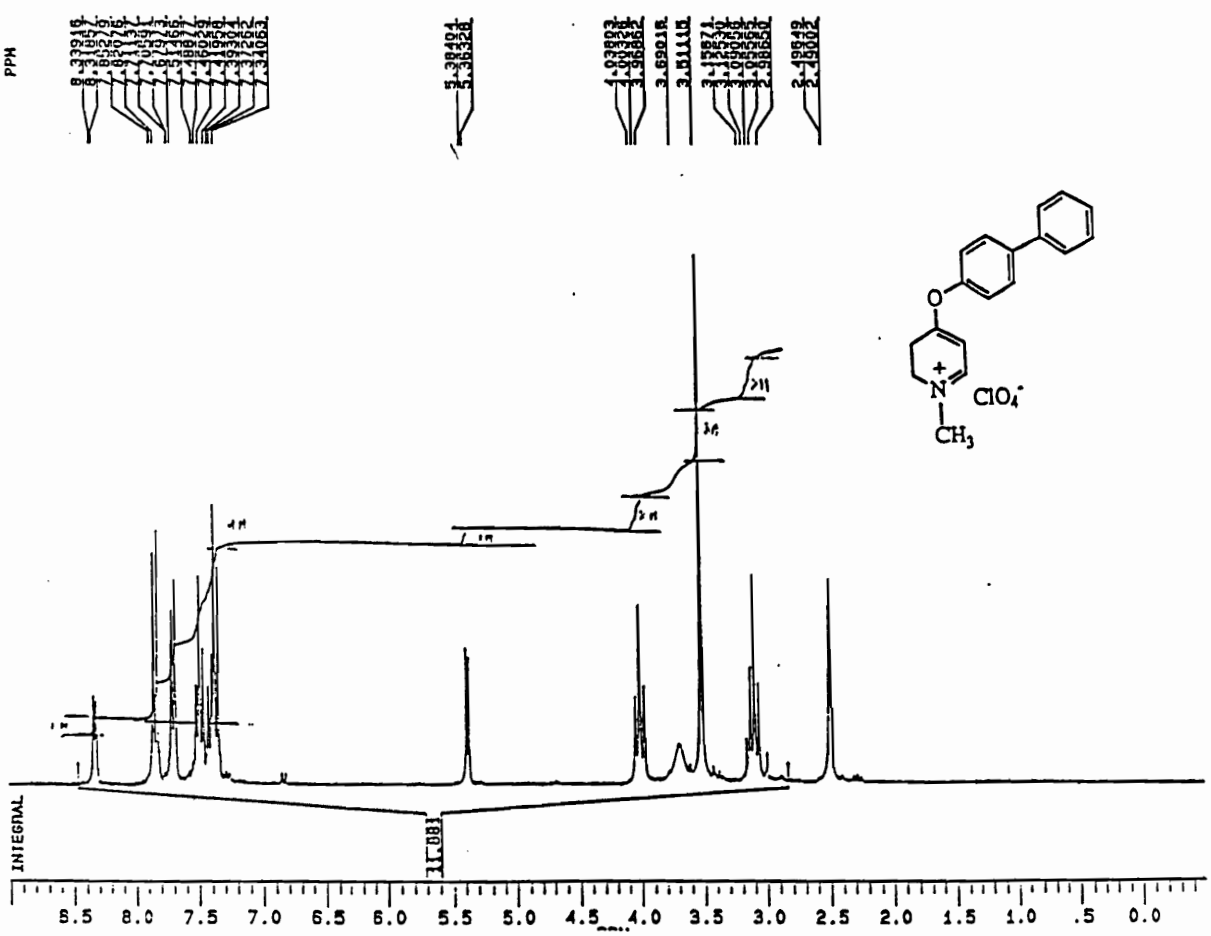

Figure. 92. ^1H NMR Spectrum (DMSO-d_6) of 1-Methyl-4-phenylphenoxy-2,3-Dihydropyridinium Perchlorate.

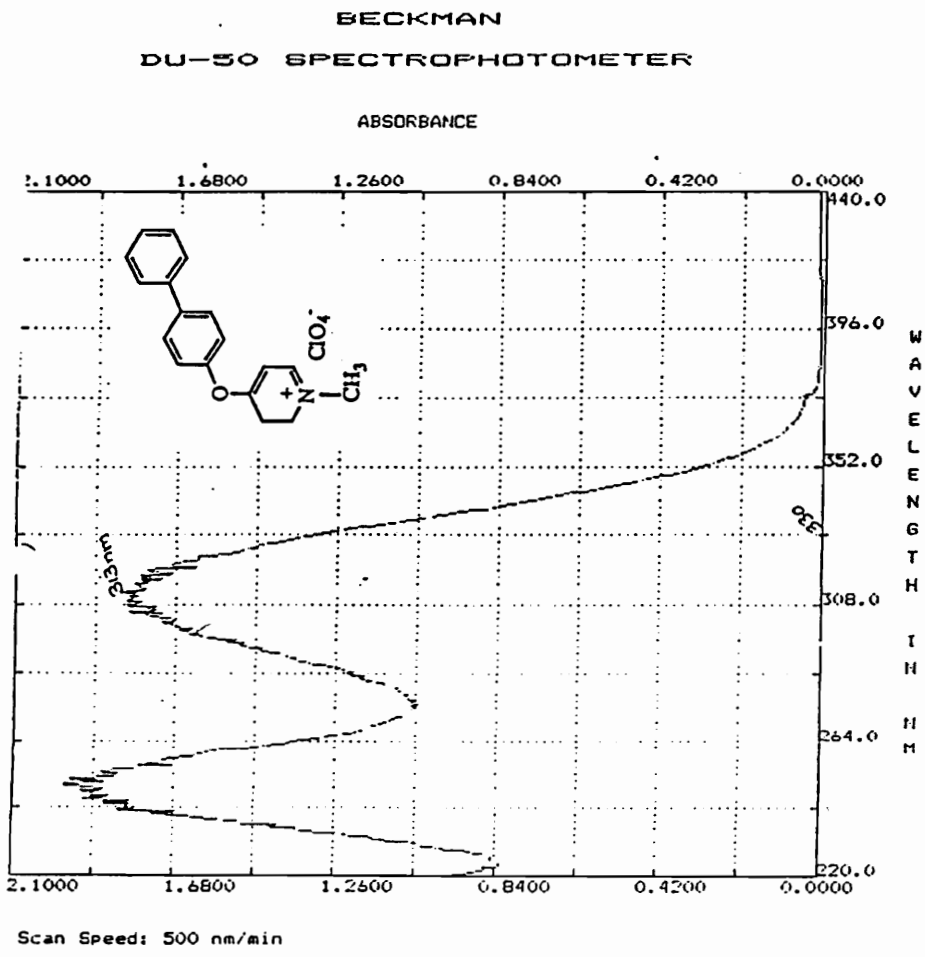

Figure. 93. UV Spectrum of 125 µM (in pH 7.4 Phosphate Buffer) 1-Methyl-4-phenylphenoxy-2,3-dihydropyridinium Perchlorate.

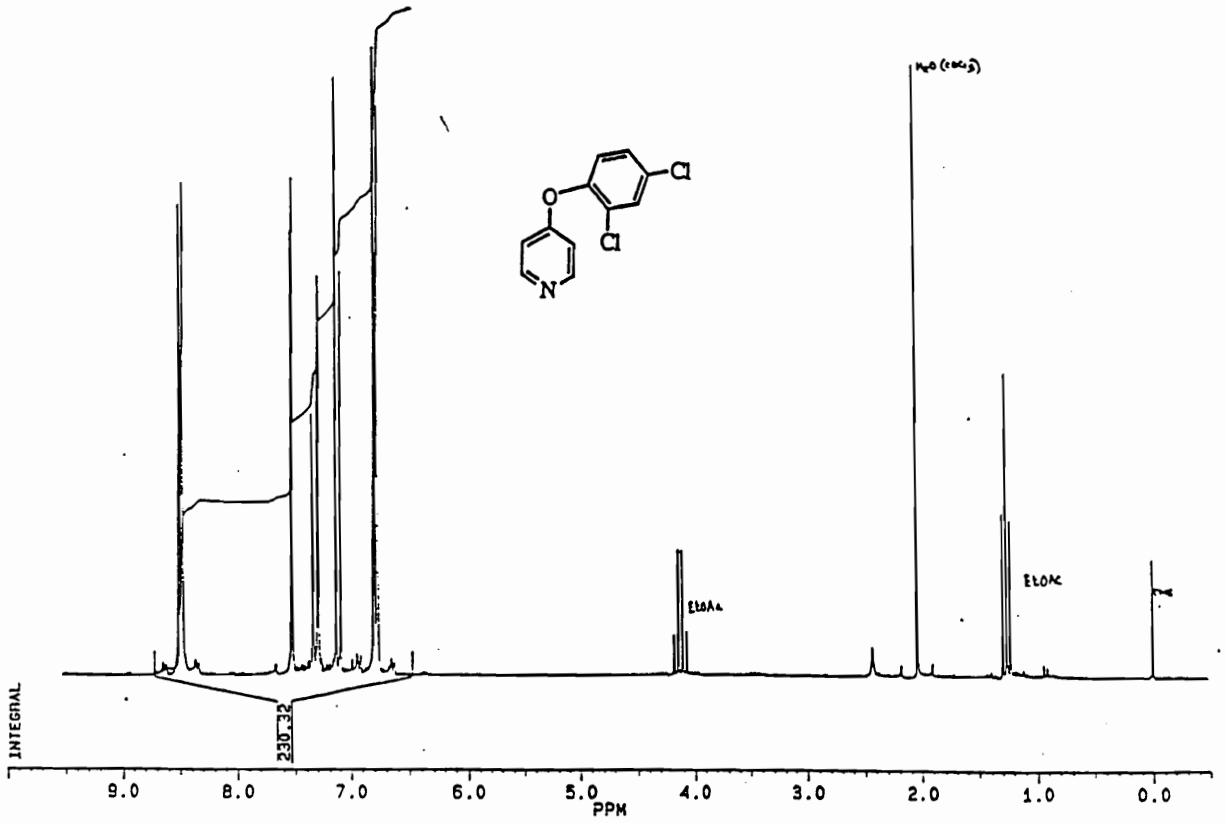

Figure. 94. ^{1}H NMR Spectrum ($CDCl_3$) of 4-(2,4-Dichlorophenoxy)pyridine.

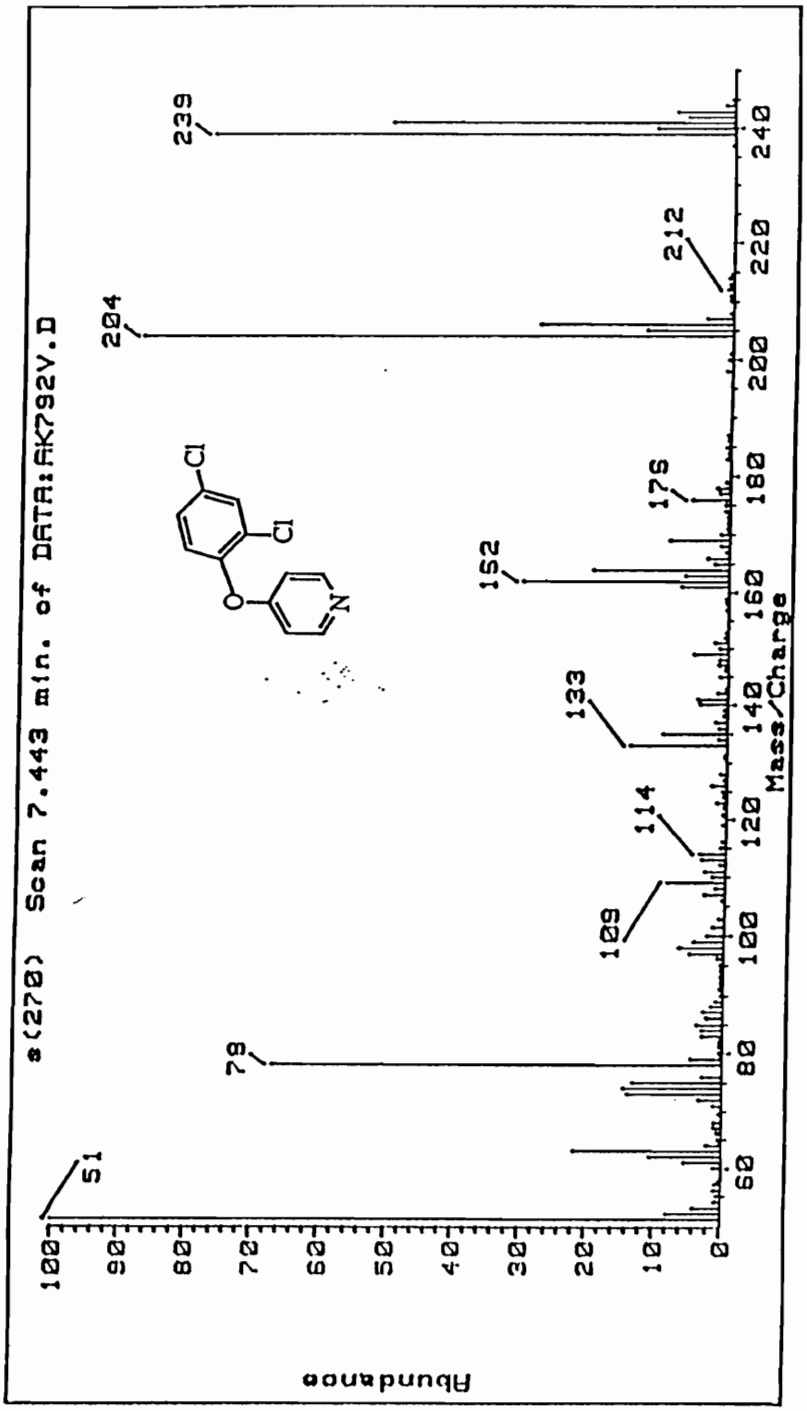

Figure. 95. GC/EIMS of 4-(2,4-Dichlorophenoxy)pyridine.

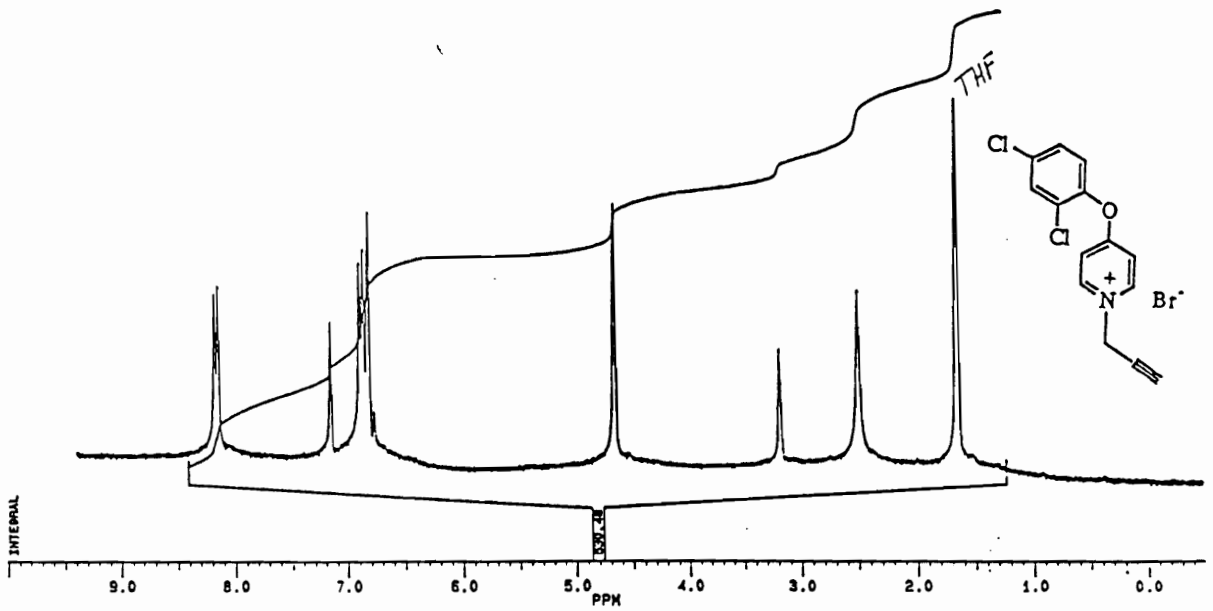

Figure. 96. ^{1}H NMR Spectrum (DMSO-d_6) of 4-(2,4-Dichlorophenoxy)-1-propargylpyridinium Iodide.

VITA

Amit Sumant Kalgutkar was born on August 27, 1965 in Bombay, India. He received his Bachelor of Science degree in Chemistry from the University of Bombay, India in 1985. In Fall of 1987, he was awarded his Master of Science degree in Organic Chemistry from the University of Bombay. He then worked as a Post-Graduate Fellow under the supervision of Dr. Sabir Mashraqui in the Department of Chemistry, University of Bombay. In Fall of 1988, the author came to the Department of Chemistry, Virginia Polytechnic Institute and State University. He then studied Drug Metabolism under the direction of Peter's Professor Dr. Neal Castagnoli, Jr. His research was sponsored by the Harvey W. Peters Research Center for Parkinson's Disease and Disorders of the Central Nervous System and NIH. He was awarded the Doctor of Philosophy degree in Chemistry from Virginia Polytechnic Institute and State University in the Fall of 1993.

Amit Sumant Kalgutkar